Gravitationally induced decoherence: from theoretical models to signatures in neutrino oscillations

Gravitativ induzierte Dekohärenz: Von theoretischen Modellen zu Signaturen in Neutrinooszillationen

Der Naturwissenschaftlichen Fakultät

der Friedrich-Alexander-Universität

Erlangen-Nürnberg

zur

Erlangung des Doktorgrades Dr. rer. nat.

vorgelegt von

Max Joseph Fahn

Als Dissertation genehmigt

von der Naturwissenschaftlichen Fakultät

der Friedrich-Alexander-Universität Erlangen-Nürnberg

Tag der mündlichen Prüfung: 11.12.2024

Gutachter/in:

Prof. Dr. Kristina Giesel
Prof. Dr. Daniel Burgarth

Table of Contents

To my family

Acknowledgements

I could not have undertaken this journey without my supervisor Prof. Dr. Kristina Giesel. I am extremely grateful for her continuous, fantastic support on my path towards the completion of this PhD thesis. The numerous fruitful discussions, the insightful comments and the invaluable feedback have made this work possible.

Furthermore, I would like to express my deepest appreciation to Prof. Dr. Daniel Burgarth for his willingness to give a second opinion on the thesis and to take the time to thoroughly read through it.

For their willingness to support my PhD as a member of the defense committee, I would like to express my deepest gratitude to Prof. Dr. Ana-Sunčana Smith and to Prof. Dr. Uli Katz.

Additionally, I would like to extend my sincere thanks to the QGRANT working group for the inspiring collaboration, in particular to Dr. Alba Domi, PD Dr. Thomas Eberl, Prof. Dr. Kristina Giesel, Lukas Hennig, Prof. Dr. Uli Katz, Roman Kemper and Michael Kobler.

I am also grateful for the support of the Institute of Quantum Gravity and all its members that I've received in the last years and the productive working atmosphere there. In particular, I would like to thank Dr. Renata Ferrero, Roman Kemper and Michael Kobler for the fruitful discussions on the project.

I would like to express my deepest appreciation to the Heinrich-Böll-Stiftung for the great ideational and financial support throughout my PhD, which enabled me to focus on this project.

Thanks should also go to the Elite Network of Bavaria, where my PhD programme was a part of. I am extremely grateful for the big variety of events and seminars and the network I could build there.

Last but of course not least, words cannot express my gratitude to my family who always supported me during my entire PhD, in particular my parents Doris and Christian, my sister Maria and my grandmother Stilla.

Declaration

The work this thesis is based on was published in the following papers:

- "A gravitationally induced decoherence model using Ashtekar variables", *Classical and Quantum Gravity 40.9 (2023), 094002, DOI 10.1088/1361-6382/acc5d5*; together with Kristina Giesel and Michael Kobler [1], published under the CC BY 4.0 License `https://creativecommons.org/licenses/by/4.0/`

- "Gravitationally induced decoherence of a scalar field: investigating the one-particle sector and its interplay with renormalisation", available as preprint *arXiv:2409.12790*; together with Kristina Giesel [2]

- "Understanding gravitationally induced decoherence parameters in neutrino oscillations using a microscopic quantum mechanical model", available as preprint *arXiv:2403.03106v3*; together with Alba Domi, Thomas Eberl, Kristina Giesel, Lukas Hennig, Ulrich Katz, Roman Kemper and Michael Kobler [3]
  This is the version of the article before peer review or editing, as submitted by an author to "Journal of Cosmology and Astroparticle Physics" (JCAP). IOP Publishing Ltd is not responsible for any errors or omissions in this version of the manuscript or any version derived from it. The Version of Record is available online at DOI 10.1088/1475-7516/2024/11/006 and [4], published under the CC BY 4.0 License `https://creativecommons.org/licenses/by/4.0/`

Part II of this thesis covers the content of the first paper [1], Part III most of the content of the second paper [2] and Part IV the third paper [3] and some minor parts of the second paper [2]. The text of these articles has been reused.
This thesis includes results of the Master's thesis "Gravitationally induced decoherence in open quantum systems using linearised gravity formulated in Ashtekar variables" submitted to the Department of Physics in 2020 [5]. This is clearly indicated in the introductory remarks of the corresponding sections. These results were included, as this PhD thesis builds on them.

Additionally, a fourth publication entitled "A gravitationally induced decoherence model for photons in the context of the relational formalism" [6] is prepared by Kristina Giesel and Roman Kemper together with the author of this thesis. The content of this work is kept out of this thesis.

Contribution of Max Joseph Fahn to the publication "A gravitationally induced decoherence model using Ashtekar variables", Classical and Quantum Gravity, 40.9 (2023), 094002.:

As a co-author, I confirm that Max Joseph Fahn contributed significantly to the results of the publication above. This involves his work on the conceptual questions and the literature research, the technical methods, the content of this article and the text manuscript. In particular, this encloses a major and significant contribution to the computations necessary to obtain the final results in the publication and their interpretation. The presentation of the work in this thesis summarises well his contributions to the publication. I agree with the use of this publication in this thesis.

Kristina Giesel

Contribution of Max Joseph Fahn to the publication "Gravitationally induced decoherence of a scalar field: Investigating the one-particle sector and the interplay between renormalisation and Markov approximation", in preparation:

As a co-author, I confirm that Max Joseph Fahn contributed significantly to the results of the publication above. This involves his work on the conceptual questions and the literature research, the technical methods, the content of this article and the text manuscript. In particular, this encloses a major and significant contribution to the computations necessary to obtain the final results in the publication and their interpretation. The presentation of the work in this thesis summarises well his contributions to the publication. I agree with the use of this publication in this thesis.

Kristina Giesel

Contribution of Max Joseph Fahn to the publication "Understanding gravitationally induced decoherence parameters in neutrino oscillations using a microscopic quantum mechanical model", available as preprint arXiv:2403.03106 and currently being reviewed:

As a co-author, I confirm that Max Joseph Fahn contributed significantly to the results of the publication above. This involves his work on the conceptual questions and the literature research, the technical methods, the content of this article and the text manuscript as well as some of the figures and comments on the numerical code. In particular, this encloses a major and significant contribution to the analytical computations necessary to obtain the final results in the publication and the interpretation of the analytical and numerical results. The presentation of the work in this thesis summarises well his contributions to the publication. I agree with the use of this publication in this thesis.

Kristina Giesel

Contribution of Max Joseph Fahn to the publication "A gravitationally induced decoherence model using Ashtekar variables", Classical and Quantum Gravity, 40.9 (2023), 094002.:

As a co-author, I confirm that Max Joseph Fahn contributed significantly to the results of the publication above. This involves his work on the conceptual questions and the literature research, the technical methods, the content of this article and the text manuscript. In particular, this encloses a major and significant contribution to the computations necessary to obtain the final results in the publication and their interpretation. The presentation of the work in this thesis summarises well his contributions to the publication. I agree with the use of this publication in this thesis.

Michael Kobler

Contribution of Max Joseph Fahn to the publication "Understanding gravitationally induced decoherence parameters in neutrino oscillations using a microscopic quantum mechanical model", available as preprint arXiv:2403.03106 and currently being reviewed:

As a co-author, I confirm that Max Joseph Fahn contributed significantly to the results of the publication above. This involves his work on the conceptual questions and the literature research, the technical methods, the content of this article and the text manuscript as well as some of the figures and comments on the numerical code. In particular, this encloses a major and significant contribution to the analytical computations necessary to obtain the final results in the publication and the interpretation of the analytical and numerical results. The presentation of the work in this thesis summarises well his contributions to the publication. I agree with the use of this publication in this thesis.

Michael Kobler

Contribution of Max Joseph Fahn to the publication "Understanding gravitationally induced decoherence parameters in neutrino oscillations using a microscopic quantum mechanical model", available as preprint arXiv:2403.03106 and currently being reviewed:

As a co-author, I confirm that Max Joseph Fahn contributed significantly to the results of the publication above. This involves his work on the conceptual questions and the literature research, the technical methods, the content of this article and the text manuscript as well as some of the figures and comments on the numerical code. In particular, this encloses a major and significant contribution to the analytical computations necessary to obtain the final results in the publication and the interpretation of the analytical and numerical results. The presentation of the work in this thesis summarises well his contributions to the publication. I agree with the use of this publication in this thesis.

Alba Domi

Contribution of Max Joseph Fahn to the publication "Understanding gravitationally induced decoherence parameters in neutrino oscillations using a microscopic quantum mechanical model", available as preprint arXiv:2403.03106 and currently being reviewed:

As a co-author, I confirm that Max Joseph Fahn contributed significantly to the results of the publication above. This involves his work on the conceptual questions and the literature research, the technical methods, the content of this article and the text manuscript as well as some of the figures and comments on the numerical code. In particular, this encloses a major and significant contribution to the analytical computations necessary to obtain the final results in the publication and the interpretation of the analytical and numerical results. The presentation of the work in this thesis summarises well his contributions to the publication. I agree with the use of this publication in this thesis.

Thomas Eberl

Contribution of Max Joseph Fahn to the publication "Understanding gravitationally induced decoherence parameters in neutrino oscillations using a microscopic quantum mechanical model", available as preprint arXiv:2403.03106 and currently being reviewed:

As a co-author, I confirm that Max Joseph Fahn contributed significantly to the results of the publication above. This involves his work on the conceptual questions and the literature research, the technical methods, the content of this article and the text manuscript as well as some of the figures and comments on the numerical code. In particular, this encloses a major and significant contribution to the analytical computations necessary to obtain the final results in the publication and the interpretation of the analytical and numerical results. The presentation of the work in this thesis summarises well his contributions to the publication. I agree with the use of this publication in this thesis.

Ulrich Katz

Contribution of Max Joseph Fahn to the publication "Understanding gravitationally induced decoherence parameters in neutrino oscillations using a microscopic quantum mechanical model", available as preprint arXiv:2403.03106 and currently being reviewed:

As a co-author, I confirm that Max Joseph Fahn contributed significantly to the results of the publication above. This involves his work on the conceptual questions and the literature research, the technical methods, the content of this article and the text manuscript as well as some of the figures and comments on the numerical code. In particular, this encloses a major and significant contribution to the analytical computations necessary to obtain the final results in the publication and the interpretation of the analytical and numerical results. The presentation of the work in this thesis summarises well his contributions to the publication. I agree with the use of this publication in this thesis.

Roman Kemper

Contribution of Max Joseph Fahn to the publication "Understanding gravitationally induced decoherence parameters in neutrino oscillations using a microscopic quantum mechanical model", available as preprint arXiv:2403.03106 and currently being reviewed:

As a co-author, I confirm that Max Joseph Fahn contributed significantly to the results of the publication above. This involves his work on the conceptual questions and the literature research, the technical methods, the content of this article and the text manuscript as well as some of the figures and comments on the numerical code. In particular, this encloses a major and significant contribution to the analytical computations necessary to obtain the final results in the publication and the interpretation of the analytical and numerical results. The presentation of the work in this thesis summarises well his contributions to the publication. I agree with the use of this publication in this thesis.

Lukas Hennig

Abstract

The search for signatures of quantum gravity effects in candidate theories of quantum gravity often focuses on symmetry reduced models such as cosmology and black holes. The main object of investigation of this thesis follows another approach and considers the effective influence of linearised quantum gravity effects on quantised matter systems formulated as open quantum systems, in particular the resulting decoherence induced in these with a focus on neutrino oscillations. To model these effects, we derive master equations for two different open quantum systems with linearised gravity as environment.

The first system consists of a scalar field coupled to linearised gravity formulated in Ashtekar variables and is meant to serve as a first step for the construction of decoherence models inspired by loop quantum gravity, which allows a mathematically rigorous canonical quantisation of full general relativity (GR). Due to the fact that GR is a gauge theory, it is essential to identify the physical degrees of freedom in order to assure a model's predictability. While field theoretical decoherence models that include gravity have so far worked with specific gauge fixings for linearised GR formulated in ADM variables, we follow in this thesis a different approach based on the relational formalism. For this, we show how suitable geometric clocks can be constructed that enable the construction of Dirac observables for the physical degrees of freedom. The advantage of this procedure is two-fold: on the one hand, it permits the formulation of the decoherence model independently of a specific gauge fixing but can be easily linked to different choices of such a gauge fixing, hence providing a method to compare different choices. On the other hand, it delivers a way to assign physical meaning to the time and space coordinates in the model, which originally are purely gauge in GR. The introduction and application of a dual version of the observable map originating from the relational formalism enables us to perform a canonical transformation to decompose the classical phase space into a physical and a gauge sector, where the Poisson algebras of the respective elementary phase space variables commute. Due to this, the reduced physical system, whose elementary phase space variables are the Dirac observables, can be quantised canonically, where in this work a Fock quantisation is used to facilitate the comparison with the literature. The methods derived in this thesis for the treatment of decoherence models involving linearised gravity in Ashtekar variables can also be applied to similar models with different matter fields such as for instance photons where these methods need to be slightly extended to take the $U(1)$ gauge symmetry into account.

Starting from a quantised model, there exist several different ways to obtain a master equation that describes the effective dynamics of the matter field under the influence of the gravitational environment. These techniques are usually employed in other areas of physics such as for instance in quantum optics or condensed matter physics. When gravity is considered as the environment, there are still many open questions regarding the applicability and validity of these methods and their interplay with a possible renormalisation. In the present thesis, we try to give some answers to these questions for specific physical systems and show some possible ways how these can be used in other systems. For this, we start from a time-convolutionless master equation for the scalar field which we derived with the projection operator technique assuming that the linearised gravitational environment is weakly coupled to the scalar field and obeys a stationary Gibbs state, which corresponds to thermal gravitational waves. Such a time-convolutionless master equation is in general not completely positive, which can lead to unphysical negative probabilities. To

circumvent this, for the description of decoherence models usually further approximations such as the Markov and the rotating wave approximations are applied to cast this equation into a completely positive Lindblad form. As mentioned above, the detailed influence of these approximations is however rather unexplored for gravity as environment and also their validity for this class of models is not yet clear. To investigate these open points and to facilitate the extraction of physical predictions from the field theoretical master equation, we project this equation onto the space of a single scalar particle. We then show how the resulting one-particle master equation can be connected to the underlying effective quantum field theory (QFT), which permits a clear physical interpretation of the involved contributions and scattering processes encoded in the master equation. Such a link has not been worked out before for gravity as environment in this class of decoherence models. Based on this, we can deliver a physical interpretation for different versions of the one-particle projection of the master equation applied in the literature and for the divergent terms in this master equation. It turns out that the latter correspond to vacuum bubbles and to the self-energy of the scalar particle. To remove them, we perform a renormalisation of the underlying effective QFT and obtain a master equation with only finite contributions. The renormalisation of the one-particle master equation for gravitationally induced decoherence at this stage is new in the literature and enables us to discuss the effects of the applications towards a Lindblad form from a physical point of view. In this work, we analyse the two most often invoked approximations for this purpose which are the Markov and rotating wave approximations. Additionally, conditions for the validity of the Markov approximation for the specific application to ultra-relativistic particles, in particular as a toy application for neutrinos, are given, which has not been discussed yet in the works on this class of gravitationally induced decoherence models in the literature.

Neutrinos represent potential candidates to exhibit features of gravitationally induced decoherence by modifications of their oscillation behaviour. Therefore, there is increasing interest in both the neutrino physics and gravitational decoherence communities to investigate this effect and its possible signatures in experimental data. Most of these analyses are based on phenomenological models that start from a Lindblad equation for a neutrino where the effective influence of gravity is represented by the Lindblad operators. As these models are not based on a microscopic theory, the Lindblad operators are unknown and therefore parametrised by free decoherence parameters. Bounds for these are then determined from experimental data by testing different possible dependencies of these decoherence parameters on the energy of the neutrino, however thereby not yielding an intuition which energy ranges and hence which detectors are favoured in the search of signatures of this decoherence effect. From a theoretical point of view it is thus of high interest to construct microscopic models that allow to resolve the structure of the dissipator in the phenomenological Lindblad equation and to give a physical interpretation of the unknown decoherence parameters. The construction of a model that provides some answers to these questions is a main part of this thesis. As a first step, we use the Lindblad form of the one-particle projection of the field theoretical master equation for a scalar field and apply it by asserting typical neutrino energies to the scalar particle, which delivers a precise form for the solution of the Lindblad equation for linearised gravity as environment, in which all appearing quantities have a clear physical interpretation due to the underlying field theoretical model.
As however a scalar particle might not be able to reproduce all the characteristics of a neutrino and in particular their oscillations appropriately, we consider as second model a quantum mechanical, microscopic toy model which couples a neutrino to a thermal bath of harmonic oscillators.

Such quantum mechanical models are usually constructed by hand with the implication that the form and the strength of the coupling of system and environment is a free, unknown parameter. In this thesis, we can provide a possible solution for this by using the results of the field theoretical model above. Another challenge is that when deriving master equations for quantum mechanical models, the environment with only finitely many degrees of freedom would lead to unphysical Poincaré recurrences after finite time intervals which correspond to recoherences. In realistic physical systems, these are usually expected to happen only after extremely long time intervals that lie far beyond the scope of measurable timescales. To cure this, a continuum limit is employed on the modes in the environment. By comparison to the field theoretical master equation discussed above, we can motivate a specific form for this limit which is often used in other contexts as for instance in quantum optics. As a next step, we also prove for the quantum mechanical model that the validity of the Markov approximation is given when applied to the specific case of ultra-relativistic neutrinos. To deduce physical implications from the final Lindblad equation, we again emphasise the relevance of a proper renormalisation, which is not always taken into account in the literature.
This Lindblad equation, arising from the microscopic model motivated by the field theoretical one, now enables the comparison of the resulting time evolution to the one obtained from phenomenological models and its general solution is very similar to the one of the field theoretical model applied to a single scalar particle. An advantage of the microscopic model in comparison to the phenomenological ones is that the parametrisation used in the latter can now be resolved which yields a physical interpretation for the decoherence parameters. We end up with two free parameters corresponding to the coupling strength, for which we discuss a possible value coming from the field theoretical model, and a temperature parameter that characterises the thermal environment. It turns out that the usual parametrisation in the phenomenological models for the considered class of models for gravitationally induced decoherence cannot be matched with the microscopic model for neutrino oscillations in matter. The reason for this is that the phenomenological models mostly assume constant Lindblad operators independently of the matter density, whereas the microscopic quantum mechanical model suggests that they are equal to the neutrino Hamiltonian which changes when the matter density does. This point of view would also be featured by GR, where the Lindblad operators would be derived from the energy-momentum tensor of the neutrino that contains the matter contribution as well.

Zusammenfassung

Der Titel der Arbeit überträgt sich ins Deutsche als "Gravitativ induzierte Dekohärenz: Von theoretischen Modellen zu Signaturen in Neutrinooszillationen".

Die Suche nach Signaturen von Quantengravitationseffekten in möglichen Kandidaten für Quantengravitationstheorien ist häufig fokussiert auf symmetriereduzierte Modelle wie die Kosmologie oder Schwarze Löcher. In dieser Arbeit wird ein anderer Ansatz verfolgt, in dem der effektive Einfluss von linearisierten Quantengravitationseffekten auf quantisierte Materiesysteme, die als offene Quantensysteme formuliert sind, analysiert wird und insbesondere die daraus resultierende Dekohärenz, die in diesen Systemen induziert wird, mit einem Fokus auf Neutrinooszillationen untersucht wird. Um diese Effekte zu modellieren, werden Mastergleichungen für zwei verschiedene offene Quantensysteme mit linearisierter Gravitation als Umgebung hergeleitet.

Das erste System besteht aus einem Skalarfeld, das an linearisierte Gravitation, formuliert in Ashtekar-Variablen, gekoppelt ist, und soll als erster Schritt für die Konstruktion von Dekohärenzmodellen inspiriert durch die Schleifenquantengravitation dienen, die eine mathematisch rigorose kanonische Quantisierung der vollen Allgemeinen Relativitätstheorie (ART) ermöglicht. Da es sich bei der ART um eine Eichtheorie handelt, ist es essentiell für die Ableitung physikalischer Vorhersagen aus einem Modell die physikalischen Freiheitsgrade zu identifizieren. Während feldtheoretische Dekohärenzmodelle die die Gravitation mit einbeziehen bisher spezifische Eichfixierungen für die linearisierte ART formuliert in ADM Variablen benutzt haben, wird in dieser Arbeit ein anderer Ansatz verfolgt, der auf dem Relationalen Formalismus basiert. Für diesen wird gezeigt, wie geeignete geometrische Uhren gefunden werden können, die die Konstruktion von Dirac-Observablen für die physikalischen Freiheitsgrade ermöglichen. Dieses Verfahren bietet zwei Vorteile: Zum einen erlaubt es die Formulierung des Dekohärenzmodells unabhängig von einer bestimmten Eichfixierung, kann aber leicht mit verschiedenen Wahlen für eine solche Eichfixierung verknüpft werden und bietet somit eine Methode zum Vergleich verschiedener Fixierungen. Andererseits bietet es eine Möglichkeit, den Zeit- und Raumkoordinaten des Modells eine physikalische Bedeutung zuzuweisen, bei denen es sich in der ART um reine Eichparameter handelt. Die Einführung und Anwendung einer dualen Version der aus dem relationalen Formalismus stammenden Observablen-Abbildung ermöglicht es, eine kanonische Transformation durchzuführen, um den klassischen Phasenraum in einen physikalischen und einen Eichteil aufzuspalten, wobei die Poisson-Algebren der entsprechenden elementaren Phasenraumvariablen kommutieren. Dadurch kann das reduzierte physikalische System, dessen elementare Phasenraumvariablen die physikalischen Dirac-Observablen sind, kanonisch quantisiert werden, wobei in dieser Arbeit eine Fock-Quantisierung verwendet wird, um den Vergleich mit der Literatur zu erleichtern. Die in dieser Arbeit abgeleiteten Methoden zur Behandlung von Dekohärenzmodellen mit linearisierter Gravitation in Ashtekar-Variablen können ebenfalls auf ähnliche Modelle angewendet werden, die aus anderen Materiefeldern bestehen, wie beispielsweise Photonen, wo diese Methoden etwas erweitert werden müssen, um die zusätzliche $U(1)$ Eichsymmetrie zu implementieren.

Ausgehend von einem quantisierten Modell gibt es verschiedene Möglichkeiten eine Mastergleichung herzuleiten, die die effektive Dynamik des Materiefeldes unter Einfluss der gravitativen Umgebung beschreibt. Diese Techniken werden in der Regel in anderen Bereichen der Physik angewandt, zum Beispiel in der Quantenoptik oder der Festkörperphysik. Wenn Gravitation als

Umgebung betrachtet wird, gibt es jedoch noch viele offene Fragen bezüglich der Anwendbarkeit und Gültigkeit dieser Methoden und ihres Zusammenwirkens mit einer möglicherweise notwendigen Renormierung. In der vorliegenden Arbeit wird versucht, einige Antworten auf diese Fragen für bestimmte physikalische Systeme zu geben und Möglichkeiten aufzuzeigen, wie diese in anderen Systemen verwendet werden können. Dazu wird mit einer zeitfaltungslosen Mastergleichung für das Skalarfeld begonnen, die mithilfe der Projektionsoperatortechnik abgeleitet wurde unter der Annahme, dass die linearisierte Gravitationsumgebung schwach an das Skalarfeld koppelt und einem stationären Gibbs-Zustand folgt, welcher thermischen Gravitationswellen entspricht. Eine solche zeitfaltungslose Mastergleichung ist im Allgemeinen nicht vollständig positiv, was zu unphysikalischen negativen Wahrscheinlichkeiten führen kann. Daher werden zur Beschreibung von Dekohärenzmodellen üblicherweise weitere Näherungen wie die Markov- und die Rotating Wave-Näherung angewendet, um diese Gleichung in eine vollständig positive Lindblad-Form zu bringen. Wie bereits erwähnt, ist der detaillierte Einfluss dieser Näherungen für Gravitation als Umgebung noch nicht weit erforscht und auch ihre Gültigkeit für diese Klasse von Modellen ist noch nicht klar. Um diese offenen Punkte zu untersuchen und um die Extraktion physikalischer Vorhersagen aus der feldtheoretischen Mastergleichung zu erleichtern, wird diese Gleichung auf den Raum eines einzelnen skalaren Teilchens projiziert. Anschließend wird gezeigt, wie die sich daraus ergebende Ein-Teilchen-Mastergleichung mit der zugrundeliegenden effektiven Quantenfeldtheorie (QFT) verbunden werden kann, was eine physikalische Interpretation der in der Mastergleichung vorkommenden Beiträge und Streuprozesse ermöglicht. Eine solche Verbindung wurde bisher noch nicht ausgearbeitet für Gravitation als Umgebung in dieser Klasse von Dekohärenzmodellen. Darauf aufbauend kann eine physikalische Interpretation für verschiedene in der Literatur verwendete Versionen der Ein-Teilchen-Projektion der Mastergleichung und für die divergenten Terme in ihr geliefert werden. Es stellt sich heraus, dass diese Divergenzen Vakuumblasen und der Selbstenergie des skalaren Teilchens entsprechen. Um sie zu entfernen wird eine Renormierung der zugrunde liegenden effektiven QFT durchgeführt, was eine Mastergleichung mit nur endlichen Beiträgen liefert. Die Renormierung der Ein-Teilchen-Mastergleichung für gravitativ induzierte Dekohärenz an dieser Stelle vor der Anwendung weiterer Näherungen ist neu in der Literatur und ermöglicht es, die Auswirkungen der Näherungen, die auf eine Lindblad-Form führen, aus physikalischer Sicht zu diskutieren. In dieser Arbeit werden die beiden dafür am häufigsten verwendeten Näherungen analysiert, die Markov- und die Rotating Wave-Näherung. Zusätzlich werden Bedingungen für die Gültigkeit der Markov-Näherung für die Anwendung auf ultra-relativistische Teilchen, insbesondere als einfaches Modell für Neutrinos, gegeben, was bisher noch nicht in den Arbeiten zu dieser Klasse von gravitativ induzierten Dekohärenzmodellen in der Literatur besprochen wurde.

Neutrinos stellen potenzielle Kandidaten dar, die Signaturen von gravitativ induzierten Dekohärenzeffekte zeigen könnten, die zu einer Veränderung ihres Oszillationsverhaltens führen könnten. Daher gibt es sowohl in der Neutrinophysik als auch in der Forschung zu gravitativ induzierter Dekohärenz ein wachsendes Interesse an der Untersuchung dieses Effekts und seiner möglichen Signaturen in experimentellen Daten. Die meisten dieser Analysen basieren auf phänomenologischen Modellen, die von einer Lindblad-Gleichung für ein Neutrino ausgehen, wobei der effektive Einfluss der Gravitation in den Lindblad-Operatoren kodiert wird. Da diese Modelle nicht auf einer mikroskopischen Theorie beruhen, sind die Lindblad-Operatoren unbekannt und werden in unbekannten Dekohärenzparametern ausgedrückt. Grenzen für deren Größe werden dann durch experimentelle Daten bestimmt, indem verschiedene mögliche Modelle ausgewertet werden, die

unterschiedliche Abhängigkeiten der Dekohärenzparameter von der Energie des Neutrinos enthalten, ohne dadurch jedoch eine Intuition zu erhalten, welche Energiebereiche und damit welche Detektoren bei der Suche nach Signaturen dieses Dekohärenzeffekts besser geeignet sind. Aus theoretischer Sicht ist es daher von großem Interesse, Modelle zu konstruieren, die es ermöglichen, die Struktur des Dissipators in der phänomenologischen Lindblad-Gleichung aufzulösen und eine physikalische Interpretation der unbekannten Dekohärenzparameter zu geben. Die Konstruktion eines Modells, das einige Antworten auf diese Fragen liefert, ist ein Hauptbestandteil dieser Arbeit. In einem ersten Schritt wird die Lindblad-Form der Ein-Teilchen-Projektion der feldtheoretischen Mastergleichung für ein skalares Feld verwendet und angewendet, indem dem skalaren Teilchen typische Neutrinoenergien zugeschrieben werden, was eine spezifische Lösung der Lindblad-Gleichung liefert, in der alle auftretenden Größen aufgrund des zugrundeliegenden feldtheoretischen Modells eine klare physikalische Interpretation besitzen.
Da jedoch ein skalares Teilchen möglicherweise nicht alle Eigenschaften eines Neutrinos, insbesondere seine Oszillationen, angemessen wiedergeben kann, wird als zweites Modell ein quantenmechanisches, mikroskopisches Spielzeugmodell betrachtet, in welchem ein Neutrino an ein thermisches Bad aus harmonischen Oszillatoren gekoppelt wird. Derartige quantenmechanische Modelle werden in der Regel künstlich von Hand konstruiert, was bedeutet, dass die Form und die Stärke der Kopplung zwischen System und Umgebung künstlich eingefügt werden muss. In dieser Arbeit wird hierfür eine mögliche Lösung geliefert durch die Verwendung der Ergebnisse des oben diskutierten feldtheoretischen Modells. Ein weiterer problematischer Punkt liegt darin, dass sich bei der Ableitung von Mastergleichungen für quantenmechanische Modelle mit endlichdimensionaler Umgebung nach bestimmen Zeitintervallen unphysikalische Poincaré-Rekurrenzen ergeben würden, die Rekohärenzen entsprechen. In realistischen physikalischen Systemen sind diese in der Regel erst nach extrem langen Zeitintervallen zu erwarten, die weit fernab der messbaren Zeitskalen liegen. Um das zu beheben, wird ein Kontinuumslimes für die Moden in der Umgebung verwendet. Durch den Vergleich mit der oben diskutierten feldtheoretischen Mastergleichung kann eine spezifische Form für diesen motiviert werden, die in anderen Bereichen, z. B. in der Quantenoptik, häufig verwendet wird. In einem nächsten Schritt wird auch für das quantenmechanische Modell bewiesen, dass die Gültigkeit der Markov-Approximation gegeben ist, wenn sie auf ultra-relativistische Neutrinos angewendet wird. Um aus der finalen Lindblad-Gleichung physikalische Folgerungen ableiten zu können, wird erneut auf die Bedeutung einer korrekten Renormierung, die in der Literatur nicht immer berücksichtigt wird, eingegangen.
Die Lindblad-Gleichung, die sich aus dem mikroskopischen Modell ergibt, welches durch das feldtheoretische Modell motiviert ist, ermöglicht nun den Vergleich der sich ergebenden Dynamik mit der aus phänomenologischen Modellen erhaltenen und ihre allgemeine Lösung weist eine sehr ähnliche Struktur auf wie die des feldtheoretischen Modells, das auf ein einzelnes skalares Teilchen angewendet wird. Ein Vorteil des mikroskopischen Modells gegenüber den phänomenologischen Modellen besteht darin, dass nun die in letzteren verwendete Parametrisierung aufgelöst und eine physikalische Interpretation für die Dekohärenzparameter gefunden werden kann. Am Ende ergeben sich zwei freie Parameter: die Kopplungsstärke, für die ein möglicher Wert basierend auf dem feldtheoretischen Modell diskutiert wird, und ein Temperaturparameter, der die thermische Gravitationsumgebung charakterisiert. Es stellt sich heraus, dass die übliche Parametrisierung in den phänomenologischen Modellen für die betrachtete Klasse an Modellen für gravitativ induzierte Dekohärenz nicht vollständig auf das mikroskopische Modell für Neutrino-Oszillationen in Materie angepasst werden kann. Der Grund hierfür ist, dass phänomenologische Modelle meist von konstanten Lindblad-Operatoren unabhängig der Materiedichte ausgehen, während das mi-

kroskopische quantenmechanische Modell ergibt, dass diese Operatoren dem Hamilton-Operator des Neutrinos entsprechen, der sich ändert sobald sich die Materiedichte ändert. Dieses Ergebnis aus dem mikroskopischen Modell wäre in Einklang mit der ART, da die Lindblad-Operatoren aus dem Energie-Impuls-Tensor des Neutrinos hergeleitet werden würden, der auch den Materiebeitrag enthält.

1. Introduction

1.1. Stories from our universe

Mankind has always been looking into the sky and wondered, what was out there. The incredible beauty of nature with its enormous amount of fascinating phenomena has led to the development of a vast number of scientific branches to construct theories that try to explain how specific parts of nature work and to perform observations to listen to the stories that come from our universe and to thereby test these theories. To understand better what is going on in the sky and beyond, physics plays an important role. While in the beginning all observable phenomena that could be viewed from our point of view on the surface of the Earth were attributed to unknown forces, their interplay and their moods, over many centuries more fundamental theories were developed that explained the observations with underlying mathematical laws.

1.1.1. Quantum and gravity

> *"From things that differ comes the most beautiful harmony."*
>
> – Heraclitus of Ephesus, *Fragments B 8*

For thousands of years, all observations were limited to visible phenomena and the theories were constructed around them. This has changed and we can also perceive information from other sources, for instance from gravitational waves, and measure particles like neutrinos that can propagate through regions light cannot pass. Today, the modern physical understanding of the world is mainly based on two fundamental theories: general relativity and the standard model of particle physics based on quantum field theory. The technical revolution of the last century, which was fuelled by the development of these two theories, gave rise to a plethora of new detection methods that allowed access to new phenomena as for instance the discovery of gravitational waves or new elementary particles. The theory of general relativity (GR) was published in 1915, approximately 110 years ago. Quantum mechanics (QM), from which quantum field theory (QFT) emerged in the subsequent years, was also mainly developed one hundred years ago and the standard model (SM) was finalised in its present formulation more than 50 years ago. Various experiments have shown since then that GR, QM/QFT and the SM seem to describe nature at a high level of accuracy in their respective regimes, that is GR for gravity and on large scales, QFT/SM for the other three fundamental forces and on small scales. Nevertheless, some issues have arisen that are not solved fully satisfying within these theories when applied to their respective regimes, for instance the singularities that GR predicts for black holes or at the Big Bang, the lack of having a rigorous, mathematically well-defined QFT for interactions, the different kinds of divergences like UV divergences arising due to having infinitesimal small lengths in QFT and the SM predicting massless neutrinos which seems to be in contrast to experimental measurements. Therefore it is clear that GR and the SM are not the end of the road of theories describing physics at the fundamental level, but only another intermediate step. However, both taught us completely new concepts that contradict our experiences from everyday life. For instance from GR we understood that time is not absolute and that spacetime is curved, while from QM we learned that the world seems to be intrinsically probabilistic.

An additional important aspect that extends the list of open issues in each of the individual theories is the lack of a commonly accepted theory that describes the interplay of gravity with

the other three forces in all regimes, that is a technique to combine both of these theories. The search for such a theory of quantum gravity (QG) is almost as old as the individual theories of GR and QM themselves. The expectation which is tied to its development is that it also resolves issues that are present in GR and QFT when considered individually. For instance, the singularity in GR at the Big Bang might only arise due to the negligence of quantum forces that might prevent such a singularity and lead to a Big Bounce or similar processes. And the UV divergences in QFT might be resolved by a quantised, minimal length. Today, there are developed several theories of QG which pursue different aims, from creating a new, grand unified theory to the attempt of quantising gravity and expressing it in a form similar to the other three fundamental forces in the SM. These theories deviate on whether they start from GR or QFT (or a completely different ansatz) and on which additional assumptions they add, if any. Two of the most prominent approaches to develop a theory of QG are String Theory [7–9] and loop quantum gravity [10–12]. String Theory attempts to create a novel grand unified theory starting from new assumptions like the world having more than four dimensions and all particles consisting of little strings. It assumes the QFT point of view where the entire universe is described with respect to a background spacetime. In contrast, the objective of loop quantum gravity is to quantise gravity in a manner compatible with the basic laws of GR. It starts from GR and uses methods to keep the theory background independent without imposing additional assumptions apart from the one that gravity is inherently quantum, which is the core assumption in any QG theory. In the past decades, there has been considerable progress in the development of QG theories and several physical phenomena were predicted, like the existence of a minimal length and a Big Bounce from loop quantum gravity and its derivatives (see for instance [11, 13, 14]), as well as the existence of new particles from String Theory (see for instance [15]) or String Cosmology (see for instance [16]).

1.1.2. Experimental signatures of quantum gravity phenomena

> *"Whatever concerns seeing, hearing, and learning, I particularly honor."*
>
> – Heraclitus of Ephesus, *Fragment 13*

With the advancing development of QG theories, it becomes increasingly more important to identify experimentally accessible physical scenarios where there is a possibility to measure signatures of QG theories in order to be able to test these different theories. Two important areas of physics for this are cosmology and Black Hole physics. In cosmology, different scenarios are being investigated on how our universe could have started, whether it was a Big Bang, a Big Bounce or something else. Based on that, the physical implications of these scenarios are analysed and signatures in experimental measurements are investigated, for instance in the cosmic microwave background or the distribution of stars and matter in our universe. As mentioned above, GR yields a singularity in this regime and thus predicts its own failure, so a more advanced theory is required to describe the beginning of our universe. Loop quantum cosmology (LQC) [13, 14, 17–19] is one attempt to construct such a theory and to give answers to these questions. This theory arises from the quantisation of a homogeneous spacetime with methods of loop quantum gravity. Due to the form of the quantisation inspired by loop quantum gravity, LQC predicts discrete geometry at the Planck level and it culminates in GR in the limit of small curvature. One conclusion from this theory is that the Big Bang can be replaced by a Big Bounce [20, 21]. The detailed measurement of the power spectrum of the cosmic microwave background by

WMAP [22] and PLANCK [23] gave rise to the question if an imprint of quantised perturbations in the early universe can be extracted from this data as another hint for processes that are not describable with GR alone, which is analysed using (loop) quantised cosmological perturbation theory [24–27]. Apart from this, also black holes represent a singularity in spacetime according to GR. Also here quantum effects could play a major role to resolve this issue and to tell us what a Black Hole looks like in its interior. The treatment of black holes in loop quantum gravity can lead indeed to a resolution of the singularity [28–31] and, motivated partly by the bounce scenario in LQC, new processes like the transition of a Black into a White Hole were proposed [32–34].
With the increasing accuracy of the new generation of detectors, also another physical process gains attention to provide potential experimental access to signatures of quantum gravity effects. This is the process of (quantum) decoherence induced by gravity. While cosmology and Black Hole physics are usually approached from the theoretical side by the application of a symmetry reduction of the full QG theory, gravitationally induced decoherence can also be investigated by using a linearised version of a QG theory in physical systems where the coupling of gravity to matter is weak, therefore working with gravitational waves.

Decoherence is a process that arises whenever two quantum mechanical systems can exchange information, but only one of them is measured in the end. This possibility to exchange information can lead to a flow of information from the system, that is measured later, into the other. In realistic quantum systems, such decoherence processes are always present, because a real system can never be shielded completely from every external influence, in particular not from gravity. So any system investigated is influenced by its surroundings and can exchange information with them. Two of the interesting points here are on the one hand the size of this decoherence effect in a given physical system and on the other hand its effect on this system under consideration. The size depends on many different factors like the other interactions present in the system or the coupling strength between the two systems. This makes it hard to generalise here, one rather has to investigate the effect of decoherence for a specific given physical setup. Also the second point, the way decoherence manifests in the system under consideration, depends among other things on the structure of the coupling of the two systems and on the basis in which physical predictions are made. By definition, the loss of information from the point of view of the measured system can lead to a classicalisation of the system under consideration, that is to the disappearance of the off-diagonal elements of the density matrix in a specific basis after certain time. The implications of this in our everyday life are still not completely understood. There exist discussions on whether decoherence might help to understand how measurements work in quantum mechanics from a fundamental level. The issue here is that an isolated quantum system obeys unitary time evolution according to the Schrödinger equation (or a Schrödinger-like equation in the field theoretical case). Whenever a measurement is performed in QM, this evolution has to be stopped and then one has to change by hand the state of the system to the eigenstate corresponding to the eigenvalue measured of the operator representing the measurement, before the unitary Schrödinger(-like) evolution continues, which is usually denotes as the measurement problem, see for instance [35–37]. Albeit this aspect is not the topic of this thesis, decoherence might yield a possible resolution of this rather phenomenological procedure, see for instance [38–40]. Furthermore, decoherence is considered to be a potential explanation of the quantum-to-classical transition which would solve the question why the world in our everyday experience appears to be classical, see for instance [41–44].

To describe physical systems that exhibit decoherence, the formalism of Open Quantum Systems is frequently used, an introduction can be found for instance in [45–47]. The idea of this technique is to consider the system one is interested in and to couple it to an environment. The detailed dynamics of the environment are not of interest, only its effective influence on the system under consideration. While the total system composed of system of interest and environment is isolated and therefore follows unitary dynamics governed by the Schrödinger equation (or a Schrödinger-like equation in the field theoretical case), the same does not hold any more when considering only the dynamics of the system of interest. Its evolution equation in density matrix formulation is called master equation and contains apart from the standard evolution, that arises when considering the system under investigation to be isolated, also additional terms resembling the influence of the environment. These additional terms lead to new effects that are not present in isolated systems: shifts in the energy levels, as it is for instance known from particles in external electromagnetic fields, energy loss into the environment and information loss into the environment, which precisely is decoherence. As any physical system interacts with an environment, this formalism has spread and is applied in many different areas of physics from quantum optics, quantum information and condensed matter physics [48–52] to cosmology [53–59] and gravitational decoherence [1, 6, 60–63]. While in cosmology or for gravitational decoherence the formalism is usually applied to analyse a desired influence of the environment on the system of interest and the aim is to have this effect as strong as possible, in quantum computing often the contrary is the case, because here the objective is to minimise external influences to make qubit states decohere as slow as possible as this decoherence destroys information saved in states and hence reduces the computational power, as discussed for instance in [64–66].

Decoherence induced by gravity has been investigated in several different approaches in the past, see [67–69] for an overview. We will name a selection of them classified similarly as in [68]. Some of these theories consider gravity to be classical, for instance the Moller-Rosenfeld theory [70, 71] or the Diosi-Penrose theory [72–75]. However, they seem to be not compatible with GR and QFT alone, but require modifications of them, as is discussed in [68, 76, 77]. Other theories consider special processes at Planck scale that lead to decoherence, for instance [78, 79]. As discussed in [68], one would expect that some effective influence of these processes is contained in GR and the deviations thereof are much smaller than effects based on GR. Another class of theories considers the point of view of treating a matter system under investigation as an open quantum system coupled to a gravitational environment which causes the matter system to decohere. In these theories GR is frequently analysed for weak gravitational interactions leading to linearised GR where the gravitational field is determined by the perturbations of the metric. In the works in [80–82], these perturbations are then modeled to follow a stochastic process, which however does one not allow to identify the physical degrees of freedom. A similar approach which assumes these linearised metric perturbations to obey the Einstein equations is used in the models in [60–63]. They are hence based on GR and QFT without the necessity to modify either of the two theories, only that linearised GR is quantised in a Fock quantisation similar to the electromagnetic field in Quantum Electrodynamics. These works discuss master equations for different matter fields, for instance a scalar field in [60, 61] or a photon field in [63], based on the ADM formulation of gravity [83], and use several different formulations of a master equation. As a mathematically rigorous quantisation of GR in ADM variables is not possible, this does however restrict the applicability of the model. Some of these works also predict the size and

form of specific decoherence effects in scalar particles and photons, such as [60, 62, 63]. For this, it is nonetheless necessary to work carefully, as the resulting effects of the master equations might change or vanish after a renormalisation. A general discussion of such a renormalisation for linearised gravity as the environment on an open quantum system independent of specific (non-)relativistic limits has not yet been discussed in these works.

1.1.3. Signatures of gravitationally induced decoherence in neutrino oscillations

"Nature loves to conceal herself."

– Heraclitus of Ephesus, *Fragment 10*

In order to gain experimental access to signatures of gravitationally induced decoherence effects, one possibility is to use tabletop experiments, see [67] for an overview and [84]. Another possibility is given by the detection and analysis of astroparticles. For these to be a suitable candidate, the gravitational influence must not be dominated by other interactions that make it non-observable. Hence for example it will be very hard to measure a gravitational decoherence effect for electromagnetically charged particles. It is at this point where neutrinos come into play: these could carry a high potential to serve as witnesses for signatures of gravitational decoherence. They are electromagnetically neutral, thus they represent optimal candidates to investigate the effect of decoherence due to gravity. In the last decades, they have lead to new discoveries that violate the standard model of particle physics in its present form: while the latter predicts neutrinos to be massless, experiments show that they are changing their flavour when propagating, so they need to have non-vanishing mass differences. These neutrino flavour oscillations give a good access point to look for signatures of decoherence effects, to analyse their size and also to compare the experimental data to different theories of quantum gravity for this decoherence effect. In the literature, there already exist several works that discuss this effect [85–106], where most of them use the phenomenological approach to start from a specific form of a master equation, usually a Lindblad equation, in which the unknown operators that represent the influence of the environment are parameterised in a specific way. This phenomenological master equation then predicts a change of the oscillation behaviour of the neutrinos, in particular in most works a damping of the oscillations and hence a classicalisation of the flavour neutrinos. In a next step, measured or simulated experimental data is analysed to find out whether there is yet a discrepancy to the standard oscillations or not for a specific detector. Analyses have been done for instance for long baseline neutrino detectors [88] like MINOS+T2K [89] or DUNE [90], or for neutrino telescopes such as IceCube [92, 105] or KM3NeT [93]. So far, no deviation from the standard oscillations have been found, so upper bounds on the magnitude of the decoherence effects could be derived. This procedure does however not give the possibility to understand in detail where these free parameters come from and what their detailed structure is. Also the question of their expected order of magnitude and in particular their dependence on the energy of the neutrinos remains unanswered by these approaches, so it is not really clear from them, which specific experiments are well-suited to look for signatures of gravitationally induced decoherence in neutrino oscillations and which are not. To better understand this process of gravitationally induced decoherence in neutrino oscillations and other astroparticles does not only give an access point to this specific quantum gravity effect as an application for candidate theories of quantum gravity, as discussed above, but would also help us to better understand the information and data carried by astroparticles coming from our universe, and thereby the stories they tell us.

1.2. Motivation and goal of this thesis

With the new effects predicted by a theory of quantum gravity being mostly out of range of experiments today, a guiding principle for the development of such a theory can be mathematical rigour and the correct limits yielding GR in the classical regime and QFT on curved spacetimes when the quantum features of gravity can be neglected. In this thesis, we are therefore interested in the approaches to gravitationally induced decoherence based on (quantised) GR and QFT. As discussed in section 1.1.2, there exist various ways to approach the theoretical description of this physical process, where only few [60–63] are based on (quantised) GR and QFT. In this section, we present a status of this approach to gravitationally induced decoherence and discuss some of its open questions. Then, we sketch the goal of this thesis and how it can provide some answers to these questions.

The four models [60–63] all formulate gravity in linearised ADM variables [83] and quantise them in a Fock quantisation. As a rigorous mathematical formulation of a quantisation of GR in ADM variables is not possible, an extension of this treatment and their techniques to open quantum systems where the gravitational environment cannot be formulated in a linearised manner yields several problems, see for instance the discussions on the Wheeler-DeWitt equation [107, 108] and the issue to define a Hilbert space [109, 110]. Additionally, the models in [60–63] use a gauge fixing for the gravitational degrees of freedom, which limits the result to this specific choice having as an effect that on the one hand a comparison to other gauge fixings is hard and on the other hand that the predictions made are problematic as they are based on the use of the unphysical time and space coordinates from GR. Due to these aspects the question arises whether one can formulate a decoherence model with gravity as the environment that enables an extension to other sectors than the linearised one and that provides a more general formulation of the physical degrees of freedom in terms of physical time and position coordinates.

The master equations in the field theoretical formulation for decoherence models with gravity as environment are often brought into Lindblad form [60, 61, 63], which has the advantage of yielding positive probabilities. In the course of this derivation, several approximations like the Markov and rotating wave approximations have to be invoked that are usually taken from other disciplines of physics like quantum optics or condensed matter systems [45, 47]. So far, a detailed analysis of the effect of these approximations for gravity as the environment is however missing. In particular, it is not clear which information is lost when applying them and which processes are suppressed. Furthermore it is not clear, if and for which classes of systems the applied approximations are a good choice for gravity as environment.

When one starts with a quantum mechanical model to study gravitationally induced decoherence, as for instance in [97, 103, 111, 112], these models are not directly based on an underlying fundamental theory, so key quantities like the form of the interaction Hamiltonian or the coupling strength between system and gravitational environment, that have a strong influence on the final decoherence, have to be put by hand into the model. This leads to the question whether it is possible to connect to such quantum mechanical models coming from a field theoretical formulation of a decoherence model, where the way GR couples to matter fixes naturally these open points in the quantum mechanical models. In [60, 62, 63], the obtained field theoretical models are projected in a specific way onto a master equation for a single particle. The relation of this projection to the different scattering processes of the underlying effective QFT is however not clear, as it is established for instance in [113] for a scalar field as system of interest and a second scalar field as environment. In particular, some terms that would arise from processes

in the underlying effective QFT are dropped by the projection chosen in [60, 62, 63] without analysing their effect. In addition, when it comes to making predictions from a decoherence model, the necessity to discuss a renormalisation that removes unphysical effects and regularises potentially divergent integrations arises. While for a QFT there exists a standard procedure to remove divergences, in [60, 62, 63] this is not applied. In [60, 63] the divergent terms are absorbed into redefinitions of fundamental parameters of the system in the final Lindblad equation, which however does not make clear how this can be connected to the standard procedure and hence how it can be generalised to other matter fields. In [62], no renormalisation is performed, but a final physical effect based on vacuum fluctuations is discussed which would be absent after a renormalisation. This hence leads to the question how a renormalisation based on the standard procedure of QFT for a master equation including gravity as the environment can be carried out and which implications this has on the final one-particle master equation as well as on the renormalisation in the quantum mechanical model.
From the experimental side, in particular focusing on neutrino oscillations, phenomenological models that are based on a master equation in Lindblad form with unknown parameters are often used to analyse gravitationally induced decoherence, for instance in [90, 96–98, 103]. These parameters are then constrained by experimental data. At this point the question arises how these parameters can be interpreted and from which underlying physical properties of the system they arise. Additionally, it would be very helpful to resolve their dependence on the neutrino's energy to be able to deduce in which energy ranges there is the highest potential that signatures of gravitationally induced decoherence are exhibited and, as an implication from that, which classes of detectors are best-suited for the search of gravitationally induced decoherence in neutrino oscillations.

The present thesis is intended to provide some answers to these questions. To achieve this, the thesis is divided into four parts. After a general introduction to master equations in the first part, in the second part, a derivation of a time-convolutionless field theoretical master equation for a scalar field coupled to linearised gravity based on GR formulated in Ashtekar variables [114, 115] is presented. As Ashtekar variables provide the classical variables of loop quantum gravity, this linearised formulation enables a generalisation to the full gravitational field and a mathematically rigorous quantisation of full GR along the lines of loop quantum gravity. To be able to compare our results with the ones in the literature, we still follow a Fock quantisation in this thesis. Furthermore, we circumvent the process of gauge fixing by the construction of suitable Dirac observables using the relational formalism [116–121]. This provides us with the possibility to compare different gauge fixings and to define physical time and position coordinates as the values of the reference fields the Dirac observables are constructed from.
In the third part of the thesis, we project this master equation onto the space of a single scalar particle and thereby discuss two different ways to perform this projection, where one is the one applied in [60, 62, 63], where some contributions from scattering processes allowed by the underlying effective QFT are dropped, and the other one contains all possible processes compatible with QFT similar to [113]. The effect of the choice of either projection is then analysed throughout the following steps of the derivation. Then, we apply the Markov and the rotating wave approximations one after another to cast the one-particle master equation into Lindblad form. This gives us the opportunity to discuss on the one hand conditions for their applicability, where we are not able to comment on the general case but focus on ultra-relativistic particles to connect later to neutrino oscillations, and on the other hand the opportunity to analyse the terms that

the individual approximations drop as well as their effect in detail. In this part, we also show how a renormalisation of the one-particle master equation based on the underlying effective QFT can be carried out following [113], identifying the divergent contribution as the self-energy of the scalar particle. This renormalisation removes the parts arising from vacuum fluctuations and permits us to discuss its interplay with the different approximations taken afterwards.
In the last part of the thesis, a time-convolutionless master equation is derived for a microscopic quantum mechanical model, where the model in [112] is extended to include a neutrino as system of interest that is coupled to a bath of harmonic oscillators that mimics an environment of gravitational waves. Here, we can indeed use the field theoretical model from the previous parts to motivate the form of the coupling in the interaction Hamiltonian as well as the coupling strength and the way to perform the continuum limit for the oscillators in the environment and can therefore provide a motivation for some of the steps that have to be put into such quantum mechanical models by hand. After the application of the Markov approximation and the discussion of its validity for the specific model, a connection to phenomenological models as for instance in [90, 96–98, 103] is established yielding a resolution of their free parameters and a physical interpretation for them. In particular, we can also show for which energy dependencies the decoherence effect arising from gravity is expected to be strong in neutrino oscillations according to the considered quantum mechanical model.

1.3. Structure and content of this thesis

In this thesis, the question is approached how gravity can be used as an environment in open quantum systems to obtain predictions for gravitationally induced decoherence effects with a particular focus on neutrino oscillations. The thesis consists of four parts that discuss after an introduction to the employed formalism two different models. The first one is based on field theory where a scalar field is coupled to linearised gravity which is later projected on the space of a single scalar particle and renormalised. The second model is a quantum mechanical toy model tailored to neutrino oscillations, where a neutrino is coupled to an environment of harmonic oscillators that mimic a gravitational waves background. While the first model gives answers to open questions in the quantum mechanical toy model like the detailed form of the coupling or its strength, the latter facilitates the connection to experiments and the application of approximations such as for instance the Markov approximation, therefore both models complement each other. The detailed structure of the thesis is as follows:

Part I

In part I of the thesis, we give an introduction to basic concepts of open quantum systems and master equations that will be employed in the following parts. We start with a discussion of the general formulation of open quantum systems and decoherence effects in section 2. After that, in section 3 the Lindblad equation [122, 123] as a completely positive, specific form of a master equation is discussed and it is derived for rather strong assumptions on the underlying microscopic system that permit to treat the time evolution of the system of interest as a quantum dynamical semigroup. As for most physical systems these assumptions are not fulfilled, we present in section 4 the projection operator formalism [124–127] which enables a microscopic derivation of a time-convolutionless master equation. Based on this, different simplifications of this master equation are discussed and the requirements for their applications to physical system are sketched. Finally,

this part of the thesis is concluded with section 5, where a simple quantum mechanical model is discussed to present some of the techniques introduced in this part of the thesis.

Part II

This part of the thesis corresponds to the work published in [1]. This subsection was partially inspired by the introduction in that work.

For the first decoherence model, which we consider in this thesis in parts II and III, we start at the classical level of the action in section 6 and couple a scalar field to linearised gravity, similar to [60–62]. However, while these work with ADM variables, we express the gravitational part of our system in Ashtekar variables [114, 115] that are the canonical variables of loop quantum gravity. This does in principle give us the opportunity to use a loop quantisation, as it is done for instance in [128, 129] for linearised gravity, and additionally provides a direct possibility to couple fermions for a future model. To facilitate the comparison of our results with the one obtained in [60–63], we later however apply a Fock quantisation to the matter system as well as to the linearised gravitational system. Before that, we discuss a way how to perturb the gravitational degrees of freedom of the entire system and include the matter degrees of freedom consistently into the perturbed formulation by means of a post-Minkowski approximation [130] in section 6.3, which generalises the treatment in [60–63]. In the classical linearised formulation, the gravitational part of the system contains gauge degrees of freedom, in Ashtekar variables even more than in ADM variables due to the presence of a gravitational Gauß constraint. While the models in the literature on gravitationally induced decoherence work with gauge fixings here, we employ the relational formalism in section 7 to construct suitable Dirac observables [116–121] that encode the physical degrees of freedom by deriving geometrical clocks from gravitational gauge degrees of freedom. In this context, we introduce a dual version of the observable map, where the role of the clocks and constraints is swapped. This facilitates the construction of commuting observables and clocks. The advantage of this approach is that it is independent from a specific choice of gauge fixing, can however be easily related to different gauge fixings by assigning suitable values to the geometric clocks, as we show in section 7.9. This formulation of the classical theory in terms of Dirac observables gives us then the opportunity to separate the phase space into a physical one, consisting of the observables for gravity and matter, and a gauge part. The sub-algebra of the physical phase space decouples from the remaining gauge degrees of freedom, so we can apply a reduced Fock quantisation only to the subspace of physical observables for linearised gravity and matter.

In section 8 we present this Fock quantisation of the reduced system. For this, we choose to normal order all appearing contributions which is different to the orderings in [60, 62, 63]. We will analyse the implications of the different orderings in part III when considering the decoherence of a single scalar particle. With this, we can apply in a next step one of the techniques to derive a first master equation from the quantised Hamiltonian of matter system and environment. We choose to work with the projection operator technique [124–127] to obtain a time-convolutionless (TCL) master equation in section 9 expressed in terms of thermal Wightman functions, where the gravitons in the environment are distributed according to a Gibbs state. Finally, we present three different forms of the master equation and compare them to the ones in [60, 62, 63]. In contrast to [60, 63], our master equation is not yet of Lindblad form. It can be directly cast into this specific form by the application of the Markov and the rotating wave approximation. As it is not yet clear, if they are justified for this specific physical system, in particular with gravity

being involved, this step will be analysed in detail in part III of this thesis for the master equation from this part being projected to the space of a single scalar particle.

Part III

This part of the thesis corresponds to the work published in [2].
In order to further analyse the model from part II and to draw physical conclusions from it, we discuss in this part of the thesis the one-particle projection of the final TCL master equation from the previous part. We start in section 10 with the projection of the master equation onto the space of a single scalar particle. For this, we consider two different projections used in the literature, which we call non-extended [60, 62, 63] and extended [113] projection. While the latter takes into account also contributions that correspond to the creation and annihilation of two scalar particles as intermediate steps which preserves the one-particle space, these terms are ignored in the non-extended projection. They lead to UV-divergent terms that can be interpreted as vacuum bubbles, for which we show a possible renormalisation, and to the violation of probability conservation in the subsystem of the scalar particle. Using either projection, there appear additional divergent terms in the one-particle master equation, which is also the case in similar models for gravitationally induced decoherence of matter fields [60, 63]. While these are treated there after the application of a Markov and rotating wave approximation in specific non- or ultra-relativistic limits, in this thesis we renormalise the one-particle master equation before performing these further steps. For this, we follow the strategy of [113], where a scalar field as system of interest is coupled to another scalar field as environment, and connect the one-particle TCL master equation in section 11 to the underlying effective quantum field theory using a set of non-covariant Feynman diagrams arising from the action of part II. Such non-covariant Feynman diagrams also arise in QED when quantised in non-covariant gauges as for instance in Coulomb gauge (see [131, 132]). This provides us with the opportunity to identify the diverging terms with the vacuum part of the scalar particle's self-energy in sections 11.1 and 11.2. After the discussion of a covariant set of Feynman diagrams in section 11.3, we perform an on-shell renormalisation of the underlying quantum field theory in 11.4 which permits us to include a suitable counter term for the divergent terms in the master equation and to obtain a renormalised version of the TCL one-particle master equation in section 11.5. In order to derive a completely positive Lindblad equation, we discuss in section 12 the application of the Markov (section 12.1) and rotating wave approximation (section 12.2). New compared to the literature is in this section that we already use the renormalised one-particle master equation, hence we can discuss the terms removed by the applications at a physical level. Albeit we cannot give general conditions on the applicability of the two approximations for gravity as environment, we deliver a condition for the applicability of the Markov approximation to ultra-relativistic scalar particles in section 12.1.1. To conclude this part of the thesis, several applications of the resulting renormalised one-particle Lindblad equation are discussed in section 13. A first aspect is the analysis of the populations of the density matrix predicted by the master equation, which we compare in section 13.1 for the different intermediate steps before and after renormalisation and before and after the application of the Markov approximation, while the rotating wave approximation does not modify them. It turns out that the vacuum effect discussed in [62] for the populations of the density matrix for a photon vanishes after the renormalisation. Additional applications that are considered are the non-relativistic (section 13.2) and ultra-relativistic (section 13.3) limit of the renormalised one-particle Lindblad equation which yields results similar to [60, 63]. The investigation of the

ultra-relativistic form of the master equation is later in part IV taken as the starting point to discuss gravitationally induced decoherence in neutrino oscillations based on the field theoretical model.

Part IV

Pieces of this part of the thesis correspond to the work published in [3] and [2]. This subsection was partially inspired by the introduction in [3].
In this part, we focus on an application of the formalism of open quantum systems to neutrino oscillations. In section 14 we give a brief introduction to neutrinos and neutrino oscillations in vacuum, discussing them in the context of Gaussian wave packets and plane waves. After that, we explain how these oscillations change when neutrinos propagate through matter. The question on how these oscillations are modified due to the presence of a gravitational environment has achieved increasing attention in the past years and was investigated by several works [85–106]. Most of these works follow a phenomenological approach based on a Lindblad equation. We introduce this class of models in section 15. One main aspect of these models is that they use a specific form of the dissipator which is parameterised with a number of unknown parameters. Their amount is then further reduced by several physical assumptions, such as energy conservation in the neutrino subsystem. We discuss some of these assumptions and their implications on a phenomenologically parameterised dissipator also in section 15. Moreover, from such a general parametrisation the dependence of the dissipator on the energy of the system of interest is not clear. Due to this, in such models several different dependencies are postulated in terms of power laws and their implication on the decoherence effect are investigated. Depending on this choice, the decoherence effect is enhanced at completely different neutrino energies and therefore from such a treatment it is not clear, from which sources neutrinos are best suited to show gravitationally induced decoherence. From the derivations in the previous parts of the thesis, it is visible that an underlying microscopic model enables to resolve the detailed structure of such a dissipator and therefore is able to answer most of the open questions in the phenomenological approach. Therefore we introduce in section 16 a quantum mechanical model based on [112] and extended to include neutrinos, where we couple as system under consideration a neutrino to a bath of harmonic oscillators that is supposed to represent an environment of gravitational waves. A key quantity in such a quantum mechanical model is the way the interaction Hamiltonian is specified. Here we follow the model in [112] and pick a coupling motivated by GR. We then derive the TCL master equation for this model, where we apply the continuum limit to the oscillators in the environment by introducing a spectral density in section 16.3 and assume that they are in a thermal state. In similar quantum mechanical models, like for instance the Caldeira-Leggett model [45, 133] or spin-boson models [45, 46, 134–136], different forms of spectral densities are used motivated by typical behaviours of the physical environments in these models. In our case, for gravity such a behaviour has not yet been studied, therefore we use the results from the previous parts of the thesis to show which form of a spectral density is a good choice for the considered model and we discuss different high-frequency cutoffs. In a next step, we apply in section 16.4 the Markov approximation which then yields a Lindblad equation. After analysing the validity of this approximation for the model under consideration, we give a proof that for one choice of the high-frequency cutoff in the spectral density the application as it is usually done in the literature, where the order of different limits is switched, is justified for the present model, and that other choices yield an equivalent result.

The Lindblad equation we obtain has a similar form as the one in the phenomenological models mentioned above. A point where they differ is that in our equation there is still a Lamb-shift term present which modifies the unitary evolution and therefore shifts the eigenenergies of the neutrino system due to the presence of the gravitational environment. In the field theoretical models such a Lamb-shift term is also present, but it requires a renormalisation, as it can be seen in part III of this thesis. Indeed, also in the quantum mechanical model it is problematic, as the shift it induces on the energies of the system depends linearly on the high-frequency cutoff from the spectral density and diverges when the latter is sent to infinity. Therefore it cannot be physical and in section 16.5 we include a counter term to renormalise it, similarly to the treatment in the Caldeira-Leggett model [45, 133]. So far the system under consideration has not been specified, apart from its contribution to the interaction Hamiltonian, as all the discussions and derivations made focused on the gravitational environment. In section 16.6 we apply this master equation to neutrino oscillations in matter, solve the resulting evolution equation and then discuss the results in section 17. First, we compare the resulting modifications on the oscillations to the predictions made by phenomenological models in section 17.1. This permits us to give a detailed expression for the generically parameterised dissipator in the phenomenological models as well as its energy dependence. The only two free parameters in the microscopic model are then the coupling strength between system and environment, as well as a temperature parameter characterising the oscillators in the environment. The analysis shows that in matter the parameters of the dissipator should depend on the matter density according to our model, which is not included in most of the phenomenological models. Hence the results and sensitivity analyses obtained on their basis deviate from the ones one would obtain when using the microscopic quantum mechanical model when considering neutrinos propagating through matter. We also discuss the implications of the renormalisation of the Lamb shift on neutrino oscillations in section 17.2, in particular by comparing two predictions for models with and without a renormalisation, and give in section 17.3 an estimate for the order of magnitude of the coupling parameter inspired by the field theoretical model in the previous parts of the thesis. Finally, in section 17.4 we apply the ultra-relativistic form of the one-particle projection of the master equation from part III to a neutrino, which yields the same form for the dissipator as the quantum mechanical toy model. Based on this, we compare several aspects of these two models enclosing the coupling strength, the requirement to introduce a spectral density in the quantum mechanical model and the applicability of the Markov approximation for ultra-relativistic particles in both models.

Part I.
Open quantum systems and master equations

In this part of the thesis, we give an introduction to open quantum systems and master equations, which will be used throughout the thesis to describe decoherence processes occurring due to the interaction of matter fields or particles with the gravitational field. After a general introduction to open quantum systems in section 2, we discuss in section 3 a very specific example of a master equation, the so-called Lindblad equation, which has the advantage of complete positivity, but also very restrictive conditions under which it holds. As these are in general not fulfilled considering gravity as an environment in the open quantum system and also in other situations where gravity does not play any role, we present in section 4 with the projection operator formalism a different method that leads to a master equation. This master equation is time-convolutionless, but in general not completely positive. In part II and IV of the thesis, we will use this procedure to obtain master equations and discuss the approximations that would cast it into a Lindblad form in part III and IV. To conclude this part of the thesis, a simple quantum mechanical decoherence model is discussed in section 5 and some of the previously introduced techniques are applied to it.

2. Open quantum systems and decoherence

In standard quantum mechanics, one is interested in the eigenvalues and dynamics of an isolated quantum system. Its unitary time evolution is then dictated by the **Schrödinger equation** which reads for a state $|\psi_S(t)\rangle$ describing the quantum system and the corresponding Hamiltonian[1] H_S:

$$\frac{\partial}{\partial t}|\psi_S(t)\rangle = -\frac{i}{\hbar}H_S|\psi_S(t)\rangle \ . \tag{2.1}$$

The solution of this equation predicts the dynamics of the probability amplitude of the state $|\psi_S(t)\rangle$ by expanding it in the eigenstates $|E_i\rangle$ of H with eigenvalues E_i and then propagating the individual eigenstates in time t with the phase factors $e^{-\frac{i}{\hbar}E_i t}$. This yields different interferences at different times, but the probability of the system to be in one of the energy eigenstates when measured will always be one, assuming proper normalisation of all involved states. The Hamiltonian H_S hence determines the energy levels of the system and the total probability is conserved.

As soon as it comes to the treatment of more particles, solving the Schrödinger equation becomes more and more challenging and for a macroscopic number of particles it is unrealistic as well as unimportant to know, store and process all the data of each individual quantum particle. In this case, one is usually only interested in averaged quantities of the system. This leads to statistical physics, where a system is described in terms of a density matrix $\rho_S(t)$ that encodes on the one hand the intrinsic quantum mechanical superposition principle, like a quantum state $\psi_S(t)$ does, and on the other hand as a new feature also the classical lack of knowledge of all the details of the state, that could be known without contradiction from quantum mechanics. The time evolution of a state is then determined by the **Liouville-von Neumann equation**

$$\frac{\partial}{\partial t}\rho_S(t) = -\frac{i}{\hbar}[H_S, \rho_S(t)] \tag{2.2}$$

with the commutator $[.,.]$. The solution to this equation is given, similarly as above, by the multiplication of the density matrix in energy basis $|E_i\rangle\langle E_j|$ with exponential phase factors

[1] In what follows, we assume H_S to be time-independent to put the focus on the concepts introduced in this section. All equations can readily be generalised to a time-dependent Hamiltonian using time-ordering operators.

$e^{-\frac{i}{\hbar}(E_i - E_j)t}$. The populations, that are the diagonal entries of $\rho_S(t)$, give the probabilities to measure the system in the state described by the corresponding diagonal element of the density matrix and the off-diagonal elements, called coherences, are a measure for interference probabilities of the corresponding states. The total probability to measure the system in one of the states is given by the sum over the populations and is constant due to the structure of the Liouville-von Neumann equation, as the cyclicity of the trace together with the commutator lead to a vanishing right hand side of equation (2.2). Therefore, the energy levels of the system are still determined by H_S and the probability is conserved.
All of these descriptions consider the quantum system to be isolated or closed and not in any contact with its surroundings. This, however, is not how our world works: there are influences from an enormous amount of sources that affect physical systems, in particular very small quantum particles. While the system can be shielded from some of these influences like electromagnetic interactions, from others this is not possible. One important contribution here is gravity, which is omnipresent and inevitable. In order to take these new class of influences into account, which we call from now on the environment, one can work with the formalism of open quantum systems: This formalism considers a system of interest not any more as a perfectly isolated physical system, but as being in contact with an environment through some specific coupling, see figure 1.

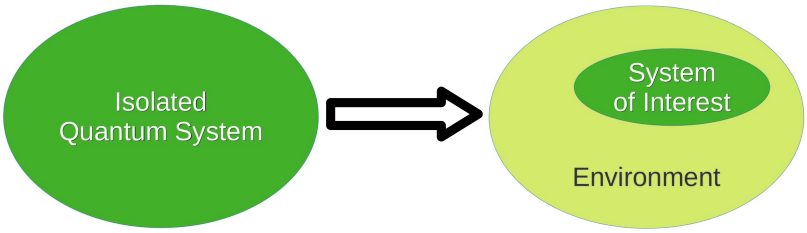

Figure 1: Transition from an isolated (closed) quantum system to an open quantum system consisting of a system of interest coupled to an environment.

While it is evident that the total system consisting of the system of interest and the environment is still isolated with evolution equation being the Liouville-von Neumann equation (2.2), one is usually only interested in the detailed dynamics of the system under investigation and in a dynamical equation for its state with the effective influence of the environment. The detailed dynamics of the environment are not of interest. Oftentimes, the environment is assumed to be very large compared to the system of interest and in a stationary state that is not influenced by the back-reaction of the system under consideration onto the environment. Then, the evolution equation that describes the system of interest's state $\rho_S(t)$ under the additional influence of the environment is given by a so-called **master equation**

$$\frac{\partial}{\partial t}\rho_S(t) = -\frac{i}{\hbar}[H_S + H_{add}, \rho_S(t)] + \mathcal{D}[\rho_S(t)]\,. \tag{2.3}$$

In comparison to the Liouville-von Neumann equation (2.2), there is an additional term in the commutator that contributes to the unitary evolution of the system under investigation, and there is another contribution in terms of a so-called dissipator $\mathcal{D}$ which is a super-operator acting on the density matrix of the system of interest. This dissipator can contain in general terms that contribute to the unitary evolution of $\rho_S(t)$, but also terms that lead to additional, new effects. From this it is evident that the energy levels of the considered system are not any more

only determined by H_S, but also influenced by the environment present through H_{add} and $\mathcal{D}$. This results in a shift of energy levels of the system of interest compared to the isolated case, and possibly also in a required renormalisation of the energy levels. From a physical point of view this result is not surprising, as for instance charged particles in an electromagnetic field also experience a similar shift of energy levels. Having said this, let us further discuss new features that arise from the master equation (2.3). Given that $\mathcal{D}[\rho_S(t)]$ can in general not be written in the form $-\frac{i}{\hbar}[H_{\mathcal{D}}, \rho_S(t)]$ with a suitable self-adjoint operator $H_{\mathcal{D}}$ but also contains real contributions to the evolution equation, quantities like energy and probability are not conserved any more within the system under investigation. As the entire system including the environment is isolated, energy or probability loss in the system of interest therefore corresponds to a flow of energy or probability into the environment. As the latter is not directly represented in (2.3), it seems that the prior conserved quantities are lost, while they are only not conserved any more in the specific considered system that represents a subsystem of the entire, isolated system. The flow of energy from this system of interest to the environment is called dissipation. Due to the constant interaction between system and environment, there is furthermore a flow of information that manifests in a decrease of the coherences of $\rho_S(t)$ with time in a certain basis. This process is called decoherence and leads to a classicalisation of the system under investigation in that specific basis, as the interference probabilities also decrease and vanish after a certain amount of time. The basis in which this effects happens depends among other things on the way the system of interest and the environment are coupled in the interaction Hamiltonian.
There exist different ways to obtain a master equation of the form (2.3). One method which is typically used when directly connecting to physical quantities and experiments is the phenomenological way to start from equation (2.3) with H_S known and to parameterise H_{add} and $\mathcal{D}$ in a suitable way with free parameters that have to be determined by the size of the new effects in experiments. Mostly, the parametrisation is based on a Lindblad form of the master equation which we will discuss in section 3. We comment on the phenomenological models more in detail in section 15 and discuss their application to gravitationally induced decoherence in neutrino oscillations in section 17.1. Another approach which we will use in part II of this thesis consists in starting from the Liouville-von Neumann equation for the total closed system $\rho_T(t)$ embracing the system under consideration and the environment with total Hamiltonian H_T:

$$\frac{\partial}{\partial t}\rho_T(t) = -\frac{i}{\hbar}[H_T, \rho_T(t)]\,. \tag{2.4}$$

To obtain the dynamics of the reduced system of interest, one then can trace out the environment $\mathcal{E}$:

$$\frac{\partial}{\partial t}\rho_S(t) = -\frac{i}{\hbar}\, tr_{\mathcal{E}}\left\{[H_T, \rho_T(t)]\right\}\,, \tag{2.5}$$

where we defined

$$\rho_S(t) := tr_{\mathcal{E}}\left\{\rho_T(t)\right\}\,. \tag{2.6}$$

While the evolution of $\rho_T(t)$ is encoded in a unitary operator $U(t, t_0)$ such that

$$\rho_T(t) = U(t, t_0)\,\rho_T(t_0)\,U^{\dagger}(t, t_0) \tag{2.7}$$

and as such reversible, the evolution of the reduced system is given in terms of a super-operator $\mathcal{V}(t, t_0)$ such that

$$\rho_S(t) = \mathcal{V}(t, t_0)\,\rho_S(t_0) \tag{2.8}$$

and is in general not unitary and hence not reversible, leading to phenomena like dissipation and decoherence. In section 4, we will start from the total, closed system that lives on a total Hilbert space $\mathcal{H}_T$

$$\mathcal{H}_T = \mathcal{H}_S \otimes \mathcal{H}_\mathcal{E} \tag{2.9}$$

composed by the Hilbert spaces of the system under investigation $\mathcal{H}_S$ and the environment $\mathcal{H}_\mathcal{E}$. From this total system, we derive different kinds of master equations tracing out the environment. For this, we assume that the total Hamiltonian can be decomposed into three different parts:

$$H_T = H_S \otimes \mathbb{1}_\mathcal{E} + \mathbb{1}_S \otimes H_\mathcal{E} + \alpha H_I \,. \tag{2.10}$$

In this decomposition, H_S is the Hamiltonian describing the uncoupled dynamics of the system of interest, $H_\mathcal{E}$ the Hamiltonian of the uncoupled environment, H_I the interaction Hamiltonian of system of interest and environment with the coupling strength determined by α.

3. The Lindblad equation

One specific form of a master equation is the Lindblad equation. In this chapter, we briefly outline how it can be derived under certain assumptions as the most general form of a quantum dynamical semigroup which is defined below in (3.7). For this, we follow the presentation in [45]. As mentioned in the previous section, the total system $\rho_T(t)$, consisting of system of interest and environment, evolves unitarily in time according to equation (2.7), while the reduced system under consideration $\rho_S(t)$ can be evolved by the application of a super operator $\mathcal{V}(t, t_0)$, see equation (2.8). Under the assumption of factorising initial conditions

$$\rho_T(t_0) = \rho_S(t_0) \otimes \rho_\mathcal{E}(t_0)\,, \tag{3.1}$$

the super operator $\mathcal{V}(t, t_0)$ has the following form which can be obtained by combining equation (2.8) with (2.7), (3.1) and (2.6):

$$\rho_S(t) = \mathcal{V}(t, t_0)\rho_S(t_0) = tr_\mathcal{E}\left\{U(t, t_0)[\rho_S(t_0) \otimes \rho_\mathcal{E}(t_0)]U^\dagger(t, t_0)\right\}\,. \tag{3.2}$$

For fixed initial and final times as well as for a fixed initial environmental state $\rho_\mathcal{E}$, this super operators is a completely positive, trace-preserving dynamical map. The property of complete positivity is a very important one for master equations, therefore we want to explain this property a bit more. Positivity of a super operator means that it maps positive operators to positive operators. In our case, the super operator encodes time evolution and the operators it is applied to are density matrices of the total/reduced system. This positivity ensures that all populations of the density matrix, that represent the probabilities of measuring the system in the corresponding state, remain non-negative under time evolution. The state of the system of interest however only represents one part of the entire system and therefore does the dynamical map only act on this part of the composite system. In order to maintain positive probabilities, it is therefore required that not only $\mathcal{V}(t, t_0)\rho_S(t_0)$ is a positive operator, but also the combined map $\mathcal{V}(t, t_0) \otimes \mathbb{1}$ acting on operators of the total system. The representation theorem of quantum operations then shows (see for instance [45, 137]) that a dynamical map like $\mathcal{V}(t, t_0)$ is completely positive if it can be written in the following way:

$$\mathcal{V}(t, t_0)\rho_S(t_0) = \sum_{A,B} \mathcal{W}_{AB}(t, t_0)\, \rho_S(t_0)\, \mathcal{W}_{AB}^\dagger(t, t_0) \tag{3.3}$$

with a countable set $\mathcal{W}_{AB}(t, t_0)$ that fulfills

$$\sum_{A,B} \mathcal{W}_{AB}^\dagger(t, t_0)\mathcal{W}_{AB}(t, t_0) = \mathbb{1}\,. \tag{3.4}$$

and is defined as

$$\mathcal{W}_{AB}(t, t_0) = \sqrt{\lambda_B}\,\langle\psi_A|\,U(t, t_0)\,|\psi_B\rangle \tag{3.5}$$

where the λ_A and $|\psi_A\rangle$ come from the spectral decomposition of $\rho_\mathcal{E}(t_0)$:

$$\rho_\mathcal{E}(t_0) = \sum_A \lambda_A\,|\psi_A\rangle\,\langle\psi_A|\,. \tag{3.6}$$

If we now consider the collection of all dynamical maps $\mathcal{V}(t, t_0)$ for a fixed initial time t_0 and times $t \geq t_0$, we obtain a one-parameter family of dynamical maps $\{\mathcal{V}(t, t_0)|t \geq t_0\}$. If the correlation

functions in the environment decay much faster than the system of interest evolves, then one can neglect memory effects in the evolution of the system under consideration. This is the so-called Markov approximation which will be discussed and applied at various stages throughout this thesis. Given this approximation holds, the one-parameter family of dynamical maps even forms a quantum dynamical semigroup

$$\mathcal{V}(t_2,t_1)\mathcal{V}(t_1,t_0)=\mathcal{V}(t_2,t_0) \qquad \text{for } t_1,t_2\geq t_0\,. \tag{3.7}$$

The crucial point here is that the evolution is local in time, which means it only depends on the present state and not any more on its entire history: To evolve the state from $\rho_S(t_0)$ to $\rho_S(t_2)$, we can first evolve it to $\rho_S(t_1)$ and then, without knowledge of the original initial state $\rho_S(t_0)$, evolve the state via $\mathcal{V}(t_2,t_1)$ from $\rho_S(t_1)$ to $\rho_S(t_2)$.

In order to write down a master equation that corresponds to this quantum dynamical semigroup, one has to define a suitable generator $\mathcal{J}$ of this group such that

$$\mathcal{V}(t,t_0)=e^{\mathcal{J}\cdot(t-t_0)}\,. \tag{3.8}$$

Such a generator exists if the semigroup is (weakly) continuous and it then defines a Markovian quantum master equation in the following manner:

$$\frac{\partial}{\partial t}\rho_S(t)=\mathcal{J}\rho_S(t)\,. \tag{3.9}$$

Similar to [45], we specialise now on the case of a finite-dimensional underlying Hilbert space for the system of interest with dimension N. We then can expand any operator acting on this Hilbert space in a complete, orthonormal basis $\{F_i\}_{i=1,\dots,N^2}$ with inner product defined via the trace:

$$\langle F_i,F_j\rangle:=tr_{\mathcal{S}}\left\{F_i^\dagger F_j\right\}=\delta_{ij}\,. \tag{3.10}$$

Choosing F_{N^2} proportional to the identity and expanding the operators $\mathcal{W}_{AB}$ in terms of the basis $\{F_i\}_{i=1,\dots,N^2}$, one can cast the master equation (3.9) into the so-called first standard form:

$$\frac{\partial}{\partial t}\rho_S(t)=-\frac{i}{\hbar}[H_L,\rho_S(t)]+\sum_{i,j=1}^{N^2-1}a_{ij}\left(F_i\rho_S(t)F_j^\dagger-\frac{1}{2}\left\{F_j^\dagger F_i,\rho_S(t)\right\}\right)\,, \tag{3.11}$$

With a positive coefficient matrix A with components a_{ij} where $i\in\{1,\dots,N^2-1\}, j\in\{1,\dots,N^2\}$ defined as

$$a_{ij}:=\lim_{\epsilon\to 0}\frac{1}{\epsilon}\sum_{A,B}\langle F_i,\mathcal{W}_{AB}(\epsilon)\rangle\langle F_j,\mathcal{W}_{AB}(\epsilon)\rangle^*\,, \tag{3.12}$$

and

$$H_L:=\frac{1}{2i}\frac{1}{\sqrt{N}}\sum_{i=1}^{N^2-1}\left(a_{iN^2}^*F_i^\dagger-a_{iN^2}F_i\right)\,. \tag{3.13}$$

More details on the derivation can be found in [45]. Due to the positivity of the coefficient matrix A, it can be diagonalised yielding the so-called diagonal form

$$\frac{\partial}{\partial t}\rho_S(t)=-\frac{i}{\hbar}[H_L,\rho_S(t)]+\sum_{i=1}^{N^2-1}\gamma_i\left(L_i\rho_S(t)L_i^\dagger-\frac{1}{2}\left\{L_i^\dagger L_i,\rho_S(t)\right\}\right) \tag{3.14}$$

with the non-negative eigenvalues γ_i of A and the so-called Lindblad operators L_i defined from the relation

$$F_i = \sum_{j=1}^{N^2-1} u_{ji} L_j \,, \tag{3.15}$$

where the u_{ij} are components of a matrix U that diagonalises the matrix A via $UAU^\dagger$. Equation (3.14) is often called the GKSL or Lindblad equation after Gorini, Kossakowski and Sudarshan, who proved in [123] the first standard form to be the most general form for the generator for a finite dimensional Hilbert space, and Lindblad, who showed in [122] that the diagonal form (3.14) is the most general form for a bounded generator if the underlying Hilbert space is separable and the sum runs over a countable set.

To summarise, while this approach is very elegant and one can directly write down a completely positive, trace preserving master equation for a given open quantum system, there is a list of conditions that need to hold in order for this master equation to be a good representation of the system's dynamics:

(1) The total state is separable at the initial time as stated in (3.1).

(2) The back-reaction of the system of interest on the environment is negligible and the environment remains approximately stationary.

(3) The timescales on which the correlations of the environment decay is much smaller than the timescale on which the system of interest evolves (Markov property) in order to obtain memorylessness which leads to a quantum dynamical semigroup.

(4) Either the underlying Hilbert space is finite-dimensional, or it is separable and the generator is bounded.

The first bullet point can be assumed to hold in several physical systems, the second one is usually in particular satisfied if one considers a large stationary environment like a thermal state which is only weakly coupled to the considered system. The third assumption has to be investigated for a specific physical system and can be seen as an approximation. The fourth point however is very problematic: For many physical systems this requirement is not fulfilled, for instance when considering harmonic oscillators or quantum fields. In order to see how these conditions enter the derivation of the Lindblad equation in detail and which intermediate master equations there are if not all of these four requirements are satisfied, we discuss in the following section 4 a different way to derive a master equation starting from the microscopic total system Hamiltonian and the Liouville-von Neumann equation (2.4). This will facilitate the possible analysis of errors made when taking the above assumptions and provide us with tools to deal with physical systems that do not fulfill all of these four requirements.

4. Projection operator formalism

This section was written independently from similar introductions in [5] and [1]. As it is based on the same references and has the same content, it might however show some similarities.
As discussed in the previous section, the Lindblad equation which is derived based on a quantum dynamical semigroup is subject to a set of requirements that limit its applicability to very few realistic physical systems. In order to be able to use similar master equations and their benefits to describe a larger class of systems, there exist different methods to derive such equations starting from an underlying Hamiltonian of the total system. In this section, we present the projection operator technique which leads to a more general form of a master equation that can be turned into a Lindblad equation when invoking several approximations. For the presentation, we closely follow [45]. A different method is for instance the influence functional approach based on work by Feynman and Vernon (see [138]). The first part 4.1 of this section will introduce the so-called Nakajima-Zwanzig projection operator technique which yields an integro-differential equation for the system of interest, that however still involves a time integration over its entire history. With the so-called time-convolutionless projection operator method that is discussed in subsection 4.2, one can then obtain a first-order differential equation that is time-local. In 4.3 we further discuss how from that equation a Redfield and a Born-Markov master equation can be obtained. To conclude, we sketch in 4.4 a general form for the environmental correlation functions which are two-point correlation functions of the environment appearing in the master equation.

4.1. Nakajima-Zwanzig projection operator method

This subsection was written independently from similar introductions in [5] and [1]. As it is based on the same references, it might however show some similarities.
In this subsection we discuss, following [45], the Nakajima-Zwanzig projection operator method, a route towards a master equation which is based on the works in [124], [125] and [139]. The starting point is a Hamiltonian describing the total system of the form (2.10). With this, the Liouville-von Neumann equation for the time evolution of the total system reads, see equation (2.4):

$$\frac{\partial}{\partial t}\rho_T(t) = -\frac{i}{\hbar}[H_T, \rho_T(t)]\,. \tag{4.1}$$

For the projection operator technique it is convenient to switch to the interaction picture, denoted by a tilde, where one then obtains

$$\frac{\partial}{\partial t}\widetilde{\rho}_T(t) = -\frac{i}{\hbar}\alpha[\widetilde{H}_I(t), \widetilde{\rho}_T(t)] \tag{4.2}$$

with the coupling parameter α that describes the coupling strength between system and environment. The evolution of the uncoupled system is now encoded in the operators while the remaining part leads to a change of the state of the system. For a general operator A we have:

$$A \longrightarrow \widetilde{A}(t) := e^{\frac{i}{\hbar}(H_S\otimes\mathbb{1}_\mathcal{E}+\mathbb{1}_S\otimes H_\mathcal{E})t} A e^{-\frac{i}{\hbar}(H_S\otimes\mathbb{1}_\mathcal{E}+\mathbb{1}_S\otimes H_\mathcal{E})t}\,, \tag{4.3}$$

$$\rho_T(t) \longrightarrow \widetilde{\rho}_T(t) := e^{\frac{i}{\hbar}(H_S\otimes\mathbb{1}_\mathcal{E}+\mathbb{1}_S\otimes H_\mathcal{E})t} \underbrace{e^{-\frac{i}{\hbar}H_T t}\rho_T(0)e^{\frac{i}{\hbar}H_T t}}_{=\rho_T(t)} e^{-\frac{i}{\hbar}(H_S\otimes\mathbb{1}_\mathcal{E}+\mathbb{1}_S\otimes H_\mathcal{E})t}\,. \tag{4.4}$$

At this point it is customary to introduce three "superoperators" called like that due to the fact that they act on other operators, in particular on elements of $\mathcal{B}(\mathcal{H}_T)$, where $\mathcal{H}_T$ denotes the

total Hilbert space of the system and $\mathcal{B}(\mathcal{H}_T)$ the set of bounded linear operators on $\mathcal{H}_T$ with the density matrix $\widetilde{\rho}_T(t)$ being one specific element thereof. These three operators are the Liouvillian and two projection operators:

$$\text{Liouvillian } \mathcal{L}(t): \qquad \widetilde{\rho}_T(t) \mapsto \mathcal{L}(t)\widetilde{\rho}_T(t) := -\frac{i}{\hbar}[\widetilde{H}_I(t), \widetilde{\rho}_T(t)] \tag{4.5}$$

$$\text{Projector } \mathcal{R} \text{ on relevant part}: \qquad \widetilde{\rho}_T(t) \mapsto \mathcal{R}\widetilde{\rho}_T(t) := \underbrace{tr_{\mathcal{E}}\{\widetilde{\rho}_T(t)\}}_{=:\widetilde{\rho}_S(t)} \otimes \rho_{\mathcal{E}} \tag{4.6}$$

$$\text{Projector } \mathcal{I} \text{ on irrelevant part}: \qquad \widetilde{\rho}_T(t) \mapsto \mathcal{I}\widetilde{\rho}_T(t) := \widetilde{\rho}_T(t) - \mathcal{R}\widetilde{\rho}_T(t)\,. \tag{4.7}$$

Here, we introduced an arbitrary, time-independent and normalised environmental reference state $\rho_{\mathcal{E}}$ that will be specified later. The two projectors indeed fulfill the mathematical requirements for projectors, in particular $\mathcal{R}^2 = \mathcal{R}, \mathcal{I}^2 = \mathcal{I}, \mathcal{R} + \mathcal{I} = \mathbb{1}_T$ and $\mathcal{R}\mathcal{I} = \mathcal{I}\mathcal{R} = 0$, which we will use in the derivation of the master equation. These projectors are now applied to the Liouville-von Neumann equation in (4.2) and yield:

$$\frac{\partial}{\partial t}\mathcal{R}\widetilde{\rho}_T(t) = \alpha\, \mathcal{R}\, \mathcal{L}(t)\ (\mathcal{R} + \mathcal{I})\ \widetilde{\rho}_T(t)\,, \tag{4.8}$$

$$\frac{\partial}{\partial t}\mathcal{I}\widetilde{\rho}_T(t) = \alpha\, \mathcal{I}\, \mathcal{L}(t)\ (\mathcal{R} + \mathcal{I})\ \widetilde{\rho}_T(t)\,. \tag{4.9}$$

In order to obtain a time evolution equation for[2] $\widetilde{\rho}_S(t) = tr_{\mathcal{E}}\{\mathcal{R}\widetilde{\rho}_T(t)\}$, the strategy is now to solve equation (4.9) for the irrelevant part of the density matrix $\mathcal{I}\widetilde{\rho}_T(t)$ and then to insert the result into equation (4.8) for the relevant part of the density matrix. Introducing the propagator $\mathcal{P}_{\mathcal{I}}(t, t_0)$ of the irrelevant part of the density matrix

$$\mathcal{P}_{\mathcal{I}}(t, t_0) := \mathcal{T}_{\leftarrow}\, e^{\alpha \int_{t_0}^{t} ds\, \mathcal{I}\, \mathcal{L}(s)}\,, \tag{4.10}$$

where $\mathcal{T}_{\leftarrow}$ denotes chronological time ordering, the solution of the evolution equation of the irrelevant part of the density matrix (4.9) reads

$$\mathcal{I}\widetilde{\rho}_T(t) = \mathcal{P}_{\mathcal{I}}(t, t_0)\, \mathcal{I}\widetilde{\rho}_T(t_0) + \alpha \int_{t_0}^{t} ds\, \mathcal{P}_{\mathcal{I}}(t, s)\, \mathcal{I}\, \mathcal{L}(s)\, \mathcal{R}\widetilde{\rho}_T(s)\,. \tag{4.11}$$

Using this in (4.8) yields:

$$\begin{aligned}\frac{\partial}{\partial t}\mathcal{R}\widetilde{\rho}_T(t) = {} & \alpha\, \mathcal{R}\, \mathcal{L}(t)\, \mathcal{R}\, \widetilde{\rho}_T(t) + \alpha\, \mathcal{R}\, \mathcal{L}(t)\, \mathcal{P}_{\mathcal{I}}(t, t_0)\, \mathcal{I}\, \widetilde{\rho}_T(t) \\ & + \alpha^2 \int_{t_0}^{t} ds\, \mathcal{R}\, \mathcal{L}(t)\, \mathcal{P}_{\mathcal{I}}(t, s)\, \mathcal{I}\, \mathcal{L}(s)\, \mathcal{R}\, \widetilde{\rho}_T(s)\,.\end{aligned} \tag{4.12}$$

This equation is called Nakajima-Zwanzig master equation [124, 125, 139] and does not yet contain any assumptions or approximations, thus it is still an exact master equation resembling the true dynamics of the system of interest. It however is hard to treat analytically, as it contains in the propagator as well as in the last term integrations over the entire history of the system from the initial time t_0 to the present time t. In the next subsection, we will discuss a method on how to proceed from this stage in order to remove this integration over the entire system's history.

[2] We assume the density matrix for the environment to be normalised, i.e. $tr_{\mathcal{E}}\{\rho_{\mathcal{E}}\} = 1$.

4.2. Time-convolutionless projection operator method

This subsection was written independently from similar introductions in [5] and [1]. As it is based on the same references, it might however show some similarities.
Given the highly complex form of the Nakajima-Zwanzig master equation (4.12), in particular the inclusion of the entire history of the system, we discuss here a method to cast this master equation into a time-local form, introduced in [126, 127, 140]. For the presentation of this method, we follow [45]. The starting points are again the evolution equations for the relevant and irrelevant part of the density matrix in (4.8) and (4.9). The solution for the irrelevant part is now modified by the introduction of another propagator $\mathcal{P}_{\mathcal{B}}(t,t_0)$ which propagates the total system back in time:

$$\mathcal{P}_{\mathcal{B}}(t,t_0) = \mathcal{T}_{\rightarrow} e^{-\alpha \int_{t_0}^{t} ds\, \mathcal{L}(s)}\,, \tag{4.13}$$

where $\mathcal{T}_{\rightarrow}$ denotes anti-chronological time ordering. This does not cause any problem, as the total system is closed and hence follows revertible, unitary dynamics. With this, the manifest time-convolution can be removed from the density matrix in the solution of the irrelevant part of the density matrix in (4.11):

$$\mathcal{I}\widetilde{\rho}_T(t) = \mathcal{P}_{\mathcal{I}}(t,t_0)\,\mathcal{I}\widetilde{\rho}_T(t_0) + \Sigma(t,t_0)\,\widetilde{\rho}_T(t) \tag{4.14}$$

with the former time convolution now being part of a new super-operator

$$\Sigma(t,t_0) := \alpha \int_{t_0}^{t} ds\, \mathcal{P}_{\mathcal{I}}(t,s)\,\mathcal{I}\,\mathcal{L}(s)\,\mathcal{R}\,\mathcal{P}_{\mathcal{B}}(t,s)\,. \tag{4.15}$$

Inserting a factor of $\mathbb{1}_T = \mathcal{R} + \mathcal{I}$ in front of the last density matrix in (4.14) permits us to solve this equation for the irrelevant part of the density matrix:

$$\mathcal{I}\widetilde{\rho}_T(t) = [1-\Sigma(t,t_0)]^{-1}\,\Sigma(t,t_0)\,\mathcal{R}\widetilde{\rho}_T(t) + [1-\Sigma(t,t_0)]^{-1}\,\mathcal{P}_{\mathcal{I}}(t,t_0)\,\mathcal{I}\widetilde{\rho}_T(t_0)\,, \tag{4.16}$$

where the propagator $\mathcal{P}_{\mathcal{I}}(t,t_0)$ was defined in equation (4.10). To derive this equation, we assumed that $[1-\Sigma(t,t_0)]$ is invertible, at least for some interval $[t_0,t]$. Such an interval exists as $\Sigma(t_0,t_0)=0$ and $\Sigma(t,t_0)$ is continuous in t, more details on that can be found in [1] in Appendix C. The size of this interval $[t_0,t]$ depends on the coupling parameter α. This solution for the irrelevant part of the density matrix can then be inserted into the equation for the relevant part (4.8) and one obtains

$$\begin{aligned}\frac{\partial}{\partial t}\mathcal{R}\widetilde{\rho}_T(t) =& \alpha\,\mathcal{R}\,\mathcal{L}(t)\left[1 + [1-\Sigma(t,t_0)]^{-1}\,\Sigma(t,t_0)\right]\mathcal{R}\widetilde{\rho}_T(t) \\ &+ \alpha\,\mathcal{R}\,\mathcal{L}(t)\,[1-\Sigma(t,t_0)]^{-1}\,\mathcal{P}_{\mathcal{I}}(t,t_0)\,\mathcal{I}\widetilde{\rho}_T(t_0)\,.\end{aligned} \tag{4.17}$$

Upon introduction of the TCL generator

$$\mathcal{G}(t,t_0) := \alpha\,\mathcal{R}\,\mathcal{L}(t)\left[1 + [1-\Sigma(t,t_0)]^{-1}\,\Sigma(t,t_0)\right]\mathcal{R} \tag{4.18}$$

and the inhomogeneity

$$\mathcal{N}(t,t_0) := \alpha\,\mathcal{R}\,\mathcal{L}(t)\,[1-\Sigma(t,t_0)]^{-1}\,\mathcal{P}_{\mathcal{I}}(t,t_0)\,\mathcal{I}\,, \tag{4.19}$$

this can be brought into the following convenient form:

$$\frac{\partial}{\partial t}\mathcal{R}\widetilde{\rho}_T(t) = \mathcal{G}(t,t_0)\,\mathcal{R}\widetilde{\rho}_T(t) + \mathcal{N}(t,t_0)\,\mathcal{I}\widetilde{\rho}_T(t_0)\,. \tag{4.20}$$

This master equation is still exact and now also local in time as it does not depend any more on the system's past history, only on the initial and present state. In order to simplify the treatment of this master equation, we now assume that the system of interest is weakly coupled to the environment, i.e. that the coupling constant α is small. This motivates us to expand the TCL generator and the inhomogeneity in a perturbation series in α. We start with the TCL generator:

$$\mathcal{G}(t,t_0) = \sum_{n=0}^{\infty} \alpha^n \mathcal{G}_n(t,t_0)\,. \tag{4.21}$$

Given the definitions of the propagators in (4.10) and (4.13) and the application of the geometric sum that yields on the interval $[t_0,t]$ where the inverse of $[1-\Sigma(t,t_0)]$ exists

$$[1-\Sigma(t,t_0)]^{-1} = \sum_{n=0}^{\infty}[\Sigma(t,t_0)]^n\,, \tag{4.22}$$

the individual $\mathcal{G}_n(t,t_0)$ can be determined from

$$\mathcal{G}(t,t_0) = \sum_{n=0}^{\infty}\alpha^n\mathcal{G}_n(t,t_0) = \alpha\,\mathcal{R}\,\mathcal{L}(t)\left[1+\sum_{m=1}^{\infty}[\Sigma(t,t_0)]^m\right]\mathcal{R} \tag{4.23}$$

and for the first orders it follows that, using $\mathcal{I} = \mathbb{1}_T - \mathcal{R}$:

$$\mathcal{G}_0(t,t_0) = 0 \tag{4.24}$$

$$\mathcal{G}_1(t,t_0) = \mathcal{R}\,\mathcal{L}(t)\,\mathcal{R} \tag{4.25}$$

$$\mathcal{G}_2(t,t_0) = \int_{t_0}^{t} ds\;\mathcal{R}\,\mathcal{L}(t)\,\mathcal{L}(s)\,\mathcal{R} - \int_{t_0}^{t} ds\;\mathcal{R}\,\mathcal{L}(t)\,\mathcal{R}\,\mathcal{L}(s)\,\mathcal{R}\,. \tag{4.26}$$

Throughout this thesis, we will focus on TCL master equations truncated after second order, so for us this expansion is only of interest until order $\mathcal{G}_2(t,t_0)$. In order to derive higher orders, it is helpful to make use of the so-called cumulant expansion developed by van Kampen in [141] and [142], which is a technique that allows one to directly write down $\mathcal{G}_n(t,t_0)$ for any n. As here we only need $n=\{0,1,2\}$, it is sufficient to calculate them directly, as done above. For the inhomogeneities one obtains in a similar fashion:

$$\mathcal{N}_0(t,t_0) = 0 \tag{4.27}$$

$$\mathcal{N}_1(t,t_0) = \mathcal{R}\,\mathcal{L}(t)\,\mathcal{I} \tag{4.28}$$

$$\mathcal{N}_2(t,t_0) = \int_{t_0}^{t} ds\;\mathcal{R}\,\mathcal{L}(t)\,\mathcal{L}(s)\,\mathcal{I} - \int_{t_0}^{t} ds\;\mathcal{R}\,\mathcal{L}(t)\,\mathcal{R}\,\mathcal{L}(s)\,\mathcal{I}\,. \tag{4.29}$$

With this expansion, the second order truncated TCL master equation [126, 127, 140] (also called TCL_2 master equation) reads

$$\begin{aligned}\frac{\partial}{\partial t}\mathcal{R}\widetilde{\rho}_T(t) = {}& \alpha\,\mathcal{R}\,\mathcal{L}(t)\,\mathcal{R}\widetilde{\rho}_T(t) + \alpha^2\int_{t_0}^{t} ds\;\mathcal{R}\,\mathcal{L}(t)\,\mathcal{L}(s)\,\mathcal{R}\widetilde{\rho}_T(t) - \alpha^2\int_{t_0}^{t} ds\;\mathcal{R}\,\mathcal{L}(t)\,\mathcal{R}\,\mathcal{L}(s)\,\mathcal{R}\widetilde{\rho}_T(t)\\ &+ \alpha\,\mathcal{R}\,\mathcal{L}(t)\,\mathcal{I}\widetilde{\rho}_T(t_0) + \alpha^2\int_{t_0}^{t} ds\;\mathcal{R}\,\mathcal{L}(t)\,\mathcal{L}(s)\,\mathcal{I}\widetilde{\rho}_T(t_0) - \alpha^2\int_{t_0}^{t} ds\;\mathcal{R}\,\mathcal{L}(t)\,\mathcal{R}\,\mathcal{L}(s)\,\mathcal{I}\widetilde{\rho}_T(t_0)\,.\end{aligned} \tag{4.30}$$

Up to this stage, we have not directly used any of the assumptions made in section 3. The only requirement so far is that the coupling between system and environment is weak, while similar microscopic derivations of a master equation also are possible for strong coupling if the Hamiltonian can be expanded in the inverse of the coupling constant, see [45]. The projection operator formalism yielded under the assumption of weak coupling the second order truncated master equation (4.30) which has a rather simple form and is valid for any kind of detailed coupling in the interaction Hamiltonian, any environment and also for an arbitrarily entangled initial state $\widetilde{\rho}_T(t_0)$. This is an outstanding point which makes the projection operator technique extremely powerful compared to similar derivations of master equations that often directly aim at the derivation of a Lindblad equation and due to that loosing track of the special features and the general picture of a given system under consideration. Examples for this are the direct microscopic derivation of the Lindblad equation for instance in [45] or [143] that are usually based on the Redfield or Born-Markov master equation that applies only to specific classes of systems. In the next subsection, we discuss in which way and under which assumptions these equations can be obtained from the TCL_2 master equation (4.30).

4.3. Redfield and Born-Markov master equations from the TCL_2 master equation

In this section we discuss, which additional assumptions and steps are necessary in order to cast the TCL_2 master equation (4.30) into a Redfield form and further into a Born-Markov master equation. These two types of master equations are often used in the literature, sometimes as an intermediate step towards a Lindblad equation. To cast the TCL_2 master equation into Redfield form, there are two assumptions that have to be taken, whose fulfillment depend on the specific physical scenario that is considered.

(a) The initial state of the total system is a product state, i.e. $\rho_T(t_0) = \rho_S(t_0) \otimes \rho_{\mathcal{E}}(t_0)$. Picking then the environmental reference state in the projection operator formalism to be equal to $\rho_{\mathcal{E}}(t_0)$, the projection onto the irrelevant part of the density matrix at initial time t_0 will vanish, i.e. $\mathcal{I}\widetilde{\rho}_T(t_0) = 0$. This implies that all inhomogeneities in the TCL_2 master equation (4.30), that is all terms in the second line, vanish. This assumption precisely is requirement (1) in section 3. While it is physically not always clear whether this assumption holds, it is often assumed in order to simplify calculations. The projection operator formalism however shows how non-vanishing inhomogeneities can be treated structurally.

(b) The second assumption is that $\mathcal{R}\,\mathcal{L}(t)\,\mathcal{R} = 0$, which removes the first and third term from the first line of the TCL_2 master equation in (4.30), as well as the last term in the second line. This condition is equivalent to

$$-\frac{i}{\hbar} tr_{\mathcal{E}} \left\{ [\widetilde{H}_I(t), \widetilde{\rho}_S(t) \otimes \rho_{\mathcal{E}}] \right\} = 0\,. \tag{4.31}$$

One condition for this to hold is that $tr_{\mathcal{E}} \left\{ \widetilde{H}_I(t)\, \rho_{\mathcal{E}} \right\} = 0$. This is in particular given if the environmental reference state, in particular therefore also the state of the environment at the initial time t_0, see assumption (a) above, is taken to be a stationary Gibbs state and the interaction Hamiltonian to be linear in the creation and annihilation operators of the environment. This will be the situation we will find throughout this thesis. This is however not in general fulfilled, one counter example would be if one considers a polymerised

environment as for instance in [144]. This assumption is related to requirement (2) in section 3.

Under these assumptions the TCL_2 master equation (4.30) obtains the following form:

$$\frac{\partial}{\partial t}\mathcal{R}\widetilde{\rho}_T(t) = \alpha^2 \int_{t_0}^{t} ds\, \mathcal{R}\, \mathcal{L}(t)\, \mathcal{L}(s)\, \mathcal{R}\widetilde{\rho}_T(t)\,, \tag{4.32}$$

which we can rewrite due to the factorising initial conditions in (a), and taking the trace with respect to the environment, as

$$\frac{\partial}{\partial t}\widetilde{\rho}_S(t) = -\frac{\alpha^2}{\hbar^2}\int_{t_0}^{t} ds\, tr_{\mathcal{E}}\left\{[\widetilde{H}_I(t), [\widetilde{H}_I(s), \widetilde{\rho}_S(t)\otimes\rho_{\mathcal{E}}]]\right\}\,, \tag{4.33}$$

where we used the definition $\widetilde{\rho}_S(t) := tr_{\mathcal{E}}\{\widetilde{\rho}_T(t)\}$ from equation (4.6). In Schrödinger picture, this master equation reads

$$\frac{\partial}{\partial t}\rho_S(t) = -\frac{i}{\hbar}[H_S, \rho_S(t)] - \frac{\alpha^2}{\hbar^2}\int_{t_0}^{t} ds\, tr_{\mathcal{E}}\left\{[H_I, [\widetilde{H}_I(s-t), \rho_S(t)\otimes\rho_{\mathcal{E}}]]\right\}\,, \tag{4.34}$$

and defining $\tau := t - s$ this becomes

$$\frac{\partial}{\partial t}\rho_S(t) = -\frac{i}{\hbar}[H_S, \rho_S(t)] - \frac{\alpha^2}{\hbar^2}\int_{0}^{t-t_0} d\tau\, tr_{\mathcal{E}}\left\{[H_I, [\widetilde{H}_I(-\tau), \rho_S(t)\otimes\rho_{\mathcal{E}}]]\right\}\,. \tag{4.35}$$

This is the so-called Redfield master equation. To arrive at this form, one can alternatively also start from the trace of the Liouville-von Neumann equation and apply the assumptions used here, where assumption (a) is implemented by the Born approximation which assumes $\rho_T(t) \approx \rho_S(t)\otimes\rho_{\mathcal{E}}$ to hold inside the double commutator, and assumption (b) is plugged in by hand. This approach is for instance discussed in [5] or [45]. Deriving a Redfield master equation in that way does however not give any technique or intuition on how to deal with different environments or non-separable initial states and therefore non-vanishing inhomogeneities. While the Redfield equation is in general not completely positive in contrast to the Lindblad equation discussed in section 3, it does in principle approximate the dynamics of a system under consideration with higher accuracy as a Lindblad equation due to the fewer amount of approximations invoked. Its use is however limited, as from a certain time t on it might predict negative probabilities. Therefore its predictions have to be treated with caution and its domain of validity has to be analysed in detail given a specific physical system. Additionally, one can test, under which circumstances the Redfield equation can be cast into a Lindblad equation and which error is committed when doing so. One major part of this thesis deals with Redfield master equations for different physical systems involving gravity as the environment, and the analysis of the required approximations to cast it into a Lindblad form.
Under the additional assumption of short memory in the environment, that is that the environmental correlation functions, that will be discussed in more details in the next subsection, are strongly peaked in τ and decay rapidly, one can apply the Markov approximation to the Redfield equation. This approximation consists in shifting the initial time from t_0 to $-\infty$ and assumes that the error made by this shift is negligible. This yields then the Born-Markov master equation

$$\frac{\partial}{\partial t}\rho_S(t) = -\frac{i}{\hbar}[H_S, \rho_S(t)] - \frac{\alpha^2}{\hbar^2}\int_{0}^{\infty} d\tau\, tr_{\mathcal{E}}\left\{[H_I, [\widetilde{H}_I(-\tau), \rho_S(t)\otimes\rho_{\mathcal{E}}]]\right\}\,. \tag{4.36}$$

This approximation precisely is condition (3) in section 3 and the resulting master equation now is completely local in time, as it does not any more depend on the initial state at t_0 as the Redfield equation did before. The Markov approximation however is a rather strong assumption and it is a priori not clear whether it is a good approximation for a given physical system. Therefore we will work throughout this thesis with the Redfield equation (4.35) and test in the different models considered in detail, whether the Markov approximation is justified or not. Apart from this route towards a Redfield master equation, there also exists the influence functional approach based on [138] which is used in the literature, e.g. in [62]. An introduction to this technique can be found for instance in [5], [1] or [45]. As is discussed in [1], for the TCL_2 master equation it yields an equivalent result as the time-convolutionless projection operator method applied in this thesis.

4.4. Environmental correlation functions

In this subsection, we introduce environmental correlation functions into the Redfield master equation (4.33) in order to set the stage for the next parts of this thesis where we will make use of these two-point correlation functions. For this, we first split the interaction Hamiltonian into a very general form:

$$\widetilde{H}_I(t) = \int d\lambda \sum_A \widetilde{S}_A(\lambda, t) \otimes \widetilde{E}^A(\lambda, t)\,, \tag{4.37}$$

where the operators $\widetilde{S}_A\lambda, t)$ act on the Hilbert space of the system of interest and the operators $\widetilde{E}^A(\lambda, t)$ act on the Hilbert space of the environment. Both operators are linked by an intrinsic, continuous parameter λ and a discrete parameter A, which can be understood as multi-index and which is summed over a finite set. Using Einstein's sum convention, we drop the explicit sum over A. Applying this in the Redfield equation (4.33) we obtain

$$\begin{aligned}\frac{\partial}{\partial t}\widetilde{\rho}_S(t) = -\frac{\alpha^2}{\hbar^2}\int_{t_0}^{t} ds \int d\lambda \int d\lambda' \Bigg(& \Big(\widetilde{S}_A(\lambda,t)\,\widetilde{S}_B(\lambda',s)\,\widetilde{\rho}_S(t) - \widetilde{S}_B(\lambda',s)\,\widetilde{\rho}_S(t)\,\widetilde{S}_A(\lambda,t)\Big) \\ & \cdot G^{>AB}(\lambda,\lambda',t,s) \\ & + \Big(-\widetilde{S}_A(\lambda,t)\,\widetilde{\rho}_S(t)\,\widetilde{S}_B(\lambda',s) + \widetilde{\rho}_S(t)\,\widetilde{S}_B(\lambda',s)\,\widetilde{S}_A(\lambda,t)\Big) \\ & \cdot G^{<AB}(\lambda,\lambda',t,s)\Bigg)\,,\end{aligned} \tag{4.38}$$

where we defined the thermal Wightman correlation functions in the same manner as in [145]:

$$G^{>AB}(\lambda,\lambda',t,s) := tr_{\mathcal{E}}\left\{\widetilde{E}^A(\lambda,t)\,\widetilde{E}^B(\lambda',s)\,\rho_{\mathcal{E}}\right\}\,, \tag{4.39}$$

$$G^{<AB}(\lambda,\lambda',t,s) := tr_{\mathcal{E}}\left\{\widetilde{E}^B(\lambda',s)\,\widetilde{E}^A(\lambda,t)\,\rho_{\mathcal{E}}\right\}\,. \tag{4.40}$$

Depending on the system under consideration and in particular on the time dependence of the $\widetilde{S}_A(\lambda, t)$ and on the parameter λ, the investigation of these functions alone might (see part IV, section 16.4, where a quantum mechanical model in which a neutrino is coupled to harmonic oscillators is investigated) or might not (see part III, section 12.1.1, where the one-particle projection of a scalar field coupled to an environment of gravitational waves is discussed) be enough

to test for the applicability of the Markov approximation. With further approximations, in particular the Markov and, depending on the specific system, also the rotating wave approximation, the master equation in (4.38) can be cast into Lindblad form. As these approximations cannot straight forwardly be applied in general, we will discuss this for the systems under consideration in this thesis individually.
In figure 2 the different master equations, the approximations required to derive them and their dependence on each other are sketched.

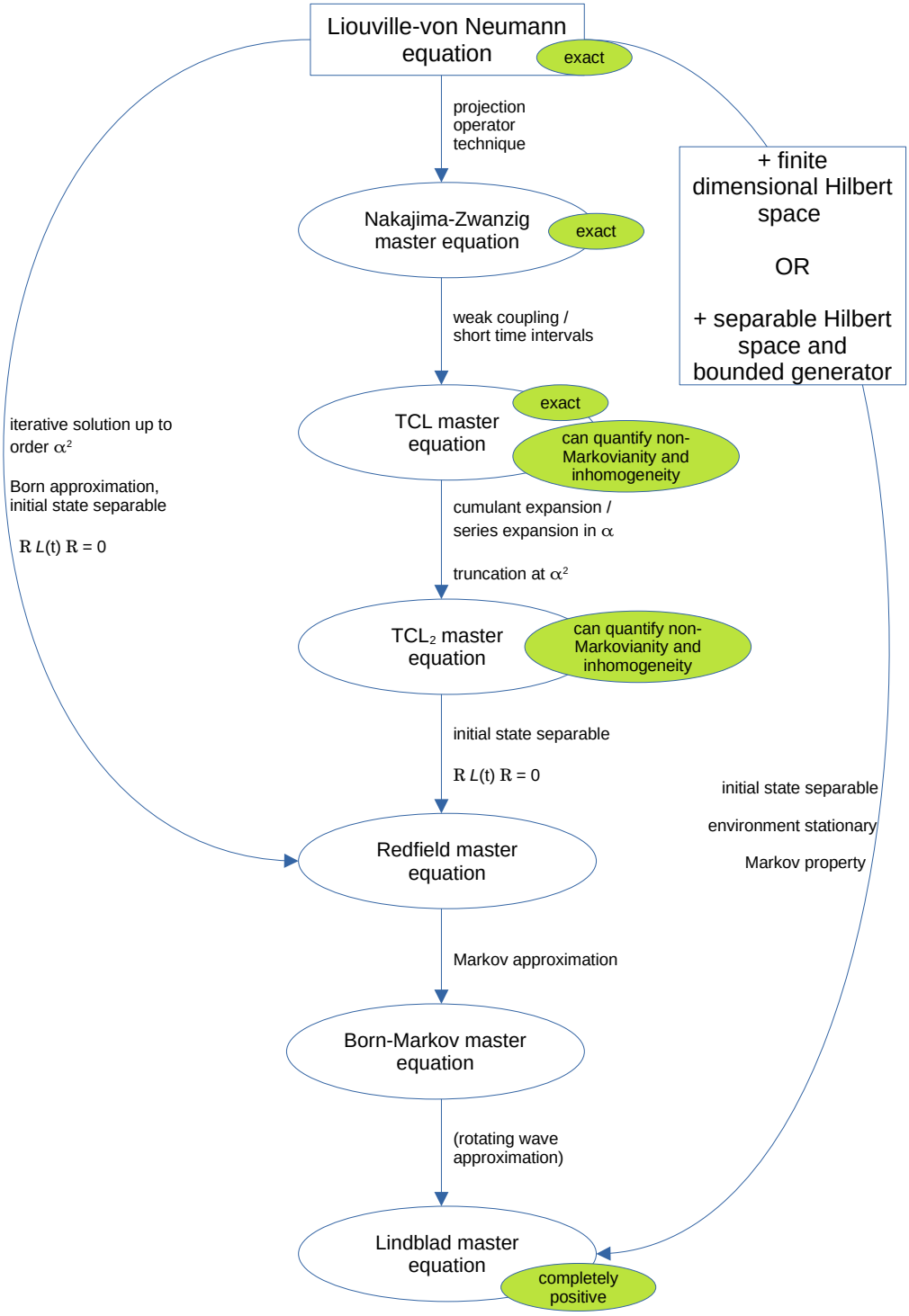

Figure 2: Overview of the different kinds of master equations discussed in this thesis and the route and approximations required for their derivations.

5. A simple quantum mechanical decoherence model

To demonstrate the path towards a master equation and some of the standard techniques discussed in the previous section of this part of the thesis, we sketch in this section a simple quantum mechanical system for which a corresponding master equation is derived. The simple model is a so-called spin-boson model that consists of a two-level system which is coupled to an environment of harmonic oscillators. This model was investigated to discuss decoherence in qubits in [134–136]. Here, we partly follow the presentation in [45, 46]. We have chosen this specific model, as it is still very well treatable analytically and is similar to the one investigated in part IV of this thesis, where we couple a neutrino described as a three-level system and hence by a different system Hamiltonian to an environment of harmonic oscillators. For the model discussed in this section, we start from the total Hamiltonian of the underlying microscopic system that has the form specified in (2.10):

$$H_T = H_S \otimes \mathbb{1}_\mathcal{E} + \mathbb{1}_S \otimes H_\mathcal{E} + H_I \,. \tag{5.1}$$

where we absorbed the coupling constant α into H_I, and with

$$H_S := \frac{\omega_0}{2}\sigma_3 \tag{5.2}$$

$$H_\mathcal{E} := \sum_i \omega_i \, b_i^\dagger b_i \tag{5.3}$$

$$H_I := \sigma_3 \otimes \sum_i \left(g_i b_i^\dagger + g_i^* b_i \right) . \tag{5.4}$$

In these definitions, $\sigma_3 = \mathrm{diag}(1, -1)$ denotes the third Pauli matrix, ω_0 the energy difference between the two levels of the system of interest, $b_i^{(\dagger)}$ the Ladder operators for the ith oscillator in the environment that fulfill $[b_i, b_j^\dagger] = \delta_{ij}$, ω_i their frequencies and $g_i^{(*)}$ the coupling constants that can in principle be different for each oscillator i. If g_i is purely real, then the interaction Hamiltonian can be rewritten as

$$H_I \propto H_S \otimes \sum_i g_i q_i \,, \tag{5.5}$$

where q_i is the position operator of oscillator i. This is the interaction Hamiltonian for the model discussed in part IV starting in section 16, which is based on [112] and couples a three-level system to an environment of harmonic oscillators, serving as a toy model for gravitationally induced decoherence in neutrino oscillations. For now, we continue with the general case where g_i is a complex number. To derive a master equation that encodes the effective influence of the environment on the two-level system, we first switch into interaction picture (denoted by a tilde), in which the interaction Hamiltonian has the following form:

$$\begin{aligned} \widetilde{H}_I(t) &= e^{\frac{i}{\hbar}(H_S \otimes \mathbb{1}_\mathcal{E} + \mathbb{1}_S \otimes H_\mathcal{E})t} H_I e^{-\frac{i}{\hbar}(H_S \otimes \mathbb{1}_\mathcal{E} + \mathbb{1}_S \otimes H_\mathcal{E})t} \\ &= \sigma_3 \otimes \sum_i \Big(g_i \underbrace{e^{\frac{i}{\hbar}H_\mathcal{E} t} b_i^\dagger e^{-\frac{i}{\hbar}H_\mathcal{E} t}}_{=:\, b_i^\dagger(t)} + g_i^* \underbrace{e^{\frac{i}{\hbar}H_\mathcal{E} t} b_i e^{-\frac{i}{\hbar}H_\mathcal{E} t}}_{=:\, b_i(t)} \Big) . \end{aligned} \tag{5.6}$$

To obtain the time evolution of the Ladder operators we use:

$$b_i^{(\dagger)}(t) = e^{i\omega_i t \, b_i^\dagger b_i} \, b_i^{(\dagger)} \, e^{-i\omega_i t \, b_i^\dagger b_i} = \sum_{m=0}^{\infty} \frac{(i\omega_i t)^m}{m!} [b_i^\dagger b_i, b_i^{(\dagger)}]_{(m)} \,, \tag{5.7}$$

where we introduced the iterated or nested commutator $[A,B]_{(m)}$ which is defined recursively in the following way:

$$[A,B]_{(m+1)} := [A,[A,B]_{(m)}]\,, \qquad [A,B]_{(0)} = B\,. \tag{5.8}$$

In the present case this yields:

$$[b_i^\dagger b_i, b_i]_{(m)} = (-1)^m b_i\,, \qquad [b_i^\dagger b_i, b_i^\dagger]_{(m)} = b_i^\dagger\,, \tag{5.9}$$

which implies

$$b_i(t) = e^{-i\omega_i t}\, b_i \qquad b_i^\dagger(t) = e^{i\omega_i t}\, b_i^\dagger \tag{5.10}$$

and thus the interaction Hamiltonian in interaction picture reads

$$\widetilde{H}_I(t) = \sigma_3 \otimes \sum_i \left(g_i e^{i\omega_i t}\, b_i^\dagger + g_i^* e^{-i\omega_i t}\, b_i \right). \tag{5.11}$$

With this, the Liouville-von Neumann equation in interaction picture (4.2) can be constructed:

$$\frac{\partial}{\partial t}\widetilde{\rho}_T(t) = -\frac{i}{\hbar}[\widetilde{H}_I(t), \widetilde{\rho}_T(t)] \tag{5.12}$$

with

$$\widetilde{\rho}_T(t) := e^{\frac{i}{\hbar}(H_S\otimes \mathbb{1}_\mathcal{E} + \mathbb{1}_S \otimes H_\mathcal{E})t}\, \rho_T(t)\, e^{-\frac{i}{\hbar}(H_S\otimes \mathbb{1}_\mathcal{E} + \mathbb{1}_S \otimes H_\mathcal{E})t}\,. \tag{5.13}$$

To show a bit the variety of the formalism of open quantum systems, in this model we will apply the time evolution of the entire system and then trace out the environment, while in the similar but slightly more complex model in part IV of the thesis, we will first trace out the environment. In the present model, we can use that the time evolution operator $\widetilde{U}(t)$ for the Liouville-von Neumann equation in interaction picture can be simplified in the following way:

$$\widetilde{U}(t) = \mathcal{T}_{\leftarrow} e^{-\frac{i}{\hbar}\int_0^t d\tau\, \widetilde{H}_I(\tau)} = e^{i\varphi(t)} e^{-\frac{i}{\hbar}\int_0^t d\tau\, \widetilde{H}_I(\tau)}\,, \tag{5.14}$$

where $\mathcal{T}_{\leftarrow}$ denotes chronological time ordering and $\varphi(t)$ is a phase factor

$$\varphi(t) := \frac{i}{2\hbar^2}\int_0^t d\tau \int_0^t d\tau'\, \Theta(\tau-\tau')\, \left[\widetilde{H}_I(\tau), \widetilde{H}_I(\tau')\right]. \tag{5.15}$$

The reason for the applicability of this simplification is the fact that the commutator

$$\left[\widetilde{H}_I(\tau), \widetilde{H}_I(\tau')\right] \propto \mathbb{1}_T\,, \tag{5.16}$$

hence instead of applying the time ordering it is sufficient to use the standard exponential series and multiply it with the correction arising from the commutations which is the phase $e^{i\varphi(t)}$. A proof of this equality can be found for instance in [45, 46]. The time evolution operator can thus be written as

$$\widetilde{U}(t) = e^{i\varphi(t)} e^{\frac{\sigma_3}{2}\otimes\sum_i \left(c_i(t)\, b_i^\dagger - c_i^*(t)\, b_i\right)} =: e^{i\varphi(t)} e^{\sigma_3 \otimes \sum_i D_i\left(\frac{c_i(t)}{2}\right)}\,, \tag{5.17}$$

where

$$c_i(t) := 2g_i \frac{1-e^{i\omega_i t}}{\hbar\omega_i} \qquad \text{and} \qquad D_i\left(\frac{c_i(t)}{2}\right) := \frac{1}{2}\left(c_i(t)\, b_i^\dagger - c_i^*(t)\, b_i\right). \tag{5.18}$$

To apply this evolution, we have to fix the initial state of the total system. As discussed in the previous section, an initially uncorrelated state simplifies the analysis, so we assume this to hold here:

$$\rho_T(0) = \widetilde{\rho}_T(0) = \rho_S(0) \otimes \rho_{\mathcal{E}}(0)\,. \tag{5.19}$$

The assumption which will be made throughout this thesis for the physical systems considered is always that the environment is very large compared to the system under consideration and is in thermal equilibrium, that is in a stationary Gibbs state. Due to the large size of the environment, the back-reaction which the system causes on the environment is neglected. From this follows

$$\rho_{\mathcal{E}}(t) = \rho_{\mathcal{E}} = \frac{1}{Z_{\mathcal{E}}} e^{-\beta H_{\mathcal{E}}} \tag{5.20}$$

with the partition sum of the environment $Z_{\mathcal{E}} := tr_{\mathcal{E}}\{e^{-\beta H_{\mathcal{E}}}\}$ that normalises the trace of the density matrix to $tr_{\mathcal{E}}\{\rho_{\mathcal{E}}\} = 1$, where $tr_{\mathcal{E}}$ denotes the trace over the environmental part of the Hilbert space and $\beta := \frac{1}{k_B \Theta}$ with the Boltzmann constant k_B and a temperature parameter Θ that characterises the Gibbs state.
The time evolution of the density matrix for the system of interest is then obtained in energy eigenbasis $\{|i\rangle, |j\rangle\}$ as

$$\widetilde{\rho}_{S,ij}(t) = \langle i|\, tr_{\mathcal{E}}\{\widetilde{U}(t)\, \widetilde{\rho}_T(0)\, \widetilde{U}^{\dagger}(t)\}\, |j\rangle\ . \tag{5.21}$$

As the interaction Hamiltonian commutes with the system Hamiltonian, the state of the system itself is apart from a possible sign flip not changed by the application of the time evolution operator. When considering the diagonal elements (populations) of the density matrix, this sign cancels. For the environmental part of the time evolution operator we have $D_i^{\dagger}\left(\frac{c_i(t)}{2}\right) = -D_i\left(\frac{c_i(t)}{2}\right)$, which also cancels for the populations. Thus the populations of the system's density matrix remain constant in time:

$$\widetilde{\rho}_{S,ii}(t) = \widetilde{\rho}_{S,ii}(0) \tag{5.22}$$

and the model is a pure dephasing model. Indeed, the fact that H_I and H_S commute implies that the interaction of the system with the environment cannot change the system's energy. For the off-diagonal elements (coherences) we find:

$$\widetilde{\rho}_{S,ij}(t) = \rho_{S,ij}(0) e^{-\Gamma(t)} \tag{5.23}$$

with a decoherence function $\Gamma(t)$ that is real and non-negative for $t \geq 0$. This function can be computed using the techniques introduced below in section 16. As the calculation is very similar to the one there, we just state the result from [45], equation (4.49) here:

$$\Gamma(t) = \sum_i \frac{4|g_i|^2}{\hbar^2 \omega_i^2} \coth\left(\frac{\beta\omega_i}{2}\right)(1 - \cos(\omega_i t))\,, \tag{5.24}$$

which, as expected, is non-negative and real for $\omega_i \geq 0$. To determine this quantity more in detail, one needs the knowledge of all the individual coupling constants g_i and frequencies ω_i of the oscillators in the environment. As this is not practical, at this stage usually a continuum limit is applied that replaces the individual oscillators by a continuum of oscillators that are characterised by a spectral density $J(\omega)$. This choice of such a spectral density has to be imposed by hand and is discussed in more detail in section 16.3. When starting in the beginning with a

microscopic model that is based on a (quantum) field theory, then the choice of a spectral density is not necessary. With such a spectral density, the decoherence function can be expressed as

$$\Gamma(t) = \int_0^\infty d\omega \, \frac{J(\omega)}{\hbar^2\omega^2} \coth\left(\frac{\beta\omega}{2}\right)(1-\cos(\omega t))\,. \tag{5.25}$$

We can split this function into a vacuum contribution that represents decoherence due to vacuum fluctuations:

$$\Gamma_{vac}(t) := \int_0^\infty d\omega \, \frac{J(\omega)}{\hbar^2\omega^2}(1-\cos(\omega t)) \tag{5.26}$$

and a thermal one that encodes the influence of the thermal environment on the system of interest:

$$\Gamma_{th}(t) = \int_0^\infty d\omega \, \frac{J(\omega)}{\hbar^2\omega^2}\left[\coth\left(\frac{\beta\omega}{2}\right)-1\right](1-\cos(\omega t))\,. \tag{5.27}$$

From the fact that $\Gamma(t) \geq 0$ for $t \geq 0$ combined with equation (5.23) it follows that the influence of the environment leads to a damping of the off-diagonal elements of the density matrix in the energy eigenbasis. To analyse this effect in detail, first a spectral density has to be picked and then often also approximations regarding the temperature parameter are invoked. As this both depends on the physical system that is being studied, we stop at this point and refer for further analysis of this model to the literature, for instance to [45, 46] and also to part IV of the thesis, where a spectral density is chosen and discussed for gravitationally induced decoherence in neutrino oscillations which is motivated by the field theoretical approach in parts II and III of this thesis.

Part II.
Gravity as environment: a master equation for gravitationally induced decoherence on a scalar field in the relational formalism

As the main application of this thesis, we discuss in this part the derivation of a master equation for a scalar field in a linearised gravitational environment. For this, we make extensive use of the techniques introduced in part I. Most of the content and results of this part were published in [1]. Some parts are based on the results from the master's thesis [5], to which we refer the reader for more details on the basic model.

6. The basic model: linearised gravity coupled to a scalar matter field

The content of this section was already published in [1] and is partially based on results of the Master's thesis [5]. It is included in this PhD thesis as it forms the basis of the PhD project and is presented here with slight modifications compared to [1] to adapt it to the flow of the thesis.
Following the approach for gravitationally induced decoherence models presented in part I of this thesis, we introduce in this section a field theoretical model that consists of a scalar field as system under consideration and linearised gravity as environment. We discuss the corresponding action, which arises from the full theory of general relativity in first place, and necessary boundary contributions in terms of Ashtekar variables for gravity in subsection 6.1. For better analytic treatment and to adopt to physical scenarios of weak coupling, we focus on linearised gravity only. For this purpose we consider the linearisation of vacuum gravity in Ashtekar variables in subsection 6.2 use the framework of a Post-Minkowski approximation to couple the scalar field, which is discussed in subsection 6.3.

6.1. The gravity-matter system formulated in Ashtekar variables

The content of this subsection was already published in [1] and is partially based on results of the Master's thesis [5]. It is included in this PhD thesis as it forms the basis of the PhD project and is presented here with slight modifications compared to [1] to adapt it to the flow of the thesis.
As the starting point for deriving the decoherence model in this part of the thesis, we choose the following action involving gravity coupled to a Klein-Gordon scalar field in the ADM decomposition [83] expressed in terms of Ashtekar variables [114, 115, 146, 147]:

$$S = \int_{\mathbb{R}} dt \int_{\sigma} d^3x \Big(\frac{1}{\kappa\beta} \dot{A}_a{}^i(\vec{x},t)\, E^a{}_i(\vec{x},t) + \dot{\phi}(\vec{x},t)\, \pi(\vec{x},t) \\ - \Big[\Lambda^i(\vec{x},t)\, G_i(\vec{x},t) + N^a(\vec{x},t)\, C_a(\vec{x},t) + N(\vec{x},t)\, C(\vec{x},t) \Big] \Big) , \tag{6.1}$$

where β is the Barbero-Immirzi parameter, $\kappa = \frac{8\pi G_N}{c^4}$ with Newton's gravitational constant G_N, c denotes the speed of light and we work with the mostly-plus signature of the metric. From here on, we will set $c = \hbar = 1$. The gravitational degrees of freedom are encoded in the Ashtekar variables consisting of an SU(2)-connection $A_a{}^i(\vec{x},t)$ and the canonically conjugate densitised triads $E^a{}_i(\vec{x},t)$. The matter sector includes the scalar field $\phi(\vec{x},t)$ as well as its canonically conjugate momentum $\pi(\vec{x},t)$, an overdot denotes a derivative with respect to the temporal coordinate. That general relativity is a fully constrained theory is reflected by the fact that apart from the symplectic potential in the action, there appears a sum of constraints $G_i(\vec{x},t)$, $C_a(\vec{x},t)$ and $C(\vec{x},t)$ only multiplied by different Lagrange multipliers $\Lambda^i(\vec{x},t)$, $N^a(\vec{x},t)$ and $N(\vec{x},t)$, where the latter two are usually referred to as the shift vector and the lapse function, respectively. In Ashtekar

variables the spatial diffeomorphism constraint reads

$$C_a(\vec{x},t) = \frac{1}{\kappa\beta} F_{ab}{}^{i}(\vec{x},t)\, E^{b}{}_{i}(\vec{x},t) + \pi(\vec{x},t)\,\partial_a\phi(\vec{x},t)\,, \tag{6.2}$$

where $F_{ab}{}^{i}(\vec{x},t) := \partial_a A_b{}^{i}(\vec{x},t) - \partial_b A_a{}^{i}(\vec{x},t) + \epsilon_{ijk} A_a{}^{j}(\vec{x},t)\, A_b{}^{k}(\vec{x},t)$ denotes the curvature related to the connection variable A. The Gauß constraint, which is absent if working in ADM variables, is given by

$$G_i(\vec{x},t) = \frac{1}{2\kappa\beta}\left(\partial_a E^{a}{}_{i}(\vec{x},t) + \epsilon_{ij}{}^{k} A_a{}^{j}(\vec{x},t)\, E^{a}{}_{k}(\vec{x},t)\right) \tag{6.3}$$

with the completely antisymmetric tensor ϵ. Finally, the Hamiltonian constraint takes the form

$$\begin{aligned} C(\vec{x},t) =& \frac{1}{2\kappa}\left(F_{ab}{}^{i}(\vec{x},t) - \frac{\beta^2+1}{\beta^2}\epsilon_{ilm}(A_a{}^{l}(\vec{x},t) - \Gamma_a{}^{l}(\vec{x},t))(A_b{}^{m}(\vec{x},t) - \Gamma_b{}^{m}(\vec{x},t))\right) \\ &\qquad\qquad \cdot \frac{\epsilon^{ijk} E^{a}{}_{j}(\vec{x},t)\, E^{b}{}_{k}(\vec{x},t)}{\sqrt{\det(E^{c}{}_{n})}} \\ &+ \frac{\pi^2(\vec{x},t)}{2\sqrt{\det(E^{c}{}_{n})}} + \frac{1}{2\sqrt{\det(E^{c}{}_{n})}}\delta^{ij} E^{a}{}_{i}(\vec{x},t)\, E^{b}{}_{j}(\vec{x},t)\,(\partial_a\phi(\vec{x},t))(\partial_b\phi(\vec{x},t)) \\ &+ \frac{\sqrt{\det(E^{c}{}_{n})}}{2}\, m^2\phi^2(\vec{x},t)\,. \end{aligned} \tag{6.4}$$

Here, m denotes the mass of the scalar field and $\Gamma_a{}^{i}$ is the spin connection, considered a functional of the densitised triads, i.e.

$$\Gamma_a{}^{i} = -\frac{1}{2}\epsilon^{ijk} E^{b}{}_{k}\left(E_a{}^{j}{}_{,b} - E_b{}^{j}{}_{,a} + E^{c}{}_{j} E_a{}^{l} E_c{}^{l}{}_{,b} + E_a{}^{j}\frac{\det(E^{c}{}_{l})_{,b}}{\det(E^{c}{}_{l})} - E_b{}^{j}\frac{\det(E^{c}{}_{l})_{,a}}{2\det(E^{c}{}_{l})}\right), \tag{6.5}$$

where we abbreviated partial derivatives with a comma, that is $E_a{}^{j}{}_{,b} := \partial_b E_a{}^{j}$, and suppressed the spatial and temporal arguments of the involved field variables. The elementary phase space variables satisfy the following Poisson algebra on the classical phase space:

$$\begin{aligned} \{E^{a}{}_{i}(\vec{x},t), E^{b}{}_{j}(\vec{y},t)\} = \{A_a{}^{i}(\vec{x},t), A_b{}^{j}(\vec{y},t)\} = 0\,, \quad \{A_a{}^{i}(\vec{x},t), E^{b}{}_{j}(\vec{y},t)\} = \beta\kappa\delta_a^b\delta_j^i\delta^3(\vec{x}-\vec{y})\,, \\ \{\phi(\vec{x},t),\phi(\vec{y},t)\} = \{\pi(\vec{x},t),\pi(\vec{y},t)\} = 0\,, \qquad \{\phi(\vec{x},t),\pi(\vec{y},t)\} = \delta^{(3)}(\vec{x}-\vec{y})\,, \end{aligned} \tag{6.6}$$

where all the remaining ones vanish. As the decoherence model presented in this part of the thesis requires to linearise the above action around a flat Minkowski background in the course of the upcoming section, we choose asymptotically flat boundary conditions [148] also addressed in [149, 150] for the case of real Ashtekar variables. With the fall-off behaviour of the Ashtekar variables discussed in section 6.2 and the linearisation of the Lagrange multipliers chosen such that both are consistent with an asymptotically flat universe, it turns out that the Gauß constraint and the gravitational part of the spatial diffeomorphism constraint do not cause any issues and need no further modification in accordance with [151]. However, the gravitational part of the Hamiltonian constraint as well as its variation is not well-defined in the asymptotically flat limit and contains divergences. To circumvent these, we introduce a suitable boundary term given by

$$T[N] = -2\int_{\partial\sigma} dS_a\, N A_b{}^{k}\epsilon^{ijk}\frac{E^{a}{}_{i} E^{b}{}_{j}}{\sqrt{\det E}} \tag{6.7}$$

to the smeared Hamiltonian constraint, which makes it well-defined and functionally differentiable. Note that on the constraint hypersurface where the Gauß constraint vanishes $T[1]$ is the so-called ADM-energy [152]. Further we assume, as is usually done, that the initial data of the matter variables have compact support, yielding matter contributions that are well-defined in the asymptotically flat case. Given this, the canonical Hamiltonian that we will work with in the following and that is consistent with our chosen boundary conditions reads

$$\begin{aligned}\mathbf{H}_{\text{can}} &= C(N) + \vec{C}(\vec{N}) + \vec{G}(\vec{\Lambda}) + T[N] \\ &= \int_\sigma d^3x \Big[\frac{1}{\kappa\beta} N^a F_{ab}{}^j E^b{}_j + N^a \pi \nabla_a \phi + \frac{1}{2\kappa\beta} \Lambda^i \partial_a E^a{}_i + \frac{1}{2\kappa\beta} \Lambda^i \epsilon_{ikl} A_a{}^k E^a{}_l \\ &\qquad - N \epsilon^{jkl} \frac{1}{\sqrt{\det E}} E^a{}_k E^b{}_l \frac{1}{2\kappa\beta^2} \epsilon_{jmn} \left(A_a{}^m A_b{}^n + (\beta^2+1) \Gamma_a{}^m \Gamma_b{}^n - 2\Gamma_a{}^m A_b{}^n \right) \\ &\qquad + \frac{1}{\sqrt{\det E}} \Big(-\frac{1}{\kappa} \epsilon^{jkl} E^a{}_k E^b{}_l A_b{}^j \partial_a N + N \frac{\pi^2}{2} + \frac{N}{2} E^a{}_i E^b{}_i (\partial_a \phi)(\partial_b \phi) \Big) \\ &\qquad + N \frac{\sqrt{\det E}}{2} \, m^2 \phi^2 \Big] , \end{aligned} \tag{6.8}$$

where

$$C(N) := \int_\sigma d^3x \; C(\vec{x},t) N(\vec{x},t) \tag{6.9}$$

$$\vec{C}(\vec{N}) := \int_\sigma d^3x \; C_a(\vec{x},t) N^a(\vec{x},t) \tag{6.10}$$

$$\vec{G}(\vec{\Lambda}) := \int_\sigma d^3x \; G_i(\vec{x},t) \Lambda^i(\vec{x},t) \, . \tag{6.11}$$

In the following two subsections we will consider a linearisation of the gravity-matter system. For this purpose we first briefly review the linearisation of the vacuum case and afterwards discuss how the scalar field can be coupled to linearised gravity in the framework of a Post-Minkowski approximation scheme.

6.2. Brief review of linearised gravity in Ashtekar variables

The content of this subsection was already published in [1] and is partially based on results of the Master's thesis [5]. It is included in this PhD thesis as it forms the basis of the PhD project and is presented here with slight modifications compared to [1] to adapt it to the flow of the thesis.
A quantisation of the full theory of general relativity is a highly complex task. In this thesis, we are mainly interested in scenarios that involve weak couplings between the matter system and the gravitational field, such as for instance the gravitational influence on neutrinos. Therefore, we will consider a linearisation of general relativity around a Minkowski spacetime and then work with a perturbation for the gravitational degrees of freedom using κ as an expansion parameter. Here we will focus on vacuum gravity using Ashtekar variables, analogous to the work in for instance [128] or [153]. We denote the linear perturbations with a prefix δ. The Ashtekar variables as well

as the Lagrange multipliers then become

$$E^a{}_i = \overline{E}^a_i + \kappa\,\delta E^a{}_i = \delta^a_i + \kappa\,\delta E^a{}_i \qquad \delta E : O(r^{-1}) \text{ even} \tag{6.12}$$

$$A_a{}^i = \overline{A}^i_a + \kappa\,\delta A_a{}^i = 0 + \kappa\,\delta A_a{}^i \qquad \delta A : O(r^{-2}) \text{ odd} \tag{6.13}$$

$$N = \overline{N} + \kappa\,\delta N = 1 + \kappa\,\delta N \qquad \delta N : O(r^{-1}) \tag{6.14}$$

$$N^a = \overline{N}^a + \kappa\,\delta N^a = 0 + \kappa\,\delta N^a \qquad \delta N^a : O(r^{-1}) \tag{6.15}$$

$$\Lambda^i = \overline{\Lambda}^i + \kappa\,\delta\Lambda^i = 0 + \kappa\,\delta\Lambda^i \qquad \delta\Lambda : O(r^{-2}) \text{ even}\,, \tag{6.16}$$

where the fall-off behaviour in the limit of spatial infinity of the first order perturbations has been chosen in accordance with the asymptotically flat boundary condition [148]. The split into background and perturbed quantities was made in a way such that the background corresponds to a Minkowski spacetime that remains unchanged by the action of the canonical Hamiltonian of the system, i.e.

$$\overline{\{E^a{}_i, \mathbf{H}_{can}\}} = 0 \tag{6.17}$$

$$\overline{\{A_a{}^i, \mathbf{H}_{can}\}} = 0\,, \tag{6.18}$$

where the overline stands for evaluation with respect to the background Minkowski spacetime. In the case of vacuum gravity (after computation of the Poisson brackets) this amounts to $\overline{E}^a_i = \delta^a_i$, $\overline{A}^i_a = 0$, $\overline{N} = 1$ and $\overline{N}^a = 0$. As one can easily compute, the spin connection vanishes in the background:

$$\begin{aligned}\Gamma_a{}^i &= \overline{\Gamma}^i_a + \kappa\,\delta\Gamma_a{}^i \approx 0 + \kappa\,\delta\Gamma_a{}^i \\ &= -\frac{\kappa}{2}\epsilon^{ijk}\delta^b_k\left[-\delta^l_a\delta^j_c\partial_b(\delta E^c{}_l) + \delta^j_c\delta^l_b\partial_a(\delta E^c{}_l) - \delta_{ac}\partial_b(\delta E^c{}_j) + \delta^j_a\delta^l_c\partial_b(\delta E^c{}_l)\right]\,.\end{aligned} \tag{6.19}$$

The Poisson algebra of the linearised gravitational variables can be inherited from (6.6):

$$\{\delta E^a{}_i(\vec{x},t), \delta E^b{}_j(\vec{y},t)\} = \{\delta A_a{}^i(\vec{x},t), \delta A_b{}^j(\vec{y},t)\} = 0\,, \qquad \{\delta A_a{}^i(\vec{x},t), \delta E^b{}_j(\vec{y},t)\} = \frac{\beta}{\kappa}\delta^b_a\delta^i_j\delta^3(\vec{x}-\vec{y})\,. \tag{6.20}$$

In the next subsection we will address how the matter contributions can be included consistently in the linearised framework.

6.3. Post-Minkowski approximation scheme

The content of this subsection was already published in [1] and is partially based on results of the Master's thesis [5]. It is included in this PhD thesis as it forms the basis of the PhD project and is presented here with slight modifications compared to [1] to adapt it to the flow of the thesis.
In the context of general relativistic perturbation theory, one usually chooses a background solution and then considers perturbations of the gravitational and matter sector around it assuming that the perturbations are small compared to the chosen background quantities. In this work we linearise around a flat Minkowski spacetime, which is a vacuum solution of general relativity. Hence, any considered perturbation in the matter sector will not be small compared to vanishing matter degrees of freedom in the vacuum case. However, we can formulate a model that involves the coupling between matter and linearised gravity in a Post-Minkowski approximation scheme.

For the model presented in this part of the thesis we will need to consider the zeroth and first order in the Post-Minkowski formalism only and this will be the underlying guiding principle of how the matter sector will be included into the Hamiltonian formulation and in particular into the constraints. We will briefly sketch the main steps that lead to the linearised action that we take as our starting point. The Post-Minkowski formalism is based on the Landau-Lifshitz formulation of general relativity, see for instance the book [130] for an introduction to the subject. One starts by introducing the so-called gothic metric defined as

$$\mathfrak{g}^{\mu\nu} := \sqrt{-\det(g_{\rho\sigma})}\, g^{\mu\nu}, \tag{6.21}$$

by means of which we can introduce the following tensor density

$$H^{\mu\nu\rho\sigma} := \mathfrak{g}^{\mu\rho}\mathfrak{g}^{\nu\sigma} - \mathfrak{g}^{\mu\sigma}\mathfrak{g}^{\nu\rho}\,, \tag{6.22}$$

where $H^{\mu\nu\rho\sigma}$ carries the same symmetries as the Riemann tensor. Following the presentation in [130] one can use (6.22) to rewrite Einstein's equations $G_{\mu\nu} = \kappa T_{\mu\nu}$ in the following form:

$$\partial_\nu\partial_\sigma H^{\mu\nu\rho\sigma} = 2\kappa(-\det(g))\,[T^{\mu\rho} + t^{\mu\rho}_{LL}]\ . \tag{6.23}$$

Here, $T^{\mu\rho}$ denotes the energy-momentum tensor of the matter degrees of freedom and $t^{\mu\rho}_{LL}$ is the so-called Landau-Lifshitz pseudotensor which consists of a sum of (contractions of) terms $\partial\mathfrak{g}\,\partial\mathfrak{g}$ and does not transform as a tensor under coordinate transformations. This quantity corresponds to the distribution of energy of the gravitational field in spacetime. If one aims at formulating the corresponding linearised theory, as a first step, one applies a partial gauge fixing on the gothic metric by the harmonic coordinate condition

$$\partial_\mu\mathfrak{g}^{\mu\nu} = 0\,. \tag{6.24}$$

For later convenience it is useful to introduce the following quantity also known as the metric potentials $\mathfrak{h}^{\mu\nu}$ that have the following relation to the gothic metric $\mathfrak{g}^{\mu\nu}$:

$$\mathfrak{g}^{\mu\nu} = \eta^{\mu\nu} - \mathfrak{h}^{\mu\nu}\,. \tag{6.25}$$

The harmonic coordinate condition then carries over to $\partial_\mu\mathfrak{h}^{\mu\nu} = 0$. In this gauge, Einstein's equations in (6.23) have the form, see e.g. equation (6.51) and (6.52) in [130]:

$$\Box\mathfrak{h}^{\mu\nu} = -2\kappa(-\det(g))\,[T^{\mu\nu}[\Phi, g] + t^{\mu\nu}_{LL}[\mathfrak{h}] + t^{\mu\nu}_{H}[\mathfrak{h}]]\,, \tag{6.26}$$

with the d'Alembertian $\Box$ in flat spacetime and

$$t^{\mu\nu}_{H}[\mathfrak{h}] := \frac{1}{2\kappa(-\det(g))}\,(\partial_\rho\mathfrak{h}^{\mu\sigma}\ \partial_\sigma\mathfrak{h}^{\nu\rho} - \mathfrak{h}^{\rho\sigma}\ \partial_\rho\partial_\sigma\mathfrak{h}^{\mu\nu})\ . \tag{6.27}$$

Among the individual contributions in (6.26) the energy-momentum tensor $T^{\mu\nu}$ depends on the matter variables here denoted by Φ and on the metric g, while the other two contributions depend on the modified gothic metric $\mathfrak{h}$ only[3]. The idea of the Post-Minkowski approximation scheme is to construct an iterative solution to (6.26). For this purpose one chooses that in lowest order the

[3]Later we consider a Klein-Gordon scalar field for the matter sector but here Φ is understood symbolically for all possible matter choices that one would like to couple in a given model

gothic metric agrees with the Minkowski metric and for higher orders considers an expansion of $\mathfrak{h}^{\mu\nu}$ in terms of powers of κ according to

$$\mathfrak{g}^{\mu\nu} = \eta^{\mu\nu} + \sum_{n=1}^{\infty} \kappa^n \, \mathfrak{h}^{\mu\nu}_{(n)} \, . \tag{6.28}$$

As in this part of the thesis we linearise our entire system around a flat Minkowski background and are therefore only interested in weak gravity, for the model under consideration here we can consider truncations of this perturbative expansion[4].
An iterative solution of Einstein's equations is constructed by the following procedure. Let us assume one has a solution for the potentials $\mathfrak{h}$ of order κ^k. Then one is able to compute the contributions of the quantities on the right hand side of (6.26) with it. Due to the prefactor κ, the right hand side will then be of order κ^{k+1}, so the entire equation will yield a solution for $\mathfrak{h}_{(k+1)}$. As can be seen from (6.28), the perturbative ansatz in the Post-Minkowski approximation scheme is constructed in a way that in the zeroth order where $\mathfrak{h} = 0$ one has $\mathfrak{g} = \eta$, from which one directly obtains $g = \eta$. With this, one can construct the right hand side of (6.26) using this zeroth order solution. As t_{LL} and t_H both contain $\mathfrak{h}$ in each summand, they vanish for $\mathfrak{h} = 0$ and the only non-trivial contribution comes from the energy-momentum tensor $T^{\mu\nu}$ on the right hand side. As in zeroth order $g = \eta$, it simplifies to the energy momentum tensor $T^{\mu\nu}$ on a flat Minkowski spacetime. Given the right hand side of (6.26), the left hand side amounts to the first order modified gothic metric, that is

$$\kappa \Box \mathfrak{h}^{\mu\nu}_{(1)} = -2\kappa T^{\mu\nu}[\Phi, \eta] \, . \tag{6.29}$$

Finally, one needs to relate $\mathfrak{h}^{\mu\nu}_{(1)}$ to the (inverse) metric perturbations $\delta h^{\mu\nu}$. Since in this work we are interested in the linearised theory only, we can use $g^{\mu\nu} = \eta^{\mu\nu} - \kappa \delta h^{\mu\nu} + O(\kappa^2)$ and obtain

$$\mathfrak{h}^{\mu\nu}_{(1)} = \delta h^{\mu\nu} - \frac{1}{2} \eta^{\mu\nu} \, \eta_{\rho\sigma} \delta h^{\rho\sigma} \, . \tag{6.30}$$

The last equation allows us to rewrite the linearised equations in a first order Minkowski approximation as

$$-\frac{\kappa}{2} \left(\Box(\delta h^{\mu\nu}) - \frac{1}{2} \eta^{\mu\nu} \, \eta_{\rho\sigma} \Box(\delta h^{\rho\sigma}) \right) = \kappa T^{\mu\nu}[\Phi, \eta] \, . \tag{6.31}$$

From (6.31) we can directly read off how the interaction term in the action needs to look like, namely

$$S_I = \frac{\kappa}{2} \int_M d^4x \; \delta h_{\mu\nu} T^{\mu\nu}[\Phi, \eta] \, . \tag{6.32}$$

The overall factor $\frac{\kappa}{2}$ takes into account that we start with an overall factor of $\frac{1}{2\kappa}$ and then consider linear perturbations of the metric $g_{\mu\nu} = \eta_{\mu\nu} + \kappa \delta h_{\mu\nu}$ yielding a factor κ^2 for second-order perturbations in the vacuum case. Note that, as expected, the same interaction contribution to the action can be obtained by minimally coupling matter to gravity and then linearising the metric degrees of freedom around a Minkowski spacetime [60–62, 154]. Let us denote the matter

[4] Note also the formal role of the expansion parameter κ that is further explained in box 6.4 in [130]: Depending on the chosen system of units, κ could also be equal to one.

Lagrangian density by $\mathcal{L}_\Phi$, then we have

$$\int_M d^4x\,\sqrt{-\det(g)}\,\mathcal{L}_\Phi \approx \int_M d^4x\,\mathcal{L}_\Phi|_{g=\eta} + \int_M d^4x\,(-\kappa\delta h^{\mu\nu})\left(\frac{\delta(\sqrt{-\det(g)}\,\mathcal{L}_\Phi)}{\delta g^{\mu\nu}}\right)\Big|_{g=\eta}$$
$$= S_\Phi^\eta + \frac{\kappa}{2}\int_M d^4x\,\delta h^{\mu\nu}T_{\mu\nu}[\Phi,\eta]\,, \tag{6.33}$$

where S_Φ^η denotes the matter action on flat spacetime. For the model discussed in this part of the thesis, we choose the matter Lagrangian of a Klein-Gordon scalar field

$$\mathcal{L}_\phi = -\frac{1}{2}g^{\mu\nu}D_\mu\phi D_\nu\phi - \frac{m^2}{2}\phi^2, \tag{6.34}$$

where D_μ denotes the torsion-free, covariant metric-compatible derivative with respect to g. Performing an ADM decomposition as we did for the vacuum case we end up with

$$S_\phi = \int dt\int_\sigma d^3x\left(\dot\phi\pi - \left[N^aC_a^\phi + NC^\phi\right]\right) \tag{6.35}$$

with

$$C_a^\phi := \pi\nabla_a\phi, \tag{6.36}$$
$$C^\phi := \frac{\pi^2}{2\sqrt{\det q}} + \frac{\sqrt{\det q}}{2}q^{ab}(\nabla_a\phi)(\nabla_b\phi) + \sqrt{\det q}\,\frac{m^2}{2}\phi^2\,, \tag{6.37}$$

where π denotes the canonically conjugate momentum associated to ϕ. If we linearise the model including the scalar field as discussed above and take into account all contributions up to first order in κ, we obtain the following constraints in the linearised theory:

$$\delta G_i = \frac{\kappa}{2\beta}\left(\partial_a(\delta E^a{}_i) + \epsilon_{ik}{}^l\delta_l^a\,\delta A_a{}^k\right), \tag{6.38}$$
$$\delta C_a = \frac{\kappa}{\beta}\delta_j^b\left(\partial_a(\delta A_b{}^j) - \partial_b(\delta A_a{}^j)\right) + \kappa\underbrace{\pi\,\partial_a\phi}_{=:p_a(\phi,\pi)}\,, \tag{6.39}$$
$$\delta C = \kappa\epsilon_j{}^{kl}\delta_k^a\delta_l^b\,\partial_a(\delta A_b{}^j) + \kappa\underbrace{\frac{1}{2}\left[\pi^2 + \partial_a\phi\,\partial^a\phi + m^2\phi^2\right]}_{=:\epsilon(\phi,\pi)}\,. \tag{6.40}$$

These constraints are also consistent with the 00 and $0a$ components of the linearised Einstein's equations that one obtains in the Post-Minkowski approximation scheme. Now these include gravitational- as well as matter contributions, where we introduced the momentum density $p_a(\phi,\pi)$ and the energy density $\epsilon(\phi,\pi)$ of the scalar field. Note that these constraints are abelian up to first order in κ. The corresponding background constraints of the zeroth order Post-Minkowski approximation scheme all vanish trivially, since $\overline{C} = \overline{C}^{geo} = 0, \overline{C}_a = \overline{C}_a^{geo} = 0$ and $\overline{G}_j = 0$. The action of the linearised theory is given by

$$S_{\rm lin} = \int dt\Bigg(\int_\sigma d^3x\left[\frac{\kappa}{\beta}\delta\dot A_a{}^i\delta E^a{}_i + \pi\dot\phi\right]$$
$$\underbrace{-\int_\sigma d^3x\left[\epsilon(\phi,\pi) + \delta N\delta C + \delta N^a\delta C_a + \delta\Lambda^i\delta G_i + \delta\mathcal{H}_I + \frac{1}{\kappa}\delta^2C^{geo}\right]}_{=\delta\mathbf{H}_{\rm can}}\Bigg) \tag{6.41}$$

with the interaction part $\delta\mathcal{H}_I := \frac{\kappa}{2}\delta h_{ab}T^{ab}$, where δh_{ab} is understood as a function of the densitised triads, and the second order of the geometrical Hamiltonian constraint $\delta^2 C^{geo}$. Note that the overall $\frac{1}{\kappa}$ in front of the geometrical term has partly been cancelled by the κ involved in the linearised quantities for N, N^a and Λ^i, while the constraints and the interaction term are still linear in κ. In the above form of the linearised action we have already made use of the fact that in the linearised framework with asymptotically flat boundary conditions the boundary term precisely cancels the first order of the (geometrical) Hamiltonian constraint in accordance with [151], i.e. $T = -\overline{N}\delta C^{geo} = -\delta C^{geo}$ where we used that $\overline{N} = 1$. Hence, neither the linearised Hamiltonian constraint with background lapse nor the boundary term do appear in the action and canonical Hamiltonian anymore.
The linearised total canonical Hamiltonian, which follows from (6.8), is given by:

$$\begin{aligned}\delta\mathbf{H}_{can} = \int_\sigma d^3x \Big[&\epsilon(\phi,\pi) + \kappa\,\delta N^a\,\pi\,\partial_a\phi + \kappa\,\delta N\,\epsilon(\phi,\pi) + \kappa\,(\partial_a\phi)\,(\partial^b\phi)\,\delta E^a{}_i\,\delta^i_b \\ &+ \frac{\kappa}{2}m^2\phi^2\,\delta E^a{}_i\,\delta^i_a - \frac{\kappa}{2}\delta E^a{}_i\,\delta^i_a\,\epsilon(\phi,\pi) + \frac{\kappa}{\beta}\delta N^a\,\delta^b_j\left(\partial_a(\delta A_b{}^j) - \partial_b(\delta A_a{}^j)\right) \\ &+ \frac{\kappa}{2\beta}\delta\Lambda^i\,\partial_a(\delta E^a{}_i) + \frac{\kappa}{2\beta}\delta\Lambda^i\,\epsilon_{ik}{}^l\,\delta^a_l\,\delta A_a{}^k - \kappa\,\epsilon_j{}^{kl}\,\delta^a_k\,\delta^b_l\,\delta A_b{}^j\,\partial_a(\delta N) \\ &- \frac{\kappa}{2\beta^2}\epsilon^{jkl}\epsilon_{jmn}\,\delta^a_k\,\delta^b_l\left(\delta A_a{}^m\delta A_b{}^n + (\beta^2+1)\delta\Gamma_a{}^m\delta\Gamma_b{}^n - 2\delta\Gamma_a{}^m\delta A_b{}^n\right)\Big]. \end{aligned} \tag{6.42}$$

Let us briefly comment on the individual contributions in different orders of κ. The κ^0-order encodes the equations of motion for the uncoupled system and environment. In our case these are the Klein-Gordon equation and the equations of motion for the background connection and densitised triad variables. Since the connection vanishes in the background and the triad is just given by $\overline{E}^a_i = \delta^a_i$ the corresponding equations of motion trivially vanish and this is again consistent with the vanishing of the background constraints that generate this trivial dynamics for the gravitational degrees of freedom. Note that the energy density of the scalar field $\epsilon(\phi,\pi)$ in κ^0-order is not part of the background constraints but just contributes to the non-vanishing part of the Hamiltonian in this order. Without the boundary term a further term that contributes to the κ^0 is the linearised Hamiltonian given by $\overline{N}\delta C^{\mathrm{geo}} = \overline{N}(\delta C - \kappa\epsilon)$. On the linearised phase space this term generates the background equations. If we compute the Poisson brackets of $\delta A_a{}^i, \delta E^a{}_i$ with $\overline{N}\delta C^{\mathrm{geo}}$ they both vanish for $\overline{N} = 1$ demonstrating again that the background equations are trivially fulfilled. In linear order in κ in the covariant case we obtain a part that is quadratic in the perturbations of all metric components. Here, this corresponds to the terms that are either quadratic in the linearised Ashtekar variables or involve them linearly together with the linearised lapse and shift variables. These terms together in $\delta\mathbf{H}_{\mathrm{can}}$ will generate the left hand side of all linearised Einstein's equations including the 00 and $0a$ component. The right hand side of the linearised Einstein's equations will be obtained from all contributions that involve gravitational as well as matter variables in the κ^1-order. These will be $\delta\mathcal{H}_I$ together with the parts where the matter variables occur in combination with the linearised lapse and shift.
As can easily be seen, most of the twenty phase space variables of the linearised theory,

$$(\phi,\pi) \qquad (\delta A_a{}^i, \delta E^b{}_j)\,, \tag{6.43}$$

are not observable, as they transform non-trivially under the linearised constraints. In the next section 7 we use the relational formalism to construct a set of independent gauge invariant quantities.

7. Construction of Dirac observables in the linearised model using geometrical clocks

The content of this section was already published in [1]. Here, it is presented with some modifications compared to [1] to adapt it to the flow of the thesis.
At this stage, we are working with a gauge theory which is to be quantised later. Then, the environmental degrees of freedom are traced out to obtain an effective reduced model for the scalar field system. Due to this, we need to take care of the gauge freedom involved in the theory. For this, one can either consider a specific gauge fixing or work at the gauge invariant level by formulating the model in terms of gauge invariant variables also known as Dirac observables in the context of general relativity. In this part of the thesis, we choose the latter strategy. Once the dynamics of the model is written by means of Dirac observables, the advantage is that it provides us with a way to split the total physical Hamiltonian, that generates the dynamics of the Dirac observables, into a system and environmental part, which we will take then as our starting point for the quantisation in section 8.

7.1. The relational formalism and the (dual) observable map

The content of this subsection was already published in [1]. Here, it is presented with some modifications compared to [1] to adapt it to the flow of the thesis.
As mentioned above, in a gauge theory we can either apply a specific gauge fixing or formulate the model in terms of gauge invariant quantities. In case we work at the level of perturbation theory, as done here, one often takes the approach that gauge invariance is guaranteed up to possible corrections that are of higher order in perturbation theory than one is truncating at. We will follow the same strategy here. To construct gauge invariant variables on the linearised phase space we consider the relational formalism [116–118] together with an observable map that maps the elementary variables of the linearised phase space to their corresponding gauge invariant quantities [119–121, 155]. The formalism is based on a choice of reference fields, one for each constraint in the system, and then the observable map returns for a given tensor field of certain rank on phase space its corresponding gauge invariant extension. Explicitly, it can be written as a power series in the reference fields weighted by contributions that involve nested Poisson brackets of the tensor fields and the constraints. The physical interpretation of these gauge invariant quantities, also known as Dirac observables in the framework of general relativity, is that they give the value of the tensor field at those values where the reference fields take specific values. For general relativity and its spatial diffeomorphism and Hamiltonian constraints this particularly means that we can formulate the dynamics of a given tensor field on phase space with respect to the reference fields and these provide a notion of physical spatial and temporal coordinates. The observable map introduced in [119–121] has the property that when applied to the chosen reference fields it maps them to phase space independent quantities and thus such a map can describe neither a canonical transformation on the full phase space one starts with nor a transformation that preserves the number of elementary phase space variables. For this reason we will slightly modify the map from [119–121] in two aspects. First we modify its action on reference fields and second we further introduce also the kind of dual version of this map to treat the choice of the reference fields and the constraints more on an equal footing, allowing to use the modified map to construct a canonical transformation for the variables $(\phi, \pi), (\delta A_a{}^i, \delta E^b{}_j)$. For the purpose of this work we can restrict our discussion to the linearised phase space. The transformation

that we aim at constructing will map the set of elementary variables $(\phi,\pi),(\delta A_a{}^i,\delta E^b{}_j)$ to a new set of canonical variables containing the Dirac observables associated with (ϕ,π), seven chosen reference fields that are canonically conjugate to the seven linearised constraints as well as two canonical pairs of further Dirac observables in the gravitational sector. Using this kind of canonical transformation for the elementary phase space variables, the physical phase space can be more easily accessed because the constraints as well as the reference fields are among the new canonical variables.

As we will discuss below for a modification of the observable maps in [119–121, 155] in our work here, we add a so called dual observable map and the combination of both allows us to construct the canonical transformation on the full phase space. Let us briefly introduce the observable map from [119–121, 155] as well as the dual one and then apply them to the model. We consider a system with a set of first class constraints $\{C_I\}$ and elementary phase space variables (q^A,p_A). Then we choose a set of reference variables $\{T^I\}$ that satisfy $\det(\{T^I,C_J\})\neq 0$ where we abbreviate $\{T^I,C_J\}:=M^I{}_J$. We can define an equivalent set of constraints given by

$$C'_I=\sum_J (M^{-1})^J{}_I C_J. \tag{7.1}$$

Then by construction we have that the constraints C'_I are weakly canonically conjugate to the T^I's. Given this, one further chooses a set of functions $\{\tau^I\}$ that can depend on the spatial and temporal coordinates by means of which one can construct an observable map which maps a function f on the phase space to its corresponding observable denoted by $\mathcal{O}_{f,\{T\}}$

$$\begin{aligned}\mathcal{O}_{f,\{T\}}(\tau^I) &= \Big[\exp(\xi^I\{C_I,\cdot\})\cdot f\Big]\Big|_{\xi^I:=T^I-\tau^I} \\ &= f+(T^I-\tau^I)\{C_I,f\}+\frac{1}{2!}(T^I-\tau^I)(T^J-\tau^J)\{C_J,\{C_I,f\}\}+\cdots,\end{aligned} \tag{7.2}$$

where the label $\{T\}$ refers to the chosen set of reference variables. The observable $\mathcal{O}_{f,\{T\}}(\tau^I)$ returns the value of f at those values where the reference variables T^I take the values τ^I. As can be shown [119, 121] we have $\{C_I,O_{f,T}\}\approx 0$ where $\approx$ denotes weak equivalence, that is on the constraint hypersurface defined by the C_I's and thus the $O_{f,\{T\}}$ are weak Dirac observables. In case the constraints C_I are already canonically conjugate to the T^I's then the $O_{f,\{T\}}$ are even strong Dirac observables and weak equalities are replaced by equality signs. Let us introduce $\mathcal{G}^I:=T^I-\tau^I$ that we can also understand as a choice of coordinate gauge fixing condition if we require $\mathcal{G}^I\approx 0$. Then (7.2) can be understood as a power series in the $\mathcal{G}^I$'s with nested Poisson brackets involving the constraints C_I that are in this case equal to the C'_I's. In case we have $\{T^I,C_J\}=\delta^I_J$, because the τ^I do not depend on phase space variables, we also obtain $\{\mathcal{G}^I,C_J\}=\delta^I_J$. Thus, the gauge fixing conditions and the constraints build canonically conjugate pairs. If this is the case, we can construct a dual version of the observable map in (7.2) where the role of the gauge fixing conditions and constraints are interchanged given by

$$\begin{aligned}\mathcal{O}^{dual}_{f,\{C\}} &= \Big[\exp(-\xi_I\{\mathcal{G}^I,\cdot\})\cdot f\Big]\Big|_{\xi_I:=C_I} \\ &= f-C_I\{\mathcal{G}^I,f\}+\frac{1}{2!}C_IC_J\{\mathcal{G}^J,\{f,\mathcal{G}^I\}\}\pm\cdots,\end{aligned} \tag{7.3}$$

where the label $\{C\}$ denotes that we have interchanged the role of gauge fixing conditions and the constraints for the dual map. This is also the reason for the additional factor of $(-1)^n$ compared to the observable map in (7.2). Note that this dual map does not depend on any functions

τ^I since the constraint hypersurface is defined by $C_I \approx 0$. Similar to $\mathcal{O}_{f,\{T\}}(\tau^I)$, which can be understood as a family of gauge invariant extensions of f parameterised by τ^I for $\mathcal{G}^I \neq 0$, the quantity $\mathcal{O}^{dual}_{f,\{C\}}$ is an extension from the $C_I \approx 0$ constraint hypersurface with the property that it commutes with all the $\mathcal{G}^I$ by construction.
Our strategy is to construct a canonical transformation to a new set of elementary variables. For this purpose, we apply a combination of the two observable maps yielding quantities that commute by construction with all constraints C_I and all $\mathcal{G}_I$'s. Hence, we can choose the set $(\mathcal{G}^I, C_I)$ as new canonical variables together with the number of independent Dirac observables obtained from the observable and its dual map associated with the set (q^I, p_I). How many independent such Dirac observables exist depends on the number of constraints.
Note that the introduction of the equivalent set of constraints in (7.1) is also called weak Abelianisation [119] and ensures that the corresponding Hamiltonian vector fields of the C_I's weakly commute. As a consequence, the order in which we apply the constraints C_I in the nested Poisson bracket is irrelevant. Now the situation relevant for us is that the constraints satisfy $\{T^I, C_J\} = \delta^I_J$ and thus the C_I's can be expressed linearly in the momenta conjugate to the T^I's. Using that the set $\{C_I\}$ is first class, this is sufficient to show that the constraints are abelian and hence their corresponding Hamiltonian vector fields commute and the order how we apply the C_I also does not matter in our case. However, if we consider the entire set $(\mathcal{G}^I, C_I)$ then the $\mathcal{G}^I$ and C_I do not commute, not even weakly and neither is the entire set first class and in general also the subset of the $\mathcal{G}^I$ is not abelian. This has the effect that the final observable that we obtain by applying the observable map in combination with its dual in general depends on the order in which we apply the two maps as well as the order in which the $\mathcal{G}^I$ occur in the nested Poisson brackets. This causes no problem for the model considered in this part of the thesis, it just means that there exist different choices of possible coordinate transformations on phase space, but important for us is rather that we can choose one among those.

7.2. The observable map in perturbation theory

The content of this subsection was already published in [1]. Here, it is presented with some modifications compared to [1] to adapt it to the flow of the thesis.
In the following we will generalise the observable map to the field theoretical setup and perturbation theory which can easily be done. In the context of perturbation theory it is sufficient to require gauge invariance or some specific form of the Poisson algebra up to corrections that are higher than the order that is considered in perturbation theory. This means we can truncate the power series for the map and its dual at some order in accordance with the desired order in perturbation theory that we consider for the linearised model. For instance if we want to compute Poisson brackets of observables up to linear order then we need to perturb both observables up to second order and collect all terms that contribute up to linear order to the final result. Such a perturbative approach for constructing observables has for instance also been used in [151, 156, 157]. Alternatively, if available, we can also take the result of the corresponding Poisson bracket in full general relativity and perturb it up to linear order. But since many quantities we work with will be known at the perturbative level only the latter option is often not possible.
The first step in the relational formalism consists of choosing suitable reference fields for the given set of constraints. In our case these will be the Hamiltonian, spatial diffeomorphism and Gauß constraint. If we are interested in results up to corrections of second order in the perturbations inside the Poisson brackets, we need to consider perturbations up to second order of these

constraints. The properties our chosen reference fields should have are:

(i) Each chosen reference field consists of linear perturbations of the elementary gravitational variables and its derivatives only. These are also known as linearised geometrical clocks.

(ii) Each chosen reference field is in lowest order canonically conjugated to one of the constraints.

(iii) Each reference field commutes in lowest order with all constraints except the one that it is in lowest order canonically conjugated to.

(iv) All reference fields mutually commute.

Let us introduce the notation

$$\delta\mathcal{C}_I(\vec{x},t) := (\delta C(\vec{x},t), \delta C_a(\vec{x},t), \delta G_i(\vec{x},t)), \quad \delta^2\mathcal{C}_I(\vec{x},t) := (\delta^2 C(\vec{x},t), \delta^2 C_a(\vec{x},t), \delta^2 G_i(\vec{x},t))$$

for the set of linearised constraints $\delta\mathcal{C}_I(\vec{x},t)$ and $\delta^2\mathcal{C}_I(\vec{x},t)$ for the set of second-order perturbations. For each of the individual constraints we have to choose one reference field and we introduce the following notation $\mathcal{G}^I(\vec{x},t)$ for this set with

$$\begin{aligned}
&\mathcal{G}^I(\vec{x},t) := (\delta\mathcal{G}(\vec{x},t), \delta\mathcal{G}^a(\vec{x},t), \delta\mathcal{G}^j(\vec{x},t))\\
&\delta\mathcal{G}(\vec{x},t) := \delta T(\vec{x},t) - \delta\tau(\vec{x},t), \quad \delta\mathcal{G}^a(\vec{x},t) := \delta T^a(\vec{x},t) - \delta\sigma^a(\vec{x},t),\\
&\delta\mathcal{G}^j(\vec{x},t) := \delta\Xi^j(\vec{x},t) - \delta\xi^j(\vec{x},t).
\end{aligned} \tag{7.4}$$

where $\delta T, \delta T^a, \delta\Xi^j$ are the individual reference fields for the Hamiltonian, spatial diffeomorphism and Gauß constraint respectively. We denote background quantities with a bar and assume that in the background the gauge fixing conditions as well as the constraints are satisfied, that is

$$\begin{aligned}
&\overline{\mathcal{G}}(\vec{x},t) := \overline{T}(\vec{x},t) - \overline{\tau}(\vec{x},t) = 0, \overline{C} = 0, \quad \overline{\mathcal{G}}^a(\vec{x},t) := \overline{T}^a(\vec{x},t) - \overline{\sigma}^a(\vec{x},t) = 0, \overline{C}_a = 0,\\
&\overline{\mathcal{G}}^j(\vec{x},t) := \overline{T}^j(\vec{x},t) - \overline{\xi}^j(\vec{x},t) = 0, \overline{G}_j = 0.
\end{aligned}$$

With the assumptions (i)-(iv) above we know that $\delta^2\mathcal{G}^I = 0$ and we further have

$$\begin{aligned}
\{\mathcal{G}^I(x), \mathcal{C}_J(y)\} :=& \quad \{\delta\mathcal{G}^I(x), \delta\mathcal{C}_J(y)\} + \{\delta\mathcal{G}^I(x), \delta^2\mathcal{C}_J(y)\} + O(\delta^2,\kappa^2)\\
=& \quad \tfrac{1}{\kappa}\delta^I_J\delta^3(\vec{x}-\vec{y}) + \{\delta\mathcal{G}^I(x), \delta^2\mathcal{C}_J(y)\} + O(\delta^2,\kappa^2),
\end{aligned} \tag{7.5}$$

where $O(\delta^2,\kappa^2)$ means that we neglect all terms that are second-order in the perturbations and/or of order κ^2 and the factor $\frac{1}{\kappa}$ has been chosen because it is also involved in the Poisson bracket of the elementary gravitational variables. This means there could be terms being of order κ^n with $n \leq 1$ that do not contribute because they involve second or higher orders of δ. That those terms can be present is caused by an asymmetry in δ and κ due to the fact that we only perturb the gravitational degrees of freedom but not the matter ones and further that the individual terms in the action involve different powers of κ from the beginning. We realise that the linearised constraints $\delta\mathcal{C}_I$ are canonically conjugated to the reference fields $\mathcal{G}^I$ but in general there can be a non-vanishing contribution in linear order coming from the Poisson bracket $\{\delta\mathcal{G}^I(x), \delta^2\mathcal{C}_J(y)\}$. To ensure that we have a vanishing contribution in linear order we will use the dual observable map as discussed below. For this purpose we need to adapt the observable map and its dual to

field theory and perturbation theory and for both maps we need the observable map up to second order. Taking this into account the observable formula up to second order reads

$$\begin{aligned}
&\mathcal{O}_{f,\{T\}}(\delta\tau,\delta\sigma^a,\delta\xi^j) = \delta f + \delta^2 f + \kappa \int_\sigma d^3y\; \delta\mathcal{G}^I(y)\{\delta\mathcal{C}_I(y),\delta f\} \\
&+\kappa \int_\sigma d^3y\; \delta^2\mathcal{G}^I(y)\{\delta\mathcal{C}_I(y),\delta f\} + \kappa \int_\sigma d^3y\; \delta\mathcal{G}^I(y)\Big(\{\delta^2\mathcal{C}_I(y),\delta f\} + \{\delta\mathcal{C}_I(y),\delta^2 f\}\Big) \\
&+\frac{\kappa^2}{2} \int_\sigma d^3y\; \delta\mathcal{G}^I(y) \int_\sigma d^3z\; \delta\mathcal{G}^J(z)\Big(\{\delta\mathcal{C}_J(z),\{\delta^2\mathcal{C}_I(y),\delta f\}\} + \{\delta\mathcal{C}_J(z),\{\delta\mathcal{C}_I(y),\delta^2 f\}\}\Big) \\
&+O(\delta^3,\kappa^3)\,,
\end{aligned} \tag{7.6}$$

where we used that $\overline{\mathcal{G}} = \overline{\mathcal{G}}^a = \overline{\mathcal{G}}^j = 0$ and allowed possible non-vanishing second-order perturbations of $\mathcal{G}^I$ that might be present if one wants to relax the assumptions (i)-(iv) from above. Because we consider perturbations around flat spacetime, in the background it holds that $\overline{C} = 0, \overline{C}_a = 0$ as well as $\overline{G}_i = 0$, all trivially vanish and hence we also have $\overline{\mathcal{G}} = 0, \overline{\mathcal{G}}^a = 0$ and $\overline{\mathcal{G}}^j = 0$. Therefore, for the background there is no gauge freedom we have to deal with and thus no corresponding observables to construct. Note that if we construct the observables for elementary phase space variables then $\delta^2 f = 0$ and the observable formula above simplifies. This construction of observables order by order in κ also plays a role when we consider the linearised Hamiltonian $\delta\mathbf{H}_{\text{can}}$ which, as can be seen from (6.42), has contributions in κ^0 and linear order in κ. The transformation behaviour under the linearised constraints of the matter variables can be found in the next section 7.4 in (7.14) and (7.18) and the results are an expression linear in κ. This again demonstrates that in the limit where κ is sent to zero, which corresponds to the situation that we consider a scalar field on Minkowski only with no coupling to linearised gravity, the elementary variables ϕ, π are suitable observables. Once we consider the coupling with linearised gravity perturbations, this is no longer the case and we need the gauge invariant version of these variables. For $\delta\mathbf{H}_{\text{can}}$ this means that in the κ^0 term we can still work with the original ϕ, π whereas for the linear order in κ we also need to construct Dirac observables for the matter sector, see for instance also the discussion in [154] in the context of the covariant theory. Note that as before, the linearised phase space in the Post-Minkowski approximation scheme involves the linear perturbations of the gravitational degrees of freedom as well as the variables (ϕ, π) for the matter sector. In a similar way we obtain the linearised dual observable map given by

$$\begin{aligned}
&\mathcal{O}^{dual}_{f,\{C\}} = \delta f + \delta^2 f - \kappa \int_\sigma d^3y\; \delta\mathcal{C}_I(y)\{\delta\mathcal{G}^I(y),\delta f\} \\
&-\kappa \int_\sigma d^3y\; \delta^2\mathcal{C}_I(y)\{\delta\mathcal{G}^I(y),\delta f\} - \kappa \int_\sigma d^3y\; \delta\mathcal{C}_I(y)\Big(\{\delta^2\mathcal{G}^I(y),\delta f\} + \{\delta\mathcal{G}^I(y),\delta^2 f\}\Big) \\
&+\frac{\kappa^2}{2} \int_\sigma d^3y\; \delta\mathcal{C}_I(y) \int_\sigma d^3z\; \delta\mathcal{C}_J(z)\Big(\{\delta\mathcal{G}^J(z),\{\delta^2\mathcal{G}^I(y),\delta f\}\} + \{\delta\mathcal{G}^J(z),\{\delta\mathcal{G}^I(y),\delta^2 f\}\}\Big) \\
&+O(\delta^3,\kappa^3)\,.
\end{aligned} \tag{7.7}$$

The alternating signs compared to the observable map in (7.2) are needed since the order of how the constraints and the reference fields enter into the Poisson bracket is switched. Note that if

we choose for instance $\mathcal{G}^I$ such that $\delta^2\mathcal{G}^I = 0$ and not the non-linear $\mathcal{C}_I$ but only the linearised parts as clocks, then we drop all terms that involve $\delta^2\mathcal{G}^I, \delta^2\mathcal{C}_I$ in the dual observable map (7.7) and this will be exactly the application we need later.

7.3. Overview of the strategy to construct Dirac observables

The content of this subsection was already published in [1]. Here, it is presented with some modifications compared to [1] to adapt it to the flow of the thesis.
After the introduction to the formalism used in this section for the construction of Dirac observables that encode the physical degrees of freedom, let us briefly sketch the strategy we follow in the next subsections, which can also be applied to a different choice of reference fields. We outline this directly for the case relevant here, namely perturbation theory up to linear order.

- First choose a set of linearised reference fields, that is $\delta^2\mathcal{G}^I = 0$, such that they form canonical pairs with the linearised constraints, that is $\{\delta\widetilde{\mathcal{G}}^I(x), \delta\mathcal{C}_J(y)\} = \delta^I_J\delta^{(3)}(x,y)$.
- In case not all reference fields and hence $\delta\widetilde{\mathcal{G}}^I(x)$ mutually commute, apply the dual observable map with the linearised constraints as clocks up to second order[5] to those that do not to obtain $\mathcal{G}^I$.
- Next apply the dual observable map up to second order neglecting the linear order to all constraints $\mathcal{C}_I$ to get the constraints $\mathcal{C}'_I$ that are abelian and canonically conjugate to the reference fields $\mathcal{G}^I$ up to corrections of second order.
- Define the observable map by means of the constraints $\mathcal{C}'_I$ using as reference fields $\mathcal{G}^I$.
- Choose next to $(\delta\mathcal{G}^I, \delta\mathcal{C}'_I)$ further independent phase space variables on the linearised phase space denoted by $(\delta q^I, \delta p_I)$.
- Apply the observable map to $(\delta q^I, \delta p_I)$ to obtain the physical gauge invariant degrees of freedom.
- Compute the algebra of the Dirac observables of $(\delta q^I, \delta p_I)$, for which relation (7.69) discussed below is helpful.
- If we further apply the dual observable map to these Dirac observables and they still satisfy the same Poisson algebra as their gauge variant counterparts, we can also say that given the set of variables $(\delta\mathcal{G}^I, \delta\mathcal{C}'_I, \delta q^I, \delta p_I)$ then applying the observable map and its dual to the entire set with the modification that we exclude the linear order in the observable map and its dual for the set $(\delta\mathcal{G}^I, \delta\mathcal{C}'_I)$ defines a canonical transformation on the entire phase space.

In our case the final application of the dual observable map on the variables $(\delta q^I, \delta p_I)$ corresponding to $\phi^{\mathrm{G}I}, \pi^{\mathrm{G}I}, \delta\mathcal{A}^i_a, \delta\mathcal{E}^a_i$ acts trivially since the original gauge variant quantities already commute with our chosen geometrical clocks. We expect that one can extend this strategy without any problems to higher orders in perturbation theory and for the aspect of constructing abelian constraints this has be done in [151]. How and if also the further steps can be generalised to higher order goes beyond the scope of this work and will be discussed more in detail elsewhere.

[5] Note that for this choice of clocks, since we apply it to the linearised clocks only, the linear terms in the power series will contribute.

7.4. Construction of reference fields

The content of this subsection was already published in [1]. Here, it is presented with some modifications compared to [1] to adapt it to the flow of the thesis.
As we will work with so-called geometrical clocks, in a first step we will choose the set of reference fields among the linearised elementary gravitational degrees of freedom. As a consequence, we will work with geometrical clocks for which $\delta^2\mathcal{G}^I = 0$ and hence they satisfy assumption (i) from section 7.2. To also fulfil (ii) we further choose $\mathcal{G}^I$ such that

$$\{\delta\mathcal{G}^I(x), \delta C_J(y)\} = \frac{1}{\kappa}\delta^I_J\delta^{(3)}(x,y),$$

where the factor $\frac{1}{\kappa}$ is chosen because it is also involved in Poisson bracket of the elementary geometrical variables. These requirements still allow several choices for suitable $\mathcal{G}^I$ and the specific choice for $\mathcal{G}^I$ taken here is motivated by the fact that we can relate the set of gauge invariant variables to a gauge fixing often chosen in the context of linearised gravity, as will be discussed in subsection 7.9. In order to construct suitable reference fields for the three sets of constraints involved in the system, we first analyse the gauge transformation they induce on the phase space variables and use them as building blocks for the construction of the reference fields. Defining the smeared linearised Gauß, Hamiltonian and spatial diffeomorphism constraints as

$$\delta G[\delta\Lambda](t) := \int_\sigma d^3y\ \delta\Lambda^i(\vec{x},t)\,\delta G_i(\vec{x},t) \tag{7.8}$$

$$\delta C[\delta N](t) := \int_\sigma d^3x\ \delta N(\vec{x},t)\,\delta C(\vec{x},t) \tag{7.9}$$

$$\overrightarrow{\delta C}[\overrightarrow{\delta N}](t) := \int_\sigma d^3x\ \delta N^a(\vec{x},t)\,\delta C_a(\vec{x},t) \tag{7.10}$$

one can evaluate the gauge transformations they infer on the phase space variables. As the Gauß constraint (6.38) does not contain matter degrees of freedom, it leaves the matter fields unchanged and just modifies the geometrical degrees of freedom:

$$\{\phi(\vec{x},t), \delta G[\delta\Lambda](t)\} = \{\pi(\vec{x},t), \delta G[\delta\Lambda](t)\} = 0 \tag{7.11}$$

$$\{\delta E^a{}_i(\vec{x},t), \delta G[\delta\Lambda](t)\} = \frac{1}{2}\epsilon^{ijk}\delta\Lambda_j(\vec{x},t)\,\delta^a_k \tag{7.12}$$

$$\{\delta A_a{}^i(\vec{x},t), \delta G[\delta\Lambda](t)\} = -\frac{1}{2}\partial_a(\delta\Lambda^i(\vec{x},t))\,. \tag{7.13}$$

For the Hamiltonian constraint (6.40) we find the following gauge transformations:

$$\{\phi(\vec{x},t), \delta C[\delta N](t)\} = \kappa\delta N(\vec{x},t)\,\pi(\vec{x},t) \tag{7.14}$$

$$\{\pi(\vec{x},t), \delta C[\delta N](t)\} = \kappa\partial_a\left[\delta N(\vec{x},t)\,\partial^a\phi(\vec{x},t)\right] - \kappa\delta N(\vec{x},t)\,m^2\,\phi(\vec{x},t) \tag{7.15}$$

$$\{\delta E^a{}_i(\vec{x},t), \delta C[\delta N](t)\} = -\beta\,\epsilon^{ijk}\,\delta^a_j\,\delta^b_k\,\partial_b(\delta N(\vec{x},t)) \tag{7.16}$$

$$\{\delta A_a{}^i(\vec{x},t), \delta C[\delta N](t)\} = 0\,. \tag{7.17}$$

Finally, the gauge transformations induced by the spatial diffeomorphism constraint (6.39) are

$$\{\phi(\vec{x},t),\overrightarrow{\delta C}[\overrightarrow{\delta N}](t)\} = \kappa\delta N^a(\vec{x},t)\,\partial_a\phi(\vec{x},t) \tag{7.18}$$

$$\{\pi(\vec{x},t),\overrightarrow{\delta C}[\overrightarrow{\delta N}](t)\} = \kappa\partial_a[\delta N^a(\vec{x},t)\,\pi(\vec{x},t)] \tag{7.19}$$

$$\{\delta E^a{}_i(\vec{x},t),\overrightarrow{\delta C}[\overrightarrow{\delta N}](t)\} = -\left(\delta^b_i\,\partial_b(\delta N^a(\vec{x},t)) - \delta^a_i\,\partial_b(\delta N^b(\vec{x},t))\right) \tag{7.20}$$

$$\{\delta A_a{}^i(\vec{x},t),\overrightarrow{\delta C}[\overrightarrow{\delta N}](t)\} = 0\,. \tag{7.21}$$

Using these, we now construct suitable reference fields for the system under consideration. Note that in [151] also geometrical clocks were used based on the ADM clocks introduced in [158] and [159]. This set of clocks is not equivalent to ours and when requiring that all clocks vanish this corresponds to a different gauge fixing, as is discussed in section 7.9.3.

7.4.1. Choice of the reference field for the linearised Gauß constraint

The content of this subsection was already published in [1]. Here, it is presented with some modifications compared to [1] to adapt it to the flow of the thesis.
As the choice of reference fields can be understood as gauge fixing constraints in a corresponding gauge fixed theory, we choose a reference field for the Gauß constraint that implements a Lorentz-like gauge condition analogous to [128] for the connection perturbation, i.e.

$$\partial^a(\delta A_a{}^i(\vec{x},t)) = 0\,. \tag{7.22}$$

Evaluation of the Poisson bracket between this condition and the Gauß constraint (6.38) using the linearised Poisson bracket (6.20) yields

$$\{\partial^a(\delta A_a{}^i(\vec{x},t)),\delta G_j(\vec{y},t)\} = -\frac{1}{2}\delta^i_j\Delta_{\vec{x}}\delta^3(\vec{x}-\vec{y})\,, \tag{7.23}$$

where $\Delta_{\vec{x}}$ denotes the Laplacian with respect to $\vec{x}$. We will drop the subscript if only one coordinate is involved. In order to have the commutation relation

$$\{\delta\Xi^i(\vec{x},t),\delta G_j(\vec{y},t)\} = \frac{1}{\kappa}\delta^i_j\delta^3(\vec{x}-\vec{y})\,, \tag{7.24}$$

we define the reference fields for the Gauß constraint as

$$\delta\Xi^i(\vec{x},t) := \frac{2}{\kappa}\partial^a\left(\delta A_a{}^i * G^\Delta\right)(\vec{x},t) = \frac{2}{\kappa}\int d^3y\;\partial^a_{\vec{x}}G^\Delta(\vec{x}-\vec{y})\,\delta A_a{}^i(\vec{y}) \tag{7.25}$$

with $\partial^a_{\vec{x}} := \frac{\partial}{\partial x_a}$. The abbreviation $G^\Delta(\vec{x}-\vec{y})$ denotes the Green's function of the Laplacian,

$$G^\Delta(\vec{x}-\vec{y}) = \int\frac{d^3k}{(2\pi)^3}\frac{1}{||\vec{k}||^2}e^{i\vec{k}(\vec{x}-\vec{y})}\,. \tag{7.26}$$

Due to the fact that the connection remains invariant under the Hamiltonian and spatial diffeomorphism constraint, this reference field also remains invariant under transformations induced by these two constraints.

7.4.2. Choice of the reference field for the linearised Hamiltonian constraint

The content of this subsection was already published in [1]. Here, it is presented with some modifications compared to [1] to adapt it to the flow of the thesis.
The Hamiltonian constraint leaves the connection invariant and only transforms a specific part of the densitised triad:

$$\{\epsilon_a{}^{cb}\delta^i_c\partial_b\delta E^a{}_i(\vec{x},t),\delta C(\vec{y},t)\} = 2\beta\Delta_{\vec{x}}\delta^3(\vec{x}-\vec{y})\,. \tag{7.27}$$

This suggests to define a reference field

$$\delta\widetilde{T}(\vec{x},t) := -\frac{1}{2\beta\kappa}\epsilon_a{}^{cb}\delta^i_c\partial_b\left(\delta E^a{}_i * G^\Delta\right)(\vec{x},t)\,. \tag{7.28}$$

However, in this form the reference field is not invariant under gauge transformations induced by the Gauß constraint:

$$\{\delta\widetilde{T}(\vec{x},t),\delta G_j(\vec{y},t)\} = -\frac{1}{2\beta\kappa}\delta^a_j\partial^{\vec{x}}_a G^\Delta(\vec{x}-\vec{y})\,, \tag{7.29}$$

where $\partial^{\vec{x}}_a$ denotes the partial derivative with respect to x^a. To cure this, we seek to subtract some combination of geometrical phase space variables that transforms precisely the same way as $\delta\widetilde{T}$ under the Gauß constraint and remains invariant under the Hamiltonian constraint. The latter is true for any combination of the connection variables, and it turns out that the trace of the connection solves the problem. Hence a good choice for a reference field corresponding to the Hamiltonian constraint is

$$\delta T(\vec{x},t) := -\frac{1}{\kappa\beta}\left[\frac{1}{2}\epsilon_a{}^{cb}\delta^i_c\partial_b\left(\delta E^a{}_i * G^\Delta\right)(\vec{x},t) + \delta^a_i\left(\delta A_a{}^i * G^\Delta\right)(\vec{x},t)\right]\,, \tag{7.30}$$

which also commutes with the spatial diffeomorphism constraint. Additionally, it commutes with the reference field for the Gauß constraint:

$$\{\delta T(\vec{x},t),\Xi^i(\vec{y},t)\} = 0\,. \tag{7.31}$$

7.4.3. Choice of the reference field for the linearised spatial diffeomorphism constraint

The content of this subsection was already published in [1]. Here, it is presented with some modifications compared to [1] to adapt it to the flow of the thesis.
In a last step we have to find a suitable reference field for the spatial diffeomorphism constraint. To fulfill the list of requirements in section 7.2, we construct it in several steps. In the end, the final reference field $\delta T^a(\vec{x},t)$ should

- consists of linearised elementary gravitational degrees of freedom only
- fulfill $\{\delta T^a(\vec{x},t),\delta C_b(\vec{y},t)\} = \frac{1}{\kappa}\delta^a_b\delta^3(\vec{x}-\vec{y})$,
- commute with the remaining linearised constraints and
- commute with the remaining reference fields.

For the first step it is helpful to realise from (7.20) that only the trace and one of the longitudinal parts of the densitised triad are modified by this constraint in the following manner:

$$\{\delta^i_c\partial^c\delta E^a{}_i(\vec{x},t),\delta C_b(\vec{y},t)\} = (\partial^a_{\vec{x}}\partial^{\vec{x}}_b - \delta^a_b\Delta_{\vec{x}})\delta^3(\vec{x}-\vec{y}) \tag{7.32}$$

$$\{\delta^i_a\delta E^a{}_i(\vec{x},t),\delta C_b(\vec{y},t)\} = 2\partial^{\vec{x}}_b\delta^3(\vec{x}-\vec{y})\,. \tag{7.33}$$

A suitable combination for a reference field that is canonically conjugated to the linearised spatial diffeomorphism constraint is therefore

$$\delta\widetilde{\widetilde{T}}^a(\vec{x},t) := \frac{1}{\kappa}\left(\delta^a_b\delta^i_c\partial^c - \frac{1}{2}\delta^i_b\partial^a\right)\left(\delta E^b{}_i * G^\Delta\right)(\vec{x},t)\,. \tag{7.34}$$

Unfortunately, this combination is not invariant under the linearised Gauß constraint:

$$\{\delta\widetilde{\widetilde{T}}^a(\vec{x},t),\delta G_j(\vec{y},t)\} = -\frac{1}{2\kappa}\epsilon_{cb}{}^a\delta^c_j\partial^b_{\vec{x}}G^\Delta(\vec{x}-\vec{y})\,. \tag{7.35}$$

To cure this, we can add a suitable form of

$$\partial_a\delta E^a{}_i(\vec{x},t)\,, \tag{7.36}$$

which is just a scalar density and therefore invariant under the linearised spatial diffeomorphism constraint. It turns out that

$$\delta\widetilde{T}^a(\vec{x},t) := \frac{1}{\kappa}\left(\delta^a_b\delta^i_c\partial^c - \frac{1}{2}\delta^i_b\partial^a + \delta^{ac}\delta^i_c\partial_b\right)\left(\delta E^b{}_i * G^\Delta\right)(\vec{x},t) \tag{7.37}$$

is invariant under the linearised Gauß constraint and still canonically conjugated to the linearised spatial diffeomorphism constraint. A quick calculation also shows that it is invariant under the gauge transformations generated by the linearised Hamiltonian constraint. Although the reference fields $\delta\widetilde{T}^a(\vec{x},t)$ mutually commute, they do not have vanishing Poisson brackets with all the remaining reference fields and violate assumption (iv). To obtain reference fields for the spatial diffeomorphism constraint we can employ the dual observables map for $\delta\widetilde{T}^a(\vec{x},t)$ yielding a quantity that by construction commutes with $\delta\mathcal{G}, \delta\mathcal{G}^a, \delta\mathcal{G}^j$ and hence with all reference fields. As clock for the dual observable map we choose the geometric part of the linearised Hamiltonian constraint, that is $\delta C - \kappa\epsilon$, because we want the final clock to depend on the geometrical degrees of freedom only, as well as the linearised Gauß constraint. Note that $\delta C - \kappa\epsilon \not\approx 0$ and as a consequence $\delta\widetilde{T}^a \not\approx \delta T^a$ but this causes no problems because two different choices of sets of clocks need not necessarily be weakly equivalent. Such that the observable formula can be applied we just need $\{\delta T^I, \delta\mathcal{C}_J\} = \{\delta\mathcal{G}^I, \delta\mathcal{C}_J\} = \delta^I_J$ which is satisfied also if we use the geometric contribution of δC only. For $\delta\widetilde{T}^a(\vec{x},t)$ the part corresponding to the spatial diffeomorphism constraint will not contribute in the dual observable map. Since we use the linearised constraint as the clock and not $\mathcal{C}_I$, we can drop all terms involving $\delta^2 C_I$. Using this together with $\delta^2\mathcal{G}^I = 0$ the dual observable map in (7.3) simplifies in this case to

$$\mathcal{O}^{dual}_{\delta\widetilde{T}^a,\{\delta C\}} =: \delta T^a = \delta\widetilde{T}^a - \kappa\int_\sigma d^3y\,(\delta C - \kappa\epsilon)(y)\{\delta T(y),\delta\widetilde{T}^a\} - \kappa\int_\sigma d^3y\,\delta G_j(y)\{\delta\Xi^j(y),\delta\widetilde{T}^a\}.$$

The explicit result we obtain has the form

$$\begin{aligned}\delta T^a(\vec{x},t) :=& \frac{1}{\kappa}\left(\delta^a_b\delta^i_c\partial^c - \frac{1}{2}\delta^i_b\partial^a + \delta^{ac}\delta^i_c\partial_b\right)\left(\delta E^b{}_i * G^\Delta\right)(\vec{x},t)\\ &+ \frac{2\beta}{\kappa^2}\left[\frac{1}{2}\delta^i_b\partial^a\partial^b\left(\delta G_i * G^{\Delta\Delta}\right)(\vec{x},t) - \delta^{ab}\delta^i_b\left(\delta G_i * G^\Delta\right)(\vec{x},t)\right]\\ &+ \frac{1}{2\kappa^2}\partial^a\left[(\delta C - \kappa\epsilon) * G^{\Delta\Delta}\right](\vec{x},t)\,,\end{aligned} \tag{7.38}$$

where $G^{\Delta\Delta}$ denotes the Green's function of the squared Laplacian, that is

$$G^{\Delta\Delta}(\vec{x}-\vec{y}) = \int \frac{d^3k}{(2\pi)^3}\frac{1}{||\vec{k}||^4}e^{i\vec{k}(\vec{x}-\vec{y})} = \int d^3z\, G^\Delta(\vec{x}-\vec{z})\, G^\Delta(\vec{y}-\vec{z})\,. \tag{7.39}$$

This reference field is defined on the entire phase space. On the constraint hypersurface, the additional constraint terms drop and we are left again with $\delta\widetilde{T}^a(\vec{x},t)$, which still commutes with the constraints in the desired way. This concludes the construction of the reference fields for the model under consideration.

7.5. An equivalent set of constraints

The content of this subsection was already published in [1]. Here, it is presented with some modifications compared to [1] to adapt it to the flow of the thesis.

Now we are in the situation, that the seven linearised constraints as well as the seven reference fields form in lowest order two abelian sub-algebras and further obey the following Poisson algebra:

$$\{\delta T(\vec{x},t),\delta C(\vec{y},t)\} = \frac{1}{\kappa}\delta(\vec{x}-\vec{y}) \qquad \{\delta T(\vec{x},t),\delta C_a(\vec{y},t)\} = 0 \qquad \{\delta T(\vec{x},t),\delta G_i(\vec{y},t)\} = 0 \tag{7.40}$$

$$\{\delta T^a(\vec{x},t),\delta C(\vec{y},t)\} = 0 \qquad \{\delta T^a(\vec{x},t),\delta C_b(\vec{y},t)\} = \frac{1}{\kappa}\delta^a_b\delta(\vec{x}-\vec{y}) \qquad \{\delta T^a(\vec{x},t),\delta G_i(\vec{y},t)\} = 0 \tag{7.41}$$

$$\{\delta \Xi^i(\vec{x},t),\delta C(\vec{y},t)\} = 0 \qquad \{\delta \Xi^i(\vec{x},t),\delta C_a(\vec{y},t)\} = 0 \qquad \{\delta \Xi^i(\vec{x},t),\delta G_j(\vec{y},t)\} = \frac{1}{\kappa}\delta^i_j\delta(\vec{x}-\vec{y})\,. \tag{7.42}$$

Since $\delta\mathcal{G}, \delta\mathcal{G}^c, \delta\mathcal{G}^j$ differ from $\delta T, \delta T^c, \delta\Xi^j$ by some phase space independent quantity only, we can replace the reference fields by the corresponding $\delta\mathcal{G}^I$s and the Poisson algebra above will not change. We have defined the Poisson algebra with a factor $\frac{1}{\kappa}$ because the gravitational degrees of freedom involve a similar factor. The reference fields have been defined such that the algebra of them and the linearised constraints no longer involves the Barbero-Immirzi parameter on the right hand side for the reason that κ is the parameter labelling the order of perturbations. Going back to the Poisson algebra of $\mathcal{G}^I$ and $\mathcal{C}_I$ in (7.5), so far we have chosen reference fields that satisfy this algebra. However, the in general non-vanishing contribution in linear order will prevent us from choosing $\mathcal{G}^I$ and $\mathcal{C}_J$ as new canonical coordinates. To achieve this we will apply the dual observable map to $\mathcal{C}_I$ and obtain an equivalent set of constraints $\mathcal{C}'_I$ satisfying

$$\{\mathcal{G}^I(x),\mathcal{C}'_J(y)\} = \{\delta\mathcal{G}^I(x),\delta\mathcal{C}'_J(y) + \delta^2\mathcal{C}'_J(y)\} = \frac{1}{\kappa}\delta^I_J\delta^{(3)}(x,y) + O(\delta^2,\kappa^2)\,. \tag{7.43}$$

With this algebra, we can then choose $\delta\mathcal{G}^I$ as new configuration variables and $\delta\mathcal{C}'_I$ as new momentum variables. Because in lowest order we already have the correct algebra relations, we only need a modification in the linear order. To accomplish this we apply the dual observable map to all $\mathcal{C}_I$ and drop the linear order terms. The latter would just abelianise the lowest order and cancel the $\mathcal{C}_I$ contribution in the observable which is something we do not want. The second order that we keep will then modify the linear order in a way that we obtain the algebra shown in (7.43). Since we want an equivalent set of constraints here we are forced to choose as clocks the linearised constraints $\delta\mathcal{C}_I$ involving also the matter contributions in δC and δC_a. Taking all this into account the equivalent constraints $\mathcal{C}'_I$ are given by

$$\begin{aligned}\mathcal{C}'_I :=& \mathcal{O}^{dual}_{\mathcal{C}_I,\{\delta C\}} = \delta\mathcal{C}_I + \delta^2\mathcal{C}_I - \kappa \int_\sigma d^3y\, \delta\mathcal{C}_I(y)\{\delta\mathcal{G}^I(y), \delta^2\mathcal{C}_I\} \\ &+ \frac{\kappa^2}{2}\int_\sigma d^3y\, \delta\mathcal{C}_J(y) \int_\sigma d^3z\, \delta\mathcal{C}_K(z)\{\delta\mathcal{G}_J(z), \{\delta\mathcal{G}_K(y), \delta^2\mathcal{C}_I\}\} + O(\delta^3, \kappa^3),\end{aligned} \tag{7.44}$$

where we used again that $\delta^2\mathcal{G}^I = 0$ in our case. Up to linear order we have $\delta\mathcal{C}'_I = \delta\mathcal{C}_I$ showing that as expected we have modified the constraint only in second order. This modifications become not relevant when we work with the constraints directly in the linearised theory since they are of second order but need to be considered when we compute Poisson brackets and want to consider the result up to linear order. For a set of mutually commuting reference fields, that we consider here, in a more general context it was proven in [151] that the constraints $\mathcal{C}'_I$ are abelian up to corrections of second order and applying this result here we have

$$\{\mathcal{C}'_I(x), \mathcal{C}'_J(y)\} = \{\delta\mathcal{C}'_I(x) + \delta^2\mathcal{C}'_I(x), \delta\mathcal{C}'_J(y) + \delta^2\mathcal{C}'_J(y)\} = 0 + O(\delta^2, \kappa^2)$$

and thus in the order of perturbation theory we consider here, we can treat them as abelian constraints. Because we can just consider higher orders in the dual observable map we can always ensure that the constraints are abelian up to a chosen order in perturbation theory and if the entire sum of the dual observable map converges even in the full unperturbed theory. Note that a similar result has already been discussed in [151] in the context of applying weak Abelianisation order by order in perturbation theory and afterwards modifying the constraints by terms that involve higher order powers of the linearised constraints. Here we can rediscover that case in the framework of the dual observable map which seems to us to be slightly more general because it cannot only be applied to the constraints as this corresponds to the case discussed in [151], but to any phase space function as we did for instance for the clock of the spatial diffeomorphism constraint before. Further, the strategy discussed in [151] separates weak Abelianisation and the addition of terms of higher order in the linearised constraints where this happens all at once here using the dual observable map from second order on.

7.6. Construction of the Dirac observables for the system under consideration

The content of this subsection was already published in [1]. Here, it is presented with some modifications compared to [1] to adapt it to the flow of the thesis.

Given the abelian constraints $\mathcal{C}'_I(x)$ discussed in the previous subsection, we can now use them in the observable map in (7.2) and construct gauge invariant quantities that commute by construction with the constraints $\mathcal{C}'_I(x)$ up to $O(\delta^2, \kappa^2)$ corrections. We want to apply the observable

map to the elementary phase space variables of the matter and gravitational degrees of freedom and use $\delta\mathcal{G}^I$ as our clocks. Therefore, we can drop all terms involving $\delta^2 f$ and $\delta^2\mathcal{G}^I$ and the observable map reduces to

$$\begin{aligned}(\delta f)^{GI}(\delta\tau,\delta\sigma^a,\delta\xi^j) &:= \mathcal{O}_{\delta f,\{\delta T\}}(\delta\tau,\delta\sigma^a,\delta\xi^j) \\ &= \mathcal{O}^{(1)}_{\delta f,\{\delta T\}}(\delta\tau,\delta\sigma^a,\delta\xi^j)+\mathcal{O}^{(2)}_{\delta f,\{\delta T\}}(\delta\tau,\delta\sigma^a,\delta\xi^j)+O(\delta^3,\kappa^3),\end{aligned} \tag{7.45}$$

where the label GI means gauge invariant with

$$\begin{aligned}\mathcal{O}^{(1)}_{\delta f,\{\delta T\}}(\delta\tau,\delta\sigma^a,\delta\xi^j) :=& \delta f+\kappa\int_\sigma d^3y\ \delta\mathcal{G}^I(y)\{\delta\mathcal{C}'_I(y),\delta f\} \\ \mathcal{O}^{(2)}_{\delta f,\{\delta T\}}(\delta\tau,\delta\sigma^a,\delta\xi^j) :=& \kappa\int_\sigma d^3y\ \delta\mathcal{G}^I(y)\{\delta^2\mathcal{C}'_I(y),\delta f\} \\ &+\frac{\kappa^2}{2}\int_\sigma d^3y\ \delta\mathcal{G}^I(y)\int_\sigma d^3z\ \delta\mathcal{G}^J(z)\Big(\{\delta\mathcal{C}'_J(z),\{\delta^2\mathcal{C}'_I(y),\delta f\}\}\Big),\end{aligned} \tag{7.46}$$

where $\mathcal{O}^{(1)}_{\delta f,\{\delta T\}}$ and $\mathcal{O}^{(2)}_{\delta f,\{\delta T\}}$ denote all contributions to the observable in linear and second order respectively. Since in this work we perturb the geometrical degrees of freedom only, for the matter sector we just replace δf by $f=\phi,\pi$ in the formula above. That this works so easily in the matter sector might not be obvious in the first place for the following reason: If we consider in $\mathcal{O}^{(1)}_{\delta f,\{\delta T\}}$ the second term, then for δf chosen from geometric degrees of freedom this will be of zeroth order and hence trivially commute with the linearised or higher order constraints. In contrast, for the matter variables the corresponding term still involves the matter variables linearly and hence does not commute with the linearised constraints or higher order ones and thus yields an additional contribution compared to the geometric case. However, since the Poisson brackets of the gravitational degrees of freedom involve a factor $\frac{1}{\kappa}$, whereas the Poisson brackets of the matter variables do not, these additional contributions come with an extra factor of κ. In the linearised theory we require for Dirac observables to commute with the constraints up to order δ and κ and hence these kind of contributions will only occur in higher orders in κ. A similar argument applies to these kind of additional contributions in $\mathcal{O}^{(2)}_{\delta f,\{\delta T\}}$ and therefore we can indeed apply the observable formula also to the matter variables. To obtain the explicit form of these Dirac

observables, we apply the observable map in (7.46) to $(\phi, \pi, \delta A_a{}^i, \delta E^a{}_i)$ and obtain

$$\begin{aligned}\phi^{GI}(\delta\sigma^c, \delta\tau, \delta\xi^j) &= \phi(\vec{x},t) - \kappa^2(\delta T(\vec{x},t) - \delta\tau(\vec{x},t))\pi(\vec{x},t) \\ &\quad - \kappa^2(\delta T^c(\vec{x},t) - \delta\sigma^c(\vec{x},t))\partial_c\phi(\vec{x},t) \\ &\quad + \mathcal{O}^{(2)}_{\phi,\{\delta T\}}(\delta\tau, \delta\sigma^a, \delta\xi^j) + O(\delta^3, \kappa^3),\end{aligned} \tag{7.47}$$

$$\begin{aligned}\pi^{GI}(\delta\sigma^c, \delta\tau, \delta\xi^j) &= \pi(\vec{x},t) - \kappa^2\partial_a[(\delta T(\vec{x},t) - \delta\tau(\vec{x},t))\partial^a\phi(\vec{x},t)] \\ &\quad - \kappa^2\partial_c[(\delta T^c(\vec{x},t) - \delta\sigma^c(\vec{x},t))\pi(\vec{x},t)] + \kappa^2(\delta T(\vec{x},t) - \delta\tau(\vec{x},t))\, m^2\phi(\vec{x},t) \\ &\quad + \mathcal{O}^{(2)}_{\pi,\{\delta T\}}(\delta\tau, \delta\sigma^a, \delta\xi^j) + O(\delta^3, \kappa^3),\end{aligned} \tag{7.48}$$

$$\begin{aligned}(\delta E^a{}_i)^{GI}(\delta\sigma^a, \delta\tau, \delta\xi^j) &= \delta E^a{}_i(\vec{x},t) - \kappa(\delta^a_i\partial_c - \delta^a_c\delta^b_i\partial_b)(\delta T^c(\vec{x},t) - \delta\sigma^c(\vec{x},t)) \\ &\quad + \kappa\beta\epsilon_c{}^{ab}\delta^c_i\partial_b(\delta T(\vec{x},t) - \delta\tau(\vec{x},t)) - \frac{\kappa}{2}\epsilon_{ij}{}^k\delta^a_k(\delta\Xi^j(\vec{x},t) - \delta\xi^j(\vec{x},t)) \\ &\quad + \mathcal{O}^{(2)}_{\delta E^a{}_i,\{\delta T\}}(\delta\tau, \delta\sigma^a, \delta\xi^j) + O(\delta^3, \kappa^2),\end{aligned} \tag{7.49}$$

$$\begin{aligned}(\delta A_a{}^i)^{GI}(\delta\sigma^a, \delta\tau, \delta\xi^j) &= \delta A_a{}^i(\vec{x},t) + \frac{\kappa}{2}\partial_a(\delta\Xi^i(\vec{x},t) - \delta\xi^i(\vec{x},t)) \\ &\quad + \mathcal{O}^{(2)}_{\delta A_a{}^i,\{\delta T\}}(\delta\tau, \delta\sigma^a, \delta\xi^j) + O(\delta^3, \kappa^2)\,,\end{aligned} \tag{7.50}$$

where we displayed only the linear order in explicit form and $(\delta\tau(\vec{x},t), \delta\sigma^c(\vec{x},t), \delta\xi^j(\vec{x},t))$ denote the spacetime functions corresponding to the reference fields $(\delta T, \delta T^c, \delta\Xi^j)$, see $\delta\mathcal{G}, \delta\mathcal{G}^c$ and $\delta\mathcal{G}^j$ in (7.4). The so constructed observables are Dirac observables for all values of the functions $(\delta\tau(\vec{x},t), \delta\sigma^c(\vec{x},t), \delta\xi^j(\vec{x},t))$ and thus each can be understood as a family of Dirac observables parameterised by $\delta\tau(\vec{x},t), \delta\sigma^c(\vec{x},t)$ and $\delta\xi^j(\vec{x},t)$ respectively. Now let us choose specific spacetime functions for $\delta\tau(\vec{x},t), \delta\sigma^c(\vec{x},t)$ and $\delta\xi^j(\vec{x},t)$. A specific choice for $\delta\tau(\vec{x},t), \delta\sigma^c(\vec{x},t)$ and $\delta\xi^j(\vec{x},t)$ can be obtained as follows: For the Gauß constraint we choose vanishing parameters $\delta\xi^j(\vec{x},t)$. The remaining parameters we associate with the temporal and spatial coordinates respectively. Taking into account that the full non-linear parameters τ and σ^c with $\tau = \overline{\tau} + \kappa\delta\tau + O(\kappa^2)$ and $\sigma^c = \overline{\sigma}^c + \kappa\delta\sigma^c + O(\kappa^2)$ should be set to t and x^c_σ respectively and that the clocks vanish in the background as well as for higher orders than the linear one, we only need to choose the linearised parameters $\delta\tau$ and $\delta\sigma^c$ yielding

$$\delta\tau(\vec{x},t) := \frac{t}{\kappa}, \quad \delta\sigma^c(\vec{x},t) := \frac{x^c_\sigma}{\kappa}, \quad \delta\xi^j(\vec{x},t) := 0, \tag{7.51}$$

with x^c_σ being the unique solution where $\delta T^c(\vec{x},t) = \frac{1}{\kappa}\sigma^c$ with $\sigma^c = \text{const}$. We reinsert these choices into $\delta\mathcal{G}, \delta\mathcal{G}^c$ and $\delta\mathcal{G}^j$, respectively, in (7.4). Then we can understand the Dirac observables as functions of $(\vec{x}_\sigma, t)$.

7.6.1. Derivation of the linear order

The content of this subsection was already published in [1]. Here, it is presented with some modifications compared to [1] to adapt it to the flow of the thesis.

In what follows, we derive the first order of the gravitational observables (7.49) and (7.50) explicitly. In order to do so, it turns out to be helpful to work in Fourier space. For these calculations we choose a certain complex basis in Fourier space, which is the same as in [128] consisting of

$$\hat{k}^a := \frac{k^a}{||\vec{k}||} \qquad m^a(\vec{k}) \qquad \overline{m}^a(\vec{k})\,, \tag{7.52}$$

where $\vec{k}$ is the momentum and we understand the plane perpendicular to it as a complex plane spanned by the two unit vectors $m^a(\vec{k})$ and $\overline{m}^a(\vec{k})$, where the bar denotes complex conjugation. This basis is orthonormal in the following manner:

$$\hat{k}^a\hat{k}_a = m^a(\vec{k})\overline{m}_a(\vec{k}) = \overline{m}^a(\vec{k})m_a(\vec{k}) = 1 \tag{7.53}$$

$$\hat{k}^a m_a(\vec{k}) = \hat{k}^a\overline{m}_a(\vec{k}) = m^a(\vec{k})m_a(\vec{k}) = \overline{m}^a(\vec{k})\overline{m}_a(\vec{k}) = 0\,. \tag{7.54}$$

The expansion of the metric in this basis is

$$q_{ab}(\vec{k}) = \hat{k}_a\hat{k}_b + m_a(\vec{k})\,\overline{m}_b(\vec{k}) + \overline{m}_a(\vec{k})\,m_b(\vec{k})\,, \tag{7.55}$$

the soldering form reads

$$\delta^i_a(\vec{k}) = \hat{k}_a\hat{k}^i + m_a(\vec{k})\,\overline{m}^i(\vec{k}) + \overline{m}_a(\vec{k})\,m^i(\vec{k})\,, \tag{7.56}$$

and we fix the orientation of the basis vectors in the complex plane relative to each other by imposing

$$\epsilon_{abc}\,\hat{k}^a\,m^b(\vec{k})\,\overline{m}^c(\vec{k}) = -i\,. \tag{7.57}$$

We additionally impose (see [5] section 5.3):

$$m^a(-\vec{k}) = \overline{m}^a(\vec{k})\,. \tag{7.58}$$

We expand the Fourier transform of the gravitational fields in this basis, following the notation in [128]:

$$\begin{aligned}\underset{\sim}{\delta E}^a{}_i(\vec{k}) =& \underset{\sim}{\delta E}^+(\vec{k})m^a(\vec{k})m_i(\vec{k}) + \underset{\sim}{\delta E}^-(\vec{k})\overline{m}^a(\vec{k})\overline{m}_i(\vec{k}) + \underset{\sim}{\delta E}^1(\vec{k})\hat{k}^a m_i(\vec{k}) + \underset{\sim}{\delta E}^{\overline{1}}(\vec{k})\hat{k}^a\overline{m}_i(\vec{k})\\ &+ \underset{\sim}{\delta E}^2(\vec{k})m^a(\vec{k})\hat{k}_i + \underset{\sim}{\delta E}^{\overline{2}}(\vec{k})\overline{m}^a(\vec{k})\hat{k}_i + \underset{\sim}{\delta E}^3(\vec{k})\hat{k}^a\hat{k}_i\\ &+ \underset{\sim}{\delta E}^4(\vec{k})m^a(\vec{k})\overline{m}_i(\vec{k}) + \underset{\sim}{\delta E}^5(\vec{k})\overline{m}^a(\vec{k})m_i(\vec{k})\end{aligned} \tag{7.59}$$

and

$$\begin{aligned}\underset{\sim}{\delta A}_a{}^i(\vec{k}) =& \underset{\sim}{\delta A}^+(\vec{k})m_a(\vec{k})m^i(\vec{k}) + \underset{\sim}{\delta A}^-(\vec{k})\overline{m}_a(\vec{k})\overline{m}^i(\vec{k}) + \underset{\sim}{\delta A}^1(\vec{k})\hat{k}_a m^i(\vec{k}) + \underset{\sim}{\delta A}^{\overline{1}}(\vec{k})\hat{k}_a\overline{m}^i(\vec{k})\\ &+ \underset{\sim}{\delta A}^2(\vec{k})m_a(\vec{k})\hat{k}^i + \underset{\sim}{\delta A}^{\overline{2}}(\vec{k})\overline{m}_a(\vec{k})\hat{k}^i + \underset{\sim}{\delta A}^3(\vec{k})\hat{k}_a\hat{k}^i\\ &+ \underset{\sim}{\delta A}^4(\vec{k})m_a(\vec{k})\overline{m}^i(\vec{k}) + \underset{\sim}{\delta A}^5(\vec{k})\overline{m}_a(\vec{k})m^i(\vec{k})\,.\end{aligned} \tag{7.60}$$

From this expansion it is evident that $\underset{\sim}{\delta A}^\pm$ and $\underset{\sim}{\delta E}^\pm$ encode the transverse traceless degrees of freedom with corresponding projectors

$$\underset{\sim}{P}^a{}_i{}^j{}_b(\vec{k}) := \overline{m}^a(\vec{k})\overline{m}_i(\vec{k})m^j(\vec{k})m_b(\vec{k}) + m^a(\vec{k})m_i(\vec{k})\overline{m}^j(\vec{k})\overline{m}_b(\vec{k}) \tag{7.61}$$

for $\underset{\sim}{\delta E}$ and $\underset{\sim}{P}_a{}^i{}_j{}^b(\vec{k}) := \delta_{ac}\delta^{il}\delta_{jm}\delta^{bd}\underset{\sim}{P}^c{}_l{}^m{}_d(\vec{k})$ for $\underset{\sim}{\delta A}$. Their position space version is given below in (7.67) and involves highly-nonlocal terms. Hence we set

$$\underset{\sim}{\delta\mathcal{E}}^a{}_i(\vec{k}) := \underset{\sim}{\delta E}^+(\vec{k})m^a(\vec{k})m_i(\vec{k}) + \underset{\sim}{\delta E}^-(\vec{k})\overline{m}^a(\vec{k})\overline{m}_i(\vec{k}) \tag{7.62}$$

$$\underset{\sim}{\delta\mathcal{A}}_a{}^i(\vec{k}) := \underset{\sim}{\delta A}^+(\vec{k})m_a(\vec{k})m^i(\vec{k}) + \underset{\sim}{\delta A}^-(\vec{k})\overline{m}_a(\vec{k})\overline{m}^i(\vec{k})\,. \tag{7.63}$$

The Dirac observables constructed in (7.49) and (7.50) can be expressed in terms of this basis up to linear order and read, where we drop the $\vec{k}$ dependency for better readability and already set $\delta\xi^j = 0$:

$$\begin{aligned}(\underset{\sim}{\delta E}^a{}_i)^{GI} =& \underset{\sim}{\delta\mathcal{E}}^a{}_i + \hat{k}^a m_i \left(\underset{\sim}{\delta E}^1 + \frac{1}{||\vec{k}||}\underset{\sim}{\delta A}^1\right) + \hat{k}^a \overline{m}_i \left(\underset{\sim}{\delta E}^{\overline{1}} - \frac{1}{||\vec{k}||}\underset{\sim}{\delta A}^{\overline{1}}\right) - m^a \hat{k}_i \frac{1}{||\vec{k}||}\underset{\sim}{\delta A}^2 \\ &+ \overline{m}^a \hat{k}_i \frac{1}{||\vec{k}||}\underset{\sim}{\delta A}^{\overline{2}} + \hat{k}^a \hat{k}_i \underset{\sim}{\delta E}^3 - m^a \overline{m}_i \frac{2}{||\vec{k}||}\underset{\sim}{\delta A}^4 + \overline{m}^a m_i \frac{2}{||\vec{k}||}\underset{\sim}{\delta A}^5 \\ &+ i\kappa \left(\delta^a_i k_c - \delta^a_c \delta^b_i k_b\right) \underset{\sim}{\delta\sigma}^c - i\beta\kappa\epsilon_c{}^{ab}\delta^c_i k_b \underset{\sim}{\delta\tau} + O(\delta^2, \kappa) \end{aligned} \tag{7.64}$$

$$(\underset{\sim}{\delta A}_a{}^i)^{GI} = \underset{\sim}{\delta\mathcal{A}}_a{}^i + \underset{\sim}{\delta A}^2 m_a \hat{k}^i + \underset{\sim}{\delta A}^{\overline{2}} \overline{m}_a \hat{k}^i + \underset{\sim}{\delta A}^4 m_a \overline{m}^i + \underset{\sim}{\delta A}^5 \overline{m}_a m^i + O(\delta^2, \kappa)\,. \tag{7.65}$$

We have that (ϕ^{GI}, π^{GI}) are already the independent Dirac observables in the matter sector. However, the 18 observables $(\delta A_a{}^i)^{GI}, (\delta E^a{}_i)^{GI}$ are not all independent, but only four of them are in total. From the explicit forms of $(\delta A_a{}^i)^{GI}$ and $(\delta E^a{}_i)^{GI}$ in Fourier space in (7.64) and (7.65) we realise that $\delta\tau$ and $\delta\sigma^c$ enter explicitly into these formulae. However, for the choice discussed here where $\delta\tau$ is linear in t and $\delta\sigma^c$ is constant the contributions both vanish because they come with spatial derivatives acting on δt and $\delta\sigma^c$. In case we choose $\delta\sigma^c$ linear in x^c then $(\delta E^a{}_i)^{GI}$ has an additional term involving a Kronecker delta that also survives when we express $(\delta E^a{}_i)^{GI}$ in terms of the independent gauge invariant degrees of freedom similar to what was observed in [158]. As a consequence, considering $(\delta E^a{}_i)^{GI}$ as an isolated quantity its fall-off behaviour gets modified and does no longer satisfy the requirement in (6.12). This however causes no issue because we need this quantity as an intermediate step only to reinsert it into the physical Hamiltonian. The final result of the physical Hamiltonian has a suitable fall-off behaviour because these critical terms are combined with scalar field contributions for which we assumed, as usually done, that the initial data has compact support, see also our discussion above (6.8). The four independent degrees of freedom in the gravitational sector are encoded in the symmetric[6] transverse-traceless part of the the variables $(\delta A_a{}^i)^{GI}, (\delta E^a{}_i)^{GI}$ and therefore the 4 independent Dirac observables in the gravitational sector are given by

$$\delta\mathcal{A}_a{}^i(\vec{x}_\sigma, t) := P_a{}^i{}_j{}^b (\delta A_b{}^j)^{GI}(\vec{x}_\sigma, t) \qquad \delta\mathcal{E}^a{}_i(\vec{x}_\sigma, t) := P^a{}_i{}^j{}_b (\delta E^b{}_j)^{GI}(\vec{x}_\sigma, t), \tag{7.66}$$

where $P_a{}^i{}_j{}^b$ and $P^a{}_i{}^j{}_b$ denote the projector on the transverse-traceless part in position space. Its explicit form is given by

$$\begin{aligned} P_a{}^i{}_j{}^b X(\vec{x}_\sigma, t) = \frac{1}{2}\Bigg\{ &\left[\delta_{aj}\delta^{bi} + \delta^b_a \delta^i_j - \delta^i_a \delta^b_j\right] X(\vec{x}_\sigma, t) + \partial_a \partial^i \partial_j \partial^b \left(X * G^{\Delta\Delta}\right)(\vec{x}_\sigma, t) \\ &+ \left[\delta_{aj}\partial^i\partial^b + \delta^{ib}\partial_a\partial_j + \delta^b_a \partial^i\partial_j + \delta^i_j \partial_a\partial^b - \delta^i_a \partial_j\partial^b - \delta^b_j \partial_a\partial^i\right] \left(X * G^{\Delta}\right)(\vec{x}_\sigma, t)\Bigg\}, \end{aligned} \tag{7.67}$$

where $\partial_i := \delta^c_i \partial_c$, $\partial^i := \delta^i_c \partial^c$, $\delta_{aj} := \delta_{ac}\delta^c_j$, and

$$P^a{}_i{}^j{}_b X(\vec{x}_\sigma, t) = \delta^{ac}\delta_{ik}\delta^{jm}\delta_{bd} P_c{}^k{}_m{}^d X(\vec{x}_\sigma, t)\,. \tag{7.68}$$

[6] If one considers the soldered version of the quantities, i.e. $\delta\mathcal{A}_{ab} := \delta\mathcal{A}_a{}^i \delta^c_i \delta_{cb}$ and analogously for $\delta\mathcal{E}^{ab} := \delta\mathcal{E}^a{}_i \delta^i_c \delta^{cb}$.

As expected, these projectors are non-local in position space but local in momentum space, as can be seen in (7.61). A comparison between the local projector in position space also often used in the literature in the context of the transverse-traceless gauge has been analysed in [160].
From now on we will drop the label σ at $\vec{x}_\sigma$ and by an abuse of notation denote it by $\vec{x}$ again and always keep in mind that these x^a coordinates are related to values that the reference field T^a takes. By construction the Dirac observables Poisson commute with all constraints $\mathcal{C}'_I$. Since the set $\mathcal{C}'_I$ is weakly equivalent to the set $\mathcal{C}_I$ the Dirac observables are weak Dirac observables with respect to $\mathcal{C}_I$ where the weak equivalence refers to the constraint hypersurface defined by the linearised constraints $\delta\mathcal{C}_I$ that, as discussed above, agree with $\delta C'_I$.

7.6.2. Algebra of the Dirac observables

The content of this subsection was already published in [1]. Here, it is presented with some modifications compared to [1] to adapt it to the flow of the thesis.
What still remains to be discussed is the algebra of the independent Dirac observables. For this purpose we will consider the relation between the algebra of Dirac observables and the observable associated to the corresponding Dirac bracket. As proven in theorem 2.2 in [155], see also [119] for an alternative proof, in general we have

$$\{O_{f,\{T\}}, O_{g,\{T\}}\} \approx O_{\{f,g\}^*,\{T\}}$$

where $\{f,g\}^*$ denotes the Dirac bracket associated with the total set $(\mathcal{G}^I, \mathcal{C}_J)$, that, when requiring $\mathcal{G}^I$ to be gauge fixing conditions, is a second class system of constraints for which a Dirac bracket can be constructed. If we have such a relation also at the perturbative level then it provides an efficient way to compute the observable algebra because if we are interested in the algebra up to linear order then we can just expand the observable on the right hand side up to linear order whereas we need to consider the observables up to second order on the left hand side. In the following we will not consider the most general case here but just discuss the necessary result we need for the model derived in this work.
As proven in Appendix A under the assumption that we have linearised clocks, that is $\mathcal{G}^I = \delta\mathcal{G}^I$ with $\delta^k\mathcal{G}^I = 0$ for all $k \geq 2$ and we consider observables of quantities $f = \delta f$ for which $\delta^k f = 0$ with $k \geq 2$, one can show that

$$\left\{O^{(1)}_{\delta f,\{\delta T\}} + O^{(2)}_{\delta f,\{\delta T\}}\,,\, O^{(1)}_{\delta g,\{\delta T\}} + O^{(2)}_{\delta g,\{\delta T\}}\right\} = \{\delta f, \delta g\}^* + O^{(1)}_{\{\delta f,\delta g\}^*,\{\delta T\}} + O(\delta^2, \kappa^2), \qquad (7.69)$$

where the Dirac bracket $\{\delta f, \delta g\}^*$ corresponds to the set $(\mathcal{G}^I = \delta\mathcal{G}^I, \mathcal{C}'_I = \mathcal{C}'^{(1)}_I + \mathcal{C}'^{(2)}_I)$. Again as above, because we do not perturb the matter degrees of freedom, we can apply the same result here if we replace δf by f again with $f = \phi, \pi$. As discussed in Appendix A, the case interesting for us is when f, g are the elementary phase space variables of the linearised theory. Given this and using that for the reference fields we have $\mathcal{G}^I = \delta\mathcal{G}^I$ as well as $\{\mathcal{G}^I(x), \mathcal{C}'_J(y)\} = \frac{1}{\kappa}\delta^I_J\delta^{(3)}(x,y) + O(\delta^2, \kappa^2)$

the explicit form of the Dirac bracket up to linear order reads

$$\begin{aligned}\{\delta f(x),\delta g(y)\}^* :=&\{\delta f(x),\delta g(y)\} - \kappa\int\limits_\sigma d^3z\{\delta f(x),\delta\mathcal{C}'_L(z)\}\delta^L_M\{\delta\mathcal{G}^M(z),\delta g(y)\}\\ &-\kappa\int\limits_\sigma d^3z\{\delta f(x),\delta^2\mathcal{C}'_L(z)\}\delta^L_M\{\delta\mathcal{G}^M(z),\delta g(y)\}\\ &+\kappa\int\limits_\sigma d^3z\{\delta g(x),\delta\mathcal{C}'_L(z)\}\delta^L_M\{\delta\mathcal{G}^M(z),\delta f(y)\}\\ &+\kappa\int\limits_\sigma d^3z\{\delta g(x),\delta^2\mathcal{C}'_L(z)\}\delta^L_M\{\delta\mathcal{G}^M(z),\delta f(y)\}+O(\delta^2,\kappa^2)\,. \end{aligned}\tag{7.70}$$

Now for δf and δg, that have the property that they commute with all $\delta\mathcal{G}^I$, the Dirac bracket reduces to the ordinary Poisson bracket. If δf and δg are further elementary phase space variables that satisfy standard canonical Poisson brackets, then their Poisson bracket is phase space independent and as a consequence, the Dirac observable of the Dirac bracket has only a zeroth order contributions that agrees with the original Poisson bracket. In the case considered here, the variables $(\phi,\pi),(\delta\mathcal{A}_a{}^i,\delta\mathcal{E}^a{}_i)$ all commute with the clocks δT^I which is equivalent to them commuting with all $\delta\mathcal{G}^I$. This can be seen in the following way: First, we note that the clocks being geometrical ones do not contain any matter variables and also the additional contributions from the dual observable map involved in the diffeomorphism clock contains the geometric degrees of freedom only. Hence, all clocks trivially commute with the matter fields (ϕ,π). To see that they also commute with the variables $(P_a{}^i_j{}^b(\delta A_b{}^j), P^a{}_i{}^j{}_b(\delta E^b{}_j))$, it is convenient to express them in Fourier space. This can be found in section 7.7 and one can see that all clocks are independent of $\delta\underset{\frown}{A}^\pm$ and $\delta\underset{\frown}{E}^\pm$. As the latter are the transverse-traceless degrees of freedom and these are elementary phase space variables, they have vanishing Poisson brackets with all remaining degrees of freedom and therefore also commute with all clocks.
Thus, for this set of variables the Dirac bracket agrees with the original Poisson bracket. Consequently, we can immediately conclude that the non-vanishing Poisson brackets of the set of Dirac observables $\phi^{GI},\pi^{GI},\delta\mathcal{A}_a{}^i,\delta\mathcal{E}^a{}_i$ read

$$\{\phi^{GI}(\vec{x},t),\pi^{GI}(\vec{y},t)\} = \delta(\vec{x}-\vec{y})+O(\delta^2,\kappa^2),\tag{7.71}$$

$$\{\delta\mathcal{A}_a{}^i(\vec{x},t),\delta\mathcal{E}^b{}_j(\vec{y},t)\} = \frac{\beta}{\kappa}P_a{}^i_j{}^b\delta(\vec{x}-\vec{y})+O(\delta^2,\kappa^2).\tag{7.72}$$

All remaining ones vanish up to corrections of order $O(\delta^2,\kappa^2)$. The matter variables satisfy the same Poisson algebra as their gauge variant counter parts and for the geometric gauge invariant degrees of freedom the Poisson bracket also involves on the right hand side the expected projector on the transverse and traceless part.

7.7. Canonical transformation

The content of this subsection was already published in [1]. Here, it is presented with some modifications compared to [1] to adapt it to the flow of the thesis.
Considering the algebra of the Dirac observables in (7.71) and (7.72) together with the Poisson algebra of the $\mathcal{G}^I$ and $\mathcal{C}'_I$ in (7.43), one can perform a canonical transformation from the set of variables

$$(\phi,\pi),\quad (\delta A_a{}^i,\delta E^a{}_i)$$

to the new set of variables

$$(\delta\mathcal{G}, C'), \quad (\delta\mathcal{G}^a, C'_a), \quad (\delta\mathcal{G}^j, G'_j), \quad (\phi^{GI}, \pi^{GI}), \quad (\delta\mathcal{A}_a{}^i, \delta\mathcal{E}^a{}_i)$$

with

$$\delta\mathcal{G} = \delta T - t, \quad \delta\mathcal{G}^a = \delta T^a - x^a_\sigma, \quad \delta\mathcal{G}^j = \delta\Xi^j. \tag{7.73}$$

As discussed in the seminal work in [158], one can reformulate the corresponding forms of the geometric clocks so that they no longer explicitly involve the coordinates. This is possible here because the way the geometric clocks are defined is non-local due to the Green's function involved in the position space representation. The equivalent local conditions are obtained by applying the Laplacian, which has the consequence that neither t nor x^a are explicitly involved any more. It are also these local quantities that are involved in the perturbed quantities, and therefore the use of such geometric clocks does not contradict the requirement that the perturbations be small. The reason is that these coordinate conditions only set certain components of the metric perturbations and their conjugate momenta to zero, see also the more detailed discussion in [158] and references therein.

Because the definition of $\mathcal{C}'_I$ involves second-order contributions, as can be seen from (7.44), in order to implement this canonical transformation on the linearised phase space we restrict $\mathcal{C}'_I$ to its linear part and, using that in our case $\delta\mathcal{C}'_I = \delta\mathcal{C}_I$, the new set of canonical variables on the linearised phase space is given by

$$(\delta\mathcal{G}, \delta C), \quad (\delta\mathcal{G}^a, \delta C_a), \quad (\delta\mathcal{G}^j, \delta G_j), \quad (\phi^{GI}, \pi^{GI}), \quad (\delta\mathcal{A}_a{}^i, \delta\mathcal{E}^a{}_i)\,. \tag{7.74}$$

To derive the explicit form of the canonical transformation, we first transform the clocks and constraints into momentum space using the basis introduced above in section 7.6.1 and end up with the following expressions:

$$\underset{\smile}{\delta\mathcal{G}} = \frac{1}{2\beta\kappa||\vec{k}||}(\underset{\smile}{\delta E^5} - \underset{\smile}{\delta E^4}) - \frac{1}{\beta\kappa||\vec{k}||^2}(\underset{\smile}{\delta A^3} + \underset{\smile}{\delta A^4} + \underset{\smile}{\delta A^5}) - \underset{\smile}{\delta\tau} \tag{7.75}$$

$$\underset{\smile}{\delta C} = \kappa||\vec{k}||(\underset{\smile}{\delta A^4} - \underset{\smile}{\delta A^5}) + \kappa\,\underset{\smile}{\epsilon} \tag{7.76}$$

$$m_a\underset{\smile}{\delta\mathcal{G}^a} = \frac{i}{\kappa||\vec{k}||}(\underset{\smile}{\delta E^{\overline{1}}} + \underset{\smile}{\delta E^{\overline{2}}}) - \frac{2\beta}{\kappa^2||\vec{k}||^2}m^i\underset{\smile}{\delta G_i} - m_a\underset{\smile}{\delta\sigma^a} \tag{7.77}$$

$$\overline{m}_a\underset{\smile}{\delta\mathcal{G}^a} = \frac{i}{\kappa||\vec{k}||}(\underset{\smile}{\delta E^1} + \underset{\smile}{\delta E^2}) - \frac{2\beta}{\kappa^2||\vec{k}||^2}\overline{m}^i\underset{\smile}{\delta G_i} - \overline{m}_a\underset{\smile}{\delta\sigma^a} \tag{7.78}$$

$$\hat{k}_a\underset{\smile}{\delta\mathcal{G}^a} = \frac{i}{2\kappa||\vec{k}||}(3\underset{\smile}{\delta E^3} - \underset{\smile}{\delta E^4} - \underset{\smile}{\delta E^5}) - \frac{3\beta}{\kappa^2||\vec{k}||^2}\hat{k}^i\underset{\smile}{\delta G_i} + \frac{i}{2\kappa||\vec{k}||^3}\left(\frac{1}{\kappa}\underset{\smile}{\delta C} - \underset{\smile}{\epsilon}\right) - \hat{k}_a\underset{\smile}{\delta\sigma^a} \tag{7.79}$$

$$m^a\underset{\smile}{\delta C_a} = -\frac{i\kappa||\vec{k}||}{\beta}\underset{\smile}{\delta A^{\overline{2}}} + \kappa m^a\,\underset{\smile}{p_a} \tag{7.80}$$

$$\overline{m}^a\underset{\smile}{\delta C_a} = -\frac{i\kappa||\vec{k}||}{\beta}\underset{\smile}{\delta A^2} + \kappa\overline{m}^a\,\underset{\smile}{p_a} \tag{7.81}$$

$$\hat{k}^a\underset{\smile}{\delta C_a} = \frac{i\kappa||\vec{k}||}{\beta}(\underset{\smile}{\delta A^4} + \underset{\smile}{\delta A^5}) + \kappa\hat{k}^a\,\underset{\smile}{p_a} \tag{7.82}$$

$$m^i\underset{\smile}{\delta G_i} = \frac{\kappa i}{2\beta}(||\vec{k}||\underset{\smile}{\delta E^{\overline{1}}} - \underset{\smile}{\delta A^{\overline{1}}} + \underset{\smile}{\delta A^{\overline{2}}}) \tag{7.83}$$

$$\overline{m}^i \delta\underset{\smile}{G}_i = \frac{\kappa i}{2\beta}(||\vec{k}||\delta\underset{\smile}{E}^1 - \delta\underset{\smile}{A}^2 + \delta\underset{\smile}{A}^1) \tag{7.84}$$

$$\hat{k}^i \delta\underset{\smile}{G}_i = \frac{\kappa i}{2\beta}(||\vec{k}||\delta\underset{\smile}{E}^3 - \delta\underset{\smile}{A}^5 + \delta\underset{\smile}{A}^4) \tag{7.85}$$

$$m_i \delta\underset{\smile}{\mathcal{G}}^i = \frac{2i}{\kappa||\vec{k}||}\delta\underset{\smile}{A}^{\overline{1}} - m_i \delta\underset{\smile}{\xi}^i \tag{7.86}$$

$$\overline{m}_i \delta\underset{\smile}{\mathcal{G}}^i = \frac{2i}{\kappa||\vec{k}||}\delta\underset{\smile}{A}^1 - \overline{m}_i \delta\underset{\smile}{\xi}^i \tag{7.87}$$

$$\hat{k}_i \delta\underset{\smile}{\mathcal{G}}^i = \frac{2i}{\kappa||\vec{k}||}\delta\underset{\smile}{A}^3 - \hat{k}_i \delta\underset{\smile}{\xi}^i \,. \tag{7.88}$$

In total, these are 14 equations that can be solved uniquely for the 14 old variables. The solution then is

$$\delta\underset{\smile}{A}^1 = -\frac{i\kappa||\vec{k}||}{2}\overline{m}_i \left[\delta\underset{\smile}{\mathcal{G}}^i + \delta\underset{\smile}{\xi}^i\right] \tag{7.89}$$

$$\delta\underset{\smile}{A}^{\overline{1}} = -\frac{i\kappa||\vec{k}||}{2} m_i \left[\delta\underset{\smile}{\mathcal{G}}^i + \delta\underset{\smile}{\xi}^i\right] \tag{7.90}$$

$$\delta\underset{\smile}{A}^2 = \frac{i\beta}{||\vec{k}||}\overline{m}^a \left(\frac{1}{\kappa}\delta\underset{\smile}{C}_a - \underset{\smile}{p}_a\right) \tag{7.91}$$

$$\delta\underset{\smile}{A}^{\overline{2}} = \frac{i\beta}{||\vec{k}||} m^a \left(\frac{1}{\kappa}\delta\underset{\smile}{C}_a - \underset{\smile}{p}_a\right) \tag{7.92}$$

$$\delta\underset{\smile}{A}^3 = -\frac{i\kappa||\vec{k}||}{2}\hat{k}_i \left[\delta\underset{\smile}{\mathcal{G}}^i + \delta\underset{\smile}{\xi}^i\right] \tag{7.93}$$

$$\delta\underset{\smile}{A}^4 = -\frac{i\beta}{2||\vec{k}||}\hat{k}^a \left(\frac{1}{\kappa}\delta\underset{\smile}{C}_a - \underset{\smile}{p}_a\right) + \frac{1}{2||\vec{k}||}\left(\frac{1}{\kappa}\delta\underset{\smile}{C} - \underset{\smile}{\epsilon}\right) \tag{7.94}$$

$$\delta\underset{\smile}{A}^5 = -\frac{i\beta}{2||\vec{k}||}\hat{k}^a \left(\frac{1}{\kappa}\delta\underset{\smile}{C}_a - \underset{\smile}{p}_a\right) - \frac{1}{2||\vec{k}||}\left(\frac{1}{\kappa}\delta\underset{\smile}{C} - \underset{\smile}{\epsilon}\right) \tag{7.95}$$

$$\delta\underset{\smile}{E}^1 = -\frac{2i\beta}{\kappa||\vec{k}||}\overline{m}^i \delta\underset{\smile}{G}_i + \frac{i\beta}{||\vec{k}||^2}\overline{m}^a \left(\frac{1}{\kappa}\delta\underset{\smile}{C}_a - \underset{\smile}{p}_a\right) + \frac{i\kappa}{2}\overline{m}^i \left[\delta\underset{\smile}{\mathcal{G}}_i + \delta\underset{\smile}{\xi}_i\right] \tag{7.96}$$

$$\delta\underset{\smile}{E}^{\overline{1}} = -\frac{2i\beta}{\kappa||\vec{k}||} m^i \delta\underset{\smile}{G}_i - \frac{i\beta}{||\vec{k}||^2} m^a \left(\frac{1}{\kappa}\delta\underset{\smile}{C}_a - \underset{\smile}{p}_a\right) - \frac{i\kappa}{2} m^i \left[\delta\underset{\smile}{\mathcal{G}}_i + \delta\underset{\smile}{\xi}_i\right] \tag{7.97}$$

$$\delta\underset{\smile}{E}^2 = -i\kappa||\vec{k}||\overline{m}_a \left[\delta\underset{\smile}{\mathcal{G}}^a + \delta\underset{\smile}{\sigma}^a\right] - \frac{i\kappa}{2}\overline{m}_i \left[\delta\underset{\smile}{\mathcal{G}}^i + \delta\underset{\smile}{\xi}^i\right] - \frac{\beta i}{||\vec{k}||^2}\overline{m}_a \left(\frac{1}{\kappa}\delta\underset{\smile}{C}^a - \underset{\smile}{p}^a\right) \tag{7.98}$$

$$\delta\underset{\smile}{E}^{\overline{2}} = -i\kappa||\vec{k}||m_a \left[\delta\underset{\smile}{\mathcal{G}}^a + \delta\underset{\smile}{\sigma}^a\right] + \frac{i\kappa}{2} m_i \left[\delta\underset{\smile}{\mathcal{G}}^i + \delta\underset{\smile}{\xi}^i\right] + \frac{\beta i}{||\vec{k}||^2} m_a \left(\frac{1}{\kappa}\delta\underset{\smile}{C}_a - \underset{\smile}{p}^a\right) \tag{7.99}$$

$$\delta\underset{\smile}{E}^3 = -\frac{2i\beta}{\kappa||\vec{k}||}\hat{k}^i \delta\underset{\smile}{G}_i - \frac{1}{||\vec{k}||^2}\left(\frac{1}{\kappa}\delta\underset{\smile}{C} - \underset{\smile}{\epsilon}\right) \tag{7.100}$$

$$\begin{aligned}\delta\underset{\smile}{E}^4 = -\kappa\beta||\vec{k}||\left[\delta\underset{\smile}{\mathcal{G}} + \delta\underset{\smile}{\tau}\right] + i\kappa||\vec{k}||\hat{k}^a \left[\delta\underset{\smile}{\mathcal{G}}_a + \delta\underset{\smile}{\sigma}_a\right] - \frac{1}{||\vec{k}||^2}\left(\frac{1}{\kappa}\delta\underset{\smile}{C} - \underset{\smile}{\epsilon}\right) + \frac{i\kappa}{2}\hat{k}^i \left[\delta\underset{\smile}{\mathcal{G}}_i + \delta\underset{\smile}{\xi}^i\right] \\ + \frac{i\beta}{||\vec{k}||^2}\hat{k}^a \left(\frac{1}{\kappa}\delta\underset{\smile}{C}_a - \underset{\smile}{p}_a\right)\end{aligned} \tag{7.101}$$

$$\underset{\smile}{\delta E}^5 = \kappa\beta||\vec{k}||\left[\underset{\smile}{\delta\mathcal{G}} + \underset{\smile}{\delta\tau}\right] + i\kappa||\vec{k}||\hat{k}^a\left[\underset{\smile}{\delta\mathcal{G}_a} + \underset{\smile}{\delta\sigma_a}\right] - \frac{1}{||\vec{k}||^2}\left(\frac{1}{\kappa}\underset{\smile}{\delta C} - \underset{\smile}{\epsilon}\right) - \frac{i\kappa}{2}\hat{k}^i\left[\underset{\smile}{\delta\mathcal{G}_i} + \underset{\smile}{\delta\xi^i}\right] - \frac{i\beta}{||\vec{k}||^2}\hat{k}^a\left(\frac{1}{\kappa}\underset{\smile}{\delta C_a} - \underset{\smile}{p_a}\right). \tag{7.102}$$

All the appearing matter degrees of freedom must be substituted by their gauge invariant extensions plus the corresponding correction terms, what can be read off from (7.47) and (7.48), from which we obtain up to first order in κ:

$$\phi(\vec{x},t) = \phi^{GI}(\delta\sigma^c,\delta\tau,\delta\xi^j) + \kappa^2(\delta T(\vec{x},t) - \delta\tau(\vec{x},t))\pi(\vec{x},t) + \kappa^2(\delta T^c(\vec{x},t) - \delta\sigma^c(\vec{x},t))\partial_c\phi(\vec{x},t) \tag{7.103}$$

$$\pi(\vec{x},t) = \pi^{GI}(\delta\sigma^c,\delta\tau,\delta\xi^j) + \kappa^2\partial_a[(\delta T(\vec{x},t) - \delta\tau(\vec{x},t))\partial^a\phi(\vec{x},t)] + \kappa^2\partial_c[(\delta T^c(\vec{x},t) - \delta\sigma^c(\vec{x},t))\pi(\vec{x},t)] - \kappa^2(\delta T(\vec{x},t) - \delta\tau(\vec{x},t))\, m^2\phi(\vec{x},t)\,. \tag{7.104}$$

Note that when considering terms where any of the gravitational variables $\underset{\smile}{\delta A}$ or $\underset{\smile}{\delta E}$ appear with a prefactor κ, then we can drop all the correction terms of order κ in (7.103) and (7.104) as they would then lead to terms of order κ^2.
An advantage of this new set of elementary phase space variables (7.74) is that it allows to clearly separate the physical degrees of freedom from the remaining gauge degrees of freedom at the level of the full phase space. The physical phase space corresponds to the subspace involving the subalgebra of all Dirac observables $(\phi^{GI},\pi^{GI}),(\delta\mathcal{A}_a{}^i,\delta\mathcal{E}^a{}_i)$ including the expected six physical degrees of freedom. The price to pay in this context is that, as far as the position space is considered, we need to work with highly non-local clocks that become local in momentum space. This is not unexpected here considering the fact that the projector to the transverse-traceless part of the gravitational perturbations is local in momentum but non-local in position space[7].

7.8. Dynamics of the Dirac observables

The content of this subsection was already published in [1]. Here, it is presented with some modifications compared to [1] to adapt it to the flow of the thesis.
In this subsection, we discuss the dynamics of our constructed Dirac observables. This is the last ingredient missing in order to take the gauge invariant formulation as the starting point for the quantisation in section 8. As we know from full general relativity, the dynamics of Dirac observables cannot be generated by the canonical Hamiltonian because by construction, all Dirac observables commute with the constraints and $\mathbf{H}_{\rm can}$ is just a linear combination of the smeared constraints. The generator of the dynamics of the Dirac observables is the so-called physical Hamiltonian [155]. If we rewrite the Hamiltonian constraint linearly in the clock momentum of the temporal reference field, that is $C = P_T + h$, then the physical Hamiltonian corresponds to the Dirac observable associated with the phase space function h. Here we need to adapt this to the framework of perturbation theory and consider the fact that in addition we have an interaction Hamiltonian as well as a non-vanishing Hamiltonian in κ^0 order. The perturbed Hamiltonian constraint up to second order is given by $C = \delta C + \delta^2 C^{\rm geo} + O(\delta^2,\kappa^2)$. The reference field δT is canonically conjugate to the linearised Hamiltonian constraint δC and

[7] In [160] it is discussed that there are situations particularly in the case of sources where a replacement of the non-local projector in position space by the also widely used local projector can yield different physical effects.

thus we can identify δC with the momentum variable conjugate to δT that we denote by δP_T, then we have[8] $C = \delta P_T + \delta^2 C^{\text{geo}} + O(\delta^2, \kappa^2)$. The Dirac observable associated with $\delta^2 C^{\text{geo}}$ corresponds to that part of the physical Hamiltonian that is generating the dynamics of the purely gravitational physical degrees of freedom. The Dirac observable corresponding to the interaction Hamiltonian $\mathcal{H}_I = \frac{\kappa}{2}\delta h_{ab} T^{ab}$ with $\delta h_{ab} = -\delta^i_b \delta_{ac} \delta E^c{}_i - \delta^i_a \delta_{bc} \delta E^c{}_i + \delta_{ab} \delta^i_c \delta E^c{}_i$ encodes the interaction between the matter and gravitational physical degrees of freedom. As we will see below when expressed in terms of the independent Dirac observables it decomposes into a term where the physical triad variables $\delta\mathcal{E}^a{}_i$ couple to the physical matter variables as well as a self-interaction term that involves a coupling between the physical matter variables only. Finally, in κ^0-order the physical Hamiltonian involves the matter Hamiltonian for the scalar field on Minkowski spacetime. Summarising the above discussion and denoting the physical Hamiltonian of the model considered in this work by $\delta\mathbf{H}$, it takes the following form:

$$\delta\mathbf{H} = \mathcal{H}_\phi + O_{\mathcal{H}_{\text{geo}},\{T\}} + O_{\mathcal{H}_I,\{T\}} \quad \text{with} \quad \mathcal{H}_\phi := \int_\sigma d^3x\, \epsilon(\vec{x}, t), \quad \mathcal{H}_{\text{geo}} := \int_\sigma d^3x\, \delta^2 C^{\text{geo}}(x)\,. \tag{7.105}$$

As can be seen below in (7.113), it can be written entirely in terms of the Dirac observables (ϕ^{GI}, π^{GI}), $(\delta\mathcal{A}_a{}^i, \delta\mathcal{E}^a{}_i)$ and therefore is by construction gauge invariant up to corrections of order $O(\delta^2, \kappa^2)$. Here, as discussed above, we insert the Dirac observables in all terms being linearly in κ but keep ϕ, π in the κ^0 contribution because at zeroth order ϕ, π are suitable observables. Because in second-order perturbation theory the constraints $\mathcal{C}'_I$ are only weakly equivalent to the original constraints $\mathcal{C}_I$ and the observable of the interaction Hamiltonian $\mathcal{H}_I$ is linear in the perturbations, we need to consider the Dirac observable of $\delta E^a{}_i$ up to second order in $\mathcal{H}_I$ when computing Poisson brackets with the constraints. Hence, as far as the set of original constraints $\mathcal{C}_I$ is considered, $\delta\mathbf{H}$ is a weak Dirac observable.

In the following, we explicitly derive the physical Hamiltonian $\delta\mathbf{H}$. Using the canonical transformation derived in the previous subsection, it is possible to express the canonical Hamiltonian $\delta\mathbf{H}_{\text{can}}$ in (6.42) in terms of the new phase space variables consisting of the physical gauge invariant degrees of freedom, the constraints and the clocks. In a first step we rewrite the Hamiltonian in the following way:

$$\begin{aligned}\delta\mathbf{H}_{\text{can}} = \int_\sigma d^3x \Big[& \epsilon(\phi,\pi) + \delta N^a\, \delta C_a + \delta N\, \delta C + \delta\Lambda^i\, \delta G_i \\ & + \kappa\, (\partial_a \phi)\, (\partial^b \phi)\, \delta E^a{}_i\, \delta^i_b + \frac{\kappa}{2} m^2 \phi^2\, \delta E^a{}_i\, \delta^i_a - \frac{\kappa}{2} \delta E^a{}_i\, \delta^i_a\, \epsilon(\phi,\pi) + \\ & - \frac{\kappa}{2\beta^2} \epsilon^{jkl} \epsilon_{jmn}\, \delta^a_k\, \delta^b_l \left(\delta A_a{}^m \delta A_b{}^n + (\beta^2+1) \delta\Gamma_a{}^m \delta\Gamma_b{}^n - 2\delta\Gamma_a{}^m \delta A_b{}^n \right) \Big], \end{aligned} \tag{7.106}$$

where in the first line there is the background matter Hamiltonian and the constraints, in the second line the interaction part and in the last line the second order of the Hamilton constraint. The first line contains the background Hamiltonian of the scalar field, which does not need to be transformed as there are no background constraints and hence it is already gauge invariant, see discussion above. In order to obtain the physical Hamiltonian as described in (7.105) in terms of the new variables, one first has to determine the observables (7.64) and (7.65) in terms of the

[8] Note that the boundary term $T[N]$ in δH_{can} cancels exactly the contribution $\overline{N}\delta C = \delta C$ in δH_{can} but since the clock momentum $\delta P_T = \delta C$ is anyway not part of the physical Hamiltonian this causes no problems.

new variables, where we already set $\delta\xi^j = 0$ as explained above in (7.51):

$$\begin{aligned}(\delta\underset{\smile}{E}^a{}_i)^{GI} =& \delta\underset{\smile}{\mathcal{E}}^a{}_i - \frac{2i\beta}{\kappa||\vec{k}||}\hat{k}^a\delta\underset{\smile}{G}_i + \frac{\beta}{\kappa||\vec{k}||^2}\epsilon^{ba}{}_i\left[\delta\underset{\smile}{C}_b - \kappa\underset{\smile}{p}_b\right] - \frac{1}{\kappa||\vec{k}||^2}\delta^a_i\left[\delta\underset{\smile}{C} - \kappa\underset{\smile}{\epsilon}\right] \\ & - i\kappa||\vec{k}||\delta\underset{\smile}{\sigma}^b\left(\delta^a_b\hat{k}_i - \delta^a_i\hat{k}_b\right) - \kappa||\vec{k}||\beta\delta\underset{\smile}{\tau}i\hat{k}_c\epsilon_i{}^{ac} + O(\delta^3,\kappa^2) \qquad (7.107)\\ (\delta\underset{\smile}{A}_a{}^i)^{GI} =& \delta\underset{\smile}{\mathcal{A}}_a{}^i + \frac{i\beta}{2\kappa||\vec{k}||}(2\hat{k}_i\delta^{ab} - \hat{k}^b\delta^a_i - \hat{k}^i\hat{k}_a\hat{k}^b)\left[\delta\underset{\smile}{C}_b - \kappa\underset{\smile}{p}_b\right] \\ & - \frac{1}{2\kappa||\vec{k}||}i\epsilon_{ba}{}^i\hat{k}^b\left[\delta\underset{\smile}{C} - \kappa\underset{\smile}{\epsilon}\right] + O(\delta^3,\kappa^2)\,. \qquad (7.108)\end{aligned}$$

The interaction part in (7.105), $O_{\mathcal{H}_I,\{T\}}$, then assumes the following form:

$$\begin{aligned}O_{\mathcal{H}_I,\{T\}} =& \kappa\int d^3k\ \underset{\smile}{\varphi}{}^b_a\ \delta\underset{\smile}{\mathcal{E}}'^a{}_i\delta^i_b + \kappa\int d^3k ik_b\delta\underset{\smile}{\sigma}'^a\left[\underset{\smile}{\varphi}{}^b_a - \delta^b_a\left(\underset{\smile}{\varphi}{}^c_c + m^2\underset{\smile}{\widetilde{V}} - \underset{\smile}{\epsilon}\right)\right] \\ & + \int\frac{d^3k}{||\vec{k}||^2}\left(-\left[\underset{\smile}{\varphi}{}^a_a + \frac{3}{2}m^2\underset{\smile}{\widetilde{V}} - \frac{3}{2}\underset{\smile}{\epsilon}\right]\left(\delta\underset{\smile}{C}' - \kappa\underset{\smile}{\epsilon}{}'\right)\right. \\ & \left. + 2i\beta k^a\delta\underset{\smile}{G}'_i\left[\underset{\smile}{\varphi}{}^b_a\delta^i_b + \left(\frac{1}{2}m^2\underset{\smile}{\widetilde{V}} - \frac{1}{2}\underset{\smile}{\epsilon}\right)\delta^i_a\right]\right) + O(\delta^3,\kappa^2) \qquad (7.109)\end{aligned}$$

with

$$\begin{aligned}\epsilon(\vec{x},t) &:= \epsilon(\phi^{GI}(\vec{x},t),\pi^{GI}(\vec{x},t)), & p_a(\vec{x},t) &:= p_a(\phi^{GI}(\vec{x},t),\pi^{GI}(\vec{x},t)),\\ \widetilde{V}(\vec{x},t) &:= \phi^{GI}(\vec{x},t)^2, & \varphi^b_a(\vec{x},t) &:= (\partial_a\phi^{GI}(\vec{x},t))(\partial^b\phi^{GI}(\vec{x},t))\,. \qquad (7.110)\end{aligned}$$

Note that an underbow denotes the spatial Fourier transform of the corresponding quantity, i.e.

$$\underset{\smile}{f}(\vec{k},t) := \frac{1}{(2\pi)^{\frac{3}{2}}}\int_{\mathbb{R}^3} d^3x\ e^{-i\vec{k}\vec{x}}f(\vec{x},t), \qquad \hat{k}^a := \frac{1}{||\vec{k}||}k^a.$$

We used here a shortened notation to improve readability where no argument means dependency on $(\vec{k},t)$ and a prime after a quantity means dependency on $(-\vec{k},t)$. The last line in (7.106)

yields $O_{\mathcal{H}_{geo},\{T\}}$:

$$
\begin{aligned}
O_{\mathcal{H}_{\text{geo}},\{T\}} =& \frac{\kappa}{2\beta^2}\int d^3k \sum_{r\in\{\pm\}} \left[\underset{\sim}{\delta A}^r \underset{\sim}{\delta A}'^r + ||\vec{k}||^2(\beta^2+1)\underset{\sim}{\delta E}^r \underset{\sim}{\delta E}'^r + 2r||\vec{k}||\underset{\sim}{\delta E}^r \underset{\sim}{\delta A}'^r\right] \\
&- \kappa\int \frac{d^3k}{||\vec{k}||^2}\Big\{ -\left(\frac{1}{\kappa}\underset{\sim}{\delta C}_a - \underset{\sim}{p}_a\right)\left(\frac{1}{\kappa}\underset{\sim}{\delta C}'_b - \underset{\sim}{p}'_b\right)(\delta^{ab} - \frac{1}{4}\hat{k}^a\hat{k}^b) \\
&\qquad + \frac{1}{4}\left(\frac{1}{\kappa}\underset{\sim}{\delta C} - \underset{\sim}{\epsilon}\right)\left(\frac{1}{\kappa}\underset{\sim}{\delta C}' - \underset{\sim}{\epsilon}'\right)\Big\} \\
&- \kappa\int d^3k\ \underset{\sim}{\delta G}_i\left[\frac{\beta^2+1}{\kappa^2}\hat{k}^i\hat{k}^j\ \underset{\sim}{\delta G}'_j + \frac{i\beta}{\kappa||\vec{k}||}\hat{k}^i\left(\frac{1}{\kappa}\underset{\sim}{\delta C}' - \underset{\sim}{\epsilon}'\right)\right. \\
&\qquad \left. - \frac{2i}{\kappa||\vec{k}||}\epsilon_{abi}\hat{k}^a\left(\frac{1}{\kappa}\underset{\sim}{\delta C}'_b - \underset{\sim}{p}'_b\right)\right] \\
&- \kappa\int d^3k\left[i\kappa||\vec{k}||\underset{\sim}{\delta\tau}\hat{k}^b\left(\frac{1}{\kappa}\underset{\sim}{\delta C}'_b - \underset{\sim}{p}'_b\right)\right] \\
&+ O(\delta^3,\kappa^2)\,.
\end{aligned}
\tag{7.111}
$$

As discussed above in (7.105), the physical Hamiltonian $\delta\mathbf{H}$ consists in zeroth order of the Hamiltonian of the scalar field on Minkowski spacetime plus the Dirac observable associated with $\delta^2 C^{\text{geo}}$ as well as the Dirac observable corresponding to the interaction Hamiltonian $\mathcal{H}_I$. In the following equations these contributions are marked in blue:

$$
\begin{aligned}
\delta\mathbf{H}_{\text{can}} =& \int_{\mathbb{R}^3} d^3x\ \epsilon(\vec{x},t) \\
&+\kappa\int_{\mathbb{R}^3} d^3k\ \frac{1}{2\beta^2}\sum_{r\in\{\pm\}}\Big(\underset{\sim}{\delta A}^r(\vec{k},t)\,\underset{\sim}{\delta A}^r(-\vec{k},t) + 2r\,||\vec{k}||\underset{\sim}{\delta E}^r(\vec{k},t)\,\underset{\sim}{\delta A}^r(-\vec{k},t) \\
&\qquad +(\beta^2+1)||\vec{k}||^2\underset{\sim}{\delta E}^r(\vec{k},t)\,\underset{\sim}{\delta E}^r(-\vec{k},t)\Big) \\
&+\kappa\int_{\mathbb{R}^3} d^3k\ \delta^i_b\underset{\sim}{\varphi}^b_a(\vec{k},t)\,\underset{\sim}{\delta\mathcal{E}}^a{}_i(-\vec{k},t) \\
&+\kappa\int d^3k i k_b\kappa\underset{\sim}{\delta\sigma}'^a\left[\underset{\sim}{\varphi}^b_a - \delta^b_a\left(\underset{\sim}{\varphi}^c_c + m^2\underset{\sim}{\widetilde{V}} - \underset{\sim}{\epsilon}\right)\right] + \kappa\int d^3k\left[i\kappa||\vec{k}||\underset{\sim}{\delta\tau}\hat{k}^b\underset{\sim}{p}'_b\right] \\
&-\kappa\int_{\mathbb{R}^3}\frac{d^3k}{||\vec{k}||^2}\Big(-\underset{\sim}{p}_c(\vec{k},t)\,\underset{\sim}{p}_d(-\vec{k},t)\left[\delta^{cd} - \frac{1}{4}\hat{k}^c\hat{k}^d\right] + \underset{\sim}{\epsilon}(\vec{k},t)\,\underset{\sim}{\epsilon}(-\vec{k},t)\left[\frac{1}{4}+\frac{3}{2}\right] \\
&\qquad -\frac{3}{2}m^2\,\underset{\sim}{\widetilde{V}}(\vec{k},t)\,\underset{\sim}{\epsilon}(-\vec{k},t) - \underset{\sim}{\varphi}^a_a(\vec{k},t)\,\underset{\sim}{\epsilon}(-\vec{k},t)\Big) \\
&+\int d^3k\ \underset{\sim}{\delta G}_i\Big(\underset{\sim}{\delta\Lambda}'^i - 2i\beta k^a\frac{1}{||\vec{k}||^2}\left[\underset{\sim}{\varphi}'^b_a\delta^i_b + \frac{1}{2}\left(m^2\underset{\sim}{\widetilde{V}}' - \epsilon'\right)\delta^i_a\right] - \frac{\beta^2+1}{\kappa^2}\hat{k}^i\hat{k}^j\ \underset{\sim}{\delta G}'_j \\
&\qquad -\frac{i\beta}{\kappa||\vec{k}||}\hat{k}^i\left(\frac{1}{\kappa}\underset{\sim}{\delta C}' - \underset{\sim}{\epsilon}'\right) + \frac{2i}{||\vec{k}||}\epsilon_{bia}\hat{k}^a\left(\frac{1}{\kappa}\underset{\sim}{\delta C}'_b - \underset{\sim}{p}'_b\right)\Big) \\
&+\int d^3k\ \underset{\sim}{\delta C}_a\left(\underset{\sim}{\delta N}'^a + \frac{1}{||\vec{k}||^2}\left(\frac{1}{\kappa}\underset{\sim}{\delta C}'_b - 2\underset{\sim}{p}'_b\right)(\delta^{ab} - \frac{1}{4}\hat{k}^a\hat{k}^b)\right)
\end{aligned}
$$

$$
\begin{aligned}
&+ \int d^3k\ \underset{\smile}{\delta C}\left(\underset{\smile}{\delta N}' - \frac{1}{||\vec{k}||^2}\left[\underset{\smile}{\varphi'^a_a} + \frac{3}{2}m^2\underset{\smile}{\widetilde{V}}' - \frac{3}{2}\underset{\smile}{\epsilon}'\right] - \frac{1}{4||\vec{k}||^2}\left(\frac{1}{\kappa}\underset{\smile}{\delta C}' - 2\underset{\smile}{\epsilon}'\right)\right)\\
&- \kappa\int d^3k\left[i||\vec{k}||\underset{\smile}{\delta\tau}\hat{k}^b\underset{\smile}{\delta C'}_b\right]\\
&+ O(\delta^3,\kappa^2)\,. \qquad (7.112)
\end{aligned}
$$

Dropping terms of order $O(\delta^3,\kappa^2)$ and higher the physical Hamiltonian reads:

$$
\begin{aligned}
\delta\mathbf{H} = &\int_{\mathbb{R}^3} d^3x\ \epsilon(\vec{x},t)\\
&+ \kappa\int_{\mathbb{R}^3} d^3k\ \frac{1}{2\beta^2}\sum_{r\in\{\pm\}}\Big(\underset{\smile}{\delta A}^r(\vec{k},t)\,\underset{\smile}{\delta A}^r(-\vec{k},t) + 2r\,||\vec{k}||\underset{\smile}{\delta E}^r(\vec{k},t)\,\underset{\smile}{\delta A}^r(-\vec{k},t)\\
&\qquad + (\beta^2+1)||\vec{k}||^2\underset{\smile}{\delta E}^r(\vec{k},t)\,\underset{\smile}{\delta E}^r(-\vec{k},t)\Big)\\
&+ \kappa\int_{\mathbb{R}^3} d^3k\ \delta^i_b\underset{\smile}{\varphi}{}^b_a(\vec{k},t)\,\underset{\smile}{\delta\mathcal{E}}{}^a{}_i(-\vec{k},t)\\
&+ \kappa\int d^3k\ ik_b\kappa\underset{\smile}{\delta\sigma}'^a\left[\underset{\smile}{\varphi}{}^b_a - \delta^b_a\left(\underset{\smile}{\varphi}{}^c_c + m^2\underset{\smile}{\widetilde{V}} - \underset{\smile}{\epsilon}\right)\right] + \kappa\int d^3k\left[i\kappa||\vec{k}||\underset{\smile}{\delta\tau}\hat{k}^b\underset{\smile}{p'}_b\right]\\
&- \kappa\int_{\mathbb{R}^3}\frac{d^3k}{||\vec{k}||^2}\Bigg(-\underset{\smile}{p}_c(\vec{k},t)\,\underset{\smile}{p}_d(-\vec{k},t)\left[\delta^{cd} - \frac{1}{4}\hat{k}^c\hat{k}^d\right] + \underset{\smile}{\epsilon}(\vec{k},t)\,\underset{\smile}{\epsilon}(-\vec{k},t)\left[\frac{1}{4}+\frac{3}{2}\right]\\
&\qquad - \frac{3}{2}m^2\,\underset{\smile}{\widetilde{V}}(\vec{k},t)\,\underset{\smile}{\epsilon}(-\vec{k},t) - \underset{\smile}{\varphi}{}^a_a(\vec{k},t)\,\underset{\smile}{\epsilon}(-\vec{k},t)\Bigg)\,. \qquad (7.113)
\end{aligned}
$$

As expected, the physical Hamiltonian differs from $\delta\mathbf{H}_{\text{can}}$ only by terms that involve the linearised constraints at least linearly and $\delta\mathbf{H}$ agrees exactly with the expression for the physical Hamiltonian shown in (7.105). As can be seen from the explicit form of the physical Hamiltonian in (7.113) for our choice of $\delta\tau$ and $\delta\sigma^c$ in (7.51), $\delta\tau$ being linear in t does not contribute to the physical Hamiltonian and $\delta\sigma^c$ is also absent if we chose it to be constant and enters via Kronecker delta in case we choose it to be linearly in x^c in exact agreement to what was found in [158] for the ADM variables. This additional Kronecker delta contribution for the second choice combines with terms including the scalar field and its derivatives respectively and has thus a suitable fall-off behaviour.

The different contributions to the Hamiltonian in the individual lines can be interpreted as follows: The first line corresponds to the Hamiltonian of a scalar field on a Minkowski background. The next two lines encode the Hamiltonian of a gravitational field in vacuum, the third integral denotes the interaction between the gravitational degrees of freedom and the matter field and finally the remaining contributions encode the gravitational self-interaction of the scalar field. Even though the latter does not contain any gravitational degrees of freedom, it only appears due to the coupling between matter and gravity and results from the coupling of the gauge degrees of freedom in the gravitational sector to the scalar field. Once these gauge degrees of freedom are expressed in terms of the independent physical degrees of freedom, we end up with this result. The latter contribution was neglected in [151] by using the argument that only the transverse-traceless components need to be considered. While in the vacuum case one can use a gauge fixing that sets all but the transverse-traceless gravitational degrees of freedom to zero, this is no longer a valid choice for a gauge-fixing if we couple the scalar field, because the constraints

involve additional contributions from the scalar field and suitable gauge fixing will result in such a contribution of gravitational self-interaction of the scalar field. Hence, to our understanding, it is not justified to neglect this contributions in the order of perturbation theory considered in [151].
This finalises the discussion on the classical model that will be the starting point for the Fock quantisation in section 8. Having identified the physical degrees of freedom in the model, now we are in the situation to separate the total system into a system and an environmental part, as usually done in the framework of decoherence models. We choose the following separation:

$$\text{system: } \phi^{GI},\, \pi^{GI} \qquad \text{environment: } \delta\mathcal{A}_a{}^i,\, \delta\mathcal{E}^a{}_i$$

and hence the gauge invariant matter sector becomes the system and the physical degrees freedom in the gravitational sector provide the environment.

7.9. Comparison to other observables and to approaches using a gauge fixing

The content of this subsection was already published in [1]. Here, it is presented with some modifications compared to [1] to adapt it to the flow of the thesis.
Apart from the strategy followed here by using the relational formalism and the observable map as well as its dual to construct suitable Dirac observables that allow the splitting of the phase space into the physical and gauge part, there exist different methods in the literature to identify the physical subspace of the theory. In this section, we want to comment on three different ways and compare them with the method applied in this thesis. In subsection 7.9.1 we start with another ansatz to construct observables for the ADM formalism pursued in [60] and then discuss two ways to gauge fix the theory instead that are implied by the clocks introduced in this work, which is discussed in subsection 7.9.2, and another one often used for the ADM variables introduced in [158], which we discuss in subsection 7.9.3. As discussed for instance in [161], for certain choices of the $\mathcal{G}^I$ one can relate a model formulated in terms of fully gauge invariant quantities to a corresponding gauge-fixed model. The observables constructed in this work also fall into this class of models, which means that the gauge-fixed Hamiltonian and the gauge invariant physical Hamiltonian formally agree if we replace all gauge invariant quantities by their gauge-fixed counter parts. Practically, this can be achieved by setting $\mathcal{G} = \mathcal{G}^a = \mathcal{G}^j = 0$, that is strongly equal to zero and then we can formally identify the Dirac observables with the gauge-fixed quantities involved in the gauge fixing discussed in subsection 7.9.2. For this specific gauge fixing, the constructed observables have a standard interpretation. The Hamiltonian of the gauge fixed theory can be obtained by inserting all constraints, gauge fixing conditions as well as the Lagrange multipliers that ensure the stability of the gauge fixing into $\delta\mathbf{H}_{\text{can}}$. As can be seen from the explicit form of $\delta\mathbf{H}_{\text{can}}$ in (7.112), the Hamiltonian of the gauge fixed theory agrees formally with $\delta\mathbf{H}$ under the identification of the Dirac observables with their corresponding gauge-fixed quantities. In order to compare our results with the existing literature, we discuss in subsection 7.9.3 the geometrical clocks used in [151] that are denoted as ADM clocks there because they were introduced in the seminal paper [158]. Also this set of geometrical clocks encodes the physical gravitational degrees of freedom in the symmetric transverse-traceless linearised connection and triad variables. The main difference we see among the two sets of geometrical clocks is how the reference field associated with the linearised Gauß constraint is chosen. In our work we choose a Lorentz-like condition if we set the corresponding gauge fixing condition $\delta\mathcal{G}^j = 0$, whereas in [151] the resulting $\delta\mathcal{G}^j = 0$ is only equivalent to a Lorentz-like condition in the vacuum case

but not if we couple a scalar field. Then the resulting reference fields for the linearised spatial diffeomorphism and Hamiltonian constraint also differ because for both sets of clocks we require that all geometrical clocks commute mutually.

7.9.1. Comparison to the observables used in [60]

The content of this subsection was already published in [1]. Here, it is presented with some modifications compared to [1] to adapt it to the flow of the thesis.
The model in [60] also considers gauge invariant quantities for the matter variables in the ADM framework and we would like to compare their quantities to the constructed Dirac observables in this work. There, an extension of the basic gauge variant matter variables ϕ and π is proposed that is required to commute with the linearised constraints. These observables take the form

$$\widetilde{\phi}(\vec{x},t) = \phi(\vec{x}-\vec{q},t-\tau) \qquad\qquad \widetilde{\pi}(\vec{x},t) = \pi(\vec{x}-\vec{q},t-\tau) - \partial_a q^a\,,$$

where $\vec{q}$ and τ, similarly to the geometrical clocks used in our work, consist of purely geometrical quantities in ADM variables. For these, as well as the matter fields in [60], the following transformation behaviour under the Hamiltonian and spatial diffeomorphism constraint respectively is used[9]:

$$\begin{aligned}
\text{Under the Hamilton constraint}: \quad & \phi \to \phi + \lambda\frac{\delta H_0}{\delta\pi} && \pi \to \pi - \lambda\frac{\delta H_0}{\delta\phi}\\
& \vec{q} \to \vec{q} && \tau \to \tau + \lambda\\
\text{Under the spatial diffeomorphism constraint}: \quad & \phi \to \phi + \kappa\lambda^a\partial_a\phi && \pi \to \pi + \kappa\partial_a(\lambda^a\pi)\\
& q^i \to q^i + \lambda^i && \tau \to \tau\,,
\end{aligned}$$

where $H_0 = \int d^3x\ \epsilon(\vec{x},t)$. Starting with the transformations under the Hamiltonian constraint, which is just $\epsilon(\vec{x},t)$ in the matter part, we obtain

$$\left\{\phi(\vec{x}), \int d^3y\ \lambda(\vec{y})\epsilon(\vec{y})\right\} = \lambda(\vec{x})\pi(\vec{x}) = \lambda(\vec{x})\frac{\delta H_0}{\delta\pi}(\vec{x})$$

which hence indeed confirms their proposed transformation of the matter field. Its momentum transforms differently reflecting the fact that it is a scalar density of weight one:

$$\left\{\pi(\vec{x}), \int d^3y\ \lambda(\vec{y})\epsilon(\vec{y})\right\} = \partial_a(\lambda(\vec{x})\partial^a\phi(\vec{x})) - \lambda(\vec{x})V'(\phi(\vec{x})) = -\lambda(\vec{x})\frac{\delta H_0}{\delta\phi}(\vec{x}) + (\partial_a\lambda(\vec{x}))\ \partial^a\phi(\vec{x}),$$

where we assumed that the scalar field obeys a Klein-Gordon equation and that the energy density possesses an arbitrary potential $V(\phi)$. The transformation behaviour used in [60] under the Hamiltonian constraint only agrees with the above expression if λ is constant, which in general cannot be assumed and hence the second term coming from the Poisson bracket needs to be included in the transformation of $\pi(\vec{x})$, which to our understanding has been omitted in [60].
Given the correct general transformation behaviours, we want to check whether the Dirac observables $\tilde{\phi}$ and $\widetilde{\pi}$ used in [60] are indeed gauge invariant. First it is worth noticing that due to the fact that we are working in a linearised theory, to our understanding the quantity $\widetilde{\phi}(\vec{x},t)$ has to

[9] Note that in [60] the transformation for π is given by $\pi \to \pi - \lambda\frac{\delta H_0}{\delta\pi}$ where we expect the $\frac{\delta}{\delta\pi}$ to be a typo and corrected this accordingly.

be understood as a Taylor expansion in the modifications truncated after linear order. In general this way of constructing observables looks like the canonical version of the strategy followed in [154]. To show this, we will add an additional κ in front of the modifications and also include it into the constraints. In [60] this was done for the spatial diffeomorphism constraint only, as its action on the matter fields indeed yields a correction term of order κ. As shown in the discussion on the Post-Minkowski approximation scheme in section 6.3, for consistency such a factor is also required in the Hamiltonian constraint. Therefore, we obtain

$$\begin{aligned}\widetilde{\phi}(\vec{x},t) &= \phi(\vec{x}-\kappa\vec{q}(\vec{x},t),t-\kappa\tau(\vec{x},t)) = \phi(\vec{x},t)-\kappa q^a(\vec{x},t)\partial_a\phi(\vec{x},t)-\kappa\tau(\vec{x},t)\dot{\phi}(\vec{x},t)\\ \widetilde{\pi}(\vec{x},t) &= \pi(\vec{x}-\kappa\vec{q}(\vec{x},t),t-\kappa\tau(\vec{x},t))-\partial_a q^a(\vec{x},t) = \pi(\vec{x},t)-\kappa q^a\partial_a\pi(\vec{x},t)-\kappa\tau\dot{\pi}(\vec{x},t)-\partial_a q^a(\vec{x},t)\,.\end{aligned}$$

Now under the Hamilton constraint $\widetilde{\phi}$ transforms as:

$$\widetilde{\phi}(\vec{x},t)\to\widetilde{\phi}(\vec{x},t)+\kappa(\lambda\pi)(\vec{x},t)-\kappa(\lambda\dot{\phi})(\vec{x},t)=\widetilde{\phi}(\vec{x},t)\,,$$

where we neglected terms of higher order in κ and see that indeed $\widetilde{\phi}$ remains invariant under the transformations induced by the Hamilton constraint. For $\widetilde{\pi}$ one obtains:

$$\widetilde{\pi}(\vec{x},t)\to\widetilde{\pi}(\vec{x},t)+\kappa(\lambda\dot{\pi})(\vec{x},t)-\kappa(\lambda\dot{\pi})(\vec{x},t)=\widetilde{\pi}(\vec{x},t)\,.$$

Thus, working with the correct transformation behaviour of π under the Hamiltonian constraint, also $\widetilde{\pi}$ remains invariant. For the spatial diffeomorphism constraint a quick calculation shows that its action on the matter fields is indeed given by the terms stated above and in [60]. Under its action we obtain:

$$\begin{aligned}\widetilde{\phi}&\to\widetilde{\phi}+\kappa\lambda^a\partial_a\phi-\kappa\lambda^a\partial_a\phi=\widetilde{\phi}\\ \widetilde{\pi}&\to\widetilde{\pi}-\kappa\lambda^a\partial_a\pi-\partial_a\lambda^a\neq\widetilde{\pi}\end{aligned}$$

which demonstrates that the $\tilde{\pi}$ proposed in [60] is no (linearised) Dirac observable with respect to the spatial diffeomorphism constraint. Thus, actual linearised observables for $\phi(\vec{x},t),\pi(\vec{x},t)$ in [60] would be given by

$$\begin{aligned}\widetilde{\phi}(\vec{x},t) &= \phi(\vec{x},t)-\kappa q^a(\vec{x},t)\partial_a\phi(\vec{x},t)-\kappa\tau(\vec{x},t)\dot{\phi}(\vec{x},t)\\ \widetilde{\pi}(\vec{x},t) &= \pi(\vec{x},t)-\kappa q^a\partial_a(q^a\pi)(\vec{x},t)-\kappa\tau\dot{\pi}(\vec{x},t)\,,\end{aligned}$$

where it is crucial that the partial derivative in the second term in $\widetilde{\pi}$ acts on both $q^a(\vec{x},t)$ and $\pi(\vec{x},t)$. Compared to our framework, the basic idea is similar to extend the matter fields with geometrical variables to obtain gauge invariant observables. Hence, the quantities q^a and τ play the role of geometrical clocks in our setup. In our approach we in addition require that q^a and τ mutually commute which yields to the requirement to use an explicit choice of geometrical clocks that satisfies this additional property.

7.9.2. Gauge fixing following from the clocks introduced in section 7.4

The content of this subsection was already published in [1]. Here, it is presented with some modifications compared to [1] to adapt it to the flow of the thesis. The gauge fixing used here is similar to the one applied in the Master's thesis [5], where no Dirac observables were constructed. The section is included here in order to have a comparison between the case when working with

Dirac observables and the case where a gauge fixing is employed, as the latter method is frequently used in the literature.

In this section we present a possible gauge fixing that naturally arises from the choice of the clocks introduced in section 7.4 in the context of constructing Dirac observables. The induced gauge fixing is obtained by setting the gauge fixing conditions $\mathcal{G}^I$ shown in (7.73) equal to zero. Evaluating the constraints in momentum space using the basis introduced in section 7.6.1 yields the following seven relations among the elementary phase space variables at every point $(\vec{k}, t)$:

$$||\vec{k}||\underset{\sim}{\delta E}^{\overline{1}} = \underset{\sim}{\delta A}^{\overline{1}} - \underset{\sim}{\delta A}^{\overline{2}} \qquad i||\vec{k}||(\underset{\sim}{\delta A}^4 + \underset{\sim}{\delta A}^5) = -\beta \hat{k}^a \underset{\sim}{p}_a \tag{7.114}$$

$$||\vec{k}||\underset{\sim}{\delta E}^1 = \underset{\sim}{\delta A}^2 - \underset{\sim}{\delta A}^1 \qquad i||\vec{k}||\underset{\sim}{\delta A}^{\overline{2}} = \beta m^a(\vec{k})\underset{\sim}{p}_a \tag{7.115}$$

$$||\vec{k}||\underset{\sim}{\delta E}^3 = \underset{\sim}{\delta A}^5 - \underset{\sim}{\delta A}^4 \qquad i||\vec{k}||\underset{\sim}{\delta A}^2 = \beta \overline{m}^a(\vec{k})\underset{\sim}{p}_a \tag{7.116}$$

$$||\vec{k}||(\underset{\sim}{\delta A}^4 - \underset{\sim}{\delta A}^5) = -\underset{\sim}{\epsilon}\,, \tag{7.117}$$

where $\underset{\sim}{\epsilon}$ and $\underset{\sim}{p}_a$ denote the three-dimensional Fourier transforms of the energy and momentum density of the scalar field. The gauge fixing conditions, obtained by requiring $\mathcal{G}^I$ to vanish and in addition choosing $\tau(t, \vec{x}) = t, \sigma^a = x^a_\sigma = \text{const}$ and $\xi^j = 0$, hence $\delta\tau = \frac{t}{\kappa}$, $\delta\sigma^a = \frac{x^a_\sigma}{\kappa} = \text{const}$, give seven additional conditions in momentum space for every $\vec{k}$ and t:

$$\underset{\sim}{\delta A}^3 = 0 \qquad \underset{\sim}{\delta E}^2 = -\underset{\sim}{\delta E}^1 \tag{7.118}$$

$$\underset{\sim}{\delta A}^1 = 0 \qquad \underset{\sim}{\delta E}^{\overline{2}} = -\underset{\sim}{\delta E}^{\overline{1}} \tag{7.119}$$

$$\underset{\sim}{\delta A}^{\overline{1}} = 0 \qquad 3\underset{\sim}{\delta E}^3 - \underset{\sim}{\delta E}^4 - \underset{\sim}{\delta E}^5 = \frac{1}{||\vec{k}||^2}\underset{\sim}{\epsilon} \tag{7.120}$$

$$\underset{\sim}{\delta E}^5 - \underset{\sim}{\delta E}^4 = \frac{2}{||\vec{k}||}\left(\underset{\sim}{\delta A}^3 + \underset{\sim}{\delta A}^4 + \underset{\sim}{\delta A}^5\right). \tag{7.121}$$

Note that $\delta\tau$ and $\delta\sigma$ were chosen to be constant in position and hence vanish in all appearing combinations in the gauge fixing conditions. Substituting these results into (7.59) and (7.60) yields an expression for $\underset{\sim}{\delta E}$ and $\underset{\sim}{\delta A}$ in terms of the physical degrees of freedom:

$$\begin{aligned}
\underset{\sim}{\delta E}^a{}_i =& \underset{\sim}{\delta E}^+ m^a m_i + \underset{\sim}{\delta E}^- \overline{m}^a \overline{m}_i + \frac{\underset{\sim}{\epsilon}}{||\vec{k}||^2}\delta^a_i \\
&+ \frac{\beta i}{||\vec{k}||^2}\underset{\sim}{p}_c\left[m^c\left(\hat{k}^a\overline{m}_i - \overline{m}^a\hat{k}_i\right) - \overline{m}^c\left(\hat{k}^a m_i - m^a\hat{k}_i\right) - \hat{k}^c\left(m^a\overline{m}_i - \overline{m}^a m_i\right)\right] \\
=& \underset{\sim}{\delta E}^+ m^a m_i + \underset{\sim}{\delta E}^- \overline{m}^a \overline{m}_i + \frac{\underset{\sim}{\epsilon}}{||\vec{k}||^2}\delta^a_i - \frac{\beta}{||\vec{k}||^2}\underset{\sim}{p}_c \epsilon^{ca}{}_i
\end{aligned} \tag{7.122}$$

$$\begin{aligned}
\underset{\sim}{\delta A}_a{}^i =& \underset{\sim}{\delta A}^+ m_a m^i + \underset{\sim}{\delta A}^- \overline{m}_a \overline{m}^i - \frac{\beta i}{||\vec{k}||}\underset{\sim}{p}_c\left[\overline{m}^c m_a \hat{k}^i + m^c\overline{m}_a\hat{k}^i - \frac{1}{2}\hat{k}^c\left(m_a\overline{m}^i + \overline{m}_a m^i\right)\right] \\
&+ \frac{\underset{\sim}{\epsilon}}{2||\vec{k}||}\left(\overline{m}_a m^i - m_a\overline{m}^i\right) \\
=& \underset{\sim}{\delta A}^+ m_a m^i + \underset{\sim}{\delta A}^- \overline{m}_a \overline{m}^i - \frac{\beta i}{||\vec{k}||}\underset{\sim}{p}_c\left[\hat{k}^i\delta^c_a - \frac{1}{2}\hat{k}^c\delta^i_a - \frac{1}{2}\hat{k}^c\hat{k}_a\hat{k}^i\right] + \frac{i\,\underset{\sim}{\epsilon}}{2||\vec{k}||}\epsilon_{ba}{}^i\hat{k}^b\,.
\end{aligned} \tag{7.123}$$

Note that one can also obtain this by setting the constraints equal to zero in the expressions shown in (7.107) and (7.108). The independent physical degrees of freedom are encoded in the matter fields (ϕ, π) as well as the symmetric transverse-traceless parts of the connection and densitised triads

$$\delta\underset{\sim}{\mathcal{A}}_a{}^i(\vec{k},t) = \delta\underset{\sim}{A}^+(\vec{k},t)\, m_a(\vec{k})\, m^i(\vec{k}) + \delta\underset{\sim}{A}^-(\vec{k},t)\, \overline{m}_a(\vec{k})\, \overline{m}^i(\vec{k}) = \underset{\sim}{P}_a{}^i{}_j{}^b(\vec{k})\delta\underset{\sim}{A}_b{}^j(\vec{k},t) \tag{7.124}$$

$$\delta\underset{\sim}{\mathcal{E}}^a{}_i(\vec{k},t) = \delta\underset{\sim}{E}^+(\vec{k},t)\, m^a(\vec{k})\, m_i(\vec{k}) + \delta\underset{\sim}{E}^-(\vec{k},t)\, \overline{m}^a(\vec{k})\, \overline{m}_i(\vec{k}) = \underset{\sim}{P}^a{}_i{}^j{}_b(\vec{k})\delta\underset{\sim}{E}^b{}_j(\vec{k},t) \tag{7.125}$$

with the projectors $\underset{\sim}{P}^a{}_i{}^j{}_b(\vec{k})$ and $\underset{\sim}{P}_a{}^i{}_j{}^b(\vec{k})$ onto the symmetric transverse-traceless parts that were defined in (7.61). As expected, with the components of $\delta\underset{\sim}{\mathcal{A}}_a{}^i, \delta\underset{\sim}{\mathcal{E}}^a{}_i(\vec{k},t)$ we end up with the six physical degrees of freedom given by

$$\delta\underset{\sim}{E}^+, \delta\underset{\sim}{E}^-, \delta\underset{\sim}{A}^+, \delta\underset{\sim}{A}^-, \phi, \pi\,. \tag{7.126}$$

Without the matter fields, one gets the well-known four phase space field degrees of freedom of gravitational waves in vacuum, corresponding to two field degrees of freedom in the Lagrangian framework, and the real scalar matter field leads to two additional phase space field degrees of freedom. Reinserting (7.122) and (7.123) into the Hamiltonian (6.42) yields the total Hamiltonian of the linearised theory on the reduced phase space, (7.113), where we used the transverse-traceless projectors

$$[P^\pm(\vec{k})]^b_a = \overline{m}_a(\pm\vec{k})\, \overline{m}^b(\pm\vec{k})\,, \tag{7.127}$$

such that

$$[P^\pm(\vec{k})]^b_a \delta^i_b\, \delta\underset{\sim}{E}^a{}_i = \delta\underset{\sim}{E}^\pm \tag{7.128}$$

$$[P^\pm(\vec{k})]^a_b\, \delta^b_i \delta\underset{\sim}{A}_a{}^i = \delta\underset{\sim}{A}^\pm \tag{7.129}$$

$$\underset{\sim}{P}^a{}_i{}^j{}_b(\vec{k}) = \sum_{r\in\{\pm\}} [P^r(\vec{k})]^a_i [P^{-r}(\vec{k})]^j_b\,. \tag{7.130}$$

However, working at the gauge invariant level and not choosing one specific gauge fixing allows us also to choose a different gauge fixing than the one discussed in this section and then the observables and their dynamics discussed in this work are still valid because everything was formulated in a gauge invariant manner. The only difference for other gauge fixing choices is that the interpretation of the gauge invariant Dirac observables and their relation to the gauge-fixed quantities is modified because then the gauge fixing does not necessarily correspond to setting all $\mathcal{G}^I$ equal to zero. Hence in this sense, if we consider a class of models where a relation to one gauge fixing is possible, then there is always a convenient choice for the reference fields in order to make such a relation as simple as possible. This was exactly our motivation for choosing the reference fields for this model the way we did, apart from the additional requirements (i) to (iii) listed in section 7.2.

7.9.3. A further gauge fixing often used for ADM variables introduced in [158]

The content of this subsection was already published in [1]. Here, it is presented with some modifications compared to [1] to adapt it to the flow of the thesis.

At this point, we would like to make a short comparison to the clocks introduced in [151] based on seminal work in [158] and [159]. Likewise to [151] we denote this set of clocks as ADM clocks. These clocks, similarly to the ones we use in this work, also do not contain the symmetric transverse-traceless gravitational degrees of freedom $\delta A^{\pm}$ and $\delta E^{\pm}$. Hence, these four phase space degrees of freedom are again identified as the physical degrees of freedom in the gravitational sector, as in our case. However, the gauge fixing used in [151] which is induced by setting the corresponding gauge fixing conditions $\delta\mathcal{G}^I = \delta T^I - \tau^I$ to zero is different from the one used in section 7.4 in this thesis, hence this set of clocks is not equivalent to the one discussed in section 7.4. This can be easily seen by considering the clock ${}^G T^i$ associated with the Gauß constraint from [151] in momentum space. Requiring that the components $m_i(\vec{k})\underset{\smile}{{}^G T^i}(\vec{k})$ and $\overline{m}_i(\vec{k})\underset{\smile}{{}^G T^i}(\vec{k})$ vanish yields $\delta\underset{\smile}{E}^1 = \delta\underset{\smile}{E}^{\overline{1}} = 0$. In contrast, the gauge fixing obtained by setting the constraints as well as gauge fixing conditions $\delta\mathcal{G}^I$ used in section 7.4 equal to zero, we can read off from the transformation introduced in section 7.7 that $\delta\underset{\smile}{E}^1 = -\frac{i\beta}{||\vec{k}||^2}\overline{m}^a \underset{\smile}{p}_a$ and $\delta\underset{\smile}{E}^{\overline{1}} = \frac{i\beta}{||\vec{k}||^2} m^a \underset{\smile}{p}_a$. This gauge fixing condition would be equivalent to the Lorenz-like condition for the Gauß constraint chosen in this work in (7.22) only for the vacuum case, as can be seen in [128][10]. Setting the gauge fixing conditions $\mathcal{G}^I_{\mathrm{ADM}}$ induced by the ADM clocks used in [151] equal to zero imposes the following set of conditions on the phase space variables:

$$\delta\underset{\smile}{E}^1 = \delta\underset{\smile}{E}^{\overline{1}} = \delta\underset{\smile}{E}^2 = \delta\underset{\smile}{E}^{\overline{2}} = 2\delta\underset{\smile}{A}^3 + \delta\underset{\smile}{A}^4 + \delta\underset{\smile}{A}^5 = \delta\underset{\smile}{E}^5 - \delta\underset{\smile}{E}^4 = \delta\underset{\smile}{E}^3 - \delta\underset{\smile}{E}^4 - \delta\underset{\smile}{E}^5 = 0\,, \quad (7.131)$$

which implies on the constraint hypersurface that

$$\delta\underset{\smile}{E}^a{}_i = \delta\underset{\smile}{\mathcal{E}}^a{}_i + \frac{\underset{\smile}{\epsilon}}{2||\vec{k}||^2}(\delta^a_i + \hat{k}^a\hat{k}_i) \quad (7.132)$$

$$\delta\underset{\smile}{A}_a{}^i = \delta\underset{\smile}{\mathcal{A}}_a{}^i - \frac{i\beta}{||\vec{k}||}\underset{\smile}{p}_b\left(\hat{k}^i\delta^b_a + \hat{k}_a\delta^{ib} - \frac{1}{2}\hat{k}^b\delta^i_a - \hat{k}_a\hat{k}^i\hat{k}^b\right) + \frac{i\,\underset{\smile}{\epsilon}}{2||\vec{k}||}\hat{k}^b\epsilon_{ba}{}^i\,. \quad (7.133)$$

In this particular gauge, the physical Hamiltonian becomes

$$\begin{aligned}
\delta\mathbf{H} = &\int_{\mathbb{R}^3} d^3x\ \epsilon(\vec{x},t) \\
&+ \kappa\int_{\mathbb{R}^3} d^3k\ \frac{1}{2\beta^2}\sum_{r\in\{\pm\}}\Big(\delta\underset{\smile}{A}^r(\vec{k},t)\,\delta\underset{\smile}{A}^r(-\vec{k},t) + 2r\,||\vec{k}||\delta\underset{\smile}{E}^r(\vec{k},t)\,\delta\underset{\smile}{A}^r(-\vec{k},t) \\
&\qquad\qquad + (\beta^2+1)||\vec{k}||^2\delta\underset{\smile}{E}^r(\vec{k},t)\,\delta\underset{\smile}{E}^r(-\vec{k},t)\Big) \\
&+ \kappa\int_{\mathbb{R}^3} d^3k\ \delta^i_b\underset{\smile}{\varphi}{}^b_a(\vec{k},t)\,\delta\underset{\smile}{\mathcal{E}}^a{}_i(-\vec{k},t) \\
&- \kappa\int_{\mathbb{R}^3}\frac{d^3k}{||\vec{k}||^2}\Bigg(-\underset{\smile}{p}_c(\vec{k},t)\,\underset{\smile}{p}_d(-\vec{k},t)\left[\delta^{cd} - \frac{3}{4}\hat{k}^c\hat{k}^d\right] + \underset{\smile}{\epsilon}(\vec{k},t)\,\underset{\smile}{\epsilon}(-\vec{k},t)\left[\frac{1}{4}+1\right] \\
&\qquad\qquad - m^2\,\underset{\smile}{\widetilde{V}}(\vec{k},t)\,\underset{\smile}{\epsilon}(-\vec{k},t) - \underset{\smile}{\varphi}{}^b_a(\vec{k},t)\,\underset{\smile}{\epsilon}(-\vec{k},t)\left[\frac{1}{2}\delta^a_b + \frac{1}{2}\hat{k}^a\hat{k}_b\right]\Bigg)
\end{aligned}$$

[10] Here, only the vacuum case of linearised gravity is considered and the gauge fixing employed is not equivalent to the one used in this work and discussed in section 7.9.2. In [128] one condition is that $\delta E^a{}_i$ is traceless, that is $\delta E^a{}_i\delta^i_a = 0$, which is not satisfied for the gauge fixing discussed above in section 7.9.2 where we have $\delta\underset{\smile}{E}^a{}_i\delta^i_a = \frac{3\,\underset{\smile}{\epsilon}}{||\vec{k}||^2}$.

$$+ O(\delta^3, \kappa^2)\,. \tag{7.134}$$

As can be readily seen, it differs from the Hamiltonian constructed from the observables used in this work in (7.113) only in the term encoding the self-interaction of the scalar field. The reason is that by choosing the clocks, different choices for physical temporal and spatial coordinates were established and these are determined by the choice of different sets of clocks that on the gauge fixed surface are equal to $\delta\tau$ and $\delta\sigma^a$ respectively. As discussed in equation (7.51), by an abuse of notation we understand the $\vec{x}$ and t arguments of the fields to be the associated values of the diffeomorphism and Hamiltonian clock, $\delta\tau$ and $\delta\sigma^a$ respectively. By inspection of the clocks, it turns out that the ADM clocks used in that work, corresponding to the parameters x^a_{ADM} and t_{ADM}, are related to the parameters used in this thesis, t and x^a, by

$$t_{ADM} = \frac{1}{2}t \tag{7.135}$$

$$x^a_{ADM} = x^a + \frac{1}{2}\partial^a(\epsilon * G^{\Delta\Delta})\,, \tag{7.136}$$

where we neglected factors of κ and β, as the notation regarding these factors in [151] partly differs from the one used in this work. We realise that in the case of vacuum gravity the choices for physical temporal and spatial coordinates agree but differ for non-vanishing momentum and energy density of the scalar field.

In comparison to the work in [60], where for the ADM constraints the same gauge fixing as in this section was used, their gauge fixed Hamiltonian appears with different prefactors in the self-interaction part compared to the one in (7.134). A reason might be that we were not able to reproduce the expression for V in their equation (6) in [60] which consists of the second order terms of the expansion of $\sqrt{q_{ab}}\,{}^{(3)}R$, where q_{ab} denotes the spatial ADM metric and ${}^{(3)}R$ the three-dimensional Ricci scalar. However, in contrast the structure of the result for this expansion given by partially the same authors in [63] could be reproduced by our computations.

In the next section, we proceed to quantise the physical degrees of freedom of the model encoded in the Dirac observables that were constructed in this section of the thesis.

8. Fock quantisation of the model

The content of this section was already published in [1] and is partially based on results of the Master's thesis [5], where however the gravitational degrees of freedom were quantised in a different manner[11]. It is included in this PhD thesis as it forms a core constituent of the basis of the PhD project and is presented here with slight modifications compared to [1] to adapt it to the flow of the thesis.

In this section we present the results of a Fock quantisation of the model under consideration in this part of the thesis. We work with units where $\hbar = c = 1$. For convenience, we choose to quantise the following scalar and tensor fields:

$$\phi^{GI}(\vec{x},t) \qquad \pi^{GI}(\vec{x},t) \qquad \delta\mathcal{E}^a{}_i(\vec{x},t) \qquad \delta\mathcal{C}_a{}^i(\vec{x},t)\,, \tag{8.1}$$

where the latter is the Fourier transform of

$$\underset{\sim}{\delta\mathcal{C}}_a{}^i(\vec{k},t) = \underset{\sim}{\delta\mathcal{C}}^+(\vec{k},t)m_a(\vec{k})m^i(\vec{k}) + \underset{\sim}{\delta\mathcal{C}}^-(\vec{k},t)\overline{m}_a(\vec{k})\overline{m}^i(\vec{k}) \tag{8.2}$$

with $\underset{\sim}{\delta\mathcal{C}}^\pm(\vec{k},t) = -\frac{1}{\beta}\left(\underset{\sim}{\delta A}^\pm(\vec{k},t) \pm ||\vec{k}||\,\underset{\sim}{\delta E}^\pm(\vec{k},t)\right)$; see section 7.6.1 for the definition of the basis $(\hat{k}_a, m_a(\vec{k}), \overline{m}_a(\vec{k}))$ in Fourier space. The reason for this choice is that by using $\delta\mathcal{C}$ instead of $\delta\mathcal{A}$ the terms in the linearised Hamiltonian containing only gravitational degrees of freedom in (7.113) can be rewritten in the following way:

$$\begin{aligned}&\kappa\int_{\mathbb{R}^3} d^3x \frac{1}{2}\left[\delta^{ab}\delta_{ij}\delta\mathcal{C}_a{}^i(\vec{x},t)\,\delta\mathcal{C}_b{}^j(\vec{x},t) + \delta_{bc}\delta^{ij}(\partial_a\delta\mathcal{E}^b{}_i(\vec{x},t))(\partial^a\delta\mathcal{E}^c{}_j(\vec{x},t))\right]\\ &= \kappa\int_{\mathbb{R}^3} d^3x \sum_{r\in\{+,-\}}\frac{1}{2}\left[\delta\mathcal{C}^r(\vec{x},t)\,\delta\mathcal{C}^r(\vec{x},t) + (\partial_a\delta E^r(\vec{x},t))(\partial^a\delta E^r(\vec{x},t))\right]\,,\end{aligned} \tag{8.3}$$

which has the same form as the energy density of two massless scalar fields $\delta E^\pm(\vec{x},t)$ since

$$\{\delta E^\pm(\vec{x},t), \delta\mathcal{C}^\pm(\vec{y},t)\} = -\frac{1}{\beta}\{\delta E^\pm(\vec{x},t), \delta A^\pm(\vec{y},t)\} = \frac{1}{\kappa}\delta^3(\vec{x}-\vec{y})\,. \tag{8.4}$$

A mode expansion of the fields and the Fock quantisation yield the following operator-valued distributions for the physical degrees of freedom:

$$\phi^{GI}(\vec{x},t) = \int_{\mathbb{R}^3}\frac{d^3k}{(2\pi)^{\frac{3}{2}}}\frac{1}{\sqrt{2\omega_k}}\left[a_k\,e^{-i\omega_k t+i\vec{k}\vec{x}} + a_k^\dagger\,e^{i\omega_k t-i\vec{k}\vec{x}}\right] \tag{8.5}$$

$$\pi^{GI}(\vec{x},t) = \int_{\mathbb{R}^3}\frac{d^3k}{(2\pi)^{\frac{3}{2}}}(-i)\sqrt{\frac{\omega_k}{2}}\left[a_k\,e^{-i\omega_k t+i\vec{k}\vec{x}} - a_k^\dagger\,e^{i\omega_k t-i\vec{k}\vec{x}}\right] \tag{8.6}$$

$$\delta\mathcal{E}^a{}_i(\vec{x},t) = \int_{\mathbb{R}^3}\frac{d^3k}{(2\pi)^{\frac{3}{2}}}\sqrt{\frac{1}{2\kappa\Omega_k}}\sum_{r\in\{\pm\}}\left[[P^r(-\vec{k})]_i^a\,b_k^r\,e^{-i\Omega_k t+i\vec{k}\vec{x}} + [P^r(\vec{k})]_i^a\,(b_k^r)^\dagger\,e^{i\Omega_k t-i\vec{k}\vec{x}}\right] \tag{8.7}$$

$$\delta\mathcal{C}_a{}^i(\vec{x},t) = \int_{\mathbb{R}^3}\frac{d^3k}{(2\pi)^{\frac{3}{2}}}(-i)\sqrt{\frac{\Omega_k}{2\kappa}}\sum_{r\in\{\pm\}}\left[[P^r(-\vec{k})]_a^i\,b_k^\pm\,e^{-i\Omega_k t+i\vec{k}\vec{x}} - [P^r(\vec{k})]_a^i\,(b_k^\pm)^\dagger\,e^{i\Omega_k t-i\vec{k}\vec{x}}\right]\,, \tag{8.8}$$

[11] Here, we quantise the observables $\delta\mathcal{E}^a{}_i$ and $\delta\mathcal{C}_a{}^i$, which consist of $\delta\mathcal{A}_a{}^i$ and $\delta\mathcal{E}^a{}_i$, as a whole, while in [5] the two physical degrees of freedom $\underset{\sim}{\delta E}^\pm$ and $\underset{\sim}{\delta C}^\pm$ were quantised individually.

where the $a_k^{(\dagger)}$ denote annihilation (creation) operator-valued distributions for scalar particles, while the $(b_k^{\pm})^{(\dagger)}$ denote annihilation (creation) operator-valued distributions for gravitons with polarisation label $\pm$. We have also introduced $\omega_k := \sqrt{\vec{k}^2 + m^2}$ and $\Omega_k := \sqrt{\vec{k}^2}$ as well as the transverse-traceless projectors $[P^r(\vec{k})]_a^i$ defined in (7.127), which play the role of the polarisation tensors of the quantised fields. From their definitions follows that $\overline{[P^r(\vec{k})]_i^a} = [P^r(-\vec{k})]_i^a$ and hence $\delta\mathcal{E}^a{}_i(\vec{x},t)^\dagger = \delta\mathcal{E}^a{}_i(\vec{x},t)$ and $\delta\mathcal{C}_a{}^i(\vec{x},t)^\dagger = \delta\mathcal{C}_a{}^i(\vec{x},t)$. Note that in contrast to [60] the polarisation tensors are different for the positive and negative frequency modes. The creation and annihilation operator-valued distributions satisfy the following commutation relations:

$$[a_k, a_l^\dagger] = \delta^3(\vec{k}-\vec{l}) \qquad [a_k, a_l] = [a_k^\dagger, a_l^\dagger] = 0 \tag{8.9}$$

$$[b_k^\pm, (b_l^\pm)^{(\dagger)}] = \delta^3(\vec{k}-\vec{l}) \qquad [b_k^\pm, b_l^\pm] = [(b_k^\pm)^{(\dagger)}, (b_l^\pm)^{(\dagger)}] = 0\,, \tag{8.10}$$

here we omit the vector arrow on the mode labels in all index positions in order to keep our notation more compact. The total Fock space consists of a tensor product of three individual bosonic Fock spaces, one for the scalar particles, one for the + polarised gravitons and one for the − polarised ones. As usual, the annihilation and creation operators for different fields or polarisations mutually commute. The Hamiltonian operator corresponding to (7.113) can then be implemented in the Schrödinger picture as

$$\begin{aligned} H = &\int_{\mathbb{R}^3} d^3k \left\{ \omega_k\, a_k^\dagger\, a_k + \Omega_k \left[(b_k^+)^\dagger\, b_k^+ + (b_k^-)^\dagger\, b_k^- \right] \right\} \\ &+ \sqrt{\frac{\kappa}{2}} \int d^3k \frac{1}{\sqrt{\Omega_k}} \sum_{r\in\{\pm\}} \left[b_k^r\, J_r^\dagger(\vec{k}) + (b_k^r)^\dagger\, J_r(\vec{k}) \right] \\ &+ \kappa U \otimes \mathbb{1}_{\mathcal{E}}\,, \end{aligned} \tag{8.11}$$

where we have introduced some kind of normal-ordered current operator for the scalar field that couples to the gravitational environment and which is quadratic in the scalar field and its derivatives:

$$\begin{aligned} J_r(\vec{k}) &:= \underbrace{\hat{\varphi}_a^b(\vec{k},0)[P^r(\vec{k})]_b^a} \\ &= \int \frac{d^3p}{(2\pi)^{\frac{3}{2}}} \frac{1}{2\sqrt{\omega_p\omega_{k+p}}} \left[p_a p^b [P^r(\vec{k})]_b^a \right] \left(2a_p^\dagger a_{k+p} + a_{-p} a_{k+p} + a_p^\dagger a_{-p-k}^\dagger \right) . \end{aligned} \tag{8.12}$$

Furthermore, U denotes a self-interaction operator that is present only due to the coupling of the scalar field to linearised gravity, as its contribution to the Hamiltonian operator will vanish if the coupling constant κ is set to zero. It involves fourth powers of the annihilation and creation operators of the scalar field and its momentum. Its contributions can be understood as additional self-interaction vertices of the scalar field that are not present in the corresponding free theory. We chose to implement this operator in a completely normal ordered form, that is $:U:$, where $:\cdot:$ denotes normal ordering. This is in contrast to the quantisation procedure of similar systems in [60, 62, 63], where either no specific ordering is mentioned [62], or the individual operators corresponding to the operators $\epsilon, p_a, \widetilde{V}, \varphi$ and J_r, introduced above and in (7.110), are normal ordered [60, 63], but no normal ordering is applied to the entire self-interaction operator U. The normal ordering will be an important point when we consider the one-particle projection of the

master equation in part III, because the self-interaction term then vanishes completely. For the normal ordered self-interaction operator we obtain

$$\begin{aligned} U :=& \int d^3k \frac{ik_b}{2}\kappa\underset{\sim}{\delta\sigma}^a(-\vec{k},0)\left[\underset{\sim}{\varphi}{}^b_a(\vec{k},0) - \delta^b_a\left(\underset{\sim}{\varphi}{}^c_c(\vec{k},0) + m^2\underset{\sim}{\widetilde{V}}(\vec{k},0) - \underset{\sim}{\epsilon}(\vec{k},0)\right)\right] \\ &- \int d^3k\left[2i\kappa||\vec{k}||\underset{\sim}{\delta\tau}(-\vec{k},0)\hat{k}^b\underset{\sim}{p}_b(\vec{k},0)\right] \\ &- \int_{\mathbb{R}^3}\frac{d^3k}{||\vec{k}||^2}\Bigg\{ - :\underset{\sim}{\hat{p}}_c(\vec{k},0)\,\underset{\sim}{\hat{p}}_d(-\vec{k},0):\left[\delta^{cd} - \frac{1}{4}\hat{k}^c\hat{k}^d\right] + :\underset{\sim}{\hat{\epsilon}}(\vec{k},0)\,\underset{\sim}{\hat{\epsilon}}(-\vec{k},0):\left[\frac{1}{4}+\frac{3}{2}\right] \\ &\qquad - \frac{3}{2}m^2\,:\underset{\sim}{\hat{\widetilde{V}}}(\vec{k},0)\,\underset{\sim}{\hat{\epsilon}}(-\vec{k},0): - :\underset{\sim}{\hat{\varphi}}{}^a_a(\vec{k},0)\,\underset{\sim}{\hat{\epsilon}}(-\vec{k},0):\Bigg\}. \end{aligned} \tag{8.13}$$

We realise that the parameters $\delta\tau$ and $\delta\sigma^c$ enter into the self-interaction operator U of the scalar field only. For our choice of $\delta\tau$ in (7.51), where $\delta\tau$ is linear in t, the term including $\delta\tau$ drops out completely. The same happens for all contributions involving $\delta\sigma^c$ if we choose it to be constant. In case we choose it to be linear in x^c, we have $\delta\sigma^c_{,a} = \delta^a_c$ and hence the corresponding contributions in Fourier space will not vanish, but x^c will also not enter explicitly into the self-interaction operator U.

Here we introduced several new operators involved in the physical Hamiltonian operator of the model based on the definitions in (7.110). First of all a (normal-ordered) operator corresponding to the scalar field's momentum density:

$$\begin{aligned} \underset{\sim}{\hat{p}}_a(\vec{k},t) :=& \frac{1}{2}\int_{\mathbb{R}^3}\frac{d^3q}{(2\pi)^{\frac{3}{2}}}q_a\sqrt{\frac{\omega_{k-q}}{\omega_q}}\Big[a_q a_{k-q}e^{-it(\omega_q+\omega_{k-q})} + a^\dagger_{-q}a_{k-q}e^{-it(\omega_{k-q}-\omega_q)} \\ &- a^\dagger_{q-k}a_q e^{it(\omega_{k-q}-\omega_q)} - a^\dagger_{-q}a^\dagger_{q-k}e^{it(\omega_q+\omega_{k-q})}\Big]. \end{aligned} \tag{8.14}$$

Additionally, an operator corresponding to the scalar field's energy density:

$$\begin{aligned} \underset{\sim}{\hat{\epsilon}}(\vec{k},t) :=& \frac{1}{4}\int_{\mathbb{R}^3}\frac{d^3q}{(2\pi)^{\frac{3}{2}}}\Bigg\{ - \sqrt{\omega_q\omega_{k-q}}\Big[a_q a_{k-q}e^{-it(\omega_q+\omega_{k-q})} - a^\dagger_{-q}a_{k-q}e^{-it(\omega_{k-q}-\omega_q)} \\ &\qquad - a^\dagger_{q-k}a_q e^{it(\omega_{k-q}-\omega_q)} + a^\dagger_{-q}a^\dagger_{q-k}e^{it(\omega_q+\omega_{k-q})}\Big] \\ &- \frac{q_a(k^a-q^a)-m^2}{\sqrt{\omega_q\omega_{k-q}}}\Big[a_q a_{k-q}e^{-it(\omega_q+\omega_{k-q})} + a^\dagger_{-q}a_{k-q}e^{-it(\omega_{k-q}-\omega_q)} \\ &\qquad + a^\dagger_{q-k}a_q e^{it(\omega_{k-q}-\omega_q)} + a^\dagger_{-q}a^\dagger_{q-k}e^{it(\omega_q+\omega_{k-q})}\Big]\Bigg\}. \end{aligned} \tag{8.15}$$

Finally, two more operators that correspond to certain different terms of the scalar field's energy momentum tensor that appear in the classical Hamiltonian, namely to ϕ^2 and $\partial_a\phi\,\partial^b\phi$:

$$\begin{aligned} \underset{\sim}{\hat{\widetilde{V}}}(\vec{k},t) :=& \frac{1}{2}\int_{\mathbb{R}^3}\frac{d^3q}{(2\pi)^{\frac{3}{2}}}\frac{1}{\sqrt{\omega_q\omega_{k-q}}}\Big[a_q a_{k-q}e^{-it(\omega_q+\omega_{k-q})} + a^\dagger_{-q}a_{k-q}e^{-it(\omega_{k-q}-\omega_q)} \\ &+ a^\dagger_{q-k}a_q e^{it(\omega_{k-q}-\omega_q)} + a^\dagger_{-q}a^\dagger_{q-k}e^{it(\omega_q+\omega_{k-q})}\Big] \end{aligned} \tag{8.16}$$

$$\underset{\sim}{\hat{\varphi}}{}_a^b(\vec{k},t) := -\frac{1}{2}\int_{\mathbb{R}^3}\frac{d^3q}{(2\pi)^{\frac{3}{2}}}\frac{q_a(k-q)^b}{\sqrt{\omega_q\omega_{k-q}}}\Big[a_q a_{k-q}e^{-it(\omega_q+\omega_{k-q})} + a^\dagger_{-q}a_{k-q}e^{-it(\omega_{k-q}-\omega_q)} + a^\dagger_{q-k}a_q e^{it(\omega_{k-q}-\omega_q)} + a^\dagger_{-q}a^\dagger_{q-k}e^{it(\omega_q+\omega_{k-q})}\Big]. \tag{8.17}$$

Note that all these constituents are symmetric in the sense that $\underset{\sim}{\epsilon}{}^\dagger(-\vec{k},t) = \underset{\sim}{\epsilon}(\vec{k},t)$, which implies $\epsilon^\dagger(\vec{x},t) = \epsilon(\vec{x},t)$, and hence also $U^\dagger = U$. In the interaction picture, which we denote by a tilde, the Hamiltonian operator that involves the gravity-matter interaction is given by

$$\widetilde{H}(t) = \underbrace{\sqrt{\kappa}\,\frac{1}{\sqrt{2}}\int d^3k\frac{1}{\sqrt{\Omega_k}}\sum_r\Big[b^r_k\,e^{-i\Omega_k t}\,J^\dagger_r(\vec{k},t) + (b^r_k)^\dagger\,e^{i\Omega_k t}\,J_r(\vec{k},t)\Big]}_{=:\widetilde{H}_{TI}(t)} + \kappa\widetilde{U}(t)\otimes\mathbb{1}_{\mathcal{E}} \tag{8.18}$$

with an appropriate current operator obtained directly from the one in the Schrödinger picture by using the time-dependent constituents,

$$\begin{aligned} J_r(\vec{k},t) :=& \underset{\sim}{\hat{\varphi}}{}_a^b(\vec{k},t)[P^r(\vec{k})]^a_b \\ =& \int\frac{d^3p}{(2\pi)^{\frac{3}{2}}}\frac{1}{2\sqrt{\omega_p\omega_{k+p}}}\Big[p_a p^b[P^r(\vec{k})]^a_b\Big]\Big(a^\dagger_p a_{k+p}e^{it(\omega_p-\omega_{k+p})} + a_{-p}a_{k+p}e^{-it(\omega_p+\omega_{k+p})} \\ &+ a^\dagger_{-p-k}a_{-p}e^{it(\omega_{k+p}-\omega_p)} + a^\dagger_p a^\dagger_{-p-k}e^{it(\omega_p+\omega_{k+p})}\Big), \end{aligned} \tag{8.19}$$

and the total normal-ordered self-interaction operator

$$\begin{aligned} \widetilde{U}(t) :=& \int d^3k\frac{ik_b}{2}\kappa\underset{\sim}{\delta\sigma}{}^a(-\vec{k},t)\Big[\underset{\sim}{\varphi}{}^b_a(\vec{k},t) - \delta^b_a\Big(\underset{\sim}{\varphi}{}^c_c(\vec{k},t) + m^2\underset{\sim}{\widetilde{V}}(\vec{k},t) - \underset{\sim}{\epsilon}(\vec{k},t)\Big)\Big] \\ &- \int d^3k\Big[2i\kappa||\vec{k}||\underset{\sim}{\delta\tau}(-\vec{k},t)\hat{k}^b\underset{\sim}{p}{}_b(\vec{k},t)\Big] \\ &- \int_{\mathbb{R}^3}\frac{d^3k}{||\vec{k}||^2}\Big\{-:\underset{\sim}{\hat{p}}{}_c(\vec{k},t)\,\underset{\sim}{\hat{p}}{}_d(-\vec{k},t):\Big[\delta^{cd} - \frac{1}{4}\hat{k}^c\hat{k}^d\Big] + :\underset{\sim}{\hat{\epsilon}}(\vec{k},t)\,\underset{\sim}{\hat{\epsilon}}(-\vec{k},t):\Big[\frac{1}{4}+\frac{3}{2}\Big] \\ &- \frac{3}{2}m^2:\underset{\sim}{\hat{\widetilde{V}}}(\vec{k},t)\,\underset{\sim}{\hat{\epsilon}}(-\vec{k},t):-:\underset{\sim}{\hat{\varphi}}{}^a_a(\vec{k},t)\,\underset{\sim}{\hat{\epsilon}}(-\vec{k},t):\Big\}. \end{aligned} \tag{8.20}$$

With this, the classical model has been carried over to the quantum field theoretical framework. In the next section, we will derive the master equation that governs the effective time evolution of the matter system without the need of tracking all the details of the gravitational degrees of freedom.

9. Field theoretical TCL master equation and analysis

The content of this section was already published in [1] and is partially based on results of the Master's thesis [5], where however no thermal Wightman functions or propagators where used and also no split of the full dissipator into Lamb-shift Hamiltonian and new dissipator. It is presented here with slight modifications compared to [1] to adapt it to the flow of the thesis.
In this section, we apply the projection operator method reviewed in subsection 4 to the model discussed in this part of the thesis. Assuming factorising initial conditions and a Gibbs state for the environment, we can take the TCL master equation (4.33) to second order in the coupling strength $\alpha = \sqrt{\kappa}$ and evaluate it for the model under consideration described by the interaction Hamiltonian operator shown in (8.18):

$$\frac{\partial}{\partial t}\widetilde{\rho}_S(t) = -i\kappa\left[\widetilde{U}(t), \widetilde{\rho}_S(t)\right] - \kappa\int_0^t ds\; tr_{\mathcal{E}}\left\{\left[\widetilde{H}_{TI}(t), \left[\widetilde{H}_{TI}(s), \widetilde{\rho}_S(t)\otimes\rho_{\mathcal{E}}\right]\right]\right\}. \tag{9.1}$$

To obtain the final master equations, we have to evaluate the trace over the environmental degrees of freedom in this expression and thus to obtain the correlation functions. As a first step, we take into account that the second term on the right hand side of equation (9.1) can be written in terms of thermal Wightman functions, using the expression of $\widetilde{H}_{TI}(t)$ in position space given by

$$\widetilde{H}_{TI}(t) = \sqrt{\kappa}\int_{\mathbb{R}^3} d^3x\; \delta^i_b\; \varphi^b_a(\vec{x},t)\; \delta\mathcal{E}^a{}_i(\vec{x},t)\,, \tag{9.2}$$

where $\varphi^b_a(\vec{x},t)$ denotes the three dimensional Fourier transforms of $\underset{\sim}{\varphi}{}^b_a(\vec{k},t)$ which was defined in (8.17). Following the procedure outlined in [145], where in our case the environmental part of the interaction is linear in the environmental fields and we use a Gibbs state for the environment, hence all one-point correlation functions vanish, we can define the thermal Wightman functions:

$$G^{>a\;b}_{\;\;i\;\;j}(\vec{x}-\vec{y},t-s) := \left\langle \delta\mathcal{E}^a{}_i(\vec{x},t)\;\delta\mathcal{E}^b{}_j(\vec{y},s)\right\rangle_{\varepsilon} = P^{a\;b}_{\;\;i\;\;j}\,G^{>}(\vec{x}-\vec{y},t-s) \tag{9.3}$$

$$G^{<a\;b}_{\;\;i\;\;j}(\vec{x}-\vec{y},t-s) := \left\langle \delta\mathcal{E}^b{}_j(\vec{y},s)\;\delta\mathcal{E}^a{}_i(\vec{x},t)\right\rangle_{\varepsilon} = P^{a\;b}_{\;\;i\;\;j}\,G^{<}(\vec{x}-\vec{y},t-s) = G^{>a\;b}_{\;\;i\;\;j}(\vec{y}-\vec{x},s-t)\,, \tag{9.4}$$

where $\left\langle\,\cdot\,\right\rangle_{\varepsilon}$ denotes the expectation value with respect to a thermal Gibbs state and $P^{a\;b}_{\;\;i\;\;j}$ is the transverse-traceless projector given in (7.67). We will prove these equalities in a moment below. Before we can evaluate this explicitly, we have to discuss an important point regarding the Gibbs state for the environment on the Fock space: Since this is not well defined, we would need to work with KMS states [162, 163] or alternatively regularise the system within a finite volume. Here, we follow the latter technique. For this purpose, we put the system into a box of volume $V = L^3$ allowing us to explicitly evaluate the thermal two-point functions and further identities that we will encounter during the derivation of the master equation. This kind of regularisation leads to the discreteness of modes that belong to the set $\mathbb{K}$ now and to a replacement of the operator-valued distributions by operators:

$$\int_{\mathbb{R}^3}\frac{d^3k}{(2\pi)^3} \longrightarrow \frac{1}{V}\sum_{\vec{k}\in\mathbb{K}} \qquad\qquad b^r_k \longrightarrow \sqrt{\frac{V}{(2\pi)^3}}\;b^r_{\vec{k}}\,, \tag{9.5}$$

where a rescaling of the operators was introduced in order to keep the exponential $e^{-\beta H_\mathcal{E}}$ dimensionless in the regularised model:

$$e^{-\beta H_\mathcal{E}} = \exp\left\{-\beta \sum_{r\in\{+,-\}} \sum_{\vec{k}\in\mathbb{K}} \Omega_{\vec{k}} \left[(b^r_{\vec{k}})^\dagger\, b^r_{\vec{k}}\right]\right\} . \tag{9.6}$$

The Gibbs state for the environment is then of the form

$$\rho_\mathcal{E} = Z_\mathcal{E}^{-1} e^{-\beta H_\mathcal{E}} \tag{9.7}$$

with the partition sum given by

$$Z_\mathcal{E} := tr_\mathcal{E}\left\{e^{-\beta H_\mathcal{E}}\right\} = \left[\prod_{j\in\mathbb{N}} \frac{1}{1-e^{-\beta\Omega_{\vec{k}_j}}}\right]^2 , \tag{9.8}$$

where the $j \in \mathbb{N}$ label the $\vec{k}_j \in \mathbb{K}$. Moreover, for the calculation we had to assume $\vec{k} = 0 \notin \mathbb{K}$, which corresponds to $\Omega_{\vec{k}} = 0$ and is the usual infrared divergence. More details on computing this partition sum can be found in Appendix B. After performing calculation in this regularisation, we remove the regulator by taking the limit $L \to \infty$.
With this regularisation, the thermal Wightman functions (9.3) and (9.4) can be computed explicitly:

$$\begin{aligned} G^{>a}{}_i{}^b{}_j(\vec{x}-\vec{y}, t-s) &= \langle \delta\mathcal{E}^a{}_i(\vec{x},t)\delta\mathcal{E}^b{}_j(\vec{y},s)\rangle_\varepsilon = tr_\mathcal{E}\left\{\delta\mathcal{E}^a{}_i(\vec{x},t)\delta\mathcal{E}^b{}_j(\vec{y},s)\rho_\mathcal{E}\right\} \\ &= \int \frac{d^3k d^3p}{2(2\pi)^3\sqrt{\Omega_k\Omega_p}} \sum_{r,u\in\{\pm\}} [P^{-r}(\vec{k})]^a_i [P^{-u}(\vec{p})]^b_j \\ &\qquad \cdot tr_\mathcal{E}\left\{\left[b^r_k e^{-i\Omega_k t + i\vec{k}\vec{x}} + (b^r_{-k})^\dagger e^{i\Omega_k t + i\vec{k}\vec{x}}\right]\left[b^u_p e^{-i\Omega_p s + i\vec{p}\vec{y}} + (b^u_{-p})^\dagger e^{i\Omega_p s + i\vec{p}\vec{y}}\right]\rho_\mathcal{E}\right\} , \end{aligned} \tag{9.9}$$

where $[P^{-r}(\vec{k})]^a_i := [P^{-r}(\vec{k})]^a_b \delta^b_i$. Using the explicit expression given above for the Gibbs state and the trace in the occupation number basis from Appendix B, we obtain the following results:

$$tr_\mathcal{E}\left\{b^r_k b^u_p \rho_\mathcal{E}\right\} = 0 \tag{9.10}$$

$$tr_\mathcal{E}\left\{b^r_k (b^u_{-p})^\dagger \rho_\mathcal{E}\right\} = \delta^{ru}\delta(\vec{k}+\vec{p}) tr_\mathcal{E}\left\{b^r_k (b^r_k)^\dagger \rho_\mathcal{E}\right\} = \delta^{ru}\delta(\vec{k}+\vec{p}) tr_\mathcal{E}\left\{[n^r_k+1]\rho_\mathcal{E}\right\} \tag{9.11}$$

$$tr_\mathcal{E}\left\{(b^r_{-k})^\dagger b^u_p \rho_\mathcal{E}\right\} = \delta^{ru}\delta(\vec{k}+\vec{p}) tr_\mathcal{E}\left\{(b^r_k)^\dagger b^r_k \rho_\mathcal{E}\right\} = \delta^{ru}\delta(\vec{k}+\vec{p}) tr_\mathcal{E}\left\{n^r_k \rho_\mathcal{E}\right\} \tag{9.12}$$

$$tr_\mathcal{E}\left\{(b^r_{-k})^\dagger (b^u_{-p})^\dagger \rho_\mathcal{E}\right\} = 0 . \tag{9.13}$$

Reinserting this back into the Wightman functions in (9.9) they simplify to

$$\begin{aligned} G^{>a}{}_i{}^b{}_j(\vec{x}-\vec{y}, t-s) &= \int \frac{d^3k}{2(2\pi)^3\Omega_k} \sum_{r\in\{\pm\}} [P^{-r}(\vec{k})]^a_i [P^{-r}(-\vec{k})]^b_j \\ &\qquad \cdot \left[(tr_\mathcal{E}\left\{n^r_k\rho_\mathcal{E}\right\}+1)e^{-i\Omega_k(t-s)+i\vec{k}(\vec{x}-\vec{y})} + tr_\mathcal{E}\left\{n^r_k\rho_\mathcal{E}\right\} e^{-i\Omega_k(s-t)+i\vec{k}(\vec{y}-\vec{x})}\right] , \end{aligned} \tag{9.14}$$

where we can use (B.8):

$$N(\Omega_k) := tr_{\mathcal{E}}\left\{n_k^r\,\rho_{\mathcal{E}}\right\} = \frac{1}{e^{\beta\Omega_k}-1} = \frac{\coth\left(\frac{\beta\Omega_k}{2}\right)}{2} - \frac{1}{2}\,. \tag{9.15}$$

This result is independent of the polarisation, hence we can evaluate the sum over the polarisations separately and obtain the transverse-traceless projector

$$\sum_{r\in\{\pm\}} [P^{-r}(\vec{k})]_i^a [P^{-r}(-\vec{k})]_j^b = \underset{\frown}{P}^{a\ b}_{i\ j}(\vec{k})\,. \tag{9.16}$$

From this follows the last equality above in the Wightman function (9.3):

$$G^{>a\ b}_{\ i\ j}(\vec{x}-\vec{y},t-s) =: P^{a\ b}_{i\ j}\,G^{>}(\vec{x}-\vec{y},t-s) \tag{9.17}$$

with

$$\begin{aligned} G^{>}(\vec{x}-\vec{y},t-s) &= \int \frac{d^3k}{2(2\pi)^{\frac{3}{2}}\Omega_k}\left[(N(\Omega_k)+1)e^{-i\Omega_k(t-s)+i\vec{k}(\vec{x}-\vec{y})} + N(\Omega_k)\,e^{-i\Omega_k(s-t)+i\vec{k}(\vec{y}-\vec{x})}\right] \\ &= \int \frac{d^4k}{2(2\pi)^{\frac{3}{2}}\Omega_k}\left[(N(\Omega_k)+1)\delta(k^0-\Omega_k) + N(\Omega_k)\delta(k^0+\Omega_k)\right] e^{-ik^0(t-s)+i\vec{k}(\vec{x}-\vec{y})} \\ &= \int \frac{d^4k}{2(2\pi)^{\frac{3}{2}}\Omega_k}[N(k^0)+1]\left[\delta(k^0-\Omega_k)+\delta(k^0+\Omega_k)\right] e^{-ik^0(t-s)+i\vec{k}(\vec{x}-\vec{y})}\,, \end{aligned} \tag{9.18}$$

where we used that $N(-\Omega_k) = -[N(\Omega_k)+1]$. Defining

$$\rho^{>}(k^0,||\vec{k}||) = [1+N(k^0)]\rho(k^0,||\vec{k}||) \quad \text{and} \quad \rho(k^0,||\vec{k}||) = \sqrt{\frac{\pi}{2}}\frac{1}{\Omega_k}\left[\delta(k^0-\Omega_k)-\delta(k^0+\Omega_k)\right]\,,$$

we can write down the Wightman function in its spectral decomposition:

$$G^{>}(\vec{x}-\vec{y},t-s) = \int \frac{d^4k}{(2\pi)^{\frac{4}{2}}}\rho^{>}(k^0,||\vec{k}||)e^{-ik^0(t-s)+i\vec{k}(\vec{x}-\vec{y})}\,. \tag{9.19}$$

For $G^{<}(\vec{x}-\vec{y},t-s)$, defined as

$$G^{<a\ b}_{\ i\ j}(\vec{x}-\vec{y},t-s) =: P^{a\ b}_{i\ j}\,G^{<}(\vec{x}-\vec{y},t-s)\,, \tag{9.20}$$

a similar derivation yields

$$G^{<}(\vec{x}-\vec{y},t-s) = \int \frac{d^4k}{(2\pi)^{\frac{4}{2}}}\rho^{<}(k^0,||\vec{k}||)e^{-ik^0(t-s)+i\vec{k}(\vec{x}-\vec{y})} \tag{9.21}$$

with

$$\rho^{<}(k^0,||\vec{k}||) = N(k^0)\rho(k^0,||\vec{k}||)\,.$$

From this spectral decomposition of the Wightman functions it is immediately possible to see the additional effect caused by the finite temperature in the environment, evident by the presence of the Bose-Einstein distribution $N(k^0)$, which vanishes for zero temperature parameter $\Theta = \beta^{-1} =$

0 of the Gibbs state. As usual, the two thermal Wightman functions can be combined to build the thermal Feynman propagator:

$$\begin{aligned}
G^{(F)a}{}_{i}{}^{b}{}_{j}(\vec{x}-\vec{y},t-s) =& \left\langle \mathcal{T}_{\leftarrow}\, \delta\mathcal{E}^{a}{}_{i}(\vec{x},t)\, \delta\mathcal{E}^{b}{}_{j}(\vec{y},s)\right\rangle_{\varepsilon} \\
=& P^{a}{}_{i}{}^{b}{}_{j}\, G^{>}(\vec{x}-\vec{y},t-s)\theta(t-s) + P^{a}{}_{i}{}^{b}{}_{j}\, G^{<}(\vec{x}-\vec{y},t-s)\theta(s-t) \\
=& P^{a}{}_{i}{}^{b}{}_{j}\left[\theta(t-s)\int \frac{d^3k}{2(2\pi)^{\frac{3}{2}}\Omega_k} e^{-i\Omega_k(t-s)+i\vec{k}(\vec{x}-\vec{y})}\right. \\
&\left. \qquad + \theta(s-t)\int \frac{d^3k}{2(2\pi)^{\frac{3}{2}}\Omega_k} e^{-i\Omega_k(s-t)+i\vec{k}(\vec{y}-\vec{x})}\right] \\
&+ P^{a}{}_{i}{}^{b}{}_{j}\int \frac{d^3k}{(2\pi)^{\frac{3}{2}}\Omega_k} N(\Omega_k)\cos[(\Omega_k(t-s)-\vec{k}(\vec{x}-\vec{y})] \\
=& G^{(F)}_{\Theta=0}{}^{a}{}_{i}{}^{b}{}_{j}(\vec{x}-\vec{y},t-s) \\
&+ P^{a}{}_{i}{}^{b}{}_{j}\int \frac{d^3k}{(2\pi)^{\frac{3}{2}}\Omega_k} N(\Omega_k)\cos[(\Omega_k(t-s)-\vec{k}(\vec{x}-\vec{y})]\,, \qquad (9.22)
\end{aligned}$$

where $\theta(t)$ denotes the Heaviside step function which is one for non-negative arguments and zero otherwise. The first part is the ordinary Feynman propagator one obtains at a vanishing temperature parameter Θ, that is when the Gibbs state merges into a vacuum state, and the second part is the thermal contribution that obviously vanishes for $\Theta = 0$. In case of vanishing temperature parameter $\Theta = 0$, we obtain $N(\Omega_k) = 0$ and find the Green's function of the zero temperature case that takes the following form:

$$\begin{aligned}
&G^{(F)}_{\Theta=0}{}^{a}{}_{i}{}^{b}{}_{j}(\vec{x}-\vec{y},t-s) \\
&\quad = P^{a}{}_{i}{}^{b}{}_{j}\left[\theta(t-s)\int \frac{d^3k}{2(2\pi)^{\frac{3}{2}}\Omega_k} e^{-i\Omega_k(t-s)+i\vec{k}(\vec{x}-\vec{y})} + \theta(s-t)\int \frac{d^3k}{2(2\pi)^{\frac{3}{2}}\Omega_k} e^{-i\Omega_k(s-t)+i\vec{k}(\vec{y}-\vec{x})}\right] \\
&\quad = P^{a}{}_{i}{}^{b}{}_{j}\int_{\mathbb{R}^4} \frac{d^4k}{(2\pi)^{\frac{4}{2}}}\frac{i}{k^2+i\epsilon} e^{-ik^0(t-s)+i\vec{k}(\vec{x}-\vec{y})} \\
&\quad = P^{a}{}_{i}{}^{c}{}_{l}\, P^{b}{}_{j}{}^{e}{}_{m}\, \delta^{dl}\delta^{fm}\left[\delta_{ce}\delta_{df}+\delta_{cf}\delta_{de}-\delta_{cd}\delta_{ef}\right]\frac{1}{2}\int_{\mathbb{R}^4} \frac{d^4k}{(2\pi)^{\frac{4}{2}}}\frac{i}{k^2+i\epsilon} e^{-ik^0(t-s)+i\vec{k}(\vec{x}-\vec{y})}\,. \qquad (9.23)
\end{aligned}$$

Thus, the results is just given by the transverse-traceless projection of the spatial part of the graviton propagator in harmonic gauge, see for instance [164] for the explicit form of the graviton propagator. Note that we chose the integration contour in the second step such that we obtain the Feynman propagator. After a four dimensional Fourier transformation of the entire thermal Green's function and again choosing the Feynman prescription we obtain:

$$\underset{\smile}{G}^{(F)a}{}_{i}{}^{b}{}_{j}(p) = \underset{\smile}{P}^{a}{}_{i}{}^{b}{}_{j}(\vec{p})\left\{\frac{i}{p^\mu p_\mu + i\epsilon} + 2\pi N(\Omega_p)\delta(p^\mu p_\mu)\right\}, \qquad (9.24)$$

which indeed has the expected form, see for instance [165]. We will use this propagator in part III of the thesis, where we connect the one-particle projected master equation to Feynman diagrams. Note that the aspect that we obtain a decomposition into the ordinary Feynman propagator and

a thermal correction is caused by the fact that we use a mode expansion that involves a splitting into positive and negative frequency modes. As a consequence, normal ordered expectation values with respect to thermal states are in general non-vanishing as for instance $\langle b_k^\dagger b_k \rangle_\varepsilon = N(\Omega_k) \neq 0$. Vanishing expectation values of normal ordered products are usually an important property in the proof of Wick's theorem. Given that we are working with a Gaussian state for the environment and an interaction Hamiltonian being linear in the environmental fields, we can calculate the relevant expectation values in the model we consider directly without the use of Wick's theorem. However, for different and more complicated models the application of Wick's theorem might be advantageous and for this purpose it is often convenient to consider a different splitting than in the zero temperature case such that the expectation values of normal ordered products with respect to thermal states also vanish. A detailed discussion on possible splittings in this context as well as the relation between different choices of splittings is presented in [166].
Now we can write down the second term on the right side of in the master equation (9.1) in terms of the thermal Wightman functions:

$$\begin{aligned}
&\kappa \int_0^t ds\, tr_{\mathcal{E}} \left\{ \left[\widetilde{H}_{TI}(t), \left[\widetilde{H}_{TI}(s), \widetilde{\rho}_S(t) \otimes \rho_{\mathcal{E}} \right] \right] \right\} = \\
&= -\kappa \int_0^t ds \int_{\mathbb{R}^3} d^3x \int_{\mathbb{R}^3} d^3y \sum_{r\in\{\pm\}} \Big\{ \left[J_r(\vec{x},t), J_r(\vec{y},s)\widetilde{\rho}_S(t) \right] G^{>}(\vec{x}-\vec{y},t-s) \\
&\qquad\qquad + \left[\widetilde{\rho}_S(t) J_r(\vec{y},s), J_r(\vec{x},t) \right] G^{<}(\vec{x}-\vec{y},t-s) \Big\} . \qquad (9.25)
\end{aligned}$$

To continue, we define the quantities $D(\vec{k},t-s)$ and $D_1(\vec{k},t-s)$, the three-dimensional Fourier transforms of the dissipation and noise kernels $D(\vec{x},t-s)$ and $D_1(\vec{x},t-s)$, related to the commutator's and anticommutator's correlation functions and also to the thermal Wightman functions $G^{>}(\vec{x}-\vec{y},t-s)$ and $G^{<}(\vec{x}-\vec{y},t-s)$ in the following manner:

$$\begin{aligned}
\left[\delta\mathcal{E}^a{}_i(\vec{x},t), \delta\mathcal{E}^b{}_j(\vec{y},s) \right] &= P^a{}_i{}^b{}_j \left[G^{>}(\vec{x}-\vec{y},t-s) - G^{<}(\vec{x}-\vec{y},t-s) \right] \\
&= i P^a{}_i{}^b{}_j \int_{\mathbb{R}^3} \frac{d^3k}{(2\pi)^{\frac{3}{2}}} e^{i\vec{k}(\vec{x}-\vec{y})}\, D(\vec{k},t-s) \qquad (9.26) \\
tr_{\mathcal{E}} \left(\left\{ \delta\mathcal{E}^a{}_i(\vec{x},t), \delta\mathcal{E}^b{}_j(\vec{y},s) \right\} \right) &= P^a{}_i{}^b{}_j \left[G^{>}(\vec{x}-\vec{y},t-s) + G^{<}(\vec{x}-\vec{y},t-s) \right] \\
&= P^a{}_i{}^b{}_j \int_{\mathbb{R}^3} \frac{d^3k}{(2\pi)^{\frac{3}{2}}} e^{i\vec{k}(\vec{x}-\vec{y})}\, D_1(\vec{k},t-s) , \qquad (9.27)
\end{aligned}$$

where we used that for the model considered here the commutator in the first equation is proportional to the identity operator and thus can be pulled out of the trace. The direct computation then yields

$$D(\vec{k},t-s) := -\frac{\sin(\Omega_k(t-s))}{\Omega_k} \qquad (9.28)$$

$$D_1(\vec{k},t-s) := \left[2N(\Omega_k)+1 \right] \frac{\cos(\Omega_k(t-s))}{\Omega_k} . \qquad (9.29)$$

Using these definitions, we obtain in Schrödinger picture the following TCL master equation for the system density operator $\rho_S(t)$:

$$\begin{aligned}\frac{\partial}{\partial t}\rho_S(t) =& -i\,[H_S + \kappa\, U, \rho_S(t)] \\ &- \frac{\kappa}{2}\int_0^t ds \sum_r \int_{\mathbb{R}^3} d^3k \,\Big\{ iD(\vec{k}, t-s)\Big[J_r(\vec{k}), \Big\{J_r(-\vec{k}, s-t), \rho_S(t)\Big\}\Big] \\ &\qquad + D_1(\vec{k}, t-s)\Big[J_r(\vec{k}), \Big[J_r(-\vec{k}, s-t), \rho_S(t)\Big]\Big]\Big\} \end{aligned} \tag{9.30}$$

with the matter system's Hamiltonian operator

$$H_S := \int_{\mathbb{R}^3} d^3k\, \omega_k\, a_k^\dagger\, a_k \tag{9.31}$$

as well as the operator U for the gravitational self-interaction of the scalar field that was defined in (8.13), the operator-valued distribution $J_r(\vec{k}, t)$ defined in (8.19) and $J_r(\vec{k}) = J_r(\vec{k}, 0)$.
To facilitate the comparison of our results with those already existing in the literature like for instance the ones in [60, 62, 63], it is of advantage to rewrite the master equation in (9.30) in two equivalent ways. The first alternative and equivalent form is given by

$$\begin{aligned}\frac{\partial}{\partial t}\rho_S(t) =& -i\,[H_S + \kappa\, U, \rho_S(t)] \\ &+ \frac{\kappa}{4}\int d^3k \sum_r \Bigg\{ \frac{\coth\left(\frac{\beta\Omega_k}{2}\right)}{\Omega_k}\Big[J_r(\vec{k}), \Big[\rho_S(t), \widetilde{J}_r^\dagger(\vec{k}, t)\Big]\Big] + \text{h.c.} \\ &\qquad + \frac{1}{\Omega_k}\Big[J_r(\vec{k}), \Big\{\rho_S(t), \widetilde{J}_r^\dagger(\vec{k}, t)\Big\}\Big] + \text{h.c.}\Bigg\}, \end{aligned} \tag{9.32}$$

with

$$\widetilde{J}_r(\vec{k}, t) := \int_0^t ds\; e^{-i\Omega_k(t-s)} J_r(\vec{k}, s-t) \tag{9.33}$$

and where h.c. denotes the Hermitian conjugate. This form of the master equation is similar to the master equations derived in [60] and [63]. While the first reference investigates also a model where a scalar field is coupled to linearised gravity, the second one replaces the scalar field by a photon field. Let us briefly discuss the similarities and difference of these models and the one considered here: At the classical level, one of the main difference is that we formulate the model in terms of Ashtekar variables whereas the models in [60, 63] are based on ADM variables. Thus, we have to deal with an additional Gauß constraint in the model that also needs to be taken into account when gauge invariance is considered. While we presented a way to work with a gauge invariant formulation of the classical theory by means of constructing suitable Dirac observables and also showed that one can construct a canonical transformation on the original phase space that provides a natural separation of the physical and gauge sector of the phase space by the transformation in section 7.7, in the papers [60, 63] a specific gauge fixing and another attempt to construct observables is used to eliminate the gauge degrees of freedom, see the discussion in section 7.9.1. Furthermore, we consider a standard boundary term [148] that ensures that the action in terms of Ashtekar variables as well as its variation are well defined and we expect that the corresponding ADM boundary term should be included in the formulation of the models in

[60, 63] as well. Note that in our case the boundary terms cancel the term in $\delta\mathbf{H}_{\text{can}}$ that is linear in the linearised geometric contribution to the Hamiltonian constraint and the remaining matter part combines with the $\frac{1}{\kappa}$ in front of the action to the energy density of the scalar field in κ^0 order. In contrast, in [60, 63] no perturbations of linear order have been considered in the canonical Hamiltonian but the κ^0 order is present. Therefore, effects of the missing boundary term cannot be seen in the final master equation when comparing the two results.
For the quantised model let us comment on the work in [63] and [60] separately, starting with the latter. One difference in the Hamiltonian operator in our result and the one in [60] is the form of the self-interaction part because we choose a different normal ordering compared to [60]. We chose to normal order the entire self-interaction part of the Hamiltonian operator, whereas in [60] only the individual contributions $\underset{\smile}{\hat{p}}_a$, $\underset{\smile}{\hat{\epsilon}}$, $\underset{\smile}{\hat{\tilde{V}}}$ and $\underset{\smile}{\hat{\varphi}}^a_b$ were normal ordered. Albeit the current operator valued distribution J_r defined in (8.12) is the same as in [60], it appears in their Hamiltonian (8.11) with a different factor of $\sqrt{2}$ compared to our coupling. This difference has no physical effect because it is absorbed at the level of the master equation for the following reason: The different factor of $\sqrt{2}$ arises because the Hamiltonian for the pure gravitational part contains an additional factor of $\frac{1}{2}$ when expressed in Ashtekar variables and working with $\delta\mathcal{E}$ and $\delta\mathcal{C}$ compared to the one in ADM variables in [60]. This leads to an additional factor $\frac{1}{\sqrt{2}}$ in our Fock quantised gravitational variables compared to the ADM variables. In addition, in terms of ADM variables the interaction term in the Hamiltonian density reads $-\frac{\kappa}{2}\delta h^{TT}_{ab}\, T^{ab}$ while in Ashtekar variables it is given by $+\kappa\delta\mathcal{E}^a{}_i\delta^{bi}\, T_{ab}$. This difference can be explained by the relation between ADM and Ashtekar variables. In the case of ADM variables, the gravitational physical degrees of freedom are given by the transverse-traceless components $\delta h^{TT}_{ab} := P^{cd}_{ab}\delta h_{cd}$ and the interaction reads $\delta h^{TT}_{ab}T^{ab}$ which is then quantised in [60] and the coupling of the gravitational gauge degrees of freedom to the energy momentum tensor is contained in the self-interaction part. In our case however, writing δh_{ab} in terms of the perturbed co-triad, that is $\delta h_{ab}(E) = -\delta^i_b\delta_{ac}\delta E^c{}_i - \delta^i_a\delta_{bc}\delta E^c{}_i + \delta_{ab}\delta^i_c\delta E^c{}_i$ and then using the symmetry of the energy-momentum tensor, we obtain $\delta h_{ab}(E)T^{ab} \to [-2\delta^i_a\delta_{bc} + \delta_{ab}\delta^i_c]\delta E^c{}_i T^{ab}$, where the gravitational physical degrees of freedom only enter in the first term and we obtain in the linearised theory just $-2\delta\mathcal{E}^a{}_i\,\delta^i_b T^b_a$. This difference already present in the classical Hamiltonian has no effect on the final equations of motion because with our convention the Poisson bracket between $\delta\mathcal{A}_a{}^i, \delta\mathcal{E}^a{}_i$ involves an additional factor of $\frac{1}{2}$ compared to the Poisson brackets used in [60, 63], cancelling the additional factor of 2. The minus sign is also cancelled because in our case the momentum variables couple to the energy momentum tensor whereas in [60, 63] the coupling is via configuration variables. This kind of cancellation carries of course over to the commutator at the quantum level.
A further difference is that the final master equation presented in [60] is of Lindblad form (3.14). This is a significant difference because, as we will show in the following, the master equation in (9.30) we obtain is not yet of Lindblad type (see section 3), but it requires further assumptions and approximations respectively to be of this form. For the purpose of discussing this, we rewrite the master equation in (9.30) in another equivalent form:

$$\begin{aligned}\frac{\partial}{\partial t}\rho_S(t) =& -i[H_S + \kappa\, U, \rho_S(t)] \\ &- \kappa\sum_r \int_{\mathbb{R}^3}\frac{d^3k}{2\Omega_k}\left\{[J_r^\dagger(\vec{k}), \widetilde{J}_r(\vec{k},t)\rho_S(t)] + N(\Omega_k)[J_r^\dagger(\vec{k}), [\widetilde{J}_r(\vec{k},t), \rho_S(t)]] + \text{h.c.}\right\}.\end{aligned} \tag{9.34}$$

In this form, one can clearly separate the dissipator into a part associated with zero temperature (terms without $N(\Omega_k)$) and a second part corresponding to finite temperature (terms including $N(\Omega_k)$). All three forms of the master equation derived in this part of the thesis are time-convolutionless. However, they cannot (yet) be brought into Lindblad form, as there are still time-dependent quantities apart from the reduced density operator itself present in the dissipator. Nevertheless, we can bring the master equation into a form which is similar to the first standard form introduced in (3.11) and which admits the splitting of the dissipator into a Lamb-shift Hamiltonian and a remaining contribution. To this extent, we start from the formulation in (9.34). First, we note that the J_r-operators can be split in the following way into pairs of creation and/or annihilation operator-valued distributions:

$$J_r(\vec{k}) = -\int \frac{d^3p}{(2\pi)^{\frac{3}{2}}} \sum_{a=1}^{4} j_r^a(\vec{k},\vec{p}) \tag{9.35}$$

$$\widetilde{J}_r(\vec{k},t) = -\int \frac{d^3p}{(2\pi)^{\frac{3}{2}}} \sum_{a=1}^{4} j_r^a(\vec{k},\vec{p})\; f(\Omega_k + \omega_a(\vec{k},\vec{p});t) \tag{9.36}$$

with

$$j_r^1(\vec{k},\vec{p}) := a_p^\dagger a_{k+p} \frac{1}{2\sqrt{\omega_p\omega_{k+p}}} \left[p_a p^b [P^{-r}(\vec{k})]_b^a\right] \qquad \omega_1(\vec{k},\vec{p}) := \omega_p - \omega_{k+p} \tag{9.37}$$

$$j_r^2(\vec{k},\vec{p}) := a_{-p-k}^\dagger a_{-p} \frac{1}{2\sqrt{\omega_p\omega_{k+p}}} \left[p_a p^b [P^{-r}(\vec{k})]_b^a\right] \qquad \omega_2(\vec{k},\vec{p}) := \omega_{k+p} - \omega_p \tag{9.38}$$

$$j_r^3(\vec{k},\vec{p}) := a_{-p} a_{k+p} \frac{1}{2\sqrt{\omega_p\omega_{k+p}}} \left[p_a p^b [P^{-r}(\vec{k})]_b^a\right] \qquad \omega_3(\vec{k},\vec{p}) := -\omega_p - \omega_{k+p} \tag{9.39}$$

$$j_r^4(\vec{k},\vec{p}) := a_p^\dagger a_{-k-p}^\dagger \frac{1}{2\sqrt{\omega_p\omega_{k+p}}} \left[p_a p^b [P^{-r}(\vec{k})]_b^a\right] \qquad \omega_4(\vec{k},\vec{p}) := \omega_p + \omega_{k+p} \tag{9.40}$$

and

$$f(\omega;t) := \int_0^t ds\; e^{-i\omega(t-s)} = \frac{i}{\omega}(e^{-i\omega t} - 1)\,. \tag{9.41}$$

Using this expansion in (9.34), the dissipator can be rewritten as

$$\mathcal{D}[\rho_S] = \frac{\kappa}{2} \sum_{r;a,b} \int_{\mathbb{R}^3} \frac{d^3k\, d^3p\, d^3l}{(2\pi)^{\frac{6}{2}}} \left\{ \Delta_{ab}(\vec{p},\vec{l};\vec{k},t) \left[j_r^b(\vec{k},\vec{l})\rho_S(t), j_r^a(\vec{k},\vec{p})^\dagger \right] + h.c. \right\}. \tag{9.42}$$

with

$$\begin{aligned} \Delta_{ab}(\vec{p},\vec{l};\vec{k},t) :=& \frac{1}{\Omega_k} \left[(N(\Omega_k)+1)\; f(\Omega_k + \omega_b(\vec{k},\vec{l});t) + N(\Omega_k)\; f(-\Omega_k + \omega_b(\vec{k},\vec{l});t) \right] \\ =& 2\int_0^t ds\; G^{>}(\vec{k},t-s) e^{-i\omega_b(\vec{k},\vec{l})(t-s)}\,, \end{aligned} \tag{9.43}$$

where $G^{>}(\vec{k}, t-s)$ denotes the three dimensional Fourier transform of the Wightman function $G^{>}(\vec{x}-\vec{y}, t-s)$. Combining the new coefficient functions in the following form

$$\begin{aligned} S_{ab}(\vec{p},\vec{l};\vec{k},t) &:= \frac{1}{2i}\left(\Delta_{ab}(\vec{p},\vec{l};\vec{k},t) - \Delta^{*}_{ba}(\vec{l},\vec{p};\vec{k},t)\right) \\ &= \frac{1}{2\Omega_k}\Bigg[[N(\Omega_k)+1]\left\{\frac{e^{-i(\Omega_k+\omega_b(\vec{k},\vec{l}))t}-1}{\Omega_k+\omega_b(\vec{k},\vec{l})} + \frac{e^{i(\Omega_k+\omega_a(\vec{k},\vec{p}))t}-1}{\Omega_k+\omega_a(\vec{k},\vec{p})}\right\} \\ &\qquad - N(\Omega_k)\left\{\frac{e^{i(\Omega_k-\omega_b(\vec{k},\vec{l}))t}-1}{\Omega_k-\omega_b(\vec{k},\vec{l})} + \frac{e^{-i(\Omega_k-\omega_a(\vec{k},\vec{p}))t}-1}{\Omega_k-\omega_a(\vec{k},\vec{p})}\right\}\Bigg] \end{aligned} \tag{9.44}$$

$$\begin{aligned} R_{ab}(\vec{p},\vec{l};\vec{k},t) &:= \Delta_{ab}(\vec{p},\vec{l};\vec{k},t) + \Delta^{*}_{ba}(\vec{l},\vec{p};\vec{k},t) \\ &= \frac{i}{\Omega_k}\Bigg[[N(\Omega_k)+1]\left\{\frac{e^{-i(\Omega_k+\omega_b(\vec{k},\vec{l}))t}-1}{\Omega_k+\omega_b(\vec{k},\vec{l})} - \frac{e^{i(\Omega_k+\omega_a(\vec{k},\vec{p}))t}-1}{\Omega_k+\omega_a(\vec{k},\vec{p})}\right\} \\ &\qquad - N(\Omega_k)\left\{\frac{e^{i(\Omega_k-\omega_b(\vec{k},\vec{l}))t}-1}{\Omega_k-\omega_b(\vec{k},\vec{l})} - \frac{e^{-i(\Omega_k-\omega_a(\vec{k},\vec{p}))t}-1}{\Omega_k-\omega_a(\vec{k},\vec{p})}\right\}\Bigg], \end{aligned} \tag{9.45}$$

we can split the dissipator into two parts:

$$\mathcal{D}[\rho_S] = -i\kappa[H_{LS}, \rho_S(t)] + \mathcal{D}_{\text{first}}[\rho_S] \tag{9.46}$$

with the Lamb-shift Hamiltonian operator

$$H_{LS} := \frac{1}{2}\int \frac{d^3k\, d^3p\, d^3l}{(2\pi)^{\frac{6}{2}}} \sum_{r;a,b} S_{ab}(\vec{p},\vec{l};\vec{k},t)\; j_r^a(\vec{k},\vec{p})^{\dagger}\, j_r^b(\vec{k},\vec{l}) \tag{9.47}$$

and a new dissipator term being in a form similar to the first standard form:

$$\begin{aligned} \mathcal{D}_{\text{first}}[\rho_S] := \frac{\kappa}{2}\int \frac{d^3k\, d^3p\, d^3l}{(2\pi)^{\frac{6}{2}}} \sum_{r;a,b} R_{ab}(\vec{p},\vec{l};\vec{k},t)\Bigg(& j_r^b(\vec{k},\vec{l})\rho_S(t) j_r^a(\vec{k},\vec{p})^{\dagger} \\ & - \frac{1}{2}\left\{ j_r^a(\vec{k},\vec{p})^{\dagger} j_r^b(\vec{k},\vec{l}), \rho_S(t)\right\}\Bigg), \end{aligned} \tag{9.48}$$

where the label 'first' refers to the dissipator in first standard form. The difference to the first standard form shown in (3.11) is that the coefficient function R_{ab} is still time-dependent and thus the corresponding master equation is not of Lindblad type. Often, a Lindblad form can be obtained for a given master equation by applying the second Markov approximation, that is by formally sending the upper limit of the integral involved in (9.43) or directly t in (9.44) and (9.45) to infinity leading to time-independent coefficients. Applying the second Markov approximation[12] for the model considered here is less trivial than in for instance some of the standard decoherence

[12] An example of a model where the second Markov approximation cannot be applied can be found in [167]. The reason here is that the chosen environmental operators are non-dynamical, yielding correlation functions with no dependence on the temporal coordinate. In the model in [167] this results in a set of effective system operators in the final master equation that depend linearly on the temporal coordinate preventing them from applying the second Markov approximation.

models in quantum mechanics discussed for instance in [45], because in the limit in which we send the upper limit of the temporal integral to infinity, we can no longer work with ordinary functions but need to consider distributions along the lines of [168]. Combined with the fact that the result obtained from the remaining integration over all modes might not have the properties ordinary test functions have, it requires a careful analysis how this limit can be taken in general. Therefore, we will analyse this approximation together with the remaining integration over the modes in detail for a single scalar particle in part III of this thesis.
If we ignore such subtleties for the moment and simply send t formally to infinity, then the master equation from [60] coincides structurally with the one in (9.32) apart from the explicit form of their last term, which is is given by $\{J_r, [\rho_S, \widetilde{J}_r^\dagger]\} + h.c.$. In contrast in our derivation we actually end up with $[J_r, \{\rho_S, \widetilde{J}_r^\dagger\}] + h.c.$, which yields different terms and from our calculation we do not see a way how their result can be reproduced. In [60] no detailed derivation of this result is presented but the authors cite [45], where however also such terms are not involved in the master equations.
As already mentioned, the master equation in [63] involves a photon field instead of a scalar field and thus the projectors involved are those that project on the physical degrees of freedom of the photon field. Most of the differences have already been pointed out above because the procedure in [63] is quite similar to the one followed in [60]. Compared to [60], more details on the derivation of the Lindblad equation are presented in [63] and it is derived by means of a Born-Markov and a (weak) rotating wave approximation, which will be discussed in more detail in part III. The form of their master equation after the Born-Markov approximation is structurally the same as the one in (9.32), also the commutator-anticommutator structure agrees.
Note that the master equation in (9.34) looks, apart from the expected differences due to their usage of ADM variables, similar to the one derived in [62], where a Dirac quantisation was carried out and the physical degrees of freedom were identified by imposing the gauge conditions in the quantum theory and specialising to the transverse-traceless degrees of freedom. In a second step, they then derived a master equation using the influence functional approach (see e.g. [45] for an introduction) for a general bosonic field. Their final master equation is a TCL master equation that, similar to the result derived in this paper, does also not exhibit Lindblad form.
The physical investigation of the final master equation is complex, as the equation is in general not completely positive, in contrast to an equation of Lindblad type. Apart from applying a second Markov approximation in order to arrive at second standard form, it is required to diagonalise the coefficient functions with respect to the labels $(a, \vec{p})$ and $(b, \vec{l})$. In this context, an application of a rotating wave approximation is beneficial, as it has for instance been used in [63]. For the model considered in our work this needs a further detailed analysis because applying the above-proposed additional approximations to cast it into a completely positive form, one looses in general some features of the dynamics of the system. This will be analysed in detail when performing the one-particle projection of the master equation in part III.

Part III.
Gravitationally induced decoherence on a single scalar particle: from field theory to quantum mechanics

The time-convolutionless master equation for a scalar field with an environment of linearised gravity, which was derived in the previous section, still makes it complicated to extract physical predictions from it. This originates in several points: firstly, its field theoretical structure makes a connection to physical systems that are considered in experiments rather hard. Secondly, it is not yet in a completely positive form, hence it might lead to unphysical negative probabilities. Thirdly, its underlying classical model was quantised in a Fock quantisation, hence the corresponding quantum field theory contains in general divergent terms when computing scattering amplitudes which have to be renormalised before one can draw physical conclusions from it and this issue is inherited to the master equation. In this part of the thesis, we tackle these problems by considering a one-particle projection of the TCL master equation.

10. Projection of the field theoretical master equation on the one-particle space

The content of this section was already published in [2]. Here, it is presented with some modifications compared to [2] to adapt it to the flow of the thesis.

In this section, we discuss how such a master equation for a single scalar particle can be obtained starting with the final field theoretical master equation from the previous part with the dissipator given in (9.46):

$$\frac{\partial}{\partial t}\rho_S(t) = -i[H_S + \kappa\, U + \kappa\, H_{LS}, \rho_S(t)] + \mathcal{D}_{\text{first}}[\rho_S(t)]\,, \tag{10.1}$$

where $\rho_S(t)$ denotes the density matrix of the scalar field and $\kappa = \frac{8\pi G_N}{c^4}$ the coupling constant between gravity and matter in general relativity with Newton's gravitational constant G_N and the speed of light c. Furthermore, there is the self-interaction U of the scalar field due to the presence of the gravitational field defined in (8.13), the Lamb-shift Hamiltonian H_{LS} defined in (9.47) and the dissipator $\mathcal{D}_{\text{first}}[\rho_S(t)]$, defined in (9.48), which is in a form similar to the first standard form (3.11) but still with time-dependent coefficients. When working with field theoretical master equations, such a one-particle projection is commonly applied to investigate some features of the master equation, see for instance the works in [60, 62, 63, 113]. There exist however different methods on how to perform this projection in detail. In [60, 62, 63] the procedure is carried out such that the final one-particle master equation is probability conserving, which requires to neglect some terms that would otherwise be present in a direct projection. In contrast, in [113] a different strategy based on Thermo Field Dynamics (TFD), which is a formulation of quantum field theory at finite temperature (see [169, 170] and for an introduction [171]), is employed, in which these terms still contribute to the one-particle master equation. Here we follow the method used in [60, 62, 63], but keep all possible terms and investigate their influence on the one-particle master equation. It will turn out that after applying an on-shell renormalisation and Markov approximation, they will not play any role for decoherence, but will remove the remaining contribution of the Lamb-shift-like term to the unitary evolution after the rotating wave approximation has been applied.

To obtain the one-particle projection of the master equation in (10.1), we replace the density matrix with the corresponding density matrix for a single particle in momentum representation

$$\rho_1(t) = \int_{\mathbb{R}^3} d^3u \int_{\mathbb{R}^3} d^3v\; \rho(\vec{u},\vec{v},t)\; a_u^\dagger\, |0\rangle\, \langle 0|\, a_v \tag{10.2}$$

in the master equation and neglect all contributions that project out of the single particle space. In this formulation, $\rho(\vec{u},\vec{v},t)$ is the (quantum mechanical) density matrix of a single particle in momentum representation.
In the following we will analyse the corresponding individual contributions in (10.1) separately and further discuss the assumptions used in the model considered here as well as compare them to the existing literature.
The first term of the master equation, representing the evolution of a free scalar particle, can be computed immediately to yield

$$-i[H_S,\rho_1(t)] = -i\int_{\mathbb{R}^3} d^3u \int_{\mathbb{R}^3} d^3v\ (\omega_u-\omega_v)\rho(\vec{u},\vec{v},t)\, a_u^\dagger\ |0\rangle\langle 0|\, a_v\,. \tag{10.3}$$

The contribution of the second term depends on the structure of the form of the operator U. The detailed expression is given in part II in equation (8.13), for the analysis here it is however enough to use that U consists of different combinations of always four creation and/or annihilation operators for the scalar field, i.e.

$$\begin{aligned} U = \int d^2k_1 \int d^2k_2 \int d^2k_3 \int d^2k_4 \Big[&\zeta_1\, a_{k_1}a_{k_2}a_{k_3}a_{k_4} + \zeta_2\, a^\dagger_{k_1}a_{k_2}a_{k_3}a_{k_4} \\ &+ \zeta_3\, a_{k_1}a^\dagger_{k_2}a_{k_3}a_{k_4} + ... + \zeta_N\, a^\dagger_{k_1}a^\dagger_{k_2}a^\dagger_{k_3}a^\dagger_{k_4}\Big]\,, \end{aligned} \tag{10.4}$$

with the coefficient distributions $\zeta_i = \zeta_i(\vec{k}_1,\vec{k}_2,\vec{k}_3,\vec{k}_4)$ that contain delta distributions that relate some of the momenta. When applying normal ordering to this operator, as it is done in part II of this thesis, then it will not contribute after the one-particle projection: in the summands of U, where the number of creation operators is not equal to the number of annihilation operators, the resulting terms would project out of the one-particle space. In the other summands, there are exactly two creation and two annihilation operators which, when normal ordered, annihilate any one-particle state. In [60, 63] the normal ordering of U is applied differently: in their work the four annihilation and/or creation operators are normal ordered pairwise[13]. In that case contributions of the form $:a^\dagger_{k_1}a_{k_2}::a^\dagger_{k_3}a_{k_4}:$ preserve the one-particle space and thus still contribute after the one-particle projection. To distinguish these two types of operator orderings, we denote the first one, where U is normal ordered, total normal ordering, and the second one partial normal ordering. Here, we continue to consider a totally normal ordered Hamiltonian.
The third term, the Lamb-shift-like Hamiltonian, as well as the fourth contribution, the dissipator, both contain the same building blocks. To evaluate them, it is sufficient to consider the following three combinations:

$$\underbrace{j_r^A(\vec{k},\vec{p})^\dagger\, j_r^B(\vec{k},\vec{l})\,\rho_1(t)}_{(I)} \quad \text{and} \quad \underbrace{\rho_1(t)\, j_r^A(\vec{k},\vec{p})^\dagger\, j_r^B(\vec{k},\vec{l})}_{(II)} \quad \text{and} \quad \underbrace{j_r^B(\vec{k},\vec{l})\,\rho_1(t)\, j_r^A(\vec{k},\vec{p})^\dagger}_{(III)}, \tag{10.5}$$

where the $j_r^A(\vec{k},\vec{p})$ denote individual and different normal-ordered current operators labeled by $A\in\{1,2,3,4\}$ that carry a polarisation label $r\in\{\pm\}$ and two momentum arguments. These current operators were defined in detail starting in equation (9.37).
At this point arises the question whether we want to enforce trace preservation in the one-particle master equation, which corresponds to probability conservation. In [60, 62, 63] this is done, which

[13] The reasoning for this is that U arises as combinations of two operators that each contain two creation and/or annihilation operators, as can be seen from its definition in (8.13).

results in the exclusion of specific terms from the one-particle master equation. These terms can be identified from the general form of the master equation in (10.1) as we will discuss now: it is evident that when applying the trace the commutator vanishes and one is left with

$$\frac{\partial}{\partial t} tr\left\{\rho_S(t)\right\} = tr\left\{\mathcal{D}[\rho_S(t)]\right\} . \tag{10.6}$$

Inserting the definition of the dissipator given in equation (9.48) then yields

$$\begin{aligned}\frac{\partial}{\partial t} tr\left\{\rho_S(t)\right\} = \frac{\kappa}{2}\int \frac{d^3k\, d^3p\, d^3l}{(2\pi)^3} \sum_{r\in\{\pm\}} \sum_{A,B=1}^{4} R_{AB}(\vec{p},\vec{l};\vec{k},t) \\ \cdot tr\left\{ j_r^B(\vec{k},\vec{l})\rho_S(t) j_r^A(\vec{k},\vec{p})^\dagger - \frac{1}{2}\left\{ j_r^A(\vec{k},\vec{p})^\dagger j_r^B(\vec{k},\vec{l}), \rho_S(t)\right\}\right\} ,\end{aligned} \tag{10.7}$$

where the R_{AB} are time-dependent coefficients. When the current operators j_r^A are individually projected onto the one-particle space, due to the cyclicity of the trace all terms in the difference of the two traces are exactly canceled and one obtains a preserved trace of the density matrix, hence probability conservation. This is the approach used for instance in [60, 62, 63]. Another option is to apply the one-particle projection in such a way that each entire term in the master equation has to preserve the one-particle space. This is for instance done in [113], where two scalar fields are considered, one as the system and the other one as the environment. In this case there will remain terms in the one-particle projection of the product of two current operators in the last term of (10.7) that have no counterpart in the first term of (10.7) and thus will not cancel in the difference of the two traces.
To keep our analysis as generic as possible, we will include these terms in this work and investigate their effect in the one-particle master equation and denote this one-particle projection the extended one-particle projection. To take them into account in our further calculations, we will introduce a factor δ_P in these contributions to be able to switch between the extended one-particle projection ($\delta_P = 1$) and the non-extended one ($\delta_P = 0$).

It remains to work out the one-particle projection for the Lamb-shift Hamiltonian (9.47) and the dissipator (9.48) of the master equation in (10.1). As just discussed, they contain the same structures of operators (I)-(III) from equation (10.5). Hence, we start with the evaluation of these three kinds of terms and consider all possible combinations (a, b) that give a one-particle state after application. To keep track of all different combination in the three cases, we do this using a table. Considering only the creation and annihilation operator valued distributions $a_k^{(\dagger)}$ in the j-operators, we find:

(I)	$j_r^a(\vec{k},\vec{p})^\dagger\, j_r^b(\vec{k},\vec{l})\, a_u^\dagger \left\vert 0\right\rangle \left\langle 0\right\vert a_v$
(1,1)	$a_{k+p}^\dagger a_p a_l^\dagger a_{l+k} a_u^\dagger \left\vert 0\right\rangle \left\langle 0\right\vert a_v = \delta^3(\vec{l}+\vec{k}-\vec{u})\, a_{k+p}^\dagger a_p a_l^\dagger \left\vert 0\right\rangle \left\langle 0\right\vert a_v$
	$= \delta^3(\vec{p}+\vec{k}-\vec{u})\, \delta^3(\vec{p}-\vec{l})\, a_u^\dagger \left\vert 0\right\rangle \left\langle 0\right\vert a_v$
(1,2)	$a_{k+p}^\dagger a_p a_{-l-k}^\dagger a_{-l} a_u^\dagger \left\vert 0\right\rangle \left\langle 0\right\vert a_v = \delta^3(\vec{l}+\vec{u})\, \delta^3(\vec{p}+\vec{l}+\vec{k})\, a_u^\dagger \left\vert 0\right\rangle \left\langle 0\right\vert a_v$
(2,1)	$a_{-p}^\dagger a_{-p-k} a_l^\dagger a_{k+l} a_u^\dagger \left\vert 0\right\rangle \left\langle 0\right\vert a_v = \delta^3(\vec{k}+\vec{l}-\vec{u})\, \delta^3(\vec{p}+\vec{l}+\vec{k})\, a_u^\dagger \left\vert 0\right\rangle \left\langle 0\right\vert a_v$
(2,2)	$a_{-p}^\dagger a_{-p-k} a_{-l-k}^\dagger a_{-l} a_u^\dagger \left\vert 0\right\rangle \left\langle 0\right\vert a_v = \delta^3(\vec{l}+\vec{u})\, \delta^3(\vec{p}-\vec{l})\, a_u^\dagger \left\vert 0\right\rangle \left\langle 0\right\vert a_v$
(4,4)	$\delta_P\, a_{-k-p} a_p a_l^\dagger a_{-k-l}^\dagger a_u^\dagger \left\vert 0\right\rangle \left\langle 0\right\vert a_v = \delta_P\, (a)$ *see below*

(II)	$a_u^\dagger \left\vert 0\right\rangle \left\langle 0\right\vert a_v\, j_r^a(\vec{k},\vec{p})^\dagger\, j_r^b(\vec{k},\vec{l})$
(1,1)	$a_u^\dagger \left\vert 0\right\rangle \left\langle 0\right\vert a_v a_{k+p}^\dagger a_p a_l^\dagger a_{l+k} = \delta^3(\vec{p}+\vec{k}-\vec{v})\, \delta^3(\vec{p}-\vec{l})\, a_u^\dagger \left\vert 0\right\rangle \left\langle 0\right\vert a_v$
(1,2)	$a_u^\dagger \left\vert 0\right\rangle \left\langle 0\right\vert a_v a_{k+p}^\dagger a_p a_{-l-k}^\dagger a_{-l} = \delta^3(\vec{k}+\vec{p}-\vec{v})\, \delta^3(\vec{p}+\vec{l}+\vec{k})\, a_u^\dagger \left\vert 0\right\rangle \left\langle 0\right\vert a_v$
(2,1)	$a_u^\dagger \left\vert 0\right\rangle \left\langle 0\right\vert a_v a_{-p}^\dagger a_{-p-k} a_l^\dagger a_{k+l} = \delta^3(\vec{p}+\vec{v})\, \delta^3(\vec{p}+\vec{l}+\vec{k})\, a_u^\dagger \left\vert 0\right\rangle \left\langle 0\right\vert a_v$
(2,2)	$a_u^\dagger \left\vert 0\right\rangle \left\langle 0\right\vert a_v a_{-p}^\dagger a_{-p-k} a_{-l-k}^\dagger a_{-l} = \delta^3(\vec{p}+\vec{v})\, \delta^3(\vec{p}-\vec{l})\, a_u^\dagger \left\vert 0\right\rangle \left\langle 0\right\vert a_v$
(4,4)	$\delta_P\, a_u^\dagger \left\vert 0\right\rangle \left\langle 0\right\vert a_v a_{-k-p} a_p a_l^\dagger a_{-k-l}^\dagger = \delta_P$ (b) *see below*

(III)	$j_r^b(\vec{k},\vec{l})\, a_u^\dagger \left\vert 0\right\rangle \left\langle 0\right\vert a_v\, j_r^a(\vec{k},\vec{p})^\dagger$
(1,1)	$a_l^\dagger a_{l+k} a_u^\dagger \left\vert 0\right\rangle \left\langle 0\right\vert a_v a_{k+p}^\dagger a_p = \delta^3(\vec{l}+\vec{k}-\vec{u})\, \delta^3(\vec{k}+\vec{p}-\vec{v})\, a_{u-k}^\dagger \left\vert 0\right\rangle \left\langle 0\right\vert a_{v-k}$
(1,2)	$a_{-l-k}^\dagger a_{-l} a_u^\dagger \left\vert 0\right\rangle \left\langle 0\right\vert a_v a_{k+p}^\dagger a_p = \delta^3(\vec{k}+\vec{p}-\vec{v})\, \delta^3(\vec{u}+\vec{l})\, a_{u-k}^\dagger \left\vert 0\right\rangle \left\langle 0\right\vert a_{v-k}$
(2,1)	$a_l^\dagger a_{k+l} a_u^\dagger \left\vert 0\right\rangle \left\langle 0\right\vert a_v a_{-p}^\dagger a_{-p-k} = \delta^3(\vec{p}+\vec{v})\, \delta^3(\vec{l}+\vec{k}-\vec{u})\, a_{u-k}^\dagger \left\vert 0\right\rangle \left\langle 0\right\vert a_{v-k}$
(2,2)	$a_{-l-k}^\dagger a_{-l} a_u^\dagger \left\vert 0\right\rangle \left\langle 0\right\vert a_v a_{-p}^\dagger a_{-p-k} = \delta^3(\vec{p}+\vec{v})\, \delta^3(\vec{u}+\vec{l})\, a_{u-k}^\dagger \left\vert 0\right\rangle \left\langle 0\right\vert a_{v-k}$

The expressions for (a) and (b) are calculated separately because, as will be discussed below, they include vacuum bubbles that require a renormalisation. By applying the commutators and commuting all annihilation operators towards the vacuum state one obtains:

$$\begin{aligned}(a) =& a_{-k-p} a_p a_l^\dagger a_{-k-l}^\dagger a_u^\dagger \left\vert 0\right\rangle \left\langle 0\right\vert a_v \\ =& [\delta^3(\vec{p}+\vec{k}+\vec{l})\delta_\xi^3(\vec{p}+\vec{k}+\vec{l}) + \delta^3(\vec{p}-\vec{l})\delta_\xi^3(\vec{p}-\vec{l}) + \delta^3(\vec{p}+\vec{k}+\vec{l})\delta^3(\vec{u}+\vec{k}+\vec{p}) \\ &+ \delta^3(\vec{p}-\vec{l})\delta^3(\vec{u}+\vec{k}+\vec{p}) + \delta^3(\vec{p}-\vec{u})\delta^3(\vec{p}-\vec{l}) + \delta^3(\vec{p}-\vec{u})\delta^3(\vec{k}+\vec{p}+\vec{l})]\, a_u^\dagger \left\vert 0\right\rangle \left\langle 0\right\vert a_v\,, \end{aligned} \tag{10.8}$$

$$\begin{aligned}(b) =& a_u^\dagger \left\vert 0\right\rangle \left\langle 0\right\vert a_v a_{-k-p} a_p a_l^\dagger a_{-k-l}^\dagger \\ =& [\delta^3(\vec{p}+\vec{k}+\vec{l})\delta_\xi^3(\vec{p}+\vec{k}+\vec{l}) + \delta^3(\vec{p}-\vec{l})\delta_\xi^3(\vec{p}-\vec{l}) + \delta^3(\vec{p}+\vec{k}+\vec{l})\delta^3(\vec{v}+\vec{k}+\vec{l}) \\ &+ \delta^3(\vec{p}-\vec{l})\delta^3(\vec{v}+\vec{k}+\vec{l}) + \delta^3(\vec{v}-\vec{l})\delta^3(\vec{p}-\vec{l}) + \delta^3(\vec{v}-\vec{l})\delta^3(\vec{k}+\vec{p}+\vec{l})]\, a_u^\dagger \left\vert 0\right\rangle \left\langle 0\right\vert a_v\,. \end{aligned} \tag{10.9}$$

Note that under the map $(\vec{u},\vec{p},\vec{l}) \leftrightarrow (\vec{v},\vec{l},\vec{p})$ we can get from (a) to (b) and vice versa. These additional terms that are present in the extended one-particle projection correspond to physical situations in QFT in which in the intermediate steps two particles are created and annihilated afterwards. This also includes the case where the original particle is left invariant and a vacuum bubble is created. These vacuum bubbles are encoded in the first two terms in both expressions, which contain the square of a Dirac delta distribution. This is a problematic term since, as can be shown, the corresponding integral over this expression still diverges when for the individual delta distributions the regularised version is considered and the regulator is removed after the

integration is performed. We will deal with this issue further below in this section where we renormalise the density matrix to handle the divergent contributions involved. For now, we replace one of the two delta distributions by a function including a regulator $\delta^3(\vec{k}) \to \delta^3_\xi(\vec{k})$, where the regulator is sent to zero after performing the corresponding integrations.

In a next step, we evaluate the entire expressions appearing in the Lamb-shift Hamiltonian and the dissipator. For each term, where the delta distributions resolve two integrals, that is for all terms but the diverging ones, we choose to resolve the integrals over the range of the variables $\vec{p}$ and $\vec{l}$ respectively. Then we are left with the integration over the variables $\vec{k}$, $\vec{u}$ and $\vec{v}$ as well as with the sum over the polarisation labels r. Considering for $\mathcal{V}_{ab}$ which is either R_{ab} or S_{ab}, that were defined above in (9.45) and (9.44), the three expressions

$$\textbf{(I):} \sum_r \int d^3p \int d^3l \; \mathcal{V}_{ab}(\vec{p},\vec{l};\vec{k},t)\; j^a_r(\vec{k},\vec{p})^\dagger\, j^b_r(\vec{k},\vec{l})\, a^\dagger_u \left|0\right\rangle \left\langle 0\right| a_v \tag{10.10}$$

$$\textbf{(II):} \sum_r \int d^3p \int d^3l \; \mathcal{V}_{ab}(\vec{p},\vec{l};\vec{k},t)\; a^\dagger_u \left|0\right\rangle \left\langle 0\right| a_v\, j^a_r(\vec{k},\vec{p})^\dagger\, j^b_r(\vec{k},\vec{l}) \tag{10.11}$$

$$\textbf{(III):} \sum_r \int d^3p \int d^3l \; \mathcal{V}_{ab}(\vec{p},\vec{l};\vec{k},t)\; j^a_r(\vec{k},\vec{p})^\dagger\, a^\dagger_u \left|0\right\rangle \left\langle 0\right| a_v\, j^b_r(\vec{k},\vec{l})\,, \tag{10.12}$$

that appear in the Lamb-shift Hamiltonian (9.47) and the dissipator (9.48), we obtain:

(I)	$\sum_r \int d^3p \int d^3l\; \mathcal{V}_{ab}(\vec{p},\vec{l};\vec{k},t)\; j^a_r(\vec{k},\vec{p})^\dagger\, j^b_r(\vec{k},\vec{l})\, a^\dagger_u \left\|0\right\rangle \left\langle 0\right\| a_v$
(1,1)	$\mathcal{V}_{11}(\vec{u}-\vec{k},\vec{u}-\vec{k};\vec{k},t)\; \rho(\vec{u},\vec{v}) \frac{1}{4\omega_u\omega_{u-k}} P_u(\vec{k})\; a^\dagger_u \left\|0\right\rangle \left\langle 0\right\| a_v$
(1,2)	$\mathcal{V}_{12}(\vec{u}-\vec{k},-\vec{u};\vec{k},t)\; \rho(\vec{u},\vec{v}) \frac{1}{4\omega_u\omega_{u-k}} P_u(\vec{k})\; a^\dagger_u \left\|0\right\rangle \left\langle 0\right\| a_v$
(2,1)	$\mathcal{V}_{21}(-\vec{u},\vec{u}-\vec{k};\vec{k},t)\; \rho(\vec{u},\vec{v}) \frac{1}{4\omega_u\omega_{u-k}} P_u(\vec{k})\; a^\dagger_u \left\|0\right\rangle \left\langle 0\right\| a_v$
(2,2)	$\mathcal{V}_{22}(-\vec{u},-\vec{u};\vec{k},t)\; \rho(\vec{u},\vec{v}) \frac{1}{4\omega_u\omega_{u-k}} P_u(\vec{k})\; a^\dagger_u \left\|0\right\rangle \left\langle 0\right\| a_v$
(4,4)	δ_P (a) *(see below)*

(II)	$\sum_r \int d^3p \int d^3l\; \mathcal{V}_{ab}(\vec{p},\vec{l};\vec{k},t)\; a^\dagger_u \left\|0\right\rangle \left\langle 0\right\| a_v\, j^a_r(\vec{k},\vec{p})^\dagger\, j^b_r(\vec{k},\vec{l})$
(1,1)	$\mathcal{V}_{11}(\vec{v}-\vec{k},\vec{v}-\vec{k};\vec{k},t)\; \rho(\vec{u},\vec{v}) \frac{1}{4\omega_v\omega_{v-k}} P_v(\vec{k})\; a^\dagger_u \left\|0\right\rangle \left\langle 0\right\| a_v$
(1,2)	$\mathcal{V}_{12}(\vec{v}-\vec{k},-\vec{v};\vec{k},t)\; \rho(\vec{u},\vec{v}) \frac{1}{4\omega_v\omega_{v-k}} P_v(\vec{k})\; a^\dagger_u \left\|0\right\rangle \left\langle 0\right\| a_v$
(2,1)	$\mathcal{V}_{21}(-\vec{v},\vec{v}-\vec{k};\vec{k},t)\; \rho(\vec{u},\vec{v}) \frac{1}{4\omega_v\omega_{v-k}} P_v(\vec{k})\; a^\dagger_u \left\|0\right\rangle \left\langle 0\right\| a_v$
(2,2)	$\mathcal{V}_{22}(-\vec{v},-\vec{v};\vec{k},t)\; \rho(\vec{u},\vec{v}) \frac{1}{4\omega_v\omega_{v-k}} P_v(\vec{k})\; a^\dagger_u \left\|0\right\rangle \left\langle 0\right\| a_v$
(4,4)	δ_P (b) *(see below)*

(III)	$\sum_r \int d^3p \int d^3l\; \mathcal{V}_{ab}(\vec{p},\vec{l};\vec{k},t)\; j^a_r(\vec{k},\vec{p})^\dagger\, a^\dagger_u \left\|0\right\rangle \left\langle 0\right\| a_v\, j^b_r(\vec{k},\vec{l})$
(1,1)	$\mathcal{V}_{11}(\vec{v}-\vec{k},\vec{u}-\vec{k};\vec{k},t)\; \rho(\vec{u},\vec{v}) \frac{1}{4\sqrt{\omega_v\omega_{v-k}\omega_u\omega_{u-k}}} P_{u,v}(\vec{k})\; a^\dagger_{u-k} \left\|0\right\rangle \left\langle 0\right\| a_{v-k}$
(1,2)	$\mathcal{V}_{12}(\vec{v}-\vec{k},-\vec{u};\vec{k},t)\; \rho(\vec{u},\vec{v}) \frac{1}{4\sqrt{\omega_v\omega_{v-k}\omega_u\omega_{u-k}}} P_{u,v}(\vec{k})\; a^\dagger_{u-k} \left\|0\right\rangle \left\langle 0\right\| a_{v-k}$
(2,1)	$\mathcal{V}_{11}(-\vec{v},\vec{u}-\vec{k};\vec{k},t)\; \rho(\vec{u},\vec{v}) \frac{1}{4\sqrt{\omega_v\omega_{v-k}\omega_u\omega_{u-k}}} P_{u,v}(\vec{k})\; a^\dagger_{u-k} \left\|0\right\rangle \left\langle 0\right\| a_{v-k}$
(2,2)	$\mathcal{V}_{22}(-\vec{v},-\vec{u};\vec{k},t)\; \rho(\vec{u},\vec{v}) \frac{1}{4\sqrt{\omega_v\omega_{v-k}\omega_u\omega_{u-k}}} P_{u,v}(\vec{k})\; a^\dagger_{u-k} \left\|0\right\rangle \left\langle 0\right\| a_{v-k}\,,$

where we defined

$$P_u(\vec{k}) := \sum_r [\vec{u}\cdot\vec{m}(-r\vec{k})]^2[\vec{u}\cdot\vec{m}(r\vec{k})]^2 = 2[\vec{u}\cdot\vec{m}(-\vec{k})]^2[\vec{u}\cdot\vec{m}(\vec{k})]^2 = P^{abcd}(\vec{k})u_a u_b u_c u_d \quad (10.13)$$

$$P_{u,v}(\vec{k}) := \sum_r [\vec{u}\cdot\vec{m}(-r\vec{k})]^2[\vec{v}\cdot\vec{m}(r\vec{k})]^2 = P^{abcd}(\vec{k})u_a u_b v_c v_d\,. \quad (10.14)$$

This contains the symmetric transverse-traceless projector which is given as

$$P^{abcd}(\vec{k}) = \frac{1}{2}[P^{ac}(\vec{k})P^{bd}(\vec{k}) + P^{ad}(\vec{k})P^{bc}(\vec{k}) - P^{ab}(\vec{k})P^{cd}(\vec{k})]\,. \quad (10.15)$$

with the transverse projector

$$P^{ab}(\vec{k}) = \delta^{ab} - \frac{k^a k^b}{\vec{k}^2}\,. \quad (10.16)$$

Next, we evaluate in more detail the coefficient functions S and R which were defined in (9.44) and (9.45). Firstly excluding all terms from the extended projection, i.e. the ones arising from the combination $(4,4)$, it turns out that the coefficients appearing in $(I)-(III)$ are equal to each other in each group:

$$\begin{aligned} &S_{11}(\vec{u}-\vec{k},\vec{u}-\vec{k};\vec{k},t) = S_{12}(\vec{u}-\vec{k},-\vec{u};\vec{k},t) = S_{21}(-\vec{u},\vec{u}-\vec{k};\vec{k},t) = S_{22}(-\vec{u},-\vec{u};\vec{k},t) \\ &= \frac{1}{\Omega_k}\Bigg\{\frac{N(k)+1}{\Omega_k+\omega_{u-k}-\omega_u}\left(\cos\left[(\Omega_k+\omega_{u-k}-\omega_u)t\right]-1\right) \\ &\qquad\qquad - \frac{N(k)}{\Omega_k-\omega_{u-k}+\omega_u}\left(\cos\left[(\Omega_k-\omega_{u-k}+\omega_u)t\right]-1\right)\Bigg\} \\ &=: S_{1P}^{(-)}(\vec{u},\vec{k},t)\,, \end{aligned} \quad (10.17)$$

$$\begin{aligned} &R_{11}(\vec{u}-\vec{k},\vec{u}-\vec{k};\vec{k},t) = R_{12}(\vec{u}-\vec{k},-\vec{u};\vec{k},t) = R_{21}(-\vec{u},\vec{u}-\vec{k};\vec{k},t) = R_{22}(-\vec{u},-\vec{u};\vec{k},t) \\ &= \frac{2}{\Omega_k}\Bigg\{\frac{N(k)+1}{\Omega_k+\omega_{u-k}-\omega_u}\sin\left[(\Omega_k+\omega_{u-k}-\omega_u)t\right] + \frac{N(k)}{\Omega_k-\omega_{u-k}+\omega_u}\sin\left[(\Omega_k-\omega_{u-k}+\omega_u)t\right]\Bigg\} \\ &=: 2R_{1P}^{(-)}(\vec{u},\vec{k},t) \end{aligned} \quad (10.18)$$

and

$$\begin{aligned} &R_{11}(\vec{v}-\vec{k},\vec{u}-\vec{k};\vec{k},t) = R_{12}(\vec{v}-\vec{k},-\vec{u};\vec{k},t) = R_{21}(-\vec{v},\vec{u}-\vec{k};\vec{k},t) = R_{22}(-\vec{v},-\vec{u};\vec{k},t) \\ &= \frac{i}{\Omega_k}\Bigg\{[N(k)+1]\left(\frac{e^{-i(\Omega_k+\omega_{u-k}-\omega_u)t}-1}{\Omega_k+\omega_{u-k}-\omega_u} - \frac{e^{i(\Omega_k+\omega_{v-k}-\omega_v)t}-1}{\Omega_k+\omega_{v-k}-\omega_v}\right) \\ &\qquad\qquad - N(k)\left(\frac{e^{i(\Omega_k-\omega_{u-k}+\omega_u)t}-1}{\Omega_k-\omega_{u-k}+\omega_u} - \frac{e^{-i(\Omega_k-\omega_{v-k}+\omega_v)t}-1}{\Omega_k-\omega_{v-k}+\omega_v}\right)\Bigg\} \\ &=: 2R_{1P}^{(2)}(\vec{u},\vec{v},\vec{k},t)\,. \end{aligned} \quad (10.19)$$

With these expressions, we can rewrite the equations for the Lamb-shift Hamiltonian and the dissipator that contain the contributions of $(a,b) \in \{1,2\}$:

$$\begin{aligned}-i[H_{LS}^{\{1,2\}},\rho_1(t)] = &-\frac{i\kappa}{2}\int \frac{d^3k\,d^3u\,d^3v}{(2\pi)^3}\rho(\vec{u},\vec{v},t)\; a_u^\dagger\,|0\rangle\,\langle 0|\,a_v\;\frac{P_u(\vec{k})}{\omega_{u-k}\omega_u}\;S_{1P}^{(-)}(\vec{u},\vec{k},t)\\ &+\frac{i\kappa}{2}\int \frac{d^3k\,d^3u\,d^3v}{(2\pi)^3}\rho(\vec{u},\vec{v},t)\; a_u^\dagger\,|0\rangle\,\langle 0|\,a_v\;\frac{P_v(\vec{k})}{\omega_{v-k}\omega_v}\;S_{1P}^{(-)}(\vec{v},\vec{k},t)\end{aligned} \tag{10.20}$$

as well as

$$\begin{aligned}\mathcal{D}^{\{1,2\}}[\rho_1(t)] = &-\frac{\kappa}{2}\int \frac{d^3k\,d^3u\,d^3v}{(2\pi)^3}\rho(\vec{u},\vec{v},t)\; a_u^\dagger\,|0\rangle\,\langle 0|\,a_v\;\frac{P_u(\vec{k})}{\omega_{u-k}\omega_u}\;R_{1P}^{(-)}(\vec{u},\vec{k},t)\\ &-\frac{\kappa}{2}\int \frac{d^3k\,d^3u\,d^3v}{(2\pi)^3}\rho(\vec{u},\vec{v},t)\; a_u^\dagger\,|0\rangle\,\langle 0|\,a_v\;\frac{P_v(\vec{k})}{\omega_{v-k}\omega_v}\;R_{1P}^{(-)}(\vec{v},\vec{k},t)\\ &+\kappa\int \frac{d^3k\,d^3u\,d^3v}{(2\pi)^3}\rho(\vec{u},\vec{v},t)\; a_{u-k}^\dagger\,|0\rangle\,\langle 0|\,a_{v-k}\;\frac{P_{u,v}(\vec{k})}{\sqrt{\omega_{u-k}\omega_u\omega_{v-k}\omega_v}}\;R_{1P}^{(2)}(\vec{u},\vec{v},\vec{k},t)\,.\end{aligned} \tag{10.21}$$

It remains to deal with the $(4,4)$-terms that arise when using the extended projection. The four summands from (a) and (b) without the terms containing the ξ-regulator yield

$$\begin{aligned}-i[H_{LS}^{\{4,4\}},\rho_1(t)] = &-\frac{i\kappa}{2}\int \frac{d^3k\,d^3u\,d^3v}{(2\pi)^3}\rho(\vec{u},\vec{v},t)\; a_u^\dagger\,|0\rangle\,\langle 0|\,a_v\;\frac{P_u(\vec{k})}{\omega_{u+k}\omega_u}\;\widetilde{S}_{1P}^{(+)}(\vec{u},\vec{k},t)\;\delta_P\\ &+\frac{i\kappa}{2}\int \frac{d^3k\,d^3u\,d^3v}{(2\pi)^3}\rho(\vec{u},\vec{v},t)\; a_u^\dagger\,|0\rangle\,\langle 0|\,a_v\;\frac{P_v(\vec{k})}{\omega_{v+k}\omega_v}\;\widetilde{S}_{1P}^{(+)}(\vec{v},\vec{k},t)\;\delta_P\end{aligned} \tag{10.22}$$

with

$$\begin{aligned}&S_{44}(-\vec{u}-\vec{k},\vec{u};\vec{k},t) = S_{44}(-\vec{u}-\vec{k},-\vec{u}-\vec{k};\vec{k},t) = S_{44}(\vec{u},\vec{u};\vec{k},t) = S_{44}(\vec{u},-\vec{u}-\vec{k};\vec{k},t)\\ &= \frac{1}{\Omega_k}\Bigg\{\frac{N(k)+1}{\Omega_k+\omega_{u+k}+\omega_u}\left(\cos\left[(\Omega_k+\omega_{u+k}+\omega_u)t\right]-1\right)\\ &\qquad\qquad -\frac{N(k)}{\Omega_k-\omega_{u+k}-\omega_u}\left(\cos\left[(\Omega_k-\omega_{u+k}-\omega_u)t\right]-1\right)\Bigg\}\\ &=: \widetilde{S}_{1P}^{(+)}(\vec{u},\vec{k},t)\,.\end{aligned} \tag{10.23}$$

After a substitution $\vec{k}\to-\vec{k}$ in the integration we find:

$$\begin{aligned}-i[H_{LS}^{\{4,4\}},\rho_1(t)] = &-\frac{i\kappa}{2}\int \frac{d^3k\,d^3u\,d^3v}{(2\pi)^3}\rho(\vec{u},\vec{v},t)\; a_u^\dagger\,|0\rangle\,\langle 0|\,a_v\;\frac{P_u(\vec{k})}{\omega_{u-k}\omega_u}\;S_{1P}^{(+)}(\vec{u},\vec{k},t)\;\delta_P\\ &+\frac{i\kappa}{2}\int \frac{d^3k\,d^3u\,d^3v}{(2\pi)^3}\rho(\vec{u},\vec{v},t)\; a_u^\dagger\,|0\rangle\,\langle 0|\,a_v\;\frac{P_v(\vec{k})}{\omega_{v-k}\omega_v}\;S_{1P}^{(+)}(\vec{v},\vec{k},t)\;\delta_P\end{aligned} \tag{10.24}$$

where

$$S_{1P}^{(+)}(\vec{u},\vec{k},t) := \widetilde{S}_{1P}^{(+)}(\vec{u},-\vec{k},t)\,. \tag{10.25}$$

The same substitution and the definition

$$R_{1P}^{(+)}(\vec{u},\vec{k},t) := \frac{1}{\Omega_k}\Bigg\{\frac{N(k)+1}{\Omega_k+\omega_{u-k}+\omega_u}\sin\left[(\Omega_k+\omega_{u-k}+\omega_u)t\right] + \frac{N(k)}{\Omega_k-\omega_{u-k}-\omega_u}\sin\left[(\Omega_k-\omega_{u-k}-\omega_u)t\right]\Bigg\} \quad (10.26)$$

lead to:

$$\begin{aligned}\mathcal{D}^{\{4,4\}}[\rho_1] = &-\frac{\kappa}{2}\int\frac{d^3k\,d^3u\,d^3v}{(2\pi)^3}\rho(\vec{u},\vec{v},t)\;a_u^\dagger\,|0\rangle\,\langle 0|\,a_v\;\frac{P_u(\vec{k})}{\omega_{u-k}\omega_u}\;R_{1P}^{(+)}(\vec{u},\vec{k},t)\;\delta_P\\ &-\frac{\kappa}{2}\int\frac{d^3k\,d^3u\,d^3v}{(2\pi)^3}\rho(\vec{u},\vec{v},t)\;a_u^\dagger\,|0\rangle\,\langle 0|\,a_v\;\frac{P_v(\vec{k})}{\omega_{v-k}\omega_v}\;R_{1P}^{(+)}(\vec{v},\vec{k},t)\;\delta_P\,. \end{aligned} \quad (10.27)$$

Defining additionally

$$S_{1P}^{(1)}(\vec{u},\vec{k},t) := S_{1P}^{(-)}(\vec{u},\vec{k},t) + S_{1P}^{(+)}(\vec{u},\vec{k},t)\;\delta_P \quad (10.28)$$

$$R_{1P}^{(1)}(\vec{u},\vec{k},t) := R_{1P}^{(-)}(\vec{u},\vec{k},t) + R_{1P}^{(+)}(\vec{u},\vec{k},t)\;\delta_P \quad (10.29)$$

gives us the opportunity to rewrite

$$\begin{aligned}-i[H_{LS},\rho_1(t)] = &-\frac{i\kappa}{2}\int\frac{d^3k\,d^3u\,d^3v}{(2\pi)^3}\rho(\vec{u},\vec{v},t)\;a_u^\dagger\,|0\rangle\,\langle 0|\,a_v\;\frac{P_u(\vec{k})}{\omega_{u-k}\omega_u}\;S_{1P}^{(1)}(\vec{u},\vec{k},t)\\ &+\frac{i\kappa}{2}\int\frac{d^3k\,d^3u\,d^3v}{(2\pi)^3}\rho(\vec{u},\vec{v},t)\;a_u^\dagger\,|0\rangle\,\langle 0|\,a_v\;\frac{P_v(\vec{k})}{\omega_{v-k}\omega_v}\;S_{1P}^{(1)}(\vec{v},\vec{k},t)\end{aligned} \quad (10.30)$$

as well as

$$\begin{aligned}\mathcal{D}[\rho_1] = &-\frac{\kappa}{2}\int\frac{d^3k\,d^3u\,d^3v}{(2\pi)^3}\rho(\vec{u},\vec{v},t)\;a_u^\dagger\,|0\rangle\,\langle 0|\,a_v\;\frac{P_u(\vec{k})}{\omega_{u-k}\omega_u}\;R_{1P}^{(1)}(\vec{u},\vec{k},t)\\ &-\frac{\kappa}{2}\int\frac{d^3k\,d^3u\,d^3v}{(2\pi)^3}\rho(\vec{u},\vec{v},t)\;a_u^\dagger\,|0\rangle\,\langle 0|\,a_v\;\frac{P_v(\vec{k})}{\omega_{v-k}\omega_v}\;R_{1P}^{(1)}(\vec{v},\vec{k},t)\\ &+\kappa\int\frac{d^3k\,d^3u\,d^3v}{(2\pi)^3}\rho(\vec{u},\vec{v},t)\;a_{u-k}^\dagger\,|0\rangle\,\langle 0|\,a_{v-k}\;\frac{P_{u,v}(\vec{k})}{\sqrt{\omega_{u-k}\omega_u\omega_{v-k}\omega_v}}\;R_{1P}^{(2)}(\vec{u},\vec{v},\vec{k},t)\,.\end{aligned} \quad (10.31)$$

This can be summarised as

$$\begin{aligned}-i[H_{LS},&\rho_1(t)] + \mathcal{D}[\rho_1] =\\ &= -\frac{\kappa}{2}\int\frac{d^3k\,d^3u\,d^3v}{(2\pi)^3}\rho(\vec{u},\vec{v},t)\;a_u^\dagger\,|0\rangle\,\langle 0|\,a_v\;\frac{P_u(\vec{k})}{\omega_{u-k}\omega_u}\;[R_{1P}^{(1)}(\vec{u},\vec{k},t) + iS_{1P}^{(1)}(\vec{u},\vec{k},t)]\\ &\quad -\frac{\kappa}{2}\int\frac{d^3k\,d^3u\,d^3v}{(2\pi)^3}\rho(\vec{u},\vec{v},t)\;a_u^\dagger\,|0\rangle\,\langle 0|\,a_v\;\frac{P_v(\vec{k})}{\omega_{v-k}\omega_v}\;[R_{1P}^{(1)}(\vec{v},\vec{k},t) - iS_{1P}^{(1)}(\vec{u},\vec{k},t)]\\ &\quad +\kappa\int\frac{d^3k\,d^3u\,d^3v}{(2\pi)^3}\rho(\vec{u},\vec{v},t)\;a_{u-k}^\dagger\,|0\rangle\,\langle 0|\,a_{v-k}\;\frac{P_{u,v}(\vec{k})}{\sqrt{\omega_{u-k}\omega_u\omega_{v-k}\omega_v}}\;R_{1P}^{(2)}(\vec{u},\vec{v},\vec{k},t)\,.\end{aligned} \quad (10.32)$$

Finally, the terms in the extended projection that contain the ξ-regulator, that is the expressions arising from the first two terms in (10.8) and (10.9), are analysed. These terms are equal for (a) and (b) and read:

$$\begin{aligned}\delta_P \lim_{\xi\to 0}\int \frac{d^3p\,d^3l\,d^3k\,d^3u\,d^3v}{(2\pi)^{\frac{3}{2}}}\; a_u^\dagger\,|0\rangle\langle 0|\,a_v\;\mathcal{V}_{44}(\vec{p},\vec{l};\vec{k},t)\frac{P_{p,l}(\vec{k})}{4\sqrt{\omega_p\omega_{k+p}\omega_l\omega_{k+l}}}\rho(\vec{u},\vec{v},t)\\ \cdot\{\delta^3(\vec{p}+\vec{k}+\vec{l})\delta_\xi^3(\vec{p}+\vec{k}+\vec{l})+\delta^3(\vec{p}-\vec{l})\delta_\xi^3(\vec{p}-\vec{l})\}\\ =\delta_P\lim_{\xi\to 0}\int\frac{d^3p\,d^3k}{(2\pi)^{\frac{3}{2}}}\;\mathcal{V}_{44}(\vec{p},\vec{p};\vec{k},t)\frac{P_p(\vec{k})}{2\omega_p\omega_{k+p}}\;\delta_\xi^3(\vec{0})\;\rho_1(t)\,,\end{aligned}\tag{10.33}$$

where we used that $\mathcal{V}_{44}(\vec{p},\vec{p};\vec{k},t)=\mathcal{V}_{44}(\vec{p},-\vec{k-p};\vec{k},t)$. Due to the equality of these terms for (a) and (b), they drop out of the Lamb-shift Hamiltonian and are only left in the dissipator term:

$$\mathcal{D}^{div}[\rho_1]=-\delta_P\frac{\kappa}{4}\lim_{\xi\to 0}\int\frac{d^3k\,d^3p}{(2\pi)^{\frac{3}{2}}}R_{44}(\vec{p},\vec{p};\vec{k},t)\frac{P_p(\vec{k})}{2\omega_p\omega_{k+p}}\delta_\xi^3(\vec{0})\;\rho_1(t)=:Z(t)\rho_1(t)\,.\tag{10.34}$$

Written in this form, it becomes evident that they do act as a multiplicative constant and do not modify the state ρ_1. Therefore they are nothing but vacuum bubbles expressed in QFT language. With the definition of $Z(t)$ above, the entire master equation for the single particle is given by

$$\frac{\partial}{\partial t}\rho_1(t)=-i[H_S+H_{LS},\rho_1(t)]+\mathcal{D}[\rho_1]+Z(t)\rho_1(t)\,,\tag{10.35}$$

where from now on the terms absorbed in $Z(t)$ are dropped from the definition of $\mathcal{D}[\rho_1]$. We can see that the diverging term $Z(t)$ can be absorbed by a renormalisation of the density matrix, likewise to a renormalisation of the wave function known from QFT:

$$\rho_1(t)\to\rho_1^{(ren)}(t):=\exp\left(\int_0^t dt'\;Z(t')\right)\rho_1(t)\,.\tag{10.36}$$

In terms of the renormalised density matrix, the one-particle master equation then reads:

$$\begin{aligned}\frac{\partial}{\partial t}\rho_1^{(ren)}(t)=&-i\int d^3u\,d^3v\;\rho^{(ren)}(\vec{u},\vec{v},t)\,|\vec{u}\rangle\langle\vec{v}|\;(\omega_u-\omega_v)\\ &-\frac{\kappa}{2}\int\frac{d^3k\,d^3u\,d^3v}{(2\pi)^3}\rho^{(ren)}(\vec{u},\vec{v},t)\;|\vec{u}\rangle\langle\vec{v}|\;\frac{P_u(\vec{k})}{\omega_{u-k}\omega_u}\;[R_{1P}^{(1)}(\vec{u},\vec{k},t)+iS_{1P}^{(1)}(\vec{u},\vec{k},t)]\\ &-\frac{\kappa}{2}\int\frac{d^3k\,d^3u\,d^3v}{(2\pi)^3}\rho^{(ren)}(\vec{u},\vec{v},t)\;|\vec{u}\rangle\langle\vec{v}|\;\frac{P_v(\vec{k})}{\omega_{v-k}\omega_v}\;[R_{1P}^{(1)}(\vec{v},\vec{k},t)-iS_{1P}^{(1)}(\vec{v},\vec{k},t)]\\ &+\kappa\int\frac{d^3k\,d^3u\,d^3v}{(2\pi)^3}\rho^{(ren)}(\vec{u},\vec{v},t)\;|\vec{u}-\vec{k}\rangle\langle\vec{v}-\vec{k}|\;\frac{P_{u,v}(\vec{k})}{\sqrt{\omega_{u-k}\omega_u\omega_{v-k}\omega_v}}\;R_{1P}^{(2)}(\vec{u},\vec{v},\vec{k},t)\,.\end{aligned}\tag{10.37}$$

To simplify the notation, we drop the label (ren) from the density matrix from this point on.

The complex combinations $R \pm iS$ can be evaluated further and one finds

$$
\begin{aligned}
&R^{(1)}_{1P}(\vec{u},\vec{k},t) \pm iS^{(1)}_{1P}(\vec{u},\vec{k},t) = \\
&= \frac{\pm i}{\Omega_k}\Bigg\{ \frac{N(k)+1}{\Omega_k+\omega_{u-k}-\omega_u}\left(e^{\mp i(\Omega_k+\omega_{u-k}-\omega_u)t}-1\right) - \frac{N(k)}{\Omega_k-\omega_{u-k}+\omega_u}\left(e^{\pm i(\Omega_k-\omega_{u-k}+\omega_u)t}-1\right) \\
&\qquad + \frac{\delta_P[N(k)+1]}{\Omega_k+\omega_{u-k}+\omega_u}\left(e^{\mp i(\Omega_k+\omega_{u-k}+\omega_u)t}-1\right) - \frac{\delta_P\, N(k)}{\Omega_k-\omega_{u-k}-\omega_u}\left(e^{\pm i(\Omega_k-\omega_{u-k}-\omega_u)t}-1\right)\Bigg\} \\
&= \int_0^t \frac{d\tau}{\Omega_k}\Big\{[N(k)+1]\, e^{\mp i(\Omega_k+\omega_{u-k}-\omega_u)\tau} + N(k)\, e^{\pm i(\Omega_k-\omega_{u-k}+\omega_u)\tau} \\
&\qquad + \delta_P[N(k)+1]\, e^{\mp i(\Omega_k+\omega_{u-k}+\omega_u)\tau} + \delta_P\, N(k)\, e^{\pm i(\Omega_k-\omega_{u-k}-\omega_u)\tau}\Big\}. \qquad (10.38)
\end{aligned}
$$

For $R^{(2)}$ we have:

$$
\begin{aligned}
R^{(2)}_{1P}(\vec{u},\vec{v},\vec{k},t) =& \frac{i}{2\Omega_k}\Bigg\{[N(k)+1]\left(\frac{e^{-i(\Omega_k+\omega_{u-k}-\omega_u)t}-1}{\Omega_k+\omega_{u-k}-\omega_u} - \frac{e^{i(\Omega_k+\omega_{v-k}-\omega_v)t}-1}{\Omega_k+\omega_{v-k}-\omega_v}\right) \\
&- N(k)\left(\frac{e^{i(\Omega_k-\omega_{u-k}+\omega_u)t}-1}{\Omega_k-\omega_{u-k}+\omega_u} - \frac{e^{-i(\Omega_k-\omega_{v-k}+\omega_v)t}-1}{\Omega_k-\omega_{v-k}+\omega_v}\right)\Bigg\} \\
=& \int_0^t \frac{d\tau}{2\Omega_k}\Big\{[N(k)+1]\, e^{-i(\Omega_k+\omega_{u-k}-\omega_u)\tau} + N(k)\, e^{i(\Omega_k-\omega_{u-k}+\omega_u)\tau} \\
&+ [N(k)+1]\, e^{i(\Omega_k+\omega_{v-k}-\omega_v)\tau} + N(k)\, e^{-i(\Omega_k-\omega_{v-k}+\omega_v)\tau}\Big\}. \qquad (10.39)
\end{aligned}
$$

Defining then

$$
C(\vec{u},\vec{k},t) = \int_0^{t-t_0} \frac{d\tau}{\Omega_k}\Big\{[N(k)+1]\, e^{-i(\Omega_k+\omega_{u-k}-\omega_u)\tau} + N(k)\, e^{i(\Omega_k-\omega_{u-k}+\omega_u)\tau}\Big\} \qquad (10.40)
$$

$$
C_P(\vec{u},\vec{k},t) = \int_0^{t-t_0} \frac{d\tau}{\Omega_k}\Big\{[N(k)+1]\, e^{-i(\Omega_k+\omega_{u-k}+\omega_u)\tau} + N(k)\, e^{i(\Omega_k-\omega_{u-k}-\omega_u)\tau}\Big\}, \qquad (10.41)
$$

where we have restored the initial time[14] t_0 that was set to 0 in part II, the one-particle master equation in momentum representation has the form

$$
\begin{aligned}
\frac{\partial}{\partial t}\rho(\vec{u},\vec{v},t) =& -i\rho(\vec{u},\vec{v},t)\,(\omega_u-\omega_v) \\
&- \frac{\kappa}{2}\int \frac{d^3k}{(2\pi)^3}\Bigg\{\frac{P_u(\vec{k})}{\omega_{u-k}\omega_u}\,\Big[C(\vec{u},\vec{k},t)+\delta_P C_P(\vec{u},\vec{k},t)\Big] \\
&\qquad + \frac{P_v(\vec{k})}{\omega_{v-k}\omega_v}\,\Big[C^*(\vec{v},\vec{k},t)+\delta_P C^*_P(\vec{v},\vec{k},t)\Big]\Bigg\}\,\rho(\vec{u},\vec{v},t) \\
&+ \frac{\kappa}{2}\int \frac{d^3k}{(2\pi)^3}\frac{P_{u,v}(\vec{k})}{\sqrt{\omega_{u+k}\omega_u\omega_{v+k}\omega_v}}\,\Big\{C(\vec{u}+\vec{k},\vec{k},t)+C^*(\vec{v}+\vec{k},\vec{k},t)\Big\}\,\rho(\vec{u}+\vec{k},\vec{v}+\vec{k},t)\,. \qquad (10.42)
\end{aligned}
$$

[14] Originally, the integration is of the form $\int_{t_0}^t d\tau e^{i\Omega(t-\tau)}$. The version given here can be achieved by substituting $t-\tau \to \tau$.

The presence of the symmetric transverse-traceless projector $P_u(\vec{k})$ and $P^{ijln}(\vec{k})$ is a consequence of the chosen Dirac observables in section 7, and thus the physical degrees of freedom of the linearised gravitational field. The term in the first line of the master equation in (10.42) represents the standard unitary evolution of the free scalar particle. The remaining terms describe the influence of the environment and encode in general different physical processes like energy shifts, dissipation and decoherence. While the expressions in lines two and three only depend on the state $\rho(\vec{u}, \vec{v}, t)$ considered at time t, the last line links this state to other states $\rho(\vec{u} + \vec{k}, \vec{v} + \vec{k}, t)$ at time t. This master equation however still has some problematic contributions that possess UV-divergences and hence needs to be UV-renormalised, as will be discussed in the next section.

11. Renormalisation of the TCL one-particle master equation

The content of this section was already published in [2]. Here, it is presented with some modifications compared to [2] to adapt it to the flow of the thesis.
Upon investigation of the individual contributions in (10.42) it becomes evident that some terms exhibit divergences as will be discussed in detail below. This raises the question of at what stage of the derivation of the master equation a renormalisation procedure should be carried out. In the literature, there are different strategies how to deal with these divergent contributions. For gravitationally induced decoherence, they have often not been computed in detail due to the reason that they are expected to not modify decoherence but only influence the unitary evolution, see for instance the discussion in [61, 62]. In [60, 63] the renormalisation of these contributions has been performed in the end after a Markov and rotating wave approximation have already been applied.
In this work, we choose the strategy to renormalise the master equation first before applying further approximations or deriving physical implications. It will turn out that effects predicted with a non-renormalised master equation might get modified or even vanish when working with the renormalised version instead. An example of this kind is also discussed later in part IV, where a quantum mechanical toy model for gravitationally induced decoherence based on the model in [112] is applied in the context of neutrino oscillations. In that case the necessary renormalisation is very trivial compared to the model considered in this part. There, the renormalisation causes the contributions of the Lamb-shift Hamiltonian to cancel exactly. Consequently, all physical implications involving contributions of the Lamb-shift Hamiltonian, as discussed for example in [85], would be absent when working with the renormalised model presented in part IV in sections 16 and 17.

In order to carry out the renormalisation, we will first identify the diverging terms. As we will discuss below in more detail, these are in particular the terms in the second and third line of the master equation (10.42) that will also be present in the case where the temperature parameter vanishes, that is for $\Theta = 0$, in which the thermal state merges into a vacuum state. They are of the form $\int d^3k \frac{1}{|\vec{k}|^3}$ and thus yield a logarithmic UV-divergence. Once these contributions are identified, we express them in the form of Feynman diagrams of the underlying effective QFT. For this purpose, we follow the strategy in [113], where a master equation for a scalar field with an environment consisting of another scalar field is presented. Here the treatment is extended so that the linearised gravitational field can be included as an environment. We will proceed in five steps: first in subsection 11.1 we will identify the divergent contributions in the master equation and then present the corresponding Feynman rules following from the underlying effective QFT based on the non-covariant formulation in subsection 11.2. Afterwards in subsection 11.3 we provide a set of equivalent, covariant Feynman rules in terms of which we perform the renormalisation of the divergent contributions in subsection 11.4. Finally we discuss the resulting renormalised one-particle master equation in subsection 11.5.

11.1. Identification of the involved UV divergences in the one-particle master equation

The content of this subsection was already published in [2]. Here, it is presented with some modifications compared to [2] to adapt it to the flow of the thesis.
Starting from the master equation in (10.42), we want to investigate which terms on the right-hand side are UV-divergent with respect to the $\int_{\mathbb{R}^3} d^3k$ integration. As the projector $P_{ijln}(\vec{k})$ is independent of the absolute value of $\vec{k}$, it does not influence the UV behaviour. Then, one can identify four different types of contributions in the integrands after performing the τ-integration and introducing the following sign factors $\sigma, \sigma_1, \sigma_2 \in \{\pm 1\}$:

(a) $\frac{1}{\omega_{u-k}\Omega_k}\frac{1}{\Omega_k+\omega_{u-k}+\sigma\omega_u}$: for large $|\vec{k}|$, i.e. for $|\vec{k}| >> |\vec{u}|, m$ this term becomes $\frac{1}{|\vec{k}|^3}$ and thus leads to a logarithmic UV-divergence under the integral.

(b) $\frac{1}{\omega_{u-k}\Omega_k}\frac{1}{\Omega_k+\omega_{u-k}+\sigma\omega_u}\rho(\vec{u}+\vec{k},\vec{v}+\vec{k},t)$: assuming that $\rho(\vec{x},\vec{y},t)$ is a proper, normalisable density matrix in position space for which the Fourier transform exists leads to the requirement that $\rho(\vec{u},\vec{v},t)$ has to decrease rapidly for large $\vec{u},\vec{v}$. Therefore this expression is UV-finite.

(c) $N(k)\frac{1}{\omega_{u-k}\Omega_k}\frac{1}{\Omega_k+\sigma_1\omega_{u-k}+\sigma_2\omega_u}$: a series expansion of the denominator of $N(k)$ yields $N(k) = \frac{1}{\beta|\vec{k}|+O(|\vec{k}|^2)}$. Hence, this term tends to zero for large $|\vec{k}|$ and also the combination $\frac{x^n}{e^x-1}$ decreases rapidly for $x \to \infty$, thus this kind of contribution is UV-finite.

(d) $N(k)\frac{1}{\omega_{u-k}\Omega_k}\frac{1}{\Omega_k+\sigma_1\omega_{u-k}+\sigma_2\omega_u}\rho(\vec{u}+\vec{k},\vec{v}+\vec{k},t)$: this contribution is a combination of cases (b) and (c) and also UV-finite.

From this analysis follows that the expressions involving $N(k)$, that would be absent in the vacuum case and are thus denoted as thermal contributions in the following, are all UV-finite. Some of the vacuum contributions, these are the ones that do not involve $N(k)$, lead to UV-divergences which we want to cure by a renormalisation. To achieve this, in the next section we show in a first step that these terms correspond exactly to the self-energy diagrams for the scalar particle in the form of Feynman diagrams.

11.2. Non-covariant Feynman rules and self-energy

The content of this subsection was already published in [2]. Here, it is presented with some modifications compared to [2] to adapt it to the flow of the thesis.
In this section we present the Feynman rules in non-covariant form corresponding to the effective quantum field theory from part II of this thesis containing a scalar field coupled to linearised gravity, where the latter is considered as the environment, which is the basis for the master equation in (10.42). Then, we rewrite these rules in the next section in a covariant form to be able to follow the strategy of [113], where a suitable renormalisation for a master equation for a scalar fields with a second scalar field as the environment is discussed. Here, we slightly extend these methods in order to apply them to the case where the linearised gravitational field is treated as the environment. The Feynman rules can be constructed from section 8:

- The **scalar field** has the standard **propagator**, which follows from its quantised mode expansion in (8.5) and (8.6), which we denote by a solid line and which reads in the mostly

plus signature convention:

$$\text{———} = \frac{-i}{k^2 + m^2 - i\epsilon}\,. \tag{11.1}$$

Here, $k^2 = -\left(k^0\right)^2 + \vec{k}^2$.

- The **propagator of the triad field** was derived in equation (9.24) and is denoted in terms of a curved line:

$$\sim\!\sim\!\sim = \frac{1}{\kappa} P^{abcd}(\vec{k}) \left[\frac{-i}{k^2 - i\epsilon} + 2\pi N(k)\delta(k^2)\right], \tag{11.2}$$

where the first summand is the vacuum and the second one the thermal part. The existing tensor structure manifests in the form of the tensor structure of the STT-projector defined above in (10.15). When contracted with a quantity that is symmetric in (ab) as well as in (cd), like it is the case for the interaction vertex introduced below, the STT-projector reduces to

$$P^{abcd}(\vec{k}) = \delta^{ac}\delta^{bd} - \frac{1}{2}\delta^{ab}\delta^{cd} + \frac{1}{2\vec{k}^4}k^a k^b k^c k^d - \frac{1}{\vec{k}^2}\left(2\delta^{ac}k^b k^d - \frac{1}{2}\delta^{ab}k^c k^d - \frac{1}{2}\delta^{cd}k^a k^b\right)\Bigg]. \tag{11.3}$$

- The coupling between the scalar field and linearised gravity is encoded in the interaction part of the total action in part II that is given as a reformulation of equation (8.18) by:

$$\begin{aligned} S_{int} &= -\int dt \int d^3x\, \mathcal{H}_{int}(\vec{x}, t) \\ &= -\int dt \int \frac{d^3k}{\vec{k}^2}\, \kappa\Big\{\vec{k}^2\, \delta\mathcal{E}_{ab}(\vec{k}, t)\, T^{ab}(-\vec{k}, t) - \frac{1}{2}T_{00}(\vec{k}, t)T^a_a(-\vec{k}, t) \\ &\qquad - \frac{1}{4}T_{00}(\vec{k}, t)T_{00}(-\vec{k}, t) + T_{0a}(\vec{k}, t)T_{0b}(-\vec{k}, t)\left(\delta^{ab} - \frac{k^a k^b}{4\vec{k}^2}\right)\Big\}, \end{aligned} \tag{11.4}$$

where $T^{\mu\nu}(\vec{k}, t)$ denotes the Fourier transform of the scalar field's energy momentum tensor[15]. The interaction vertex between the scalar and the triad field can then be read off and is related to T_{ab}. Due to the fact that T_{ab} depends on derivatives of the scalar field, the expression for the triad-scalar-field vertex is different depending on the direction of the momenta involved in the diagrams. Considering the Fourier transform of $T_{ab}(\vec{x}, t)$, where the the scalar fields can be factorised, we find the expression $\widetilde{T}_{ab}(p, q)\phi(p)\phi(q)$ with

$$\widetilde{T}_{ab}(p, q) := \frac{1}{2}\delta_{ab}[-p_0 q_0 + \vec{p}\cdot\vec{q} - m^2] - \frac{1}{2}[p_a q_b + p_b q_a]\,. \tag{11.5}$$

[15] In position space, its components are given by

$$\begin{aligned} T^{00} &= T_{00} = \frac{1}{2}\left[\pi^2 + (\partial_a\phi)\,(\partial^a\phi) + m^2\phi^2\right] = \epsilon(\phi, \pi)\,, \\ T^{0a} &= T^{a0} = -\delta^{ab}\, T_{0b} = -\delta^{ab}\,\pi\,\partial_b\phi = -\delta^{ab}\, p_b(\phi, \pi)\,, \\ T^{ab} &= \delta^{ac}\,\delta^{bd}\, T_{cd} = \frac{\delta^{ab}}{2}\left[\pi^2 - (\partial_c\phi)\,(\partial^c\phi) - m^2\phi^2\right] + (\partial^a\phi)\,(\partial^b\phi)\,. \end{aligned}$$

Hence, the **triad-scalar-field-vertex** is given by

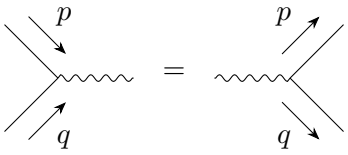

$$= i\kappa \tilde{T}_{ab}(\sigma_p p, \sigma_q q)\,,$$

where σ_p is $+$ if particle p is incoming and $-$ if it is outgoing.

- The remaining terms in the interaction part of the action (11.4) give rise to an additional **second order vertex** which cannot be split into first order vertices due to the lack of a suitable intermediate particle in this effective field theory. They have the form

$$-\kappa \int d^3x \int d^3y \frac{-\frac{1}{4}T_{00}(\vec{x})T_{00}(\vec{y}) + T_{0a}(\vec{x})T_{0b}(\vec{y})\delta^{ab} - \frac{1}{4}\left(T_{00}(\vec{x})T^a_a(\vec{y}) + T^a_a(\vec{x})T_{00}(\vec{y})\right)}{4\pi||\vec{x}-\vec{y}||}$$
$$-\kappa \int d^3x \int d^3y \int d^3z \frac{-\frac{1}{4}\partial^a_{\vec{x}}T_{0a}(\vec{x})\;\partial^b_{\vec{y}}T_{0b}(\vec{y})}{(4\pi)^2||\vec{x}-\vec{z}||||\vec{y}-\vec{z}||}\,. \tag{11.6}$$

The corresponding symmetrised Feynman rule reads:

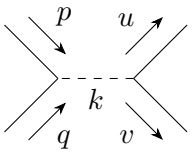

$$= -\tfrac{i\kappa}{\vec{k}^2} NI(p,q,u,v)$$

with

$$NI(p,q,u,v) := \Bigg[-\frac{1}{4}\tilde{T}_{00}(p,q)\tilde{T}_{00}(-u,-v) + \tilde{T}_{0a}(p,q)\tilde{T}_{0b}(-u,-v)\left(\delta^{ab} - \frac{k^a k^b}{4\vec{k}^2}\right)$$
$$-\frac{1}{4}\widetilde{T}_{00}(p,q)\widetilde{T}^a_a(-u,-v) - \frac{1}{4}\widetilde{T}^a_a(p,q)\widetilde{T}_{00}(-u,-v)\Bigg], \tag{11.7}$$

with $\vec{k}$ defined using momentum conservation as $\vec{k} = \vec{p} + \vec{q} = \vec{u} + \vec{v}$. Note that a similar vertex does also appear in QED when quantised in Coulomb gauge and there it represents the Coulomb interaction, see for instance [131, 132].

- As **external lines** we only have the scalar field in the cases we are interested in here. This follows the standard case for a quantised scalar field, the detailed expressions are however not required for the following discussions.

Equipped with these Feynman rules, we will now show in the subsequent section that the divergent contributions in the one-particle master equation can be identified exactly with the contribution of the self-energy diagram constructed with the above Feynman rules. In the model considered here this corresponds to the following Feynman diagram:

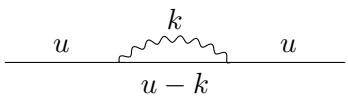

(11.8)

With the Feynman rules introduced above, the amplitude represented by this diagram and denoted by $\Pi(u^2)$ has the form

$$\begin{aligned}
\Pi(u^2) :=& \int_{\mathbb{R}^4} \frac{d^4k}{(2\pi)^4} \frac{1}{\kappa} P^{abcd}(\vec{k}) \left[\frac{-i}{k^2 - i\epsilon} + 2\pi N(k)\delta(k^2) \right] \left[i\kappa \widetilde{T}_{ab}(u, -(u-k)) \right] \\
& \cdot \frac{-i}{(u-k)^2 + m^2 - i\epsilon} \left[i\kappa \widetilde{T}_{cd}(u-k, -u) \right] \\
=& \kappa u_a u_b u_c u_d \int_{\mathbb{R}^4} \frac{d^4k}{(2\pi)^4} P^{abcd}(\vec{k}) \left[\frac{-i}{k^2 - i\epsilon} + 2\pi N(k)\delta(k^2) \right] \frac{1}{(u-k)^2 + m^2 - i\epsilon} \\
=& \kappa \int_{\mathbb{R}^3} \frac{d^3k}{2(2\pi)^3} P_u(\vec{k}) \Bigg\{ \frac{(\Omega_k + \omega_{u-k})}{\Omega_k \omega_{u-k} (\Omega_k + \omega_{u-k} + u^0 - i\epsilon)(\Omega_k + \omega_{u-k} - u^0 - i\epsilon)} \\
& - N(\Omega_k) \Bigg[\frac{1}{\Omega_k (u^0 - \Omega_k + \omega_{u-k} - i\epsilon)(u^0 - \Omega_k - \omega_{u-k} + i\epsilon)} \\
& + \frac{1}{\Omega_k (u^0 + \Omega_k + \omega_{u-k} - i\epsilon)(u^0 + \Omega_k - \omega_{u-k} + i\epsilon)} \Bigg] \Bigg\} \\
=& \Pi_{vac}(u^2) + \Pi_\Theta(u^2)
\end{aligned} \tag{11.9}$$

In the first step the definition of $\widetilde{T}_{ab}$ in (11.5) was used and in the second step the k^0-integration was performed, where for the vacuum part the residue theorem was applied. In the last step, we have defined the vacuum and thermal contribution to the self-energy as

$$\begin{aligned}
\Pi_{vac}(u^2) :=& \kappa \int_{\mathbb{R}^3} \frac{d^3k}{2(2\pi)^3} P_u(\vec{k}) \Bigg\{ \frac{(\Omega_k + \omega_{u-k})}{\Omega_k \omega_{u-k} (\Omega_k + \omega_{u-k} + u^0 - i\epsilon)(\Omega_k + \omega_{u-k} - u^0 - i\epsilon)} \qquad (11.10) \\
\Pi_\Theta(u^2) :=& -\kappa \int_{\mathbb{R}^3} \frac{d^3k}{2(2\pi)^3} P_u(\vec{k}) N(\Omega_k) \Bigg[\frac{1}{\Omega_k (u^0 - \Omega_k + \omega_{u-k} - i\epsilon)(u^0 - \Omega_k - \omega_{u-k} + i\epsilon)} \\
& + \frac{1}{\Omega_k (u^0 + \Omega_k + \omega_{u-k} - i\epsilon)(u^0 + \Omega_k - \omega_{u-k} + i\epsilon)} \Bigg] \Bigg\}. \qquad (11.11)
\end{aligned}$$

If we now want to identify contributions in the one-particle master equation with the self-energy, the following subtlety results: a key difference between the master equation in (10.42) and standard quantum field theory is that the latter is constructed for the limit $t_0 \to -\infty$, $t \to \infty$ when evaluating scattering amplitudes. To take this into account, we apply the method presented in [113] for situations where there is a finite temporal interval. In this way, we can transform the self-energy diagram into the second line of the right-hand side of the master equation in (10.42):

$$\Xi(\omega_u, \vec{u}, t_0, t) := \int_{t_0}^{t} d\tau \int_{\mathbb{R}} du^0 \, \Pi(u^2) \cos[(u^0 - \omega_u)(t-\tau)] = \int_0^{t-t_0} d\tau \int_{\mathbb{R}} du^0 \, \Pi(u^2) \cos[(u^0 - \omega_u)\tau] \,. \tag{11.12}$$

The standard QFT-limit can be recovered, in which $t \to \infty$ and $t_0 \to -\infty$, and using this the integral over the temporal interval can be rewritten as a δ-distribution as $\int_0^\infty d\tau \cos[(u^0 - \omega_u)\tau] = \frac{1}{2} \int_{-\infty}^{\infty} d\tau e^{-i(u^0 - \omega_u)\tau} = \pi\delta(u^0 - \omega_u)$, that will set the external momentum u on-shell.

After evaluating the u^0 integration we obtain for finite times t and t_0:

$$\Xi(\omega_u, \vec{u}, t_0, t) = \frac{\kappa}{2} \int_{\mathbb{R}^3} \frac{d^3k}{(2\pi)^3} P_u(\vec{k}) \frac{\pi i}{2\omega_{u-k}} \left[C(\vec{u}, \vec{k}, t - t_0) + C_P(\vec{u}, \vec{k}, t - t_0) \right] , \tag{11.13}$$

which indeed, multiplied by a factor $\frac{2i}{\pi\omega_u}$, can be identified with the first term on the right hand side of the second line of the one-particle master equation in (10.42) in the extended one-particle projection. Given this results, it is now also easy to discuss the case of the non-extended one-particle projection: the master equation for this case, i.e. for $\delta_P = 0$, can just be obtained by replacing the cosine in (11.12) by $\frac{1}{2} e^{-i(u^0-\omega_u)\tau}$. We find that in the QFT-limit the difference between the extended and non-extended one-particle projection manifests itself in a factor of 2. To obtain the second term in the second line of (10.42), we can follow the same steps and just have to replace $\vec{u}$ by $\vec{v}$ and take the complex conjugate.

With the results in this subsection we have shown that the UV-divergent terms in the one-particle master equation correspond to the self-energies of the scalar particle. What remains is to discuss the renormalisation of this self-energy. In order to be able to apply the standard procedure for renormalisation in this case, however, we first derive the corresponding covariant Feynman rules of the model considered here.

11.3. Covariant Feynman rules

The content of this subsection was already published in [2]. Here, it is presented with some modifications compared to [2] to adapt it to the flow of the thesis.
To be able to employ the standard renormalisation technique for the loop associated with the scalar particle's self-energy, we introduce in this section the covariant Feynman rules corresponding to the effective QFT under consideration here. For this, we follow [131, 132], where the procedure is outlined for QED.

In a first step we will demonstrate that specific sums of non-covariant Feynman diagrams add up to the corresponding covariant Feynman diagram. For this purpose, we consider the sum of the second order vertex in (11.6) with a second order combination of the non-covariant scalar field-triad vertex, shown below (11.5). As will be derived below, the second order vertex in (11.6) is precisely that term which restores covariance if we work with a fully covariant triad propagator and a covariant vertex.
We will restrict our discussions mainly to a Coulomb-scattering type of diagram here which is sufficient for our later applications. At the end of this section we will also briefly discuss the diagram associated with the scalar particle's self-energy. In the case of the Coulomb-scattering type diagram, the above mentioned equivalence in terms of Feynman diagrams reads

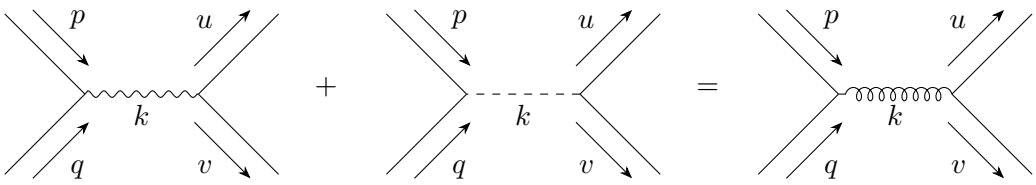

where the curly line corresponds to the covariant triad propagator. Next, we will present the covariant Feynman rules, then specialise them to the case of the Coulomb-scattering type diagram to show the above equivalence. The corresponding covariant Feynman rules for the propagators and vertices discussed in the last subsection are as follows:

- The **scalar propagator** remains unchanged

$$\text{———} = \frac{-i}{k^2 + m^2 - i\epsilon}\,. \tag{11.14}$$

- The **covariant triad propagator** becomes

$$\text{〰〰} = \frac{1}{\kappa}\frac{-i}{k^2 - i\epsilon} P_{\mu\nu\rho\sigma} \tag{11.15}$$

  with

$$P_{\mu\nu\rho\sigma} := \frac{1}{2}[\eta_{\mu\rho}\eta_{\nu\sigma} + \eta_{\mu\sigma}\eta_{\nu\rho} - \eta_{\mu\nu}\eta_{\rho\sigma}]\,. \tag{11.16}$$

  In the context of a linearised gravitational environment there is no multi-triad vertex and therefore in the effective QFT considered in this work the triad propagator always couples only to the scalar field-triad-vertex, see also below. The latter is symmetric in $(\mu\nu)$ as well as in $(\rho\sigma)$. This allows us to slightly simplify the projector $P_{\mu\nu\rho\sigma}$ whenever it occurs in combination with scalar field-triad-vertices and express it as

$$P_{\mu\nu\rho\sigma} := \eta_{\mu\rho}\eta_{\nu\sigma} - \frac{1}{2}\eta_{\mu\nu}\eta_{\rho\sigma}\,. \tag{11.17}$$

- The **covariant vertex** is given by

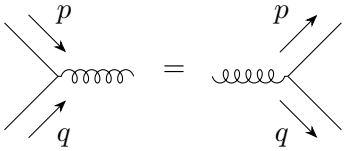

$$= \tfrac{-i\kappa}{2}(-2\tilde{T}^{\mu\nu}(\sigma_p p, \sigma_q q) + \eta^{\mu\nu}\tilde{T}^{\rho}_{\rho}(\sigma_p p, \sigma_q q))\,,$$

  where

$$\widetilde{T}^{\mu\nu}(p,q) = \frac{1}{2}\eta^{\mu\nu}\left(p_\rho q^\rho - m^2\right) - \frac{1}{2}(p^\mu q^\nu + p^\nu q^\mu)\,. \tag{11.18}$$

  Whenever this is combined with a triad propagator, the second term of the vertex contribution vanishes because we have

$$\eta^{\mu\nu}\widetilde{T}^{\alpha}_{\alpha}[\eta_{\mu\rho}\eta_{\nu\sigma} + \eta_{\mu\sigma}\eta_{\nu\rho} - \eta_{\mu\nu}\eta_{\rho\sigma}] = 2\eta_{\rho\sigma}\widetilde{T}^{\alpha}_{\alpha} - 2\eta_{\rho\sigma}\widetilde{T}^{\alpha}_{\alpha} = 0\,, \tag{11.19}$$

  where we used that $\eta^{\mu\nu}\eta_{\mu\nu} = 4$. Hence, for processes like Coulomb scattering we can replace the expression for the vertex with

$$i\kappa\widetilde{T}^{\mu\nu}(\sigma_p p, \sigma_q q)\,. \tag{11.20}$$

- Since the second order vertex was used to obtain a covariant propagator and vertex, there is no analogue of the second order vertex in the covariant case.

- The **external lines** for the scalar field remain unmodified and the ones for the triad field are not important for this work.

These covariant Feynman rules are in accordance with the ones[16] presented in [172, 173], where also a scalar field is coupled to a linearised gravitational field, except for the usual differences caused by the choice of different signatures for the metric, as they use the mostly minus signature. Using momentum conservation, i.e. $k = p + q = u + v$, yields

$$k^\mu \widetilde{T}_{\mu 0}(p,q) = k^0 \widetilde{T}_{00}(p,q) + k^a \widetilde{T}_{a0}(p,q) = \frac{1}{2}[q_0(p_0^2 - \vec{p}^2 - m^2) + p_0(q_0^2 - \vec{q}^2 - m^2)] = 0\,, \quad (11.21)$$

$$k^\mu \widetilde{T}_{\mu a}(p,q) = k^0 \widetilde{T}_{0a}(p,q) + k^b \widetilde{T}_{ba}(p,q) = \frac{1}{2}[q_a(p_0^2 - \vec{p}^2 - m^2) + p_a(q_0^2 - \vec{q}^2 - m^2)] = 0\,. \quad (11.22)$$

If the scalar field is on-shell, which we assume for a moment for the Coulomb-scattering diagram, then the right hand side of both expressions vanishes. With this, one can directly show the equivalence of using the covariant set of Feynman rules for the Coulomb scattering diagrams discussed above of this: the left hand side of the equality for the Coulomb-scattering diagrams at the beginning of this subsection is expressed in terms of the non-covariant Feynman rules and the first diagram, which we label **A**, reads

$$\begin{aligned}
\mathbf{A} =& \frac{1}{2}(-i\kappa)^2 \widetilde{T}_{ab}(p,q)\widetilde{T}_{cd}(-u,-v)\frac{-i}{\kappa}\frac{1}{k^2}P^{abcd}(\vec{k}) \\
&= \frac{i\kappa}{2k^2}\widetilde{T}_{ab}(p,q)\widetilde{T}_{cd}(-u,-v)\left[\left(\delta^{ac} - \frac{k^a k^c}{\vec{k}^2}\right)\left(\delta^{bd} - \frac{k^b k^d}{\vec{k}^2}\right) - \frac{1}{2}\left(\delta^{ab} - \frac{k^a k^b}{\vec{k}^2}\right)\left(\delta^{cd} - \frac{k^c k^d}{\vec{k}^2}\right)\right] \\
&= \frac{i\kappa}{k^2}\Bigg[\frac{1}{2}\widetilde{T}_{ab}(p,q)\widetilde{T}^{ab}(-u,-v) - \frac{1}{4}\widetilde{T}^a_a(p,q)\widetilde{T}^b_b(-u,-v) + \frac{1}{4\vec{k}^4}k^a k^b k^c k^d \widetilde{T}_{ab}(p,q)\widetilde{T}_{cd}(-u,-v) \\
&\quad - \frac{1}{\vec{k}^2}\Big\{\widetilde{T}_{ab}(p,q)\widetilde{T}^a_c(-u,-v)k^b k^c - \frac{1}{4}\widetilde{T}_{ab}(p,q)\widetilde{T}^c_c(-u,-v)k^a k^b \\
&\qquad\qquad - \frac{1}{4}\widetilde{T}^a_a(p,q)\widetilde{T}_{cd}(-u,-v)k^c k^d\Big\}\Bigg]\,,
\end{aligned} \quad (11.23)$$

where the overall factor of $\frac{1}{2}$ arises due to the fact that it is a diagram of second order in the expansion of the Dyson series. Next, we can make use of energy-momentum conservation (11.21) and (11.22), as we assumed the scalar particles to be on-shell, and find

$$k^a k^b \widetilde{T}_{ab}(p,q) = -k^0 k^b \widetilde{T}_{0b}(p,q) = (k^0)^2 \widetilde{T}_{00}(p,q) \quad (11.24)$$

$$k^a \widetilde{T}_{ab}(p,q) = -k^0 \widetilde{T}_{0b}(p,q) \quad (11.25)$$

$$k^a \widetilde{T}_{0a}(p,q) = -k^0 \widetilde{T}_{00}(p,q) \quad (11.26)$$

which leads to

$$\begin{aligned}
\mathbf{A} = \frac{i\kappa}{k^2}\Bigg[&\frac{1}{2}\widetilde{T}_{ab}(p,q)\widetilde{T}^{ab}(-u,-v) - \frac{1}{4}\widetilde{T}^a_a(p,q)\widetilde{T}^b_b(-u,-v) + \frac{(k^0)^4}{4\vec{k}^4}\widetilde{T}_{00}(p,q)\widetilde{T}_{00}(-u,-v) \\
&- \frac{(k^0)^2}{\vec{k}^2}\Big\{\widetilde{T}_{a0}(p,q)\widetilde{T}^a_0(-u,-v) - \frac{1}{4}\widetilde{T}_{00}(p,q)\widetilde{T}^c_c(-u,-v) - \frac{1}{4}\widetilde{T}^a_a(p,q)\widetilde{T}_{00}(-u,-v)\Big\}\Bigg]\,.
\end{aligned} \quad (11.27)$$

[16] Their vertex has one incoming and one outgoing scalar particle, hence is equivalent to $i\kappa\widetilde{T}^{\mu\nu}(p,-q)$ in the notation used here.

Combining this with the expression for the second term in the above Feynman diagram for Coulomb-like scattering, which we call **B** and which reads

$$\begin{aligned}\mathbf{B} =& -\frac{i\kappa}{\vec{k}^2}\Bigg[-\frac{1}{4}\tilde{T}_{00}(p,q)\tilde{T}_{00}(-u,-v)+\tilde{T}_{0a}(p,q)\tilde{T}_{0b}(-u,-v)\left(\delta^{ab}-\frac{k^a k^b}{4\vec{k}^2}\right)\\ &\qquad -\frac{1}{4}\widetilde{T}_{00}(p,q)\widetilde{T}^a_a(-u,-v)-\frac{1}{4}\widetilde{T}^a_a(p,q)\widetilde{T}_{00}(-u,-v)\Bigg]\\ =& -\frac{i\kappa}{k^2}\Bigg[-\frac{k^2}{4\vec{k}^2}\tilde{T}_{00}(p,q)\tilde{T}_{00}(-u,-v)+\frac{k^2}{\vec{k}^2}\tilde{T}_{0a}(p,q)\tilde{T}^a_0(-u,-v)-\frac{k^2(k^0)^2}{4\vec{k}^4}\tilde{T}_{00}(p,q)\tilde{T}_{00}(-u,-v)\\ &\qquad -\frac{k^2}{4\vec{k}^2}\widetilde{T}_{00}(p,q)\widetilde{T}^a_a(-u,-v)-\frac{k^2}{4\vec{k}^2}\widetilde{T}^a_a(p,q)\widetilde{T}_{00}(-u,-v)\Bigg],\end{aligned} \tag{11.28}$$

one can obtain

$$\begin{aligned}\mathbf{A}+\mathbf{B} =& \frac{i\kappa}{k^2}\Bigg[\left(\frac{(k^0)^4+k^2\vec{k}^2+k^2(k^0)^2}{4\vec{k}^4}\right)\tilde{T}_{00}(p,q)\tilde{T}_{00}(-u,-v)-\left(\frac{(k^0)^2+k^2}{\vec{k}^2}\right)\tilde{T}_{0a}(p,q)\tilde{T}^a_0(-u,-v)\\ &\quad +\frac{1}{2}\widetilde{T}_{ab}(p,q)\widetilde{T}^{ab}(-u,-v)-\frac{1}{4}\widetilde{T}^a_a(p,q)\widetilde{T}^b_b(-u,-v)\\ &\quad +\left(\frac{(k^0)^2+k^2}{4\vec{k}^2}\right)\widetilde{T}_{00}(p,q)\widetilde{T}^c_c(-u,-v)+\left(\frac{(k^0)^2+k^2}{4\vec{k}^2}\right)\widetilde{T}^a_a(p,q)\widetilde{T}_{00}(-u,-v)\Bigg]\\ =& \frac{i\kappa}{k^2}\Bigg[\frac{1}{4}\tilde{T}_{00}(p,q)\tilde{T}_{00}(-u,-v)-\tilde{T}_{0a}(p,q)\tilde{T}^a_0(-u,-v)+\frac{1}{2}\widetilde{T}_{ab}(p,q)\widetilde{T}^{ab}(-u,-v)\\ &\quad -\frac{1}{4}\widetilde{T}^a_a(p,q)\widetilde{T}^b_b(-u,-v)+\frac{1}{4}\widetilde{T}_{00}(p,q)\widetilde{T}^c_c(-u,-v)+\frac{1}{4}\widetilde{T}^a_a(p,q)\widetilde{T}_{00}(-u,-v)\Bigg].\end{aligned} \tag{11.29}$$

On the other hand, we get with the covariant Feynman rules for the right side of the Coulomb-like scattering diagram above[17], which we name **C**:

$$\begin{aligned}\mathbf{C} =& \frac{1}{2}\frac{i\kappa}{k^2}\widetilde{T}_{\mu\nu}(p,q)\widetilde{T}_{\rho\sigma}(-u,-v)\left(\eta^{\mu\rho}\eta^{\nu\sigma}-\frac{1}{2}\eta^{\mu\nu}\eta^{\rho\sigma}\right)\\ =& \frac{i\kappa}{2k^2}\left[\widetilde{T}_{\mu\nu}(p,q)\widetilde{T}^{\mu\nu}(-u,-v)-\frac{1}{2}\widetilde{T}^\mu_\mu(p,q)\widetilde{T}^\rho_\rho(-u,-v)\right]\\ =& \frac{i\kappa}{4k^2}\Bigg[2\widetilde{T}_{00}(p,q)\widetilde{T}^{00}(-u,-v)+2\widetilde{T}_{ab}(p,q)\widetilde{T}^{ab}(-u,-v)+4\widetilde{T}_{0a}(p,q)\widetilde{T}^{0a}(-u,-v)\\ &\quad -\widetilde{T}^0_0(p,q)\widetilde{T}^0_0(-u,-v)-\widetilde{T}^0_0(p,q)\widetilde{T}^c_c(-u,-v)-\widetilde{T}^a_a(p,q)\widetilde{T}^0_0(-u,-v)-\widetilde{T}^a_a(p,q)\widetilde{T}^b_b(-u,-v)\Bigg]\end{aligned}$$

[17] Note that this diagram is again of second order in the expansion of the Dyson series, hence we obtain a factor of $\frac{1}{2}$.

$$= \frac{i\kappa}{k^2}\Bigg[\frac{1}{4}\widetilde{T}_{00}(p,q)\widetilde{T}_{00}(-u,-v)\widetilde{T}_{0a}(p,q)\widetilde{T}^{0a}(-u,-v) + \frac{1}{2}\widetilde{T}_{ab}(p,q)\widetilde{T}^{ab}(-u,-v) - \\ - \frac{1}{4}\widetilde{T}^a_a(p,q)\widetilde{T}^b_b(-u,-v) + \frac{1}{4}\widetilde{T}_{00}(p,q)\widetilde{T}^c_c(-u,-v) + \frac{1}{4}\widetilde{T}^a_a(p,q)\widetilde{T}_{00}(-u,-v)\Bigg]. \tag{11.30}$$

Note that we use the mostly plus signature of the metric, hence pulling a temporal index results in a sign change. By comparing (11.29) and (11.30) we can see that they are identical, therefore we indeed have that the non-covariant and the covariant Feynman rules produce the same result for Coulomb-like scattering.

As a next step we would like to show a similar equivalence between the non-covariant and covariant Feynman rules for the self-energy diagram, namely the following equivalence in terms of Feynman diagrams:

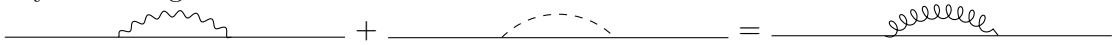

The diverging term in the one-particle master equation actually only contains the first of the two Feynman diagrams on the left hand side. However, the second term is the self-energy contribution which vanishes in the one-particle projection of the master equation, so we can add this diagram as in the one-particle master equation its contribution vanishes for normal ordering.
The equivalence for the Feynman diagrams on both sides of this equation is however much more difficult to prove compared to the Coulomb scattering diagram, which is also the case in QED, since the momentum inside the loop is not on-shell, which prevents a similar calculations as done for the Coulomb scattering tree level graph as there will remain correction terms to the relations in (11.24) - (11.26). Given that, to prove this equivalence goes beyond the scope of this work here and we refer here to the fact that the covariant set of Feynman rules can also be derived from the same underlying action using a different approach and gauge, which are then used for instance in [172, 173]. Hence, independently of the derivation, we expect that they describe the same physics. Based on this, it is now possible to specify the expression corresponding to the scalar particle self-energy diagram in covariant form and renormalise it, which will be discussed in detail in the next subsection. As mentioned at the beginning of this subsection, such a replacement of non-covariant by covariant Feynman rules along the lines presented here is also employed in QED when quantising in Coulomb gauge, as for instance in [131, 132].

11.4. UV-renormalisation of the self-energy of the scalar particle

The content of this subsection was already published in [2]. Here, it is presented with some modifications compared to [2] to adapt it to the flow of the thesis.
In terms of the Feynman rules introduced in the previous section, the self-energy diagram for the vacuum propagator, which was defined in (11.10), can be expressed as

$$\begin{aligned}\Pi_{vac}(u^2) = \int \frac{d^4k}{(2\pi)^4}\left[i\kappa\widetilde{T}^{\mu\nu}(u,-(u-k))\right]\left[i\kappa\widetilde{T}^{\rho\sigma}(u-k,-u)\right]\frac{1}{\kappa}\frac{-i}{k^2-i\epsilon} \\ \cdot\frac{1}{2}\left[\eta_{\mu\rho}\eta_{\nu\sigma}+\eta_{\mu\sigma}\eta_{\nu\rho}-\eta_{\mu\nu}\eta_{\rho\sigma}\right]\frac{-i}{(u-k)^2+m^2-i\epsilon} \\ = \frac{\kappa}{2}\int d^4k \frac{u^2k^2+2m^2uk-2m^4}{[(k+u)^2-i\epsilon][k^2+m^2-i\epsilon]}\,.\end{aligned} \tag{11.31}$$

As the thermal part $\Pi_\Theta(u^2)$ defined in (11.11) is not divergent, as it has been discussed in subsection 11.1, we only consider the vacuum part here. For the renormalisation we follow the strategy in [174]. Using dimensional regularisation with $d = 4 - \epsilon$, the STT-projector is slightly modified in d dimensions and reads (see e.g. [173]):

$$P_{\mu\nu\rho\sigma} := \frac{1}{2}[\eta_{\mu\rho}\eta_{\nu\sigma} + \eta_{\mu\sigma}\eta_{\nu\rho} - \frac{2}{2-\epsilon}\eta_{\mu\nu}\eta_{\rho\sigma}]\,. \tag{11.32}$$

Due to this, the expression for the self-energy diagram slightly changes and becomes (for $\epsilon \ll 1$):

$$\Pi_{vac}(u^2) = \frac{\kappa}{2}\mu^\epsilon \int d^dk \frac{u^2k^2 + 2m^2uk - 2m^4\left(1+\frac{\epsilon}{4}\right)}{[(k+u)^2 - i\epsilon][k^2+m^2-i\epsilon]}\,, \tag{11.33}$$

which coincides with the expression derived in [173]. Here, we rescaled $\kappa \to \kappa\mu^\epsilon$ to keep the dimension of κ for any value of d. As later we will encounter also IR-divergences, we introduce a small artificial triad mass λ in the triad propagator that becomes

$$\frac{1}{\kappa}\frac{-i}{k^2+\lambda^2-i\epsilon}P_{\mu\nu\rho\sigma}\,. \tag{11.34}$$

With this, the self-energy diagram reads

$$\Pi_{vac}(u^2) = \frac{\kappa}{2}\mu^\epsilon \int d^dk \frac{u^2k^2 + 2m^2uk - 2m^4\left(1+\frac{\epsilon}{4}\right)}{[(k+u)^2 + \lambda^2 - i\epsilon][k^2+m^2-i\epsilon]}\,, \tag{11.35}$$

which will be evaluated in what follows.

11.4.1. Computation of the loop integral

The content of this subsection was already published in [2]. Here, it is presented with some modifications compared to [2] to adapt it to the flow of the thesis.
In a first step we use the identity

$$\frac{1}{x-i\epsilon} = i\int_0^\infty dz\; e^{-iz(x-i\epsilon)} \tag{11.36}$$

in order to rewrite equation (11.35) as

$$\begin{aligned}\Pi_{vac}(u^2) &= -\frac{\kappa}{2}\mu^\epsilon \int d^dk \left[u^2k^2 + 2m^2uk - 2m^4\left(1+\frac{\epsilon}{4}\right)\right] \\ &\qquad\qquad \cdot \int_0^\infty dz_1 \int_0^\infty dz_2\; e^{-iz_1(k^2+m^2-i\epsilon)} e^{-iz_2((k+u)^2+\lambda^2-i\epsilon)} \\ &= -\frac{\kappa}{2}\mu^\epsilon \int_0^\infty dz_1 \int_0^\infty dz_2 \int d^dk \left[u^2k^2 + 2m^2uk - 2m^4\left(1+\frac{\epsilon}{4}\right)\right] \\ &\qquad\qquad \cdot e^{-i(z_1+z_2)\left(k+\frac{z_2u}{z_1+z_2}\right)^2 - \left[\epsilon(z_1+z_2)+i\lambda^2z_2+im^2z_1+iu^2z_2 - i\frac{z_2^2u^2}{z_1+z_2}\right]}\,.\end{aligned} \tag{11.37}$$

Substituting $k \to k - \frac{z_2 u}{z_1+z_2}$ then yields

$$\Pi_{vac}(u^2) = -\frac{\kappa}{2}\mu^\epsilon \int_0^\infty dz_1 \int_0^\infty dz_2 \int d^d k \Big[u^2 k^2 - 2u^2 \frac{z_2 u k}{z_1+z_2} + \frac{z_2^2 u^4}{(z_1+z_2)^2} + 2m^2 u k - 2m^2 \frac{z_2 u^2}{z_1+z_2} - 2m^4 \left(1+\frac{\epsilon}{4}\right) \Big] \cdot e^{-i(z_1+z_2)k^2 - \left[\epsilon(z_1+z_2) + i(\lambda^2+u^2)z_2 + i m^2 z_1 - i\frac{z_2^2 u^2}{z_1+z_2}\right]} . \tag{11.38}$$

Due to symmetry, all terms linear in k vanish and only terms of two different kinds remain for which the k-integrations can be performed directly:

$$\int d^d k \; e^{-i(z_1+z_2)k^2} = \sqrt{\frac{-\pi i}{z_1+z_2}}^d , \tag{11.39}$$

$$\int d^d k \; k^2 \, e^{-i(z_1+z_2)k^2} = i\frac{d}{d(z_1+z_2)} \int d^d k \; e^{-i(z_1+z_2)k^2} = \frac{d}{2\pi} \sqrt{\frac{-\pi i}{z_1+z_2}}^{d+2} . \tag{11.40}$$

Employing these, one can rewrite the self-energy as:

$$\Pi_{vac}(u^2) = -\frac{\kappa}{2}\mu^\epsilon \int_0^\infty dz_1 \int_0^\infty dz_2 \; e^{-\left[\epsilon(z_1+z_2) + i(\lambda^2+u^2)z_2 + i m^2 z_1 - i\frac{z_2^2 u^2}{z_1+z_2}\right]} \cdot \left\{ \sqrt{\frac{-\pi i}{z_1+z_2}}^d \left[\frac{z_2^2 u^4}{(z_1+z_2)^2} - 2m^2 \frac{z_2 u^2}{z_1+z_2} - 2m^4 \left(1+\frac{\epsilon}{4}\right) \right] + \frac{u^2 d}{2\pi} \sqrt{\frac{-\pi i}{z_1+z_2}}^{d+2} \right\} . \tag{11.41}$$

To continue, we use[18]

$$1 = \lim_{\xi \to 0} \int_\xi^\infty \frac{d\beta}{\beta} \, \delta\left(1 - \frac{z_1+z_2}{\beta}\right) . \tag{11.42}$$

By substituting $z_1 \to z_1\beta$ and $z_2 \to z_2\beta$ we then obtain

$$\begin{aligned} &\Pi_{vac}(u^2) = \\ &= -\frac{\kappa}{2}\mu^\epsilon \int_0^\infty dz_1 \int_0^\infty dz_2 \lim_{\xi\to 0} \int_\xi^\infty d\beta \; \delta(1-(z_1+z_2))\beta \, e^{-\beta\left[\epsilon(z_1+z_2) + i(\lambda^2+u^2)z_2 + i m^2 z_1 - i\frac{z_2^2 u^2}{z_1+z_2}\right]} \\ &\qquad \cdot \left\{ \sqrt{\frac{-\pi i}{\beta(z_1+z_2)}}^d \left[\frac{z_2^2 u^4}{(z_1+z_2)^2} - 2m^2 \frac{z_2 u^2}{z_1+z_2} - 2m^4 \left(1+\frac{\epsilon}{4}\right) \right] \right. \end{aligned}$$

[18] This equality can be shown by using that $\delta(f(x)) = \sum_i \frac{\delta(x-x_i)}{|f'(x_i)|}$, where x_i are the points for which $f(x_i) = 0$, $f'(x_i) \neq 0$ holds. That carries here over to $\int_\xi^\infty d\beta \; \frac{z_1+z_2}{\beta} \delta(\beta - (z_1+z_2))$, where we used that $z_1 + z_2 \geq 0$ which allowed us to drop the absolute value.

$$
\begin{aligned}
&\qquad\qquad + \frac{u^2 d}{2\pi}\sqrt{\frac{-\pi i}{\beta(z_1+z_2)}}^{d+2}\Bigg\} \\
&= -\frac{\kappa}{2}\mu^\epsilon \int_0^1 dz \lim_{\xi\to 0}\int_\xi^\infty d\beta\; \beta\, e^{-\beta\left[\epsilon + i(\lambda^2+u^2)z + im^2(1-z) - iz^2u^2\right]} \\
&\qquad\qquad \cdot\left\{\sqrt{\frac{-\pi i}{\beta}}^{d}\left[z^2u^4 - 2m^2zu^2 - 2m^4\left(1+\frac{\epsilon}{4}\right)\right] + \frac{u^2 d}{2\pi}\sqrt{\frac{-\pi i}{\beta}}^{d+2}\right\} \\
&= -\frac{\kappa}{2}\mu^\epsilon \int_0^1 dz \lim_{\xi\to 0}\int_\xi^\infty d\beta\; e^{-i\beta\left[-i\epsilon + (\lambda^2+u^2)z + m^2(1-z) - z^2u^2\right]} \\
&\qquad\qquad \cdot\Bigg\{ -\pi^2\frac{\beta^{\frac{\epsilon}{2}}}{\beta}\sqrt{-i\pi}^{-\epsilon}\left[z^2u^4 - 2m^2zu^2 - 2m^4\left(1+\frac{\epsilon}{4}\right)\right] \\
&\qquad\qquad\qquad + i\pi^2\frac{4-\epsilon}{2}u^2\sqrt{-i\pi}^{-\epsilon}\frac{\beta^{\frac{\epsilon}{2}}}{\beta^2}\Bigg\},
\end{aligned}
\tag{11.43}
$$

where in the last step we used $d = 4 - \epsilon$. Next, we perform the β-integration, that is

$$
\lim_{\xi\to 0}\int_\xi^\infty d\beta\; e^{-i\beta a}\,\frac{\beta^{\frac{\epsilon}{2}}}{\beta^n}\,, \tag{11.44}
$$

where we already set $\epsilon = 0$ in the exponential, with $a = (\lambda^2+u^2)z + m^2(1-z) - z^2u^2$ and $n \in \{1,2\}$. To obtain the result, we apply the residue theorem. For $a > 0$ the contour can be closed by a quarter circle from ∞ to $-i\infty + \xi$ and a line from $-i\infty + \xi$ to ξ. With this, the pole at $\beta = 0$ can be avoided. The integral then becomes

$$
\lim_{\xi\to 0}\int_\xi^\infty d\beta\; e^{-i\beta a}\,\frac{\beta^{\frac{\epsilon}{2}}}{\beta^n} = -\lim_{\xi\to 0}\int_0^\infty dt\; e^{-t}(t+i\xi a)^{\frac{\epsilon}{2}-n}(-i)^{\frac{\epsilon}{2}-n+1}a^{-\frac{\epsilon}{2}+n-1}\,, \tag{11.45}
$$

where we substituted $t = \beta a$. Expanding the term $(t+i\xi a)^{\frac{\epsilon}{2}-n}$ for small ξ yields

$$
(t+i\xi a)^{\frac{\epsilon}{2}-n} = t^{\frac{\epsilon}{2}-n} + i\xi a\left(\frac{\epsilon}{2}-n\right)t^{\frac{\epsilon}{2}-n-1} + O(\xi^2)\,. \tag{11.46}
$$

With the definition of the Gamma function

$$
\Gamma(z) = \int_0^\infty dt\; t^{z-1}e^{-t} \tag{11.47}
$$

it then follows that

$$
\lim_{\xi\to 0}\int_\xi^\infty d\beta\; e^{-i\beta a}\,\frac{\beta^{\frac{\epsilon}{2}}}{\beta^n} = (ia)^{n-1-\frac{\epsilon}{2}}\left[\Gamma\left(\frac{\epsilon}{2}-n+1\right) + \lim_{\xi\to 0}O(\xi)\right] = (ia)^{n-1-\frac{\epsilon}{2}}\Gamma\left(\frac{\epsilon}{2}-n+1\right). \tag{11.48}
$$

For $a < 0$, the contour is closed by a quarter circle from ∞ to $i\infty + \xi$ and a line from $i\infty + \xi$ to ξ. The result turns out to be the same as for the case $a > 0$. This thus yields

$$\begin{aligned}
&\Pi_{vac}(u^2) = \\
&= -\frac{\kappa}{2}\mu^\epsilon \int_0^1 dz \left\{ -\pi^2 \sqrt{-i\pi}^{-\epsilon} \left[z^2u^4 - 2m^2zu^2 - 2m^4\left(1+\frac{\epsilon}{4}\right)\right] i^{-\frac{\epsilon}{2}} \right. \\
&\qquad \cdot [(\lambda^2+u^2)z + m^2(1-z) - z^2u^2]^{-\frac{\epsilon}{2}}\Gamma\left(\frac{\epsilon}{2}\right) \\
&\qquad \left. + i\pi^2\left(2-\frac{\epsilon}{2}\right)u^2\sqrt{-i\pi}^{-\epsilon} i^{1-\frac{\epsilon}{2}}[(\lambda^2+u^2)z + m^2(1-z) - z^2u^2]^{1-\frac{\epsilon}{2}}\Gamma\left(\frac{\epsilon}{2}-1\right)\right\}.
\end{aligned} \tag{11.49}$$

Next, we expand all terms in ϵ and then perform the z-integration which results in

$$\begin{aligned}
\Pi_{vac}(u^2) = &-\frac{\pi^2\kappa}{\epsilon}\left[2m^2(m^2+u^2)+\lambda^2u^2\right] \\
&+\frac{\pi^2\kappa}{2u^2}\left\{u^2[2m^2(m^2+u^2)(\gamma_E-2)+\lambda^2(u^2(\gamma_E-1)-m^2)]\right. \\
&\quad + m^2(m^2+2u^2+\lambda^2)\sqrt{(m^2+u^2)^2-2\lambda^2(m^2-u^2)+\lambda^4} \\
&\quad\quad \cdot\left[\operatorname{arctanh}\left(\frac{m^2+u^2-\lambda^2}{\sqrt{(m^2+u^2)^2-2\lambda^2(m^2-u^2)+\lambda^4}}\right)\right. \\
&\quad\quad\quad \left.\left. - \operatorname{arctanh}\left(\frac{m^2-u^2-\lambda^2}{\sqrt{(m^2+u^2)^2-2\lambda^2(m^2-u^2)+\lambda^4}}\right)\right] \\
&\quad + \ln(\pi)[u^4\lambda^2 + 2m^2u^2(m^2+u^2)] + \ln\left(\frac{\lambda}{m}\right)[m^6 - 3m^2u^2\lambda^2 - m^2\lambda^4] \\
&\quad + \ln(\lambda)[3u^2m^4 + 2u^4(m^2+\lambda^2)] + \ln(m)[u^2m^2(2u^2+m^2)] \\
&\quad\quad \left. - \ln(\mu^2)[2u^2m^2(m^2+u^2)+\lambda^2u^4]\right\} \\
&+ O(\epsilon)
\end{aligned} \tag{11.50}$$

Given this, it becomes evident that the pole in ϵ arises from the term $-\frac{\pi^2\kappa}{\epsilon}\left[2m^2(m^2+u^2)+\lambda^2u^2\right]$, which yields in the limit of vanishing graviton mass $-\frac{\pi^2\kappa}{\epsilon}\left[2m^2(m^2+u^2)\right]$. Hence the divergent part can be isolated such that one obtains

$$\Pi_{vac}(u^2) = -\frac{2\pi^2\kappa m^2}{\epsilon}(m^2+u^2) + \Pi_{vac}^{\text{reg}}(u^2) \tag{11.51}$$

with the finite, regularised part $\Pi^{\text{reg}}_{vac}(u^2)$ given as

$$\begin{aligned}\Pi^{\text{reg}}_{vac}(u^2) =&\frac{\pi^2\kappa}{2u^2}\Bigg\{u^2[2m^2(m^2+u^2)(\gamma_E-2)+\lambda^2(u^2(\gamma_E-1)-m^2)]\\ &+m^2(m^2+2u^2+\lambda^2)\sqrt{(m^2+u^2)^2-2\lambda^2(m^2-u^2)+\lambda^4}\\ &\cdot\left[\operatorname{arctanh}\left(\frac{m^2+u^2-\lambda^2}{\sqrt{(m^2+u^2)^2-2\lambda^2(m^2-u^2)+\lambda^4}}\right)\right.\\ &\left.-\operatorname{arctanh}\left(\frac{m^2-u^2-\lambda^2}{\sqrt{(m^2+u^2)^2-2\lambda^2(m^2-u^2)+\lambda^4}}\right)\right]\\ &+\ln(\pi)[u^4\lambda^2+2m^2u^2(m^2+u^2)]+\ln\left(\frac{\lambda}{m}\right)[m^6-3m^2u^2\lambda^2-m^2\lambda^4]\\ &+\ln(\lambda)[3u^2m^4+2u^4(m^2+\lambda^2)]+\ln(m)[u^2m^2(2u^2+m^2)]\\ &-\ln(\mu^2)[2u^2m^2(m^2+u^2)+\lambda^2u^4]\Bigg\}.\end{aligned} \tag{11.52}$$

The infinite part then has to be renormalised by introducing a suitable counter term. As the finite part of this counter term can in principle be chosen arbitrarily, $\Pi^{\text{reg}}_{vac}(u^2)$ can still change. In our case, we choose the finite part of the counter term according to the on-shell renormalisation procedure. This then yields for the final renormalised loop $\Pi^{R}_{vac}(u^2)$:

$$\Pi^{R}_{vac}(u^2) := \Pi^{\text{reg}}_{vac}(u^2) - \Pi^{\text{reg}}_{vac}(-m^2) - (u^2+m^2)\frac{\partial}{\partial u^2}\Pi^{\text{reg}}_{vac}(-m^2)\,. \tag{11.53}$$

This specific form is determined by the on-shell renormalisation scheme that sets the pole of the scalar propagator to m^2 and also fixes its residue according to the following two conditions:

$$\Pi^{R}_{vac}(u^2=-m^2) \stackrel{!}{=} 0 \tag{11.54}$$

$$\frac{\partial}{\partial u^2}\Pi^{R}_{vac}(u^2=-m^2) \stackrel{!}{=} 0\,. \tag{11.55}$$

It can readily be seen that the definition in (11.53) satisfies these two conditions. Note that in [173], they apply a similar procedure without fixing the residue of the pole and therefore also not including an artificial triad mass, because for their purposes it is sufficient to fix the pole of the propagator.
Applied to (11.50), one obtains for the additional terms in equation (11.53):

$$\begin{aligned}&\Pi^{\text{reg}}_{vac}(-m^2) =\\ &=-\frac{\pi^2\kappa}{2}\lambda\Bigg\{(m^2-\lambda^2)\sqrt{\lambda^2-4m^2}\left[\operatorname{arctanh}\left(\frac{2m^2-\lambda^2}{\lambda\sqrt{\lambda^2-4m^2}}\right)+\operatorname{arctanh}\left(\frac{\lambda}{\sqrt{\lambda^2-4m^2}}\right)\right]\\ &\quad+\lambda^3\ln\left(\frac{m}{\lambda}\right)+m^2\lambda\left[\gamma_E+\ln\left(\frac{\pi\lambda^5}{\mu^2m^3}\right)\right]\Bigg\}.\end{aligned} \tag{11.56}$$

as well as

$$\begin{aligned}
&\frac{\partial}{\partial u^2}\Pi^{\mathrm{reg}}_{vac}(-m^2) = \\
&= \frac{\pi^2\kappa}{2m^2}\Bigg\{\frac{5m^4\lambda + 2m^2\lambda^3 - \lambda^5}{\sqrt{\lambda^2-4m^2}}\left[\operatorname{arctanh}\left(\frac{\lambda^2-2m^2}{\lambda\sqrt{\lambda^2-4m^2}}\right) - \operatorname{arctanh}\left(\frac{\lambda}{\sqrt{\lambda^2-4m^2}}\right)\right] \\
&\qquad + (2\gamma_E - 3)m^4 + m^2\lambda^2(\gamma_E - 2 + \ln(\pi)) + (m^4 - \lambda^4)\ln\left(\frac{m}{\lambda}\right) \\
&\qquad + 2m^2\lambda^2\ln(\lambda) + 2m^4\ln(m\pi\lambda) - m^2(2m^2+\lambda^2)\ln\left(\mu^2\right)\Bigg\}. \qquad (11.57)
\end{aligned}$$

If we had not introduced the small triad mass λ, then this last expression would be divergent, see for instance [173, 174]. Hence we continue to work now with $\Pi^R_{vac}(u^2)$.
These considerations suggest that we have to include the following counter term:

$$\delta\Pi(u^2) = \frac{2\pi^2\kappa m^2}{\epsilon}(m^2+u^2) - \Pi^{\mathrm{reg}}_{vac}(-m^2) - (u^2+m^2)\frac{\partial}{\partial u^2}\Pi^{\mathrm{reg}}_{vac}(-m^2) \qquad (11.58)$$

such that

$$\Pi(u^2) + \delta\Pi(u^2) = \Pi^R_{vac}(u^2) + \Pi_\Theta(u^2)\,, \qquad (11.59)$$

where $\Pi_\Theta(u^2)$ denotes the finite thermal contribution to the loop defined in (11.11). From (11.56) we have for $\lambda \to 0$:

$$\Pi^{\mathrm{reg}}_{vac}(-m^2) = 0\,, \qquad (11.60)$$

thus

$$\delta\Pi(u^2) = \left[\frac{2\pi^2\kappa m^2}{\epsilon} - \frac{\partial}{\partial u^2}\Pi^{\mathrm{reg}}_{vac}(-m^2)\right](m^2+u^2)\,, \qquad (11.61)$$

where the expression in the square brackets only depends on m^2. In order to implement a suitable counter term, we introduce a renormalised mass m_R by $m^2 = m_R^2 + m_R^2\delta_m$, where m denotes the bare mass we have used so far and δ_m a mass counter-term, as well as a renormalised wave function $\varphi_R = \frac{1}{\sqrt{Z_2}}\varphi$. Then the renormalised scalar field propagator (a Greens function containing twice φ) reads up to the one-loop contribution:

$$iG^{(1)}(u^2) = \frac{1}{Z_2}\frac{-i}{u^2+m^2} = \frac{-i}{u^2+m_R^2} + \frac{-i}{u^2+m_R^2}[-i(u^2\delta_2 + m_R^2(\delta_2+\delta_m)) + \Pi(u^2)]\frac{-i}{u^2+m_R^2} + O(\kappa^2)\,, \qquad (11.62)$$

where we expanded $Z_2 = 1 + \delta_2$. From this follows that

$$-i(u^2\delta_2 + m_R^2(\delta_2+\delta_m)) \stackrel{!}{=} \delta\Pi(u^2) \qquad (11.63)$$

and it becomes evident that only the wave function has to be renormalised in the following manner:

$$\delta_m = 0 \qquad\qquad \delta_2 = i\left[\frac{2\pi^2\kappa m_R^2}{\epsilon} - \frac{\partial}{\partial u^2}\Pi^{\mathrm{reg}}(-m_R^2)\right]. \qquad (11.64)$$

Due to the counter-term, We have to replace in the old set of Feynman rules m by m_R and obtain the following additional Feynman rule of order κ:

$$\text{——}\otimes\text{——} = -i\delta_2(u^2 + m_R^2)\,. \tag{11.65}$$

To simplify notation, we continue to use m, in particular as we have seen that $m_R = m$. The result is therefore an additional counter-term in the Lagrangian which leads in renormalised perturbation theory to an additional interaction of order κ that we have to include when evaluating the loop. Then the former diverging term $\Pi(u^2)$ becomes finite and only $\Pi^R_{vac}(u^2)$ is left. This yields a modification of the right hand side of the master equation which is derived in the following subsection.

11.4.2. Contribution to the master equation

The content of this subsection was already published in [2]. Here, it is presented with some modifications compared to [2] to adapt it to the flow of the thesis.
In order to see the effect of the renormalisation on the master equation, one has to evaluate the following expression, as discussed at the end of subsection 11.2:

$$\Xi_R(\omega_u, \vec{u}, t_0, t) = \int_{t_0}^{t} d\tau \int_{\mathbb{R}} du^0\ \Pi^R_{vac}(u^2)\ \cos[(u^0 - \omega_u)(t-\tau)]\,. \tag{11.66}$$

Substituting $t - \tau \to \tau$ yields

$$\Xi_R(\omega_u, \vec{u}, t_0, t) = \int_{0}^{t-t_0} d\tau \int_{\mathbb{R}} du^0\ \Pi^R_{vac}(u^2)\ \cos[(u^0 - \omega_u)\tau] \tag{11.67}$$

and due to symmetry it holds that

$$\begin{aligned}\int_{\mathbb{R}} du^0\ \Pi^R_{vac}(u^2)\ \cos[(u^0 - \omega_u)\tau] &= \int_{\mathbb{R}} du^0\ \Pi^R_{vac}(\vec{u}^2 - u_0^2)\ [\cos(u^0\tau)\cos(\omega_u\tau) + \sin(u^0\tau)\sin(\omega_u\tau)] \\ &= \cos(\omega_u\tau)\int_{\mathbb{R}} du^0\ \Pi^R_{vac}(\vec{u}^2 - u_0^2)\ \cos(u^0\tau)\,. \end{aligned}\tag{11.68}$$

To solve the integrations, we first consider all terms that depend on u^0 in the form $(u^2 + m^2) = (\omega_u^2 - u_0^2)$ with $\omega_u = \sqrt{\vec{u}^2 + m^2}$.
To evaluate this, we would like to use the distributional integration $\int_{\mathbb{R}} du^0\ \cos(u^0\tau) = \pi\delta(\tau)$. However, in order for this to be true, we would need to have a Schwartz function paired with the distribution under the τ integration and its integration domain should be $\mathbb{R}$. To have this, we modify the cosine slightly and we will see when evaluating the integration that this modification does not affect the final value. We introduce the Schwartz function $S_c(\omega_u\tau)$ which coincides on the interval $[\epsilon, t-t_0-\epsilon]$ with $\cos(\omega_u\tau)$, where $\epsilon \ll 1$. On the interval $[-\epsilon, \epsilon]$ it is a smooth function constructed in such a way that $S_c(0) = \frac{1}{2}\cos(0) = \frac{1}{2}$, $\frac{d^2}{d\tau^2}S_c(\omega_u\tau)|_{\tau=0} = \frac{1}{2}\frac{d^2}{d\tau^2}\cos(\omega_u\tau)|_{\tau=0} = -\frac{\omega_u^2}{2}$ and $S_c(\omega_u\tau) = 0$ for $\tau < \epsilon$. For $[t - t_0 - \epsilon, t - t_0 + \epsilon]$ it is also constructed as a smooth function from $S_c(\omega_u(t - t_0 - \epsilon)) = \cos(t - t_0 - \epsilon)$ to 0 for $S_c(\omega_u\tau)$ for $\tau > t - t_0 + \epsilon$. The construction is

in such a way, that $S_c(\omega_u\tau)$ is a Schwartz function on $\mathbb{R}$. Then we have:

$$\begin{aligned}
&\int_0^{t-t_0} d\tau \cos(\omega_u\tau) \int_{\mathbb{R}} du^0\ (\omega_u^2 - u_0^2)\ \cos(u^0\tau) \\
&= \int_{\mathbb{R}} d\tau\ S_c(\omega_u\tau) \left[\pi\delta(\tau)\,\omega_u^2 + \frac{d^2}{d\tau^2}\int_{\mathbb{R}} du^0\ \cos(u^0\tau)\right] \\
&= \int_{\mathbb{R}} d\tau\ S_c(\omega_u\tau) \left[\pi\delta(\tau)\,\omega_u^2 + \pi\frac{d^2}{d\tau^2}\delta(\tau)\right] \\
&= \int_{\mathbb{R}} d\tau\ \left[\pi\delta(\tau)\,\omega_u^2\, S_c(\omega_u\tau) + \pi\delta(\tau)\,\frac{d^2}{d\tau^2}S_c(\omega_u\tau)\right] \\
&= \pi\left[\frac{\omega_u^2}{2} - \frac{\omega_u^2}{2}\right] = 0\,.
\end{aligned} \tag{11.69}$$

Using this[19], what remains is

$$\begin{aligned}
\frac{\pi^2\kappa}{2}\int_0^{t-t_0} d\tau\ \cos(\omega_u\tau)\int_{\mathbb{R}} du^0\ \cos(u^0\tau)\Bigg\{&(m^4-\lambda^4)\frac{m^2+u^2}{u^2}\ln\left(\frac{\lambda}{m}\right) \\
&+ m^2\frac{m^2+2u^2+\lambda^2}{u^2}\sqrt{(m^2+u^2)^2 - 2\lambda^2(m^2-u^2)+\lambda^4}\cdot \\
&\cdot\Bigg[\operatorname{arctanh}\left(\frac{m^2+u^2-\lambda^2}{\sqrt{(m^2+u^2)^2 - 2\lambda^2(m^2-u^2)+\lambda^4}}\right) \\
&\quad - \operatorname{arctanh}\left(\frac{m^2-u^2-\lambda^2}{\sqrt{(m^2+u^2)^2 - 2\lambda^2(m^2-u^2)+\lambda^4}}\right)\Bigg] \\
&+ \lambda(m^2-\lambda^2)\sqrt{\lambda^2-4m^2}\Bigg[\operatorname{arctanh}\left(\frac{2m^2-\lambda^2}{\lambda\sqrt{\lambda^2-4m^2}}\right) \\
&\quad + \operatorname{arctanh}\left(\frac{\lambda}{\sqrt{\lambda^2-4m^2}}\right)\Bigg]\Bigg\},
\end{aligned} \tag{11.70}$$

which is independent of μ. Before explicitly evaluating the integrations, we simplify the integrands by taking the limit $\lambda \to 0$ where possible, as λ was only introduced as artificial small graviton mass to be able to fix the residuum of the pole in the propagator. As $\operatorname{arctanh}(i0)$ and $\operatorname{arctanh}(i\infty)$ are finite, the last two lines vanish. Also, $\lim_{\lambda\to 0}\lambda^4\ln(\lambda) = 0$ and, when expanding the square root in the second line, we find that $\lim_{\lambda\to 0}\lambda\operatorname{arctanh}(1+\lambda) = 0$ as $\operatorname{arctanh}(x) = \frac{1}{2}\ln(1+x) - \frac{1}{2}\ln(1-x)$.

[19] And once also using that hence $\ln(m)u^2m^2 \to -\ln(m)m^4$

This leaves us with

$$\frac{\pi^2\kappa}{2}\int_0^{t-t_0} d\tau\ \cos(\omega_u\tau)\int_{\mathbb{R}} du^0\ \cos(u^0\tau)\left\{m^4\frac{m^2+u^2}{u^2}\ln\left(\frac{\lambda}{m}\right)\right.$$
$$+ m^2\frac{m^2+2u^2}{u^2}(m^2+u^2)\cdot$$
$$\cdot\left[\operatorname{arctanh}\left(\frac{m^2+u^2-\lambda^2}{\sqrt{(m^2+u^2)^2-2\lambda^2(m^2-u^2)+\lambda^4}}\right)\right.$$
$$\left.\left.-\operatorname{arctanh}\left(\frac{m^2-u^2}{m^2+u^2}\right)\right]\right\}. \tag{11.71}$$

From the above named relation $\operatorname{arctanh}(x)=\frac{1}{2}\ln(1+x)-\frac{1}{2}\ln(1-x)$ follows that

$$\operatorname{arctanh}\left(\frac{x}{y}\right)=\frac{1}{2}\ln\left(\frac{x+y}{y-x}\right). \tag{11.72}$$

This yields for the last line:

$$\operatorname{arctanh}\left(\frac{m^2-u^2}{m^2+u^2}\right)=\frac{1}{2}\ln\left(\frac{m^2}{u^2}\right). \tag{11.73}$$

For the line before, we expand the argument in second order for small λ and obtain

$$\operatorname{arctanh}\left(\frac{m^2+u^2-\lambda^2}{\sqrt{(m^2+u^2)^2-2\lambda^2(m^2-u^2)+\lambda^4}}\right)\approx\operatorname{arctanh}\left(1-\frac{2\lambda^2u^2}{(m^2+u^2)^2}\right). \tag{11.74}$$

Higher orders will not contribute in the final limit $\lambda\to 0$. Expressing the arctanh again in terms of logarithms, we obtain

$$\operatorname{arctanh}\left(1-\frac{2\lambda^2u^2}{(m^2+u^2)^2}\right)=\frac{1}{2}\ln\left(2-\frac{2\lambda^2u^2}{(m^2+u^2)^2}\right)-\frac{1}{2}\ln\left(\frac{2\lambda^2u^2}{(m^2+u^2)^2}\right)$$
$$\approx\frac{1}{2}\ln(2)-\frac{1}{2}\ln\left(\frac{2\lambda^2u^2}{(m^2+u^2)^2}\right), \tag{11.75}$$

where we neglected terms of order λ^2 and higher. With these simplifications one then finds that

$$\begin{aligned}
\Xi_R(\omega_u,\vec{u},t_0,t) &= \\
&= \frac{\pi^2\kappa}{2}\int_0^{t-t_0} d\tau\ \cos(\omega_u\tau)\int_{\mathbb{R}} du^0\ \cos(u^0\tau)\left\{m^4\frac{m^2+u^2}{u^2}\ln\left(\frac{\lambda}{m}\right)\right. \\
&\qquad\qquad - \frac{m^2}{2}\frac{m^2+2u^2}{u^2}(m^2+u^2)\cdot \\
&\qquad\qquad \left.\cdot\left[\ln\left(\frac{2\lambda^2u^2}{(m^2+u^2)^2}\right)+\ln\left(\frac{m^2}{2u^2}\right)\right]\right\} \\
&= \frac{\pi^2\kappa}{2}\int_0^{t-t_0} d\tau\ \cos(\omega_u\tau)\int_{\mathbb{R}} du^0\ \cos(u^0\tau)\left\{m^4\frac{m^2+u^2}{u^2}\ln\left(\frac{\lambda}{m}\right)\right. \\
&\qquad\qquad - \frac{m^2}{2}\frac{m^2+2u^2}{u^2}(m^2+u^2)\cdot \\
&\qquad\qquad \left.\cdot\ln\left(\frac{\lambda^2m^2}{(m^2+u^2)^2}\right)\right\}. \qquad (11.76)
\end{aligned}$$

The next step is to solve the following two integrations:

$$\textbf{(A)} \qquad m^4\ln\left(\frac{\lambda}{m}\right)\int_{\mathbb{R}} du^0\ \cos(u^0\tau)\,\frac{\omega_u^2-u_0^2}{\vec{u}^2-u_0^2} \qquad (11.77)$$

$$\textbf{(B)} \qquad -\frac{m^2}{2}\int_{\mathbb{R}} du^0\ \cos(u^0\tau)\,\frac{m^2+2\vec{u}^2-2u_0^2}{\vec{u}^2-u_0^2}(\omega_u^2-u_0^2)\ln\left(\frac{\lambda^2m^2}{(\omega_u^2-u_0^2)^2}\right). \qquad (11.78)$$

We start with **(A)**:

$$\int_{\mathbb{R}} du^0\ \cos(u^0\tau)\,\frac{\omega_u^2-u_0^2}{\vec{u}^2-u_0^2} = -\int_{\mathbb{R}} du^0\ e^{iu^0\tau}\,\frac{\omega_u^2-u_0^2}{(u^0-|\vec{u}|)(u^0+|\vec{u}|)}\,. \qquad (11.79)$$

Applying the residue theorem by closing the contour with a semi-circle in the upper half plane leaves us with the contributions of the poles that lie on the contour, hence contribute $+\frac{1}{2}$ their residua, yielding

$$-\int_{\mathbb{R}} du^0\ e^{iu^0\tau}\,\frac{\omega_u^2-u_0^2}{(u^0-|\vec{u}|)(u^0+|\vec{u}|)} = -\pi i\left[e^{i|\vec{u}|\tau}\frac{m^2}{2|\vec{u}|}-e^{-i|\vec{u}|\tau}\frac{m^2}{2|\vec{u}|}\right] = \frac{\pi m^2}{|\vec{u}|}\sin(|\vec{u}|\tau)\,. \qquad (11.80)$$

Therefor we have

$$\textbf{(A)} \ = \frac{\pi m^6}{|\vec{u}|}\sin(|\vec{u}|\tau)\ln\left(\frac{\lambda}{m}\right). \qquad (11.81)$$

We proceed with **(B)**:

$$\begin{aligned}
&\int_{\mathbb{R}} du^0\ \cos(u^0\tau)\,\frac{m^2+2\vec{u}^2-2u_0^2}{\vec{u}^2-u_0^2}(\omega_u^2-u_0^2)\ln\left(\frac{\lambda^2m^2}{(\omega_u^2-u_0^2)^2}\right) \\
&= -\int_{\mathbb{R}} du^0\ e^{iu^0\tau}\,\frac{m^2+2\vec{u}^2-2u_0^2}{(u^0-|\vec{u}|)(u^0+|\vec{u}|)}(\omega_u^2-u_0^2)\ln\left(\frac{\lambda^2m^2}{(\omega_u^2-u_0^2)^2}\right). \qquad (11.82)
\end{aligned}$$

We apply the residue theorem once again. The integrand has singularities at $u^0 = \pm|\vec{u}|$. Working with the principal value logarithm, i.e. the complex logarithm with branch cut at the negative real axis, the logarithm here does not have any branch cuts given that $\omega_u > 0$, hence the equation $\frac{\lambda^2 m^2}{(\omega_u^2 - u_0^2)^2} \stackrel{!}{=} -\alpha$ with $\alpha \in \mathbb{R}, \alpha > 0$ does not have any solution for $u^0 \in \mathbb{C}$. Due to the prefactor $(\omega_u^2 - u_0^2)$, there is no singularity in $u^0 = \pm\omega_u$. We pick a closed integration contour from $-\infty$ to $-|\vec{u}| - \epsilon$, then go in a semi-circle clockwise around the pole to $-|\vec{u}| + \epsilon$, continue to $|\vec{u}| - \epsilon$, again go around the singularity in a semi-circle clockwise to $|\vec{u}| + \epsilon$, continue to $+\infty$ and close it with a semicircle in the upper half-plane. The closed contour does not contain any singularities, hence its contribution vanishes. Due to the exponential $e^{iu^0\tau}$, also the semi-circle at infinite radius in the upper half-plane vanishes. Hence only the contributions of the singularities at $u^0 = \pm|\vec{u}|$ remain. As we went for the closed contour around them clockwise, the singularity contributions have to be evaluated counter-clockwise and added to the closed contour. We start by investigating the one at $u^0 = +|\vec{u}|$ and replace $u^0 = |\vec{u}| + \epsilon e^{i\phi}$:

$$
\begin{aligned}
&- \lim_{\epsilon\to 0} \int_0^\pi d\phi \; i\epsilon e^{i\phi} e^{i\tau\epsilon e^{i\phi} + i\tau|\vec{u}|} \frac{m^2 - 4|\vec{u}|\epsilon e^{i\phi} - 2\epsilon^2 e^{2i\phi}}{\epsilon e^{i\phi}(2|\vec{u}| + \epsilon e^{i\phi})} (m^2 - 2|\vec{u}|\epsilon e^{i\phi} - \epsilon^2 e^{2i\phi}) \\
&\qquad\qquad \cdot \ln\left(\frac{\lambda^2 m^2}{(m^2 - 2|\vec{u}|\epsilon e^{i\phi} - \epsilon^2 e^{2i\phi})^2}\right) \\
&= -i \lim_{\epsilon\to 0} \int_0^\pi d\phi \; e^{i\tau|\vec{u}|} \frac{m^2 - 4|\vec{u}|\epsilon e^{i\phi} - 2\epsilon^2 e^{2i\phi}}{2|\vec{u}| + \epsilon e^{i\phi}} (m^2 - 2|\vec{u}|\epsilon e^{i\phi} - \epsilon^2 e^{2i\phi}) \\
&\qquad\qquad \cdot \ln\left(\frac{\lambda^2 m^2}{(m^2 - 2|\vec{u}|\epsilon e^{i\phi} - \epsilon^2 e^{2i\phi})^2}\right) \\
&= -i \lim_{\epsilon\to 0} \int_0^\pi d\phi \; e^{i\tau|\vec{u}|} m^2 \frac{1}{2|\vec{u}|} m^2 \ln\left(\frac{\lambda^2 m^2}{(m^2 - 2|\vec{u}|\epsilon e^{i\phi} - \epsilon^2 e^{2i\phi})^2}\right) \\
&= -i \frac{m^4}{2|\vec{u}|} e^{i\tau|\vec{u}|} \lim_{\epsilon\to 0} \int_0^\pi d\phi \; \ln\left(\frac{\lambda^2}{m^2}\right) \\
&= -i \frac{\pi m^4}{|\vec{u}|} e^{i\tau|\vec{u}|} \ln\left(\frac{\lambda}{m}\right) ,
\end{aligned}
\tag{11.83}
$$

where in the first step we expanded $e^{i\tau\epsilon e^{i\phi} + i\tau|\vec{u}|} = e^{i\tau|\vec{u}|}(1 + O(\epsilon))$ and neglected all but the zeroth order due to the limit, in the second step we expanded $\frac{1}{2|\vec{u}| + \epsilon e^{i\phi}} = \frac{1}{2|\vec{u}|}\left(1 - \frac{\epsilon}{2|\vec{u}|} e^{i\phi} + O(\epsilon)\right)$ and applied the limit to the terms depending on ϵ where possible. In the third step, we expanded

$$
\ln\left(\frac{\lambda^2 m^2}{(m^2 - 2|\vec{u}|\epsilon e^{i\phi} - \epsilon^2 e^{2i\phi})^2}\right) = \ln\left(\frac{\lambda^2}{m^2}\right) + \epsilon \frac{4|\vec{u}|}{m^2} e^{i\phi} + O(\epsilon^2) \,. \tag{11.84}
$$

For the other singularity at $u^0 = -|\vec{u}|$ we find analogously for $u^0 = -|\vec{u}| + \epsilon e^{i\phi}$:

$$
\begin{aligned}
&- \lim_{\epsilon\to 0} \int_0^\pi d\phi \; i\epsilon e^{i\phi} e^{i\tau\epsilon e^{i\phi} - i\tau|\vec{u}|} \frac{m^2 + 4|\vec{u}|\epsilon e^{i\phi} - 2\epsilon^2 e^{2i\phi}}{\epsilon e^{i\phi}(-2|\vec{u}| + \epsilon e^{i\phi})} (m^2 + 2|\vec{u}|\epsilon e^{i\phi} - \epsilon^2 e^{2i\phi}) \\
&\qquad\qquad \cdot \ln\left(\frac{\lambda^2 m^2}{(m^2 + 2|\vec{u}|\epsilon e^{i\phi} - \epsilon^2 e^{2i\phi})^2}\right) \\
&= +i \lim_{\epsilon\to 0} \int_0^\pi d\phi \; e^{-i\tau|\vec{u}|} m^2 \frac{1}{2|\vec{u}|} m^2 \ln\left(\frac{\lambda^2 m^2}{(m^2 + 2|\vec{u}|\epsilon e^{i\phi} - \epsilon^2 e^{2i\phi})^2}\right)
\end{aligned}
$$

$$= i\frac{m^4}{2|\vec{u}|}e^{-i\tau|\vec{u}|}\lim_{\epsilon\to 0}\int_0^\pi d\phi\ \ln\left(\frac{\lambda^2}{m^2}\right)$$
$$= i\frac{\pi m^4}{|\vec{u}|}e^{-i\tau|\vec{u}|}\ln\left(\frac{\lambda}{m}\right). \tag{11.85}$$

Combining these two yields

$$\mathbf{(B)} = -\frac{\pi m^6}{|\vec{u}|}\sin(|\vec{u}|\tau)\ln\left(\frac{\lambda}{m}\right) = -\mathbf{(A)}\,. \tag{11.86}$$

From this follows that we have

$$\Xi_R(\omega_u,\vec{u},t_0,t) = 0\,. \tag{11.87}$$

Hence we have that the contribution of the renormalised vacuum loop terms to the master equation vanishes:

$$\Xi_R(\omega_u,\vec{u},t_0,t) = \int_{t_0}^t d\tau\int_{\mathbb{R}} du^0\ \Pi^R_{vac}(u^2)\cos[(u^0-\omega_u)(t-\tau)] = 0\,, \tag{11.88}$$
$$\Xi_R(\omega_v,\vec{v},t_0,t) = \int_{t_0}^t d\tau\int_{\mathbb{R}} dv^0\ \Pi^R_{vac}(v^2)\cos[(v^0-\omega_v)(t-\tau)] = 0\,. \tag{11.89}$$

Due to the way the renormalised quantities entered in the master equation, the result is now independent of the scale μ as well as of the artificial graviton mass λ, whose limit to zero can therefore be taken without problems. Therefore neither the dimensional constant μ, nor the artificial triad mass λ play a role in the physical predictions made with the master equation.

11.5. Renormalised one-particle master equation

The content of this subsection was already published in [2]. Here, it is presented with some modifications compared to [2] to adapt it to the flow of the thesis.

With the renormalisation carried out in the previous subsections, a first renormalised version of the one-particle master equation (10.42), where only the former diverging terms are modified, reads:

$$\begin{aligned}\frac{\partial}{\partial t}\rho(\vec{u},\vec{v},t) =& -i\rho(\vec{u},\vec{v},t)\ (\omega_u-\omega_v)\\ &-\frac{\kappa}{2}\int\frac{d^3k}{(2\pi)^3}\Big\{\frac{P_u(\vec{k})}{\omega_{u-k}\omega_u}\ \Big[C^R(\vec{u},\vec{k},t)+\delta_P C^R_P(\vec{u},\vec{k},t)\Big]\\ &\qquad+\frac{P_v(\vec{k})}{\omega_{v-k}\omega_v}\ \Big[\Big(C^R(\vec{v},\vec{k},t)\Big)^*+\delta_P\Big(C^R_P(\vec{v},\vec{k},t)\Big)^*\Big]\Big\}\ \rho(\vec{u},\vec{v},t)\\ &+\frac{\kappa}{2}\int\frac{d^3k}{(2\pi)^3}\frac{P_{ijln}(\vec{k})\,u^iu^jv^lv^n}{\sqrt{\omega_{u+k}\omega_u\omega_{v+k}\omega_v}}\ \Big\{C(\vec{u}+\vec{k},\vec{k},t)+C^*(\vec{v}+\vec{k},\vec{k},t)\Big\}\ \rho(\vec{u}+\vec{k},\vec{v}+\vec{k},t)\end{aligned} \tag{11.90}$$

with

$$C^R(\vec{u},\vec{k},t) = 2\int_0^{t-t_0}\frac{d\tau}{\Omega_k}N(k)\ \cos[\Omega_k\tau]e^{-i(\omega_{u-k}-\omega_u)\tau} \tag{11.91}$$
$$C^R_P(\vec{u},\vec{k},t) = 2\int_0^{t-t_0}\frac{d\tau}{\Omega_k}N(k)\ \cos[\Omega_k\tau]e^{-i(\omega_{u-k}+\omega_u)\tau} \tag{11.92}$$

and

$$C(\vec{u},\vec{k},t)=\int_0^{t-t_0}\frac{d\tau}{\Omega_k}\Big\{[N(k)+1]\,e^{-i(\Omega_k+\omega_{u-k}-\omega_u)\tau}+N(k)\,e^{i(\Omega_k-\omega_{u-k}+\omega_u)\tau}\Big\}. \tag{11.93}$$

At the level of the operator equation, the renormalisation removed the Θ-independent terms from the terms in the second and third line of (11.90), hence leaving us with the following dissipator:

$$\begin{aligned}\mathcal{D}[\rho_S]=-\frac{\kappa}{2}\sum_{r\in\{+,-\}}\sum_{a,b=1}^{4}\int_{\mathbb{R}^3}\frac{d^3k\,d^3p\,d^3l}{(2\pi)^3}\frac{1}{\Omega_k}\Big\{&-\Big(j_r^b(\vec{k},\vec{l})\rho_S(t)j_r^a(\vec{k},\vec{p})^\dagger\Big)\;f(\Omega_k+\omega_b(\vec{k},\vec{l}))+h.c.\\&+N(k)\;\Big[j_r^a(\vec{k},\vec{p})^\dagger,\Big[j_r^b(\vec{k},\vec{l}),\rho_S(t)\Big]\Big]\;f(\Omega_k+\omega_b(\vec{k},\vec{l}))+h.c.\Big\}.\end{aligned} \tag{11.94}$$

If working with the non-extended projection $\delta_P=0$, then there was probability conservation before the renormalisation, i.e. $\int d^3u\frac{\partial}{\partial t}\rho(\vec{u},\vec{u},t)=0$. Now, due to the vacuum term in (11.93) this probability conservation is destroyed. As the renormalisation is a purely technical procedure that should not change the physics, in particular not basic principles as probability conservation, we also replace $C(\vec{u},\vec{k},t)$ by $C^R(\vec{u},\vec{k},t)$ in the last line of the master equation. Another reason for this is that the term in the last line of the master equation is based on the same QFT as the terms in the second and third line, hence they should be renormalised in the same way[20]. The final renormalised one-particle master equation is thus

$$\begin{aligned}\frac{\partial}{\partial t}\rho(\vec{u},\vec{v},t)=&-i\rho(\vec{u},\vec{v},t)\;(\omega_u-\omega_v)\\&-\frac{\kappa}{2}\int\frac{d^3k}{(2\pi)^3}\Big\{\frac{P_u(\vec{k})}{\omega_{u-k}\omega_u}\;\Big[C^R(\vec{u},\vec{k},t)+\delta_P C_P^R(\vec{u},\vec{k},t)\Big]\\&\qquad+\frac{P_v(\vec{k})}{\omega_{v-k}\omega_v}\;\Big[\Big(C^R(\vec{v},\vec{k},t)\Big)^*+\delta_P\Big(C_P^R(\vec{v},\vec{k},t)\Big)^*\Big]\Big\}\rho(\vec{u},\vec{v},t)\\&+\frac{\kappa}{2}\int\frac{d^3k}{(2\pi)^3}\frac{P_{ijln}(\vec{k})\,u^iu^jv^lv^n}{\sqrt{\omega_{u+k}\omega_u\omega_{v+k}\omega_v}}\;\Big\{C^R(\vec{u}+\vec{k},\vec{k},t)+\Big(C^R(\vec{v}+\vec{k},\vec{k},t)\Big)^*\Big\}\\&\qquad\cdot\rho(\vec{u}+\vec{k},\vec{v}+\vec{k},t)\end{aligned} \tag{11.95}$$

and the dissipator at operator level

$$\begin{aligned}\mathcal{D}[\rho_S]=-\frac{\kappa}{2}\sum_{r\in\{+,-\}}\sum_{a,b=1}^{4}\int_{\mathbb{R}^3}\frac{d^3k\,d^3p\,d^3l}{(2\pi)^3}\frac{N(k)}{\Omega_k}\\\cdot\Big\{\Big[j_r^a(\vec{k},\vec{p})^\dagger,\Big[j_r^b(\vec{k},\vec{l}),\rho_S(t)\Big]\Big]\;f(\Omega_k+\omega_b(\vec{k},\vec{l}))+h.c.\Big\}.\end{aligned} \tag{11.96}$$

[20] If one keeps these terms, they will drop from the dissipator part in the Markov approximation and from the Lamb-shift Hamiltonian after the rotating wave approximation, hence not form part of a Lindblad equation derived using these two approximations.

Compared to the expression before renormalisation given in equation (9.34), one can see that the effect of the renormalisation is hence that the vacuum contribution in the entire dissipator (and therefore also in the Lamb-shift Hamiltonian) vanishes.

In part IV of this thesis, we analyse a quantum mechanical model based on the model in [112], where a system is coupled to an environment of harmonic oscillators. The bath of harmonic oscillators mimics the thermal gravitational waves and the model serves as toy model for gravitationally induced decoherence. We find there, that a renormalisation in that model is also necessary, which will remove the Lamb-shift Hamiltonian after the Markov approximation as it depends on an unphysical high-frequency cutoff for the oscillators in the environment. In section 16.5 we analyse this renormalisation and compare it with the one performed here for the one-particle master equation and also the one used in QED in [45].

This concludes the discussion on the renormalisation of the one-particle master equation. In the next section, we discuss how one can apply specific physical approximations to draw physical implications from the renormalised one-article master equation.

12. Application of the Markov and rotating wave approximations to transform the TCL one-particle master equation into Lindblad form

The content of this section was already published in [2]. Here, it is presented with some modifications compared to [2] to adapt it to the flow of the thesis.

The renormalised TCL one-particle master equation (11.95) describes the evolution of a single scalar particle in an environment filled with thermal gravitational waves. Since this master equation is not in Lindblad form, we cannot directly conclude that it is completely positive and provides physically meaningful implications based on positive probabilities for all chosen time intervals. For such models, one usually has to investigate case by case whether further assumptions such as the Markov and rotating wave approximation are justified that are usually used to obtain a master equation in Lindblad form. It is often possible to understand from the involved time scales in the system and environment of the open quantum model in which scenarios these approximations are a good choice, see for example [45] for a discussion in quantum optics. For models with finitely many degrees of freedom, there are also results that suggest time scales which allow to judge when the Markov approximation can be applied that are completely determined by the properties of the environment, such as its spectral density as well as the coupling constant, which encodes the strength of the coupling to the system in the interaction Hamiltonian [175].

The derivation of master equations in the context of field theoretical models with gravity as an environment is less well explored in the literature in comparison and has been presented in the context of gravitationally induced decoherence recently for instance in [6, 60–63]. While the works in [6, 61, 62] focus on the derivation of a TCL master equation, in [60, 63] a Lindblad equation is used, for which further approximations are employed, among these the Markov approximation and the rotating wave approximation.

Compared to the above-mentioned open quantum mechanical models for gravitationally induced decoherence, a detailed analysis of the applicability of such approximations is much more challenging and beyond the scope of this article. An important difference to the present work is that in [60, 63] the approximations are applied on the non-renormalised one-particle master equation. Given the results of the last section, we can instead perform the Markov and rotating wave approximations for the renormalised one-particle master equation and investigate whether applying these approximations before or after renormalisation leads to differences in the final one-particle master equation, considering both the extended and non-extended one-particle projection.

In this section we consider both approximations separately, in subsection 12.1 we discuss the Markov approximation and in subsection 12.2 the rotating wave approximation. In addition, for the case of an ultra-relativistic limit, we also specify some conditions when the Markov approximation can be used for the model considered here.

12.1. Markov approximation

The content of this subsection was already published in [2]. Here, it is presented with some modifications compared to [2] to adapt it to the flow of the thesis.

The Markov approximation consists in the assumption that the correlation functions of the environment are strongly peaked around the initial time and decay rapidly. If this is given, the integral $\int_0^{t-t_0} d\tau$ over these environmental correlation functions has the main contribution from around

their peak. Thus the error obtained when shifting the initial time $t_0 \to -\infty$ and therefore the upper integration limit $t - t_0 \to \infty$ is negligibly small. As a consequence, the parameters involved in the dissipator of the final Lindblad equation will no longer depend on the temporal coordinate.

As discussed above for a field theoretical model, even in the single particle sector, to develop generic criteria for which the Markov approximation can be applied that can easily be checked for a given model, is difficult. For instance the methods developed in [175] strongly rely on the fact that the model is formulated in a quantum mechanical context. Motivated by the physical applications in section 17.4 to ultra-relativistic particles, in particular neutrinos and their oscillations, as a first step, we investigate this special case more in detail in this context and present in the next subsection a condition under which the Markov approximation can be applied for the model under consideration.

12.1.1. Applicability of the Markov approximation for ultra-relativistic particles

The content of this subsection was already published in [2]. Here, it is presented with some modifications compared to [2] to adapt it to the flow of the thesis.
In general, the Markov approximation can be applied if the timescales τ_B on which the correlation functions decay are much smaller than the timescales τ_R on which the state of the system varies (see [45]). The identification of these timescales is however hard without solving the one-particle master equation before the application of the approximation. As the Markov approximation corresponds to sending $t_0 \to -\infty$ and hence $\int_0^{t-t_0} d\tau \longrightarrow \int_0^{\infty} d\tau$, we will analyse the error one makes when extending the integration domain from $t - t_0$ to ∞. If the integrand is strongly peaked around $\tau = 0$, which is usually assumed when deriving Markovian master equations, then the error of the additional contribution should be negligible. For this, we analyse the different parts of the renormalised one-particle master equation in (11.95):

$$\begin{aligned}\frac{\partial}{\partial t}\rho(\vec{u},\vec{v},t) =& -i\rho(\vec{u},\vec{v},t)\,(\omega_u-\omega_v)\\ &-\frac{\kappa}{2}\int\frac{d^3k}{(2\pi)^3}\Big\{\frac{P_u(\vec{k})}{\omega_{u-k}\omega_u}\,\Big[C^R(\vec{u},\vec{k},t)+\delta_P C_P^R(\vec{u},\vec{k},t)\Big]\\ &\qquad+\frac{P_v(\vec{k})}{\omega_{v-k}\omega_v}\,\Big[\Big(C^R(\vec{v},\vec{k},t)\Big)^*+\delta_P\Big(C_P^R(\vec{v},\vec{k},t)\Big)^*\Big]\Big\}\rho(\vec{u},\vec{v},t)\\ &+\frac{\kappa}{2}\int\frac{d^3k}{(2\pi)^3}\frac{P_{ijln}(\vec{k})\,u^iu^jv^lv^n}{\sqrt{\omega_{u+k}\omega_u\omega_{v+k}\omega_v}}\,\Big\{C^R(\vec{u}+\vec{k},\vec{k},t)+\Big(C^R(\vec{v}+\vec{k},\vec{k},t)\Big)^*\Big\}\\ &\qquad\cdot\rho(\vec{u}+\vec{k},\vec{v}+\vec{k},t)\end{aligned} \tag{12.1}$$

with

$$C^R(\vec{u},\vec{k},t) = 2\int_0^{t-t_0}\frac{d\tau}{\Omega_k}N(k)\,\cos[\Omega_k\tau]e^{-i(\omega_{u-k}-\omega_u)\tau} \tag{12.2}$$

$$C_P^R(\vec{u},\vec{k},t) = 2\int_0^{t-t_0}\frac{d\tau}{\Omega_k}N(k)\,\cos[\Omega_k\tau]e^{-i(\omega_{u-k}+\omega_u)\tau}\,. \tag{12.3}$$

We start with the real part of C^R in the second line, which will later lead to decoherence. The term we have to take into account is

$$\begin{aligned}
&-\frac{\kappa}{2}\int\frac{d^3k}{(2\pi)^3}\frac{P_u(\vec{k})}{\omega_{u-k}\omega_u}\int_0^{t-t_0}\frac{d\tau}{\Omega_k}N(k)\left[\cos((\Omega_k+\omega_{u-k}-\omega_u)\tau)+\cos((\Omega_k-\omega_{u-k}+\omega_u)\tau)\right]\\
&=-\frac{\kappa}{2(2\pi)^2}\int_0^\infty dk\int_0^\pi d\theta\,\frac{u^4}{2}\frac{\sin^5(\theta)}{\omega_{u-k}\omega_u}kN(k)\\
&\qquad\cdot\left[\frac{\sin((k+\omega_{u-k}-\omega_u)(t-t_0))}{k+\omega_{u-k}-\omega_u}+\frac{\sin((k-\omega_{u-k}+\omega_u)(t-t_0))}{k-\omega_{u-k}+\omega_u}\right],
\end{aligned}\tag{12.4}$$

where in the second line we went to spherical coordinates with $\vec{k}_z||\vec{u}$ and performed the τ-integration. The main contribution from the integrand will come from small k, because for $k=0$ the denominator tends to zero and $N(k)$ decreases rapidly for large k. For the Markov approximation however the behaviour depending on $(t-t_0)$ is important. To extract this, we first substitute

$$\mu:=\omega_{u-k}=\sqrt{\omega_u^2+k^2-2uk\cos(\theta)}\tag{12.5}$$

and assume, already adapting the scenario of section 17.4 where we will apply the one-particle master equation to ultra-relativistic particles, that $\omega_u\approx u$, where $u:=|\vec{u}|$, which then yields

$$\mu(0)=|k-u|\qquad\qquad\mu(\pi)=k+u\qquad\qquad d\theta=d\mu\frac{\mu}{uk\sin(\theta)}\tag{12.6}$$

as well as

$$\sin^2(\theta)=1-\frac{(u^2+k^2-\mu^2)^2}{4u^2k^2}\,.\tag{12.7}$$

Using this and defining $\Delta t:=t-t_0$, equation (12.4) reads

$$\begin{aligned}
&-\frac{u^2\kappa}{4(2\pi)^2}\int_0^\infty dk\;N(k)\int_{|k-u|}^{k+u}d\mu\;\left[1-\frac{(u^2+k^2-\mu^2)^2}{4u^2k^2}\right]^2\\
&\qquad\cdot\left[\frac{\sin((k+\mu-\omega_u)\Delta t)}{k+\mu-\omega_u}+\frac{\sin((k-\mu+\omega_u)\Delta t)}{k-\mu+\omega_u}\right].
\end{aligned}\tag{12.8}$$

Now we make some assumptions on the involved quantities motivated by the application to ultra-relativistic neutrinos to simplify the integration. In order to continue, we assume that

$$u\gg\frac{1}{c\beta}\,,\tag{12.9}$$

where $u:=|\vec{u}|$ and c denotes the speed of light. The reason why β and thus the temperature parameter Θ are involved here is because we use a Gibbs state to trace out the environmental and thus gravitational degrees of freedom. To resolve the absolute value in the μ-integration, we split the k-integration into two regions, one with $k<u$ and another one with $k>u$:

$$\int_0^u dk\;N(k)\int_{u-k}^{u+k}+\int_u^\infty dk\;N(k)\int_{k-u}^{u+k}\,.\tag{12.10}$$

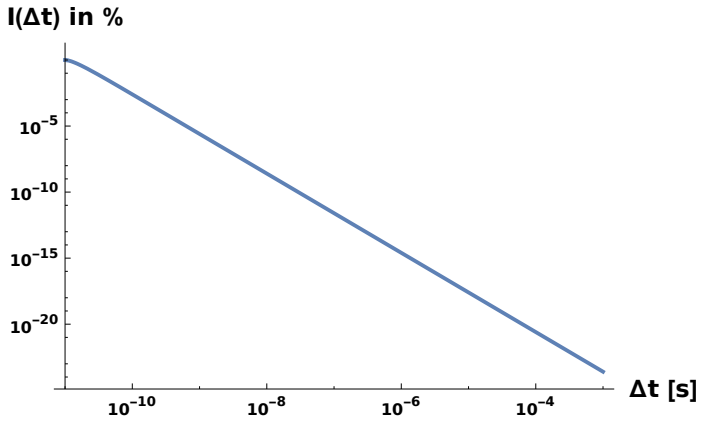

Figure 3: Decay of the integral $I(\Delta t)$ in (12.12) for different values of u and β (see main text) in percent normalised such that $I(10^{-11}s) = 1$. *This plot was originally published in [2].*

The second integral is now negligible compared to the first one, as on the one hand side the dominant contribution of the integrand is around $k = 0$ where the root of the denominator lies, and on the other hand due to condition (12.9) for $k > u \gg \frac{1}{c\beta}$ also $N(k)$ will strongly damp the integrand in that region. Hence we only continue with the first integral:

$$-\frac{u^2\kappa}{4(2\pi)^2}\int_0^u dk\; N(k)\int_{u-k}^{k+u} d\mu\;\left[1-\frac{(u^2+k^2-\mu^2)^2}{4u^2k^2}\right]^2 \cdot\left[\frac{\sin((k+\mu-\omega_u)\Delta t)}{k+\mu-\omega_u}+\frac{\sin((k-\mu+\omega_u)\Delta t)}{k-\mu+\omega_u}\right]. \quad (12.11)$$

The μ-integration can be solved and one obtains

$$\begin{aligned}-\frac{u^2\kappa}{4(2\pi)^2}\int_0^u dk\frac{N(k)}{k^4(\Delta t)^8u^4} &\cdot\Big[16k\Delta t(45+(\Delta t)^2(-6k^2+(-27+4k^2(\Delta t)^2)u^2+(\Delta t)^2u^4))\\ &+4k\Delta t(135+2(\Delta t)^2(-3k^2+(-36+k^2(\Delta t)^2)u^2+(\Delta t)^2u^4))\cos(2k\Delta t)\\ &-6(105+2(\Delta t)^2(-15k^2+(-30+7k^2(\Delta t)^2)u^2+(\Delta t)^2u^4))\sin[2k\Delta t]\Big].\end{aligned} \quad (12.12)$$

This can be integrated numerically. For[21] the three different values of $u = 2.4\cdot 10^{22}\frac{1}{s}, u = 2.4\cdot 10^{24}\frac{1}{s}, u = 2.4\cdot 10^{26}\frac{1}{s}$ and for the two values of $\beta = 10^{-11}s, \beta = 10^{-13}s$ one obtains that the result vanishes rapidly for increasing times Δt, see figure 3.
It hence is visible that the error made when not only considering time until $t - t_0$ but until ∞ is negligible, given that its value drops rapidly when increasing $t - t_0$. In section 17.4 typical

[21] We restored units in the following way: $\beta = \hbar\widetilde{\beta}$, $u = \frac{\widetilde{u}}{\hbar}$, where $\widetilde{u}$ has dimension of energy (Joule) and $\widetilde{\beta}$ has dimension of inverse energy (one over Joule). The above values then correspond to $\widetilde{u} = 0.1GeV, \widetilde{u} = 10GeV, \widetilde{u} = 1TeV$ and temperatures $T \approx 5K, T \approx 500K$.

propagation times of neutrinos through the Earth are used, which are of the order $t-t_0 \approx 10^{-2}s$.

In the general case, in which we do not specify to ultra-relativistic neutrinos, the integration boundaries for the μ-integration in (12.8) would be $\mu(0) = \sqrt{m^2+(k-u)^2}$ as well as $\mu(\pi) = \sqrt{m^2+(k+u)^2}$. As the temperature parameter Θ characterising the environment is finite, one can always find a parameter $\widetilde{k}$ such that $\widetilde{k} \gg \frac{1}{c\beta}$ and hence the k-integration can be approximated $\int_0^\infty dk \approx \int_0^{\widetilde{k}} dk$, since $N(k)$ damps the result strongly on the remaining interval. The general integration of this quantity goes beyond the scope of this work. To facilitate its computation, one can use the specific properties of the considered model similarly to the way it is applied to ultra-relativistic neutrinos in this work.
Next, we consider the real terms arising from the extended projection in line two of equation (12.1). The same steps for the ultra-relativistic conditions as above yield

$$-\frac{u^2\kappa}{4(2\pi)^2}\int_0^u dk\; N(k)\int_{u-k}^{k+u} d\mu\;\left[1-\frac{(u^2+k^2-\mu^2)^2}{4u^2k^2}\right]^2 \cdot\left[\frac{\sin((k+\mu+\omega_u)\Delta t)}{k+\mu+\omega_u}+\frac{\sin((k-\mu-\omega_u)\Delta t)}{k-\mu-\omega_u}\right]. \quad (12.13)$$

Note that in contrast to the previous case, now the denominator is never zero, hence the contribution of this term is less dominant than the one of the previous terms. Solving the μ-integration and plotting the term with the same parameters as above again shows that the result vanishes rapidly for increasing values of $t-t_0$. The absolute value of the integral is however several orders of magnitude below the contribution in (12.12), hence it is negligible compared to the above term. For the imaginary terms in the second line of (12.1), one can perform the same analysis and also obtains a strong decay in $t-t_0$ for the terms. The analogous arguments (if $v \gg \frac{1}{c\beta}$ with $v := |\vec{v}|$) hold for the terms in the third line of (12.1). For the last line, also the wave function ρ depends on $\vec{k}$, but as the structure of the involved terms is very similar and the same main arguments can be carried over (roots of the denominator, same main quantities u, v, β and damping due to $N(k)$), also the behaviour of this term depending on $t-t_0$ is similar as above. Hence the Markov approximation is justified here under the above named assumptions of ultra-relativistic particles that fulfil

$$u, v \gg \frac{1}{c\beta}\,, \quad (12.14)$$

If another than the ultra-relativistic case is considered, this condition could be violated, and therefore a more comprehensive analysis is needed to understand when and under what conditions the Markov approximation can be applied, which we envisage for future work.

12.1.2. Evaluation of the Markov approximation

The content of this subsection was already published in [2]. Here, it is presented with some modifications compared to [2] to adapt it to the flow of the thesis.
Before applying the Markov approximation to the renormalised one-particle master equation, we briefly discuss the main steps that are involved. The first step is to replace the upper limit of

the τ-integration with ∞ and to then perform the integration using the identity

$$\int_0^{t-t_0} d\tau\, e^{-i\omega\tau} \longrightarrow \int_0^{\infty} d\tau\, e^{-i\omega\tau} = \int_{-\infty}^{\infty} d\tau\, \Theta(\tau) e^{-i\omega\tau} = 2\pi \int_{-\infty}^{\infty} dx\, \Theta(x) e^{-2\pi i\omega x}$$
$$= \pi\delta(\omega) - PV\left(\frac{i}{\omega}\right), \tag{12.15}$$

where PV denotes the Cauchy principal value, and secondly the evaluation of the $\vec{k}$-integration which simplifies due to the first step. With this, the affected terms in the master equation can then be split into two classes: one class that consists of contributions involving the delta distribution that will yield a real contribution to the master equation and hence lead to decoherence. We evaluate these terms in subsection 12.1.2.1. Another class that contains terms including the principal value, which result in an imaginary contribution that affects the unitary evolution, is evaluated in subsection 12.1.2.2.

12.1.2.1. Evaluation of the delta terms

The content of this subsection was already published in [2]. Here, it is presented with some modifications compared to [2] to adapt it to the flow of the thesis.

In this subsection, we investigate the terms containing the delta distribution. The delta distribution parts of the terms in lines two and three of (12.1) become

$$-\frac{\pi\kappa}{2}\int \frac{d^3k}{(2\pi)^3}\Bigg\{\frac{P_u(\vec{k})}{\omega_{u-k}\omega_u}\,\frac{N(k)}{\Omega_k}\Bigg[\delta(\Omega_k-\omega_{u-k}+\omega_u)+\delta(\Omega_k+\omega_{u-k}-\omega_u)$$
$$+\delta_P\delta(\Omega_k-\omega_{u-k}-\omega_u)+\delta_P\delta(\Omega_k+\omega_{u-k}+\omega_u)\Bigg]$$
$$+\frac{P_v(\vec{k})}{\omega_{v-k}\omega_v}\,\frac{N(k)}{\Omega_k}\Bigg[\delta(\Omega_k-\omega_{v-k}+\omega_v)+\delta(\Omega_k+\omega_{v-k}-\omega_v)$$
$$+\delta_P\delta(\Omega_k-\omega_{v-k}-\omega_v)+\delta_P\delta(\Omega_k+\omega_{v-k}+\omega_v)\Bigg]\Bigg\}. \tag{12.16}$$

To evaluate the delta distributions, we first have to determine the zeroes of the arguments. As the part for v is exactly the same as the one for u, we focus on the latter one. The four equations to solve then read, expressing the $\vec{k}$-integration in spherical coordinates (k,θ,ϕ) and picking them such that $\vec{u}||\vec{k}_z$:

$$\pm k = \sqrt{\omega_u^2 + k^2 - 2uk\cos(\theta)} - \omega_u \tag{12.17}$$
$$\pm k = \sqrt{\omega_u^2 + k^2 - 2uk\cos(\theta)} + \omega_u\,, \tag{12.18}$$

where $u := |\vec{u}|$. With the limits set by the spherical coordinates, i.e. $k \in \{0,\infty\}$ and $\cos(\theta) \in \{-1,1\}$ it is evident that the right hand side of the equation in the second line is always positive, hence $\delta(\Omega_k+\omega_{u-k}+\omega_u)=0$. For the positive sign in the second line we find

$$(k-\omega_u) = \sqrt{\omega_u^2 + k^2 - 2uk\cos(\theta)}$$
$$\iff k\omega_u = uk\cos(\theta)\,, \tag{12.19}$$

which is solved for $k = 0$. There is no other solution, as the remaining equation $\omega_u = \sqrt{m^2 + u^2} = u\cos(\theta)$ is never fulfilled for $m > 0$. Note however that $k = 0$ is here only a solution of the squared equation and not of the original one[22] in (12.18), hence we also have $\delta(-\Omega_k + \omega_{u-k} + \omega_u) = 0$. This means that here all additional terms arising from the extended projection vanish. For the two equations in the first line we have

$$\begin{aligned} &(\pm k + \omega_u) = \sqrt{\omega_u^2 + k^2 - 2uk\cos(\theta)} \\ \iff\ &\mp k\omega_u = uk\cos(\theta)\,. \end{aligned} \tag{12.20}$$

This is solved by $k = 0$, which is also a solution to both non-squared equations. Apart from that, there is no other solution as again $|\mp\omega_u| = |\mp\sqrt{m^2 + u^2}| > u$ while $|u\cos(\theta)| \leq u$. From this we obtain

$$\delta(\pm\Omega_k - \omega_{u-k} + \omega_u) = \frac{\delta(k)}{\left|\pm 1 + \frac{u\cos(\theta)}{\omega_u}\right|} = \frac{\delta(k)}{1 \pm \frac{u\cos(\theta)}{\omega_u}}\,. \tag{12.21}$$

Applying this to the original expression in spherical coordinates, we find

$$\begin{aligned} -\frac{\pi\kappa}{2}\frac{1}{(2\pi)^2}\int_0^\infty dk \int_0^\pi d\theta\; k\sin(\theta)\Bigg\{ &\frac{P_u(\vec{k})}{\omega_{u-k}\omega_u}\, N(k)\left[\frac{\delta(k)}{1 + \frac{u\cos(\theta)}{\omega_u}} + \frac{\delta(k)}{1 - \frac{u\cos(\theta)}{\omega_u}}\right] \\ &+ \frac{P_v(\vec{k})}{\omega_{v-k}\omega_v}\, N(k)\left[\frac{\delta(k)}{1 + \frac{v\cos(\theta)}{\omega_v}} + \frac{\delta(k)}{1 - \frac{v\cos(\theta)}{\omega_v}}\right]\Bigg\}, \end{aligned} \tag{12.22}$$

where in the second line we picked different spherical coordinates with $\vec{v} || \vec{k}_z$ and defined $v := |\vec{v}|$. Evaluation of the delta yields, using

$$P_u(k, \theta, \phi) = \frac{1}{2}\left[u^2 - \frac{(uk\cos(\theta))^2}{k^2}\right]^2 = \frac{u^4}{2}\left[1 - \cos^2(\theta)\right]^2 = \frac{u^4}{2}\sin^4(\theta) = P_u(\theta, \phi) \tag{12.23}$$

and with l'Hospital's limit

$$\lim_{k\to 0} k\, N(k) = \lim_{k\to 0} \frac{k}{e^{\beta k} - 1} = \lim_{k\to 0} \frac{1}{\beta e^{\beta k}} = \frac{1}{\beta}\,, \tag{12.24}$$

[22] If $x = x_s$ is a solution to the equation $f(x) = g(x)$, then it is also to the squared version $f(x)^2 = g(x)^2$, but not necessarily vice versa.

the following result[23], where we get an additional factor of $\frac{1}{2}$ as the point $k = 0$, where the delta distribution does not vanish, lies at the edge of the integration area:

$$\begin{aligned}
&-\frac{\pi\kappa}{8\beta}\frac{1}{(2\pi)^2}\int_0^\pi d\theta\ \sin^5(\theta)\left\{\frac{u^4}{\omega_u^2}\left[\frac{1}{1+\frac{u\cos(\theta)}{\omega_u}}+\frac{1}{1-\frac{u\cos(\theta)}{\omega_u}}\right]+\frac{v^4}{\omega_v^2}\left[\frac{1}{1+\frac{v\cos(\theta)}{\omega_v}}+\frac{1}{1-\frac{v\cos(\theta)}{\omega_v}}\right]\right\}\\
&=\frac{\pi\kappa}{4\beta}\frac{1}{(2\pi)^2}\int_0^\pi d\theta\ \sin^5(\theta)\left\{\frac{u^2}{\cos^2(\theta)-\frac{\omega_u^2}{u^2}}+\frac{v^2}{\cos^2(\theta)-\frac{\omega_v^2}{v^2}}\right\}\\
&=\frac{\pi\kappa}{4\beta}\frac{1}{(2\pi)^2}\left[-\frac{10}{3}(u^2+v^2)+2(\omega_u^2+\omega_v^2)-\frac{2}{\omega_u u}m^4\,\mathrm{arccoth}\left(\frac{\omega_u}{u}\right)-\frac{2}{\omega_v v}m^4\,\mathrm{arccoth}\left(\frac{\omega_v}{v}\right)\right].
\end{aligned} \tag{12.25}$$

Next, we compute the last line of equation (12.1). The terms containing the delta distributions read

$$\begin{aligned}
&\frac{\pi\kappa}{2}\int\frac{d^3k}{(2\pi)^3}P_{ijln}(\vec{k})\frac{u^iu^jv^lv^n}{\sqrt{\omega_{u+k}\omega_u\omega_{v+k}\omega_v}}\frac{N(k)}{\Omega_k}\\
&\qquad\cdot\Big\{\delta(\Omega_k+\omega_u-\omega_{u+k})+\delta(\Omega_k-\omega_u+\omega_{u+k})\\
&\qquad\quad+\delta(\Omega_k+\omega_v-\omega_{v+k})+\delta(\Omega_k-\omega_v+\omega_{v+k})\Big\}\,\rho(\vec{u}+\vec{k},\vec{v}+\vec{k},t)\,.
\end{aligned} \tag{12.26}$$

Proceeding the same way as above it follows that

$$\delta(\pm\Omega_k+\omega_u-\omega_{u+k})=\frac{\delta(k)}{\left|1\mp\frac{u\cos(\alpha_{uk})}{\omega_u}\right|}=\frac{\omega_u\delta(k)}{\omega_u\mp u\cos(\alpha_{uk})}\,, \tag{12.27}$$

where α_{uk} is the angle between $\vec{u}$ and $\vec{k}$. Due to the presence of the two directions $\vec{u}$ and $\vec{v}$ in the prefactor, it is not possible to pick $\vec{k}_z$ parallel to both $\vec{u}$ and $\vec{v}$, as in general $\vec{u}||\vec{v}$ does not hold. Given that $P_{ijln}(\vec{k}) = P_{ijln}(\theta,\phi)$, the delta distribution can be applied and one obtains[24]

$$\begin{aligned}
&\frac{\pi\kappa}{2(2\pi)^3\beta}\int_0^\pi d\theta\int_0^{2\pi}d\phi\sin(\theta)P_{ijln}(\theta,\phi)\frac{u^iu^jv^lv^n}{\omega_u\omega_v}\\
&\qquad\cdot\left\{\frac{\omega_u^2}{\omega_u^2-u^2\cos^2(\alpha_{uk})}+\frac{\omega_v^2}{\omega_v^2-v^2\cos^2(\alpha_{vk})}\right\}\rho(\vec{u},\vec{v},t)\,.
\end{aligned} \tag{12.28}$$

[23] Note that here the terms that were renormalised would have dropped out as they have 1 instead of $N(k)$ and hence one would have gotten $\lim_{k\to 0} k\cdot 1 = 0$. This is consistent with the literature, e.g. with [60, 63], where the renormalisation after application of the Markov approximation in the one-particle master equation does not affect the decoherence part which comes from the delta terms.

[24] Note that a factor $\frac{1}{2}$ arises due to the fact that the point $k = 0$ where the delta distribution is not equal to zero is at the edge of the integration interval.

Now we choose in the first term the spherical coordinates such that $\vec{u}||\vec{k}_z$ and in the second one $\vec{v}||\vec{k}_z$ and obtain

$$\frac{\pi\kappa}{2(2\pi)^3\beta}\int_0^\pi d\theta\int_0^{2\pi}d\phi\sin(\theta)P_{ijln}(\theta,\phi)\frac{u^iu^jv^lv^n}{\omega_u\omega_v}\left\{\frac{\omega_u^2}{\omega_u^2-u^2\cos^2(\theta)}+\frac{\omega_v^2}{\omega_v^2-v^2\cos^2(\theta)}\right\}\rho(\vec{u},\vec{v},t)\,. \tag{12.29}$$

The only quantity depending on ϕ is $P_{ijln}(\theta,\phi)$. The appearing contraction is, assuming $\vec{u}||\vec{k}_z$:

$$\begin{aligned}P_{ijln}(\theta,\phi)u^iu^jv^lv^n&=\left[\vec{u}\cdot\vec{v}-\frac{(\vec{u}\cdot\vec{k})(\vec{v}\cdot\vec{k})}{\vec{k}^2}\right]^2-\frac{1}{2}\left[\vec{u}^2-\frac{(\vec{u}\cdot\vec{k})^2}{\vec{k}^2}\right]\left[\vec{v}^2-\frac{(\vec{v}\cdot\vec{k})^2}{\vec{k}^2}\right]\\&=\left[\vec{u}\cdot\vec{v}-u\cos(\theta)(\vec{v}\cdot\hat{\vec{k}})\right]^2-\frac{1}{2}\left[u^2-u^2\cos^2(\theta)\right]\left[v^2-(\vec{v}\cdot\hat{\vec{k}})^2\right]\\&=(\vec{u}\cdot\vec{v})^2+u^2\cos^2(\theta)(\vec{v}\cdot\hat{\vec{k}})^2-2u\cos(\theta)(\vec{u}\cdot\vec{v})(\vec{v}\cdot\hat{\vec{k}})\\&\qquad-\frac{1}{2}u^2\sin^2(\theta)\left[v^2-(\vec{v}\cdot\hat{\vec{k}})^2\right]\,,\end{aligned} \tag{12.30}$$

where the unit vector $\hat{\vec{k}}$ is defined as

$$\hat{\vec{k}}=\begin{pmatrix}\sin(\theta)\cos(\phi)\\\sin(\theta)\sin(\phi)\\\cos(\theta)\end{pmatrix}\,. \tag{12.31}$$

From this follows that

$$\begin{aligned}&\int_0^{2\pi}d\phi\;P_{ijln}(\theta,\phi)u^iu^jv^lv^n\\&\quad=2\pi(\vec{u}\cdot\vec{v})^2+u^2\cos^2(\theta)[2\pi\cos^2(\theta)v_z^2+\pi\sin^2(\theta)(v_x^2+v_y^2)]-4\pi uv_z\cos^2(\theta)(\vec{u}\cdot\vec{v})\\&\qquad-\frac{\pi u^2}{2}\sin^2(\theta)[2v^2-2v_3^2\cos^2(\theta)-\sin^2(\theta)(v_1^2+v_2^2)]\\&\quad=\pi\Big[2(\vec{u}\cdot\vec{v})^2-\frac{u^2}{2}(v^2+v_z^2)\Big]+\pi\cos^2(\theta)\Big[u^2(v^2+v_z^2)-4uv_z(\vec{u}\cdot\vec{v})\Big]\\&\qquad+\pi\cos^4(\theta)\Big[\frac{u^2}{2}(3v_z^2-v^2)\Big]\\&\quad=-\pi\frac{u^2}{2}(v^2-3v_z^2)+\pi\cos^2(\theta)u^2(v^2-3v_z^2)-\pi\cos^4(\theta)\frac{u^2}{2}(v^2-3v_z^2)\\&\quad=-\frac{\pi}{2}u^2(v^2-3v_z^2)\Big[1-\cos^2(\theta)\Big]^2\\&\quad=-\frac{\pi}{2}u^2(v^2-3v_z^2)\sin^4(\theta)\,,\end{aligned} \tag{12.32}$$

where we used in the second step that we chose the coordinate system such that $\vec{u}=u\vec{e}_z$, hence $\vec{u}\cdot\vec{v}=uv_z$. The θ-integration then has the form

$$\begin{aligned}&-\frac{\pi}{2}u^2(v^2-3v_z^2)\int_0^\pi d\theta\;\sin^5(\theta)\frac{\omega_u^2}{\omega_u^2-u^2\cos^2(\theta)}\\&=-\pi\omega_u(v^2-3v_z^2)\Big[\frac{5}{3}\omega_u-\frac{\omega_u^3}{u^2}+\frac{m^4}{u^3}\mathrm{arctanh}\left(\frac{u}{\omega_u}\right)\Big]\,.\end{aligned} \tag{12.33}$$

Due to symmetry, we get the same result for the other term just with the replacement $u \leftrightarrow v$, as for the corresponding terms we can analogously choose $\vec{v} = v\vec{e}_z$. The contribution of the last line of equation (12.1) is therefore[25]:

$$\frac{\kappa}{16\pi\beta}\left\{\frac{\omega_u}{\omega_v}\left(v^2 - 3\frac{(\vec{u}\cdot\vec{v})^2}{u^2}\right)\left[\frac{5}{3} - \left(1+\frac{m^2}{u^2}\right) + \frac{m^4}{\omega_u u^3}\operatorname{arctanh}\left(\frac{u}{\omega_u}\right)\right]\right.$$
$$\left. + \frac{\omega_v}{\omega_u}\left(u^2 - 3\frac{(\vec{u}\cdot\vec{v})^2}{v^2}\right)\left[\frac{5}{3} - \left(1+\frac{m^2}{v^2}\right) + \frac{m^4}{\omega_v v^3}\operatorname{arctanh}\left(\frac{v}{\omega_v}\right)\right]\right\}. \tag{12.34}$$

Collecting all contributions from the delta terms yields

$$\frac{\kappa}{16\pi\beta}\left\{-\frac{10}{3}(u^2+v^2) + 2(\omega_u^2+\omega_v^2) - \frac{2}{\omega_u u}m^4\operatorname{arctanh}\left(\frac{u}{\omega_u}\right) - \frac{2}{\omega_v v}m^4\operatorname{arctanh}\left(\frac{v}{\omega_v}\right)\right.$$
$$- \frac{\omega_u}{\omega_v}\left(v^2 - 3\frac{(\vec{u}\cdot\vec{v})^2}{u^2}\right)\left[\frac{2}{3} - \frac{m^2}{u^2} + \frac{m^4}{\omega_u u^3}\operatorname{arctanh}\left(\frac{u}{\omega_u}\right)\right]$$
$$\left. - \frac{\omega_v}{\omega_u}\left(u^2 - 3\frac{(\vec{u}\cdot\vec{v})^2}{v^2}\right)\left[\frac{2}{3} - \frac{m^2}{v^2} + \frac{m^4}{\omega_v v^3}\operatorname{arctanh}\left(\frac{v}{\omega_v}\right)\right]\right\}. \tag{12.35}$$

This is the final form of the real part of the dissipator that causes decoherence. The rotating wave approximation which is carried out as a next step leaves this part of the master equation invariant.

12.1.2.2. Evaluation of the Cauchy principal value contributions

The content of this subsection was already published in [2]. Here, it is presented with some modifications compared to [2] to adapt it to the flow of the thesis.

For the Markov approximation, it remains to compute the terms that contain the Cauchy principal value in (12.1) after the approximation (12.15). The terms in line two of (12.1) read

$$\frac{i\kappa}{2}\int\frac{d^3k}{(2\pi)^3}\frac{u^4}{2}\frac{\sin^4(\alpha_{uk})}{\omega_{u-k}\omega_u}\frac{N(k)}{\Omega_k}\left[PV\left(\frac{1}{\Omega_k+\omega_{u-k}-\omega_u}\right) - PV\left(\frac{1}{\Omega_k-\omega_{u-k}+\omega_u}\right)\right.$$
$$\left. + \delta_P PV\left(\frac{1}{\Omega_k+\omega_{u-k}+\omega_u}\right) - \delta_P PV\left(\frac{1}{\Omega_k-\omega_{u-k}-\omega_u}\right)\right], \tag{12.36}$$

where α_{uk} is the angle between $\vec{u}$ and $\vec{k}$. It can be seen that the term inside the principal value causes problems for $\vec{k}\to\vec{0}$. Thus we exclude a small region of radius ϵ around $\vec{k}=\vec{0}$, perform the integration and take the limit $\epsilon\to 0$ in the end. We then obtain in spherical coordinates[26]

[25] Here it is important to use the coordinate independent expressions $uv_z = (\vec{u}\cdot\vec{v})$ and $vu_z = (\vec{u}\cdot\vec{v})$, as we picked different coordinate systems when evaluating the two sets of terms.

[26] Note that the change of coordinates could have been done before applying the second Markov approximation, hence also before introducing the principal value.

with $\vec{k}_z||\vec{u}$:

$$\lim_{\epsilon\to 0}\frac{i\kappa u^4}{4(2\pi)^2\omega_u}\int_\epsilon^\infty dk\int_0^\pi d\theta\ \sin^5(\theta)\frac{1}{\omega_{u-k}}kN(k)\Bigg[\frac{1}{\Omega_k+\omega_{u-k}-\omega_u}-\frac{1}{\Omega_k-\omega_{u-k}+\omega_u}$$
$$+\delta_P\frac{1}{\Omega_k+\omega_{u-k}+\omega_u}-\delta_P\frac{1}{\Omega_k-\omega_{u-k}-\omega_u}\Bigg]. \tag{12.37}$$

For $\delta_P=1$ this can be simplified to

$$\begin{aligned}&\lim_{\epsilon\to 0}\frac{i\kappa u^4}{4(2\pi)^2\omega_u}\int_\epsilon^\infty dk\int_0^\pi d\theta\ \sin^5(\theta)\frac{1}{\omega_{u-k}}kN(k)\left[\frac{2u\cos(\theta)\omega_{u-k}}{k\omega_u^2-ku^2\cos^2(\theta)}\right]\\&=\lim_{\epsilon\to 0}\frac{i\kappa u^5}{2(2\pi)^2\omega_u}\left[\int_\epsilon^\infty dk\ N(k)\right]\underbrace{\left[\int_0^\pi d\theta\frac{\cos(\theta)\sin^5(\theta)}{\omega_u^2-u^2\cos^2(\theta)}\right]}_{=0}\\&=\lim_{\epsilon\to 0}0=0\,.\end{aligned} \tag{12.38}$$

Without the principal value the k-integration would diverge:

$$\int_0^\infty dk\ N(k)=\int_0^\infty dk\ \frac{1}{e^{\beta k}-1}=\frac{i\pi}{\beta}-\lim_{\epsilon\to 0}\frac{2}{\beta}\text{arctanh}\left(1-2e^{\epsilon\beta}\right). \tag{12.39}$$

Without prior renormalisation, some terms arising due to the additional term present in the non-renormalised coefficients $C(\vec{u},\vec{k},t)$ in (11.93) compared to the renormalised one would remain here and lead to logarithmic divergences, as expected from the discussion in section 11.1.
For the non-extended projection, i.e. for $\delta_P=0$, the situation is more complicated. In that case we find, again using spherical coordinates and implementing the principal value by excluding a sphere of radius ϵ around the critical point $\vec{k}=\vec{0}$:

$$\begin{aligned}&\lim_{\epsilon\to 0}\frac{i\kappa u^4}{4(2\pi)^2\omega_u}\int_\epsilon^\infty dk\int_0^\pi d\theta\ \sin^5(\theta)\frac{1}{\omega_{u-k}}kN(k)\left[\frac{1}{\Omega_k+\omega_{u-k}-\omega_u}-\frac{1}{\Omega_k-\omega_{u-k}+\omega_u}\right]\\&=-\lim_{\epsilon\to 0}\frac{i\kappa u^4}{2(2\pi)^2\omega_u}\int_\epsilon^\infty dk\int_0^\pi d\theta\ \sin^5(\theta)kN(k)\frac{1-\frac{\omega_u}{\omega_{u-k}}}{k^2-(\omega_{u-k}-\omega_u)^2}\,.\end{aligned} \tag{12.40}$$

The θ-integration leads to a complicated result that can be simplified when considering e.g. the ultra-relativistic limit. Then it yields, where the limit $\epsilon\to 0$ can be taken also before the integration:

$$\begin{aligned}&-\frac{i\kappa u^4}{105(2\pi)^2\omega_u}\left\{-4\int_0^u dk\ N(k)\left(\frac{k^3}{u^4}-7\frac{k}{u^2}\right)+\int_u^\infty dk\ N(k)\left(35\frac{1}{u}-14\frac{u}{k^2}+3\frac{u^3}{k^4}\right)\right\}\\&=-\frac{i\kappa u^4}{105(2\pi)^2\omega_u}\\&\quad\cdot\left\{4\left[\frac{\pi^4}{15\beta^4u^4}-\frac{7\pi^2}{6\beta^2u^2}-6\frac{\ln(1-e^{-\beta u})}{\beta u}+4\frac{\text{Li}_2(e^{-\beta u})}{\beta^2u^2}-6\frac{\text{Li}_3(e^{-\beta u})}{\beta^3u^3}-6\frac{\text{Li}_4(e^{-\beta u})}{\beta^4u^4}\right]\right.\\&\qquad\left.+35-35\frac{\ln\left(e^{\beta u}-1\right)}{\beta u}-14u\int_u^\infty dk\ \frac{N(k)}{k^2}+3u^3\int_u^\infty dk\ \frac{N(k)}{k^4}\right\}.\end{aligned} \tag{12.41}$$

Here, $\mathrm{Li}_s(x)$ denotes the poly-logarithm function defined by

$$\mathrm{Li}_s(x) := \sum_{n=1}^{\infty} \frac{x^n}{n^s}\,. \tag{12.42}$$

The remaining two integrations cannot be performed analytically, but they can be solved numerically given a specific temperature Θ and a value for u, and are finite as long as $u > 0$.
For the terms in line three of (12.1) we get the same results when replacing $\vec{u} \to \vec{v}$ and applying complex conjugation. For the terms in line four we obtain:

$$\begin{aligned}
&\frac{i\kappa}{2(2\pi)^3}\frac{1}{\sqrt{\omega_u\omega_v}}\int d^3k\; P_{ijln}(\vec{k})\frac{u^i u^j v^l v^n}{\sqrt{\omega_{u+k}\omega_{v+k}}}\frac{N(k)}{\Omega_k}\rho(\vec{u}+\vec{k},\vec{v}+\vec{k},t)\\
&\qquad\left\{\mathrm{PV}\left(\frac{1}{\Omega_k+\omega_u-\omega_{u+k}}\right)-\mathrm{PV}\left(\frac{1}{\Omega_k-\omega_u+\omega_{u+k}}\right)\right.\\
&\qquad\left.-\mathrm{PV}\left(\frac{1}{\Omega_k+\omega_v-\omega_{v+k}}\right)+\mathrm{PV}\left(\frac{1}{\Omega_k-\omega_v+\omega_{v+k}}\right)\right\}.
\end{aligned} \tag{12.43}$$

Without further specification of ρ, this cannot be simplified further at this point.
In summary, after the second Markov approximation we hence have

$$\begin{aligned}
\frac{\partial}{\partial t}\rho(\vec{u},\vec{v},t) =& -i\rho(\vec{u},\vec{v},t)\;(\omega_u-\omega_v)\\
&+\frac{\kappa}{16\pi\beta}\left\{-\frac{10}{3}(u^2+v^2)+2(\omega_u^2+\omega_v^2)-\frac{2m^4}{\omega_u u}\,\mathrm{arctanh}\left(\frac{u}{\omega_u}\right)-\frac{2m^4}{\omega_v v}\,\mathrm{arctanh}\left(\frac{v}{\omega_v}\right)\right.\\
&\qquad-\frac{\omega_u}{\omega_v}\left(v^2-3\frac{(\vec{u}\cdot\vec{v})^2}{u^2}\right)\left[\frac{2}{3}-\frac{m^2}{u^2}+\frac{m^4}{\omega_u u^3}\mathrm{arctanh}\left(\frac{u}{\omega_u}\right)\right]\\
&\qquad\left.-\frac{\omega_v}{\omega_u}\left(u^2-3\frac{(\vec{u}\cdot\vec{v})^2}{v^2}\right)\left[\frac{2}{3}-\frac{m^2}{v^2}+\frac{m^4}{\omega_v v^3}\mathrm{arctanh}\left(\frac{v}{\omega_v}\right)\right]\right\}\rho(\vec{u},\vec{v},t)\\
&+\frac{i\kappa}{2(2\pi)^3}\frac{1}{\sqrt{\omega_u\omega_v}}\int d^3k\; P_{ijln}(\vec{k})\frac{u^i u^j v^l v^n}{\sqrt{\omega_{u+k}\omega_{v+k}}}\frac{N(k)}{\Omega_k}\rho(\vec{u}+\vec{k},\vec{v}+\vec{k},t)\\
&\qquad\left\{\mathrm{PV}\left(\frac{1}{\Omega_k+\omega_u-\omega_{u+k}}\right)-\mathrm{PV}\left(\frac{1}{\Omega_k-\omega_u+\omega_{u+k}}\right)\right.\\
&\qquad\left.-\mathrm{PV}\left(\frac{1}{\Omega_k+\omega_v-\omega_{v+k}}\right)+\mathrm{PV}\left(\frac{1}{\Omega_k-\omega_v+\omega_{v+k}}\right)\right\}\\
&-(1-\delta_P)\frac{i\kappa\,\rho(\vec{u},\vec{v},t)}{2(2\pi)^2}\lim_{\epsilon\to 0}\left[\frac{u^4}{\omega_u}\int_\epsilon^\infty dk\int_0^\pi d\theta\;\sin^5(\theta)kN(k)\frac{1-\frac{\omega_u}{\omega_{u-k}}}{k^2-(\omega_{u-k}-\omega_u)^2}\right.\\
&\qquad\left.-\frac{v^4}{\omega_v}\int_\epsilon^\infty dk\int_0^\pi d\theta\;\sin^5(\theta)kN(k)\frac{1-\frac{\omega_v}{\omega_{v-k}}}{k^2-(\omega_{v-k}-\omega_v)^2}\right].
\end{aligned} \tag{12.44}$$

The contributions in lines two to four arose from the delta distributions and are real, so they cause decoherence in the evolution of the scalar particle. The remaining terms are imaginary

and therefore contribute to the unitary evolution of the density matrix. When working with the extended one-particle projection, then the expressions in the last two lines vanish. The real part in lines two to four remains unaffected by the rotating wave approximation that will be applied in the next subsection, hence it already possesses its final form.
In the existing literature, the master equation in the one-particle picture is usually directly specified or derived for the non-relativistic (see e.g. [60] for scalar particles) or the ultra-relativistic case (see e.g. [63] for photons). In these cases, the dissipator has a simpler form and there are no arctanh-terms present as it is the case here in the general master equation, where neither the non- nor the ultra-relativistic limits have been applied yet.
To further compare with the existing literature, in section 17.4 we will consider the non- and ultra-relativistic limit of this master equation above and show that the arctanh does not appear in either limit. Thus, it indeed leads to the results obtained in the literature.
Another difference to similar work in [60, 63] is that the master equation in the present work has already been renormalised, i.e. all vacuum contributions that are independent of the temperature parameter Θ have been removed in these terms, which arise due to the gravitational influence in (12.44), which in particular contains all vacuum fluctuations of the gravitational field. This can be seen by setting the temperature parameter equal to zero, as then all terms including the gravitational influence vanish.

12.2. Rotating wave approximation

The content of this subsection was already published in [2]. Here, it is presented with some modifications compared to [2] to adapt it to the flow of the thesis.
After having applied the Markov approximation, the rotating wave approximation is usually a next step in order to cast the master equation into a completely positive Lindblad form. The physical idea behind the approximation is to take into account that detectors only have a finite resolution and cannot resolve arbitrarily fast oscillations, but only measure a coarse-grained result. In the literature, there exist different ways to apply the rotating wave approximation. One possibility is, following the nomenclature in [176], the pre-trace RWA, where the approximation is applied at the level of the interaction Hamiltonian by dropping counter-rotating terms. This is often employed e.g. in quantum optics and leads to the Jaynes-Cummings model, see [177, 178], which is nowadays extensively studied for instance in quantum technology, see [179]. This pre-trace RWA, which is also applicable in closed quantum systems, has been studied from several angles yielding different results in the last years among other things on its higher order corrections and a renormalisation of the resulting series (see [180]) as well as also on the bounds of its applicability (see [181]). From the analysis in [176] it follows that in open quantum systems the second version of the RWA, the post-trace rotating wave approximation which is applied at the level of the master equation after tracing out the environment, yields dynamics which are expected to be closer to the true system dynamics. This analysis in [176] is carried out for quantum mechanical models and we expect that more work is required to extend it to the full field theoretical case. Nevertheless, we take this discussion as a motivation to apply in this work the post-trace RWA, which was also employed in similar analyses, for instance in [63]. This post-trace RWA is implemented by considering the master equation in the interaction picture and then dropping terms that rotate very fast compared to the other ones.

For the application of the post-trace RWA we proceed in the standard way by considering the

master equation in interaction picture and removing all terms that oscillate fast (see e.g. [45, 63]). For this we start in the field theory and consider the full dissipator from equation (9.34):

$$\mathcal{D}[\rho_S] = -\frac{\kappa}{2}\sum_{r\in\{+,-\}}\sum_{a,b=1}^{4}\int_{\mathbb{R}^3}\frac{d^3k\,d^3p\,d^3l}{(2\pi)^3}\frac{1}{\Omega_k}\Big\{\Big[j_r^a(\vec{k},\vec{p})^\dagger, j_r^b(\vec{k},\vec{l})\rho_S(t)\Big]\ f(\Omega_k+\omega_b(\vec{k},\vec{l})) + h.c. \\ +N(k)\ \Big[j_r^a(\vec{k},\vec{p})^\dagger, \Big[j_r^b(\vec{k},\vec{l}),\rho_S(t)\Big]\Big]\ f(\Omega_k+\omega_b(\vec{k},\vec{l})) + h.c.\Big\}, \tag{12.45}$$

where $f(\omega;t) := \int_0^{t-t_0} d\tau\ e^{-i\omega\tau}$ and we assume that the Markov approximation has already been applied, thus the former functions $f(\omega;t)$ are now distributions $f(\omega) = \pi\delta(\omega) - iPV\left(\frac{1}{\omega}\right)$ independent of time. The different ω_a and j_a^r were defined starting in (9.37). Taking into account that the renormalisation removed the terms that are independent of $N(k)$, the dissipator becomes (see (11.96)):

$$\mathcal{D}[\rho_S] = -\frac{\kappa}{2}\sum_{r\in\{+,-\}}\sum_{a,b=1}^{4}\int_{\mathbb{R}^3}\frac{d^3k\,d^3p\,d^3l}{(2\pi)^3}\frac{N(k)}{\Omega_k} \\ \cdot\Big\{\Big[j_r^a(\vec{k},\vec{p})^\dagger, \Big[j_r^b(\vec{k},\vec{l}),\rho_S(t)\Big]\Big]\ f(\Omega_k+\omega_b(\vec{k},\vec{l})) + h.c.\Big\}. \tag{12.46}$$

The basis for the RWA is the dissipator in interaction picture, which is obtained by substituting

$$j_r^a(\vec{k},\vec{p}) \longrightarrow j_r^a(\vec{k},\vec{p})e^{i\omega_a(\vec{k},\vec{p})t}\,. \tag{12.47}$$

Thus we get as time-dependent frequencies that cause oscillations terms of the form

$$e^{\pm i[\omega_a(\vec{k},\vec{p})-\omega_b(\vec{k},\vec{l})]t}\,. \tag{12.48}$$

Next we apply the RWA, which means that we discard all the rapidly oscillating terms and only keep those where $\omega_a(\vec{k},\vec{p}) = \omega_b(\vec{k},\vec{l})$ holds. For $a=3$ and $a=4$ this means that only $b=3$ and $b=4$ survive. However, from the definition of the $\omega_a(\vec{k},\vec{p})$ follows that $\omega_1(\vec{k},\vec{p}) = \omega_2(\vec{k},-\vec{k}-\vec{p})$, so also terms of the form $a=1$, $b=2$ and vice versa will remain. To simplify this, we introduce $J_r^A(\vec{k},\vec{p})$ and $\omega^A(\vec{k},\vec{p})$ with $A\in\{2,3,4\}$, similar as in [63], such that

$$J_r^2(\vec{k},\vec{p}) := 2j_r^1(\vec{k},\vec{p}) \qquad \omega^2(\vec{k},\vec{p}) := \omega_1(\vec{k},\vec{p}) = \omega_2(\vec{k},-\vec{k}-\vec{p}) = \omega_p - \omega_{k+p} \tag{12.49}$$

$$J_r^3(\vec{k},\vec{p}) := j_r^3(\vec{k},\vec{p}) \qquad \omega^3(\vec{k},\vec{p}) := \omega_3(\vec{k},\vec{p}) = -\omega_p - \omega_{k+p} \tag{12.50}$$

$$J_r^4(\vec{k},\vec{p}) := j_r^4(\vec{k},\vec{p}) \qquad \omega^4(\vec{k},\vec{p}) := \omega_4(\vec{k},\vec{p}) = \omega_p + \omega_{k+p}\,. \tag{12.51}$$

Making use of the fact that $j_r^1(\vec{k},\vec{p}) = j_r^2(\vec{k},-\vec{k}-\vec{p})$, we can rewrite the dissipator in terms of a sum over capital letters A,B:

$$\mathcal{D}[\rho_S] = -\frac{\kappa}{2}\sum_{r\in\{+,-\}}\sum_{A,B=2}^{4}\int_{\mathbb{R}^3}\frac{d^3k\,d^3p\,d^3l}{(2\pi)^3}\frac{N(k)}{\Omega_k} \\ \cdot\Big\{\Big[J_r^A(\vec{k},\vec{p})^\dagger, \Big[J_r^B(\vec{k},\vec{l}),\rho_S(t)\Big]\Big]\ f(\Omega_k+\omega^B(\vec{k},\vec{l})) + h.c.\Big\}. \tag{12.52}$$

The RWA-requirement to keep only the terms where $\omega^A(\vec{k},\vec{p}) = \omega^B(\vec{k},\vec{l})$ then keeps the following summands

$$A = B = 2 \qquad A = B = 3 \qquad A = B = 4 \tag{12.53}$$

completely, which were also exactly the same summands that survived the one-particle projection, while for the remaining six summands it yields the following conditions:

$$A = 2,\ B = 3: \quad \omega_p - \omega_{k+p} + \omega_l + \omega_{k+l} = 0 \tag{12.54}$$
$$A = 2,\ B = 4: \quad \omega_p - \omega_{k+p} - \omega_l - \omega_{k+l} = 0 \tag{12.55}$$
$$A = 3,\ B = 4: \quad -\omega_p - \omega_{k+p} - \omega_l - \omega_{k+l} = 0\,, \tag{12.56}$$

and for the other three summands the same conditions with the role of $\vec{p}$ and $\vec{l}$ swapped. For mass $m > 0$, which implies $\omega_k > 0$, the last condition is never fulfilled. For $m = 0$ there is a solution, namely $\vec{k} = \vec{p} = \vec{l} = 0$. The first condition reads

$$\omega_{k+p} = \omega_p + \omega_l + \omega_{k+l}\,. \tag{12.57}$$

This is never fulfilled, as we show in the following (where we define $p := ||\vec{p}||, l := ||\vec{l}||, k := ||\vec{k}||$ and assume[27] $m > 0$):

$$\omega_{k+p} \leq \sqrt{(k+p)^2 + m^2} < \sqrt{p^2+m^2} + \sqrt{l^2+m^2} + \sqrt{(k-l)^2+m^2} \leq \omega_p + \omega_l + \omega_{k+l}\,. \tag{12.58}$$

The inequality in the middle can be proven by considering the square of both sides (as each summand individually is positive, the direction of the inequality remains unaffected), which yields:

$$kp + kl < m^2 + l^2 + \sqrt{p^2+m^2}\sqrt{(k-l)^2+m^2} + \sqrt{p^2+m^2}\sqrt{l^2+m^2} + \sqrt{l^2+m^2}\sqrt{(k-l)^2+m^2}\,. \tag{12.59}$$

We can now estimate the right hand side downwards as

$$\begin{aligned} &m^2 + l^2 + p|k-l| + pl + l|k-l| \\ &\quad < m^2 + l^2 + \sqrt{p^2+m^2}\sqrt{(k-l)^2+m^2} + \sqrt{p^2+m^2}\sqrt{l^2+m^2} + \sqrt{l^2+m^2}\sqrt{(k-l)^2+m^2}\,, \end{aligned} \tag{12.60}$$

which yields

$$kp + kl < m^2 + l^2 + p|k-l| + pl + l|k-l| \tag{12.61}$$

to be proven. Due to the absolute value, we consider two different cases: Let's first assume that $k > l$. Then the inequality reads

$$kp + kl < m^2 + kp + kl\,, \tag{12.62}$$

[27] Afterwards we comment on the case $m = 0$.

which is true as long as $m > 0$. In the second case, i.e. for $l \geq k$, we are left with

$$kp + kl < m^2 + 2l^2 + 2pl - pk - kl\,, \tag{12.63}$$

or equivalently

$$0 < m^2 + 2[l^2 - kl] + 2[pl - pk]\,. \tag{12.64}$$

However, as we are considering the case $l \geq k$, both brackets yield non-negative results and thus the inequality is fulfilled for $m > 0$. Hence (12.54) does also not have any solutions as long as $m > 0$. For $m = 0$ we have to solve the following equality:

$$|\vec{k} + \vec{p}| - p \stackrel{!}{=} |\vec{k} + \vec{l}| - l\,. \tag{12.65}$$

However, we also have

$$|\vec{k} + \vec{p}| - p \leq k \leq |k - l| + l \leq |\vec{k} + \vec{l}| - \vec{l}, \tag{12.66}$$

hence in order for equation (12.65) to hold, all $\leq$ signs must become equalities. For the first one this is the case if $\vec{k} \parallel \vec{p}$ and for the last one if $\vec{k} \parallel -\vec{l}$. For the one in the middle, we have to consider two cases on how to resolve $|k-l|$. If $k \geq l$, then we can directly drop the absolute value and the middle $\leq$ becomes an equality. In case $k < l$ we find $|k - l| + l = 2l - k > 2k - k = k$, so there is no equality. Hence for $m = 0$ the following solutions exist:

$$\vec{k} \parallel \vec{p} \quad \wedge \quad \vec{k} \parallel -\vec{l} \quad \wedge \quad k \geq l\,. \tag{12.67}$$

It remains to investigate (12.55). Isolating ω_p on one side and following the same argumentation as above (squaring the inequality and estimating downwards the rights hand side) we end up with

$$kp + kl < k^2 + m^2 + l^2 + l|k - p| + |k - p||k - l| + l|k - l|\,. \tag{12.68}$$

Here we have to consider four different cases:

- $k \geq p$ and $k \geq l$: We obtain $2kp < 2k^2 + m^2$, which has no solution for $m > 0$ and for $m = 0$ and $k = p$ we get solutions, thus $k \geq l, k = p, \vec{k} \parallel -\vec{l}, \vec{k} \parallel -\vec{p}$.

- $k \geq p$ and $k < l$: We obtain $0 < m^2 + 2l^2 - 2pl$ which has no solution for $m \geq 0$.

- $k < p$ and $k \geq l$: We obtain $0 < m^2$, which has only for $m = 0$ a solution, thus there $k \geq l, k < p, \vec{k} \parallel -\vec{l}, \vec{k} \parallel -\vec{p}$.

- $k < p$ and $k < l$: We obtain $0 < m^2 + 2[(p - k)(l - k) + l(l - k)]$ and thus no solution as every bracket is positive.

Summarising, for equality (12.55) we get again no solution if $m > 0$ and for $m = 0$ we have

$$\vec{k} \parallel -\vec{p} \quad \wedge \quad \vec{k} \parallel -\vec{l} \quad \wedge \quad p \geq k \geq l\,. \tag{12.69}$$

So in total, for a positive mass non of the non-diagonal terms survives the rotating wave approximation. If the mass is zero, the following non-diagonal terms survive:

$$A=2,B=3: \qquad \vec{k}\parallel\vec{p} \quad\wedge\quad \vec{k}\parallel-\vec{l} \quad\wedge\quad k\geq l \tag{12.70}$$

$$A=2,B=4: \qquad \vec{k}\parallel-\vec{p} \quad\wedge\quad \vec{k}\parallel-\vec{l} \quad\wedge\quad p\geq k\geq l \tag{12.71}$$

$$A=3,B=4: \qquad \vec{k}=\vec{l}=\vec{p}=0 \tag{12.72}$$

$$A=3,B=2: \qquad \vec{k}\parallel\vec{l} \quad\wedge\quad \vec{k}\parallel-\vec{p} \quad\wedge\quad k\geq p \tag{12.73}$$

$$A=4,B=2: \qquad \vec{k}\parallel-\vec{l} \quad\wedge\quad \vec{k}\parallel-\vec{p} \quad\wedge\quad l\geq k\geq p \tag{12.74}$$

$$A=4,B=3: \qquad \vec{k}=\vec{l}=\vec{p}=0\,. \tag{12.75}$$

If we plug these special cases into the dissipator, which contains a projection of $\vec{l}$ and also of $\vec{p}$ onto the plane perpendicular to $\vec{k}$, all extra terms containing $\vec{k}\parallel\pm\vec{l}$ and $\vec{k}\parallel\pm\vec{p}$ vanish. Then only the special solution $\vec{k}=\vec{l}=\vec{p}=0$ remains in all six cases (due to polar coordinates and thus also spherical coordinates being non-unique for zero radius, in that case still all directions are possible). However, as this is only one point regarding the radius integrations, it will vanish under the integral. Thus all the extra correction terms vanish[28] and we are left with the dissipator after the RWA in the form

$$\mathcal{D}[\rho_S]=-\frac{\kappa}{2}\sum_{r\in\{+,-\}}\sum_{A=2}^{4}\int_{\mathbb{R}^3}\frac{d^3k\,d^3p\,d^3l}{(2\pi)^3}\frac{N(k)}{\Omega_k} \cdot\left\{\left[J_r^A(\vec{k},\vec{p})^\dagger,\left[J_r^A(\vec{k},\vec{l}),\rho_S(t)\right]\right]\ f(\Omega_k+\omega^A(\vec{k},\vec{l}))+h.c.\right\}\Bigg|_{\omega^A(\vec{k},\vec{p})=\omega^A(\vec{k},\vec{l})}. \tag{12.76}$$

In order to explicitly write the Hermitian conjugate, we split $f(\omega)=f_\delta(\omega)+f_{PV}(\omega)$, as the two parts behave differently under complex conjugation (the first part is real, the second one purely imaginary) and compute them in the following two subsections.

12.2.1. Computation of the delta terms in the RWA

The content of this subsection was already published in [2]. Here, it is presented with some modifications compared to [2] to adapt it to the flow of the thesis.

The delta terms remains unaffected by the complex conjugation[29], thus we get, using that the

[28] The same is the case for the result in [63]: There appear the $L^{++}_{(\sigma,\lambda)}(\vec{k},\vec{p})$ in the $J^1_{(\sigma,\lambda)}(\vec{k},\vec{p})$ with $\vec{k}\parallel\vec{p}$. To show this, one can use the definition $L^{++}_{(\sigma,\lambda)}(\vec{k},\vec{p})=\sqrt{\Omega_p\Omega_{p+k}}(\epsilon_{-\sigma}(\vec{k})\cdot\epsilon_{-\lambda}(\vec{p}))(\epsilon_{-\sigma}(\vec{k})\cdot\epsilon_\lambda(\vec{k}+\vec{p}))$ and that one can express the circular polarisation in terms of two linear polarisations $\epsilon_s(\vec{k})=\frac{1}{\sqrt{2}}[\epsilon^1(\vec{k})+is\epsilon^2(\vec{k})]$ with $\epsilon^2(\vec{k}):=\frac{\hat{u}_0\times\hat{k}}{|\sin\gamma_{u_0k}|}$ with an arbitrary unit vector $\hat{u}_0$ that is not (anti-)parallel to $\vec{k}$ and the angle γ_{u_0k} between $\hat{u}_0$ and $\vec{k}$, as well as $\epsilon^1(\vec{k}):=\epsilon^2(\vec{k})\times\hat{k}$, see also [182]. As $\vec{p}\parallel\vec{k}$, we can see that $\epsilon_s(\vec{k})=\epsilon_s(\vec{p})=\epsilon_s(\vec{k}+\vec{p})$. Using also $\epsilon_{-s}(\vec{k})=\epsilon_s^*(\vec{k})$ and $\epsilon_s^*(\vec{k})\epsilon_t(\vec{k})=\delta_{ts}$ which can be proven right away, we get that $[\epsilon_\sigma^*(\vec{k})\cdot\epsilon_{-\lambda}(\vec{k})][\epsilon_\sigma^*(\vec{k})\cdot\epsilon_\lambda(\vec{k})]=0$, thus all additional terms containing J^1 vanish, as in our case, and only additional terms with $\vec{k}=\vec{p}=\vec{l}=0$ remain, which are of measure zero.

[29] As $\int_{\mathbb{R}}dx\,f(x)\delta^*(x)=\left[\int_{\mathbb{R}}dx\,f^*(x)\delta(x)\right]^*=[f^*(0)]^*=f(0)=\int_{\mathbb{R}}dx\,f(x)\delta(x)$ for a test function $f:\mathbb{R}\mapsto\mathbb{C}$, from which one can conclude that $\delta^*(x)=\delta(x)$.

terms in the first line, which are independent of $N(k)$, vanished due to the Markov approximation:

$$\mathcal{D}_\delta[\rho_S] = \kappa \sum_{r\in\{+,-\}} \sum_{A=2}^{4} \int_{\mathbb{R}^3} \frac{d^3k\, d^3p\, d^3l}{(2\pi)^3} \frac{f_\delta(\Omega_k + \omega^A(\vec{k},\vec{l}))}{\Omega_k} N(k) \cdot \Bigg\{ \left(J_r^A(\vec{k},\vec{p})^\dagger \rho J_r^A(\vec{k},\vec{l}) - \frac{1}{2}\left\{\rho, J_r^A(\vec{k},\vec{l}) J_r^A(\vec{k},\vec{p})^\dagger\right\}\right) + \left(J_r^A(\vec{k},\vec{l}) \rho J_r^A(\vec{k},\vec{p})^\dagger - \frac{1}{2}\left\{\rho, J_r^A(\vec{k},\vec{p})^\dagger J_r^A(\vec{k},\vec{l})\right\}\right) \Bigg\}\Bigg|_{\omega^A(\vec{k},\vec{p})=\omega^A(\vec{k},\vec{l})} . \tag{12.77}$$

Using the following equalities:

$$J_r^2(\vec{k},\vec{p})^\dagger = J_r^2(-\vec{k},\vec{k}+\vec{p}) \qquad \omega^2(-\vec{k},\vec{p}+\vec{k}) = -\omega^2(\vec{k},\vec{p}) \tag{12.78}$$

$$J_r^3(\vec{k},\vec{p})^\dagger = J_r^4(-\vec{k},-\vec{p}) \qquad \omega^3(-\vec{k},-\vec{p}) = -\omega^4(\vec{k},\vec{p}) \tag{12.79}$$

$$J_r^4(\vec{k},\vec{p})^\dagger = J_r^3(-\vec{k},-\vec{p}) \qquad \omega^4(-\vec{k},-\vec{p}) = -\omega^3(\vec{k},\vec{p})\,, \tag{12.80}$$

we can simplify the δ-part of the dissipator and obtain

$$\mathcal{D}_\delta[\rho_S] = \kappa \sum_{r\in\{+,-\}} \sum_{A=2}^{4} \int_{\mathbb{R}^3} \frac{d^3k\, d^3p\, d^3l}{(2\pi)^3} \frac{f_\delta(\Omega_k + \omega^A(\vec{k},\vec{l})) + f_\delta(\Omega_k - \omega^A(\vec{k},\vec{l}))}{\Omega_k} N(k) \cdot \Bigg\{ \left(J_r^A(\vec{k},\vec{l}) \rho J_r^A(\vec{k},\vec{p})^\dagger - \frac{1}{2}\left\{\rho, J_r^A(\vec{k},\vec{p})^\dagger J_r^A(\vec{k},\vec{l})\right\}\right) \Bigg\}\Bigg|_{\omega^A(\vec{k},\vec{p})=\omega^A(\vec{k},\vec{l})} . \tag{12.81}$$

Additionally, all terms involving the extended projection, i.e. all terms where $A = 3$ or $A = 4$, vanished due to the Markov approximation, hence the δ-part of the dissipator simplifies even further:

$$\mathcal{D}_\delta[\rho_S] = \kappa \sum_{r\in\{+,-\}} \int_{\mathbb{R}^3} \frac{d^3k\, d^3p\, d^3l}{(2\pi)^3} \frac{f_\delta(\Omega_k + \omega^2(\vec{k},\vec{l})) + f_\delta(\Omega_k - \omega^2(\vec{k},\vec{l}))}{\Omega_k} N(k) \cdot \Bigg\{ \left(J_r^2(\vec{k},\vec{l}) \rho J_r^2(\vec{k},\vec{p})^\dagger - \frac{1}{2}\left\{\rho, J_r^2(\vec{k},\vec{p})^\dagger J_r^2(\vec{k},\vec{l})\right\}\right) \Bigg\}\Bigg|_{\omega^2(\vec{k},\vec{p})=\omega^2(\vec{k},\vec{l})} . \tag{12.82}$$

As shown above, $f_\delta \propto \delta(k)$, hence the RWA condition reads

$$\omega^2(\vec{k},\vec{p}) = \omega_p - \omega_{k+p} = 0 = \omega_l - \omega_{k+l} = \omega^2(\vec{k},\vec{l}) \tag{12.83}$$

and is therefore automatically fulfilled, thus it can be dropped. One can furthermore evaluate the f_δ and obtains, using (12.21):

$$f_\delta(\Omega_k + \omega^2(\vec{k},\vec{l})) + f_\delta(\Omega_k - \omega^2(\vec{k},\vec{l})) = \pi\delta(k) \left[\frac{1}{1 + \frac{l\cos(\theta_l)}{\omega_l}} + \frac{1}{1 - \frac{l\cos(\theta_l)}{\omega_l}} \right] = \delta(k) \frac{2\pi}{1 - \frac{l^2\cos^2(\theta_l)}{\omega_l^2}}\,, \tag{12.84}$$

where θ_l denotes the angle between $\vec{k}$ and $\vec{l}$ and $l = |\vec{l}|$, $k = |\vec{k}|$. This yields

$$\mathcal{D}_\delta[\rho_S] = \kappa \sum_{r\in\{+,-\}} \int_{\mathbb{R}^3} \frac{d^3k\, d^3p\, d^3l}{(2\pi)^3} \frac{\delta(k)}{\Omega_k} \frac{2\pi}{1 - \frac{l^2\cos^2(\theta_l)}{\omega_l^2}} N(k) \cdot \left\{ \left(J_r^2(\vec{k},\vec{l})\rho J_r^2(\vec{k},\vec{p})^\dagger - \frac{1}{2}\left\{\rho, J_r^2(\vec{k},\vec{p})^\dagger J_r^2(\vec{k},\vec{l})\right\}\right)\right\}. \quad (12.85)$$

The rotating wave condition further implies

$$\begin{aligned} &\frac{\partial}{\partial|k|}\omega^2(\vec{k},\vec{p}) = \frac{\partial}{\partial|k|}\omega^2(\vec{k},\vec{l}) \\ &\iff \frac{k + p\cos(\theta_p)}{\omega_{k+p}} = \frac{k + l\cos(\theta_l)}{\omega_{k+l}}\,. \end{aligned} \quad (12.86)$$

We therefore can use that

$$\delta(k)\frac{2\pi}{1 - \frac{l^2\cos^2(\theta_l)}{\omega_l^2}} = 2\pi\delta(k)\frac{1}{1 - \frac{(k+l\cos(\theta_l))^2}{\omega_{k+l}^2}} = 2\pi\delta(k)\frac{1}{\sqrt{1 - \frac{(k+l\cos(\theta_l))^2}{\omega_{k+l}^2}}}\frac{1}{\sqrt{1 - \frac{(k+p\cos(\theta_p))^2}{\omega_{k+p}^2}}} \quad (12.87)$$

and, defining the Lindblad operators

$$L_r(\vec{k}) := \int_{\mathbb{R}^3} d^3p\, \frac{1}{\sqrt{1 - \frac{(k+p\cos(\theta_p))^2}{\omega_{k+p}^2}}} J_r^2(\vec{k},\vec{p})\,, \quad (12.88)$$

we can recast the dissipator in Lindblad form:

$$\mathcal{D}_\delta[\rho_S] = \kappa \sum_{r\in\{+,-\}} \int_{\mathbb{R}^3} \frac{d^3k}{(2\pi)^2}\delta(k)\frac{N(k)}{\Omega_k}\left(L_r(\vec{k})\rho L_r(\vec{k})^\dagger - \frac{1}{2}\left\{\rho, L_r(\vec{k})^\dagger L_r(\vec{k})\right\}\right). \quad (12.89)$$

As the rotating wave approximation dropped the same terms as the single-particle projection and led to a condition on the frequencies that is already implemented in $\delta(k)$, which is present in every term of the δ-part of the dissipator after the Markov approximation, the RWA does not change the form of the δ-part of the dissipator compared to its form after the Markov approximation in (12.35).

12.2.2. Computation of the Cauchy principal value terms in the RWA

The content of this subsection was already published in [2]. Here, it is presented with some modifications compared to [2] to adapt it to the flow of the thesis.

The contributions involving the Cauchy principal value, denoted as the PV-part of the dissipator (12.76) in the following reads after renormalisation, which removes the terms independent of

$N(k)$:

$$\begin{aligned}\mathcal{D}_{PV}[\rho_S] &= -\frac{\kappa}{2}\sum_{r\in\{+,-\}}\sum_{A=2}^{4}\int_{\mathbb{R}^3}\frac{d^3k\,d^3p\,d^3l}{(2\pi)^3}\frac{N(k)}{\Omega_k} \\ &\quad\cdot\left\{\left[J_r^A(\vec{k},\vec{p})^\dagger,\left[J_r^A(\vec{k},\vec{l}),\rho_S(t)\right]\right]\ f_{PV}(\Omega_k+\omega^A(\vec{k},\vec{l}))+h.c.\right\}\Bigg|_{\omega^A(\vec{k},\vec{p})=\omega^A(\vec{k},\vec{l})}.\end{aligned} \tag{12.90}$$

As $f(\omega)$ is purely imaginary, it switches sign under the Hermitian conjugation and we obtain:

$$\begin{aligned}\mathcal{D}_{PV}[\rho_S] &= -\frac{\kappa}{2}\sum_{r\in\{+,-\}}\sum_{A=2}^{4}\int_{\mathbb{R}^3}\frac{d^3k\,d^3p\,d^3l}{(2\pi)^3}\frac{N(k)}{\Omega_k} \\ &\quad\cdot\left\{\left[\left[J_r^A(\vec{k},\vec{p})^\dagger,J_r^A(\vec{k},\vec{l})\right],\rho_S(t)\right]\ f_{PV}(\Omega_k+\omega^A(\vec{k},\vec{l}))\right\}\Bigg|_{\omega^A(\vec{k},\vec{p})=\omega^A(\vec{k},\vec{l})}.\end{aligned} \tag{12.91}$$

We can then rewrite this part of the dissipator as

$$\mathcal{D}_{PV}[\rho_S] = -i\frac{\kappa}{2}\left[V_{LS},\rho\right] \tag{12.92}$$

with

$$\begin{aligned}V_{LS} &= -\sum_{r\in\{+,-\}}\sum_{A=2}^{4}\int_{\mathbb{R}^3}\frac{d^3k\,d^3p\,d^3l}{(2\pi)^3}\frac{N(k)}{\Omega_k} \\ &\quad\cdot PV\left(\frac{1}{\Omega_k+\omega^A(\vec{k},\vec{l})}\right)\left[J_r^A(\vec{k},\vec{p})^\dagger,J_r^A(\vec{k},\vec{l})\right]\Bigg|_{\omega^A(\vec{k},\vec{p})=\omega^A(\vec{k},\vec{l})}.\end{aligned} \tag{12.93}$$

Note that the rotating wave approximation hence removed the imaginary terms in the fifth to seventh line of the Markovian master equation in (12.44), while it did not change the other imaginary terms. These were vanishing when working with the extended projection, hence in that case we find $V_{LS}=0$. If the non-extended projection is used, only the terms for $A=2$ are left and there the RWA condition is already implemented in the one-particle projection, as the case $(1,1)$ includes $\delta(\vec{p}-\vec{l})$, see table (I) and (II) at the beginning of section 10. Hence the RWA does not change anything in the remaining PV-terms. The final one-particle master equation

then becomes

$$\begin{aligned}\frac{\partial}{\partial t}\rho(\vec{u},\vec{v},t) =& -i\rho(\vec{u},\vec{v},t)\ (\omega_u-\omega_v)\\ &+\frac{\kappa}{16\pi\beta}\Bigg\{-\frac{10}{3}(u^2+v^2)+2(\omega_u^2+\omega_v^2)-\frac{2m^4}{\omega_u u}\operatorname{arctanh}\left(\frac{u}{\omega_u}\right)-\frac{2m^4}{\omega_v v}\operatorname{arctanh}\left(\frac{v}{\omega_v}\right)\\ &\quad-\frac{\omega_u}{\omega_v}\left(v^2-3\frac{(\vec{u}\cdot\vec{v})^2}{u^2}\right)\left[\frac{2}{3}-\frac{m^2}{u^2}+\frac{m^4}{\omega_u u^3}\operatorname{arctanh}\left(\frac{u}{\omega_u}\right)\right]\\ &\quad-\frac{\omega_v}{\omega_u}\left(u^2-3\frac{(\vec{u}\cdot\vec{v})^2}{v^2}\right)\left[\frac{2}{3}-\frac{m^2}{v^2}+\frac{m^4}{\omega_v v^3}\operatorname{arctanh}\left(\frac{v}{\omega_v}\right)\right]\Bigg\}\rho(\vec{u},\vec{v},t)\\ &-(1-\delta_P)\frac{i\kappa\,\rho(\vec{u},\vec{v},t)}{2(2\pi)^2}\lim_{\epsilon\to 0}\Bigg[\frac{u^4}{\omega_u}\int_\epsilon^\infty dk\int_0^\pi d\theta\ \sin^5(\theta)kN(k)\frac{1-\frac{\omega_u}{\omega_{u-k}}}{k^2-(\omega_{u-k}-\omega_u)^2}\\ &\quad-\frac{v^4}{\omega_v}\int_\epsilon^\infty dk\int_0^\pi d\theta\ \sin^5(\theta)kN(k)\frac{1-\frac{\omega_v}{\omega_{v-k}}}{k^2-(\omega_{v-k}-\omega_v)^2}\Bigg].\end{aligned}\tag{12.94}$$

It can be seen when comparing this result to (12.44) that the effect of the rotating wave approximation is to remove the remaining part of the Lamb-shift in the extended projection. In the non-extended projection, there still survives one term of the Lamb-shift which corresponds to the last two lines in (12.94). Apart from that, the rotating wave approximation causes no further modifications on the master equation. This is due to the fact that all other terms that would be removed by the approximation were already dropped when performing the one-particle projection of the master equation. The general dissipator at the operator level can however be written in Lindblad form after the RWA, see (12.89).
With this, we have derived the final form of the renormalised one-particle master equation after Markov and rotating wave approximation. In the next section, we discuss some applications and investigate some features of the master equation at different intermediate stages before, during and after the applied approximations.

13. Applications of the one-particle master equation

The content of this section was already published in [2]. Here, it is presented with some modifications compared to [2] to adapt it to the flow of the thesis.
In this section, we discuss some applications of the one-particle master equation derived in the previous sections. We start with analysing the evolution of the populations of the one-particle density matrix with a special focus on the interplay between the renormalisation and Markov and rotating wave approximations in subsection 13.1 and compare the results to [62] where the evolution of the populations of the non-renormalised TCL master equation is derived. Next we discuss the non-relativistic limit of the one-particle master equation in subsection 13.2 and compare the results to the ones in [60]. Furthermore, we investigate the ultra-relativistic limit in section 13.3 and compare it to [63]. This enables us to later discuss in section 17.4 the relation to the quantum mechanical model for gravitationally induced decoherence in neutrino oscillations introduced in part IV of this thesis.

13.1. Evolution of the populations of the one-particle master equation

The content of this subsection was already published in [2]. Here, it is presented with some modifications compared to [2] to adapt it to the flow of the thesis.
We start by analysing the dynamics of the populations, that is the diagonal elements, in momentum representation predicted by the master equation at different stages in the derivation of the final Lindblad equation. We have chosen this application because it is an example that allows us to discuss and compare the implications that arise depending on the stage of the calculation at which the renormalisation procedure is performed.
To investigate the evolution of the populations, we take the different versions of the master equation and compute it for $\rho(\vec{k},t) := \rho(\vec{k},\vec{k},t)$ before and after the renormalisation as well as after the Markov approximation. As the rotating wave approximation only affects the Lamb-shift Hamiltonian, the dynamics of the populations will not get modified after its application.

13.1.1. Before renormalisation

The content of this subsection was already published in [2]. Here, it is presented with some modifications compared to [2] to adapt it to the flow of the thesis.
The dynamics of the populations in the one-particle master equation (10.42) before renormalisation and further approximations can be obtained by evaluating the master equation for $\rho(\vec{k},t) := \rho(\vec{k},\vec{k},t)$. In this case, we have no contribution from the unitary dynamics and in the dissipator all imaginary parts will vanish[30] and one obtains a dissipator that is purely real. In this subsection we adapt the notation to the one used in [62] in order to better facilitate the

[30] As all coefficients now enter in the form $C + C^*$.

comparison with their results:

$$\dot{\rho}(\vec{k},t) = -\kappa \int \frac{d^3k'}{(2\pi)^3} \frac{P_k(\vec{k}'-\vec{k})}{\Omega_{k'-k}\omega_{k'}\omega_k} \cdot \\ \cdot \Bigg\{ \Bigg[[N(k'-k)+1] \frac{\sin(\chi(t-t_0))}{\chi} + N(k'-k)\frac{\sin(\chi'(t-t_0))}{\chi'} \\ + \delta_P [N(k'-k)+1] \frac{\sin(\eta(t-t_0))}{\eta} + \delta_P N(k'-k)\frac{\sin(\eta'(t-t_0))}{\eta'} \Bigg] \rho(\vec{k},t) \\ - \left[[N(k'-k)+1] \frac{\sin(\chi'(t-t_0))}{\chi'} + N(k'-k)\frac{\sin(\chi(t-t_0))}{\chi} \right] \rho(\vec{k}',t) \Bigg\} \tag{13.1}$$

with $\dot{\rho}(\vec{k},t) = \partial_t \rho(\vec{k},t)$ and $\chi := \Omega_{k'-k} - \omega_k + \omega_{k'}$, $\chi' := \Omega_{k'-k} + \omega_k - \omega_{k'}$, $\eta := \Omega_{k'-k} + \omega_k + \omega_{k'}$ and $\eta' := \Omega_{k'-k} - \omega_k - \omega_{k'}$ as well as $P_k(\vec{k}'-\vec{k}) = P_{ijln}(\vec{k}'-\vec{k})k^i k^j k^l k^n$. Using that $P_{ijln}(\vec{k}-\vec{k}')(\vec{k}-\vec{k}')^i = 0$ as $P_{ijln}(\vec{k}-\vec{k}')$ projects onto the symmetric transverse traceless part and therefore removes the longitudinal part $\propto \vec{k}-\vec{k}'$, which can be seen from the definition in (10.15), we can use

$$P_{ijln}(\vec{k}-\vec{k}')k^i = P_{ijln}(\vec{k}-\vec{k}')k'^i \tag{13.2}$$

and hence rewrite

$$P_k(\vec{k}'-\vec{k}) = P_{ijln}(\vec{k}'-\vec{k})k^i k^j k'^l k'^n \,. \tag{13.3}$$

From equation (13.1) one can also once more see the implication of the chosen projection, i.e. whether $\delta_P = 0$ or $\delta_P = 1$, on the probability conservation, which was discussed below equation (10.7). When working with the non-extended projection $\delta_P = 0$, then we have

$$\int_{\mathbb{R}^3} d^3k \; \dot{\rho}(\vec{k},t) = 0 \tag{13.4}$$

due to symmetry and thus probability in the scalar particle's subsystem is conserved. If working with the extended one-particle projection $\delta_P = 1$ instead, it can be seen in equation (13.1) that the terms containing η and η' lack a symmetric counterpart to be cancelled and hence in that case probability conservation is not given any more, as it was also discussed below equation (10.7).

In [62] the dynamics of the population for a master equation of a photon coupled to linearised gravity are discussed. We obtain an agreement with their result if we specialise to a massless scalar particle and choose as the initial time $t_0 = 0$. In addition we need to consider the non-extended one particle projection (i.e. $\delta_P = 0$), in order to adapt to their chosen normal ordering as well as choose the temperature parameter Θ to be zero. The latter corresponds to a vacuum state of the gravitational waves environment. Inserting these assumptions in the evolution of the populations this equation becomes

$$\dot{\rho}(\vec{k},t) = -\kappa \int \frac{d^3k'}{(2\pi)^3} \frac{P_k(\vec{k}'-\vec{k})}{\Omega_{k'-k}\omega_{k'}\omega_k} \left[\frac{\sin(\chi t)}{\chi} \rho(\vec{k},t) - \frac{\sin(\chi' t)}{\chi'} \rho(\vec{k}',t) \right] , \tag{13.5}$$

which has a very similar form as the one in [62] for a photon. The only difference arises due to the fact that for the photons in [62] the polarisation vectors couple to the symmetric transverse

traceless projector while here for the scalar particles, as they do not carry any polarisation, This role is taken over by the momentum, which is the only direction-dependent quantity that scalar particles possess.

13.1.2. After renormalisation

The content of this subsection was already published in [2]. Here, it is presented with some modifications compared to [2] to adapt it to the flow of the thesis.
As discussed in section 11.5, the effect of the renormalisation was that the vacuum part in the one-particle master equations, these are the contributions not involving $N(\vec{k})$, vanishes. At the practical level this can be implemented by replacing everywhere $N(k'-k)+1 \to N(k'-k)$. Then the dynamics of the populations becomes

$$\begin{aligned}\dot{\rho}(\vec{k},t) = -\kappa \int \frac{d^3k'}{(2\pi)^3} \frac{P_k(\vec{k}'-\vec{k})}{\Omega_{k'-k}\omega_{k'}\omega_k} \cdot N(k'-k) \cdot \Bigg\{ \Bigg[&\frac{\sin(\chi(t-t_0))}{\chi} + \frac{\sin(\chi'(t-t_0))}{\chi'} \\ &+ \delta_P \frac{\sin(\eta(t-t_0))}{\eta} + \delta_P \frac{\sin(\eta'(t-t_0))}{\eta'} \Bigg] \rho(\vec{k},t) \\ &- \left[\frac{\sin(\chi'(t-t_0))}{\chi'} + \frac{\sin(\chi(t-t_0))}{\chi} \right] \rho(\vec{k}',t) \Bigg\}. \end{aligned} \tag{13.6}$$

We realise that now all terms depend on $N(k'-k)$. As a consequence, the entire evolution of the populations is trivial, that is $\dot{\rho}(\vec{k},t)$ vanishes, if we consider the specific case of a vanishing temperature parameter $\Theta = 0$ yielding directly $N(k'-k) = 0$ for all k, k'. The comparison to the non-renormalised master equation shows that the physical properties of the two one-particle master equations are quite different as far as the dynamics of the populations is concerned. For this reason the discussions and physical implications drawn in [62] based on the dynamics of the populations in the non-renormalised equation (13.5) are problematic, as the evolution of the diagonal terms vanishes after renormalisation in the zero temperature limit.

13.1.3. After the Markov approximation

The content of this subsection was already published in [2]. Here, it is presented with some modifications compared to [2] to adapt it to the flow of the thesis.
Due to the fact that for the diagonal elements the coefficients always enter in the form $C + C^*$, only real terms in the one-particle master equation after the second Markov approximation in

(12.44) remain:

$$\begin{aligned}\frac{\partial}{\partial t}\rho(\vec{k},t) =&\dot{\rho}(\vec{k},t)\\ =&\frac{\kappa}{16\pi\beta}\Bigg\{-\frac{20}{3}k^2+4\omega_k^2-\frac{4}{\omega_k k}m^4\,\mathrm{arctanh}\left(\frac{k}{\omega_k}\right)\\ &+4k^2\left[\frac{2}{3}-\frac{m^2}{k^2}+\frac{m^4}{\omega_k k^3}\mathrm{arctanh}\left(\frac{k}{\omega_k}\right)\right]\Bigg\}\rho(\vec{k},t)\\ =&0\,. \end{aligned} \tag{13.7}$$

This means that the Markov approximation removes the dynamics of the populations also in the case of non-vanishing temperature and independently of the extended projection δ_P. It therefore also restores probability conservation, as it removes all terms from the extended projection in the dissipator. The rotating wave approximation only affects the imaginary parts of the master equation, thus it does not change the evolution of the populations any more.
This result that the dynamics of the populations vanishes is also obtained in [60] for a non-relativistic one-particle master equation that was renormalised after the application of Markov and rotating wave approximation, and for the one of a photon after renormalisation and application of the same two approximations in [63].

13.2. Non-relativistic limit

The content of this subsection was already published in [2]. Here, it is presented with some modifications compared to [2] to adapt it to the flow of the thesis.
In the following, we apply the renormalised one-particle master equation after Markov and rotating wave approximation (12.94) to non-relativistic particles in order to compare the decoherence with the one derived in [60]. In the non-relativistic limit we have $\frac{u^2}{m^2}\ll 1$ and $\frac{v^2}{m^2}\ll 1$ and due to this the one-particle master equation simplifies. In this case we can expand the arctanh as

$$-2m^2\frac{m}{u}\frac{1}{\sqrt{1+\frac{u^2}{m^2}}}\mathrm{arctanh}\left(\frac{u}{m}\frac{1}{\sqrt{1+\frac{u^2}{m^2}}}\right)=-2m^2\frac{m}{u}\left[\frac{u}{m}-\frac{2}{3}\frac{u^3}{m^3}+\frac{8}{15}\frac{u^5}{m^5}+O\left(\frac{u^6}{m^6}\right)\right]. \tag{13.8}$$

Given this we find for the contribution from lines two to four in (12.94), which is the part leading to decoherence, the following expression:

$$\frac{\kappa}{16\pi\beta}\left\{-\frac{16}{15}\frac{u^4+v^4}{m^2}-\frac{16}{15}\frac{u^2v^2}{m^2}(1-3\cos^2(\gamma)\right\}=-\frac{\kappa}{5\pi\beta m^2}\left[\frac{1}{3}(u^4+v^4)+u^2v^2\left(\frac{1}{3}-\cos^2(\gamma)\right)\right], \tag{13.9}$$

where γ is defined as the angle between $\vec{u}$ and $\vec{v}$, i.e. $\vec{u}\cdot\vec{v}=uv\cos(\gamma)$. We work with the extended projection $\delta_P=1$ here, as a consequence there is no Lamb-shift contribution left and the master

equation becomes

$$\begin{aligned}\frac{\partial}{\partial t}\rho(\vec{u},\vec{v},t) &= -i\rho(\vec{u},\vec{v},t)(\omega_u-\omega_v) - \frac{\kappa}{5\pi\beta m^2}\left[\frac{1}{3}(\vec{u}^4+\vec{v}^4)+\vec{u}^2\vec{v}^2\left(\frac{1}{3}-\cos^2(\gamma)\right)\right]\rho(\vec{u},\vec{v},t)\\ &= -i\rho(\vec{u},\vec{v},t)\left(\frac{u^2}{2m}-\frac{v^2}{2m}\right) - \frac{\kappa}{5\pi\beta m^2}\left[\frac{1}{3}(\vec{u}^4+\vec{v}^4)+\vec{u}^2\vec{v}^2\left(\frac{1}{3}-\cos^2(\gamma)\right)\right]\rho(\vec{u},\vec{v},t)\,,\end{aligned} \tag{13.10}$$

where we used in the last step $\omega_u = \sqrt{\vec{u}^2+m^2} = m\sqrt{\frac{u^2}{m^2}+1} \approx m+\frac{u^2}{2m}$ and likewise for ω_v. The master equation (60) in [60], where a Lindblad equation is used after Markov and rotating wave approximation to also describe a scalar field coupled to a linearised gravitational field, reads in momentum representation[31]

$$\frac{\partial}{\partial t}\rho(\vec{u},\vec{v},t) = -i\rho(\vec{u},\vec{v},t)\left(\frac{u^2}{2m_R}-\frac{v^2}{2m_R}\right) - \frac{2\kappa}{3\beta m_R^2}\left[\frac{1}{3}(\vec{u}^4+\vec{v}^4)-\frac{1}{3}\vec{u}^2\vec{v}^2\left(1+\cos^2(\gamma)\right)\right]\rho(\vec{u},\vec{v},t)\,. \tag{13.11}$$

While in that work, they use the same underlying physical system, one of the differences is that there a gauge fixing is used while in this work the elementary physical variables were identified in section 7 by choosing geometrical clocks with respect to which suitable Dirac observables were constructed. Additionally, the Hamiltonian used in [60] is not completely normal ordered, while here we worked with a completely normal ordered one. A more detailed discussion of these two points can be found in section 8. Furthermore, the renormalisation is carried out in a different manner: in this work it is done before the Markov and rotating wave approximation are applied. In contrast in [60] the final master equation is renormalised after the application of these two approximations and after going into the non-relativistic limit. Their renormalisation procedure involves the introduction of a cutoff $\Lambda \ll m$ which is later absorbed in a redefinition of the renormalised mass $m \to m_R$, while here we found in equation (11.64) that only the wave function needs to be renormalised, see section 11.4. In [60] compared to our result here, there are some additional unitary terms left due to using the non-extended one-particle projection. These contributions are proportional to the UV-cutoff Λ and to $\frac{u^4}{m_R^2}$, which is why they are dropped in [60] from the final master equation in the non-relativistic limit, even though in the limit $\Lambda \to \infty$ they would diverge. As our results demonstrate, using the extended projection and a renormalisation before the application of the approximations hence removes the necessity to drop diverging terms by hand.
Additional differences between (13.10) and (13.11) are the prefactor in front of the dissipator and the structure inside the square brackets. In these two points the results derived here do not agree with the results in [60]. Particularly regarding the last point, our result however agrees with a similar derivation for photons in [63] where more intermediate steps are provided and where the final structure in the square brackets is the same as in (13.10).

13.3. Ultra-relativistic limit

The content of this subsection was already published in [2]. Here, it is presented with some modifications compared to [2] to adapt it to the flow of the thesis.

[31] In [60] a different κ_{AH} is used that is related to the κ used here by $\kappa_{AH} = 2\kappa$.

In this subsection we apply the one-particle master equation to ultra-relativistic particles. Possible applications are one-particle master equations for photons as discussed in [63] as well as gravitationally induced decoherence in neutrino oscillations as discussed in part IV of this thesis, where a quantum mechanical toy model is used.

In the ultra-relativistic limit we have $\frac{m^2}{u^2} \ll 1$ as well as $\frac{m^2}{v^2} \ll 1$. Taking this into account, we neglect all terms of order $O\left(\frac{m^2}{u^2}\right)$ and $O\left(\frac{m^2}{v^2}\right)$ respectively and higher order contributions. Note, that this also includes terms involving arctanh function because

$$\frac{m^2}{u^2}\frac{1}{\sqrt{1+\frac{m^2}{u^2}}}\text{arctanh}\left(\frac{1}{\sqrt{1+\frac{m^2}{u^2}}}\right) = O\left(\frac{m^2}{u^2}\right) .$$

This leads to the the following simplification for the decoherence term in (12.94):

$$\frac{\kappa}{16\pi\beta}\left\{ -\frac{4}{3}(u^2+v^2) - \frac{4}{3}\Big[uv - 3(\vec{u}\cdot\vec{v})^2\Big]\right\} = -\frac{\kappa}{4\pi\beta}\left[\frac{1}{3}(u^2+v^2) + uv\left(\frac{1}{3}-\cos^2(\gamma)\right)\right] . \quad (13.12)$$

The remaining computation of the imaginary part in the dissipator can be found in (12.41). Combining all results, the renormalised one-particle master equation in the ultra-relativistic limit can be written in the form

$$\begin{aligned}
\frac{\partial}{\partial t}\rho(\vec{u},\vec{v},t) =& -i\rho(\vec{u},\vec{v},t)\,(u-v) \\
&- \frac{\kappa}{4\pi\beta}\left[\frac{1}{3}(u^2+v^2) + uv\left(\frac{1}{3}-\cos^2(\gamma)\right)\right]\rho(\vec{u},\vec{v},t) \\
&- (1-\delta_P)\frac{i\kappa u^4\,\rho(\vec{u},\vec{v},t)}{105(2\pi)^2\omega_u}\left\{4\left[\frac{\pi^4}{15\beta^4u^4} - \frac{7\pi^2}{6\beta^2u^2} - 6\frac{\ln(1-e^{-\beta u})}{\beta u} + 4\frac{\text{Li}_2(e^{-\beta u})}{\beta^2u^2}\right.\right. \\
&\qquad\left. - 6\frac{\text{Li}_3(e^{-\beta u})}{\beta^3u^3} - 6\frac{\text{Li}_4(e^{-\beta u})}{\beta^4u^4}\right] + 35 - 35\frac{\ln\left(e^{\beta u}-1\right)}{\beta u} \\
&\qquad\left. - 14u\int_u^\infty dk\,\frac{N(k)}{k^2} + 3u^3\int_u^\infty dk\,\frac{N(k)}{k^4}\right\} \\
&+ (1-\delta_P)\frac{i\kappa v^4\,\rho(\vec{u},\vec{v},t)}{105(2\pi)^2\omega_v}\left\{4\left[\frac{\pi^4}{15\beta^4v^4} - \frac{7\pi^2}{6\beta^2v^2} - 6\frac{\ln(1-e^{-\beta v})}{\beta v} + 4\frac{\text{Li}_2(e^{-\beta v})}{\beta^2v^2}\right.\right. \\
&\qquad\left. - 6\frac{\text{Li}_3(e^{-\beta v})}{\beta^3v^3} - 6\frac{\text{Li}_4(e^{-\beta v})}{\beta^4v^4}\right] + 35 - 35\frac{\ln\left(e^{\beta v}-1\right)}{\beta v} \\
&\qquad\left. - 14v\int_v^\infty dk\,\frac{N(k)}{k^2} + 3v^3\int_v^\infty dk\,\frac{N(k)}{k^4}\right\} , \qquad (13.13)
\end{aligned}$$

where γ denotes the angle between $\vec{u}$ and $\vec{v}$ and $\text{Li}_s(x)$ denotes the poly-logarithm function defined in (12.42). In the extended projection, i.e. for $\delta_P = 1$, this becomes

$$\frac{\partial}{\partial t}\rho(\vec{u},\vec{v},t) = -i\rho(\vec{u},\vec{v},t)\,(u-v) - \frac{\kappa}{4\pi\beta}\left[\frac{1}{3}(u^2+v^2) + uv\left(\frac{1}{3}-\cos^2(\gamma)\right)\right]\rho(\vec{u},\vec{v},t) , \quad (13.14)$$

which can be rewritten in terms of an operator equation as

$$\frac{\partial}{\partial t}\hat{\rho}(t) = -i[\hat{H}, \hat{\rho}(t)] + \frac{\kappa}{8\pi\beta}\left(\delta^{il}\delta^{jm} - \frac{1}{3}\delta^{ij}\delta^{lm}\right)\left[\frac{\hat{p}_i\hat{p}_j}{\hat{p}_0}, \left[\hat{\rho}(t), \frac{\hat{p}_l\hat{p}_m}{\hat{p}_0}\right]\right], \tag{13.15}$$

with $\hat{p}_0 := \sqrt{\hat{p}_n\hat{p}^n + \xi_{m^2}\mathbb{1}}$. In this definition, ξ_{m^2} is a small regulator that removes the eigenvalue zero from the spectrum of $\hat{p}_0$, as in that case the operator would not be invertible. For massive particles, this regulator corresponds to the mass squared m^2 which is still present in the ultra-relativistic limit, even though very small compared to the other summand. This is, up to a factor of 2, the same result for decoherence as derived in [63] for gravitationally induced decoherence of photons. This difference of a factor of 2 is already present when comparing the field theoretical models of [63] and part II of this thesis. Note that in [63] the derivation and in particular the application of the approximations is performed without a prior renormalisation of the one-particle master equation, which is done in the end to get rid of the diverging Lamb-shift term. As expected from the analysis in this work, they find a logarithmic divergence in the end. The derivation of the master equation in [63] is very similar to the one in [60], hence we refer for a detailed comparison to the discussion in subsection 13.2. The renormalisation in [63] is done after performing the approximations and the ultra-relativistic limit such that the detailed procedure depends on the cutoff frequency Λ and its relation to the photon frequency ω_u (in our case the scalar particle's frequency). In the end in [63] the electric and magnetic fields as well as the coupling constant are renormalised.
In section 17.4, we will use this ultra-relativistic form of the master equation (13.14), apply it to neutrino oscillations and compare its results with the quantum mechanical toy model for gravitationally induced decoherence on neutrino oscillations discussed in part IV of this thesis.

Part IV.
Gravitationally induced decoherence in neutrino oscillations: quantum mechanical toy models

After having derived a master equation for gravitationally induced decoherence on a scalar field from an underlying action in full field theory based on linearised general relativity, we discuss different approaches in this part of the thesis. As the derivation of the previous model in parts II and III is a complex task, in particular to get to the physical predictions which we obtained at the end of part III, there exist different ways towards a similar master equation which we discuss in this part of the thesis. Among these are phenomenological models, where a specific form of the master equation is assumed as starting point, often a Lindblad form with unknown operators. These operators are parameterised adopted to the given physical problem and then are fitted to experimental data in order to obtain values (or at least bounds) for the unknown parameters. In this part of the thesis, we will focus on these models for gravitationally induced decoherence on neutrino oscillations. For this, we will first discuss the general process of neutrino oscillations and its theoretical description in section 14 and then introduce phenomenological models that tackle the gravitational influence in this process in section 15. After that, we present the construction of a quantum mechanical toy model based on the Hamiltonian of a closed system where a neutrino is coupled to a bath of harmonic oscillators that model a gravitational waves environment in section 16. In the end, we compare the predictions made by this model to the one derived in the previous parts from field theory and also to phenomenological models in the literature in section 17.

14. Neutrinos and their oscillations

14.1. Neutrinos

Neutrinos are nowadays probably the most mysterious constituent of the standard model of particle physics (see e.g. [183–187] for introductory books on neutrino physics and [188–190] for discussions of open points in neutrino oscillations). They are produced in various processes in (at least) three different flavours as electron, muon or tauon neutrinos. Although they were theoretically postulated already almost 100 years ago by Wolfgang Pauli to explain the conservation of energy and angular momentum in the beta decay, the experimental discovery of the three different neutrino flavours took several more decades and resulted in the detection of the electron neutrino by Reines and Cowan in 1956, the muon neutrino by Lederman and Schwartz in 1962 and the tauon neutrino by Kodama et al. at Fermilab in 2001. From the analysis of the decay of the Z^0 boson in [191] follows that one expects precisely three different neutrino flavours (and their corresponding anti-particles) that participate in the weak interaction. There could be more neutrino flavours which would be called "sterile", because they should not interact weakly. As neutrinos do not possess electromagnetic charge, they do not couple to the electromagnetic field, neither do they interact via strong interactions. They however interact with the gravitational field, as they have a non-vanishing energy-momentum tensor.
In 1956, Wu and colleagues discovered that the weak interaction violates parity maximally in the sense that left- and right-chiral leptons do not participate in the same manner in the weak interaction. It turned out that only left-chiral leptons interact weakly while right-chiral ones do not. For electrically charged particles like the electron this means that right-chiral electrons still participate in the electromagnetic interaction and can therefore also be detected. Based on this, in 1958 Goldhaber and his group showed that only left-chiral electron neutrinos exist, which implies that there are only right-chiral electron anti-neutrinos. If there are right-chiral electron neutrinos, then it is very hard to detect them, because they would be sterile as they do

only interact gravitationally. In the standard model, this is assumed to also hold for muon and tauon neutrinos. The theoretical description of lepton families in the standard model and the conservation of lepton number then lead to the conclusion that neutrinos have to be massless, because of the non-existence of right-chiral neutrinos there is no possibility to include a neutrino mass term into the Lagrangian of the standard model.
In the late 1960, Davis discovered in his famous Homestake experiment that the flavour ratio of neutrinos coming from the sun was measured to be different than expected from the theoretical calculations. This started the solar neutrino puzzle, a riddle that was debated in the neutrino community for several decades. While in the beginning the known model of the sun was questioned, the answer to the puzzle was a new effect in neutrino physics: neutrino oscillations. Proposed already in 1968 by Pontecorvo, the experimental evidence was found only in 1998 by Super-Kamiokande as well as in 2001 by the Sudbury Neutrino Observatory. The key idea of neutrino oscillations is that neutrinos are created and interact weakly as distinct flavour states, propagate however in a different basis, the mass basis, which is related to the flavour basis by a unitary transformation. The discovered oscillations then depend on the differences of the neutrino masses in mass basis, which shows that neutrinos are required to have mass, in contrast to the standard model.
Such a mass term can be included in two ways as an extension of the standard model: As they do not have electric charge, neutrinos could either exist as Dirac particles, where one could distinguish between a neutrino and its anti-particle, or as Majorana particles, which would mean that neutrinos are their own anti-particles. While a Dirac mass term could be generated from the Higgs mechanism, this is not possible for a Majorana mass term, at least not with a scalar Higgs field that is included in the standard model. In what follows, we work with Dirac neutrinos.
We begin the discussions with neutrino oscillations in vacuum. There are three neutrino mass eigenstates $|\nu_i\rangle$ with $i \in \{1,2,3\}$ which are the solution of the Dirac equation and hence determine the neutrino propagation in time. The flavour states of the neutrino, in which the latter interact weakly, are described by $|\nu_\alpha\rangle$ with $\alpha \in \{e,\mu,\tau\}$ and these two sets of states are related by a unitary transformation U, called PMNS matrix:

$$|\nu_\alpha\rangle = U_{\alpha i}\,|\nu_i\rangle \ , \tag{14.1}$$

where we use Einstein's sum convention. For Dirac neutrinos such a transformation in N dimensions can in general be parameterised by $\frac{N(N-1)}{2}$ angles and $\frac{(N-1)(N-2)}{2}$ phases, which leads for three neutrinos to three angles $\Theta_{12}, \Theta_{13}, \Theta_{23}$ and one phase $e^{i\delta}$. Using these, a parametrisation for the PMNS matrix is

$$U = \begin{pmatrix} c_{12}c_{13} & s_{12}c_{13} & s_{13}e^{-i\delta} \\ -s_{12}c_{23} - c_{12}s_{23}s_{13}e^{i\delta} & c_{12}c_{23} - s_{12}s_{23}s_{13}e^{i\delta} & s_{23}c_{13} \\ s_{12}s_{23} - c_{12}c_{23}s_{13}e^{i\delta} & -c_{12}s_{23} - s_{12}c_{23}s_{13}e^{i\delta} & c_{23}c_{13} \end{pmatrix} \tag{14.2}$$

where $s_{ij} := \sin(\Theta_{ij})$ and $c_{ij} := \cos(\Theta_{ij})$. Due to their property of mixing the different neutrino mass states, the three angles are usually called mixing angles. If the phase $e^{i\delta}$ is not equal to 1, then neutrino oscillations would violate the CP symmetry. For Majorana neutrinos, one would have two additional phases in three dimensions. The most recent values obtained for the mixing angles and the CP-violating phase are regularly published by the particle data group, see [192] for the most recent version.

14.2. Time evolution

In order to obtain the time evolution of a neutrino, one has to solve the corresponding Dirac equation. Each solution will then be a product of an $L_2(\mathbb{R}^3)$ function solving the spatial part of the equation and a vectorial component encoding the spinorial and internal degrees of freedom. In most of the treatments of neutrino oscillations, the calculation is simplified and the spatial part as well as the spinor structure are neglected. Here, we neglect the spinorial structure and first discuss the remaining parts and show in the end how one can connect to the simplified model only using the internal degrees of freedom. We start with the vacuum case, where the Hamiltonian is diagonal in mass basis, hence the mass states are the energy eigenstates in which any given neutrino state has to be expanded in order to determine its time evolution. The matter case will be discussed in section 14.2.3. In the presentation we follow in parts [188–190, 193]. For a flavour state $|\nu_\alpha(t, t_I, \vec{x}_I)\rangle$ created at an initial spacetime point $(t_I, \vec{x}_I)$ and expanded in the mass basis one obtains

$$|\nu_\alpha(t, t_I, \vec{x}_I)\rangle = \sum_i U_{\alpha i} \, |\Psi_i(t, t_I, \vec{x}_I)\rangle \otimes |\nu_i\rangle \ . \tag{14.3}$$

To determine the exact form of $|\Psi_i(t, t_I, \vec{x}_I)\rangle$, we start with a wave packet with momenta $\vec{p}$ distributed according to a distribution function $w_i(\vec{p}-\vec{p}_i)$ with mean momentum $\vec{p}_i$. The relativistic energy-momentum relation $E_i(\vec{p}) = \sqrt{c^2\vec{p}^2 + m_i^2c^4}$ then leads to the following time evolution of the the wave packet expressed in momentum eigenstates:

$$|\Psi_i(t, t_I, \vec{x}_I)\rangle = \int d^3p \; w_i(\vec{p} - \vec{p}_i) e^{-i\vec{p}\vec{x}_I} e^{-\frac{i}{\hbar}E_i(\vec{p})(t-t_I)} \, |\vec{p}\rangle \tag{14.4}$$

with momentum eigenstates $|\vec{p}\rangle$. In order to be able to make predictions for detections at a certain spacetime point[32], we switch to position space by inserting $\int d^3x \, |\vec{x}\rangle \, \langle\vec{x}|$ and find

$$|\nu_\alpha(t, t_I, \vec{x}_I)\rangle = \sum_i \int d^3x \; U_{\alpha i} \Psi_i(\vec{x}, \vec{x}_I, t, t_I) \, |\vec{x}\rangle \otimes |\nu_i\rangle \ , \tag{14.5}$$

where we used $\langle\vec{x}, \vec{p}\rangle = \frac{1}{(2\pi)^{\frac{3}{2}}} e^{i\vec{p}\vec{x}}$ and defined the wave functions $\Psi_i(\vec{x}, \vec{x}_I, t, t_I)$ given as

$$\Psi_i(\vec{x}, \vec{x}_I, t, t_I) = \int \frac{d^3p}{(2\pi)^{\frac{3}{2}}} \; w_i(\vec{p} - \vec{p}_i) e^{i\vec{p}(\vec{x}-\vec{x}_I) - iE_i(\vec{p})(t-t_I)} \, . \tag{14.6}$$

In order to obtain the transition probabilities of one flavour into another (or the same one), we assume that the idealised detector measures a flavour neutrino at spacetime point $(t_F, \vec{x}_F)$ in state $|\vec{x}_F\rangle \otimes |\nu_\beta\rangle$, which leads to the oscillation probability

$$\begin{aligned} P(\nu_\alpha \to \nu_\beta)(\vec{x}_F, \vec{x}_I, t_F, t_I) &= \left|\left(\langle\vec{x}_F| \otimes \langle\nu_\beta|\right) |\nu_\alpha(t_F, t_I, \vec{x}_I)\rangle\right|^2 = \left|\sum_i U_{\alpha i} U^*_{\beta i} \Psi_i(\vec{x}_F, \vec{x}_I, t_F, t_I)\right|^2 \\ &= \sum_{i,j} U_{\alpha i} U^*_{\alpha j} U^*_{\beta i} U_{\beta j} \Psi_i(\vec{x}_F, \vec{x}_I, t_F, t_I) \Psi^*_j(\vec{x}_F, \vec{x}_I, t_F, t_I) \, . \end{aligned} \tag{14.7}$$

[32] Physically, this is impossible as there are always uncertainties regarding the exact detection time and location. For a discussion we refer to [189], where alternative approaches that take this into account are discussed. We comment on the implications of a realistic detector model further below. For the analyses in this thesis, however, the idealised assumption on a specific detection time and position are sufficient.

To proceed, we make further assumptions on the specific form of the wave packet distribution functions $w_i(\vec{p}-\vec{p_i})$. We discuss two different cases: First, we consider a more involved version using Gaussian wave packets in section 14.2.1 and then simplify to the case of plane waves in section 14.2.2.

14.2.1. Neutrinos as Gaussian wave packets

For a wave packet of Gaussian shape, the momentum distribution function has the following form:

$$w_i(\vec{p}-\vec{p_i}) = \frac{1}{(2\pi\sigma^2)^{\frac{3}{4}}} e^{-\frac{(\vec{p}-\vec{p}_i)^2}{4\sigma^2}} \tag{14.8}$$

with the mean momenta $\vec{p_i}$ and width σ. Assuming a small width σ, we can expand the energy $E_i(\vec{p})$ that appears in the wave function $\Psi_i(\vec{x},\vec{x}_I,t,t_I)$ in (14.6) around $\vec{p}=\vec{p_i}$ and obtain, neglecting terms of higher order:

$$E_i(\vec{p}) \approx E_i(\vec{p_i}) + \frac{c^2\vec{p_i}}{E_i(\vec{p_i})}(\vec{p}-\vec{p_i})\,. \tag{14.9}$$

Defining the group velocity $\vec{v}_i$ of the wave packet

$$(\vec{v}_i)_j = \frac{\partial E_i(\vec{p})}{\partial p_j} \qquad \Longrightarrow \qquad \vec{v}_i = \frac{c^2\vec{p_i}}{E_i(\vec{p_i})} \tag{14.10}$$

and using that

$$E_i(\vec{p_i}) - \frac{c^2\vec{p_i}^2}{E_i(\vec{p_i})} = \frac{m_i^2c^4}{E_i(\vec{p_i})}\,, \tag{14.11}$$

the wave function $\Psi_i(\vec{x},\vec{x}_I,t,t_I)$ in (14.6) becomes

$$\begin{aligned}\Psi_i(\vec{x},\vec{x}_I,t,t_I) &= \frac{1}{(2\pi\sigma^2)^{\frac{3}{4}}} e^{-i(t-t_I)\frac{m_i^2c^4}{E_i(\vec{p_i})}} \int \frac{d^3p}{(2\pi)^{\frac{3}{2}}}\, e^{-\frac{(\vec{p}-\vec{p}_i)^2}{4\sigma^2}} e^{i\vec{p}[(\vec{x}-\vec{x}_I)-\vec{v}_i(t-t_I)]} \\ &= \frac{1}{(2\pi\sigma^2)^{\frac{3}{4}}} e^{-i(t-t_I)\frac{m_i^2c^4}{E_i(\vec{p_i})}} e^{i\vec{p_i}[(\vec{x}-\vec{x}_I)-\vec{v}_i(t-t_I)]} \int \frac{d^3p}{(2\pi)^{\frac{3}{2}}}\, e^{-\frac{\vec{p}^2}{4\sigma^2}+i\vec{p}[(\vec{x}-\vec{x}_I)-\vec{v}_i(t-t_I)]}\,.\end{aligned} \tag{14.12}$$

Applying the formula for a Gaussian integral in three dimensions,

$$\int d^3p\; e^{-\frac{1}{2}A_{ij}p^ip^j+iB_ip^i} = \sqrt{\frac{(2\pi)^3}{\det(A)}} e^{-\frac{1}{2}\vec{B}^TA^{-1}\vec{B}} \tag{14.13}$$

with a real, symmetric positive-definite matrix A and a real vector $\vec{B}$ that are in our case

$$A_{ij} = \frac{1}{2\sigma^2}\delta_{ij}, \qquad A^{-1}_{ij} = 2\sigma^2\delta_{ij} \qquad \text{and} \qquad B_i = \left[(\vec{x}-\vec{x}_I)-\vec{v}_i(t-t_I)\right]_i \tag{14.14}$$

with A being indeed real, symmetric and positive-definite, we find that

$$\begin{aligned}\Psi_i(\vec{x},\vec{x}_I,t,t_I) &= \frac{1}{(2\pi\sigma^2)^{\frac{3}{4}}} e^{-i(t-t_I)\frac{m_i^2c^4}{E_i(\vec{p_i})}} e^{i\vec{p_i}[(\vec{x}-\vec{x}_I)-\vec{v}_i(t-t_I)]} \frac{\sqrt{(4\pi\sigma^2)^3}}{(2\pi)^{\frac{3}{2}}} e^{-\sigma^2[(\vec{x}-\vec{x}_I)-\vec{v}_i(t-t_I)]^2} \\ &= \left(\frac{2\sigma^2}{\pi}\right)^{\frac{3}{4}} e^{i\vec{p_i}(\vec{x}-\vec{x}_I)-iE_i(\vec{p_i})(t-t_I)} e^{-\sigma^2[(\vec{x}-\vec{x}_I)-\vec{v}_i(t-t_I)]^2}\,.\end{aligned} \tag{14.15}$$

From this we can determine the oscillation probabilities from equation (14.7):

$$P(\nu_\alpha \to \nu_\beta)(\vec{x}_F, \vec{x}_I, t_F, t_I) = \left(\frac{2\sigma^2}{\pi}\right)^{\frac{3}{2}} \sum_{i,j} U_{\alpha i} U^*_{\alpha j} U^*_{\beta i} U_{\beta j} e^{i(\vec{p}_i - \vec{p}_j)(\vec{x}_F - \vec{x}_I) - i(E_i(\vec{p}_i) - E_j(\vec{p}_j))(t_F - t_I)} \cdot e^{-\sigma^2[(\vec{x}_F - \vec{x}_I) - \vec{v}_i(t_F - t_I)]^2} e^{-\sigma^2[(\vec{x}_F - \vec{x}_I) - \vec{v}_j(t_F - t_I)]^2}. \tag{14.16}$$

The problem which arises here is that in order to compute the explicit probability, one needs to insert the propagation length $\vec{x}_F - \vec{x}_I$ and additionally the propagation time $t_F - t_I$, which is not measured in neutrino experiments. What is measured is only the particles that were created at point $\vec{x}_I$ and detected at $\vec{x}_F$, so a common procedure to analyse standard oscillations is to average over the time interval $\Delta t := t_F - t_I$. One can indeed see from the form of the probability that the real exponentials damp the oscillations and are minimal for $\vec{x}_F - \vec{x}_I = \vec{v}_{i/j}\Delta t$, hence if the propagation time is equal to the propagated distance times the group velocity. For times much lower or larger, the probability will be highly suppressed, as expected. Defining the propagation length $\vec{L} := \vec{x}_F - \vec{x}_I$ we then have:

$$P(\nu_\alpha \to \nu_\beta)(\vec{L}) = \left(\frac{2\sigma^2}{\pi}\right)^{\frac{3}{2}} \sum_{i,j} U_{\alpha i} U^*_{\alpha j} U^*_{\beta i} U_{\beta j} e^{i(\vec{p}_i - \vec{p}_j)\vec{L}} \cdot \frac{1}{N_T} \int_0^\infty d(\Delta t)\; e^{-i(E_i(\vec{p}_i) - E_j(\vec{p}_j))\Delta t} e^{-\sigma^2\left[\vec{L} - \vec{v}_i \Delta t\right]^2} e^{-\sigma^2\left[\vec{L} - \vec{v}_j \Delta t\right]^2} \tag{14.17}$$

with a normalisation constant N_T that cannot directly be determined due to the infinite size of the time interval. It is therefore usually determined later by requiring normalised oscillation probabilities. As $t_F > t_I$, the integration domain is $\Delta t > 0$. For the integration over the time interval we find:

$$\begin{aligned}
&\int_0^\infty d(\Delta t)\; e^{-i(E_i(\vec{p}_i) - E_j(\vec{p}_j))\Delta t} e^{-\sigma^2\left[\vec{L} - \vec{v}_i \Delta t\right]^2} e^{-\sigma^2\left[\vec{L} - \vec{v}_j \Delta t\right]^2} \\
&= e^{-2\sigma^2 \vec{L}^2} \int_0^\infty d(\Delta t)\; e^{-\sigma^2(\Delta t)^2(\vec{v}_i^2 + \vec{v}_j^2) + (\Delta t)[2\sigma^2 \vec{L}\cdot(\vec{v}_i + \vec{v}_j) - i(E_i(\vec{p}_i) - E_j(\vec{p}_j))]} \\
&= e^{-2\sigma^2 \vec{L}^2} \frac{\sqrt{\pi}}{2\sigma\sqrt{\vec{v}_i^2 + \vec{v}_j^2}} e^{\frac{[2\sigma^2 \vec{L}\cdot(\vec{v}_i + \vec{v}_j) - i(E_i(\vec{p}_i) - E_j(\vec{p}_j))]^2}{4\sigma^2(\vec{v}_i^2 + \vec{v}_j^2)}} \\
&\qquad \cdot \left[1 + \operatorname{erf}\left(\frac{2\sigma^2 \vec{L}\cdot(\vec{v}_i + \vec{v}_j) - i(E_i(\vec{p}_i) - E_j(\vec{p}_j))}{2\sigma\sqrt{\vec{v}_i^2 + \vec{v}_j^2}}\right)\right].
\end{aligned} \tag{14.18}$$

From this point on the calculations become pretty involved, also due to the Gaussian error function. One way to circumvent this is to extend the integration domain for the time difference Δt from $-\infty$ to ∞, which is often employed in the literature, e.g. in [188–190, 193, 194]. This then leads to a final oscillation formula which encodes next to the standard oscillations also limitations arising from the finite size of the region where the wave packet is created (or detected, when working with a finite size detector) as well as from wave packet separations. When considering decoherence, such an extension of the domain of the time integration is highly problematic, see

for instance the discussion in [195], as for $t_F < t_I$ one obtains unphysical recoherences that violate the second law of thermodynamics. Therefore in the case we are interested in in this thesis, this procedure is not satisfying, which is discussed more in detail at the end of section 16.6. To analyse the model introduced in section 16, it is however sufficient to simplify the theoretical treatment in terms of wave packets and to use plane waves instead, which will be discussed in the next section. The treatment of decoherence in terms of wave packets is not yet fully clear in the literature due to the above named failure of the standard procedure. The attempt to circumvent it by ignoring the dissipator in the time average, adding it afterwards by hand and directly imposing e.g. the equal energy condition yields contradictory results compared to the ones derived from the plane wave ansatz, see [195], as it does not derive the time evolution predicted by the open quantum system. This aspect will be discussed in more detail at the end of section 16.6. It is noteworthy to mention that the plane wave ansatz is however neither directly capable of describing spreads in the wave packet of the particle nor the creation or detection of the particle in a finite region.

14.2.2. Neutrinos as plane waves

For a plane wave with well-defined momentum $\vec{p}_i$, the momentum distribution function is a delta distribution:

$$w_i(\vec{p} - \vec{p}_i) = (2\pi)^{\frac{3}{2}} \delta^3(\vec{p} - \vec{p}_i)\,. \tag{14.19}$$

Using this in the expression for the wave function in equation (14.6) we find

$$\Psi_i(\vec{x}, \vec{x}_I, t, t_I) = e^{i\vec{p}_i(\vec{x}-\vec{x}_I) - iE_i(\vec{p}_i)(t-t_I)}\,. \tag{14.20}$$

The oscillation probability in equation (14.7) then becomes

$$P(\nu_\alpha \to \nu_\beta)(\vec{x}_F, \vec{x}_I, t_F, t_I) = \sum_{i,j} U_{\alpha i} U^*_{\alpha j} U^*_{\beta i} U_{\beta j} e^{i(\vec{p}_i - \vec{p}_j)(\vec{x}_F - \vec{x}_I) - i(E_i(\vec{p}_i) - E_j(\vec{p}_j))(t_F - t_I)}\,. \tag{14.21}$$

Introducing the time interval $\Delta t := t_F - t_I$ and the propagation length $\vec{L} := \vec{x}_F - \vec{x}_I$ this yields the well-known standard formula for neutrino oscillations:

$$P(\nu_\alpha \to \nu_\beta)(\vec{L}, \Delta t) = \sum_{i,j} U_{\alpha i} U^*_{\alpha j} U^*_{\beta i} U_{\beta j} e^{i(\vec{p}_i - \vec{p}_j)\vec{L} - i(E_i(\vec{p}_i) - E_j(\vec{p}_j))\Delta t}\,. \tag{14.22}$$

As it was already discussed in the case of a Gaussian wave packet, here both the propagation length and the time between neutrino production and detection appear. In experiments, one only measures the former, so we still have to get rid of the time interval Δt. To do so, there exist different methods when working with plane waves that employ the fact that a plane wave has a well-defined momentum (in contrast to a wave packet) and hence also a well-defined energy. This circumvents the procedure of an averaging in time that is problematic when including decoherence, which was discussed in the previous section. We present here with the equal momentum and equal energy conditions two commonly used methods to replace the time interval that both lead to the same oscillation probabilities in standard oscillations when considering relativistic neutrinos. Additional methods such as the equal velocity conditions or the conservation of energy-momentum condition can be found for instance in [189] and also yield the same oscillation probabilities for standard relativistic neutrino oscillations.
We assume that the propagation of the neutrinos is happening approximately in one dimension,

i.e. $\vec{p}_i||\vec{L}||\vec{p}_j$, so we get $\vec{p}_{i/j}\cdot\vec{L} = |\vec{p}_{i/j}||\vec{L}| =: p_{i/j}L$. The reason for this assumption is that we are interested in rather long baselines where the wave packet separation, which was mentioned in the previous subsection, strongly suppresses propagation in more than one dimension. Furthermore, we are later only interested in ultra-relativistic neutrinos where $|\vec{p}_i| \gg m_i c$ which allows us to expand the relativistic energy-momentum relation.

- **Equal energy condition:** here the assumption is that $E_i(\vec{p}_i) = E_j(\vec{p}_j) =: E$. This implies that the coefficient of Δt in the oscillation probability in equation (14.22) vanishes and one can use that
$$p_i - p_j = \sqrt{E^2 - m_i^2} - \sqrt{E^2 - m_j^2} \approx \frac{m_j^2 - m_i^2}{2E}\,. \tag{14.23}$$
- **Equal momentum condition:** in this case, one starts from the requirement that $p_i = p_j =: p$. Then this implies that
$$E_i(p_i) - E_j(p_j) = \sqrt{p^2 + m_i^2} - \sqrt{p^2 + m_j^2} \approx \frac{m_i^2 - m_j^2}{2p} \approx \frac{m_i^2 - m_j^2}{2E}\,, \tag{14.24}$$
where in the last step we defined the mean energy $E := \frac{E_i + E_j}{2}$ and used
$$p = \frac{1}{2}\sqrt{E_i^2 - m_i^2} + \frac{1}{2}\sqrt{E_j^2 - m_j^2} = \frac{E_i + E_j}{2} + O\left(\frac{m_i^2}{E_i}, \frac{m_j^2}{E_j}\right) \approx E\,. \tag{14.25}$$
Additionally approximating the speed of the neutrino by the speed of light (as the correction terms will again involve the neutrino mass) permits to replace $\Delta t \approx \frac{L}{c}$, which then yields the same form of the oscillation probabilities as obtained using the equal energy condition.

In both cases we obtain for the oscillation probabilities:
$$P(\nu_\alpha \to \nu_\beta)(\vec{L}, \Delta t) = \sum_{i,j} U_{\alpha i} U_{\alpha j}^* U_{\beta i}^* U_{\beta j} e^{-i\frac{m_i^2 - m_j^2}{2E}L}\,. \tag{14.26}$$

In a simplified yet often used quantum mechanical description, this can be derived from the underlying Hamiltonian defined in (16.93), see for instance [187].

14.2.3. Propagation through matter

For the model analysed in section 16, we are particularly interested in neutrinos that propagate through the Earth. The matter of the Earth consists mostly of atoms. As neutrinos participate in the weak interaction, they couple to the electrons in matter and interact by exchanging a $W^\pm$ boson (charged current, only electron neutrinos) or a Z boson (neutral current, also muon and tauon neutrinos). As the former has a significantly higher cross section and therefore is dominating, we drop the neutral current interaction in the simple toy model we are constructing for use in section 16. As the interaction with matter happens in flavour basis, the contribution to the Hamiltonian in mass basis is expected to be (see for instance [186, 187]):
$$\hat{U}^\dagger \hat{H}_{mat} \hat{U} \qquad \text{with } \hat{H}_{mat} = G_m \begin{pmatrix} 1 & 0 & 0 \\ 0 & 0 & 0 \\ 0 & 0 & 0 \end{pmatrix} \tag{14.27}$$

and a coupling constant G_m. From the underlying standard model and from experimental measurements, this coupling constant was determined to be $G_m = \pm\sqrt{2}G_f N_e$, where the sign discriminates between neutrinos (+) and anti-neutrinos (−), G_f denotes the Fermi coupling constant and N_e is the electron density present at the neutrino's position. In simulations of neutrino oscillations, the Earth is divided into different layers of constant density N_e to predict the evolution of the neutrino. This concludes the general introduction on neutrino oscillations. In the next section, we discuss some phenomenological models from the literature for gravitationally induced decoherence in neutrino oscillations that also build on the plane wave approximation and the matter effects discussed in this section.

15. An introduction to the phenomenological approach

The question how the standard neutrino oscillations introduced in the previous section are altered by different physical effects, partly also new physics, is widely explored in the literature. One particular effect which we also investigate in this part of the thesis is gravitationally induced decoherence in neutrino oscillations. This effect is expected to change the oscillation probabilities of the neutrino flavour oscillations and has been investigated in a large amount of works in the literature, for instance in [85–106]. Most of these works follow a phenomenological ansatz in order to determine the influence of gravity on the neutrino oscillations. To understand this approach, we introduce in this section the class of phenomenological models which is mostly used in the above cited works. In the following sections we will then present a different model which is based on an underlying quantum mechanical toy model for the neutrino and an environment composed of harmonic oscillators that serve as gravitational waves.
The process of gravitationally induced decoherence in neutrino oscillations has been investigated phenomenologically for more than two decades. While earlier works mainly focused on the two neutrino case, as for instance [96–98, 102, 103, 106], later also the three neutrino case was investigated, e.g. in [86, 88, 95, 99]. The procedure is very similar in most of the literature: starting from a phenomenological model which consists of a Lindblad equation for the quantum mechanical neutrino, the dissipator is parameterised in a general form. In the next step, physical conditions are applied to reduce the number of free parameters in the dissipator and often different scenarios are considered such that in the end only one free parameter remains. After this, measured or simulated experimental data is used to constrain the free parameters where the argument is the following: So far, no deviation of the standard oscillations has been measured. This implies that given a specific sensitivity of a detector, it is capable of yielding information in new parameter regions and can set new upper bounds if its collected data does not show deviations from the standard oscillations. Such analyses have been carried out for several detectors that resolve different energy ranges and for neutrinos coming from different sources, for instance for ANTARES [102], DUNE [90, 94, 99], IceCube/DeepCore [92, 105], JUNO [91] or Km3NeT [93].
In this section we introduce the phenomenological model and arguing to be able to compare it to our model in the following sections. The starting point of the phenomenological models is usually the Lindblad equation, which was discussed in detail in section 3 of this thesis. It is taken to describe as system of interest a neutrino system consisting of two or three different flavour/mass states in the quantum mechanical picture (see the previous section for a discussion of the advantages and disadvantages of this approach):

$$\frac{d}{dt}\hat{\rho}_S(t) = -\frac{i}{\hbar}\left[\hat{H}_S, \hat{\rho}_S(t)\right] + \mathcal{D}[\hat{\rho}_S(t)] \tag{15.1}$$

with the dissipator having Lindblad form (3.14)

$$\mathcal{D}[\hat{\rho}_S(t)] = \sum_{i=1}^{N^2-1}\left(\hat{A}_i\hat{\rho}_S(t)\hat{A}_i^\dagger - \frac{1}{2}\left\{\hat{A}_i^\dagger\hat{A}_i, \hat{\rho}_S(t)\right\}\right), \tag{15.2}$$

where the coefficient γ_i from equation (3.14) was absorbed in the definition of the Lindblad operators $\hat{A}_i$. The Hilbert space of the neutrino is N-dimensional, where N is the number of considered neutrino families, in the phenomenological models usually two or three. To proceed, the individual components of the master equation are expanded in a certain basis which often

consists of the generators of the $SU(N)$, i.e. for the two neutrino model the unit matrix and the Pauli matrices, for the three neutrino model the unit matrix and the Gell-Mann matrices. In this section, we will discuss directly the three flavour case, as this is the one we use for the toy model in the next sections. The two flavour case however works similarly and is discussed in more detail for instance in [97, 103]. In three dimensions, the eight Gell-Mann matrices along with the unit matrix are N^2 basis matrices λ_μ which read (for convenience, we have normalised the Gell-Mann matrices with a factor $\frac{1}{2}$ and the unit matrix with a factor $\frac{1}{\sqrt{6}}$, similarly to [101]):

$$\lambda_0 = \frac{1}{\sqrt{6}}\begin{pmatrix}1&0&0\\0&1&0\\0&0&1\end{pmatrix} \qquad \lambda_1 = \frac{1}{2}\begin{pmatrix}0&1&0\\1&0&0\\0&0&0\end{pmatrix} \qquad \lambda_2 = \frac{1}{2}\begin{pmatrix}0&-i&0\\i&0&0\\0&0&0\end{pmatrix}$$
$$\lambda_3 = \frac{1}{2}\begin{pmatrix}1&0&0\\0&-1&0\\0&0&0\end{pmatrix} \qquad \lambda_4 = \frac{1}{2}\begin{pmatrix}0&0&1\\0&0&0\\1&0&0\end{pmatrix} \qquad \lambda_5 = \frac{1}{2}\begin{pmatrix}0&0&-i\\0&0&0\\i&0&0\end{pmatrix}$$
$$\lambda_6 = \frac{1}{2}\begin{pmatrix}0&0&0\\0&0&1\\0&1&0\end{pmatrix} \qquad \lambda_7 = \frac{1}{2}\begin{pmatrix}0&0&0\\0&0&-i\\0&i&0\end{pmatrix} \qquad \lambda_8 = \frac{1}{\sqrt{12}}\begin{pmatrix}1&0&0\\0&1&0\\0&0&-2\end{pmatrix}. \tag{15.3}$$

The numbering of the Gell-Mann matrices is not unique, sometimes the diagonal matrices, which are here λ_0, λ_3 and λ_8, are listed first. To expand the operators of the Lindblad equation in this basis, we can use the fact that

$$tr\left(\lambda_\mu\,\lambda_\nu\right) = \frac{1}{2}\delta_{\mu\nu}\,. \tag{15.4}$$

where Greek indices are used for all nine matrices $\{\lambda_0, \lambda_1, ..., \lambda_8\}$, while roman ones indicate the eight matrices $\{\lambda_1, ..., \lambda_8\}$. In this representation, the density matrix and the system Hamiltonian in the Lindblad equation become nine dimensional vectors with components

$$\rho_\mu(t) := 2\,tr\left(\hat{\rho}_S(t)\,\lambda_\mu\right) \tag{15.5}$$
$$h_\mu := 2\,tr\left(\hat{H}_S\,\lambda_\mu\right). \tag{15.6}$$

The factor of two was added due to the factor of $\frac{1}{2}$ in the trace such that

$$\hat{\rho}_S(t) = \rho^\mu(t)\,\lambda_\mu \tag{15.7}$$
$$\hat{H}_S = h^\mu\,\lambda_\mu \tag{15.8}$$

hold. The same is also true for the Lindblad operators $\hat{A}_i$. Here, often the entire dissipator is transformed into Gell-Mann basis yielding an 9×9-dimensional matrix

$$D_{\mu\nu}\rho^\nu := 2\,tr\left(\mathcal{D}[\hat{\rho}_S]\,\lambda_\mu\right) \tag{15.9}$$

which implies

$$\mathcal{D}[\hat{\rho}_S] = D_{\mu\nu}\lambda^\mu\rho^\nu\,. \tag{15.10}$$

This dissipator then has in general 81 unknown complex parameters and is not yet the one for a Lindblad equation. At this stage, several different physical assumptions are imposed on the dissipator to reduce the number of free parameters drastically. Some examples are:

- **Hermiticity**: For the dissipator to be Hermitian we require

$$\mathcal{D}[\hat{\rho}_S]^\dagger \stackrel{!}{=} \mathcal{D}[\hat{\rho}_S] \tag{15.11}$$

which is equivalent to, using in equation (15.10) that $\lambda_\mu^\dagger = \lambda_\mu$ and $\hat{\rho}_S^\dagger(t) = \hat{\rho}_S(t)$ which implies $\rho_\mu^*(t) = \rho_\mu(t)$,

$$D_{\mu\nu}^* = D_{\mu\nu}\,, \tag{15.12}$$

hence instead of 81 complex free parameters we end up with 81 real ones.

- **Probability conservation** in the neutrino system: for the probability to be conserved, we have that

$$0 \stackrel{!}{=} tr\left(\frac{d}{dt}\hat{\rho}_S(t)\right) = tr\left(\mathcal{D}[\hat{\rho}_S(t)]\right) = D_{\mu\nu}\rho^\nu tr\left(\lambda^\mu\right)\,, \tag{15.13}$$

from which we can conclude that $D_{0\nu} = 0$, as the trace of the unit matrix does not vanish in contrast to the traces of the individual Gell-Mann matrices. This removes 9 parameters. From a physical point of view, probability conservation in the neutrino subsystem is not necessarily required, see the discussions in part III of this thesis. Nevertheless, this assumption is almost always taken in phenomenological models. One example where also a dissipator that violates probability conservation is discussed is [95].

- **Complete positivity**: This corresponds to the physical requirement to obtain positive probabilities for predictions in the neutrino subsystem even when considered a part of a larger system when a measurement according to an operator is performed on the entire system that acts trivial on the other part(s) of the total system. As discussed in part III of the thesis, the approximations required to cast a map into complete positive form might increase the error compared to the original master equation.
On the level of the dissipator complete positivity means that it can be written in Lindblad form, see section 3. Then we can expand the dissipator in Lindblad form in the Gell-Mann basis using that for each operator $\hat{O}$ we have $\hat{O} = \lambda_\mu\, 2\, tr\left(\hat{O}\lambda^\mu\right)$ and find:

$$\mathcal{D}[\hat{\rho}_S(t)] = 8\left(\lambda_\mu\lambda_\rho\lambda_\sigma - \frac{1}{2}\lambda_\sigma\lambda_\mu\lambda_\rho - \frac{1}{2}\lambda_\rho\lambda_\sigma\lambda_\mu\right)\, tr\left(\lambda^\rho\hat{\rho}_S(t)\right)\, \sum_i tr\left(\lambda^\mu\hat{A}_i\right)\, tr\left(\lambda^\sigma\hat{A}_i^\dagger\right)\,. \tag{15.14}$$

At this point we can use that

$$[\lambda_\mu, \lambda_\nu] = i f_{\mu\nu\sigma}\lambda^\sigma\,, \tag{15.15}$$

where the f_{abc} are the fully antisymmetric $SU(2)$ structure constants and the $f_{\mu\nu\sigma}$ are equal to them for all indices greater than zero and vanish otherwise. Using this identity in (15.14) yields:

$$\begin{aligned}
&\left(\lambda_\mu\lambda_\rho\lambda_\sigma - \frac{1}{2}\lambda_\sigma\lambda_\mu\lambda_\rho - \frac{1}{2}\lambda_\rho\lambda_\sigma\lambda_\mu\right)\\
&= \left(\lambda_\mu\lambda_\rho\lambda_\sigma - \frac{1}{2}\lambda_\mu\lambda_\sigma\lambda_\rho - \frac{1}{2}\lambda_\rho\lambda_\mu\lambda_\sigma - \frac{i}{2}f_{\sigma\mu a}\lambda^a\lambda_\rho - \frac{i}{2}f_{\sigma\mu a}\lambda_\rho\lambda^a\right)\\
&= -\frac{i}{2}\left(f_{\sigma\rho a}\lambda_\mu\lambda^a + f_{\rho\mu a}\lambda^a\lambda_\sigma + f_{\sigma\mu a}\lambda^a\lambda_\rho + f_{\sigma\mu a}\lambda_\rho\lambda^a\right)\\
&= -\frac{i}{2}\left(f_{\sigma\rho a}\lambda_\mu\lambda^a + f_{\rho\mu a}\lambda^a\lambda_\sigma + f_{\sigma\mu a}(\lambda^a\lambda_\rho + \lambda_\rho\lambda^a)\right)
\end{aligned} \tag{15.16}$$

and hence

$$\mathcal{D}[\hat{\rho}_S(t)] = -\frac{i}{2}\left(f_{\sigma\rho a}\lambda_\mu\lambda^a - f_{\mu\rho a}\lambda^a\lambda_\sigma + f_{\sigma\mu a}(\lambda^a\lambda_\rho + \lambda_\rho\lambda^a)\right)\,\rho^\rho(t)\,\sum_i a_i^\mu\,\left(a_i^\sigma\right)^*\,. \quad (15.17)$$

where we defined $a_i^\mu := 2\,tr\left(\lambda^\mu \hat{A}_i\right)$ and used that, given the hermiticity of the λ^σ,

$$2\,tr\left(\lambda^\sigma \hat{A}_i^\dagger\right) = 2\,tr\left((\lambda^\sigma \hat{A}_i)^\dagger\right) = 2\,tr\left((\lambda^\sigma \hat{A}_i)^T\right)^* = \left(a_i^\sigma\right)^*\,. \quad (15.18)$$

Now we split the last part into real and imaginary term in the following manner:

$$\sum_i a_i^\mu\,\left(a_i^\sigma\right)^* =: a_R^{\mu\sigma} + i a_I^{\mu\sigma}\,, \quad (15.19)$$

with

$$a_R^{\mu\sigma} = \sum_i [\Re(a_i^\mu)\Re(a_i^\sigma) + \Im(a_i^\mu)\Im(a_i^\sigma)] = a_R^{\sigma\mu} \quad (15.20)$$

$$a_I^{\mu\sigma} = \sum_i [\Im(a_i^\mu)\Re(a_i^\sigma) - \Re(a_i^\mu)\Im(a_i^\sigma)] = -a_I^{\sigma\mu} \quad (15.21)$$

where $\Re$ and $\Im$ denote the real and imaginary part respectively, from which it follows that

$$\begin{aligned}\mathcal{D}[\hat{\rho}_S(t)] &= -\frac{i}{2}\left(f_{\sigma\rho a}\lambda_\mu\lambda^a - f_{\mu\rho a}\lambda^a\lambda_\sigma + f_{\sigma\mu a}(\lambda^a\lambda_\rho + \lambda_\rho\lambda^a)\right)\,\rho^\rho(t)\,\left(a_R^{\mu\sigma} + i a_I^{\mu\sigma}\right)\\ &= -\frac{i}{2}\left(a_R^{\mu\sigma} f_{\sigma\rho a}[\lambda_\mu,\lambda^a] + i a_I^{\mu\sigma} f_{\sigma\rho a}\{\lambda_\mu,\lambda^a\} + i a_I^{\mu\sigma} f_{\sigma\mu a}\{\lambda^a,\lambda_\rho\}\right)\rho^\rho(t)\,. \end{aligned} \quad (15.22)$$

Also the anti-commutator of two λ^μ matrices can be expanded as a combination of the λ^μ:

$$\{\lambda_\mu,\lambda^a\} = \sqrt{\frac{2}{3}}\left(\delta_{\mu 0}\lambda^a + \delta_\mu^a\lambda^0\right) + d_\mu{}^{ab}\lambda_b\,, \quad (15.23)$$

where $d_0{}^{ab} = 0$ (as well as any other d containing at least one index with value 0) and $d_c{}^{ab} := 2\,tr\left(\lambda_c\{\lambda^a,\lambda^b\}\right)$. Using this, we obtain

$$\begin{aligned}&\mathcal{D}[\hat{\rho}_S(t)] = -\frac{i}{2}\left(a_R^{\mu\sigma} f_{\sigma\rho a}[\lambda_\mu,\lambda^a] + i a_I^{\mu\sigma} f_{\sigma\rho a}\{\lambda_\mu,\lambda^a\} + i a_I^{\mu\sigma} f_{\sigma\mu a}\{\lambda^a,\lambda_\rho\}\right)\rho^\rho(t)\\ &= \frac{1}{2}\left(a_R^{\mu\sigma} f_{\sigma\rho a} f_\mu{}^{ab}\lambda_b + a_I^{\mu\sigma}\left(\sqrt{\frac{2}{3}}\lambda^a(\delta_{\mu 0}f_{\sigma\rho a} + \delta_{\rho 0}f_{\sigma\mu a}) + \lambda_c(f_{\sigma\rho a}d^{\mu ac} + f_{\sigma\mu a}d^{\rho ac})\right)\right)\rho^\rho(t)\\ &= \frac{1}{2}\left(a_R^{\mu\sigma} f_{\sigma\rho a} f_\mu{}^a{}_\nu + a_I^{\mu\sigma}\left(\sqrt{\frac{2}{3}}(\delta_{\mu 0}f_{\sigma\rho\nu} + \delta_{\rho 0}f_{\sigma\mu\nu}) + (f_{\sigma\rho a}d^{\mu a}{}_\nu + f_{\sigma\mu a}d^{\rho a}{}_\nu)\right)\right)\lambda^\nu\rho^\rho(t)\,. \end{aligned} \quad (15.24)$$

In this form, one can read off $D_{\nu\rho}$ such that

$$\mathcal{D}[\hat{\rho}_S(t)] = D_{\nu\rho}\lambda^\nu\rho^\rho(t)\,. \quad (15.25)$$

From this form it is evident that we have $D_{0\rho} = 0$ which implies probability conservation in the neutrino subsystem, see the previous bullet point. This indeed directly follows when applying the trace on the dissipator in Lindblad form in equation (15.2) and using the cyclicity of the trace. Note that complete positivity and also the way how the $a_{R/I}^{\mu\nu}$ matrices are defined also impose conditions on them. For details we refer to the literature, e.g. to [101, 106].

- **Increasing von Neumann entropy** in the neutrino system: from the work in [196] it follows that for Hermitian Lindblad operators, the von Neumann-entropy of the neutrino system never decreases in time. For such a choice of Hermitian Lindblad operators $\hat{A}_i^\dagger = \hat{A}_i$ we have that $(a_i^\mu)^* = a_i^\mu$ which implies $a_I^{\mu\sigma} = 0$. Due to this we obtain in that case for the dissipator in equation (15.24):

$$\mathcal{D}[\hat{\rho}_S(t)] = \frac{1}{2} a_R^{\mu\sigma} f_{\sigma\rho a} f_\mu{}^a{}_\nu \lambda^\nu \rho^\rho(t)\,. \tag{15.26}$$

  This condition for the Lindblad operators is used for instance in [86, 101, 103].

- **Energy conservation** in the neutrino system: This is equivalent to requiring that

$$[\hat{A}_i, \hat{H}_S] = 0\,, \tag{15.27}$$

  where $\hat{H}_S$ is the Hamiltonian of the neutrino system. Assuming we are in the basis where $\hat{H}_S$ is diagonal, i.e. the effective mass basis (which is equivalent to the vacuum mass basis for propagation in vacuum), this relation becomes in Gell-Mann representation:

$$4\,tr\left(\hat{A}_i\lambda^\mu\right)\,tr\left(\hat{H}_S\lambda^\nu\right)\,[\lambda_\mu,\lambda_\nu] = 4if_{\mu\nu a}\lambda^a\,tr\left(\hat{A}_i\lambda^\mu\right)\,tr\left(\hat{H}_S\lambda^\nu\right) = 0\,. \tag{15.28}$$

  From the specific form of the λ^μ at the beginning of this section it follows that for diagonal $\hat{H}_S$ the expression $tr\left(\hat{H}_S\lambda^\nu\right)$ is only non-zero for $\nu \in \{0,3,8\}$. This implies that in order for equation (15.28) to hold, we need that $tr\left(\hat{A}_i\lambda^\mu\right) = 0$ for $\mu \in \{1,2,4,5,6,7\}$, so $\hat{A}_i$ also has to be a diagonal matrix, which yields that the only non-vanishing elements of $a_{R/I}^{\mu\nu}$ are the ones where $\mu,\nu \in \{0,3,8\}$. From the explicit values of the f_{abc}, where the non-vanishing ones are

$$f_{123} = 1; \qquad f_{147} = f_{165} = f_{246} = f_{257} = f_{345} = f_{376} = \frac{1}{2}; \qquad f_{458} = f_{678} = \frac{\sqrt{3}}{2}\,, \tag{15.29}$$

  one can conclude that for Hermitian Lindblad operators this implies that the dissipator is diagonal in Gell-Mann basis and assumes the following form:

$$\begin{aligned} D_{\mu\nu} = \mathrm{diag}\Bigg(0, -\frac{1}{2}a_R^{33}, -\frac{1}{2}a_R^{33}, 0, -\frac{1}{8}a_R^{33} - \frac{\sqrt{3}}{4}a_R^{38} - \frac{3}{8}a_R^{88}, -\frac{1}{8}a_R^{33} - \frac{\sqrt{3}}{4}a_R^{38} - \frac{3}{8}a_R^{88}, \\ -\frac{1}{8}a_R^{33} + \frac{\sqrt{3}}{4}a_R^{38} - \frac{3}{8}a_R^{88}, -\frac{1}{8}a_R^{33} + \frac{\sqrt{3}}{4}a_R^{38} - \frac{3}{8}a_R^{88}, 0\Bigg)\,. \end{aligned} \tag{15.30}$$

  This contains three independent parameters and can be reexpressed as

$$D_{\mu\nu} = \mathrm{diag}(0, -\Gamma_1, -\Gamma_1, 0, -\Gamma_2, -\Gamma_2, -\Gamma_3, -\Gamma_3, 0) \tag{15.31}$$

  by defining

$$\Gamma_1 := \frac{1}{2}a_R^{33} = \frac{1}{2}(\vec{a}^3)^2 \geq 0 \tag{15.32}$$

$$\Gamma_2 := \frac{1}{8}a_R^{33} + \frac{\sqrt{3}}{4}a_R^{38} + \frac{3}{8}a_R^{88} = \frac{1}{2}\left(\frac{1}{2}\vec{a}^3 + \frac{\sqrt{3}}{2}\vec{a}^8\right)^2 \geq 0 \tag{15.33}$$

$$\Gamma_3 := \frac{1}{8}a_R^{33} - \frac{\sqrt{3}}{4}a_R^{38} + \frac{3}{8}a_R^{88} = \frac{1}{2}\left(\frac{1}{2}\vec{a}^3 - \frac{\sqrt{3}}{2}\vec{a}^8\right)^2 \geq 0\,, \tag{15.34}$$

where we used the notation from [101] and defined $\vec{a}^{\mu} := (a_1^{\mu}, ..., a_8^{\mu})$. Similar expressions can be found for instance in [106].

The dissipator in (15.31) is frequently used as starting point in the phenomenological models. From the discussion in this section it becomes clear which assumptions enter the master equation in order to obtain it. Using the explicit representation of the $\rho^{\mu}(t)$,

$$\begin{aligned}
&\rho^0(t) = \frac{1}{\sqrt{6}}(\rho_{11}(t) + \rho_{22}(t) + \rho_{33}(t)) \qquad \rho^1(t) = \frac{1}{2}(\rho_{12}(t) + \rho_{21}(t)) \qquad \rho^2(t) = \frac{i}{2}(\rho_{12}(t) - \rho_{21}(t)) \\
&\rho^3(t) = \frac{1}{2}(\rho_{11}(t) - \rho_{22}(t)) \qquad \rho^4(t) = \frac{1}{2}(\rho_{13}(t) + \rho_{31}(t)) \qquad \rho^5(t) = \frac{i}{2}(\rho_{13}(t) - \rho_{31}(t)) \\
&\rho^6(t) = \frac{1}{2}(\rho_{23}(t) + \rho_{32}(t)) \qquad \rho^7(t) = \frac{i}{2}(\rho_{23}(t) - \rho_{32}(t)) \qquad \rho^8(t) = \frac{1}{\sqrt{12}}(\rho_{11}(t) + \rho_{22}(t) - 2\rho_{33}(t))
\end{aligned} \tag{15.35}$$

we can transform the master equation back into the original representation as 3×3-matrices in the effective mass basis. For the dissipator in equation (15.31) one then obtains:

$$\begin{aligned}
\mathcal{D}[\hat{\rho}_S(t)] &= -\frac{1}{2}\begin{pmatrix} 0 & \Gamma_1(\rho^1(t) - i\rho^2(t)) & \Gamma_2(\rho^4(t) - i\rho^5(t)) \\ \Gamma_1(\rho^1(t) + i\rho^2(t)) & 0 & \Gamma_3(\rho^6(t) - i\rho^7(t)) \\ \Gamma_2(\rho^4(t) + i\rho^5(t)) & \Gamma_3(\rho^6(t) + i\rho^7(t)) & 0 \end{pmatrix} \\
&= -\frac{1}{2}\begin{pmatrix} 0 & \Gamma_1\rho_{12}(t) & \Gamma_2\rho_{13}(t) \\ \Gamma_1\rho_{21}(t) & 0 & \Gamma_3\rho_{23}(t) \\ \Gamma_2\rho_{31}(t) & \Gamma_3\rho_{32}(t) & 0 \end{pmatrix}.
\end{aligned} \tag{15.36}$$

The master equation that corresponds to this dissipator is in the effective mass basis where $\hat{H}_S = \mathrm{diag}(H_1, H_2, H_3)$:

$$\begin{aligned}
&\frac{d}{dt}\hat{\rho}_S(t) = -\frac{i}{\hbar}\left[\hat{H}_S, \hat{\rho}_S(t)\right] + \mathcal{D}[\hat{\rho}_S(t)] \\
&= \begin{pmatrix} 0 & \left(-\frac{i}{\hbar}(H_1 - H_2) - \frac{\Gamma_1}{2}\right)\rho_{12}(t) & \left(-\frac{i}{\hbar}(H_1 - H_3) - \frac{\Gamma_2}{2}\right)\rho_{13}(t) \\ \left(-\frac{i}{\hbar}(H_2 - H_1) - \frac{\Gamma_1}{2}\right)\rho_{21}(t) & 0 & \left(-\frac{i}{\hbar}(H_2 - H_3) - \frac{\Gamma_3}{2}\right)\rho_{23}(t) \\ \left(-\frac{i}{\hbar}(H_3 - H_1) - \frac{\Gamma_2}{2}\right)\rho_{31}(t) & \left(-\frac{i}{\hbar}(H_3 - H_2) - \frac{\Gamma_3}{2}\right)\rho_{32}(t) & 0 \end{pmatrix}.
\end{aligned} \tag{15.37}$$

The solution of this equation can be written down immediately in the effective mass basis assuming a constant system Hamiltonian:

$$\rho_{ii}(t) = \rho_{ii}(0) \qquad \text{and for } i \neq j: \qquad \rho_{ij}(t) = e^{-\frac{i}{\hbar}(H_i - H_j)t - \Gamma_{ij}t}\rho_{ij}(0)\,, \tag{15.38}$$

where $\Gamma_{12} = \Gamma_{21} = \frac{\Gamma_1}{2}$, $\Gamma_{13} = \Gamma_{31} = \frac{\Gamma_2}{2}$ and $\Gamma_{23} = \Gamma_{32} = \frac{\Gamma_3}{2}$. In the phenomenological models, the next step is then the analysis to constrain the three decoherence parameters Γ_1, Γ_2 and Γ_3 that change the neutrino oscillations in flavour basis. To reduce their amount, different approximations are considered where some of these Gamma parameters are set equal to each other or equal to zero. Their definitions starting in (15.32) show however that these choices are problematic in general and not necessarily justified for any system. Finally, they are in most phenomenological models assumed to have a specific unknown dependence on the neutrino energy:

$$\Gamma_{ij} = \gamma_{ij}\left(\frac{E}{GeV}\right)^n, \tag{15.39}$$

where n is assumed to be $n \in \{-2, -1, 0, 1, 2\}$ and γ_{ij} is a constant. Different dependencies on the power of the energy lead to different detectors being more favourable to measure gravitationally induced decoherence, so the sensitivity of various detectors is analysed in detail for different values of n. An important remark here is that in almost all models γ_{ij} and n are taken to be constant, even when the system Hamiltonian changes because the neutrino propagates through different layers of matter with changing density. An exception to this assumptions represents the work in [103], where for a two flavour system a dissipator is constructed that commutes with the system Hamiltonian in every density layer, thus also changes when the system Hamiltonian does. In the following two sections, we derive a master equation for gravitationally induced decoherence in neutrino oscillations based on a microscopic quantum mechanical toy model. That approach allows to resolve the structure and energy dependence of the Γ parameters based on the underlying action of the total system and do not need to make any of the assumptions listed in this section to arrive at a dissipator that has a simple form: starting from the microscopic toy model, we will naturally arrive at a dissipator whose Lindblad operators are the system Hamiltonian $\hat{H}_S$. With the Markov approximation, whose validity is explicitly tested for the model under consideration, this dissipator has Lindblad form and thus probabilities are conserved and it is completely positive. As the system Hamiltonian is Hermitian and commutes with itself, also the von Neumann-entropy of the neutrino system does not decrease with time and the energy is conserved in the neutrino subsystem. This then yields indeed a dissipator of the form (15.36), where the structure of the individual Γ parameters is however fixed from the underlying microscopic model, up to two physical parameters that characterise on the one hand the coupling strength between neutrino system and gravitational environment as well as on the other hand the environmental state.

16. Quantum mechanical model: setup and derivation of the master equation

Parts of the content of this section were already published in [3]. Here, they are presented with some modifications compared to [3] to adapt them to the flow of the thesis and extended with further content and calculations.

The quantum mechanical toy model investigated in this part of the thesis is inspired from the field theory models for gravitationally induced decoherence [1, 60–63], where the one in [1] was discussed in the previous parts of the thesis, that all consider linearised gravity as the environment to which a given matter system is coupled. Because general relativity as well as generic matter systems involve gauge symmetries, some work is necessary in order to get the corresponding physical Hamiltonian of the total system that usually is the starting point of the decoherence model. This has been implemented in [1, 60–63] either by gauge fixing [60–63] or by the construction of gauge invariant observables [1], see section 7, by means of choosing a suitable dynamical reference system. The classical total Hamiltonian $\hat{H}_T$ in all these models has the form discussed in (2.10):

$$\hat{H}_T = \hat{H}_S \otimes \hat{\mathbb{1}}_{\mathcal{E}} + \hat{\mathbb{1}}_S \otimes \hat{H}_{\mathcal{E}} + \alpha \hat{H}_I \,, \tag{16.1}$$

where $\hat{H}_S$ encodes the dynamics of the system usually chosen to be some matter, $\hat{H}_{\mathcal{E}}$ is the Hamiltonian for the environment, here linearised gravity, and $\hat{H}_I$ describes their interaction. Once a frame of reference has been chosen, the form of each Hamiltonian can be derived from the underlying action, and in particular the form of the interaction Hamiltonian $\hat{H}_I$ is determined by the way matter and (linearised) gravity are coupled, namely via the energy-momentum tensor of the matter to the metric. Thus, on the one hand it is an advantage to know the underlying field theory model because the microscopic Hamiltonian that enters any decoherence models can rather be derived than needing to be chosen, which results in decoherence models with less ambiguities. On the other hand as the results in [1, 60–63] illustrate, the final form of the master equation which encodes the dynamics of the system's density matrix when the environmental degrees of freedom have been traced out, is very complicated and hence technically challenging, as is evident from parts II and III of this thesis. To broaden the techniques to treat gravitationally induced decoherence in matter systems, in this part of the thesis we consider the quantum mechanical toy model for gravitationally induced decoherence introduced in the seminal work of Xu and Blencowe in [112]. This model is strongly inspired by the field theory models and hence mimics the usual gravitational coupling in the quantum mechanical toy model. To the knowledge of the authors in [3], although this model exists in the literature it has only been applied to investigate gravitationally induced decoherence in the context of neutrino oscillations in [195] where the authors however conclude that the model will lead to no decoherence effect if they apply the equal-energy condition, which was introduced in section 14.2.2 in this thesis, motivated in their work from the wave packet approach. We will consider the slightly generalised model of [112] such that we can also apply it to neutrino oscillations and present the derivation of the corresponding master equation, which was not included in the presentation in [112] in detail to show that from our results non-vanishing decoherence effects are possible for this model.

16.1. Basic quantum mechanical model and master equation

Parts of the content of this subsection were already published in [3]. Here, they are presented with some modifications compared to [3] to adapt them to the flow of the thesis and extended with

further content and calculations.
In [112], a harmonic oscillator is considered as matter system and its dynamics are derived working with coherent states for the bath. Based on this, the decoherence on an initial superposition of coherent states is studied. Here, we want to consider the model in a more general context to be able to apply it later to neutrino oscillations. Therefore, we will leave the choice of the system's Hamiltonian generic in this section and only specify to neutrinos later. The only assumption we make for H_S is that it is time-independent. Likewise to the field theory case, the total Hamiltonian splits into the individual contributions which are then quantised in a quantum mechanical context. In this part we put hats on all operators and drop the tensor product with the identity to simplify readability and to have the notation more similar to [112] and the phenomenological models. The total Hamiltonian for the model under consideration is then

$$\hat{H}_T = \hat{H}_S + \hat{H}_\mathcal{E} + \hat{H}_I = \underbrace{\hat{H}_S^{(0)} + \hat{H}_S^{(C)}}_{\hat{H}_S} + \underbrace{\frac{1}{2}\sum_{i=1}^{N}\left[\frac{\hat{p}_i^2}{\mu} + \mu\omega_i^2\hat{q}_i^2\right]}_{\hat{H}_\mathcal{E}} - \underbrace{\hat{H}_S \otimes \sum_{i=1}^{N} g_i\hat{q}_i}_{\hat{H}_I}\,, \tag{16.2}$$

where here the specific form of $\hat{H}_\mathcal{E}$ and $\hat{H}_I$ are inspired from the field theory model, the coupling constant g_i has dimensions of inverse length and $\hat{H}_S^{(C)}$ denotes a counter term of the form $\hat{H}_S^{(C)} = \sum_{i=1}^{N}\frac{\hbar g_i^2}{2\mu\omega_i^2}(\hat{H}_S^{(0)})^2$. This counter term is needed as it will later remove the unphysical contribution of the Lamb shift. It is included analogously to the treatment of the Caldeira-Leggett model [133], see for instance [112], and can be understood as a tiny, due to g_i^2, frequency dependent correction to the unitary evolution of the non-renormalised and thus the bare system's Hamiltonian $\hat{H}_S^{(0)}$. The environment serves as a toy model for gravitational waves that interact with the system under consideration. To resemble this, N independent harmonic oscillators with unit mass[33] μ were chosen explaining the form of $\hat{H}_\mathcal{E}$. In later applications in section 16.6, the system will be chosen as a neutrino. The lesson from the field theory models is that the interaction Hamiltonian, which includes the energy-momentum tensor and the metric, can be modeled by an interaction Hamiltonian operator, as shown in [112], that involves a coupling between the system's Hamiltonian $\hat{H}_S$ and the position operator of the environmental degrees of freedom $\hat{q}_i$. In field theory, this is replaced by a coupling of the energy-momentum tensor of the system to the metric, which is in the classical theory the configuration variable of the environment. The coupling constant g_i, which has dimension of inverse length, can in principle be different for each oscillator.
Position and momentum operators of the oscillators in the environment fulfil the usual commutation relations:

$$[\hat{q}_i, \hat{p}_j] = i\hbar\delta_{ij}\,. \tag{16.3}$$

Assuming that the interaction is small (i.e. g_i is small) compared to the evolution in the absence of coupling to the environment, a time-convolutionless (TCL) master equation truncated at second order in the coupling g_i (see equation (4.35)) provides a good approximation to the effective dynamics of the system, which is obtained after the degrees of freedom of the environment have been worked out. In order to use equation (4.35), we assumed, as it was discussed in section 4.3, to have factorising initial conditions, i.e. $\hat{\rho}(t_0) = \hat{\rho}_S(t_0)\otimes\hat{\rho}_\mathcal{E}$, and a Gibbs state $\hat{\rho}_\mathcal{E} = \frac{1}{Z}e^{-\beta\hat{H}_\mathcal{E}}$ for the environment. The latter includes the partition function $Z = \mathrm{Tr}_\mathcal{E}\left(e^{-\beta\hat{H}_\mathcal{E}}\right)$, where $\beta = \frac{1}{k_B\Theta}$ with

[33] Introduced to obtain correct dimensions.

the Boltzmann constant k_B and similar to [60] we denote the involved 'temperature' parameter of the environment by Θ, which characterises the bath of the oscillators in the environment that mimic the thermal gravitational wave background in this toy model. The master equation then assumes a simple form, since the interaction Hamiltonian H_I contains a time-independent system Hamiltonian $\hat{H}_S$:

$$\frac{d}{dt}\hat{\rho}_S(t) = -\frac{i}{\hbar}\left[\hat{H}_S, \hat{\rho}_S(t)\right] - \frac{1}{\hbar^2}\int_0^{t-t_0} d\tau \, \mathrm{Tr}_{\mathcal{E}}\left(\left[\hat{H}_I, \left[\hat{H}_I(-\tau), \hat{\rho}_S(t)\otimes\hat{\rho}_{\mathcal{E}}\right]\right]\right) . \tag{16.4}$$

The density matrix of the matter system evaluated at temporal coordinate t is denoted by $\hat{\rho}_S(t)$ and $\hat{H}_I(\tau)$ is the interaction Hamiltonian operator in the interaction picture evaluated at time τ, i.e. $\hat{H}_I(\tau) := e^{\frac{i}{\hbar}(\hat{H}_S+\hat{H}_{\mathcal{E}})\tau}\hat{H}_I e^{-\frac{i}{\hbar}(\hat{H}_S+\hat{H}_{\mathcal{E}})\tau}$. A detailed discussion of the derivation of equation (16.4) can be found in section 4 of this thesis. Here we continue from this form and plug in the interaction Hamiltonian to obtain for the integrand of the last term:

$$\begin{aligned}\mathrm{Tr}_{\mathcal{E}}\left(\left[\hat{H}_I, \left[\hat{H}_I(-\tau), \hat{\rho}_S(t)\otimes\hat{\rho}_{\mathcal{E}}\right]\right]\right) = \sum_{i,j=1}^{N} \Big\{ & C_{ij}(-\tau)\left(\hat{H}_S^2\,\hat{\rho}_S(t) - \hat{H}_S\,\hat{\rho}_S(t)\,\hat{H}_S\right) \\ & + C_{ji}(\tau)\left(\hat{\rho}_S(t)\hat{H}_S^2 - \hat{H}_S\,\hat{\rho}_S(t)\,\hat{H}_S\right)\Big\}, \end{aligned} \tag{16.5}$$

where we defined the dimensionless correlation functions

$$C_{ij}(-\tau) := g_i g_j \mathrm{Tr}_{\mathcal{E}}\left(\hat{q}_i\,\hat{q}_j(-\tau)\,\hat{\rho}_{\mathcal{E}}\right) \tag{16.6}$$

and we used the cyclicity of the trace as well as the following identity:

$$\begin{aligned} g_i g_j \mathrm{Tr}_{\mathcal{E}}\left(\hat{q}_j(-\tau)\,\hat{q}_i\,\hat{\rho}_{\mathcal{E}}\right) &= g_i g_j \mathrm{Tr}_{\mathcal{E}}\left(e^{-\frac{i}{\hbar}(\hat{H}_S+\hat{H}_{\mathcal{E}})\tau}\hat{q}_j e^{\frac{i}{\hbar}(\hat{H}_S+\hat{H}_{\mathcal{E}})\tau}\,\hat{q}_i\,\hat{\rho}_{\mathcal{E}}\right) \\ &= g_i g_j \mathrm{Tr}_{\mathcal{E}}\left(\hat{q}_j\, e^{\frac{i}{\hbar}(\hat{H}_S+\hat{H}_{\mathcal{E}})\tau}\hat{q}_i e^{-\frac{i}{\hbar}(\hat{H}_S+\hat{H}_{\mathcal{E}})\tau}\, e^{\frac{i}{\hbar}(\hat{H}_S+\hat{H}_{\mathcal{E}})\tau}\hat{\rho}_{\mathcal{E}} e^{-\frac{i}{\hbar}(\hat{H}_S+\hat{H}_{\mathcal{E}})\tau}\right) \\ &= g_i g_j \mathrm{Tr}_{\mathcal{E}}\left(\hat{q}_j\,\hat{q}_i(\tau)\,\hat{\rho}_{\mathcal{E}}\right) \\ &= C_{ji}(\tau)\,, \end{aligned} \tag{16.7}$$

where we employed that the Gibbs state $\hat{\rho}_{\mathcal{E}}$ is stationary. Hence, we only have one specific form of the correlation function that we have to compute, namely $C_{ij}(-\tau)$. We will do the explicit computation in subsection 16.2. Note that due to the specific from of the interaction Hamiltonian in (16.2), each particle in the environment is coupled to the same operator of the system, i.e. the Hamiltonian. Therefore, the sum over the particles in the environment only appears in the correlation functions and not in the operators of the system, which is different to the coupling investigated so far in parts II and III, where the two parts of the interaction Hamiltonian were tied together by a sum over the spatial (and internal) indices as well as by the same spacetime evaluation point. This is not the case here, which simplifies the calculations. Defining two quantities Λ and Γ, which both have the dimension of time,

$$\Lambda(t-t_0) := \frac{i}{2}\int_0^{t-t_0} d\tau \sum_{i,j=1}^{N}\left(C_{ij}(-\tau) - C_{ji}(\tau)\right) \tag{16.8}$$

$$\Gamma(t-t_0) := \int_0^{t-t_0} d\tau \sum_{i,j=1}^{N}\left(C_{ij}(-\tau) + C_{ji}(\tau)\right), \tag{16.9}$$

permits us to rewrite the master equation (16.4) in the following form:

$$\frac{d}{dt}\hat{\rho}_S(t) = -\frac{i}{\hbar}\left[\hat{H}_S, \hat{\rho}_S(t)\right] + \frac{i\Lambda(t-t_0)}{\hbar^2}\left[\hat{H}_S^2, \hat{\rho}_S(t)\right] + \frac{\Gamma(t-t_0)}{\hbar^2}\left(\hat{H}_S\hat{\rho}_S(t)\hat{H}_S - \frac{1}{2}\left\{\hat{H}_S^2, \hat{\rho}_S(t)\right\}\right). \tag{16.10}$$

As $\Lambda(t-t_0)$ and $\Gamma(t-t_0)$ are already of second order in the coupling g_i, after which the master equation was truncated, one can replace $\hat{H}_S$ by $\hat{H}_S^{(0)}$ in all but the first term, as the correction term $\hat{H}_S^{(C)}$ is also of second order in g_i, which yields

$$\begin{aligned}\frac{d}{dt}\hat{\rho}_S(t) = &-\frac{i}{\hbar}\left[\hat{H}_S, \hat{\rho}_S(t)\right] + \frac{i\Lambda(t-t_0)}{\hbar^2}\left[\left(\hat{H}_S^{(0)}\right)^2, \hat{\rho}_S(t)\right] \\ &+ \frac{\Gamma(t-t_0)}{\hbar^2}\left(\hat{H}_S^{(0)}\hat{\rho}_S(t)\hat{H}_S^{(0)} - \frac{1}{2}\left\{\left(\hat{H}_S^{(0)}\right)^2, \hat{\rho}_S(t)\right\}\right).\end{aligned} \tag{16.11}$$

The first term of the master equation is the standard unitary evolution of the matter system itself. The second term, usually referred to as the Lamb shift contribution, leads to a renormalisation of the energy levels of the matter systems due to the presence of the environment, and the third term is the dissipator present in open quantum systems. An analogous contribution to the Lamb shift, which results here directly from the derivation of the master equation, is also present in the field theoretical model. In addition, in the field theory model a further gravitationally induced self-interaction term for the matter system is present, such a term is not involved in the quantum mechanical toy model because on the one hand it is strongly related to the gauge symmetries in general relativity and the construction of gauge invariant quantities, see part II and III of this thesis, and on the other hand whether it is present in the 1-particle projection also depends on the normal ordering chosen in the field theory model, see the discussion in part III. In the field theoretical case, a renormalisation must normally be carried out for this contribution. We discuss this point for the quantum mechanical toy model below after computing the correlation functions. The dissipator resembles the remaining effective interaction of the gravitational wave environment with the matter system. Both contributions would be absent if one treats the neutrinos as a closed quantum system.

16.2. Computation of the correlation functions

As a next step, we want to compute the correlation functions $C_{ij}(-\tau)$, which were defined in equation (16.6). Evaluating the trace in occupation number basis, in which the Gibbs state is

$$\hat{\rho}_{\mathcal{E}} = \frac{1}{Z}\bigotimes_{i=1}^{N}\sum_{n_i\in\mathbb{N}} e^{-\beta\epsilon_{n,i}}\left|n_i\right\rangle\left\langle n_i\right| \tag{16.12}$$

with eigenenergies $\epsilon_{n,i} = \hbar\omega_i\left(n_i + \frac{1}{2}\right)$, we obtain:

$$C_{ij}(-\tau) = \frac{g_i g_j}{Z}\prod_{l=1}^{N}\sum_{n_l\in\mathbb{N}} e^{-\beta\epsilon_{n,l}}\left\langle n_l\right|\hat{q}_{i,l}\,\hat{q}_{j,l}(-\tau)\left|n_l\right\rangle, \tag{16.13}$$

where $\hat{q}_{i,l}$ is the projection of $\hat{q}_i$ onto the operators on the Hilbert space of particle l, which is the identity for $i \neq l$ and $\hat{q}$ for $i = l$. Expanding the position operators in ladder operators $a_i^{(\dagger)}$ that

fulfill $[a_i, a_j^\dagger] = \delta_{ij}$ yields

$$\hat{q}_i = \sqrt{\frac{\hbar}{2\mu\omega_i}}(\hat{a}_i^\dagger + \hat{a}_i)\,, \tag{16.14}$$

where $\hat{a}_i^{(\dagger)}$ again acts as ladder operator on the Hilbert space of particle i and as identity on the Hilbert spaces of the other particles. For the time evolution we find:

$$\hat{a}_i^{(\dagger)}(-\tau) = e^{-i\omega_i\tau\,\hat{a}_i^\dagger\hat{a}_i}\,\hat{a}_i^{(\dagger)}\,e^{i\omega_i\tau\,\hat{a}_i^\dagger\hat{a}_i} = \sum_{m=0}^{\infty}\frac{(-i\omega_i\tau)^m}{m!}[\hat{a}_i^\dagger\hat{a}_i, \hat{a}_i^{(\dagger)}]_{(m)}\,, \tag{16.15}$$

where the iterated commutator $[A, B]_{(m)}$ is defined recursively:

$$[A, B]_{(m+1)} := [A, [A, B]_{(m)}]\,, \qquad [A, B]_{(0)} = B\,. \tag{16.16}$$

For the application here we find:

$$[\hat{a}_i^\dagger\hat{a}_i, \hat{a}_i]_{(m)} = (-1)^m\hat{a}_i\,, \qquad [\hat{a}_i^\dagger\hat{a}_i, \hat{a}_i^\dagger]_{(m)} = \hat{a}_i^\dagger\,, \tag{16.17}$$

from which it follows that

$$\hat{a}_i(-\tau) = e^{i\omega_i\tau}\,\hat{a}_i\,, \qquad \hat{a}_i^\dagger(-\tau) = e^{-i\omega_i\tau}\,\hat{a}_i^\dagger\,. \tag{16.18}$$

Using the orthogonality of the occupation basis states and the normalisation of the Gibbs state, we can simplify the correlation functions (16.13) now further:

$$C_{ij}(-\tau) = \delta_{ij}\frac{g_i^2}{Z_i}\sum_{n_i\in\mathbb{N}} e^{-\beta\epsilon_{n,i}}\,\langle n_i|\,\hat{q}_{i,i}\,\hat{q}_{i,i}(-\tau)\,|n_i\rangle\,, \tag{16.19}$$

where $Z_i := \mathrm{Tr}_{\mathcal{E},i}\left(e^{-\beta\hat{H}_{\mathcal{E},i}}\right)$ with the partial trace summing only over the Hilbert space of particle i and $\hat{H}_{\mathcal{E},i}$ being the Hamiltonian of oscillator i. With the decomposition of the position operator in ladder operators we obtain

$$\begin{aligned}
C_{ij}(-\tau) &= \delta_{ij}\frac{\hbar g_i^2}{2\mu\omega_i}\frac{1}{Z_i}\sum_{n_i\in\mathbb{N}} e^{-\beta\epsilon_{n,i}}\,\langle n_i|\,e^{-i\omega_i\tau}(\hat{a}_{i,i}\,\hat{a}_{i,i}^\dagger) + e^{i\omega_i\tau}(\hat{a}_{i,i}^\dagger\,\hat{a}_{i,i})\,|n_i\rangle \\
&= \delta_{ij}\frac{\hbar g_i^2}{2\mu\omega_i}\frac{1}{Z_i}\sum_{n_i\in\mathbb{N}} e^{-\beta\epsilon_{n,i}}\left(e^{-i\omega_i\tau} + 2\cos(\omega_i\tau)\,\langle n_i|\,\hat{a}_{i,i}^\dagger\,\hat{a}_{i,i}\,|n_i\rangle\right) \\
&= \delta_{ij}\frac{\hbar g_i^2}{2\mu\omega_i}\left(e^{-i\omega_i\tau} + \frac{2}{Z_i}\cos(\omega_i\tau)\sum_{n_i\in\mathbb{N}} n_i e^{-\beta\epsilon_{n,i}}\right)\,.
\end{aligned} \tag{16.20}$$

To continue, we use a similar procedure as in Appendix B, in the present case we however also have to consider the zero-point energy of the harmonic oscillator:

$$\begin{aligned}
\frac{1}{Z_i}\sum_{n_i\in\mathbb{N}} n_i e^{-\beta\epsilon_{n,i}} &= \frac{1}{Z_i}\sum_{n_i\in\mathbb{N}} n_i e^{-\beta\hbar\omega_i\left(n_i+\frac{1}{2}\right)} \\
&= -\frac{1}{\hbar\omega_i}\frac{1}{Z_i}\frac{\partial}{\partial\beta}\left[\sum_{n_i\in\mathbb{N}} e^{-\beta\hbar\omega_i\left(n_i+\frac{1}{2}\right)}\right] - \frac{1}{Z_i}\frac{1}{2}\sum_{n_i\in\mathbb{N}} e^{-\beta\hbar\omega_i\left(n_i+\frac{1}{2}\right)} \\
&= -\frac{1}{\hbar\omega_i}\frac{\partial}{\partial\beta}\ln Z_i - \frac{1}{2}\,.
\end{aligned} \tag{16.21}$$

Using

$$Z_i = e^{-\frac{1}{2}\beta\hbar\omega_i} \sum_{n_i\in\mathbb{N}} \left(e^{-\beta\hbar\omega_i}\right)^{n_i} = \frac{e^{-\frac{1}{2}\beta\hbar\omega_i}}{1-e^{-\beta\hbar\omega_i}} \tag{16.22}$$

and thus

$$\frac{\partial}{\partial\beta}\ln Z_i = \frac{\partial}{\partial\beta}\left(-\frac{1}{2}\beta\hbar\omega_i - \ln\left(1-e^{-\beta\hbar\omega_i}\right)\right) = -\frac{\hbar\omega_i}{2} - \hbar\omega_i\frac{e^{-\beta\hbar\omega_i}}{1-e^{-\beta\hbar\omega_i}} = -\frac{\hbar\omega_i}{2} + \frac{\hbar\omega_i}{1-e^{\beta\hbar\omega_i}}\,. \tag{16.23}$$

From this we can conclude that

$$\frac{1}{Z_i}\sum_{n_i\in\mathbb{N}} n_i e^{-\beta\epsilon_{n,i}} = -\frac{1}{1-e^{\beta\hbar\omega_i}} \tag{16.24}$$

and therefore we find for the correlation function (16.20) using $\frac{1}{e^{\beta\hbar\omega_i}-1} = \frac{1}{2}\left[\coth\left(\frac{\beta\hbar\omega_i}{2}\right)-1\right]$:

$$\begin{aligned} C_{ij}(-\tau) &= \delta_{ij}\frac{\hbar g_i^2}{2\mu\omega_i}\left(e^{-i\omega_i\tau} - 2\cos(\omega_i\tau)\frac{1}{1-e^{\beta\hbar\omega_i}}\right) \\ &= \delta_{ij}\frac{\hbar g_i^2}{2\mu\omega_i}\left(-i\sin(\omega_i\tau) + \cos(\omega_i\tau)\coth\left(\frac{\beta\hbar\omega_i}{2}\right)\right)\,, \end{aligned} \tag{16.25}$$

and we can see that $C_{ji}(\tau) = C_{ij}^*(-\tau)$. From these explicit expressions, we can now also give the specific expressions for $\Lambda(t-t_0)$ and $\Gamma(t-t_0)$ that were defined in (16.8) and (16.9):

$$\Lambda(t-t_0) = \int_0^{t-t_0} d\tau \sum_{i=1}^{N}\frac{\hbar g_i^2}{2\mu\omega_i}\sin(\omega_i\tau) \tag{16.26}$$

$$\Gamma(t-t_0) = 2\int_0^{t-t_0} d\tau \sum_{i=1}^{N}\frac{\hbar g_i^2}{2\mu\omega_i}\cos(\omega_i\tau)\coth\left(\frac{\beta\hbar\omega_i}{2}\right)\,. \tag{16.27}$$

In order to evaluate these further, one usually introduces a so-called spectral density that characterises the strength with which different frequencies in the environment contribute to the interaction with the matter system. To compute things, this spectral density is then picked as a continuous function resembling the continuum limit of the oscillators in the environment. This will be discussed in detail in the next subsection.

16.3. Spectral density

Parts of the content of this subsection were already published in [3]. Here, they are presented with some modifications compared to [3] to adapt them to the flow of the thesis and extended with further content.

Next, we introduce a spectral density

$$J(\omega) = \sum_{i=1}^{N}\frac{\hbar g_i^2}{2\mu\omega_i}\delta(\omega-\omega_i)\,, \tag{16.28}$$

where $\delta(.)$ denotes the Dirac delta function and $J(\omega)$ has dimension of time. With this, the two coefficient functions $\Lambda(t-t_0)$ and $\Gamma(t-t_0)$ that appear in the master equation can be reexpressed

as

$$\Lambda(t-t_0) = \int_0^{t-t_0} d\tau \int_0^\infty d\omega\ J(\omega)\sin(\omega\tau) \tag{16.29}$$

$$\Gamma(t-t_0) = 2\int_0^{t-t_0} d\tau \int_0^\infty d\omega\ J(\omega)\cos(\omega\tau)\coth\left(\frac{\beta\hbar\omega}{2}\right). \tag{16.30}$$

Given that not all the oscillators in the environment are neither known in detail, nor of interest, one often approximates $J(\omega)$ by a smooth function in ω, see e.g. [45]. The usual requirements for this function are that it is linear in ω for small ω and that it tends to zero for large ω. Note that such a spectral density is also chosen, for example, in the Caldeira-Leggett model for quantum Brownian motion, and the linear dependence is crucial in this case to obtain the friction term present in that model after renormalisation. These spectral densities with such a linear behavior are usually called Ohmic spectral densities. Many models used in the existing literature [45, 47, 112] use an Ohmic spectral density and differ only by the chosen cutoff function, see for instance also [197] for an application of the Drude regularisation. Note that a different than linear behaviour for small ω would for the model considered here lead to IR divergences for all ω^m with $m \leq 0$, $m \in \mathbb{Z}$ and partly also to a rather not physically reasonable scaling with the inverse temperature parameter Θ in the decoherence term. The latter corresponds to a strong decoherence effect when the temperature is low that becomes infinite for $\Theta = 0$, that is when the Gibbs state corresponds to a vacuum state. For $m \geq 2$ with $m \in \mathbb{N}$ there exist no decoherence effects in the model considered in this work. At the end of this section we show that building on the field theoretical model from part II and III, linearity in ω for small ω is reasonable, while a cutoff for larger ω corresponds to the UV-divergences in field theory that also have to be renormalised there.

Since the choice of a particular spectral density is an assumption that goes into every model, we are interested in how the final result of the master equation depends on this choice. Therefore, we considered a few choices in this work that also include the most prominent ones used in the existing literature like the Lorentz-Drude and the exponential cutoff. These are shown below:

$$\text{Lorentz-Drude cutoff: } J(\omega) = \frac{2}{\pi}\eta^2\omega\frac{\Omega^2}{\Omega^2+\omega^2} \tag{16.31}$$

$$\text{Quartic cutoff: } J(\omega) = \frac{2}{\pi}\eta^2\omega\frac{(2\Omega)^4}{((2\Omega)^2+\omega^2)^2} \tag{16.32}$$

$$\text{Exponential cutoff: } J(\omega) = \frac{2}{\pi}\eta^2\omega e^{-\frac{2\omega}{\pi\Omega}} \tag{16.33}$$

$$\text{Gaussian cutoff: } J(\omega) = \frac{2}{\pi}\eta^2\omega e^{-\frac{\omega^2}{\pi\Omega^2}}. \tag{16.34}$$

In these functions, η^2 is a free parameter whose role we will discuss further below and Ω is a cutoff frequency used as regulator for the otherwise divergent integrals. Evaluating the $\int d\omega$ integral in (16.29) and (16.30) yields the integrands $I_\Lambda(\tau)$ and $I_\Gamma(\tau)$ defined as

$$\Lambda(t-t_0) = \int_0^{t-t_0} d\tau\ I_\Lambda(\tau) \tag{16.35}$$

$$\Gamma(t-t_0) = 2\int_0^{t-t_0} d\tau\ I_\Gamma(\tau). \tag{16.36}$$

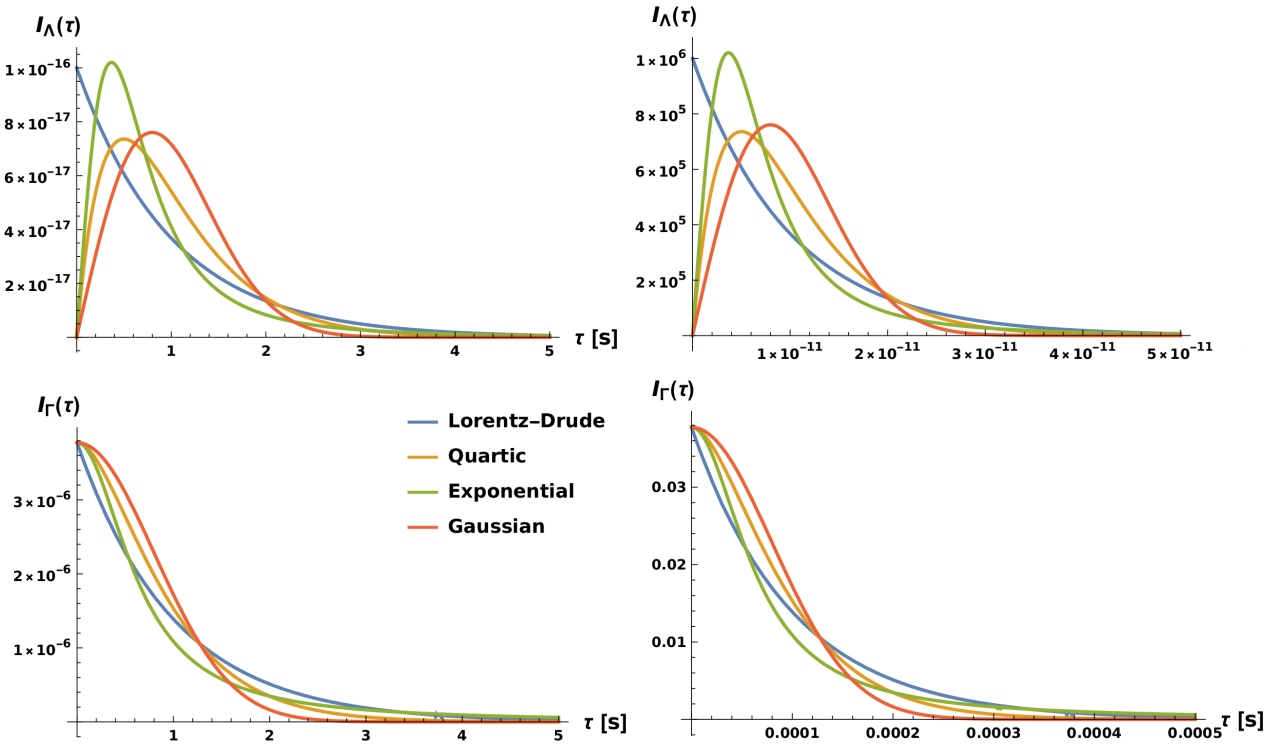

Figure 4: Integrands $I_\Lambda(\tau)$ (first row) and $I_\Gamma(\tau)$ (second row) defined in (16.35) and (16.36) for the different cutoff functions and with parameter values $\eta = 10^{-8}$ s, $\Theta = 0.9K$ and $\Omega = 1Hz$ (first column), $\Omega = 100GHz$ (second column, first row) and $\Omega = 10KHz$ (second column, second row). *This plot was originally published in [3].*

A plot of these functions is shown in figure 4.

Before we apply the Markov approximation in the next section, we want to discuss how reasonable the choice of a spectral density like the ones discussed in this section is, based on the field theoretical model presented in part II and III of this thesis. To motivate such a choice of spectral density, in particular the linear dependence on ω for small ω, we compare the quantum mechanical model with the field theoretical one in part II, where for simplicity we drop all indices in the latter. In the field theoretical case, the role of the configuration variable is taken over by the densitised triad $\widehat{\delta E}$ and the canonically conjugated momentum is $\widehat{\delta C}$, which is a combination of the connection and the densitised triad. Their quantisation is introduced in equations (8.7) and (8.8). To obtain the same commutation relations and environmental Hamiltonian as for the quantum mechanical model discussed in this part of the thesis, we redefine $\widehat{\widetilde{\delta E}} := \sqrt{\kappa}\widehat{\delta E}$ and $\widehat{\widetilde{\delta C}} := \sqrt{\kappa}\widehat{\delta C}$, where $\kappa = \frac{8\pi G_N}{c^4}$ is the coupling constant in general relativity, containing Newton's gravitational constant G_N and the speed of light c. The reason for this redefinition is the fact that their original algebra (see equation (8.4)) contains a factor κ^{-1}. In terms of these rescaled

variables we obtain (see also equations (8.4) and (8.3)):

$$\left[\widehat{\widetilde{\delta E}}, \widehat{\widetilde{\delta C}}\right] = i\hbar\delta \qquad\qquad \hat{H}_E = \frac{1}{2}\int d^3k \left[\widehat{\widetilde{\delta C}}(\vec{k})^2 + \Omega_k^2 \widehat{\widetilde{\delta E}}(\vec{k})^2\right], \tag{16.37}$$

where the frequencies are defined as $\Omega_k := \sqrt{\vec{k}^2}$ and δ represents the Dirac and Kronecker deltas relating the arguments and labels of $\widehat{\widetilde{\delta E}}$ and $\widehat{\widetilde{\delta C}}$ which we suppress here for better readability. In the interaction Hamiltonian (see equation (6.41) and below), one then couples the energy momentum tensor to the metric, which corresponds to contractions of $\widehat{\widetilde{\delta E}}$, hence

$$\hat{H}_I \sim \int d^3k \frac{\sqrt{\kappa}}{2} \hat{T} \otimes \widehat{\widetilde{\delta E}}\,, \tag{16.38}$$

where $\sim$ means "corresponds to". From this analogue one can deduce $g_i \sim \sqrt{\kappa}$. When computing correlation functions and hence Λ and Γ, the terms appearing are of the form (see equations (8.7) and (9.3)), introducing a function $h(\vec{k})$ that contains all remaining detailed contributions:

$$\int d^3k \frac{\kappa}{2\Omega_k} h(\vec{k}) \tag{16.39}$$

compared to the expressions appearing here in (16.29) and (16.30) using (16.28):

$$\hbar^2 \sum_{i=1}^{N} \frac{g_i^2}{2\mu\omega_i} h(\omega_i)\,. \tag{16.40}$$

Assuming for simplicity that $h(\vec{k}) = h(\Omega_k)$, we can rewrite the integration in (16.39) in spherical coordinates:

$$\int d^3k \frac{\kappa}{2\Omega_k} h(\Omega_k) = \int_0^\infty d\Omega\; 2\pi\kappa\Omega h(\Omega)\,. \tag{16.41}$$

Motivated by this analogue, we take the following continuum limit for the quantum mechanical model:

$$\hbar^2 \sum_{i=1}^{N} \frac{g_i^2}{2\mu\omega_i} h(\omega_i) \longrightarrow \hbar^2 \int_0^\infty d\omega\; 2\pi\kappa\omega h(\omega)\,. \tag{16.42}$$

This suggests to use as spectral density $J(\omega)$, which appears in integrals as $\int d\omega J(\omega) f(\omega)$, the following smooth function:

$$J(\omega) = \hbar^2 \sum_{i=1}^{N} \frac{g_i^2}{2\mu\omega_i} \delta(\omega - \omega_i) \longrightarrow \frac{2\pi\kappa\hbar}{c}\omega\,, \tag{16.43}$$

where we inserted additional inverse factors of $\hbar$ and c to obtain the correct dimensions, as the work in part II and III is in natural units. To cure UV-divergence, we have to add a suitable cutoff, see the discussion above. From this comparison, it is not possible to read off the precise numerical prefactors. We will do this below in section 17.4 by using the ultra-relativistic form of the one-particle projection of the field theoretical master equation from section 13.3.

16.4. Markov approximation

The content of the introduction of this subsection was already published in [3]. Here, it is presented with some modifications compared to [3] to adapt it to the flow of the thesis.
Equipped with the different spectral densities, we now want to investigate if for the present model a Markov approximation is applicable. As discussed below in Figure 8 in section 17.2, for thermal gravitational waves a reasonable cutoff frequency is $\Omega = 100GHz$. Hence, in the case of $I_\Lambda(\tau)$, the integrand decays rapidly on timescales of $\tau = 10^{-10}s$ which is much smaller than the timescale on which the core system varies, that is determined for the neutrinos investigated in this part of the thesis by $\left(\frac{1}{\hbar}\frac{\Delta m^2}{2E}\right)^{-1}$, which[34] is around the order of magnitude of $1s$. Furthermore, the plots for $I_\Gamma(\tau)$ suggest that $\Gamma(t-t_0)$ is independent of Ω for $t-t_0$ sufficiently large enough, as the two axes scale inversely to each other with the same ratio. Already for $\Omega = 10KHz$, where $I_\Gamma(\tau)$ is numerically still well computable, the timescale on which $I_\Gamma(\tau)$ decays is much lower than the one on which the system state varies. This means that the environment rapidly "forgets" about the history of the system and thus the Markovian approximation for a memoryless process is justified. Therefore, in both cases the error committed when shifting the initial time $t_0 \to -\infty$ and hence the upper integration limit of the τ integration to $+\infty$ is negligible. Given that, we perform the Markov approximation for the further analysis. In what follows, we present the calculation of Λ and Γ in the Markov limit using two different spectral densities.

16.4.1. Markov limit using a Lorentz-Drude cutoff

With the Lorentz-Drude cutoff form of the spectral density we find in the Markov approximation

$$\Lambda := \lim_{t_0\to-\infty} \Lambda(t-t_0) = \frac{2}{\pi}\eta^2 \int_0^\infty d\tau \int_0^\infty d\omega\, \omega \frac{\Omega^2}{\Omega^2+\omega^2}\sin(\omega\tau) \tag{16.44}$$

$$\Gamma := \lim_{t_0\to-\infty} \Gamma(t-t_0) = \frac{4}{\pi}\eta^2 \int_0^\infty d\tau \int_0^\infty d\omega\, \omega \frac{\Omega^2}{\Omega^2+\omega^2}\cos(\omega\tau)\coth\left(\frac{\beta\hbar\omega}{2}\right). \tag{16.45}$$

We use this spectral density here as it is often used in the literature. The way in which it is usually applied is to switch the order of the τ and ω integration because then the calculation is simplified. Let us do this for a moment and afterwards perform the integrals again in the correct order to show that we obtain the same results. When switching the order of the integrals, we can use

$$\int_0^\infty d\tau\, e^{-i\omega\tau} = \pi\delta(\omega) - PV\left(\frac{i}{\omega}\right), \tag{16.46}$$

where PV denotes the Cauchy principal value. From this follows that

$$\int_0^\infty d\tau\, \sin(\omega\tau) = PV\left(\frac{1}{\omega}\right) \qquad \text{and} \qquad \int_0^\infty d\tau\, \cos(\omega\tau) = \pi\delta(\omega). \tag{16.47}$$

With this we obtain

$$\Lambda = \frac{2}{\pi}\eta^2 \int_0^\infty d\omega\, \frac{\Omega^2}{\Omega^2+\omega^2} = \Omega\eta^2 \tag{16.48}$$

$$\Gamma = 2\eta^2\left[\omega\coth\left(\frac{\beta\hbar\omega}{2}\right)\right]_{\omega=0} = \frac{4\eta^2}{\beta\hbar} = \frac{4\eta^2 k_B\Theta}{\hbar}. \tag{16.49}$$

[34] As the dominant contribution to the neutrino evolution comes from the part $e^{\frac{i}{\hbar}\frac{\Delta m^2}{2E}t}$ and the matter effects have a similar order of magnitude.

In the first line, we have dropped the principal value as the expression is unproblematic at $\omega = 0$. In the second line, we have included a factor of $\frac{1}{2}$ as the contributing point $\omega = 0$ lies at the border of the integration area and we have used l'Hospital's theorem to obtain the value at $\omega = 0$ in the second step. We hence obtain a linear dependence of Λ on the cutoff Ω and a linear dependence of Γ on the temperature parameter Θ.
To check this result, we now perform the same calculation without switching the order of the integrations. We start with Λ:

$$\Lambda = \frac{2}{\pi}\eta^2 \int_0^\infty d\tau \int_0^\infty d\omega\, \omega \frac{\Omega^2}{\Omega^2+\omega^2} \sin(\omega\tau) = \frac{\eta^2}{i\pi} \int_0^\infty d\tau \int_{-\infty}^\infty d\omega\, \omega \frac{\Omega^2}{\Omega^2+\omega^2} e^{i\omega\tau}\,. \tag{16.50}$$

Next, we apply the residue theorem for the ω integration closing the contour in a semicircle in the upper half-plane (for $\tau > 0$) or the lower half-plane (for $\tau < 0$). The poles of the integrand lie at $\omega = \pm i\Omega$ and thus for any τ there will be one pole included. One then obtains

$$\begin{aligned}\Lambda &= \frac{\eta^2}{i\pi} \int_0^\infty d\tau \left\{ 2\pi i \Theta(\tau) \left[\frac{\omega\Omega^2}{\omega + i\Omega} e^{i\omega\tau} \right]_{\omega = i\Omega} - 2\pi i \Theta(-\tau) \left[\frac{\omega\Omega^2}{\omega - i\Omega} e^{i\omega\tau} \right]_{\omega = -i\Omega} \right\} \\ &= \eta^2\Omega^2 \int_0^\infty d\tau\, e^{-\Omega|\tau|} \mathrm{sgn}(\tau) = \eta^2\Omega^2 \int_0^\infty d\tau\, e^{-\Omega\tau} = \Omega\eta^2\,,\end{aligned} \tag{16.51}$$

which coincides with the result from above. For Γ, using the expansion of the hyperbolic cotangent in terms of Matsubara frequencies:

$$\coth\left(\frac{\beta\hbar\omega}{2}\right) = \frac{2}{\hbar\beta} \sum_{n=-\infty}^{\infty} \frac{\omega}{\omega^2 + \nu_n^2} \qquad \text{with the Matsubara frequencies } \nu_n = \frac{2\pi n}{\hbar\beta}\,, \tag{16.52}$$

we find the following expression:

$$\begin{aligned}\Gamma &= \frac{4}{\pi}\eta^2 \int_0^\infty d\tau \int_0^\infty d\omega\, \omega \frac{\Omega^2}{\Omega^2+\omega^2} \cos(\omega\tau) \coth\left(\frac{\beta\hbar\omega}{2}\right) \\ &= \frac{4}{\pi\hbar\beta}\eta^2 \int_0^\infty d\tau \int_{-\infty}^\infty d\omega \sum_{n=-\infty}^{\infty} \frac{\Omega^2}{\Omega^2+\omega^2} \frac{\omega^2}{\omega^2+\nu_n^2} e^{i\omega\tau}\,.\end{aligned} \tag{16.53}$$

To continue, we switch the order of the sum and the ω-integration to apply once again the residue theorem. This switch is not necessarily well-defined. As it is extensively used in the literature, we perform it here as well, but will investigate it in detail when using the quartic cutoff in the next section. Then we have

$$\begin{aligned}\Gamma &= \frac{4}{\pi\hbar\beta}\eta^2 \int_0^\infty d\tau \int_{-\infty}^\infty d\omega \sum_{n=-\infty}^{\infty} \frac{\Omega^2}{\Omega^2+\omega^2} \frac{\omega^2}{\omega^2+\nu_n^2} e^{i\omega\tau} \\ &= \frac{8}{\pi\hbar\beta}\eta^2 \int_0^\infty d\tau \sum_{n=1}^{\infty} \int_{-\infty}^\infty d\omega\, \frac{\Omega^2}{\Omega^2+\omega^2} \frac{\omega^2}{\omega^2+\nu_n^2} e^{i\omega\tau} + \frac{4}{\pi\hbar\beta}\eta^2 \int_0^\infty d\tau \int_{-\infty}^\infty d\omega\, \frac{\Omega^2}{\Omega^2+\omega^2} e^{i\omega\tau}\,.\end{aligned} \tag{16.54}$$

For the residue theorem, we again close the path in a semi-circle in the upper or lower half-plane, depending on whether τ is positive or negative. In the first term, there are four poles: In

addition to the two also present in the second term, $\omega = \pm i\Omega$, we also have poles at $\omega = \pm i|\nu_n|$. Application of the residue theorem then yields for the first term

$$\begin{aligned}
&\frac{8\eta^2}{\pi\hbar\beta} 2\pi i\Omega^2 \int_0^\infty d\tau\, \mathrm{sgn}(\tau) \sum_{n=1}^\infty \left\{ \frac{-\mathrm{sgn}(\tau)\Omega^2}{2i\Omega(\nu_n^2-\Omega^2)} e^{-\mathrm{sgn}(\tau)\Omega\tau} + \frac{-\mathrm{sgn}(\tau)\nu_n^2}{2i|\nu_n|(\Omega^2-\nu_n^2)} e^{-\mathrm{sgn}(\tau)|\nu_n|\tau} \right\} \\
&= \frac{8\eta^2\Omega^2}{\hbar\beta} \int_0^\infty d\tau \sum_{n=1}^\infty \frac{\Omega e^{-\Omega|\tau|} - |\nu_n| e^{-|\nu_n||\tau|}}{\Omega^2-\nu_n^2} = \frac{8\eta^2\Omega^2}{\hbar\beta} \lim_{T\to\infty} \sum_{n=1}^\infty \int_0^T d\tau\, \frac{\Omega e^{-\Omega\tau} - |\nu_n| e^{-|\nu_n|\tau}}{\Omega^2-\nu_n^2} \\
&= \frac{8\eta^2\Omega^2}{\hbar\beta} \lim_{T\to\infty} \sum_{n=1}^\infty \frac{-e^{-\Omega T} + e^{-|\nu_n|T}}{\Omega^2-\nu_n^2}\,. \qquad (16.55)
\end{aligned}$$

For the second term in (16.54) we find

$$\frac{4}{\pi\hbar\beta}\eta^2 \int_0^\infty d\tau\, 2\pi i \frac{\Omega^2}{2i\Omega} e^{-\Omega|\tau|} = \frac{4\eta^2}{\hbar\beta}\,. \qquad (16.56)$$

Combining both terms we have that

$$\Gamma = \frac{8\eta^2\Omega^2}{\hbar\beta} \lim_{T\to\infty} \sum_{n=1}^\infty \frac{-e^{-\Omega T} + e^{-|\nu_n|T}}{\Omega^2-\nu_n^2} + \frac{4\eta^2}{\hbar\beta}\,. \qquad (16.57)$$

The second term already contains the Markov limit, for the first one we can see that, if we switch the order of the limit and the sum (which is not necessarily justified, more on that in the following section), this expression vanishes, so in total we get

$$\Gamma = \frac{4\eta^2}{\hbar\beta} = \frac{4\eta^2 k_B\Theta}{\hbar} \qquad (16.58)$$

and therefor also the same result as in the case above. When working with the Markov limit, a similar derivation using the Lorentz-Drude spectral density is often found in the literature. As it is evident from the derivation presented here, it involves two steps which might be problematic because they consist in the switching of two limits. To get a clean version of the application of the Markov approximation, we present the approximation for the model under consideration using the quartic cutoff form of the spectral density in the next section and proving with it that the problematic steps are mathematically well-defined for it. The results we obtain are equal to the ones obtained here with the Lorentz-Drude cutoff.

16.4.2. Markov limit using a quartic cutoff

In this section we again apply the Markov approximation to determine the two quantities Λ and Γ that appear in the master equation. To solve the problem of interchanging limits that arose in the previous section when using the Lorentz-Drude cutoff, we present here proofs using the quartic cutoff to show that for this choice of cutoff the switch of limits is justified and confirm the results obtained in the previous section. For Λ we did not encounter any issues, so we follow the same path as before and have in Markov approximation using the quartic cutoff:

$$\Lambda = \frac{32}{\pi}\eta^2 \int_0^\infty d\tau \int_0^\infty d\omega\, \omega \frac{\Omega^4}{(4\Omega^2+\omega^2)^2} \sin(\omega\tau) = \frac{16}{\pi i}\eta^2 \int_0^\infty d\tau \int_{-\infty}^\infty d\omega\, \omega \frac{\Omega^4}{(4\Omega^2+\omega^2)^2} e^{i\omega\tau}\,. \qquad (16.59)$$

Now we can apply the residue theorem. We have two poles of second order at $\omega = \pm 2i\Omega$ and close the contour depending on the sign of τ with a semi-circle in the upper ($\tau > 0$) or the lower ($\tau < 0$) half-plane. The pole contributions turn out to be

$$\pm 2\pi i \frac{d}{d\omega}\left[\frac{\omega\Omega^4}{(\omega \pm 2i\Omega)^2} e^{i\omega\tau}\right]_{\omega=\pm 2i\Omega} = \pm\frac{\pi i}{4}\tau\Omega^3 e^{\mp 2\Omega\tau}\,. \tag{16.60}$$

With this we find

$$\Lambda = 4\eta^2\Omega^3 \int_0^\infty d\tau\ |\tau| e^{-2\Omega|\tau|} = 4\eta^2\Omega^3 \int_0^\infty d\tau\ \tau e^{-2\Omega\tau} = \Omega\eta^2\,, \tag{16.61}$$

which coincides with the expression found using the Lorentz-Drude cutoff in (16.51). This also explains the different prefactors of Ω in the definition of the different spectral densities in equations (16.31)-(16.34): they were chosen such that all Λ coincide no matter which spectral density is picked, as the cutoff Ω was introduced arbitrarily and should not have any physical relevance, see discussion below at the end of section 16.6.
Next we continue with Γ for which we have with the quartic cutoff:

$$\begin{aligned}
\Gamma =& \frac{64}{\pi}\eta^2 \int_0^\infty d\tau \int_0^\infty d\omega\ \omega \frac{\Omega^4}{(4\Omega^2+\omega^2)^2} \cos(\omega\tau) \coth\left(\frac{\beta\hbar\omega}{2}\right) \\
=& \frac{64}{\pi\hbar\beta}\eta^2 \int_0^\infty d\tau \int_{-\infty}^\infty d\omega \sum_{n=-\infty}^{\infty} \frac{\omega^2}{\omega^2+\nu_n^2} \frac{\Omega^4}{(4\Omega^2+\omega^2)^2} e^{i\omega\tau} \\
=& \frac{64}{\pi\hbar\beta}\eta^2 \int_0^\infty d\tau \int_{-\infty}^\infty d\omega\ \frac{\Omega^4}{(4\Omega^2+\omega^2)^2} e^{i\omega\tau} \\
&+ \frac{128}{\pi\hbar\beta}\eta^2 \int_0^\infty d\tau \int_{-\infty}^\infty d\omega \sum_{n=1}^{\infty} \frac{\omega^2}{\omega^2+\nu_n^2} \frac{\Omega^4}{(4\Omega^2+\omega^2)^2} e^{i\omega\tau}\,.
\end{aligned} \tag{16.62}$$

Now we can apply the residue theorem directly to the first term and obtain, using that we have poles of second order at $\omega = \pm 2i\Omega$ and that we can close the contour with a semi-circle in the upper half-plane for $\tau > 0$ and in the lower half-plane for $\tau < 0$:

$$\int_{-\infty}^\infty d\omega\ \frac{\Omega^4}{(4\Omega^2+\omega^2)^2} e^{i\omega\tau} = \pm 2\pi i \frac{d}{d\omega}\left[\frac{\Omega^4}{(\omega \pm 2i\Omega)^2} e^{i\omega\tau}\right]_{\omega=\pm 2i\Omega} = \frac{\pi\Omega}{16} e^{-2\Omega|\tau|}(1 + 2\Omega|\tau|)\,. \tag{16.63}$$

To solve the second term in (16.62), we would like to follow a similar procedure. For this, we however have to switch the order of the sum over n and the integration over ω. This corresponds to switching the order of two limits. To prove that this is a well-defined operation here, we use the theorem of Lebesgue (dominated convergence theorem). The term we have to investigate for this is

$$\int_{-\infty}^\infty d\omega \sum_{n=1}^{\infty} \frac{\omega^2}{\omega^2+\nu_n^2} \frac{\Omega^4}{(4\Omega^2+\omega^2)^2} e^{i\omega\tau} = 2\int_0^\infty d\omega \sum_{n=1}^{\infty} \cos(\omega\tau) \frac{\omega^2\Omega^4}{(\omega^2+\nu_n^2)(\omega^2+4\Omega^2)^2}\,. \tag{16.64}$$

Let

$$F(\omega) := \sum_{n=1}^{\infty} \frac{\omega^2\Omega^4}{(\omega^2+\nu_n^2)(\omega^2+4\Omega^2)^2} \qquad f_N(\omega) := \sum_{n=1}^{N} \cos(\omega\tau) \frac{\omega^2\Omega^4}{(\omega^2+\nu_n^2)(\omega^2+4\Omega^2)^2} \tag{16.65}$$

which implies

$$\lim_{N\to\infty} f_N(\omega) = f(\omega) := \sum_{n=1}^{\infty} \cos(\omega\tau) \frac{\omega^2\Omega^4}{(\omega^2+\nu_n^2)(\omega^2+4\Omega^2)^2}\,. \tag{16.66}$$

As every summand in $F(\omega)$ is non-negative, we have that

$$|f_N(\omega)| \leq \sum_{n=1}^{N} \frac{\omega^2\Omega^4}{(\omega^2+\nu_n^2)(\omega^2+4\Omega^2)^2} \leq F(\omega)\,. \tag{16.67}$$

Using the definition of the hyperbolic cotangent, we obtain

$$\begin{aligned} F(\omega) &= \frac{1}{2}\sum_{n=-\infty}^{\infty} \frac{\omega^2\Omega^4}{(\omega^2+\nu_n^2)(\omega^2+4\Omega^2)^2} - \frac{\Omega^4}{2(\omega^2+4\Omega^2)^2} \\ &= \frac{\hbar\beta}{4}\coth\left(\frac{\beta\hbar\omega}{2}\right)\frac{\omega\Omega^4}{(\omega^2+4\Omega^2)^2} - \frac{\Omega^4}{2(\omega^2+4\Omega^2)^2}\,, \end{aligned} \tag{16.68}$$

from which we find that, using the triangle inequality in the first step:

$$\int_0^\infty d\omega |F(\omega)| \leq \frac{\hbar\beta}{4}\int_0^\infty d\omega\ \coth\left(\frac{\beta\hbar\omega}{2}\right)\frac{\omega\Omega^4}{(\omega^2+4\Omega^2)^2} + \underbrace{\int_0^\infty d\omega\ \frac{\Omega^4}{2(\omega^2+4\Omega^2)^2}}_{=\frac{\pi\Omega}{64}}\,. \tag{16.69}$$

For the first term we can see that due to its finite value at $\omega = 0$ and the fact that it has no singularities on the positive real axis, the integration over a finite interval will give a finite value $\omega \in (0,\xi)$, so we can use, picking $\xi > \frac{2}{\sqrt{3}}\Omega$ such that $\frac{\omega\Omega^4}{(\omega^2+4\Omega^2)^2}$ is decreasing for $\omega \in (\xi,\infty)$:

$$\begin{aligned} \int_0^\infty d\omega |F(\omega)| \leq& \frac{\hbar\beta}{4}\int_0^\xi d\omega\ \coth\left(\frac{\beta\hbar\omega}{2}\right)\frac{\omega\Omega^4}{(\omega^2+4\Omega^2)^2} \\ &+ \frac{\hbar\beta}{4}\int_\xi^\infty d\omega\ \coth\left(\frac{\beta\hbar\omega}{2}\right)\frac{\omega\Omega^4}{(\omega^2+4\Omega^2)^2} + \frac{\pi\Omega}{64} \\ \leq& \text{finite} + \frac{\hbar\beta}{4}\int_\xi^\infty d\omega\ \coth\left(\frac{\beta\hbar\omega}{2}\right)\frac{\omega\Omega^4}{(\omega^2+4\Omega^2)^2} \\ \leq& \text{finite} + \frac{\hbar\beta}{4}\coth\left(\frac{\beta\hbar\xi}{2}\right)\int_\xi^\infty d\omega\ \frac{\omega\Omega^4}{(\omega^2+4\Omega^2)^2} \\ =& \text{finite} + \frac{\hbar\beta}{4}\coth\left(\frac{\beta\hbar\xi}{2}\right)\frac{\Omega^4}{2\xi^2+8\Omega^2} < \infty \end{aligned} \tag{16.70}$$

and hence

$$F(\omega) \in L^1([0,\infty])\,. \tag{16.71}$$

Given that, we can apply the dominated convergence theorem and obtain

$$2\int_0^\infty d\omega\ \sum_{n=1}^{\infty} \cos(\omega\tau)\frac{\omega^2\Omega^4}{(\omega^2+\nu_n^2)(\omega^2+4\Omega^2)^2} = 2\int_0^\infty d\omega\ f(\omega) = 2\lim_{N\to\infty}\int_0^\infty d\omega\ f_N(\omega)\,, \tag{16.72}$$

hence we can indeed switch the order of the Matsubara sum and the ω integration in the term of the last line of equation (16.62). With this we obtain

$$\Gamma = \frac{64}{\pi\hbar\beta}\eta^2 \int_0^\infty d\tau\ \frac{\pi\Omega}{16} e^{-2\Omega\tau}(1+2\Omega\tau) + \frac{128}{\pi\hbar\beta}\eta^2 \int_0^\infty d\tau\ \sum_{n=1}^\infty \int_{-\infty}^\infty d\omega\ \frac{\omega^2}{\omega^2+\nu_n^2}\frac{\Omega^4}{(4\Omega^2+\omega^2)^2} e^{i\omega\tau}\,. \tag{16.73}$$

The residue theorem is now readily applied to the second term with first-order poles at $\omega = \pm i|\nu_n|$ as well as second-order poles at $\omega = \pm 2i\Omega$. This yields for $\mathrm{sgn}(\tau) \gtrless 0$, closing the contour with a semi-circle in the upper/lower half-plane:

$$\begin{aligned}
&\int_{-\infty}^\infty d\omega\ \frac{\omega^2}{\omega^2+\nu_n^2}\frac{\Omega^4}{(4\Omega^2+\omega^2)^2} e^{i\omega\tau} \\
&= \pm 2\pi i \left[e^{i\omega\tau} \frac{\omega^2\Omega^4}{(\omega \pm i|\nu_n|)(\omega^2+4\Omega^2)^2} \right]_{\omega=\pm i|\nu_n|} \pm 2\pi i \frac{d}{d\omega} \left[e^{i\omega\tau} \frac{\omega^2\Omega^4}{(\omega^2+\nu_n^2)(\omega\pm 2i\Omega)^2} \right]_{\omega=\pm 2i\Omega} \\
&= -\pi e^{-|\nu_n||\tau|} \frac{|\nu_n|\Omega^4}{(4\Omega^2-\nu_n^2)^2} + \frac{\pi\Omega^3}{4} e^{-2\Omega|\tau|} \frac{\nu_n^2(1-2\Omega|\tau|)+4\Omega^2(1+2\Omega|\tau|)}{(\nu_n^2-4\Omega^2)^2}\,.
\end{aligned} \tag{16.74}$$

Thus we find

$$\begin{aligned}
\Gamma =& \frac{64}{\pi\hbar\beta}\eta^2 \int_0^\infty d\tau\ \frac{\pi\Omega}{16} e^{-2\Omega\tau}(1+2\Omega\tau) - \frac{128}{\hbar\beta}\eta^2 \int_0^\infty d\tau\ \sum_{n=1}^\infty e^{-|\nu_n||\tau|} \frac{|\nu_n|\Omega^4}{(4\Omega^2-\nu_n^2)^2} \\
&+ \frac{32\Omega^3}{\hbar\beta}\eta^2 \int_0^\infty d\tau\ e^{-2\Omega|\tau|} \sum_{n=1}^\infty \frac{\nu_n^2(1-2\Omega|\tau|)+4\Omega^2(1+2\Omega|\tau|)}{(\nu_n^2-4\Omega^2)^2}\,.
\end{aligned} \tag{16.75}$$

Using

$$\begin{aligned}
&\sum_{n=1}^\infty \frac{2\Omega|\tau|(4\Omega^2-\nu_n^2)}{(4\Omega^2-\nu_n^2)^2} = |\tau| \sum_{n=1}^\infty \frac{2\Omega}{4\Omega^2-\nu_n^2} = \frac{|\tau|}{2} \sum_{n=-\infty}^\infty \frac{2\Omega}{4\Omega^2-\nu_n^2} - \frac{|\tau|}{4\Omega} = \frac{\hbar\beta|\tau|}{4}\cot(\beta\hbar\Omega) - \frac{|\tau|}{4\Omega}\,, \\
&\sum_{n=1}^\infty \frac{(4\Omega^2+\nu_n^2)}{(4\Omega^2-\nu_n^2)^2} = -\frac{1}{8\Omega^2} + \frac{\hbar^2\beta^2}{8}\csc^2(\beta\hbar\Omega)\,,
\end{aligned} \tag{16.76}$$

where $\csc(x) = \frac{1}{\sin(x)}$, we can simplify Γ:

$$\begin{aligned}
\Gamma =& \frac{64}{\pi\hbar\beta}\eta^2 \int_0^\infty d\tau\ \frac{\pi\Omega}{16} e^{-2\Omega\tau}(1+2\Omega\tau) - \frac{128}{\hbar\beta}\eta^2 \int_0^\infty d\tau\ \sum_{n=1}^\infty e^{-|\nu_n||\tau|} \frac{|\nu_n|\Omega^4}{(4\Omega^2-\nu_n^2)^2} \\
&+ \frac{32\Omega^3}{\hbar\beta}\eta^2 \int_0^\infty d\tau\ e^{-2\Omega|\tau|} \left[\frac{\hbar\beta|\tau|}{4}\cot(\beta\hbar\Omega) - \frac{|\tau|}{4\Omega} - \frac{1}{8\Omega^2} + \frac{\hbar^2\beta^2}{8}\csc^2(\beta\hbar\Omega) \right] \\
=& \frac{4\eta^2}{\hbar\beta} - \frac{128}{\hbar\beta}\eta^2 \int_0^\infty d\tau\ \sum_{n=1}^\infty e^{-|\nu_n||\tau|} \frac{|\nu_n|\Omega^4}{(4\Omega^2-\nu_n^2)^2} \\
&+ \frac{32\Omega^3}{\hbar\beta}\eta^2 \left[\frac{\hbar\beta}{16\Omega^2}\cot(\beta\hbar\Omega) - \frac{1}{16\Omega^3} - \frac{1}{16\Omega^3} + \frac{\hbar^2\beta^2}{16\Omega}\csc^2(\beta\hbar\Omega) \right] \\
=& \frac{4\eta^2}{\hbar\beta} - \frac{128}{\hbar\beta}\eta^2 \int_0^\infty d\tau\ \sum_{n=1}^\infty e^{-|\nu_n||\tau|} \frac{|\nu_n|\Omega^4}{(4\Omega^2-\nu_n^2)^2} + 2\eta^2\Omega\cot(\beta\hbar\Omega) - \frac{4\eta^2}{\hbar\beta} + 2\hbar\beta\Omega^2\eta^2\csc^2(\beta\hbar\Omega)\,.
\end{aligned} \tag{16.77}$$

The remaining sum yields the Hurwitz-Lerch transcendent for which the evaluation of the time integration is difficult. To circumvent this, we apply Lebesgue's theorem of dominated convergence once again to show that we can perform the time integration before evaluating the sum. We focus on the case $\tau \geq 0$ and we also have that $\nu_n \geq 0$. Let

$$\widetilde{F}(\tau) := \sum_{n=1}^{\infty} \underbrace{e^{-\frac{2\pi}{\hbar\beta}\tau} \frac{\nu_n \Omega^4}{(4\Omega^2 - \nu_n^2)^2}}_{\geq 0} = -e^{-\frac{2\pi}{\hbar\beta}\tau} \frac{\Omega^3 \hbar^2 \beta^2}{32\pi^2} \left[\psi^{(1)}\left(1 + \frac{\Omega\hbar\beta}{\pi}\right) - \psi^{(1)}\left(1 - \frac{\Omega\hbar\beta}{\pi}\right) \right], \tag{16.78}$$

where $\psi^{(1)}(x)$ denotes the first derivative of the digamma function. It is finite as long as its argument is not equal to a non-positive integer, in particular for $\frac{\Omega\hbar\beta}{\pi}$ not being a positive integer. As we can pick the cutoff frequency Ω arbitrarily and it will drop out of physical predictions later, we can assume this to be true. Now setting

$$\widetilde{f}_N(\tau) := \sum_{n=1}^{N} e^{-|\nu_n||\tau|} \frac{|\nu_n| \Omega^4}{(4\Omega^2 - \nu_n^2)^2} \tag{16.79}$$

$$\widetilde{f}(\tau) := \sum_{n=1}^{\infty} e^{-|\nu_n||\tau|} \frac{|\nu_n| \Omega^4}{(4\Omega^2 - \nu_n^2)^2}, \tag{16.80}$$

we have that

$$\lim_{N\to\infty} \widetilde{f}_N(\tau) = \widetilde{f}(\tau) \qquad \text{and} \qquad |f_N(\tau)| \leq \widetilde{F}(\tau). \tag{16.81}$$

Combined with

$$\int_0^{\infty} d\tau \, |\widetilde{F}(\tau)| = \frac{\Omega^3 \hbar^3 \beta^3}{64\pi^3} \left| \psi^{(1)}\left(1 + \frac{\Omega\hbar\beta}{\pi}\right) - \psi^{(1)}\left(1 - \frac{\Omega\hbar\beta}{\pi}\right) \right| < \infty \tag{16.82}$$

we can once again apply the theorem of dominated convergence to solve the remaining time integration in (16.77):

$$\begin{aligned}
&-\frac{128}{\hbar\beta}\eta^2 \int_0^{\infty} d\tau \sum_{n=1}^{\infty} e^{-|\nu_n||\tau|} \frac{|\nu_n|\Omega^4}{(4\Omega^2 - \nu_n^2)^2} = -\frac{128}{\hbar\beta}\eta^2 \sum_{n=1}^{\infty} \int_0^{\infty} d\tau \, e^{-|\nu_n|\tau} \frac{|\nu_n|\Omega^4}{(4\Omega^2 - \nu_n^2)^2} \\
&= -\frac{128}{\hbar\beta}\eta^2 \sum_{n=1}^{\infty} \frac{\Omega^4}{(4\Omega^2 - \nu_n^2)^2} = -\frac{128}{\hbar\beta}\eta^2 \left[-\frac{1}{32} + \frac{\Omega\hbar\beta}{64} \cot(\beta\hbar\Omega) + \frac{\Omega^2\beta^2\hbar^2}{64} \csc^2(\beta\hbar\Omega) \right] \\
&= \frac{4\eta^2}{\hbar\beta} - 2\Omega\eta^2 \cot(\beta\hbar\Omega) - 2\Omega^2\eta^2\hbar\beta \csc^2(\beta\hbar\Omega).
\end{aligned} \tag{16.83}$$

Using this in (16.77) yields the final result for Γ with the quartic cutoff and proofs of all the intermediate steps:

$$\Gamma = \frac{4\eta^2}{\hbar\beta} = \frac{4\eta^2 k_B \Theta}{\hbar}, \tag{16.84}$$

which indeed coincides with the value found using the Lorentz-Drude cutoff in the previous section.

16.5. Renormalisation and Lindblad equation

Parts of the content of this subsection were already published in [3] and [2]. Here, they are presented with some modifications compared to [3] and [2] to adapt them to the flow of the thesis and extended with further content and calculations.

From the discussion in the previous section we have obtained the master equation (16.11) in the Markovian limit:

$$\begin{aligned}\frac{d}{dt}\hat{\rho}_S(t) = &-\frac{i}{\hbar}\left[\hat{H}_S, \hat{\rho}_S(t)\right] + \frac{i\Omega\eta^2}{\hbar^2}\left[\left(\hat{H}_S^{(0)}\right)^2, \hat{\rho}_S(t)\right] \\ &+ \frac{4\eta^2}{\hbar^2}\frac{k_B\Theta}{\hbar}\left(\hat{H}_S^{(0)}\hat{\rho}_S(t)\hat{H}_S^{(0)} - \frac{1}{2}\left\{\left(\hat{H}_S^{(0)}\right)^2, \hat{\rho}_S(t)\right\}\right) . \end{aligned} \tag{16.85}$$

As expected, Γ is independent of Ω. When introducing any of the above named spectral densities, the corresponding counter term is the same for all choices of the cutoff in the spectral density and given by, using here in the intermediate step the Lorentz-Drude cutoff:

$$\hat{H}_S^{(C)} = \frac{1}{\hbar}\int_0^\infty d\omega \frac{J(\omega)}{\omega}(\hat{H}_S^{(0)})^2 = \frac{1}{\hbar}\frac{2\eta^2}{\pi}\int_0^\infty d\omega \frac{\Omega^2}{\Omega^2+\omega^2}(\hat{H}_S^{(0)})^2 = \frac{\Omega\eta^2}{\hbar}(\hat{H}_S^{(0)})^2 , \tag{16.86}$$

which precisely cancels the Lamb-shift contribution in the second order TCL master equation in Markovian limit yielding:

$$\frac{d}{dt}\hat{\rho}_S(t) = -\frac{i}{\hbar}\left[\hat{H}_S^{(0)}, \hat{\rho}_S(t)\right] + \frac{4\eta^2}{\hbar^2}\frac{k_B\Theta}{\hbar}\left(\hat{H}_S^{(0)}\hat{\rho}_S(t)\hat{H}_S^{(0)} - \frac{1}{2}\left\{(\hat{H}_S^{(0)})^2, \hat{\rho}_S(t)\right\}\right) . \tag{16.87}$$

This master equation includes still two free parameters, η which is related to the coupling parameter between the system and the environment, and the environmental temperature parameter Θ that enters via $\beta = \frac{1}{k_B\Theta}$ in the Gibbs state, where k_B denotes the Boltzmann constant.

In order to compare the master equation (16.87) better to the existing phenomenological models later, we note that (16.87) can be written in Lindblad form

$$\frac{d}{dt}\hat{\rho}_S(t) = -\frac{i}{\hbar}\left[\hat{H}_S^{(0)}, \hat{\rho}_S(t)\right] + \frac{4\eta^2}{\hbar^2}\frac{k_B\Theta}{\hbar}\left(\hat{L}\hat{\rho}_S(t)\hat{L}^\dagger - \frac{1}{2}\left\{\hat{L}^\dagger\hat{L}, \hat{\rho}_S(t)\right\}\right) . \tag{16.88}$$

with the choice of the Lindblad operator $\hat{L} = \hat{H}_S^{(0)}$ using that $\hat{H}_S^{(0)}$ is self-adjoint, that is $\hat{L}^\dagger = \hat{L}$ and thus $\hat{L}^\dagger\hat{L} = \hat{L}^2$. For instance [198] also chooses a Lindblad operator proportional to the Hamiltonian of the system for a decoherence model inspired by discrete quantum gravity. In many phenomenological models, the Lindblad equation is taken as the starting point, often omitting the second term containing the contributions of the Lamb shift as well as a counter term. Then the model is characterised by a selection of Lindblad operators $\hat{L}_i$, of which there can generally be more than one, usually chosen to be either linear with the position and/or momentum operators of the matter system such that they can be written linearly in annihilation and creation operators, see for instance [45] for the standard examples or [199] for a non-perturbative treatment of multi-time expectation values in open quantum systems for specific environments. The advantage of starting with a microscopic model as in (16.2) is that, for example, the functions $\Lambda(t-t_0)$ and $\Gamma(t-t_0)$ can be derived and calculated directly, resulting in a model with less ambiguities at the level of the Lindblad equation. Furthermore, the choice of the Lindblad

operator, following the field theoretical models [1, 60–63], is directly linked to the property of how linearised gravity couples to matter, and therefore in this sense is also determined by the microscopic model. We discuss in the application to neutrino oscillations a comparison between the renormalised and non-renormalised model in section 17.2. It is worth noting that for the special case of zero temperature $\Theta = 0$, in which the Gibbs state is only the vacuum state and thus the gravitational environment is assumed to be in a vacuum state, no decoherence effects are present, since in the model presented here the dissipator is linear in Θ. Note that this is a property of the gravitational environment and independent of the chosen system under consideration and will thus also apply to the case of neutrinos in the next section.

Before we continue with this application to neutrinos, we would like to discuss and compare the renormalisation applied for this quantum mechanical model to the one for the one-particle projection of the field theoretical model in section 11. The quantum mechanical master equation in the present section consists of a dissipator term and a Lamb-shift, where the latter contained divergences and was finally removed by the renormalisation. The form of the coupling in the quantum mechanical model in equation (16.2) implies that the coefficients Λ of the Lamb-shift and Γ of the dissipator in the final Lindblad equation only depend on the environment. From their form before the Markov approximation in equations (16.29) and (16.30) it becomes evident that the Lamb-shift term is independent of the temperature parameter Θ. Thus the Lamb-shift contribution only encodes vacuum effects, while the prefactor Γ of the dissipator depends on Θ and yields a non-vanishing contribution for $\Theta = 0$. The counter term then removed the Lamb-shift contribution completely, as it depends on the unphysical cutoff frequency Ω, while the prefactor of the dissipator is not altered, as here the dependency on Ω vanishes after the Markov approximation.

Next, let us discuss to what extent it is possible to connect the renormalisation and its effects of the one-particle master equation presented above in section 11 with the renormalisation applied in the quantum mechanical toy model. For this purpose first we discuss the two forms of the original full field theoretical master equation derived in part II of this thesis. The first form is given in equation (9.30):

$$\begin{aligned}\frac{\partial}{\partial t}\rho_S(t) = &- i\left[H_S + \kappa\, U, \rho_S(t)\right] \\ &- \frac{\kappa}{2}\int_0^t ds \sum_r \int_{\mathbb{R}^3} d^3k \left\{ iD(\vec{k}, t-s)\left[J_r(\vec{k}), \left\{J_r(-\vec{k}, s-t), \rho_S(t)\right\}\right]\right. \\ &\left. + D_1(\vec{k}, t-s)\left[J_r(\vec{k}), \left[J_r(-\vec{k}, s-t), \rho_S(t)\right]\right]\right\},\end{aligned} \tag{16.89}$$

where D and D_1 are two coefficients defined in equation (9.28) and (9.29) that arise from combinations of the environmental correlation functions similar to Λ and Γ in the quantum mechanical model. They read:

$$D(\vec{k}, t-s) := -\frac{\sin(\Omega_k(t-s))}{\Omega_k} \tag{16.90}$$

$$D_1(\vec{k}, t-s) := \coth\left(\frac{\beta\Omega_k}{2}\right)\frac{\cos(\Omega_k(t-s))}{\Omega_k}\,. \tag{16.91}$$

The operators $J_r(\vec{k},t)$ and $J_r(\vec{k}) := J_r(\vec{k},0)$ were defined in equation (8.19) and contain a combination of two creation and/or annihilation operators of the scalar field along with their time evolution. As a first difference to the master equation for the quantum mechanical model it turns out that the term proportional to D in (16.89) cannot be written as a simple commutator, as it is the case with the Lamb-shift contribution in the quantum mechanical toy model. If the system operator J were to commute with the system Hamiltonian, then this would be possible, which is precisely the case in the quantum mechanical toy model. Then this would imply that the Lamb-shift is independent of the temperature parameter Θ and therefore a pure vacuum effect.
For the field theoretical model, a similar form where one has a Lamb-shift contribution and a dissipator is the one given when using the dissipator in the form of equation (9.46). Here, the coefficients of the Lamb-shift term are S_{ab} and the prefactors of the dissipator are R_{ab}. From their definitions in (9.44) and (9.45) one can see that in general they have a different form as Λ and Γ in (16.29) and (16.30) above and the Lamb-shift for the field theoretical model includes vacuum as well as thermal contributions. A similar result is obtained in [45], where quantum electrodynamics is discussed from the point of view of open quantum systems with the standard interaction Hamiltonian of QED. There, the resulting Lamb-shift Hamiltonian is therefore split into a vacuum part, denoted as Lamb-shift and a thermal part, denoted as Stark-shift.
As discussed above, we would expect that if in the field theoretical model the system operator in the interaction Hamiltonian commutes with the system Hamiltonian, that we can then recover the form of the quantum mechanical model. Indeed, if we had $[J, H_S] = 0$, then the phases $e^{\pm i\omega_a(\vec{k},\vec{p})t}$ and $e^{\pm i\omega_b(\vec{k},\vec{l})t}$ coming from the time evolution of the J operators would vanish in the definitions of S_{ab} and R_{ab} in (9.44) and (9.45). This allows the remaining terms to be combined into a form similar to Λ and Γ. In particular the thermal contribution of the Lamb-shift would vanish, as it is the case in the quantum mechanical toy model.
Let us now compare the renormalisations of the two models: in the quantum mechanical model, the effect of the renormalisation is to remove the Lamb-shift Hamiltonian which only consisted of a vacuum part. The renormalisation applied in the one-particle projection of the field theoretical master equation in section 11 removes the vacuum parts in the Lamb-shift Hamiltonian and the dissipator. The thermal part of the Lamb-shift Hamiltonian however remains. From the discussion of the open QED model from [45], one would expect a similar result in a quantum mechanical model where a thermal contribution in the Lamb-shift is present. The dissipator of the quantum mechanical model is left unmodified by the renormalisation, in particular the vacuum contribution is present there. This is in contrast to the procedure for the one-particle projection, where the renormalisation removes all vacuum terms, also the ones from the dissipator, see in particular the discussion in section 11.5. In the quantum mechanical toy model, these contributions were however removed at a later stage when the Markov approximation was applied and hence also not present in the final Lindblad equation (16.88).

16.6. Solution of the master equation for neutrino oscillations

The content of this subsection was already published in [3]. Here, it is presented with some modifications compared to [3] to adapt it to the flow of the thesis.
In this section, we evaluate and solve the master equation (16.87) for neutrinos with three different flavors as the matter system. To adapt the model to neutrinos, we choose the following

Hamiltonian operator for the system:

$$\hat{H}_S^{(0)} = \hat{H}_{vac} + \hat{U}^\dagger \hat{H}_{mat} \hat{U}, \tag{16.92}$$

where the second term takes into account that the neutrinos propagates through the (different layers of the) Earth. This Hamiltonian contains the neutrino Hamiltonian in vacuum in the mass basis given as

$$\hat{H}_{vac} = \begin{pmatrix} E_1 & 0 & 0 \\ 0 & E_2 & 0 \\ 0 & 0 & E_3 \end{pmatrix} = E\mathbb{1}_3 + \frac{c^4}{6E} \begin{pmatrix} -\Delta m_{21}^2 - \Delta m_{31}^2 & 0 & 0 \\ 0 & \Delta m_{21}^2 - \Delta m_{32}^2 & 0 \\ 0 & 0 & \Delta m_{31}^2 + \Delta m_{32}^2 \end{pmatrix}, \tag{16.93}$$

where we used that $E_i \approx E + \frac{m_i^2 c^4}{2E}$ and that we can modify the Hamiltonian by a constant matrix such that the difference $(E_i - E_j)$ is not modified because in the final equation only powers of the energy difference will contribute. Here the mass differences squared are denoted by $\Delta m_{ij}^2 = m_i^2 - m_j^2$, the mean neutrino energy by $E = \frac{1}{3}(E_1 + E_2 + E_3)$ and the PMNS matrix by $\hat{U}$. The matter contribution, that takes into account the electron density of the Earth, is given as discussed in section 14.2.3 by

$$\hat{H}_{mat} = \pm\sqrt{2} G_f N_e \begin{pmatrix} 1 & 0 & 0 \\ 0 & 0 & 0 \\ 0 & 0 & 0 \end{pmatrix}, \tag{16.94}$$

where the sign depends on whether neutrinos $(+)$ or antineutrinos $(-)$ are involved, G_f is the Fermi coupling constant and N_e the electron density in the considered layer of the Earth.
Due to the different orders of magnitude of E compared to $\frac{\Delta m_{ij}^2 c^4}{6E}$, working with $\hat{H}_{vac}$ as specified in (16.93) requires very high numerical precision and hence high computational effort. To simplify the computation, one can proceed as follows: Splitting $\hat{H}_S^{(0)}$ into two parts in the following way:

$$\hat{H}_S^{(0)} = E\mathbb{1}_3 + \hat{H}_S^{(\Delta)}, \tag{16.95}$$

the characteristic polynomial reads:

$$\det\left(\hat{H}_S^{(0)} - \lambda\mathbb{1}_3\right) = \det\left(\hat{H}_S^{(\Delta)} - \lambda^{(\Delta)}\mathbb{1}_3\right) = 0, \tag{16.96}$$

where $\lambda^{(\Delta)} = \lambda - E$ are the eigenvalues of $\hat{H}_S^{(\Delta)}$. For the eigenvectors $v^{(\Delta)}$ of $\hat{H}_S^{(\Delta)}$ we find:

$$\hat{H}_S^{(\Delta)} v^{(\Delta)} = \lambda^{(\Delta)} v^{(\Delta)} \iff \hat{H}_S^{(0)} v^{(\Delta)} - E v^{(\Delta)} = \lambda v^{(\Delta)} - E v^{(\Delta)} \iff \hat{H}_S^{(0)} v^{(\Delta)} = \lambda v^{(\Delta)}, \tag{16.97}$$

thus $\hat{H}_S^{(0)}$ and $\hat{H}_S^{(\Delta)}$ have the same eigenvectors. Hence, one can work with $\hat{H}_S^{(\Delta)}$ and its eigenvectors throughout the calculation and just has to use in the final results in for instance (16.106) that $\widetilde{H}_i = \lambda_{S,i}^{(\Delta)} + E$, where $\lambda_{S,i}^{(\Delta)}$ are the eigenvalues of $\hat{H}_S^{(\Delta)}$. As the evolution of the neutrino in the end only depends on terms of the form $\left(\widetilde{H}_i - \widetilde{H}_j\right)$, the mean neutrino energy E will always cancel.
In the literature, often different forms of $\hat{H}_{vac}$ are used that differ from the one presented here by the addition of a constant matrix in mass basis such that energy differences agree for all

choices[35]. As it has been just discussed, such a constant shift in energy yields the same result as long as the final solution of the master equation only depends on energy differences $(E_i - E_j)$ or powers thereof because constant terms that agree for all i and j, such as for instance the mean neutrino energy E, are just canceled in the difference. While the equation (16.92) is formulated in terms of the vacuum mass basis, to solve the master equation it is advantageous to work in the effective mass basis in which $\hat{H}_S^{(0)}$ is diagonal. This basis always changes when N_e changes, i.e. when we consider different layers of the Earth. We denote all quantities in the effective mass basis with a tilde and the transformation matrix from flavour to effective mass basis by $\hat{\tilde{V}}$. If we define the diagonal matrix of the system in the effective mass basis $\hat{\tilde{H}}_S := \hat{\tilde{V}}^\dagger \hat{U} \hat{H}_S^{(0)} \hat{U}^\dagger \hat{\tilde{V}}$, the master equation in terms of the effective mass basis can be written as

$$\frac{d}{dt}\hat{\tilde{\rho}}_S(t) = -\frac{i}{\hbar}\left[\hat{\tilde{H}}_S, \hat{\tilde{\rho}}_S(t)\right] + \frac{4\eta^2}{\hbar^2}\frac{k_B\Theta}{\hbar}\left(\hat{\tilde{H}}_S\hat{\tilde{\rho}}_S(t)\hat{\tilde{H}}_S - \frac{1}{2}\left\{\hat{\tilde{H}}_S^2, \hat{\tilde{\rho}}_S(t)\right\}\right). \tag{16.99}$$

As we have already seen from (16.88), the dissipator involves second powers of the system's Hamiltonian and it is linear in the temperature parameter Θ of the gravitational environment. A consequence of the second property is that there is no decoherence effect at a temperature of zero, e.g. when the environment is in a vacuum state.
Now we solve the master equation (16.99) in effective mass basis. To make the derivation of a solution structurally better accessible, we rewrite the master equation in the following form:

$$\frac{d}{dt}\rho(t) = -\frac{i}{\hbar}\left[H, \rho(t)\right] + l\left(H\rho(t)H - \frac{1}{2}\left\{H^2, \rho(t)\right\}\right) \tag{16.100}$$

with the scalar prefactor $l = \frac{4\eta^2}{\hbar^2}\frac{k_B T}{\hbar}$. For better readability, we dropped all hats and tildes and indices, also for $H := \hat{\tilde{H}}_S$. To solve this equation, we consider the three summands individually. As all operators that appear apart from the density matrix commute and are time-independent, we can solve the master equation for each summand individually and then combine the solutions.

- For the first summand we find:

$$\frac{d}{dt}\rho^{(1)}(t) = -\frac{i}{\hbar}\left[H, \rho^{(1)}(t)\right] \quad \Longrightarrow \quad \rho^{(1)}(t) = e^{-\frac{i}{\hbar}Ht}\rho^{(1)}(0)e^{\frac{i}{\hbar}Ht}. \tag{16.101}$$

- The third summand yields:

$$\frac{d}{dt}\rho^{(2)}(t) = -\frac{l}{2}\left\{H^2, \rho^{(2)}(t)\right\} \quad \Longrightarrow \quad \rho^{(2)}(t) = e^{-\frac{l}{2}H^2t}\rho^{(2)}(0)e^{-\frac{l}{2}H^2t}. \tag{16.102}$$

- For the second summand we obtain:

$$\frac{d}{dt}\rho^{(3)}(t) = l \cdot H\rho^{(3)}(t)H \quad \Longrightarrow \quad \rho^{(3)}(t) = \sum_{n=0}^{\infty}\frac{(lt)^n}{n!}H^n\rho^{(3)}(0)H^n. \tag{16.103}$$

[35] See for instance [86, 87, 106] where this is used to work with a matrix in which one of the diagonal elements is zero:

$$\hat{H}_{vac} = \frac{c^4}{2E}\begin{pmatrix} 0 & 0 & 0 \\ 0 & \Delta m_{21}^2 & 0 \\ 0 & 0 & \Delta m_{31}^2 \end{pmatrix} \tag{16.98}$$

Combining these in a suitable form, the total solution then reads:

$$\begin{aligned}\rho(t) &= \sum_{n=0}^{\infty} \frac{(lt)^n}{n!} H^n e^{-\frac{i}{\hbar}Ht - \frac{l}{2}H^2 t} \rho(0) e^{\frac{i}{\hbar}Ht - \frac{l}{2}H^2 t} H^n \\ &=: \sum_{n=0}^{\infty} \frac{(lt)^n}{n!} H^n F \rho(0) F^\dagger H^n \,, \end{aligned} \tag{16.104}$$

where we defined $F := e^{-\frac{i}{\hbar}Ht - \frac{l}{2}H^2 t}$. Since F and H^n are diagonal in the effective mass basis, we can evaluate the matrix product directly and obtain:

$$\rho_{ij}(t) = \sum_{n=0}^{N} \frac{(lt)^n}{n!} \rho_{ij}(0) F_i F_j^* H_i^n H_j^n = \rho_{ij}(0) F_i F_j^* e^{l H_i H_j t} \,, \tag{16.105}$$

where a star denotes complex conjugation and we refer to the components of the diagonal matrices as $F_i := F_{ii}$ and $H_i := H_{ii}$. Reinserting the original expressions, this yields the solution:

$$\widetilde{\rho}_{ij}(t) = \widetilde{\rho}_{ij}(0) \cdot e^{-\frac{i}{\hbar}\left(\widetilde{H}_i - \widetilde{H}_j\right)t - \frac{2\eta^2}{\hbar^2}\frac{k_B \Theta}{\hbar}\left(\widetilde{H}_i - \widetilde{H}_j\right)^2 t} \,, \tag{16.106}$$

where $\widetilde{\rho}_{ij}(t)$ denotes the matrix elements of $\hat{\widetilde{\rho}}_S(t)$ and $\widetilde{H}_i$ denotes the elements of the diagonal matrix $\hat{\widetilde{H}}_S$. As expected from the form of the dissipator, the decoherence term is quadratic in the difference of the energy eigenvalues $(\tilde{H}_i - \tilde{H}_j)^2$. In flavour basis we explicitly obtain

$$\rho_{ij}(t) = \rho_{mn}(0) \widetilde{V}_{km}^\dagger \widetilde{V}_{nl} \widetilde{V}_{ik} \widetilde{V}_{lj}^\dagger e^{-\frac{i}{\hbar}\left(\widetilde{H}_k - \widetilde{H}_l\right)t - \frac{2\eta^2 k_B \Theta}{\hbar^3}\left(\widetilde{H}_k - \widetilde{H}_l\right)^2 t} \tag{16.107}$$

where $\widetilde{V}_{ij}$ denote the matrix elements of $\hat{\widetilde{V}}$. The first term corresponds to the standard oscillation term which is non-vanishing for $\Delta m_{ij}^2 \neq 0$. The second terms is the additional contribution due to coupling to the gravitational environment. Note, that as discussed above due to the counter term that we introduced in (16.86) the final solution does not involve a Lamb shift contribution and is thus independent of the cutoff frequency.

A model that also included a Lamb shift contribution is the one in [85] where due to such a contribution the model allows neutrino oscillations to be present even if the initial mass difference vanishes. Although it is not directly obvious from the parameter in which the authors in [85] encode the Lamb shift contribution (denoted as ω_3 in (3.1) in [85]), to our understanding the final value of this parameter depends on a choice of test function that needs to be introduced to regularise an otherwise infinite integral (see (A.14) in [85]). Although the derivation in [85] starts with a field theory setup, as far as we understand the derivation, carried over to the toy model presented here, such a test function would correspond to the cutoff frequency because the final value of ω_3 will in general depend on the chosen test function. Thus, it looks like they obtain a shift in the neutrino energy eigenvalues that still depends on some regulator and we would expect that similar to what happens here in the toy model and in the field theoretical models in part III of this thesis as well as in [1, 60–63] a suitable renormalisation procedure needs to be applied to obtain a cutoff independent effect. Such an effect might be potentially non-vanishing for the model in [85] in contrast to our case since they use a different coupling to the environment but this needs to be checked carefully. In addition, even if we consider the non-renormalised version of the model presented in this part of the thesis, no massless neutrino oscillations will be allowed

by the model. The reason for this is that in the model considered here the Lamb shift contribution cannot be chosen independently of the differences of the squared neutrino masses Δm_{ij}^2 due to the fact that the neutrino energy couples to the environment, whereas in our understanding this is not the case in [85] demonstrating again that physical properties of the existing models crucially depend on the coupling to the environment. To demonstrate that working with a model where no renormalisation has been applied and the Lamb shift contribution is taken as a real physical contribution, we refer to figure 8 in section 17.2 where the toy model with and without a Lamb shift contribution is compared and thus is shown that if this non-physical effect is not removed, one might draw incorrect physical conclusions.

Let us further comment on the work in [195], where the model from [112] is also considered in a two-neutrino scenario, but the conclusion is drawn that no decoherence effects occur for this model when they apply the equal-energy condition. In contrast, the results in the earlier work in [200], where a similar contribution in the decoherence terms was obtained for the special case of vacuum oscillations, as well as our results show decoherence effects where both models apply the equal-momentum condition in the quantum mechanical context using plane waves, see section 14.2.2 for details.
The use of the equal-energy condition in the paper in [195] is to our understanding motivated by the wave packet approach, where the derivation of the probabilities for neutrino oscillations includes an average over the detection time, see section 14.2.1. For standard neutrino oscillations without decoherence effects caused by some coupling to the environment, such an average over the detection time leads to a delta function that is compatible with the application of the equal-energy condition. Since the derivation of our master equation in this section is done using plane waves, the model discussed in this part of the thesis does not include decoherence effects caused by considering wave packets instead of plane waves, and we apply the equal-momentum condition to the model. A complete generalisation of the model presented in this part of the thesis within the wave packet approach is beyond the scope of this work. However, from the derivation with plane waves, we can already see that the average over the detection time becomes more subtle when decoherence effects due to coupling with an environment are present, as mentioned in section 14.2.1. Firstly, the expression for the probability of neutrino oscillations in the presence of decoherence effects includes an additional exponential time-dependent damping term. Therefore, the integrand relevant to the average over the detection time changes and thus the result is no longer simply a delta function. Since the average over the detection time is usually performed as an integral from $-\infty$ to $+\infty$, the exponential decay for negative values of the time coordinate appears problematic, as also discussed in [195]. As discussed in [201], an interesting question is whether there is a symmetry of time reversibility in open quantum systems. For the Lindblad equation, they show in [201] that it can be extended to the negative real time axis if the absolute value for the time coordinate in the dissipator term is taken into account. This has two effects: First, in this case the average over the detection time can be formed, and second, the relevant integral for the kind of models considered here and in [195] can be solved analytically, leading to a Lorentz function instead of a delta function. Thus, if decoherence effects are present in the wave packet approach, the argument with the delta function motivating the use of the equal-energy condition cannot be transferred exactly from the situation in which no decoherence effects are present to the situation in which decoherence effects are involved. Furthermore, the exact shape of the Lorentz function depends on the particular decoherence model, and thus the final result of the average over the detection time as well.

17. Quantum mechanical and field theoretical model applied to neutrino oscillations

The content of this section was already published in [3] and [2]. Here, it is presented with some modifications compared to [3] and [2] to adapt it to the flow of the thesis.
Quantum decoherence in the neutrino sector has been investigated with long baseline neutrino detectors [88], such as MINOS+T2K [89], the future DUNE [90] and reactor experiments such as Daya Bay, RENO and the future JUNO [91], where the treatment of neutrino oscillations can be well approximated by the vacuum amplitudes, and neutrino telescopes such as IceCube [92, 105] and KM3NeT [93], where matter effects play a relevant role. All such analyses are based on a class of phenomenological quantum decoherence (PQD) models that can vary by the power with which the mean neutrino energy enters into the decoherence term as well as the number of non-vanishing decoherence parameters, see section 15. In order to interpret the PQD model in terms of the microscopic gravitationally induced quantum decoherence model (GQD) presented in this work, and in order to see the differences among them, we investigate their behavior in different situations. In the following, we first present a short summary of the main results and then discuss them in detail in sections 17.1-17.3. To connect to the field theoretical model from part II and III of this thesis, we also apply the ultra-relativistic form of the one-particle projected master equation from section 13.3 to a neutrino and compare the results with the quantum mechanical model from this part of the thesis in section 17.4.

The model considered in this part of the thesis has the property that only squared differences of neutrino energies enter into the contribution responsible for decoherence. It will be shown that one of the consequences is that the model considered here is only compatible with a subclass of phenomenological models with an energy dependence E^{-2}, which directly follows from gravitationally induced decoherence that suggest a specific coupling between the neutrinos and the environment inspired by general relativity and linearised gravity respectively. That one does not obtain an energy dependence of E^n for $n > 0$ is caused by the fact that for this coupling only the squared energy differences are involved in the decoherence contribution and those scale with E^{-2} in the case of neutrinos. Furthermore, the corresponding decoherence parameters in the phenomenological models cannot be chosen independently from Δm^2_{ij}. The latter means that setting some of the decoherence parameters involved to zero or equal to each other leads to inconsistencies in the model if it is not assumed at the same time that these Δm^2_{ij} vanish or are identical, respectively.

Additionally, our results show that in the vacuum case we can obtain an exact match between the aforementioned subclass of the $n = -2$ PQD models and the GQD model presented here if we choose the decoherence parameters involved in the PQD model appropriately. One might conclude that it should be possible to already set bounds to our free parameters η, which is related to the coupling constant in the interaction Hamiltonian, and the temperature parameter Θ of the gravitational waves, based on current upper limits of the PQD γ_{ij} parameters. However, all the present analyses [88, 89, 93] make some assumptions while fitting the data, such as setting one of the $\gamma_{ij} = 0$ or two of them equal to each other, which are not compatible with the model considered here. It follows that it is not possible to directly constrain η and Θ from current bounds on γ_{ij}.

Interestingly, in the non-vacuum case such a match with the specific subclass of PQD models cannot be achieved with those phenomenological models that assume constant decoherence parameters in each layer of the Earth, as many models do, due to the fact that in the model presented here these parameters do vary. As a consequence, we obtain deviations in the oscillation probabilities in matter that can become large enough in the GeV energy regime to be resolved by neutrino telescopes, such as KM3NeT/ORCA [202]. There exist models that also take matter effects in the decoherence parameters into account, see for instance [87, 94], it is however discussed below that it is also not straight forward to match the model considered here with those. All oscillation probability plots presented in this section are evaluated for neutrinos propagating through the Earth, hence considering the non-negligible matter effects. Specifically, the oscillograms have been made with the public tool *OscProb* [203], where a new class modelling the GQD presented here has been developed by the authors of [3]. For the Earth density profile, the PREM model with 425 layers has been used [204].

17.1. Comparison to existing phenomenological models

The content of this subsection was already published in [3]. Here, it is presented with some modifications compared to [3] to adapt it to the flow of the thesis. The numerical calculations and the plots were created by one of the coauthors of [3] other than the author of this thesis. They are included in this thesis, as they improve the analysis of the results of the model.
In several works, such as in [96, 100, 103–105], a phenomenological model based on a Lindblad equation is used to model decoherence in neutrino oscillations with a solution of the form

$$\widetilde{\rho}_{ij}(t) = \widetilde{\rho}_{ij}(0) \cdot e^{-\frac{i}{\hbar}\left(\widetilde{H}_i - \widetilde{H}_j\right)t - \Gamma_{ij}t}\,, \tag{17.1}$$

where Γ_{ij} is usually parameterised as

$$\Gamma_{ij} = \gamma_{ij} E^n\,, \tag{17.2}$$

see section 15 for details. In vacuum, the model presented in this work can be related to this class of phenomenological models by identifying

$$\gamma_{ij} = \frac{\eta^2 c^8 k_B \Theta}{2\hbar^3}(\Delta m^2_{ij})^2 \quad \text{and} \quad n = -2, \tag{17.3}$$

where k_B denotes the Boltzmann constant. Hence, the quantum mechanical model considered in this part of the thesis has the property that the γ_{ij} are related to the square of the squared mass differences Δm^2_{ij}. The only two free parameters left in γ_{ij} are η, that encodes the strength of the coupling of the neutrinos to the gravitational environment, and Θ, which is the temperature of the environment of thermal gravitational waves. If one considers cosmological models in which the usual inflationary epoch is preceded by a radiation-dominated era, a thermal gravitational wave background can be produced in the early universe. In these models, it is assumed that the thermal gravitons decouple at a temperature of the order of the Planck temperature and exhibit a black-body spectrum [205, 206]. As the universe expands, the black-body spectrum of the gravitons is maintained, but the temperature is strongly red-shifted. The estimates for the temperature of the thermal gravitational wave background in the present epoch are $\Theta \simeq 0.9K$, see [207], and thus below the temperature of the cosmic microwave background of $\Theta \simeq 2.72K$.

Furthermore, because the energy eigenvalues always involve the combination $\Delta m_{ij}^2/E$, this model suggests that the decoherence parameters depend inversely on the squared mean neutrino energy. This dependence stems from the form of the interaction Hamiltonian which was motivated by the way in which gravity couples to matter according to general relativity. Compared to the phenomenological models, the approach presented here has the advantage that, if we assume that we obtain a value of the temperature parameter of thermal gravitational waves from other experiments, the Γ_{ij} only depend on one free parameter η. In order to constrain the free γ_{ij} parameters, in some phenomenological models, as for instance in [88, 93, 104], additional requirements are included where some of the γ_{ij} are set to zero or equal to each other. These limits then result each in one single free parameter γ. However, from (17.3) it can be seen that such choices correspond to either setting some of the Δm_{ij}^2 equal to zero or equal to each other, which stands in contradiction to experiments. In addition to that, the physical interpretation of this parameter is harder to access compared to the situation where the underlying microscopic model is known.

In matter, those phenomenological models that assume constant decoherence parameters γ_{ij} cannot be matched by specific choices of parameters to the model derived here. The reason for this is that while in the phenomenological models γ_{ij} is fixed at a certain value independently of the matter density, in the model presented in this part of the thesis, the decoherence parameter depends on $(\widetilde{H}_i - \widetilde{H}_j)$, which are the energy values of the neutrino that depend on the matter density and thus the different layers in the Earth. In the microscopic model, matter effects are included directly via its coupling to the environment. This dependence is caused by the fact that in matter the vacuum Hamiltonian is extended by the additional operator $\hat{H}_{mat}$ which depends on the electron density N_e in the considered matter layer, see (16.92), and thus the final Hamiltonian and therefore also the decoherence parameter changes in each layer. This leads to the conclusion that the model presented here takes the effect of the different Earth layers into account in the coupling to the environment and can thus not be formulated with a single value for γ_{ij} as it is done for the phenomenological models in (17.2). This is shown in Figure 5, where a discrepancy between PQD and GQD appears when the neutrino travels through layers of increasing density within the Earth. The effect becomes relevant for neutrino trajectories passing through the Earth core. The decoherence effects considered in [87] also involve contributions from the matter Hamiltonian of the neutrinos. However, it is not so simple to match these models and the one considered here as the models in [87, 94] involve only the sub-leading contribution of decoherence effects in order to be able to still work with analytical expressions for the oscillations probabilities and this is used to perform an analysis for DUNE and T2HK in [94].

In the context of the Lindblad equation, the phenomenological models with constant decoherence parameters γ_{ij} in matter can be identified with a model where the Lindblad operator is chosen to be the neutrino Hamiltonian in vacuum, whereas the model presented here chooses the full neutrino Hamiltonian as the Lindblad operator. If we restrict to the vacuum case, both models obviously agree but deviate in the matter case. From the point of view of the gravitational environment it is not very clear why the thermal gravitational background should only couple to the vacuum energy of the neutrino even if a non-vanishing matter density is present.
A further consequence of this is that bounds on decoherence effects of neutrino detectors that have been derived using the PQD models can only constrain η in the vacuum case. Although there are upper limits on the gamma parameters from neutrino experiments where matter effects are

negligible, such as the results of the MINOS+T2K data [89], the baselines and neutrino energies of such experiments allow a vacuum treatment of neutrino oscillations. However, in [89], they fit the data assuming three scenarios which are not fully compatible with our choice of parameters. Therefore, we cannot directly translate current upper limits on the gammas into upper limits for our parameters.

For the matter case, a further sensitivity analysis is needed because the deviation in the oscillation probabilities predicted when using the PQD model with a decoherence parameter independent of the matter density or the one presented here (GQD) is a measurable effect as can be seen in Figure 6, where the constants γ_{ij} were chosen to be equal to the decoherence parameters in the GQD model in vacuum such that the (PQD) and the (GQD) model perfectly match in the vacuum case. From the corresponding oscillograms in Figure 7 it becomes visible that the probabilities can deviate by up to 10% for $\eta = 10^{-8}$ s and $\Theta = 0.9K$.

Figure 7 shows the difference in neutrino oscillation probabilities for the PQD and GQD models in Earth as a function of the neutrino energy and the cosine of the zenith angle, where up-going events have $\cos\theta_Z = -1$. The choice of the η value matches the PQD γ_{ij} values in vacuum near to current experimental upper bounds. As it can be seen, differences up to 10% can be observed, highlighting the different decoherence behaviour of the two models that arise when including matter effects. It follows that the model considered here can be independently constrained with respect to the PQD model by neutrino telescopes optimised for the GeV energy range, such as KM3NeT/ORCA [202].

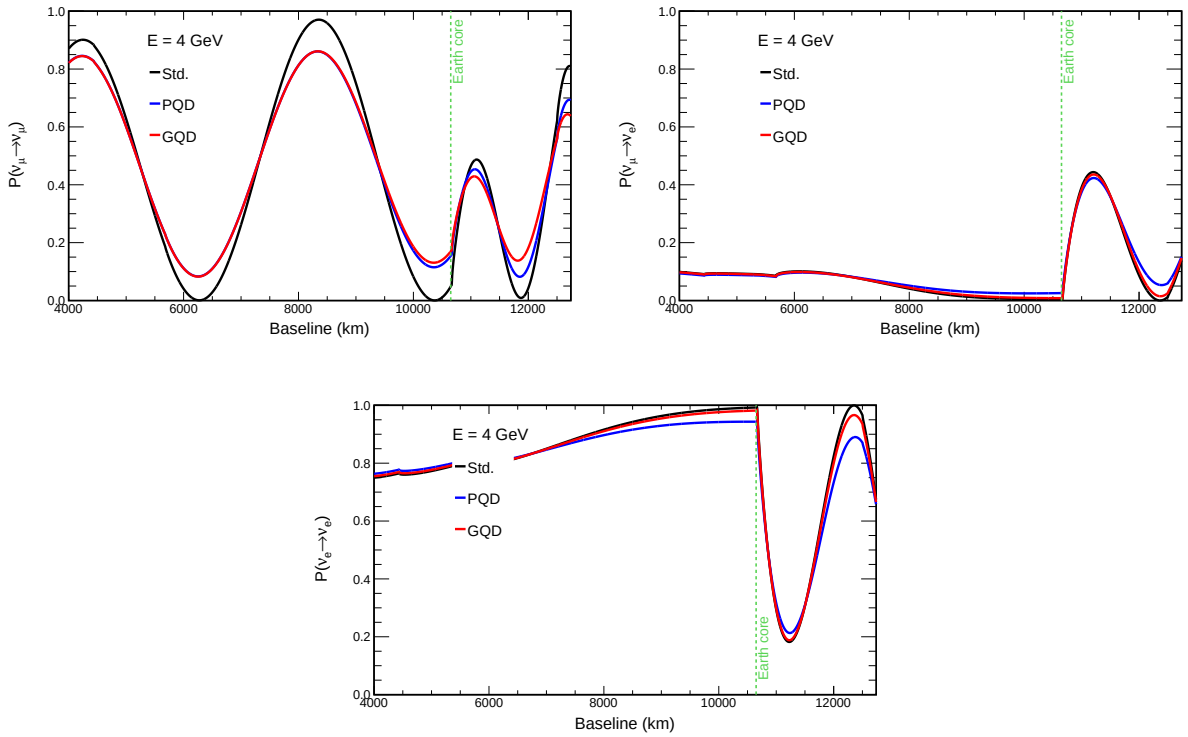

Figure 5: Neutrino oscillation probabilities in matter for a $4GeV$ neutrino as a function of the travelled baseline in Earth. The plots compare standard oscillations without decoherence (Std.) with the quantum mechanical model in this part of the thesis (GQD) and a phenomenological model with $n = -2$ (PQD). The GQD model parameters are set to $\eta = 10^{-8}s$ and $\Theta = 0.9K$ which implies for the PQD model in vacuum $\gamma_{21} = 1.00694 \cdot 10^{-25}, \gamma_{31} = 1.08067 \cdot 10^{-22}$ and $\gamma_{32} = 1.0157 \cdot 10^{-22}$. The Earth matter effects are accounted for via the PREM model [204]. The clear discontinuity for neutrino trajectories passing inside of the Earth core is due to the net change in density between mantle and core. The plots have been created with *OscProb* [203]. *This plot was originally published in [3] and created by one of the coauthors other than the author of this thesis. It is included in this thesis, as it improves the analysis of the results of the model.*

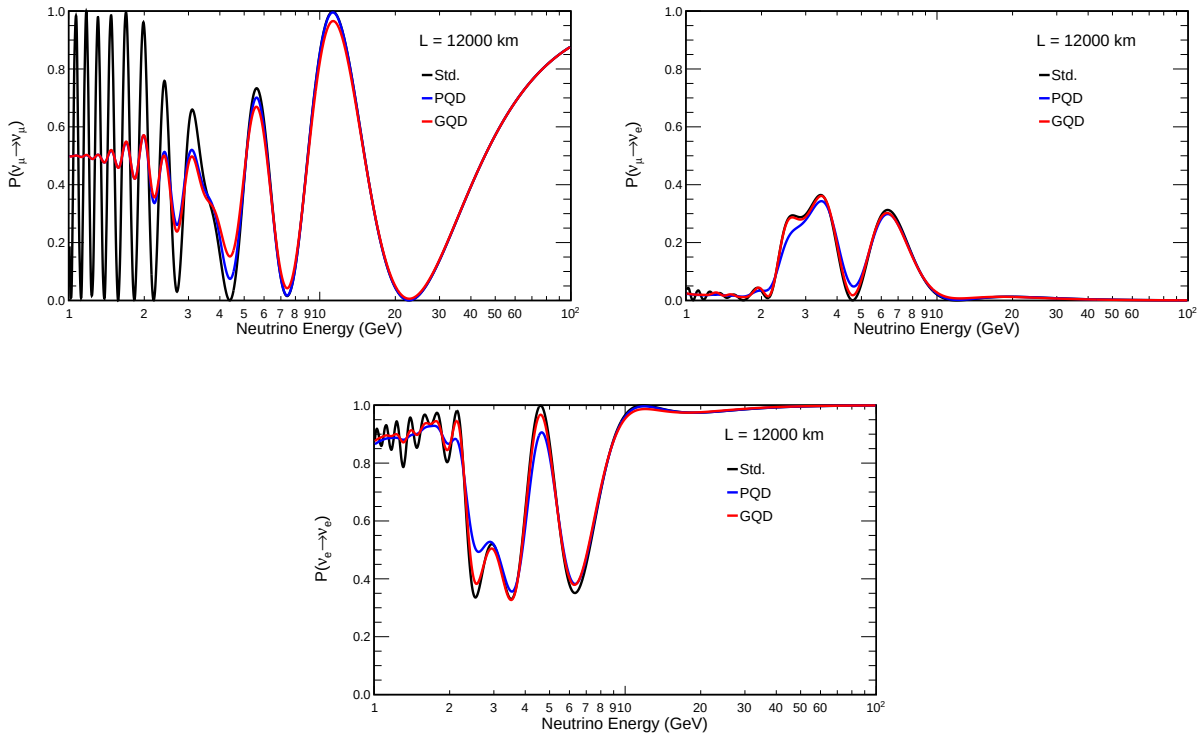

Figure 6: Neutrino oscillation probabilities in matter for a baseline of $12000km$, corresponding to $\cos\theta_{Zenith} = -0.94$, which is a trajectory passing through the Earth's core. The plots compare standard oscillations without decoherence (Std.) with the quantum mechanical model in this part of the thesis (GQD) and a phenomenological model with $n = -2$ (PQD). For the GQD model $\eta = 10^{-8}s$ and $\Theta = 0.9K$ are assumed which implies for the PQD model $\gamma_{21} = 1.00694 \cdot 10^{-25}, \gamma_{31} = 1.08067 \cdot 10^{-22}$, and $\gamma_{32} = 1.0157 \cdot 10^{-22}$ in order to have these two models coinciding in vacuum. The Earth matter effects are accounted for via the PREM model [204]. The difference between constant decoherence parameters independent of the Earth matter density (PQD) and a parameter depending on the Earth matter density (GQD) is evident. The plots have been made with *OscProb* [203]. *This plot was originally published in [3] and created by one of the coauthors other than the author of this thesis. It is included in this thesis, as it improves the analysis of the results of the model.*

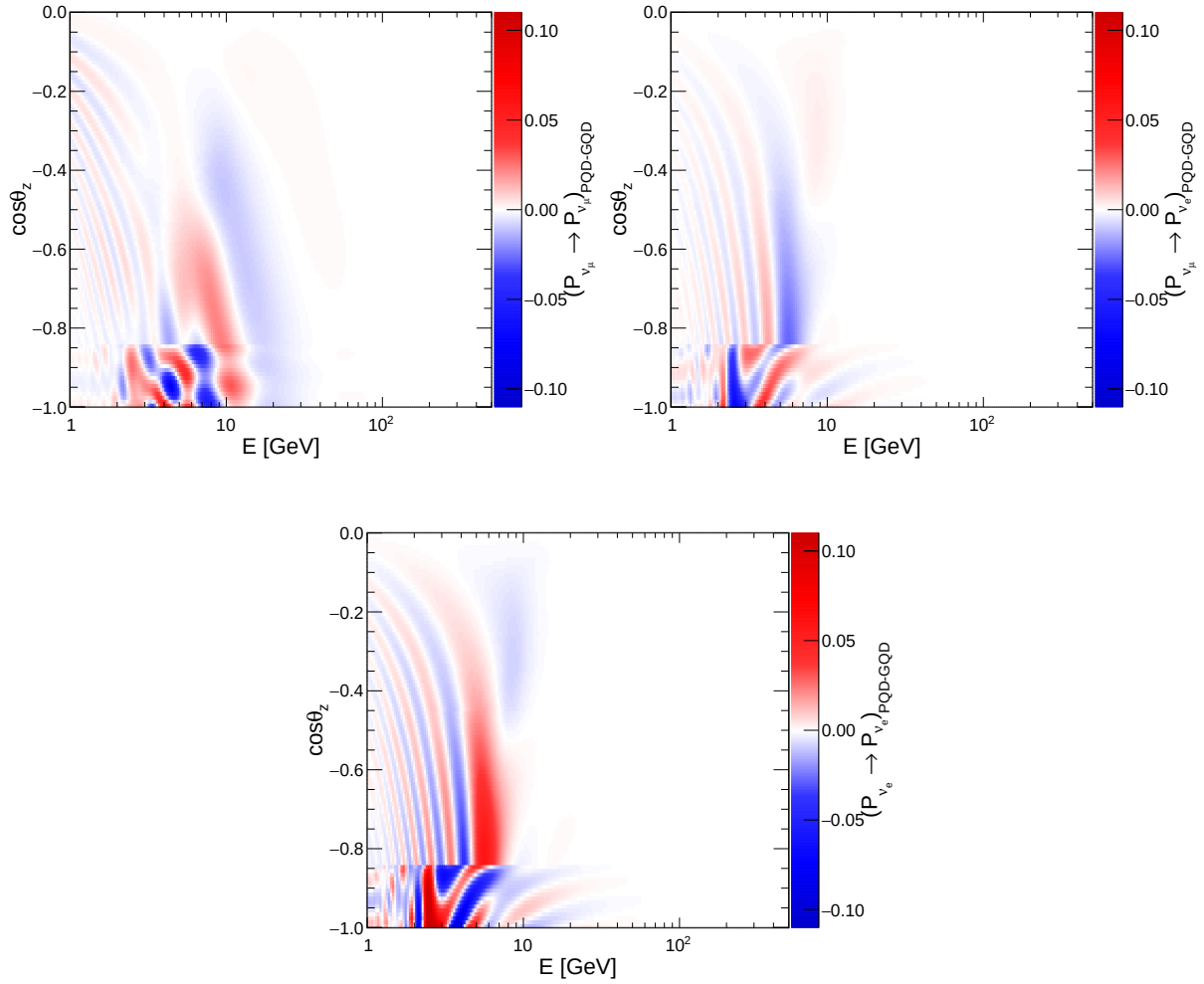

Figure 7: Difference of neutrino oscillation probabilities in matter for the quantum mechanical model in this part of the thesis (GQD) and a phenomenological model for $n = -2$ (PQD). For the GQD model $\eta = 10^{-8}s$ and $\Theta = 0.9K$ are assumed which implies for the PQD model $\gamma_{21} = 1.00694 \cdot 10^{-25}, \gamma_{31} = 1.08067 \cdot 10^{-22}$, and $\gamma_{32} = 1.0157 \cdot 10^{-22}$ such that both models coincide in vacuum. The Earth matter effects are accounted for via the PREM model [204]. The difference between constant decoherence parameters independent of the Earth matter density (PQD) and a parameter depending on the Earth matter density (GQD) is evident. The plots have been made with *OscProb* [203]. *This plot was originally published in [3] and created by one of the coauthors other than the author of this thesis. It is included in this thesis, as it improves the analysis of the results of the model.*

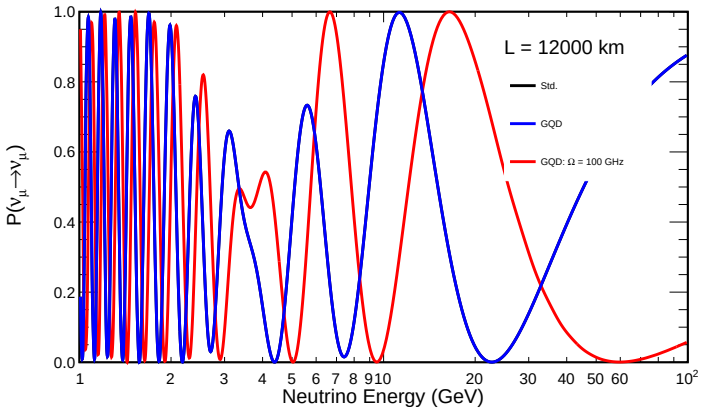

Figure 8: Comparison of the quantum mechanical model presented in this part of the thesis (GQD) with (blue) and without (red) renormalisation. In the latter case, the cutoff-dependent Lamb-shift contribution is still present in the unrenormalised Hamiltonian. The cutoff frequency has been chosen to be $\Omega = 100GHz$ corresponding to the maximal frequency of thermal gravitational waves at temperature $\Theta = 0.9K$, see for instance [207], and $\eta = 10^{-37}s$ for which the oscillations with $\Omega = 100GHz$ do not get too fast. The value $\Omega = 100GHz$ was chosen because it corresponds approximately to the maximal frequency of the black-body spectrum for $\Theta = 0.9K$. Considering the Lamb-shift as a real physical effect is problematic because its contribution still depends on the cutoff frequency Ω and diverges when Ω is sent to infinity, which shows that a renormalisation procedure is required. The plot has been made with *OscProb* [203]. *This plot was originally published in [3] and created by one of the coauthors other than the author of this thesis. It is included in this thesis, as it improves the analysis of the results of the model.*

17.2. Effect of the renormalisation

The content of this subsection was already published in [3]. Here, it is presented with some modifications compared to [3] to adapt it to the flow of the thesis. The numerical calculations and the plots were created by one of the coauthors of [3] other than the author of this thesis. They are included in this thesis, as they improve the analysis of the results of the model.

In Figure 8 a comparison of the quantum mechanical model presented in this part of the thesis (GQD) with and without renormalisation is shown. As expected, in the GQD model the contribution of the Lamb shift in the non-renormalised Hamiltonian $H_S^{(0)}$ in (16.2) leads to an energy-dependent phase shift in the oscillations. However, as discussed in section 16.6, such a phase shift is non-physical because it still depends on the chosen cutoff frequency Ω and diverges in the limit $\Omega \to \infty$. After renormalising the neutrino Hamiltonian and considering the limit value $\Omega \to \infty$, the contribution of the Lamb-shift is not present, as it is exactly cancelled by the counter term introduced in (16.86). Thus, these results show on the one hand that for the model considered in this work it is a justified procedure to not consider the Lamb-shift as well as the counter term at the level of the Lindblad equation, which is often done but needs in general a detailed analysis for each individual model separately. On the other hand, as already discussed

in the context of massless neutrino oscillations in [85], it further demonstrates that any physical interpretation of effects caused by the Lamb-shift term without a detailed analysis of the renormalised model can be problematic.

17.3. Coupling strength inspired from linearised gravity

The content of this subsection was already published in [3]. Here, it is presented with some modifications compared to [3] to adapt it to the flow of the thesis. The numerical calculations and the plots were created by one of the coauthors of [3] other than the author of this thesis. They are included in this thesis, as they improve the analysis of the results of the model.
In the model studied in this work, η is a free parameter which represents the coupling strength between the neutrinos and the gravitational environment. It cannot be specified by the microscopic model in (16.2), as it depends on the g_i which are in turn not specified. As discussed, the existing constraints from experimental data in [88, 89, 93] cannot be used to further constrain η because the assumptions used for the decoherence parameter in these analyses are not compatible with the model considered in this work. Hence, a detailed investigation on the sensitivities of different neutrino detectors is needed to obtain such upper bounds.

From the theoretical point of view, the estimated value of η is determined by the way general relativity couples to matter. However, to the knowledge of the authors of [3] no full field theoretical model for neutrinos has been derived so far, so there is yet no definite answer to the size of η. By comparison to full field theoretical models like [60, 63] or the one presented in part II and III of this thesis, it is nevertheless possible to attempt a first rather naive estimate for a suitable order of magnitude for the coupling parameter η. Using the model from part II, such an estimate can be found by solving this master equation applied to the ultra-relativistic case from section 13.3. This is done in detail in section 17.4. The resulting value for η, obtained in equation (17.8) to be $\eta \approx 10^{-44}s$, is rather tiny and corresponds to a γ_{ij} in the phenomenological models (for $n = -2$) of the order $\gamma_{ij} \approx 10^{-54}\frac{eV^2}{s}$. For such a tiny value of η, using similar temperature parameters Θ as above, one would not be able to detect modifications from the standard neutrino oscillations. This can also be seen from Figure 9 where the modification in the probability for the neutrino oscillations are shown for three different values of η.

Specifically, for $\eta = 10^{-9}s$, the GQD model is already almost not distinguishable from the standard scenario. For $\eta = 10^{-8}s$, the modifications start to become non-negligible and they become large already at $\eta = 10^{-7}s$, which corresponds, in vacuum, to values for the γ_{ij} parameters of the PQD models of the order $\gamma_{ij} \approx 10^{-21}\frac{eV^2}{s}$.
Does this mean that, taking this estimate seriously, the effect of gravitationally induced decoherence will be too tiny? The answer to this question is not so simple and under debate in the current literature. For instance in [60, 63] it is discussed that the interpretation of the temperature parameter Θ as the temperature of the thermal gravitational waves is too restrictive. They also conclude that for $\Theta = 0.9K$ the η that follows from the QFT model is too small to cause a detectable decoherence effect. However, they argue that Θ should rather be interpreted as an effective parameter, which for $\Theta = 0$ includes gravitons in a vacuum state where no decoherence effects are present. For the choice[36] of $\Theta \simeq 0.9K$, this corresponds to cosmic thermal gravita-

[36] In [60, 63] $\Theta = 2.7K$ is chosen, the temperature of the cosmic microwave background. To the knowledge of the

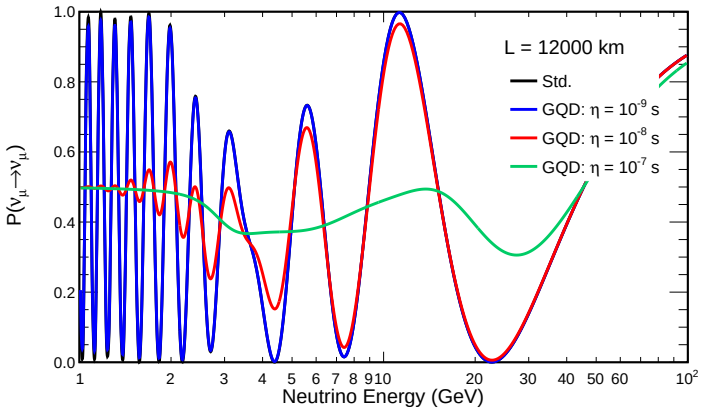

Figure 9: Effect of η, the neutrino coupling parameter to the gravitational environment, on the muon neutrino disappearance probability when propagating through the Earth. Here, $\Theta = 0.9K$ is assumed. The considered baseline takes a neutrino trajectory that passes through the Earth's core. The plot has been made with *OscProb* [203]. *This plot was originally published in [3] and created by one of the coauthors other than the author of this thesis. It is included in this thesis, as it improves the analysis of the results of the model.*

tional waves. For higher values of an effective Θ parameter they suggest that it can for instance be given if one chooses a quantum state for the environment that mimics a classical stochastic noise with an astrophysical origin such as a background caused by all rotating neutron stars in the galaxy. Another possibility they discuss is that, assuming that classical spacetimes arise from an underlying theory of quantum gravity at the thermodynamic level, a classical spacetime such as flat Minkowski spacetime is a macrostate and its emergence is therefore accompanied by classicalised thermodynamic fluctuations, which may be stronger than any quantum fluctuations in perturbative quantum gravity.

Therefore, Θ, which is understood as an effective parameter in their discussion, cannot be determined by a QFT model based on linearised gravity. Other decoherence models with a similar parameter involved can be found in [208–211], where either the parameter is not further specified or the value of the Planck temperature is discussed which is an obvious but not very restrictive upper bound for such an effective temperature parameter. To address this point, Figure 10 shows the effect of the temperature of the gravitational environment for neutrino oscillation probabilities in Earth as a function of the neutrino energy for a fixed value of η. As it can be seen, a small variation in the temperature has visible effects in oscillation probabilities which could potentially be resolved by neutrino telescopes such as KM3NeT/ORCA.

In addition, we show in Figure 11 exemplary how the modifications of the probabilities for the oscillations compared between the case with and without decoherence vary with the temperature for atmospheric neutrinos. As expected, for higher temperatures the parameter η can be smaller to still obtain deviations in the oscillation probabilities. Figure 11 also shows the plot for different neutrino energies. For smaller energies, the values of η, from that on deviations of the standard oscillations are seen, can be slightly smaller, which is due to the fact that the

authors of [3], the temperature of thermal gravitational waves is expected to be somewhat lower, see e.g. [207].

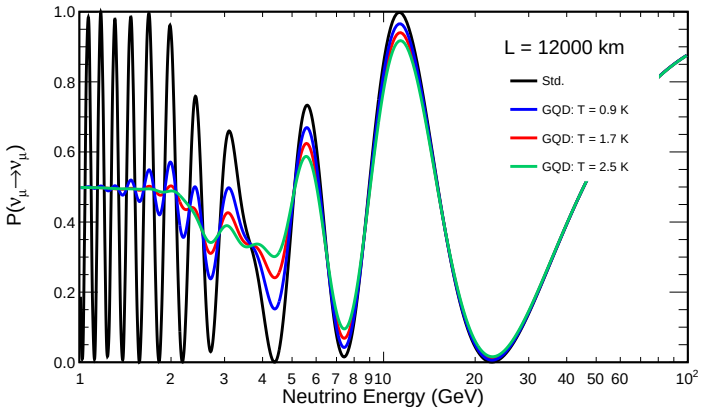

Figure 10: Effect of the temperature of the gravitational environment Θ, in the plot denoted as T, on the muon neutrino disappearance probability in Earth. Here, $\eta = 10^{-8}s$ is assumed. The plot has been made with *OscProb* [203]. *This plot was originally published in [3] and created by one of the coauthors other than the author of this thesis. It is included in this thesis, as it improves the analysis of the results of the model.*

mean neutrino energy enters with an inverse second power in the decoherence term. As for these plots we investigated atmospheric neutrinos that have as the maximum propagation length the trajectory through the Earth, the analysis of the Θ and η ranges is in this sense restricted as we expect decoherence effects to become larger for larger propagation lengths.

An additional aspect which is related to this and becomes relevant in the case of neutrino oscillations is that we can also enhance the decoherence effect if we consider longer propagation lengths of the neutrinos. In this case, where one wants to consider cosmic neutrinos, for example, a QFT model based on linearised gravity around a flat Minkowski spacetime, as in [60, 61, 63] or in part II and III of this thesis, might be too simple as one would have to consider more complex models that involve gravitational waves in a FLRW spacetime as a more realistic setting, for which the estimate is also expected to change due to the presence of a non-trivial scale factor in cosmological spacetimes. From the point of view of quantum gravity, it therefore remains an exciting question whether decoherence effects in neutrino oscillations are actually measured and, if so, which theoretical models can then satisfactorily explain such measurements.

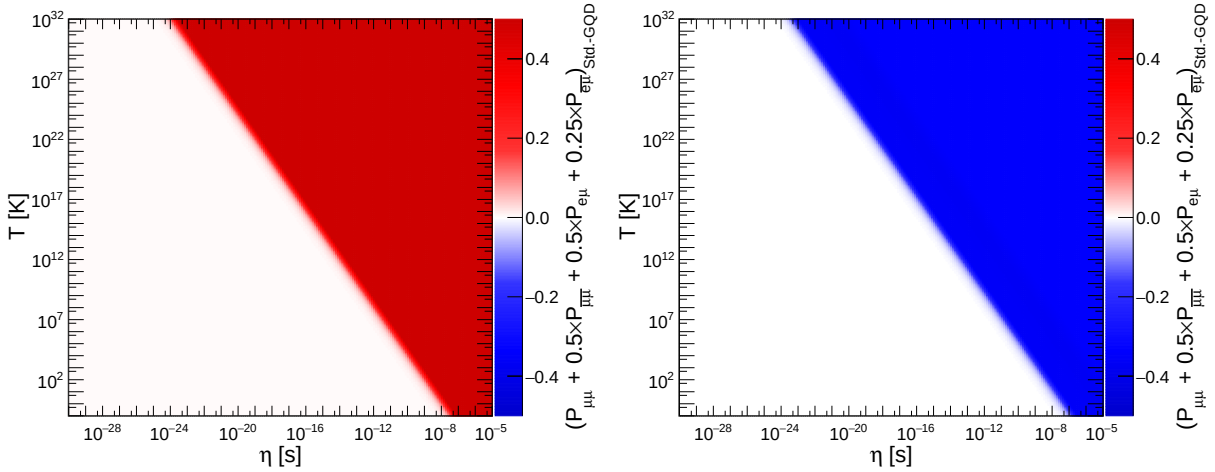

Figure 11: Difference in atmospheric neutrino oscillation probabilities between the standard (Std.) scenario and GQD, as a function of η and temperature Θ (in this plot denoted as T), the latter starting at $0.1K$ and going up to the Planck temperature. Here, upgoing neutrinos ($\cos\theta_{Zenith} = -1.0$) with an energy of $6GeV$ (left) and $18GeV$ (right) are considered. The assumed ratio between neutrino flavours and neutrinos vs. antineutrinos is a simplified approximation of the atmospheric neutrino flux. Matter effects are included via the PREM model [204]. The plots have been made with *OscProb* [203]. *This plot was originally published in [3] and created by one of the coauthors other than the author of this thesis. It is included in this thesis, as it improves the analysis of the results of the model.*

17.4. Application of the Lindblad one-particle master equation from part III to neutrino oscillations and comparison with the quantum mechanical toy model

The content of this subsection was already published in [2]. Here, it is presented with some modifications compared to [2] to adapt it to the flow of the thesis.
Finally, we want to discuss the relation of the results obtained in this part of the thesis with the one derived from the one-particle projection of the field theoretical model in part III. For this purpose, we consider the decoherence of neutrinos predicted by the ultra-relativistic one-particle master equation for a scalar particle derived in section 13.3.

This connection is of interest to us in several respects: first due to the quantum mechanical nature of the the quantum mechanical toy model, the coupling parameter encoding the strength for the coupling between system and environment cannot be determined from first principles. Instead a free parameter was introduced, that after introduction of a spectral density was denoted by η, similar to what was done also in [112]. Second, the quantum mechanical model requires the choice of a spectral density to derive the final master equation together with an appropriate cut-off function that regulates the integral over the frequency domain, see section 16.3. We have considered four different commonly used cut-off functions and we have shown that the final Lindblad master equation cannot distinguish between the different choices. The one-particle master equation in part III was derived from an underlying field theory model presented in part II, so the situation is different there. As the matter, which is a scalar field in that field theoretical model, couples to linearised gravity, the coupling constant in the interaction Hamiltonian is naturally build into the model and given by the square root of $\kappa = \frac{8\pi G_N}{c^4}$, where G_N is Newton's constant, see equation (8.11). Furthermore, due to the field theoretical character of the model, it is not necessary to introduce a spectral density by hand, since the interaction Hamiltonian contains an integral over all modes from the beginning. As a third aspect we want to compare the application of the Markov approximation in the quantum mechanical toy model and in the one-particle master equation derived in part III.
Even though the equation derived in part III is, taken strictly, only applicable to scalar particles, we still apply it to the case of neutrinos in order to discuss the relation with the results obtained from the quantum mechanical toy model. That this can be done in this context is due to the reason that the quantum mechanical toy model treats the neutrinos as plane waves and thus does not take the full spinorial nature of neutrinos into account.
We assume that the two momenta $\vec{u}$ and $\vec{v}$ of the scalar particles in section 13.3 are approximately parallel to each other in order to have intersection probability and to be able to measure them in a neutrino detector. With this, the one-particle master equation in the ultra-relativistic limit (13.14) becomes

$$\frac{\partial}{\partial t}\rho(\vec{u},\vec{v},t) = -\,i\rho(\vec{u},\vec{v},t)\,(u-v) - \frac{\kappa}{12\pi\beta}(u-v)^2\rho(\vec{u},\vec{v},t)\,. \tag{17.4}$$

As for ultra-relativistic particles we have $\hat{H}\hat{\rho} \approx u\hat{\rho}$, we indeed obtain the same form for the master equation as in the quantum mechanical toy model in the effective mass basis given in equation (16.99):

$$\frac{\partial}{\partial t}\hat{\rho}(t) = -i[\hat{H},\hat{\rho}(t)] + \frac{\kappa}{6\pi\beta}\left(\hat{H}\hat{\rho}(t)\hat{H} - \frac{1}{2}\left\{\hat{H}^2,\hat{\rho}(t)\right\}\right)\,. \tag{17.5}$$

The master equation above can be solved in the energy eigenbasis, where we denote the energy eigenvalues by E_i. With respect to this basis we denote the individual elements of $\hat{\rho}$ by ρ_{ij} whose solutions read

$$\rho_{ij}(t) = \rho_{ij}(0) e^{-i(E_i - E_j)t - \frac{\kappa}{12\pi\beta}(E_i - E_j)^2 t} \,. \tag{17.6}$$

This result agrees, up to the different prefactor of 2 in front of the decoherence term mentioned in subsection 13.3, with the one obtained for the one-particle projection evaluated for motion in one dimension for a photon in [63].

We will now discuss the comparison of the three aspects mentioned above. We start with the comparison of the coupling parameter. Such a comparison can be obtained by comparing the prefactors of the decoherence terms in both models. For the one-particle projected master equation we have

$$\frac{\kappa}{12\pi\beta} = \frac{2G_N k_B \Theta}{3c^4} \to \frac{2G_N k_B \Theta}{3\hbar^2 c^5} \,, \tag{17.7}$$

where we restored the correct units in the last step. Comparing with the decoherence rate in the quantum mechanical model, which can be read off from equation (16.106) and is $\frac{2\eta^2 k_B \Theta}{\hbar^3}$, and introducing the Planck length ℓ_P, we find that

$$\eta^2 = \frac{\hbar G_N}{3c^5} = \frac{\ell_P^2}{3c^2} \approx 10^{-87} s^2 \,. \tag{17.8}$$

Similar results of the coupling strength can be found in [60, 63]. As the one-particle master equation considers the case of a scalar field with a thermal gravitational background, more work is needed in order to develop more sophisticated models for neutrinos or fermions in general to derive a similar master equation for a fermionic system under consideration and for more general environments. In addition, the model is based on linearising gravity around a flat Minkowski background, whereas it would be interesting to also consider decoherence models for longer propagation distances and consider master equations based on a model on a cosmological background as the presence of a scale factor could modify the decoherence effect, as analysed for instance in [212–214].

Compared to the quantum mechanical model, in the one-particle projection of the field theoretical model it was not necessary to introduce a spectral density, as mentioned above, which is a kind of continuum limit for the frequencies of the oscillators in the environment that is typically used in similar quantum mechanical models to avoid Poincare recurrences, see for instance [45]. Furthermore, the cut-off function that needed to be used in the quantum mechanical model to regularise divergent integrals is not required for the one-particle master equation. Instead, the divergent contributions in the one-particle master equation could be linked to Feynman diagrams of a corresponding effective field theory in section 11.2 giving a clearer physical interpretation than in the quantum mechanical toy model. With that given, the divergent contributions were treated using a standard renormalisation procedure known from quantum field theory in section 11.4 that would be applied also in other situations in quantum field theory where such kind of diagrams play a role.

Not entirely unrelated to the latter paragraph is the discussion of the application of the Markov approximation in the field theoretical one-particle master equation and in the quantum mechanical toy model. In the latter, due to its simplicity compared to the one-particle master equation

in part III, it was explicitly shown in section 16.3 that the environmental correlation functions are strongly peaked around the initial time and decay rapidly after the peak. Such environmental correlation functions depend on both the chosen spectral density and the chosen cut-off function. For the field theoretical master equation however, none of these choices are made, but the corresponding quantities are determined and set from the beginning when formulating the model. In section 12.1 a condition was discussed under which the Markov approximation can be applied for the ultra-relativistic limit to the one-particle master equation of part III. Considering here the application to neutrinos we can discuss whether this condition is satisfied in this application and how it relates to the application of the Markov approximation in the quantum mechanical toy model in section 16.4. The condition applied in part III, equation (12.14), states that the Markov approximation is justified if[37]

$$u, v \gg \frac{k_B \Theta}{c} \,. \tag{17.9}$$

In the case of ultra-relativistic neutrinos where we neglect their masses, this is equivalent to

$$E_u, E_v \gg k_B \Theta \,, \tag{17.10}$$

where E_u and E_v denote the neutrino energies. Typical neutrino energies investigated in this part of the thesis start at energies of $1GeV \approx 1.6 \cdot 10^{-10} J$. Given the Boltzmann constant $k_B \approx 1.4 \cdot 10^{-23} \frac{J}{K}$ and the temperature parameter Θ of the thermal gravitational waves of around $1K$ used in this part of the thesis, is the condition for the applicability of the Markov approximation in part III

$$1.6 \cdot 10^{-10} J \gg 1.4 \cdot 10^{-23} J \,. \tag{17.11}$$

Both sides of the inequality still differ by more than ten orders of magnitude, so the approximation can also be used for neutrinos with lower energies or for higher values of the temperature parameters. Thus, we can conclude given the proof presented in section 12.1.1, the application of the Markov approximation to the physical scenario used in this part of the thesis is not only justified at the level of the quantum mechanical model as shown in section 16.4, but also if one derives that model from the one-particle master equation of the QFT model.

Finally, compared to the quantum mechanical toy model, the more general one-particle master equation derived in part III also allows to consider the generalisation to decoherence models with wave packets, whereas for the quantum mechanical toy model plane waves were considered. This is due to the general form of the one particle density matrix defined in (10.2) as

$$\rho_1(t) = \int_{\mathbb{R}^3} d^3u \int_{\mathbb{R}^3} d^3v \; \rho(\vec{u}, \vec{v}, t) \; a_u^\dagger \left|0\right\rangle \left\langle 0\right| a_v \,. \tag{17.12}$$

When choosing suitable initial conditions for $\rho(\vec{u}, \vec{v}, 0)$, one can model different descriptions for neutrinos like wave packets or plane waves, where the latter just correspond to delta distributions in this context.

---

[37] Note that this is not an if and only if here.

18. Conclusion

In this thesis, different ways to include quantised gravity as an environment for an open quantum system were discussed in order to work on the search for signatures of quantum gravity effects for instance in neutrino oscillations and to thereby provide an additional area of application to analyse possible imprints of quantum gravity models. The results of this work extend and generalise the formulation of theoretical models for gravitationally induced decoherence compared to the literature and several of the open questions and problematic points that were named in section 1.2 could be answered. Additionally, some implications for experiments that search for these decoherence effects in neutrino oscillations were discussed.

18.1. A field theoretical model formulated in Ashtekar variables using Dirac observables

With general relativity (GR) and quantum field theory (QFT) being the best theories to describe nature at fundamental level today, we analysed in part II of the thesis a model in which linearised gravity as described by GR was coupled to a scalar field using a Post Minkowski approximation. The gravitational part of this total system was formulated in Ashtekar variables. This is different from similar works in the literature that also consider decoherence models based on linearised gravity and bosonic matter fields as for instance [60–63], as they use ADM variables. The formulation of linearised gravity in terms of Ashtekar variables enabled us to complete the first step towards a decoherence model inspired by loop quantum gravity, which permits a mathematically rigorous quantisation of GR. With this, we could extend the formulation of the models in the literature [60–63] that had been working with ADM variables before. As the formulation in Ashtekar variables only affects the gravitational part of the system, the formalism employed in this thesis can be readily generalised to other matter fields, for instance to a photon field, as it was done in [6]. Due to the internal structure of the Ashtekar variables, it can directly be used to couple fermionic fields, for which the ADM formulation would have to be reformulated first in terms of tetrads. Further new points in our model are the inclusion of a boundary term and the construction of Dirac observables for both matter and gravitational sector to identify the physical degrees of freedom instead of a gauge fixing. The usage of Ashtekar variables brings in a Gauß constraint that extends the set of ADM constraints. We have shown how suitable geometrical clocks can be constructed for these constraints to derive Dirac observables that encode the physical degrees of freedom based on the relational formalism. To construct these Dirac observables, we introduced a dual version of the observable map which facilitates the construction of quantities that commute also with the geometric clocks. Due to this property, we were able to map with a canonical transformation the basic phase space variables onto these observables as well as the clocks and constraints which permits to split the phase space into a physical and a gauge part whose algebras decouple. In decoherence models, it is important to implement the gauge invariance and to work with the physical degrees of freedom to obtain a physically meaningful interpretation of the resulting processes [215, 216]. As our geometric clocks only depend on gravitational phase space degrees of freedom, they remain valid when different matter is coupled and one only has to extend their set by suitable clocks for the gauge degrees of freedom in the matter field, for instance with a clock for the electromagnetic Gauß constraint when working with photons [6]. Therefore, the formulation of decoherence models in terms of Dirac observables for a linearised gravitational environment in Ashtekar variables is facilitated by the methods provided

in this work.
To conclude the classical treatment of the system, we compared the Dirac observables to other observables and gauge fixings in the literature in [5, 60, 151]. The difference one obtains in the physical Hamiltonian when choosing one of these other methods lies in the self-interaction term of the scalar field that does later not play a role in a one-particle master equation when normal ordered in the quantisation procedure.

Due to the decoupling of the sub-algebra that contains the physical degrees of freedom from the remaining gauge degrees of freedom, we used a reduced phase space quantisation to quantise only the former in a Fock quantisation. The resulting Hamiltonian of the total system was normal-ordered, which differs from the orderings chosen in [60, 62, 63]. This leads to a difference in the self-interaction term of the scalar field compared to these works. In particular in the one-particle projection of the master equation, the self-interaction term vanishes completely when working with a normal ordered Hamiltonian, which we discussed in the next part of the thesis. As a next step, the time-convolutionless projection operator technique was invoked to obtain a time-convolutionless master equation for the scalar field truncated after second order in the coupling. For this, the coupling was assumed to be weak and the environment of gravitational waves to be determined by a Gibbs state moderated by a temperature parameter Θ. This master equation was expressed in terms of thermal Wightman functions and the thermal Feynman propagator of the underlying effective QFT was introduced for the linearised gravitational field. At the end of part II, the resulting master equation was compared with equations for similar models in [60–63]. The main difference at the quantum level to the master equations in [60], which is also formulated for a scalar field, and to [63] formulated for a photon field is that these two are stated in Lindblad form. This requires further approximations, for instance the Markov and rotating wave approximations, that strongly depend on the environment and its influence on the system. As they have not yet been analysed for gravity, we refrained from casting the master equation into Lindblad form at this stage and just briefly sketched how these approximations can be applied. Instead, we discussed their applications and implications in the context of the one-particle equation in the following part of the thesis.

18.2. Analysis and effects of two different versions of the one-particle projection of the field theoretical master equation

One of the results of part II of the thesis was that it is highly complex to derive physical predictions from the final master equation for the scalar field. Therefore in part III of the thesis this equation was projected onto the one-particle space to obtain the evolution of a single scalar particle. For this projection, the density matrix was replaced by the density matrix of a single particle and only terms in the master equation that preserve the one-particle space were kept. At the level of the one-particle master equation, we were able to show how the individual terms of this master equation can be connected and interpreted based on the underlying effective QFT where linearised gravity is coupled to a scalar field. For this, we extended the discussion from [113] where two scalar fields are coupled as system of interest and environment. From this connection, it was possible to discuss and compare the different versions of the one-particle projection of a master equation used in [113] (which we called extended projection) on the one side and in [60, 62, 63] on the other side (which we denoted as non-extended projection). We could conclude that the main difference is that in the latter case terms that violate probability conservation in the TCL one-particle

master equation are dropped, that however represent valid scattering processes in the underlying effective QFT. These are included in the extended projection along with divergent terms that we could trace back to vacuum bubbles in the underlying effective QFT and renormalise. The Markov approximation repaired probability conservation in the renormalised one-particle master equation in the extended projection, but when dropping these terms in the non-extended projection, a part of the temperature dependent Lamb shift survived in the end, in contrast to case when using the extended projection.

18.3. Renormalisation of the one-particle master equation and the quantum mechanical toy model

The necessity of a renormalisation arose in both the one-particle projected field theoretical model discussed in part III and the quantum mechanical toy model discussed in part IV. In the former, we used the connection to the underlying effective QFT to identify the problematic diverging contributions as the self-energy term of the scalar field's propagator. For this, we rewrote the Feynman rules, which were in non-covariant form due to the initial ADM split of the system in part II, into a covariant form and then renormalised the mass and wave function to include the UV divergent terms. To maintain IR finiteness, a small artificial graviton mass was included that could be sent to zero in the end which allowed an extension of a similar renormalisation procedure for a linearised gravitational field in [173], where propagation in a thermal gravitational background is analysed. Following the standard renormalisation procedure in QFT, we could renormalise the self-energy contribution and obtain a finite one-particle master equation right after the projection where all terms arising from vacuum fluctuations were removed by this procedure. This allows a clear interpretation of the terms and processes the master equation encodes and permits the discussion of the physical implications of the later applied approximations. In similar works in the literature [60, 63], a renormalisation is only carried out after application of further approximations (Markov, rotating wave) and the specialisation of the master equation to a non-relativistic [60] or ultra-relativistic [63] limit. This procedure does not directly clarify the connection to the standard procedure in QFT and the possibility to give a physical interpretation of the influence of the invoked approximations on the master equation. This particular point, that it is highly problematic to draw physical conclusions from the master equation before a proper renormalisation, is emphasised by the analysis of the results in [62] and [85]: the final decoherence effect predicted in [62] on photons in vacuum without a renormalisation is absent in our model after the renormalisation and the massless neutrino oscillations predicted in the quantum mechanical model in [85] vanish in our quantum mechanical toy model when the Lamb-shift is renormalised properly. The discussion of both the one-particle master equation based on field theory and the microscopic quantum mechanical toy model gave us the possibility to compare the two ways to renormalise the corresponding master equations. One key point in this comparison was the fact that the interaction Hamiltonian in the quantum mechanical model commutes with the Hamiltonian of the system of interest, which leads to a vanishing thermal contribution in the Lamb-shift Hamiltonian. Due to this, the latter consists only of a vacuum part and is completely removed by the renormalisation. In the dissipator, both renormalisations differ: while in the one-particle projection the vacuum part is also removed here, it is not modified in the quantum mechanical model, but vanishes after the Markov approximation. As a consequence, both dissipators have the same form in the final Lindblad equations and depend linearly on the temperature parameter.

18.4. Application of Markov and rotating wave approximations in the one-particle master equation and the quantum mechanical toy model

Another result of the present thesis focuses on the application of the Markov and the rotating wave approximations to obtain a Lindblad form for the master equation. With the renormalisation of the one-particle master equation carried out before the application of these approximations, which has not yet been considered in similar works that exist in the literature so far [60, 63], we could interpret their influence and discuss, which physical processes are suppressed by them. As it was discussed in the introduction, neutrinos potentially provide a good candidate for the search of gravitationally induced decoherence. Therefore, for the further analysis in particular an ultra-relativistic scalar particle was investigated. It was shown that in the one-particle master equation for an ultra-relativistic scalar particle the Markov approximation is justified if the temperature parameter of the environment is not too high and we provided a starting point on how to test its validity for other physical scenarios. In the quantum mechanical model, we could also prove the validity of the Markov approximation, in this context by just using properties of the environment. There, we also provided a mathematically rigorous proof for the application of the approximation with a specific choice of cutoff in the spectral density, which we called quartic cutoff, that yields the same result as the frequently used Lorentz-Drude and exponential cutoffs. From the results of the field theoretical decoherence model, we could motivate a spectral density which is linear in the frequency ω of the oscillators of the environment for small ω when working with gravity as environment. To conclude part III of the thesis and the analysis of the field theoretical model, different applications were discussed. Firstly, the influence of the renormalisation and of the two approximations on the populations of the density matrix were investigated. This led to the insights that the Markov approximation removes their time evolution and thereby restores probability conservation if not present before (as it is the case if working with the extended one-particle projection). Additionally, we could show that the final effect obtained in [62] in a one-particle TCL master equation for the populations of a photon coupled to a gravitational waves environment in the vacuum state is not present any more after a renormalisation. Afterwards, the non-relativistic and the ultra-relativistic limit were analysed, where the model was applied as a toy model to neutrino oscillations which enabled us to confirm the final form of the dissipator obtained by the quantum mechanical toy model in part IV and to give an estimate for the order of magnitude of the coupling parameter η that appears in the spectral density of that toy model.

18.5. The microscopic quantum mechanical model and its implications on phenomenological models

It is evident from the discussions of parts II and III of the thesis that a model for gravitationally induced decoherence based on the field theoretical formulation is rather complicated and in particular the route towards physical predictions is not straight forward but rather involved. To extend the possible techniques and to make the connection to experiments and phenomenological models more direct, we have discussed in part IV of the thesis a microscopic quantum mechanical toy model based on [112] which was extended in this thesis to be capable of handling neutrinos as system of interest. After an introduction to neutrinos, the treatment of their oscillations with wave packets and plane waves as well as a presentation of phenomenological models and their involved approximations, we defined the microscopic quantum mechanical toy model with a neutrino as system of interest and an environment consisting of a finite collection of harmonic

oscillators to model gravitational waves. The coupling of the model was taken from [112] and is inspired by GR and the coupling in field theoretical models as for instance the one in part II of this thesis. For the derivation of the master equation a continuum limit for the oscillators in the environment was performed, as it is usually done in similar models, by choosing a specific spectral density. As discussed above, from a comparison to the environment of linearised gravity in part II a spectral density linear in the oscillator frequency was favoured, as it is also the case for instance in quantum optics. It turned out that the resulting Lamb-shift was then depending on the unphysical high-frequency cutoff which hence required a renormalisation that we discussed by including a suitable counter term in the original Hamiltonian. After the renormalisation, we ended up with a Lindblad equation without Lamb-shift, which we solved for a neutrino as matter particle. This final evolution equation contains only two free parameters, one being the coupling strength of the neutrino to the gravitational environment and the other one the temperature parameter that characterises the Gibbs state of this environment.
From this quantum mechanical toy model we could provide a resolution and a physical interpretation of the decoherence parameters used in the phenomenological models that directly start with a Lindblad equation which they parameterise with unknown parameters. We obtained the detailed way how the properties of the environment enter into these parameters and furthermore that they depend on the inverse of the squared neutrino energies. An important result is that the usual procedure applied in phenomenological models, as for instance in [86, 95, 105], to reduce the number of unknown parameters by setting some of these parameters equal to zero or to each other, corresponds to setting their masses equal to each other or zero, which contradicts experimentally obtained results. In vacuum, the decoherence parameters in the phenomenological model based on a Lindblad equation could be matched to our microscopic model with the choice $n = -2$ and $\gamma_{ij} = \frac{\eta^2 c^8 k_B \Theta}{2\hbar^3}(\Delta m_{ij}^2)^2$. This dependence on the neutrino energy gives valuable insights on the energy ranges of neutrinos whose oscillations are most favoured to show signatures of gravitationally induced decoherence according to this model and therefore also helps to identify neutrino detectors that are well-suited to search for this effect. The match of our model with the phenomenological ones is however not possible for matter oscillations: Here the general parametrisation of the dissipator in the phenomenological models corresponds to still using the vacuum part of the system Hamiltonian in the interaction Hamiltonian and therefore as Lindblad operator, while our microscopic toy model suggests in that case to use the full system Hamiltonian in matter. One would also expect the latter from GR, given that gravity couples to the full energy-momentum tensor of the particles and not only to its vacuum part. As we have discussed using plots for oscillations of atmospheric neutrinos, this negligence of the matter part in the Lindblad operator can lead to deviations of up to ten percent. Therefore the sensitivities obtained for different neutrino detectors based on the phenomenological approach as for instance in [86, 99, 105] have to be taken with caution, as they are often based on the analysis of oscillations in matter working with a phenomenological model. The microscopic quantum mechanical toy model discussed in this thesis hence provides a suggestion how the phenomenological models can be improved to adapt them more to the physics that one would expect to follow from GR.

18.6. Outlook

The field theoretical model investigated in this thesis consisted of a scalar field as matter content, and we analysed its implications on a toy model for decoherence in neutrino oscillations. This rises the question if a field theoretical model based on a fermionic field can provide one with

some more details and improvements for the toy model, which are not encoded in the scalar field. In the classical formulation, we constructed Dirac observables for both matter and gravity and quantised the physical part of the phase space. The observables for the gravitational part of the system were built independently of the matter field. This implies that the treatment presented here can be extended to different matter fields, as it has been done for instance in [6] for photons. In that case, an additional clock for the Gauß constraint of the photon is constructed while for the gravitational field the clocks from this thesis could be used. From these results along with the discussion in [62] for a general bosonic field, we expect that for other bosonic fields a treatment very similar to the one in the present thesis is possible. An open question is how this can be generalised to also include fermionic fields, which would be the natural candidate to describe neutrinos from the field theoretical point of view. The construction of such a gravitationally induced decoherence model for a fermionic field is thus a further step, along with its connection to quantum mechanical models as for instance the one in [82], where however a stochastic and classical gravitational field and a classical electromagnetic field are considered as environment.
The field theoretical model discussed in this work is meant to be a first step towards the development of a decoherence model inspired by loop quantum gravity (LQG) for the influence of gravity on matter. A possible next step consists in replacing the Fock quantisation of the linearised gravitational environment by an LQG inspired quantisation. This could potentially already show some specific features of a loop quantisation in the final master equation. The works in [128, 129] discuss a loop quantisation of linearised gravity in Ashtekar variables and show how one can connect it to a Fock quantisation and identify gravitons. A first toy model for a decoherence model for gravity itself formulated with LQG was used in the context of black holes in [167]. Also an LQG inspired quantisation of the quantum mechanical model is a subsequent possible next step. A first analysis in this direction is available in [144], where a master equation for a free particle coupled to an environment composed of free particles via a polymerised position-position coupling is derived and investigated.
To obtain a Lindblad equation, we have applied the Mark and the rotating wave approximation to the one-particle master equation. While we have found a condition under which the Markov approximation is applicable to ultra-relativistic particles, the question for conditions for its general applicability to master equations that contain (linearised) gravity as environment is however still open, which we were able to discuss at least in the quantum mechanical toy model in this work, where the analysis only depends on the properties of the environment and the involved time scales. Similar conditions and analyses for the applicability of the rotating wave approximation would also be of high interest, as there exist hints that it may lead to unphysical processes like causality violations and superluminal signaling in relativistic regimes [217, 218]. This point rises the question whether alternative versions of the Markov approximation, that directly yield a completely positive master equation in Lindblad form, can circumvent these issues and if they are applicable to gravity as environment. Such approximations enclose for instance the one discussed in [219, 220], where not only the density matrix, as in the standard Markov approximation, but also the system operators in Schrödinger picture is expanded in $s-t$ around $s=0$ in equation (4.34). Other possibilities are generalisations to the field theoretical formulation of the approximations for quantum mechanical models in [221], where complete positivity is obtained by replacing an arithmetic mean of the spectral density by a geometric one, or the one in [175], which does not require other assumptions than the ones made to derive the Redfield equation.
On the experimental side, as the microscopic model can yield more detailed dynamics for the

description of gravitationally induced decoherence in neutrino oscillations in matter compared to the phenomenological model, as we have shown in this thesis, further sensitivity analyses for neutrino detectors are of interest. In particular, one can make use of the modification of the phenomenological model with a non-constant decoherence parameter that depends on the Earth's density as proposed by the microscopic quantum mechanical toy model in this work due to the relevance of the matter effects that were discussed here. In addition, one can employ that for this quantum mechanical toy model detectors that measure lower-energetic neutrinos are favoured for the search of signatures of decoherence due to quantum gravity in neutrino oscillations in this class of models.

Appendices

Appendix A Details on the computation of the algebra of the Dirac observables

The content of this Appendix was already published in [1]. Here, it is presented with some modifications compared to [1] to adapt it to the flow of the thesis.
In this Appendix, we show some more details on the calculation of the algebra of the Dirac observables. In section A.1 we discuss the relation between the algebra of the Dirac observables and the Dirac observable of the Dirac bracket mentioned in the main text in section 7.6.2. In section A.2 we then compute as a consistency check the Poisson algebra of the linearised Dirac observables and discuss their relation to the canonical Poisson bracket.

A.1 Computing the algebra of the Dirac observables by means of using the Dirac observable of the corresponding Dirac bracket

The content of this Appendix was already published in [1]. Here, it is presented with some modifications compared to [1] to adapt it to the flow of the thesis. It is presented in an Appendix, as it was mainly done by one of the co-authors in [1] other than the author of this thesis. As it is however part of the proof for the algebra of the Dirac observables in section 7.6.2, it is included in this thesis.
In this Appendix, we show how the algebra of the Dirac observables is related to the Dirac observable of the Dirac bracket. Here we will discuss the special case and order in perturbation theory that is relevant for the model under consideration in this part of the thesis and we refer the reader for the proof of the general case to [120, 155]. In the application where we need this relation we will assume that we consider linearised geometrical clocks $\delta T^I(x)$ with $\delta^2 T^I(x) = 0$ that only depend on the gravitational degrees of freedom. We then introduce $\delta\mathcal{G}^I(x) := \delta T^I - \tau^I(x)$ that mutually commute with a set of constraints $\mathcal{C}'_J(x)$ up to corrections of order δ^2 that is

$$M^I_J(x,y) := \{\delta\mathcal{G}^I(x), \delta\mathcal{C}'_J(y)\} = \frac{1}{\kappa}\delta^I_J\delta^{(3)}(x,y) + O(\delta^2).$$

From the definition of $M^I_J(x,y)$ above follows that its inverse is simply given by

$$(M^{-1})^I_J(x,y) := \kappa\delta^I_J\delta^{(3)}(x,y) + O(\delta^2,\kappa^2)$$

with

$$\int d^3z\; M^I_J(x,z)(M^{-1})^J_K(z,y) = \delta^I_K\delta^{(3)}(x,y).$$

Note that we chose to denote the constraints with a prime here following the notation used in the main text. This is exactly the setup needed to analyse the algebra of Dirac observables for the model in this part of the thesis. Since we only perturb the gravitational degrees of freedom but not the matter ones, it is convenient to discuss these two types separately. We will start with the geometric sector and afterwards discuss in detail how the results can be carried over to the

algebra of the matter variables. In the framework of field theory the Dirac bracket $\{\cdot,\cdot\}^*$ reads

$$\begin{aligned}\{f(x),g(y)\}^* &= \{f(x),g(y)\} \\ &\quad -\int d^3z' \int d^3z'' \{f(x),\mathcal{C}'_L(z')\}(M^{-1})^L_M(z',z'')\{\mathcal{G}^M(z''),g(y)\} \\ &\quad +\int d^3z' \int d^3z'' \{g(y),\mathcal{C}'_L(z')\}(M^{-1})^L_M(z',z'')\{\mathcal{G}^M(z''),f(x)\} \\ &= \{f(x),g(y)\} - \int d^3z \{f(x),\mathcal{C}'_L(z)\}\delta^L_M\{T^M(z),g(y)\} \\ &\quad +\int d^3z \{g(y),\mathcal{C}'_L(z)\}\delta^L_M\{T^M(z),f(x)\}\,,\end{aligned} \tag{A.1}$$

where we used the explicit form of $(M^{-1})^J_K(z,y)$ together with the fact that inside the Poisson bracket we can replace $\mathcal{G}^M$ by T^M because they differ only by a phase space independent function. Quantities involving gravitational variables are perturbed in the model in this part of the thesis. Let us denote their linear and second-order perturbations by δf and $\delta^2 f$ respectively. Then we consider the perturbation of the Dirac bracket up to linear order that is given by

$$\begin{aligned}\{f(x),g(y)\}^* &= \{\delta f(x),\delta g(y)\} - \kappa\int d^3z \{\delta f(x),\delta\mathcal{C}'_L(z)\}\delta^L_M\{\delta T^M(z),\delta g(y)\} \\ &\quad +\kappa\int d^3z \{\delta g(y),\delta\mathcal{C}'_L(z)\}\delta^L_M\{\delta T^M(z),\delta f(x)\} \\ &\quad +\{\delta f(x),\delta^2 g(y)\} + \{\delta^2 f(x),\delta g(y)\} \\ &\quad -\kappa\int d^3z \{\delta^2 f(x),\delta\mathcal{C}'_L(z)\}\delta^L_M\{\delta T^M(z),\delta g(y)\} \\ &\quad -\kappa\int d^3z \{\delta f(x),\delta^2\mathcal{C}'_L(z)\}\delta^L_M\{\delta T^M(z),\delta g(y)\} \\ &\quad -\kappa\int d^3z \{\delta f(x),\delta\mathcal{C}'_L(z)\}\delta^L_M\{\delta T^M(z),\delta^2 g(y)\} \\ &\quad +\kappa\int d^3z \{\delta^2 g(y),\delta\mathcal{C}'_L(z)\}\delta^L_M\{\delta T^M(z),\delta f(x)\} \\ &\quad +\kappa\int d^3z \{\delta g(y),\delta^2\mathcal{C}'_L(z)\}\delta^L_M\{\delta T^M(z),\delta f(x)\} \\ &\quad +\kappa\int d^3z \{\delta g(y),\delta\mathcal{C}'_L(z)\}\delta^L_M\{\delta T^M(z),\delta^2 f(x)\} + O(\delta^2,\kappa^2).\end{aligned} \tag{A.2}$$

For elementary phase space variables we have $\delta^2 f = 0$ and $\delta^2 g = 0$, so the Dirac bracket simplifies to

$$\begin{aligned}\{f(x),g(y)\}^* &= \{\delta f(x),\delta g(y)\} \\ &\quad -\kappa\int d^3z \{\delta f(x),\delta\mathcal{C}'_L(z)\}\delta^L_M\{\delta T^M(z),\delta g(y)\} \\ &\quad +\kappa\int d^3z \{\delta g(y),\delta\mathcal{C}'_L(z)\}\delta^L_M\{\delta T^M(z),\delta f(x)\} \\ &\quad -\kappa\int d^3z \{\delta f(x),\delta^2\mathcal{C}'_L(z)\}\delta^L_M\{\delta T^M(z),\delta g(y)\} \\ &\quad +\kappa\int d^3z \{\delta g(y),\delta^2\mathcal{C}'_L(z)\}\delta^L_M\{\delta T^M(z),\delta f(x)\} + O(\delta^2,\kappa^2).\end{aligned} \tag{A.3}$$

(A.4)

The Dirac observable associated with δf is up to second order given by

$$\begin{aligned} O_{\delta f,\{T\}} &= \delta f - \kappa \int d^3z \delta\mathcal{G}^K(z)\{\delta f, \delta\mathcal{C}'_K(z)\} - \kappa \int d^3z \delta\mathcal{G}^K(z)\{\delta f, \delta^2\mathcal{C}'_K(z)\} \\ &\quad -\frac{\kappa^2}{2}\int d^3z \int d^3z' \delta\mathcal{G}^K(z)\delta\mathcal{G}^L(z')\{\{\delta f, \delta^2\mathcal{C}'(z)\}, \delta\mathcal{C}'_M(z')\} + O(\delta^3,\kappa^2) \quad \text{(A.5)} \\ &=: O^{(1)}_{\delta f,\{T\}} + O^{(2)}_{\delta f,\{T\}} + O(\delta^3,\kappa^2), \quad \text{(A.6)} \end{aligned}$$

where, as in the main text, we include all terms of order δ and δ^2 in $O^{(1)}_{\delta f,\{T\}}$ and $O^{(2)}_{\delta f,\{T\}}$ respectively.
Given this, the aim is now to show the following: For linearised quantities $\delta f, \delta g$ with $\delta^2 f = 0$ and $\delta^2 g = 0$ and for a set of constraints $\mathcal{C}'_I$ and reference fields $\mathcal{G}^I$, that satisfy $\{\mathcal{G}^I(x), \mathcal{C}'_J(y)\} = \delta^I_J\delta^{(3)}(x,y) + O(\delta^2,\kappa^2)$, we have

$$\{O_{\delta f,\{T\}}, O_{\delta g,\{T\}}\} = O_{\{\delta f,\delta g\}^*,\{T\}} + O(\delta^2,\kappa^2), \quad \text{(A.7)}$$

where the crucial property for our later application is that we have a strong equality here and not a weak one that is present in the general case [120, 155]. For the purpose of showing the equality in (A.7) we introduce the following notation:

$$\begin{aligned} \{f,g\}^*|_{\delta^0} &:= \{\delta f(x), \delta g(y)\} - \kappa\int d^3z \{\delta f(x), \delta\mathcal{C}'_L(z)\}\delta^L_M\{\delta T^M(z), \delta g(y)\} \quad \text{(A.8)} \\ &\quad +\kappa\int d^3z \{\delta g(y), \delta\mathcal{C}'_L(z)\}\delta^L_M\{\delta T^M(z), \delta f(x)\} \\ \{f,g\}^*|_{\delta^1} &:= -\kappa\int d^3z \{\delta f(x), \delta^2\mathcal{C}'_L(z)\}\delta^L_M\{\delta T^M(z), \delta g(y)\} \\ &\quad +\kappa\int d^3z \{\delta g(y), \delta^2\mathcal{C}'_L(z)\}\delta^L_M\{\delta T^M(z), \delta f(x)\}, \end{aligned}$$

where we again used that $\delta^2 f = \delta^2 g = 0$ and that we can replace $\delta\mathcal{G}^M$ by δT^M inside the Poisson brackets. Given this notation we can write $O_{\{\delta f,\delta g\}^*,\{T\}}$ up to linear order as

$$\begin{aligned} O_{\{\delta f,\delta g\}^*,\{T\}} &= \{f,g\}^*|_{\delta^0} + \{f,g\}^*|_{\delta^1} - \kappa\int d^3z \delta\mathcal{G}^K(z)\{\{f,g\}^*|_{\delta^1}, \delta\mathcal{C}'_K(z)\} + O(\delta^2,\kappa^2) \\ &= \{f,g\}^*|_{\delta^0} + \{f,g\}^*|_{\delta^1} \\ &\quad -\kappa^2\int d^3z\int d^3z' \delta\mathcal{G}^L(z)\Big(-\delta^K_M\{\delta T^M(z'), \delta g\}\{\{\delta f, \delta^2\mathcal{C}'_K(z')\}, \delta\mathcal{C}'_L(z)\} \\ &\qquad\qquad -\delta^K_M\{\delta T^M(z'), \delta f\}\{\{\delta g, \delta^2\mathcal{C}'_K(z')\}, \delta\mathcal{C}'_L(z)\}\Big) \\ &\quad +O(\delta^2,\kappa^2). \quad \text{(A.9)} \end{aligned}$$

Hence, we need to show that $\{O^{(1)}_{\delta f,\{T\}} + O^{(2)}_{\delta f,\{T\}}, O^{(1)}_{\delta g,\{T\}} + O^{(2)}_{\delta g,\{T\}}\}$ agrees with the right hand side of (A.9). To confirm this, we insert the Dirac observables of δf and δg up to second order in (A.5) into the Poisson bracket and collect all terms in the individual orders. In order δ^0 we obtain

$$\begin{aligned} \delta^0: &\quad \{\delta f(x), \delta g(y)\} - \kappa\int d^3z \{\delta f(x), \delta T^L(z)\}\{\delta g(y), \delta\mathcal{C}'_L(z)\} \quad \text{(A.10)} \\ &\quad -\kappa\int d^3z \{\delta T^L(z), \delta g(y)\}\{\delta f(x), \delta\mathcal{C}'_L(z)\} \\ &= \{f(x), g(y)\}^*|_{\delta^0}, \end{aligned}$$

where we used the antisymmetry of the Poisson bracket and replaced $\delta\mathcal{G}^M$ by δT^M inside the Poisson bracket. For the linear order in δ the result is given by

$$\begin{aligned}\delta^1: \quad & \underbrace{-\kappa\int d^3z\mathcal{G}^M(z)\{\delta f(x),\{\delta g(y),\delta^2\mathcal{C}'_M(z)\}\}}_{=:A_1}\underbrace{-\kappa\int d^3z\{\delta f(x),\delta T^M(z)\}\{\delta g(y),\delta^2\mathcal{C}'_M(z)\}}_{=:B_1}\\ & \underbrace{-\kappa\int d^3z\mathcal{G}^K(z)\{\{\delta f(x),\delta^2\mathcal{C}'_K(z)\},\delta g(y)\}}_{=:A_2}\underbrace{-\kappa\int d^3z\{\delta T^K(z),\delta g(y)\}\{\delta f(x),\delta^2\mathcal{C}'_K(z)\}}_{=:B_2}\\ & \underbrace{-\kappa^2\int d^3z\int d^3z'\{\delta f(x),\delta T^M(z)\}\delta\mathcal{G}^N(z')\{\{\delta g(y),\delta^2\mathcal{C}'_M(z)\},\delta\mathcal{C}'_N(z')\}}_{:=C_1}\\ & \underbrace{-\kappa^2\int d^3z\int d^3z'\{\delta T^K(z),\delta g(y)\}\delta\mathcal{G}^L(z')\{\{\delta f(x),\delta^2\mathcal{C}'_K(z)\},\delta\mathcal{C}'_L(z')\}}_{:=C_2}. \qquad (A.11)\end{aligned}$$

Now let us discuss the individual contributions separately. First we show that $A_1 + A_2 = 0$. Using the Jacobi identity for A_1 we obtain

$$\begin{aligned}A_1 &= -\kappa\int d^3z\mathcal{G}^M(z)\{\delta f(x),\{\delta g(y),\delta^2\mathcal{C}'_M(z)\}\} \qquad (A.12)\\ &= \kappa\int d^3z\mathcal{G}^M(z)\Big(\{\delta g(y),\{\delta^2\mathcal{C}'_M(z),\delta f(x)\}\}+\underbrace{\{\delta^2\mathcal{C}'_M(z),\underbrace{\{\delta f(x),\delta g(y)\}}_{\sim\delta^0}\}}_{=0}\Big)\\ &= \kappa\int d^3z\mathcal{G}^M(z)\{\delta g(y),\{\delta^2\mathcal{C}'_M(z),\delta f(x)\}\}\\ &= \kappa\int d^3z\mathcal{G}^M(z)\{\{\delta f(x),\delta^2\mathcal{C}'_M(z)\},\delta g(y)\}\\ &= -A_2. \qquad (A.13)\end{aligned}$$

Comparing $B_1 + B_2$ with $\{f,g\}^*|_{\delta^1}$ in (A.8) and using the antisymmetry of the Poisson bracket we realise that we have

$$B_1 + B_2 = \{f,g\}^*|_{\delta^1}. \qquad (A.14)$$

Comparing $C_1 + C_2$ with the last two terms in (A.9) and applying a suitable relabelling of the integration variables it turns out that these two expressions are exactly identical. Thus, collecting all intermediate results we have shown

$$O_{\{\delta f,\delta g\}^*,\{T\}} = A_1 + A_2 + B_1 + B_2 + C_1 + C_2 + O(\delta^2,\kappa^2) = \{O_{\delta f,\{T\}}, O_{\delta g,\{T\}}\} + O(\delta^2,\kappa^2),$$

which is exactly the equality in (A.7) we wanted to prove.
Now let us discuss the case of elementary variables from the matter sector. Because we use geometrical clocks if we consider for δf and δg both matter variables, then, since these will commute with all geometrical clocks, we immediately have $\{\delta f,\delta g\}^* = \{\delta f,\delta g\}$ so that we can work with the Poisson bracket instead of the Dirac bracket in (A.7) and, as discussed in the main text, the observable algebra simplifies drastically. The other case is if we consider the algebra of observables of one geometric and one matter quantity and, without loss of generality, let us

assume that δf contains geometric and δg matter variables. Then in general the Dirac bracket can differ from the Poisson bracket by those terms where δf is involved in a Poisson bracket with the geometric clocks. In this case the proof just presented carries over if we replace δg by g for the following reason: The Poisson bracket $\{g(y), \delta\mathcal{C}'_L(z)\}$ for $g(y)$ a function of elementary matter variables is of order δ^0 and hence also contributes in this case to the δ^0-order of the Dirac bracket. The second relevant Poisson bracket $\{g(y), \delta^2\mathcal{C}'_L(z)\}$ is, as before, of order δ^1 because in the order of perturbation theory we consider, the contributions to this Poisson bracket come from terms that involve the gravitational perturbations linearly and the matter variables in quadratic order, so that the final result will still be of order δ^1. Therefore, we can also apply the equality shown in (A.7) to matter variables by simply replacing δf by f and δg by g if we restrict f and g to be elementary phase space variables from the set $\phi(x), \pi(y)$. Furthermore, because the Poisson brackets of the matter variables do not involve a factor $\frac{1}{\kappa}$ in contrast to the gravitational variables, additional factors of κ can arise when the Dirac bracket with matter variables is considered. The application we need in the main text is even a more special case, so we will not discuss these terms more in detail here since they will not be needed in any further computation. The main motivation for presenting this proof here in detail was to understand under which assumptions regarding perturbation theory we can ensure that the Dirac bracket agrees with the Poisson bracket and how, if this is not the case, the explicit form of the Dirac observable of the Dirac bracket looks like in perturbation theory.

A.2 Poisson algebra of linearised Dirac observables

The content of this Appendix was already published in [1]. Here, it is presented with some modifications compared to [1] to adapt it to the flow of the thesis.

In this Appendix, we compute the Poisson algebra of the linearised Dirac observables explicitly and show that the zeroth order contributions are given by the standard canonical Poisson brackets, a result that we use in the main text of this work. In the notation of the main text for all observables $O_{f,\{T\}} = O^{(1)}_{f,\{T\}} + O^{(2)}_{f,\{T\}} + O(\delta^3, \kappa^3)$ we will neglect the contributions coming from $O^{(2)}_{f,\{T\}} + O(\delta^3, \kappa^3)$. This means that the explicit computations presented in this Appendix here do only consider the zeroth order result of the corresponding Poisson algebra. This causes no problem since we also know that this as well as the linear contribution to the Poisson algebra already form the relation to the Dirac observable of the corresponding Dirac bracket as discussed in the main text. The computation presented here should be rather understood as double checking our results for the explicit form of the Dirac observables that would yield incorrect results for the algebra in zeroth order if they were not computed correctly. For the gauge invariant geometrical degrees of freedom, one can use the following way to obtain their algebra:

$$\{\delta A_a{}^i(\vec{x},t), \delta E^b{}_j(\vec{y},t)\} = \frac{\beta}{\kappa}\delta^i_j\delta^b_a\delta(\vec{x}-\vec{y}) \implies \{\delta\underset{\smile}{A}_a{}^i(\vec{k},t), \delta\underset{\smile}{E}^b{}_j(\vec{p},t)\} = \frac{\beta}{\kappa}\delta^i_j\delta^b_a\delta(\vec{k}+\vec{p}) \quad \text{(A.15)}$$

and hence for $r, u \in \{\pm\}$:

$$\begin{aligned}\{\delta\underset{\smile}{A}^r(\vec{k},t), \delta\underset{\smile}{E}^u(\vec{p},t)\} &= \overline{m}^a(r\vec{k})\overline{m}_i(r\vec{k})\overline{m}_b(u\vec{p})\overline{m}^j(u\vec{p})\ \{\delta\underset{\smile}{A}_a{}^i(\vec{k},t), \delta\underset{\smile}{E}^b{}_j(\vec{p},t)\} \\ &= \frac{\beta}{\kappa}\overline{m}^a(r\vec{k})\overline{m}_i(r\vec{k})m_a(u\vec{k})m^b(u\vec{k})\delta(\vec{k}+\vec{p}) \\ &= \delta^{ru}\frac{\beta}{\kappa}\delta(\vec{k}+\vec{p})\,. \end{aligned} \quad \text{(A.16)}$$

Analogously, one can show that $\{\delta\underset{\smile}{A}^r(\vec{k},t),\delta\underset{\smile}{A}^u(\vec{p},t)\} = \{\delta\underset{\smile}{E}^r(\vec{k},t),\delta\underset{\smile}{E}^u(\vec{p},t)\} = 0$. From this point and from the fact that $O^{(1)}_{\delta\mathcal{A}_a{}^i,\{\delta T\}}(\vec{x},t) = O^{(1)}_{P\delta A_a{}^i,\{\delta T\}}(\vec{x},t) = PO^{(1)}_{\delta A_a{}^i,\{\delta T\}}(\vec{x},t) = PA_a{}^i(\vec{x},t)$, and similarly for δE, follows that

$$\begin{aligned}\{O^{(1)}_{\delta\mathcal{A}_a{}^i,\{\delta T\}}(\vec{x},t), O^{(1)}_{\delta\mathcal{E}^b{}_j,\{\delta T\}}(\vec{y},t)\} &= \int \frac{d^3kd^3p}{(2\pi)^3} e^{i\vec{k}\vec{x}+i\vec{p}\vec{y}} \underset{\smile}{P}_a{}^i{}_l{}^c(\vec{k})\underset{\smile}{P}^b{}_j{}^m{}_d(\vec{p})\{\delta\underset{\smile}{A}_c{}^l(\vec{k},t),\delta\underset{\smile}{E}^d{}_m(\vec{p},t)\}\\ &= \frac{\beta}{\kappa}\int \frac{d^3k}{(2\pi)^3} e^{i\vec{k}(\vec{x}-\vec{y})}\underset{\smile}{P}_a{}^i{}_l{}^c(\vec{k})\underset{\smile}{P}^b{}_j{}^l{}_c(-\vec{k})\\ &= \frac{\beta}{\kappa}\int \frac{d^3k}{(2\pi)^3} e^{i\vec{k}(\vec{x}-\vec{y})}\underset{\smile}{P}_a{}^i{}_j{}^b(\vec{k})\\ &= \frac{\beta}{\kappa}P_a{}^i{}_j{}^b\delta(\vec{x}-\vec{y})\,, \end{aligned} \tag{A.17}$$

where we used in the fourth line that $\underset{\smile}{P}^b{}_j{}^l{}_c(-\vec{k}) = \underset{\smile}{P}^b{}_j{}^l{}_c(\vec{k}) = \underset{\smile}{P}^l{}_c{}^b{}_j(\vec{k})$, as well as

$$\{O^{(1)}_{\delta\mathcal{A}_a{}^i,\{\delta T\}}(\vec{x},t), O^{(1)}_{\delta\mathcal{A}_b{}^j,\{\delta T\}}(\vec{y},t)\} = 0 \tag{A.18}$$

$$\{O^{(1)}_{\delta\mathcal{E}^a{}_i,\{\delta T\}}(\vec{x},t), O^{(1)}_{\delta\mathcal{E}^b{}_j,\{\delta T\}}(\vec{y},t)\} = 0\,. \tag{A.19}$$

For the matter variables we obtain, dropping terms in $O(\delta^2,\kappa^2)$ and higher:

$$\{O^{(1)}_{\phi,\{\delta T\}}(\vec{x},t), O^{(1)}_{\phi,\{\delta T\}}(\vec{y},t)\} = -\kappa^2(\delta\mathcal{G}^c(\vec{x},t))\delta^3(\vec{x}-\vec{y}) + \kappa^2(\delta\mathcal{G}^c(\vec{y},t))\delta^3(\vec{x}-\vec{y}) = 0 \tag{A.20}$$

$$\begin{aligned}\{O^{(1)}_{\pi,\{\delta T\}}(\vec{x},t), O^{(1)}_{\pi,\{\delta T\}}(\vec{y},t)\} = \kappa^2((\partial^y_a\,\delta\mathcal{G}(\vec{y},t) + \partial^x_a\,\delta\mathcal{G}(\vec{x},t))\partial^a_y\delta^3(\vec{x}-\vec{y})\\ + (\delta\mathcal{G}(\vec{y},t) - \delta\mathcal{G}(\vec{x},t))\Delta\delta^3(\vec{x}-\vec{y})]\end{aligned} \tag{A.21}$$

$$\{O^{(1)}_{\phi,\{\delta T\}}(\vec{x},t), O^{(1)}_{\pi,\{\delta T\}}(\vec{y},t)\} = \delta^3(\vec{x}-\vec{y}) - \kappa^2\partial^y_a[\delta\mathcal{G}^a(\vec{y},t)\delta^3(\vec{x}-\vec{y})] - \kappa^2\,\delta\mathcal{G}^a(\vec{x},t)\partial^x_a\delta^3(\vec{x}-\vec{y})\,. \tag{A.22}$$

Due to the presence of derivatives acting on the delta distributions, it is not immediately evident that all additional terms (which are of $O(\kappa)$ due to the presence of a factor κ^{-1} in the reference fields) vanish. To see this, it is convenient to consider the smeared version of the linearised observables, then it turns out that:

$$\int d^3x\int d^3y\; f(\vec{x})g(\vec{y})\{O^{(1)}_{\pi,\{\delta T\}}(\vec{x},t), O^{(1)}_{\pi,\{\delta T\}}(\vec{y},t)\} = 0 \tag{A.23}$$

$$\int d^3x\int d^3y\; f(\vec{x})g(\vec{y})\{O^{(1)}_{\phi,\{\delta T\}}(\vec{x},t), O^{(1)}_{\pi,\{\delta T\}}(\vec{y},t)\} = \int d^3x\; f(\vec{x})g(\vec{x})\,. \tag{A.24}$$

Hence we indeed end up with the desired algebra also for the matter observables:

$$\begin{aligned}\{O^{(1)}_{\phi,\{\delta T\}}(\vec{x},t), O^{(1)}_{\phi,\{\delta T\}}(\vec{y},t)\} &= 0\\ \{O^{(1)}_{\pi,\{\delta T\}}(\vec{x},t), O^{(1)}_{\pi,\{\delta T\}}(\vec{y},t)\} &= 0\\ \{O^{(1)}_{\phi,\{\delta T\}}(\vec{x},t), O^{(1)}_{\pi,\{\delta T\}}(\vec{y},t)\} &= \delta^3(\vec{x}-\vec{y})\,.\end{aligned} \tag{A.25}$$

As $O^{(1)}_{\delta\mathcal{A}_a{}^i,\{\delta T\}}$ and $O^{(1)}_{\delta\mathcal{E}^a{}_i,\{\delta T\}}$ commute with the clocks and do not depend on the original matter fields, all Poisson brackets among the $(O^{(1)}_{\delta\mathcal{A},\{\delta T\}}, O^{(1)}_{\delta\mathcal{E},\{\delta T\}})$ vanish up to $O(\delta^2,\kappa^2)$ and the $(O^{(1)}_{\phi,\{\delta T\}}, O^{(1)}_{\pi,\{\delta T\}})$ vanish up to $O(\kappa^2)$.

Appendix B Evaluation of the partition sum in the box

The content of this Appendix was already published in [1]. It is taken from the Master's thesis [5] and only included here in the Appendix for the benefit of the reader to be able to follow the derivations in the main text of this thesis in section 9, which makes use of the regularisation discussed in this Appendix. It is presented here with slight modifications compared to [1] to adapt it to the flow of the thesis.

In this Appendix, we will discuss the computation of the partition sum, working with a regularisation established by formulating the theory in a box of finite volume introduced in equation (9.5). Given that the two number operators $n_k^+ := (b_k^+)^\dagger b_k^+$ and $n_k^- := (b_k^-)^\dagger b_k^-$ mutually commute, as they live on different Hilbert spaces, the density matrix of the environment can be written in terms of the following tensor product:

$$\rho_{\mathcal{E}} = \rho_{\mathcal{E}+} \otimes \rho_{\mathcal{E}-}, \tag{B.1}$$

where

$$\rho_{\mathcal{E}r} = \frac{1}{Z_{\mathcal{E}r}} \exp\left\{-\beta \sum_{\vec{k}\in\mathbb{K}} \Omega_k n_k^r\right\}, \tag{B.2}$$

with $r \in \{+,-\}$, $Z_{\mathcal{E}r} := tr_{\mathcal{E}r}\{\rho_{\mathcal{E}r}\}$ and $tr_{\mathcal{E}r}$ denoting the partial trace over the r-part of the environmental Hilbert space $\mathcal{H}_{\mathcal{E}} = \mathcal{H}_{\mathcal{E}+} \otimes \mathcal{H}_{\mathcal{E}-}$.

At this point, we introduce an alternative notation for the summation over the discrete $\vec{k}$-vectors. Instead of summing over all elements of the set $\mathbb{K}$ that contains the discrete, permitted $\vec{k}$-vectors, we want to sum over an index running over the natural numbers. Such a bijection exists, because each possible $\vec{k}$ consists of three components $k_x, k_y, k_z \in \frac{\pi\mathbb{Z}}{L}$ with L denoting the length of the box. Thus, we can identify an element $\vec{k} \in \mathbb{K}$ uniquely by providing three numbers. A bijection between $\mathbb{Z}^3$ and $\mathbb{N}$ can be constructed therefore we can sum over $j \in \mathbb{N}$ instead of $\vec{k} \in \mathbb{K}$.

We use this notation and rewrite the number operator in terms of the occupation number basis of the corresponding part of the Hilbert space:

$$n_i^r = \sum_{n_1^r=0}^{\infty} \sum_{n_2^r=0}^{\infty} ... \sum_{n_i^r=1}^{\infty} ... \, n_i^r \, |n_1^r, n_2^r, ..., n_i^r, ...\rangle \langle n_1^r, n_2^r, ..., n_i^r, ...| \, , \tag{B.3}$$

where the individual $n_i^r \in \mathbb{N}_0$ on the right hand side are the eigenvalues of the occupation number operator and $|n_1^r, n_2^r, ..., n_i^r, ...\rangle$ the corresponding eigenstates. Due to the orthonormality of different Fock states $|n_1^r, n_2^r, ...\rangle$ we obtain

$$\exp\left\{-\beta \sum_{j\in\mathbb{N}} \Omega_j n_j^r\right\} = \sum_{n_1^r=0}^{\infty} \sum_{n_2^r=0}^{\infty} ... \prod_{i\in\mathbb{N}} e^{-\beta \, n_i^r \Omega_i} \, |n_1^r, n_2^r, ...\rangle \langle n_1^r, n_1^r, ...| \, . \tag{B.4}$$

From the regularisation, where we consider the system to be in a finite box, we can express the partial trace in terms of Fock states and find:

$$tr_{\mathcal{E}r}\{.\} = \sum_{n_1^r=0}^{\infty} \sum_{n_2^r=0}^{\infty} ... \langle n_1^r, n_2^r, ...| \, . \, |n_1^r, n_2^r, ...\rangle \, . \tag{B.5}$$

We can use this expression to evaluate the partition sum of the Gibbs state:

$$Z_{\mathcal{E}r} = tr_{\mathcal{E}r}\left(\exp\left\{-\beta\sum_{j\in\mathbb{N}}\Omega_j n_j^r\right\}\right) = \sum_{n_1^r=0}^{\infty}\sum_{n_2^r=0}^{\infty}...\prod_{j\in\mathbb{N}} e^{-\beta\, n_j^r\Omega_j} = \sum_{n_1^r=0}^{\infty}\sum_{n_2^r=0}^{\infty}...\prod_{j\in\mathbb{N}}\left[e^{-\beta\,\Omega_j}\right]^{n_j^r}$$
$$= \left(\sum_{n_1^r=0}^{\infty}\left[e^{-\beta\,\Omega_1}\right]^{n_1^r}\right)\cdot\left(\sum_{n_2^r=0}^{\infty}\left[e^{-\beta\,\Omega_2}\right]^{n_2^r}\right)\cdot ... = \prod_{i\in\mathbb{N}}\left(\sum_{n_i^r=0}^{\infty}\left[e^{-\beta\,\Omega_i}\right]^{n_i^r}\right) = \prod_{i\in\mathbb{N}}\frac{1}{1-e^{-\beta\,\Omega_i}}\,. \tag{B.6}$$

In the last step we assumed that $\vec{k}=0$, which corresponds to $\Omega_k = 0$, is not contained in the set $\mathbb{K}$, which is the usual infrared divergence present in quantum field theory. Then $e^{-\beta\,\Omega_i} < 1$ always holds and the expression is a geometric series.
In actual applications it is important that the partition sum is finite. This is indeed the case, a proof can be found for instance in [5]. The final partition sum for part r of the environment in (B.6) is independent of this label r, so we get the same result for $r = +$ and $r = -$ respectively. From (B.1) one can then see that the partition sum of the total environmental Gibbs state is thus just given by the square of (B.6):

$$Z_{\mathcal{E}} = \left[\prod_{j\in\mathbb{N}}\frac{1}{1-e^{-\beta\,\Omega_j}}\right]^2\,. \tag{B.7}$$

Making use of the regularisation, we can also compute the following trace which appears in the main text:

$$N(\Omega_k) := tr_{\mathcal{E}}\left\{n_k^r\,\rho_{\mathcal{E}}\right\} = \frac{1}{Z_{\mathcal{E}r}}\sum_{\substack{n_1^r=0\\ \tilde{n}_1^r=0}}^{\infty}...\sum_{\substack{n_K^r=0\\ \tilde{n}_K^r=0}}^{\infty}\langle n_1^r,...,n_K^r|\,n_k^r e^{-\beta\sum_{j=1}^{K}\tilde{n}_j^r\Omega_j}|\tilde{n}_1^r,...,\tilde{n}_K^r\rangle$$
$$\cdot\langle\tilde{n}_1^r,...,\tilde{n}_K^r|n_1^r,...,n_K^r\rangle$$
$$= \frac{1}{Z_{\mathcal{E}r}}\sum_{n_1^r=0}^{\infty}...\sum_{n_K^r=0}^{\infty}\langle n_1^r,...,n_K^r|\,n_k^r e^{-\beta\sum_{j=1}^{K}n_j^r\Omega_j}|n_1^r,...,n_K^r\rangle$$
$$= \frac{1}{-\beta}\frac{1}{Z_{\mathcal{E}r}}\frac{\partial}{\partial\Omega_k}\sum_{n_1^r=0}^{\infty}...\sum_{n_K^r=0}^{\infty}\langle n_1^r,...,n_K^r|\,e^{-\beta\sum_{j=1}^{K}n_j^r\Omega_j}|n_1^r,...,n_K^r\rangle$$
$$= \frac{1}{-\beta Z_{\mathcal{E}r}}\frac{\partial Z_{\mathcal{E}r}}{\partial\Omega_k} = \frac{1}{-\beta}\frac{\partial}{\partial\Omega_k}\ln(Z_{\mathcal{E}r}) = \frac{1}{-\beta}\frac{\partial}{\partial\Omega_k}\left[-\sum_{j=1}^{K}\ln\left(1-e^{-\beta\Omega_j}\right)\right]$$
$$= \frac{e^{-\beta\Omega_k}}{1-e^{-\beta\Omega_k}} = \frac{1}{e^{\beta\Omega_k}-1}\,. \tag{B.8}$$

As expected, this yields the Bose-Einstein distribution.

References

[1] Max Joseph Fahn, Kristina Giesel, and Michael Kobler. "A gravitationally induced decoherence model using Ashtekar variables". In: *Class. Quant. Grav.* 40.9 (2023), p. 094002. DOI: 10.1088/1361-6382/acc5d5. arXiv: 2206.06397 [gr-qc].

[2] Max Joseph Fahn and Kristina Giesel. "Gravitationally induced decoherence of a scalar field: investigating the one-particle sector and its interplay with renormalisation". In: (Sept. 2024). arXiv: 2409.12790 [hep-th].

[3] Alba Domi, Thomas Eberl, Max Joseph Fahn, Kristina Giesel, Lukas Hennig, Ulrich Katz, Roman Kemper, and Michael Kobler. "Understanding gravitationally induced decoherence parameters in neutrino oscillations using a microscopic quantum mechanical model". Mar. 2024. arXiv: 2403.03106v3 [gr-qc].

[4] Alba Domi, Thomas Eberl, Max Joseph Fahn, Kristina Giesel, Lukas Hennig, Ulrich Katz, Roman Kemper, and Michael Kobler. "Understanding gravitationally induced decoherence parameters in neutrino oscillations using a microscopic quantum mechanical model". In: *JCAP* 11 (2024), p. 006. DOI: 10.1088/1475-7516/2024/11/006.

[5] Max Joseph Fahn. "Gravitationally induced decoherence in open quantum systems using linearised gravity formulated in Ashtekar variables." Master's thesis. Friedrich-Alexander-Universität Erlangen-Nürnberg, Supervisor: Kristina Giesel, 2020.

[6] Max Joseph Fahn, Kristina Giesel, and Roman Kemper. "A gravitationally induced decoherence model for photons in the context of the relational formalism." In preparation.

[7] Barton Zwiebach. *A first course in string theory*. Cambridge university press, 2004.

[8] Katrin Becker, Melanie Becker, and John H Schwarz. *String theory and M-theory: A modern introduction*. Cambridge university press, 2006.

[9] David Tong. "String Theory". Jan. 2009. arXiv: 0908.0333 [hep-th].

[10] Carlo Rovelli. *Quantum Gravity*. Cambridge Monographs on Mathematical Physics. Cambridge University Press, 2004. DOI: 10.1017/CBO9780511755804.

[11] Thomas Thiemann. *Modern Canonical Quantum General Relativity*. Cambridge Monographs on Mathematical Physics. Cambridge University Press, 2007. DOI: 10.1017/CBO9780511755682.

[12] Carlo Rovelli and Francesca Vidotto. *Covariant Loop Quantum Gravity: An Elementary Introduction to Quantum Gravity and Spinfoam Theory*. Cambridge University Press, 2014. DOI: 10.1017/CBO9781107706910.

[13] Abhay Ashtekar and Parampreet Singh. "Loop Quantum Cosmology: A Status Report". In: *Class. Quant. Grav.* 28 (2011), p. 213001. DOI: 10.1088/0264-9381/28/21/213001. arXiv: 1108.0893 [gr-qc].

[14] Ivan Agullo and Alejandro Corichi. "Loop quantum cosmology". In: *Springer Handbook of Spacetime*. Springer, 2014, pp. 809–839.

[15] Luis E Ibanez and Angel M Uranga. *String theory and particle physics: An introduction to string phenomenology*. Cambridge University Press, 2012.

[16] Michele Cicoli, Joseph P. Conlon, Anshuman Maharana, Susha Parameswaran, Fernando Quevedo, and Ivonne Zavala. "String cosmology: From the early universe to today". In: *Phys. Rept.* 1059 (2024), pp. 1–155. DOI: 10.1016/j.physrep.2024.01.002. arXiv: 2303.04819 [hep-th].

[17] Martin Bojowald. "Loop quantum cosmology". In: *Living Reviews in Relativity* 11 (2008), pp. 1–131.

[18] Ivan Agullo and Parampreet Singh. "Loop Quantum Cosmology". In: *Loop Quantum Gravity: The First 30 Years*. Ed. by Abhay Ashtekar and Jorge Pullin. WSP, 2017, pp. 183–240. DOI: 10.1142/9789813220003_0007. arXiv: 1612.01236 [gr-qc].

[19] Bao-Fei Li and Parampreet Singh. "Loop Quantum Cosmology: Physics of Singularity Resolution and its Implications". Apr. 2023. arXiv: 2304.05426 [gr-qc].

[20] Martin Bojowald. "Quantization ambiguities in isotropic quantum geometry". In: *Class. Quant. Grav.* 19 (2002), pp. 5113–5230. DOI: 10.1088/0264-9381/19/20/306. arXiv: gr-qc/0206053.

[21] Abhay Ashtekar, Tomasz Pawlowski, and Parampreet Singh. "Quantum Nature of the Big Bang: Improved dynamics". In: *Phys. Rev. D* 74 (2006), p. 084003. DOI: 10.1103/PhysRevD.74.084003. arXiv: gr-qc/0607039.

[22] G. Hinshaw et al. "Nine-Year Wilkinson Microwave Anisotropy Probe (WMAP) Observations: Cosmological Parameter Results". In: *Astrophys. J. Suppl.* 208 (2013), p. 19. DOI: 10.1088/0067-0049/208/2/19. arXiv: 1212.5226 [astro-ph.CO].

[23] P. A. R. Ade et al. "Planck 2015 results. XIII. Cosmological parameters". In: *Astron. Astrophys.* 594 (2016), A13. DOI: 10.1051/0004-6361/201525830. arXiv: 1502.01589 [astro-ph.CO].

[24] Beatriz Elizaga Navascués, Mercedes Martín-Benito, and Guillermo A. Mena Marugán. "Hybrid models in loop quantum cosmology". In: *Int. J. Mod. Phys. D* 25.08 (2016), p. 1642007. DOI: 10.1142/S0218271816420074. arXiv: 1608.05947 [gr-qc].

[25] Edward Wilson-Ewing. "Testing loop quantum cosmology". In: *Comptes Rendus Physique* 18 (2017), pp. 207–225. DOI: 10.1016/j.crhy.2017.02.004. arXiv: 1612.04551 [gr-qc].

[26] Max Joseph Fahn, Kristina Giesel, and Michael Kobler. "Dynamical Properties of the Mukhanov-Sasaki Hamiltonian in the context of adiabatic vacua and the Lewis-Riesenfeld invariant". In: *Universe* 5.7 (2019), p. 170. DOI: 10.3390/universe5070170. arXiv: 1812.11122 [gr-qc].

[27] Muxin Han, Haida Li, and Hongguang Liu. "Manifestly gauge-invariant cosmological perturbation theory from full loop quantum gravity". In: *Phys. Rev. D* 102.12 (2020), p. 124002. DOI: 10.1103/PhysRevD.102.124002. arXiv: 2005.00883 [gr-qc].

[28] Abhay Ashtekar and Martin Bojowald. "Quantum geometry and the Schwarzschild singularity". In: *Class. Quant. Grav.* 23 (2006), pp. 391–411. DOI: 10.1088/0264-9381/23/2/008. arXiv: gr-qc/0509075.

[29] Leonardo Modesto. "Loop quantum black hole". In: *Classical and Quantum Gravity* 23.18 (2006), p. 5587.

[30] Beatriz Elizaga Navascués, Alejandro García-Quismondo, and Guillermo A. Mena Marugán. "Hamiltonian formulation and loop quantization of a recent extension of the Kruskal spacetime". In: *Phys. Rev. D* 106.4 (2022), p. 043531. DOI: 10.1103/PhysRevD.106.043531. arXiv: 2208.00425 [gr-qc].

[31] Abhay Ashtekar, Javier Olmedo, and Parampreet Singh. "Regular black holes from loop quantum gravity". In: *Regular Black Holes: Towards a New Paradigm of Gravitational Collapse*. Springer, 2023, pp. 235–282. arXiv: 2301.01309 [gr-qc].

[32] Hal M. Haggard and Carlo Rovelli. "Quantum-gravity effects outside the horizon spark black to white hole tunneling". In: *Phys. Rev. D* 92.10 (2015), p. 104020. DOI: 10.1103/PhysRevD.92.104020. arXiv: 1407.0989 [gr-qc].

[33] Norbert Bodendorfer, Fabio M. Mele, and Johannes Münch. "Mass and Horizon Dirac Observables in Effective Models of Quantum Black-to-White Hole Transition". In: *Class. Quant. Grav.* 38.9 (2021), p. 095002. DOI: 10.1088/1361-6382/abe05d. arXiv: 1912.00774 [gr-qc].

[34] Antoine Rignon-Bret and Carlo Rovelli. "Black to white transition of a charged black hole". In: *Phys. Rev. D* 105.8 (2022), p. 086003. DOI: 10.1103/PhysRevD.105.086003. arXiv: 2108.12823 [gr-qc].

[35] Eugene P Wigner. "The problem of measurement". In: *American Journal of Physics* 31.1 (1963), pp. 6–15.

[36] A. J. Leggett. "The Quantum Measurement Problem". In: *Science* 307.5711 (2005), pp. 871–872. DOI: 10.1126/science.1109541. eprint: https://www.science.org/doi/pdf/10.1126/science.1109541. URL: https://www.science.org/doi/abs/10.1126/science.1109541.

[37] Časlav Brukner. "On the quantum measurement problem". In: *Quantum [un] speakables II: half a century of Bell's theorem* (2017), pp. 95–117.

[38] Dennis Dieks. "Resolution of the measurement problem through decoherence of the quantum state". In: *Physics Letters A* 142.8-9 (1989), pp. 439–446.

[39] Maximilian Schlosshauer. "Decoherence, the Measurement Problem, and Interpretations of Quantum Mechanics". In: *Rev. Mod. Phys.* 76 (2004), pp. 1267–1305. DOI: 10.1103/RevModPhys.76.1267. arXiv: quant-ph/0312059.

[40] David Wallace. "Decoherence and its role in the modern measurement problem". In: *Philosophical Transactions of the Royal Society A: Mathematical, Physical and Engineering Sciences* 370.1975 (2012), pp. 4576–4593.

[41] D. Giulini, C. Kiefer, E. Joos, J. Kupsch, I. O. Stamatescu, and H. D. Zeh. *Decoherence and the appearance of a classical world in quantum theory*. 1996.

[42] Wojciech H Zurek. "Decoherence and the transition from quantum to classical-revisited". In: *Los Alamos Science* 27 (2002), pp. 86–109.

[43] Maximilian Schlosshauer and Kristian Camilleri. "What classicality? Decoherence and Bohr's classical concepts". In: *AIP Conference Proceedings*. Vol. 1327. 1. American Institute of Physics. 2011, pp. 26–35.

[44] Maximilian Schlosshauer. "The quantum-to-classical transition and decoherence". Apr. 2014. arXiv: 1404.2635 [quant-ph].

[45] Heinz-Peter Breuer, Francesco Petruccione, et al. *The theory of open quantum systems*. Oxford University Press on Demand, 2002.

[46] K. Hornberger. "Introduction to Decoherence Theory". In: *Lecture Notes in Physics*. Springer Berlin Heidelberg, pp. 221–276. ISBN: 9783540881698. DOI: 10.1007/978-3-540-88169-8_5. URL: http://dx.doi.org/10.1007/978-3-540-88169-8_5.

[47] Ulrich Weiss. *Quantum dissipative systems*. Singapore: World Scientific, 2012. ISBN: 9789812791795.

[48] Claude Cohen Tannoudji, Gilbert Grynberg, and J Dupont-Roe. *Atom-photon interactions*. New York, NY (United States); John Wiley and Sons Inc., 1992.

[49] Howard J Carmichael. *Statistical methods in quantum optics 1: master equations and Fokker-Planck equations*. Vol. 1. Springer Science & Business Media, 1999.

[50] Sushanta Dattagupta and Sanjay Puri. *Dissipative phenomena in condensed matter: some applications*. Vol. 71. Springer Science & Business Media, 2004.

[51] Dieter Heiss. *Fundamentals of quantum information: quantum computation, communication, decoherence and all that*. Vol. 587. Springer, 2008.

[52] Miguel Orszag. *Quantum optics: including noise reduction, trapped ions, quantum trajectories, and decoherence*. Springer, 2016.

[53] Jonathan J. Halliwell. "Decoherence in quantum cosmology". In: *Phys. Rev. D* 39 (10 1989), pp. 2912–2923. DOI: 10.1103/PhysRevD.39.2912.

[54] David Polarski and Alexei A. Starobinsky. "Semiclassicality and decoherence of cosmological perturbations". In: *Class. Quant. Grav.* 13 (1996), pp. 377–392. DOI: 10.1088/0264-9381/13/3/006. arXiv: gr-qc/9504030.

[55] Raymond LaFlamme and Jorma Louko. "Reduced density matrices and decoherence in quantum cosmology". In: *Phys. Rev. D* 43 (1991), pp. 3317–3331. DOI: 10.1103/PhysRevD.43.3317.

[56] Cliff P. Burgess, R. Holman, and D. Hoover. "Decoherence of inflationary primordial fluctuations". In: *Phys. Rev. D* 77 (2008), p. 063534. DOI: 10.1103/PhysRevD.77.063534. arXiv: astro-ph/0601646.

[57] D. Boyanovsky. "Effective field theory during inflation: Reduced density matrix and its quantum master equation". In: *Phys. Rev. D* 92.2 (2015), p. 023527. DOI: 10.1103/PhysRevD.92.023527. arXiv: 1506.07395 [astro-ph.CO].

[58] T. J. Hollowood and J. I. McDonald. "Decoherence, discord and the quantum master equation for cosmological perturbations". In: *Phys. Rev. D* 95.10 (2017), p. 103521. DOI: 10.1103/PhysRevD.95.103521. arXiv: 1701.02235 [gr-qc].

[59] Jerome Martin and Vincent Vennin. "Observational constraints on quantum decoherence during inflation". In: *JCAP* 05 (2018), p. 063. DOI: 10.1088/1475-7516/2018/05/063. arXiv: 1801.09949 [astro-ph.CO].

[60] C. Anastopoulos and B. L. Hu. "A Master Equation for Gravitational Decoherence: Probing the Textures of Spacetime". In: *Class. Quant. Grav.* 30 (2013), p. 165007. DOI: 10.1088/0264-9381/30/16/165007. arXiv: 1305.5231 [gr-qc].

[61] M. P. Blencowe. "Effective Field Theory Approach to Gravitationally Induced Decoherence". In: *Phys. Rev. Lett.* 111.2 (2013), p. 021302. DOI: 10.1103/PhysRevLett.111.021302. arXiv: 1211.4751 [quant-ph].

[62] Teodora Oniga and Charles H. T. Wang. "Quantum gravitational decoherence of light and matter". In: *Phys. Rev. D* 93.4 (2016), p. 044027. DOI: 10.1103/PhysRevD.93.044027. arXiv: 1511.06678 [quant-ph].

[63] Michalis Lagouvardos and Charis Anastopoulos. "Gravitational decoherence of photons". In: *Class. Quant. Grav.* 38.11 (2021), p. 115012. DOI: 10.1088/1361-6382/abf2f3. arXiv: 2011.08270 [gr-qc].

[64] Peter W Shor. "Scheme for reducing decoherence in quantum computer memory". In: *Physical review A* 52.4 (1995), R2493. DOI: 10.1103/physreva.52.r2493.

[65] D. A. Lidar, I. L. Chuang, and K. B. Whaley. "Decoherence free subspaces for quantum computation". In: *Phys. Rev. Lett.* 81 (1998), p. 2594. DOI: 10.1103/PhysRevLett.81.2594. arXiv: quant-ph/9807004.

[66] Bao-Jie Liu, Lei-Lei Yan, Yuan Zhang, Man-Hong Yung, Erjun Liang, Shi-Lei Su, and Chong-Xin Shan. "Decoherence-suppressed nonadiabatic holonomic quantum computation". In: *Phys. Rev. Res.* 5.1 (2023), p. 013059. DOI: 10.1103/PhysRevResearch.5.013059. arXiv: 2204.06249 [quant-ph].

[67] Angelo Bassi, André Großardt, and Hendrik Ulbricht. "Gravitational Decoherence". In: *Class. Quant. Grav.* 34.19 (2017), p. 193002. DOI: 10.1088/1361-6382/aa864f. arXiv: 1706.05677 [quant-ph].

[68] Charis Anastopoulos and Bei-Lok Hu. "Gravitational decoherence: A thematic overview". In: *AVS Quantum Sci.* 4.1 (2022), p. 015602. DOI: 10.1116/5.0077536. arXiv: 2111.02462 [gr-qc].

[69] Sandro Donadi and Angelo Bassi. "Seven nonstandard models coupling quantum matter and gravity". In: *AVS Quantum Sci.* 4.2 (2022), p. 025601. DOI: 10.1116/5.0089318. arXiv: 2202.13542 [quant-ph].

[70] C Moller. "Les Theories Relativistes de la Gravitation Colloques Internationaux CNRX 91 edited by A Lichnerowicz and M.-A. Tonnelat (Paris: CNRS)(1962). L. Rosenfeld". In: *Nucl. Phys* 40 (1963), p. 353.

[71] Leon Rosenfeld. "On quantization of fields". In: *Nuclear Physics* 40 (1963), pp. 353–356. DOI: 10.1016/0029-5582(63)90279-7.

[72] Roger Penrose and Chris J Isham. *Quantum concepts in space and time*. Clarendon, 1986.

[73] Lajos Diosi. "A universal master equation for the gravitational violation of quantum mechanics". In: *Physics letters A* 120.8 (1987), pp. 377–381. DOI: 10.1016/0375-9601(87)90681-5.

[74] Lajos Diósi. "Models for universal reduction of macroscopic quantum fluctuations". In: *Physical Review A* 40.3 (1989), p. 1165. DOI: 10.1103/PhysRevA.40.1165.

[75] Roger Penrose. "On gravity's role in quantum state reduction". In: *General relativity and gravitation* 28 (1996), pp. 581–600. DOI: 10.1007/BF02105068.

[76] B. L. Hu. "Gravitational Decoherence, Alternative Quantum Theories and Semiclassical Gravity". In: *J. Phys. Conf. Ser.* 504 (2014). Ed. by Gerhard Grössing, Hans-Thomas Elze, Johannes Mesa Pascasio, and Jan Walleczek, p. 012021. DOI: 10.1088/1742-6596/504/1/012021. arXiv: 1402.6584 [gr-qc].

[77] C. Anastopoulos and B. L. Hu. "Problems with the Newton-Schrödinger equations". In: *New J. Phys.* 16 (2014), p. 085007. DOI: 10.1088/1367-2630/16/8/085007. arXiv: 1403.4921 [quant-ph].

[78] John R. Ellis, N. E. Mavromatos, and Dimitri V. Nanopoulos. "String theory modifies quantum mechanics". In: *Phys. Lett. B* 293 (1992), pp. 37–48. DOI: 10.1016/0370-2693(92)91478-R. arXiv: hep-th/9207103.

[79] Luis J. Garay. "Space-time foam as a quantum thermal bath". In: *Phys. Rev. Lett.* 80 (1998), pp. 2508–2511. DOI: 10.1103/PhysRevLett.80.2508. arXiv: gr-qc/9801024.

[80] Pieter Kok and Ulvi Yurtsever. "Gravitational decoherence". In: *Phys. Rev. D* 68 (2003), p. 085006. DOI: 10.1103/PhysRevD.68.085006. arXiv: gr-qc/0306084.

[81] H. -P. Breuer, E. Goklu, and C. Lammerzahl. "Metric fluctuations and decoherence". In: *Class. Quant. Grav.* 26 (2009), p. 105012. DOI: 10.1088/0264-9381/26/10/105012. arXiv: 0812.0420 [gr-qc].

[82] Lorenzo Asprea, Angelo Bassi, Hendrik Ulbricht, and Giulio Gasbarri. "Gravitational Decoherence and the Possibility of Its Interferometric Detection". In: *Phys. Rev. Lett.* 126.20 (2021), p. 200403. DOI: 10.1103/PhysRevLett.126.200403. arXiv: 1912.12732 [gr-qc].

[83] Stanley Deser, R. Arnowitt, and C. W. Misner. "Consistency of Canonical Reduction of General Relativity". In: *J. Math. Phys.* 1 (1960), p. 434. DOI: 10.1063/1.1703677.

[84] Sandro Donadi, Kristian Piscicchia, Catalina Curceanu, Lajos Diósi, Matthias Laubenstein, and Angelo Bassi. "Underground test of gravity-related wave function collapse". In: *Nature Phys.* 17.1 (2021), pp. 74–78. DOI: 10.1038/s41567-020-1008-4. arXiv: 2111.13490 [quant-ph].

[85] F. Benatti and R. Floreanini. "Massless neutrino oscillations". In: *Phys. Rev. D* 64 (2001), p. 085015. DOI: 10.1103/PhysRevD.64.085015. arXiv: hep-ph/0105303.

[86] Joao A. B. Coelho and W. Anthony Mann. "Decoherence, matter effect, and neutrino hierarchy signature in long baseline experiments". In: *Phys. Rev. D* 96.9 (2017), p. 093009. DOI: 10.1103/PhysRevD.96.093009. arXiv: 1708.05495 [hep-ph].

[87] Jose Carpio, E. Massoni, and A. M. Gago. "Revisiting quantum decoherence for neutrino oscillations in matter with constant density". In: *Phys. Rev. D* 97.11 (2018), p. 115017. DOI: 10.1103/PhysRevD.97.115017. arXiv: 1711.03680 [hep-ph].

[88] Valentina De Romeri, Carlo Giunti, Thomas Stuttard, and Christoph A. Ternes. "Neutrino oscillation bounds on quantum decoherence". In: *JHEP* 09 (2023), p. 097. DOI: 10.1007/JHEP09(2023)097. arXiv: 2306.14699 [hep-ph].

[89] A. L. G. Gomes, R. A. Gomes, and O. L. G. Peres. "Quantum decoherence and relaxation in long-baseline neutrino data". In: *JHEP* 10 (2023), p. 035. DOI: 10.1007/JHEP10(2023)035. arXiv: 2001.09250 [hep-ph].

[90] J. A. Carpio, E. Massoni, and A. M. Gago. "Testing quantum decoherence at DUNE". In: *Phys. Rev. D* 100.1 (2019), p. 015035. DOI: 10.1103/PhysRevD.100.015035. arXiv: 1811.07923 [hep-ph].

[91] Jun Wang et al. "Damping signatures at JUNO, a medium-baseline reactor neutrino oscillation experiment". In: *JHEP* 06 (2022), p. 062. DOI: 10.1007/JHEP06(2022)062. arXiv: 2112.14450 [hep-ex].

[92] IceCube Collaboration. "Searching for Decoherence from Quantum Gravity at the IceCube South Pole Neutrino Observatory". July 2023. arXiv: 2308.00105 [hep-ex].

[93] Nadja Lessing and KM3NeT Collaboration. "Search for Quantum Decoherence in Neutrino Oscillations with KM3NeT ORCA6". In: *PoS* ICRC2023 (2023), p. 1025. DOI: 10.22323/1.444.1025.

[94] G. Barenboim, A. Calatayud-Cadenillas, A. M. Gago, and C. A. Ternes. "Quantum Decoherence effects on precision measurements at DUNE and T2HK". Feb. 2024. arXiv: 2402.16395 [hep-ph].

[95] Thomas Stuttard and Mikkel Jensen. "Neutrino decoherence from quantum gravitational stochastic perturbations". In: *Phys. Rev. D* 102.11 (2020), p. 115003. DOI: 10.1103/PhysRevD.102.115003. arXiv: 2007.00068 [hep-ph].

[96] E. Lisi, A. Marrone, and D. Montanino. "Probing possible decoherence effects in atmospheric neutrino oscillations". In: *Phys. Rev. Lett.* 85 (2000), pp. 1166–1169. DOI: 10.1103/PhysRevLett.85.1166. arXiv: hep-ph/0002053.

[97] F. Benatti and R. Floreanini. "Open system approach to neutrino oscillations". In: *JHEP* 02 (2000), p. 032. DOI: 10.1088/1126-6708/2000/02/032. arXiv: hep-ph/0002221.

[98] Alexander Sakharov, Nick Mavromatos, Anselmo Meregaglia, Andre Rubbia, and Sarben Sarkar. "Exploration of Possible Quantum Gravity Effects with Neutrinos. I. Decoherence in Neutrino Oscillations Experiments". In: *J. Phys. Conf. Ser.* 171 (2009). Ed. by J. Bernabeu, F. J. Botella, N. E. Mavromatos, and V. A. Mitsou, p. 012038. DOI: 10.1088/1742-6596/171/1/012038. arXiv: 0903.4985 [hep-ph].

[99] G. Balieiro Gomes, D. V. Forero, M. M. Guzzo, P. C. De Holanda, and R. L. N. Oliveira. "Quantum Decoherence Effects in Neutrino Oscillations at DUNE". In: *Phys. Rev. D* 100.5 (2019), p. 055023. DOI: 10.1103/PhysRevD.100.055023. arXiv: 1805.09818 [hep-ph].

[100] A. M. Gago, E. M. Santos, W. J. C. Teves, and R. Zukanovich Funchal. "Quantum dissipative effects and neutrinos: Current constraints and future perspectives". In: *Phys. Rev. D* 63 (2001), p. 073001. DOI: 10.1103/PhysRevD.63.073001. arXiv: hep-ph/0009222.

[101] A. M. Gago, E. M. Santos, W. J. C. Teves, and R. Zukanovich Funchal. "A Study on quantum decoherence phenomena with three generations of neutrinos". In: (Aug. 2002). arXiv: hep-ph/0208166.

[102] Dean Morgan, Elizabeth Winstanley, Jurgen Brunner, and Lee F. Thompson. "Probing quantum decoherence in atmospheric neutrino oscillations with a neutrino telescope". In: *Astropart. Phys.* 25 (2006), pp. 311–327. DOI: 10.1016/j.astropartphys.2006.03.001. arXiv: astro-ph/0412618.

[103] Marcelo M. Guzzo, Pedro C. de Holanda, and Roberto L. N. Oliveira. "Quantum Dissipation in a Neutrino System Propagating in Vacuum and in Matter". In: *Nucl. Phys. B* 908 (2016), pp. 408–422. DOI: 10.1016/j.nuclphysb.2016.04.030. arXiv: 1408.0823 [hep-ph].

[104] A. L. G. Gomes, R. A. Gomes, and O. L. G. Peres. "Quantum decoherence and relaxation in long-baseline neutrino data". In: *JHEP* 10 (2023), p. 035. DOI: 10.1007/JHEP10(2023)035. arXiv: 2001.09250 [hep-ph].

[105] Pilar Coloma, Jacobo Lopez-Pavon, Ivan Martinez-Soler, and Hiroshi Nunokawa. "Decoherence in Neutrino Propagation Through Matter, and Bounds from IceCube/DeepCore". In: *Eur. Phys. J. C* 78.8 (2018), p. 614. DOI: 10.1140/epjc/s10052-018-6092-6. arXiv: 1803.04438 [hep-ph].

[106] Roberto L. N. Oliveira. "Dissipative Effect in Long Baseline Neutrino Experiments". In: *Eur. Phys. J. C* 76.7 (2016), p. 417. DOI: 10.1140/epjc/s10052-016-4253-z. arXiv: 1603.08065 [hep-ph].

[107] Bryce S. DeWitt. "Quantum Theory of Gravity. I. The Canonical Theory". In: *Phys. Rev.* 160 (5 1967), pp. 1113–1148. DOI: 10.1103/PhysRev.160.1113. URL: https://link.aps.org/doi/10.1103/PhysRev.160.1113.

[108] C. M. Dewitt and J. A. Wheeler, eds. *Battelle rencontres - 1967 lectures in mathematics and physics: Seattle, WA, USA, 16 - 31 July 1967*. New York, NY: W. A. Benjamin, 1968.

[109] K Kuchar. *Quantum Gravity 2: a Second Oxford Symposium ed CJ Isham, R Penrose and DW Sciama*. 1981.

[110] C. J. Isham. "Canonical quantum gravity and the problem of time". In: *NATO Sci. Ser. C* 409 (1993). Ed. by L. A. Ibort and M. A. Rodriguez, pp. 157–287. arXiv: gr-qc/9210011.

[111] C. Anastopoulos. "Quantum theory of nonrelativistic particles interacting with gravity". In: *Phys. Rev. D* 54 (1996), pp. 1600–1605. DOI: 10.1103/PhysRevD.54.1600. arXiv: gr-qc/9511004.

[112] Qidong Xu and M. P. Blencowe. "Zero-dimensional models for gravitational and scalar QED decoherence". In: *New J. Phys.* 24.11 (2022), p. 113048. DOI: 10.1088/1367-2630/aca427. arXiv: 2005.02554 [quant-ph].

[113] Clare Burrage, Christian Käding, Peter Millington, and Jiří Minář. "Open quantum dynamics induced by light scalar fields". In: *Phys. Rev. D* 100.7 (2019), p. 076003. DOI: 10.1103/PhysRevD.100.076003. arXiv: 1812.08760 [hep-th].

[114] A. Ashtekar. "New Variables for Classical and Quantum Gravity". In: *Phys. Rev. Lett.* 57 (1986), pp. 2244–2247. DOI: 10.1103/PhysRevLett.57.2244.

[115] Abhay Ashtekar, Joseph D. Romano, and Ranjeet S. Tate. "New Variables for Gravity: Inclusion of Matter". In: *Phys. Rev. D* 40 (1989), p. 2572. DOI: 10.1103/PhysRevD.40.2572.

[116] Carlo Rovelli. "What Is Observable in Classical and Quantum Gravity?" In: *Class. Quant. Grav.* 8 (1991), pp. 297–316. DOI: 10.1088/0264-9381/8/2/011.

[117] Carlo Rovelli. "QUANTUM REFERENCE SYSTEMS". In: *Class. Quant. Grav.* 8 (1991), pp. 317–332. DOI: 10.1088/0264-9381/8/2/012.

[118] Carlo Rovelli. “Partial observables”. In: *Phys. Rev.* D65 (2002), p. 124013. DOI: 10.1103/PhysRevD.65.124013. arXiv: gr-qc/0110035 [gr-qc].

[119] B. Dittrich. “Partial and complete observables for Hamiltonian constrained systems”. In: *Gen. Rel. Grav.* 39 (2007), pp. 1891–1927. DOI: 10.1007/s10714-007-0495-2. arXiv: gr-qc/0411013 [gr-qc].

[120] B. Dittrich. “Partial and complete observables for canonical general relativity”. In: *Class. Quant. Grav.* 23 (2006), pp. 6155–6184. DOI: 10.1088/0264-9381/23/22/006. arXiv: gr-qc/0507106.

[121] A. S. Vytheeswaran. “Gauge unfixing in second class constrained systems”. In: *Annals Phys.* 236 (1994), pp. 297–324. DOI: 10.1006/aphy.1994.1114.

[122] Goran Lindblad. “On the generators of quantum dynamical semigroups”. In: *Communications in Mathematical Physics* 48.2 (1976), pp. 119–130. DOI: 10.1007/BF01608499.

[123] Vittorio Gorini, Andrzej Kossakowski, and Ennackal Chandy George Sudarshan. “Completely positive dynamical semigroups of N-level systems”. In: *Journal of Mathematical Physics* 17.5 (1976), pp. 821–825. DOI: 10.1063/1.522979.

[124] Sadao Nakajima. “On Quantum Theory of Transport Phenomena Steady Diffusion”. In: *Progress of Theoretical Physics* 20 (1958), pp. 948–959. DOI: 10.1143/PTP.20.948.

[125] Robert Zwanzig. “Ensemble Method in the Theory of Irreversibility”. In: *The Journal of Chemical Physics* 33.5 (1960), pp. 1338–1341. DOI: 10.1063/1.1731409.

[126] Fumiaki Shibata, Yoshinori Takahashi, and Natsuki Hashitsume. “A generalized stochastic liouville equation. Non-Markovian versus memoryless master equations”. In: *Journal of Statistical Physics* 17 (1977), pp. 171–187.

[127] S Chaturvedi and F Shibata. “Time-convolutionless projection operator formalism for elimination of fast variables. Applications to Brownian motion”. In: *Zeitschrift für Physik B Condensed Matter* 35.3 (1979), pp. 297–308.

[128] Abhay Ashtekar, Carlo Rovelli, and Lee Smolin. “Gravitons and loops”. In: *Phys. Rev. D* 44 (1991), pp. 1740–1755. DOI: 10.1103/PhysRevD.44.1740. arXiv: hep-th/9202054.

[129] Madhavan Varadarajan. “Gravitons from a loop representation of linearized gravity”. In: *Phys. Rev. D* 66 (2002), p. 024017. DOI: 10.1103/PhysRevD.66.024017. arXiv: gr-qc/0204067.

[130] E. Poisson and C. M. Will. *Gravity: Newtonian, Post-Newtonian, Relativistic*. Cambridge University Press, 2014.

[131] Steven Weinberg. *The quantum theory of fields: Volume 1, foundations*. Cambridge university press, 2005.

[132] David Tong. *Quantum Field Theory (Lecture Notes)*. 2007. URL: https://www.damtp.cam.ac.uk/user/tong/qft/qft.pdf.

[133] A. O. Caldeira and A. J. Leggett. “Influence of dissipation on quantum tunneling in macroscopic systems”. In: *Phys. Rev. Lett.* 46 (1981), p. 211. DOI: 10.1103/PhysRevLett.46.211.

[134] David P. DiVincenzo. "Two-bit gates are universal for quantum computation". In: *Phys. Rev. A* 51 (1995), pp. 1015–1022. DOI: 10.1103/PhysRevA.51.1015. arXiv: cond-mat/9407022.

[135] W. G. Unruh. "Maintaining coherence in quantum computers". In: *Phys. Rev. A* 51 (1995), p. 992. DOI: 10.1103/PhysRevA.51.992. arXiv: hep-th/9406058.

[136] G. Massimo Palma, Kalle-Antti Suominen, and Artur K. Ekert. "Quantum computers and dissipation". In: *Proc. Roy. Soc. Lond. A* 452 (1996), pp. 567–584. DOI: 10.1098/rspa.1996.0029. arXiv: quant-ph/9702001.

[137] Karl Kraus. "General state changes in quantum theory". In: *Annals of Physics* 64.2 (1971), pp. 311–335. DOI: 10.1016/0003-4916(71)90108-4.

[138] R. P. Feynman and F. L. Vernon Jr. "The Theory of a general quantum system interacting with a linear dissipative system". In: *Annals Phys.* 24 (1963). Ed. by L. M. Brown, pp. 118–173. DOI: 10.1016/0003-4916(63)90068-X.

[139] Ilya Prigogine. *Non-equilibrium statistical mechanics*. Courier Dover Publications, 2017.

[140] Fumiaki Shibata and Toshihico Arimitsu. "Expansion formulas in nonequilibrium statistical mechanics". In: *Journal of the Physical Society of Japan* 49.3 (1980), pp. 891–897.

[141] N.G. Van Kampen. "A cumulant expansion for stochastic linear differential equations. I". In: *Physica* 74.2 (1974), pp. 215–238. ISSN: 0031-8914. DOI: https://doi.org/10.1016/0031-8914(74)90121-9.

[142] N.G. Van Kampen. "A cumulant expansion for stochastic linear differential equations. II". In: *Physica* 74.2 (1974), pp. 239–247. ISSN: 0031-8914. DOI: https://doi.org/10.1016/0031-8914(74)90122-0.

[143] Carlos Alexandre Brasil, Felipe Fernandes Fanchini, and Reginaldo de Jesus Napolitano. "A simple derivation of the Lindblad equation". In: *Revista Brasileira de Ensino de Fisica* 35 (2013), pp. 01–09.

[144] Kristina Giesel and Michael Kobler. "An Open Scattering Model in Polymerized Quantum Mechanics". In: *Mathematics* 10.22 (2022), p. 4248. DOI: 10.3390/math10224248. arXiv: 2207.08749 [gr-qc].

[145] D. Boyanovsky. "Effective Field Theory out of Equilibrium: Brownian quantum fields". In: *New J. Phys.* 17.6 (2015), p. 063017. DOI: 10.1088/1367-2630/17/6/063017. arXiv: 1503.00156 [hep-ph].

[146] J. Fernando Barbero G. "Real Ashtekar variables for Lorentzian signature space times". In: *Phys. Rev. D* 51 (1995), pp. 5507–5510. DOI: 10.1103/PhysRevD.51.5507. arXiv: gr-qc/9410014.

[147] Giorgio Immirzi. "Real and complex connections for canonical gravity". In: *Class. Quant. Grav.* 14 (1997), pp. L177–L181. DOI: 10.1088/0264-9381/14/10/002. arXiv: gr-qc/9612030.

[148] T. Thiemann. "Generalized boundary conditions for general relativity for the asymptotically flat case in terms of Ashtekar's variables". In: *Class. Quant. Grav.* 12 (1995), pp. 181–198. DOI: 10.1088/0264-9381/12/1/016. arXiv: gr-qc/9910008.

[149] Alejandro Corichi, Irais Rubalcava, and Tatjana Vukasinac. "Hamiltonian and Noether charges in first order gravity". In: *Gen. Rel. Grav.* 46 (2014), p. 1813. DOI: 10.1007/s10714-014-1813-0. arXiv: 1312.7828 [gr-qc].

[150] Miguel Campiglia. "Note on the phase space of asymptotically flat gravity in Ashtekar-Barbero variables". In: *Class. Quant. Grav.* 32.14 (2015), p. 145011. DOI: 10.1088/0264-9381/32/14/145011. arXiv: 1412.5531 [gr-qc].

[151] Bianca Dittrich and Johannes Tambornino. "A Perturbative approach to Dirac observables and their space-time algebra". In: *Class. Quant. Grav.* 24 (2007), pp. 757–784. DOI: 10.1088/0264-9381/24/4/001. arXiv: gr-qc/0610060.

[152] Tullio Regge and Claudio Teitelboim. "Role of Surface Integrals in the Hamiltonian Formulation of General Relativity". In: *Annals Phys.* 88 (1974), p. 286. DOI: 10.1016/0003-4916(74)90404-7.

[153] Bianca Dittrich and Thomas Thiemann. "Testing the master constraint programme for loop quantum gravity. IV. Free field theories". In: *Class. Quant. Grav.* 23 (2006), pp. 1121–1142. DOI: 10.1088/0264-9381/23/4/004. arXiv: gr-qc/0411141.

[154] Steven Giddings and Sean Weinberg. "Gauge-invariant observables in gravity and electromagnetism: black hole backgrounds and null dressings". In: *Phys. Rev. D* 102.2 (2020), p. 026010. DOI: 10.1103/PhysRevD.102.026010. arXiv: 1911.09115 [hep-th].

[155] Thomas Thiemann. "Reduced phase space quantization and Dirac observables". In: *Class. Quant. Grav.* 23 (2006), pp. 1163–1180. DOI: 10.1088/0264-9381/23/4/006. arXiv: gr-qc/0411031 [gr-qc].

[156] Bianca Dittrich and Johannes Tambornino. "Gauge invariant perturbations around symmetry reduced sectors of general relativity: Applications to cosmology". In: *Class. Quant. Grav.* 24 (2007), pp. 4543–4586. DOI: 10.1088/0264-9381/24/18/001. arXiv: gr-qc/0702093.

[157] Kristina Giesel, Adrian Herzog, and Parampreet Singh. "Gauge invariant variables for cosmological perturbation theory using geometrical clocks". In: *Class. Quant. Grav.* 35.15 (2018), p. 155012. DOI: 10.1088/1361-6382/aacda2. arXiv: 1801.09630 [gr-qc].

[158] Richard Arnowitt, Stanley Deser, and Charles W Misner. "The dynamics of general relativity, Gravitation: An introduction to current research". In: *Chap* 7 (1962), pp. 227–265.

[159] Karel Kuchař. "Ground state functional of the linearized gravitational field". In: *Journal of Mathematical Physics* 11.12 (1970), pp. 3322–3334. DOI: 10.1063/1.1665133.

[160] Abhay Ashtekar and Béatrice Bonga. "On the ambiguity in the notion of transverse traceless modes of gravitational waves". In: *Gen. Rel. Grav.* 49.9 (2017), p. 122. DOI: 10.1007/s10714-017-2290-z. arXiv: 1707.09914 [gr-qc].

[161] K. Giesel, S. Hofmann, T. Thiemann, and O. Winkler. "Manifestly Gauge-Invariant General Relativistic Perturbation Theory. I. Foundations". In: *Class. Quant. Grav.* 27 (2010), p. 055005. DOI: 10.1088/0264-9381/27/5/055005. arXiv: 0711.0115 [gr-qc].

[162] Ryogo Kubo. "Statistical mechanical theory of irreversible processes 1. General theory and simple applications in magnetic and conduction problems". In: *J. Phys. Soc. Jap.* 12 (1957), pp. 570–586. DOI: 10.1143/JPSJ.12.570.

[163] Paul C. Martin and Julian Schwinger. "Theory of Many-Particle Systems. I". In: *Phys. Rev.* 115 (6 1959), pp. 1342–1373. DOI: 10.1103/PhysRev.115.1342.

[164] John F. Donoghue, Mikhail M. Ivanov, and Andrey Shkerin. "EPFL Lectures on General Relativity as a Quantum Field Theory". Feb. 2017. arXiv: 1702.00319 [hep-th].

[165] Jurjen F. Koksma, Tomislav Prokopec, and Michael G. Schmidt. "Decoherence in an Interacting Quantum Field Theory: Thermal Case". In: *Phys. Rev. D* 83 (2011), p. 085011. DOI: 10.1103/PhysRevD.83.085011. arXiv: 1102.4713 [hep-th].

[166] T. S. Evans and Daniele A. Steer. "Wick's theorem at finite temperature". In: *Nucl. Phys. B* 474 (1996), pp. 481–496. DOI: 10.1016/0550-3213(96)00286-6. arXiv: hep-ph/9601268.

[167] Alexandre Feller and Etera R. Livine. "Surface state decoherence in loop quantum gravity, a first toy model". In: *Class. Quant. Grav.* 34.4 (2017), p. 045004. DOI: 10.1088/1361-6382/aa525c. arXiv: 1607.00182 [gr-qc].

[168] B.L. Burrows and D.J. Colwell. "The fourier transform of the unit step function." In: *International Journal of Mathematical Education in Science and Technology* 21(4) (1990), pp. 629–635. DOI: 10.1143/PTP.14.351.

[169] T. Arimitsu and H. Umezawa. "A General Formulation of Nonequilibrium Thermo Field Dynamics". In: *Prog. Theor. Phys.* 74 (1985). Ed. by A. Arimitsu, H. Ezawa, H. Matsumoto, K. Nakamura, and Y. Yamanaka, p. 429. DOI: 10.1143/PTP.74.429.

[170] Y. Takahashi and H. Umezawa. "Thermo field dynamics". In: *Int. J. Mod. Phys. B* 10 (1996), pp. 1755–1805. DOI: 10.1142/S0217979296000817.

[171] Faqir C. Khanna, Adolfo P. C. Malbouisson, Jorge M. C. Malbouisson, and Ademir R. Santana. *Thermal quantum field theory - Algebraic aspects and applications*. 2009.

[172] John F. Donoghue. "General relativity as an effective field theory: The leading quantum corrections". In: *Phys. Rev. D* 50 (1994), pp. 3874–3888. DOI: 10.1103/PhysRevD.50.3874. arXiv: gr-qc/9405057.

[173] Daniel Arteaga, Renaud Parentani, and Enric Verdaguer. "Propagation in a thermal graviton background". In: *Phys. Rev. D* 70 (2004), p. 044019. DOI: 10.1103/PhysRevD.70.044019. arXiv: gr-qc/0311065.

[174] Brian Hatfield. *Quantum Field Theory Of Point Particles And Strings*. CRC Press, May 2019. ISBN: 978-0-429-49323-2. DOI: 10.1201/9780429493232.

[175] Frederik Nathan and Mark S. Rudner. "Universal Lindblad equation for open quantum systems". In: *Physical Review B* 102.11 (Sept. 2020). ISSN: 2469-9969. DOI: 10.1103/physrevb.102.115109. URL: http://dx.doi.org/10.1103/PhysRevB.102.115109.

[176] Chris Fleming, NI Cummings, Charis Anastopoulos, and Bei-Lok Hu. "The rotating-wave approximation: consistency and applicability from an open quantum system analysis". In: *Journal of Physics A: Mathematical and Theoretical* 43.40 (2010), p. 405304. DOI: 10.1088/1751-8113/43/40/405304.

[177] E. T. Jaynes and F. W. Cummings. "Comparison of quantum and semiclassical radiation theories with application to the beam maser". In: *IEEE Proc.* 51 (1963), pp. 89–109. DOI: 10.1109/PROC.1963.1664.

[178] Bruce W Shore and Peter L Knight. "The jaynes-cummings model". In: *Journal of Modern Optics* 40.7 (1993), pp. 1195–1238. URL: https://api.semanticscholar.org/CorpusID:123519002.

[179] Jonas Larson and Themistoklis Mavrogordatos. *The Jaynes–Cummings model and its descendants: modern research directions*. IoP Publishing, 2021.

[180] Peng Wang, Erik Hiltunen, and John C. Schotland. "Rotating wave approximation and renormalized perturbation theory". Nov. 2023. arXiv: 2311.02670 [quant-ph].

[181] Daniel Burgarth, Paolo Facchi, Robin Hillier, and Marilena Ligabò. "Taming the Rotating Wave Approximation". In: *Quantum* 8 (2024), p. 1262. DOI: 10.22331/q-2024-02-21-1262. arXiv: 2301.02269 [quant-ph].

[182] Hing-Tong Cho and Bei-Lok Hu. "Quantum noise of gravitons and stochastic force on geodesic separation". In: *Phys. Rev. D* 105.8 (2022), p. 086004. DOI: 10.1103/PhysRevD.105.086004. arXiv: 2112.08174 [gr-qc].

[183] Carlo Giunti and Chung W Kim. *Fundamentals of neutrino physics and astrophysics*. Oxford university press, 2007.

[184] Vernon Barger, Danny Marfatia, and Kerry Whisnant. *The physics of neutrinos*. Princeton University Press, 2012.

[185] Antonio Ereditato. "State Of The Art Of Neutrino Physics, The: A Tutorial For Graduate Students And Young Researchers". In: (2018).

[186] Judith Oberauer and Lothar Oberauer. *Neutrinophysik*. Springer, 2019.

[187] Kai Zuber. *Neutrino physics*. Taylor & Francis, 2020.

[188] C. Giunti. "Neutrino wave packets in quantum field theory". In: *JHEP* 11 (2002), p. 017. DOI: 10.1088/1126-6708/2002/11/017. arXiv: hep-ph/0205014.

[189] Daniel Kruppke. "On theories of neutrino oscillations". Diploma Thesis, 2007.

[190] Evgeny Kh. Akhmedov and Alexei Yu. Smirnov. "Paradoxes of neutrino oscillations". In: *Phys. Atom. Nucl.* 72 (2009), pp. 1363–1381. DOI: 10.1134/S1063778809080122. arXiv: 0905.1903 [hep-ph].

[191] Particle Data Group. "Review of Particle Physics". In: *Chin. Phys. C* 40.10 (2016), p. 100001. DOI: 10.1088/1674-1137/40/10/100001.

[192] Particle Data Group. "Review of particle physics". In: *Physical Review D* 110.3 (2024), p. 030001. DOI: 10.1103/PhysRevD.110.030001.

[193] C. Giunti, C. W. Kim, and U. W. Lee. "When do neutrinos cease to oscillate?" In: *Phys. Lett. B* 421 (1998), pp. 237–244. DOI: 10.1016/S0370-2693(98)00014-8. arXiv: hep-ph/9709494.

[194] Amélie Chatelain and Maria Cristina Volpe. "Neutrino decoherence in presence of strong gravitational fields". In: *Phys. Lett. B* 801 (2020), p. 135150. DOI: 10.1016/j.physletb.2019.135150. arXiv: 1906.12152 [hep-ph].

[195] Vittorio D'Esposito and Giulia Gubitosi. "Constraints on quantum spacetime-induced decoherence from neutrino oscillations". In: *Phys. Rev. D* 110.2 (2024), p. 026004. DOI: 10.1103/PhysRevD.110.026004. arXiv: 2306.14778 [hep-ph].

[196] Fabio Benatti and Heide Narnhofer. “Entropy behaviour under completely positive maps”. In: *letters in mathematical physics* 15 (1988), pp. 325–334.

[197] H. Grabert, U. Weiss, and P. Talkner. “Quantum theory of the damped harmonic oscillator”. In: *Z. Physik B-Condensed Matter* 55 (1984), pp. 87–94. DOI: 10.1007/BF01307505.

[198] Rodolfo Gambini, Rafael A. Porto, and Jorge Pullin. “Decoherence from discrete quantum gravity”. In: *Class. Quant. Grav.* 21 (2004), pp. L51–L57. DOI: 10.1088/0264-9381/21/8/L01. arXiv: gr-qc/0305098.

[199] Andrea Smirne, Dario Tamascelli, James Lim, Martin B. Plenio, and Susana F. Huelga. “Non-Perturbative Treatment of Open-System Multi-Time Expectation Values in Gaussian Bosonic Environments”. In: *Open Systems & Information Dynamics* 29.04 (2022), p. 2250019. DOI: 10.1142/S1230161222500196. arXiv: 2209.00293 [quant-ph].

[200] Stephen L. Adler. “Comment on a proposed Super-Kamiokande test for quantum gravity induced decoherence effects”. In: *Phys. Rev. D* 62 (2000), p. 117901. DOI: 10.1103/PhysRevD.62.117901. arXiv: hep-ph/0005220.

[201] Thomas Guff and Andrea Rocco. “Time-Reversal Symmetry in Open Classical and Quantum Systems”. Nov. 2023. arXiv: 2311.08486 [quant-ph].

[202] KM3NeT Collaboration. “Letter of intent for KM3NeT 2.0”. In: *J. Phys. G* 43.8 (2016), p. 084001. DOI: 10.1088/0954-3899/43/8/084001. arXiv: 1601.07459 [astro-ph.IM].

[203] J. A. B. Coelho et al. “OscProb”. In: *Zenodo* (2024). DOI: https://doi.org/10.5281/zenodo.10666396.

[204] Adam M. Dziewonski and Don L. Anderson. “Preliminary reference Earth model”. In: *Physics of the Earth and Planetary Interiors* 25.4 (1981), pp. 297–356. ISSN: 0031-9201. DOI: https://doi.org/10.1016/0031-9201(81)90046-7.

[205] Edward W. Kolb and Michael S. Turner. *The Early Universe*. Vol. 69. 1990. ISBN: 978-0-201-62674-2. DOI: 10.1201/9780429492860.

[206] M. Gasperini, Massimo Giovannini, and G. Veneziano. “Squeezed thermal vacuum and the maximum scale for inflation”. In: *Phys. Rev. D* 48 (1993), R439–R443. DOI: 10.1103/PhysRevD.48.R439. arXiv: gr-qc/9306015.

[207] Massimo Giovannini. “Primordial backgrounds of relic gravitons”. In: *Prog. Part. Nucl. Phys.* 112 (2020), p. 103774. DOI: 10.1016/j.ppnp.2020.103774. arXiv: 1912.07065 [astro-ph.CO].

[208] G. J. Milburn. “Intrinsic decoherence in quantum mechanics”. In: *Phys. Rev. A* 44.9 (1991), p. 5401. DOI: 10.1103/PhysRevA.44.5401.

[209] G. J. Milburn. “Lorentz invariant intrinsic decoherence”. In: *New J. Phys.* 8 (2006), p. 96. DOI: 10.1088/1367-2630/8/6/096. arXiv: gr-qc/0308021.

[210] H. -P. Breuer, E. Goklu, and C. Lammerzahl. “Metric fluctuations and decoherence”. In: *Class. Quant. Grav.* 26 (2009), p. 105012. DOI: 10.1088/0264-9381/26/10/105012. arXiv: 0812.0420 [gr-qc].

[211] Lajos Diosi. “Intrinsic time-uncertainties and decoherence: Comparison of 4 models”. In: *Braz. J. Phys.* 35 (2005). Ed. by Hans-Thomas Elze, pp. 260–265. DOI: 10.1590/S0103-97332005000200009. arXiv: quant-ph/0412154.

[212] Daniel Boriero, Dominik J. Schwarz, and Hermano Velten. "Flavour composition and entropy increase of cosmological neutrinos after decoherence". In: *Universe* 5.10 (2019), p. 203. DOI: 10.3390/universe5100203. arXiv: 1704.06139 [astro-ph.CO].

[213] Daniel Pfenniger and Veruska Muccione Geneva Observatory. "Cosmological Neutrino Entanglement and Quantum Pressure". In: *Astron. Astrophys.* 456 (2006), p. 45. DOI: 10.1051/0004-6361:20054496. arXiv: astro-ph/0605354.

[214] A. E. Bernardini. "Cosmological neutrino entropy changes due to flavor statistical mixing". In: *EPL* 103.3 (2013), p. 30005. DOI: 10.1209/0295-5075/103/30005. arXiv: 1204.1504 [astro-ph.CO].

[215] J. Wilson-Gerow. "A study of the quantum-to-classical transition in gravity, and a study of the consequences of constraints in gauge theory path-integrals." Master's thesis. University of British Colombia, Supervisor: Philip Stamp, 2017.

[216] Jordan Wilson-Gerow and P. C. E. Stamp. "Gauge invariant propagators and states in quantum electrodynamics". In: *Annals Phys.* 442 (2022), p. 168898. DOI: 10.1016/j.aop.2022.168898. arXiv: 2011.05305 [hep-th].

[217] Eduardo Martin-Martinez. "Causality issues of particle detector models in QFT and Quantum Optics". In: *Phys. Rev. D* 92.10 (2015), p. 104019. DOI: 10.1103/PhysRevD.92.104019. arXiv: 1509.07864 [quant-ph].

[218] Nicholas Funai and Eduardo Martin-Martinez. "Faster-than-light signaling in the rotating-wave approximation". In: *Phys. Rev. D* 100.6 (2019), p. 065021. DOI: 10.1103/PhysRevD.100.065021. arXiv: 1905.02235 [quant-ph].

[219] Greg Kaplanek and Erickson Tjoa. "Effective master equations for two accelerated qubits". In: *Phys. Rev. A* 107.1 (2023), p. 012208. DOI: 10.1103/PhysRevA.107.012208. arXiv: 2207.13750 [quant-ph].

[220] Thomas Colas, Julien Grain, and Vincent Vennin. "Benchmarking the cosmological master equations". In: *Eur. Phys. J. C* 82.12 (2022), p. 1085. DOI: 10.1140/epjc/s10052-022-11047-9. arXiv: 2209.01929 [hep-th].

[221] Dragomir Davidović. "Completely positive, simple, and possibly highly accurate approximation of the Redfield equation". In: *Quantum* 4 (2020), p. 326.